

14th International Symposium
**WATER MANAGEMENT AND
HYDRAULIC ENGINEERING 2015**

September 8th to 10th 2015, Brno, Czech Republic

Editors: Jaromír Říha, Tomáš Julínek, Karel Adam

Organized by:

Brno University of Technology
Faculty of Civil Engineering



In collaboration with:

University of Zagreb
Faculty of Civil Engineering, Zagreb, Croatia



Gdansk University of Technology
Faculty of Civil and Environmental Engineering, Gdansk, Poland



Slovak University of Technology in Bratislava
Faculty of Civil Engineering, Bratislava, Slovak Republic



BOKU University of Natural Resources and Applied Life Sciences
Institute of Water Management, Hydrology and Hydraulic Engineering



Vienna, Austria

Ss. Cyril and Methodius University in Skopje
Faculty of Civil Engineering, Skopje



14th International Symposium

WATER MANAGEMENT AND HYDRAULIC ENGINEERING 2015

Editors: Jaromír Říha, Tomáš Julínek, Karel Adam

Papers have been double-blind peer reviewed before final submission to the conference. Initially, paper abstracts were read and selected by the conference Scientific Committee as possible papers for the conference.

WMHE2015's Publication Ethics and Publication Malpractice Statement is based, on the guidelines and standards developed by the Committee on Publication Ethics (COPE). Publication Ethics and Publication Malpractice Statement defines responsibilities of authors, reviewers, members of Scientific Committee and editors.

Reviewers:

Aleš Dráb, Petr Hlavínek, Jan Jandora, Andrej Šoltész, Miroslav Špano,
Ladislav Tuhovčák

Many thanks to the reviewers who helped ensure the quality of the published manuscripts.

Published in 2015

First edition

© 2015 Institute of Water Structures, FCE, BUT

Front cover photos by Institute of Water Structures, FCE, BUT

All rights reserved. No part of this book may be reproduced in any form or by any means without written permission from editors.

Print version with full text papers **ISBN: 978-80-214-5230-5**

Print version with full text papers **ISSN: 2410-5910**

Conference web page: wmhe.fce.vutbr.cz

SYMPOSIUM CHAIRMEN

CHAIRMAN

Jaromír Říha (*BUT, Faculty of Civil Engineering, Brno, Czech Republic*)

Co-CHAIRMEN

Romuald Szymkiewicz (*Gdansk University of Technology, Faculty of Civil and Environmental Engineering, Gdansk, Poland*)

Davor Malus (*University of Zagreb, Faculty of Civil Engineering, Zagreb, Croatia*)

Andrej Šoltész (*SUT, Faculty of Civil Engineering, Bratislava, Slovak Republic*)

Christine Sindelar (*BOKU, Vienna, Austria*)

Cvetanka Popovska (*Ss. Cyril and Methodius University, FCE, Skopje, Macedonia*)

SCIENTIFIC ADVISORY COMMITTEE

Jan Jandora, Aleš Dráb

(BUT, Faculty of Civil Engineering, Brno, Czech Republic)

Ján Szolgay, Peter Dušička, Štefan Stanko

(SUT, Faculty of Civil Engineering, Bratislava, Slovakia)

Neven Kuspilić, Živko Vuković, Goran Lončar

University of Zagreb, FCE, Zagreb, Croatia

Michał Szydłowski, Hanna Obarska-Pempkowiak, Jerzy Sawicki

Gdansk University of Technology, FCEE, Gdansk, Poland

Helmut Habersack, Willibald Loiskandl, Johannes Hübl

BOKU, Vienna, Austria

Milorad Jovanovski, Petko Pelivanoski, Violeta Gešovska

Ss. Cyril and Methodius University, FCE, Skopje, Macedonia

ORGANIZING COMMITTEE

Tomáš Julínek, Karel Adam, Jan Vrubel, David Duchan, Pavla Kozlová

(BUT, FCE, Brno, Czech Republic)

Content

Preface	7
Keynote lectures	
240 Years Dresden Gauge – 1000 Years Floods of the Elbe (Labe) River (<i>R. Pohl</i>).....	9
Seepage Problems at Areas Protected against Floods (<i>T. Julínek, J. Říha</i>).....	20
Development of Automated Approaches for Hydropower Potential Estimations and Prospective Hydropower Plants Siting (<i>N. Badenko, T. Ivanov, O. Nikonova, V. Oleshko</i>).....	32
Braided river gravel reach hydrodynamics: a field example (<i>A. Radecki-Pawlik, J. Bencal, M. Kowalski, B. Radecki-Pawlik</i>).....	46
Hydraulics and hydromechanics	
Parameters of wind driven waves on Nove Mlyny water reservoir (<i>P. Pelikán, M. Šlezinger</i>).....	55
Physical and Mathematical Modelling for Canoe Slalom Whitewater and the 2016 Olympic Games in Rio de Janeiro (<i>J. Pollert jun., J. Pollert sen., J. Procházka, P. Chmátal, B. Campbell, J. Felton, D. Dungworth</i>).....	65
Calculating erosion rates of river bank sediment by combining field measurements of erodibility parameters and small-scale topographic features – A case study at the Danube River (<i>M. Pfemeter, M. Klösch, E. J. Langendoen, H. Habersack</i>).....	77
Modelling of open channel flow with FLOW-3D (<i>D. Duchan, T. Julínek</i>)	87
Quantification of hydrodynamic load on the bridge deck using numerical simulations (<i>M. Špano, A. Dráb</i>)	95
Water hammer analysis-impact of the pipe material in water supply system (<i>G. Taseski, C. Popovska</i>).....	103
Numerical analysis of the impact of breakwater culvert to the sea exchange in the Adriatic marinas (<i>G. Loncar, H. Mostecak, T. Polak</i>).....	111
The CFD analyses of the lateral spillway using different turbulence models (<i>M. Orfánus, A. Šoltész</i>).....	121
Hydrology and river basin management	
Analysis and visualization of irrigation distribution systems (<i>M. Čistý, Z. Bajtek, L. Celar</i>).....	131
Stormwater and snowmelt runoff storage control and flash flood hazard forecasting in the urbanized coastal basin (<i>M. Szydłowski, P. Zima, K. Weinerowska-Bords, P. Mikos- Studnicka, J. Hakiel, D. Szawurska</i>).....	141
Determining Czech Republic’s minimum residual discharges (<i>P. Balvin, A. Vizina, M. Nesládková, L. Kašpárek</i>).....	151
Predicting output flood wave on the section of the Drava River (<i>M. Šperac, T. Mijušković-Svetinović, A Rabi</i>).....	162
Climate and land use changes impacts on small catchment areas (<i>T. Dadić, L. Tadić</i>)	171
The influence of the synthetic rainfall hyetograph on runoff from urban catchment (<i>K. Mazurkiewicz, M. Sowiński</i>).....	181

Evaluation of reservoir degradation state by Autonomous Underwater Vehicle (V. Sočuvka, Y. Velísková).....	191
--	-----

Sanitary and environmental engineering

Reasons why Onsite Wastewater Treatment Systems are not Systematically Used in the Republic of Croatia (D. Malus).....	199
Membrane Technology in Surface Water Treatment for Drinking Purposes (D. Barloková, J. Ilavský, M. Kunštek, J. Buchlovičová).....	209
Possibilities for recycling of sewage sludge (D. Vouk, D. Nakić, N. Štirmer, D. Malus).....	219
The Greenhouse Gas Emissions for Several Water Utility Companies in Croatia (I. Halkijević, Z. Vuković, D. Vouk).....	229
The Comparison of Green and Conventional Stormwater Management – Zagreb Case Study (I. Halkijević, M. Kuspilić, Z. Vuković).....	235
Technical Audit of Water Supply Systems (L. Tuhovčák, T. Kučera, M. Tauš).....	245
Defining the time of closing the valve at small hydro power plant on the main pipeline of the water supply system (G. Taseski, C. Popovska, P. Pelivanoski).....	254
Runoff quality from green roofs (M. Sokáč).....	264
Efficacy of sorption materials for metals removal from water (R. Biela, T. Kučera)	271

Sustainable water use, water resources, flood risks

Flood Warning System for Valašsko – Horní Vsacko (V. Kolečkář, J. Kubík, R. Říhová).....	280
The Adriatic Sea Wave Energy Analysis (E. Ocvirk, K. Duvnjak, M. Kaciga).....	289
Dispersion tracking experiments in different streams types (M. Sokáč).....	298
Cross border water resources and water supply management – DRINKADRIA project (B. Karleuša, P. Banovec, I. Radman, J. Rubinić).....	307
The operational water consumption of energy production: Czech Republic case study (L. Ansorge, M. Zeman).....	317
Concept of Restoration and Preservation of River Odra’s Biodiversity and Eco-system Services (BIO -ODRA) (D. Kunštek).....	329
Environmental damage due to floods assessment (M. Zeleňáková, L. Gaňová).....	339
Multicriteria analysis method for flood risk assessment (J. Kozubík, A. Dráb).....	348
Overview of water resource based human carrying capacity assessment models (M. Kuspilić, Z. Vuković, I. Halkijević).....	357
Considering Uncertainties in Design of Stormwater Infiltration Facility (D. Duchan, J. Říha).....	365
Hydraulic assessment of flood protection measures in Small Carpathians (A. Janík, A. Šoltész).....	379

Geotechnical engineering, groundwater hydraulics, erosion control

Effect of soil erosion on filters behavior in hydraulic structures (S. Azirou, A. Benamar, A. Tahakourt).....	391
Investigations and Analysis of Levee Failures during recent Floods in Saxony and Saxony-Anhalt (Germany) (T. Heyer, J. Stamm).....	401

Methodology for determination of rock mass characteristics for hydrotechnical tunnels (<i>Z. Zafirovski, I. Peshevski, M. Jovanovski</i>).....	411
Effect of designed material pits on filtration stability of the subsoil of polder Borša (<i>D. Grambličková, E. Bednářová, M. Minárik, E. Kolesárová, M. Bakeš</i>).....	419
Changes in groundwater level regime along channel due to surface water level fluctuations (<i>P. Dušek</i>).....	428
Experiences on the use of polymer coated steel net for the protection of dykes against the intrusion of beavers (<i>P. Di Pietro, J. Adamec</i>)	439
Modelling of the impact on groundwater regime due to construction of the proposed hydraulic structure on the Danube River (<i>M. Nahálkova, D. Baroková, A. Šoltész</i>)	449

Hydraulic structures, monitoring

Arch dam behaviour evaluation by comparison of numerical model and monitoring data (<i>S. Mitovski, L. Petkovski, G Kokalanov</i>)	457
Flood zone modelling and flood losses estimation using GIS and numerical hydrodynamic models (<i>N. V. Badenko, T. S. Ivanov, S. P. Kotlyar, K. A. Osmolovsky, M. V. Petroshenko, V. A. Prokofyev</i>)	467
Analysis of SHPP Brodraci influence on production of HPP Ozalj (<i>E. Ocvirk, G. Gilja, J. Berbič</i>)	479
Temperature measurement methods on the water structures (<i>O. Černý, J. Hodák</i>).....	487
Using high-precision total station operating in ATR mode and robust adjustment of geodetic networks for safety supervision over waterworks (<i>T. Macháček, V. Krnáč</i>)	498
The effect of flow regime on navigation near the Water Structure (<i>A. Palkovičová</i>)....	509
Kolárovo Water Structure - selected results of the hydraulic research (<i>L. Možiešik, M. Orfánus, J. Rumann, P. Šulek, P. Dušička</i>)	518
Monitoring of the embankment dam and effectiveness of remedial measures by EIS method (<i>J. Pařílková, I. Pavlík, M. Novák, J. Veselý</i>).....	530
Classification of dam failures for adopting limit states (<i>K. Adam, J. Vrabel</i>).....	540
Restoration of the stilling basin of the Drtijšćica dam (<i>N. Humar, A. Kryžanowski</i>)....	550
Use of gabion structures as flood mitigation in hydraulic works (<i>J. Adamec, L. Luboš</i>)	560
Influence of Genetic Algorithms Parameters on the Optimization of Hydrothermal Coordination Problem (<i>P. Šulek, T. Kinczer, P. Dušička</i>)	570
Application of artificial intelligence methods in solving problems of hydrotechnics (<i>S. Kelčík, R. Květon</i>)	580
Modeling of long-term sedimentation in the Osijek port basin (<i>G. Gilja, N. Kuspilić</i>)	590

Preface

The 14th Water Management and Hydraulic Engineering (WMHE) conference follows 39 years of tradition in organizing similar conferences focused on new technologies, practices and strategies in water resources and water management, and also in related disciplines such as environmental engineering, geotechnics and others. The main goal of the conference is to share transboundary and interdisciplinary knowledge and experience between scientists and experts from Central Europe, from older and new EU member states as well as from South-East European candidate countries.

In 1976 the first conference of this type was organized as a bilateral activity between the faculties of Gdańsk University (Poland) and Zagreb University (Croatia). Since 1998, the Slovak University of Technology, the Ss. Cyril and Methodius University in Skopje (Macedonia) and the BOKU University of Natural Resources and Applied Life Sciences, Vienna (Austria), have joined this biannual conference series. In 2013 the WMHE conference was organized by the Slovak University of Technology. At this event, Brno University of Technology (BUT), Faculty of Civil Engineering (FCE), Czech Republic, joined the group and was honoured to become the organiser of the 14th conference to be held in Brno on 8 - 10 September 2015. Countries such as France, Germany and Russia will attend this event as new participants.

The conference was announced on the Internet via the creation of a dedicated web site <http://wmhe.fce.vutbr.cz>.

The following thematic topics have been chosen:

1. Hydraulics and hydromechanics
2. Hydrology and river basin management
3. Sanitary and environmental engineering
4. Sustainable water use, water resources, flood risks
5. Geotechnical engineering, groundwater hydraulics, erosion control
6. Hydraulic structures, monitoring

During the conference the presentation of papers will be organized in corresponding thematic sessions.

Special thanks should go to Prof. Petr Štěpánek, the Rector of Brno University of Technology, and to Prof. Rostislav Drochytka, the Dean of the Faculty of Civil Engineering, for their support which has greatly aided the preparation of the conference on the Faculty grounds.

The members of the Organizing Committee are also grateful to all members of the staff of the Institute of Water Structures (BUT, FCE) for their efforts in preparing the conference and technical visits. Finally, special acknowledgements are extended to the reviewers of submitted papers for their aid in producing the Conference Proceedings.

In Brno, September 2015

Editors

240 Years Dresden Gauge – 1000 Years Floods of the Elbe (Labe) River

R. Pohl

(Institute of Hydraulic Engineering and Applied Hydromechanics, Technische Universität Dresden,
D-01062 Dresden, Germany, reinhard.pohl@tu-dresden.de.)

Abstract

The statistical evaluation of flood records requires long and reliable data series to extrapolate the peak discharges and related recurrence intervals as well as possible trends. As the distribution functions for the hydraulic design are usually fitted to the discharge values historic stage-discharge-relations must be found to convert the measured stage values to discharges. Using the historic flow cross sections water profile calculations with 1D and 2D models have been carried out to specify stage-discharge-curves for each period in the past. The recalculated values allowed an update of the flood statistics with surprising results.

This paper reconsiders the use of historical hydrologic data in urban areas which have changed due to changing river beds, cross sections and flood plain areas. The resulting development of the vulnerability and resilience in the Elbe valley at Dresden will be considered and compared with the situation at other places in the world.

Keywords

historical flood records, stage-discharge-curve, peak discharge, recurrence period, flood resilience

1. INTRODUCTION

For the Elbe (Labe, Albis) River at Dresden descriptive historic flood information has been handed down for more than 1000 years. Quantitative information are available (with gaps) since 1501 [Pötzsch 1784]. For 240 years the Dresden gauge at the Augustus-Bridge has been in operation. Referring to this data the history of the water course, the flow regime and the morphology was investigated to review the stage discharge relation. One motive for this investigation was the discrepancy with a lower discharge at a higher stage in 2002 compared with 1845.

2. FLOOD RECORDS AND MEASUREMENTS

In the second half of the 18th century the systematic gauging of the Elbe water level was started in Dresden and other towns on the river. 1775 C. G. Pötzsch fixed an iron staff gauge at the Augustus-Bridge (today German Elbe-km 55.600, catchment area 53096 km², mean discharge 324 m³/s). The regular reading of the water level begun on 1st January 1776. The gauge datum was the „lower navigable

water level“. At that time the depth was measured in Dresden ells (= 0.5752 m) and Dresden inches (= 0.0236 m). Starting with the beginning hydrologic year 1901 the values have been published in the hydrographic yearbook and in 1930 a water level recorder was set into operation. Until December 1st 1935 the gauge datum was at 105.657 m asl and from this day at 102.657 m asl. After the readjustment to the new land surveying system DHHN 12 (Deutsches Haupthöhennetz 1912) the datum was at 102.73 m asl without changing the position. Since 1st February 2004 the reference system has been changed over to DHHN 92 (Deutsches Haupthöhennetz 1992). The datum of the Dresden gauge is now 102.68 m asl.

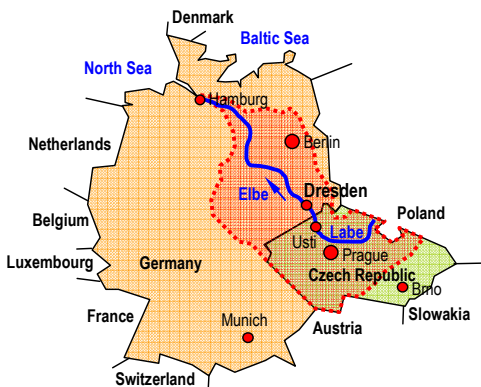


Fig. 1 Elbe/Labe, watershed.

2.1 Sources of historical data.

Precise records of water stages are to be found at many European rivers only after the middle of the 18th century. The information from the time before is often diffuse or consists only of the description of the damages. Due to the less developed measuring techniques and calculation methods the discharge data are almost always missing. And due to the exceptional character of extreme flood events which happened only once in one’s lifetime the chroniclers sometime overstated. The handed down water level data can be inexact and often it does not fit into the present reference system.

Reliable stage data can be derived from flood marks at historical buildings. Here it must be ensured that the marks are in their original place. This is guaranteed best when they are engraved in a natural stone building front or column. One of the oldest marks of this kind at the upper Elbe river from 1501 A.D. is to be found in the town of Meissen (Elbe-Lane, opposite the former monastery of the Order of St. Francis) 25 km downstream of the Dresden gauge.

Regarding historical flood information we can distinguish written, pictorial and material sources. The first group includes e.g. handwritings, gauge books, old projects, navigation documents, chronicles, damage reports, inspection reports, tax lists and parish registers. Photographs, technical drawings, inundation and river

maps, levee maps, painted or photographed views of cities, water mills, banks, bridges as well as landscapes belong to the pictorial witnesses of the past. The 3rd group includes flood marks, inscriptions, epigraphs, sediments, findings of washed away objects and things which can be dated by Carbon-14-analysis, dendrochronology or pollen analysis.

2.2 Extraordinary Floods

One of the three most severe floods in Dresden was the winter flood on 31st March 1845. Fig. 3 (top) shows the large inundation area in the city of Dresden and the downstream rural area which is nowadays a part of the city. Sudden thawing of a 1.50 m thick ice cover on 27th March caused an ice break-up with ice jam upstream the Bridge (today Augustus bridge). On 29th March a large part of the historic city of Dresden was inundated. Many people had to be rescued through the windows by means of boats. Major damages occurred. Also the only Elbe bridge at that time was damaged and the middle pier with the crucifix got broken.

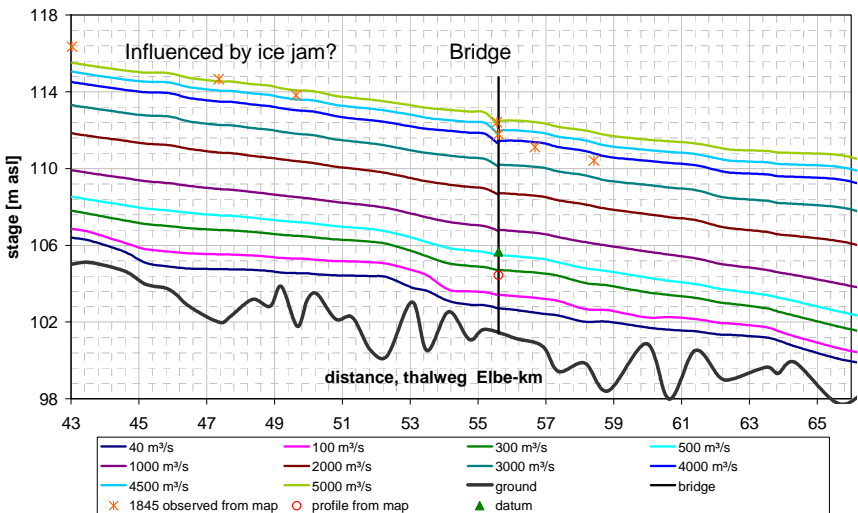


Fig. 2 Recalculated profiles with the bed morphology of 1845 for several discharges with $n = 0,035 \text{ s/m}^{1/3}$ from Elbe-km 50,25 to 60,64. Reference level for the cross sections = navigable water level 2°34' below gauge datum (s. a. Siglow 2007)

The highest water level of the Elbe within living memory was measured on 17th August 2002 during a summer flood. Although the water level was higher than in 1845 less area of the city was inundated (Fig. 3 mid). This is due to changes of the cross section and to the rise of the ground elevation in the city. Just 5 days before the city centre was inundated by the tributaries from the near Ore Mountains (Erzgebirge) which cross the urban area flowing towards the Elbe river. Due to the smaller watersheds they have a short concentration time to peak of only few hours.

3. MODIFICATION OF STAGE-DISCHARGE CURVES

The official hindcast of the 1845 peak water level at the Dresden gauge was 10 ells and 16 inches. A first estimation by the author concerning the related discharge yielded little less than 4000 m³/s [Pohl 2007] with assumed cross sections derived from the handed down information. To improve the accuracy of the calculation in a second step the historical Elbe river map from 1850/55 (scale 1:12000) was used to establish a historical digital terrain model for 1845 and other years. Herein not only the cross sections but also the water stages and inundation areas during the 1845 flood as well as a longitudinal profile with descriptions of landmarks and the gauge datum with the navigable water level (2 ells 3 inches below gauge datum 104.44 m asl) have been drawn. Additional required further quantities were measured in the map.

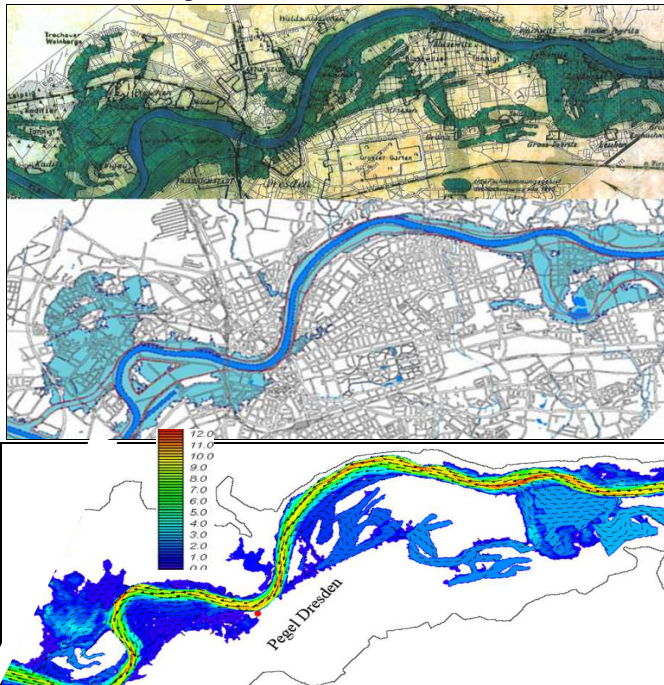


Fig. 3 : Inundation maps for the Elbe in Dresden.- top: 1845, mid: 2002 (www.dresden.de), bottom: own hydronumerical Calculation with a DTM for 1845 (s.a. Kirsch, Pohl 2011)

Comparing the historical and the today's map it is obvious that the width of the Elbe until the middle of the 19th century was about twice compared to the today's width. This is due to the river training for better navigability beginning in the second half of that century. However the deepening due to erosion was less than expected and amounts only between 0 and 60 cm. [Faulhaber 2000] found, that

upstream from Elbe-km 121 the lowering of the water level elevation was on average 25 cm from the end of the 19th century to the mid of the 20th century. Also in the period before the bed erosion seems to have been relatively moderately.

The water level calculation with different channel roughness values (Fig. 4) yields spreading stage-discharge-curves. It can be derived from Fig. 2 that the water level measured 1845 (red star mark) corresponds to a discharge of almost 4000 m³/s, at the gauge downstream the bridge.

Due to the new stage-discharge-relations the flow rates greater than 3000 m³/s were overestimated in the past and have to be reduced and values below 2000 m³/s have to be increased moderately. The bridge afflux beyond 2000 m³/s at the old bridge until their reconstruction (1906-1910) rebuilt bridge is indicated in Fig. 2.

The above mentioned water-level-profile calculations were carried out for definite points in time with its respective morphologic situations such as 1845, 1890, 1940, 2002, 2006. Strictly speaking for every year an individual stage-discharge-relation would be required to yield discharge values from the handed down stage records. In the present study the flow rates were interpolated by using a weighted mean between the years above. Before 1845 the flow cross sections were assumed to be not affected by human activities and therefore approximately constant for the time being. This is why the stage-discharge-curve of 1845 was also applied for the floods before.

4. FLOOD ANALYSIS, FLOOD STATISTICS, TRENDS

Studies like the present one are made to improve the understanding of hydraulic processes in the past on the one hand and on the other hand to improve the flood forecast for the future. For the second issue an annual updating of the flood statistics is required.

Due to the existing statistics the 2002 flood had a recurrence interval of some 150 years and the 2013 peak flow is in the range of 60 years using best fitted repartition functions. Other investigations with a partial annual series from 1936 to 1995 predicted a recurrence period of 200 years for only 3600 m³/s [Nestmann & Büchele 2002] which seems to be an underestimation of the discharge and the probability as well.

With the corrected discharge values a new statistical evaluation has been done by means of the program HQ-EX (DHI-WASY). It becomes visible that the 2002 flood with a peak discharge of $Q = 4581$ m³/s was less frequent than originally assumed. Instead of 150 years the return period is some 500 years now (depending on the selected distribution function - Fig. 5). The 2002 (and round about the 1890) flood become a “centennial flood”.

When yielding so different values the question about trends arises. From Fig. 6 a decreasing trend can be derived. But it is also obvious that due to several human activities at the river and in the watershed the statistical universe (basic population) might have changed. Especially flood protection measures like construction

of dams in the 20th century could be an explanation for the generally decreasing trend.

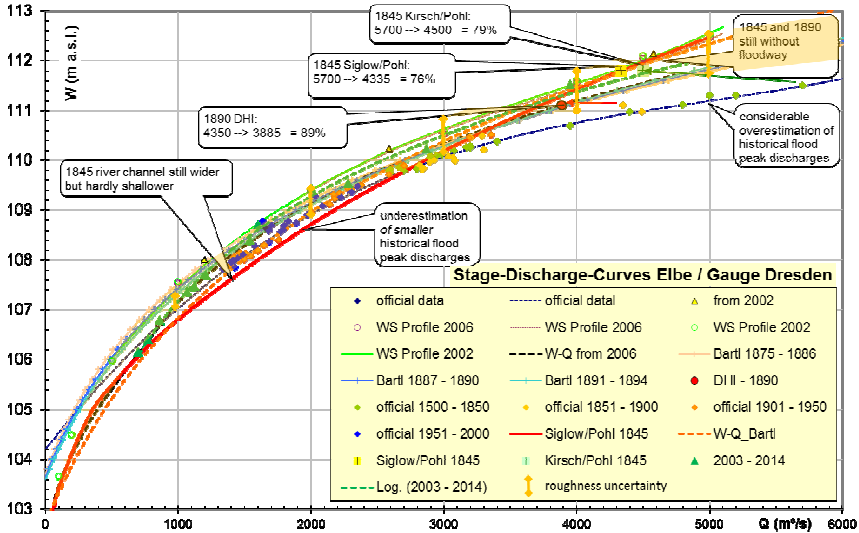


Fig. 4 Comparison of the Stage-Discharge-Relations at the Dresden Gauge with Dispersion due to Roughness Estimations.

Beobachtungszeitraum: 1805 - 2014 Anzahl der Fehljahre: 0
 Berechnungszeitraum: 1501 - 2014 Anzahl Jahres-HQ: 403, davon historische HQ: 13
 Einzugsgebiet [km²]: 50000.0

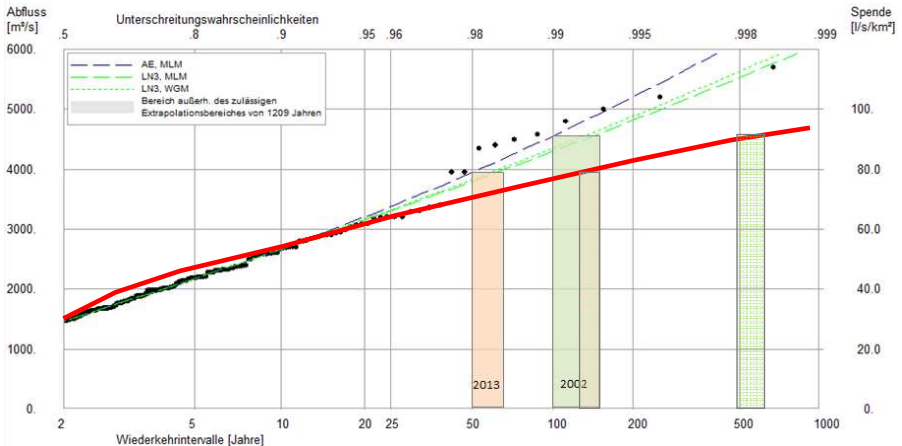


Fig. 5 Annual Peak Discharges and related Return Periods at the Dresden Gauge. Plotting Positions and best fitted Distribution Functions. Upper Curves: existing Statistics. Lower Curves: modified Values without Plotting Positions

On the other hand due to the revised series the peak discharge of 2002 was the biggest value at all, that means an all-time record from the mathematical point of view. This value strongly influences the trend of partial series (Fig. 6).

Insofar it is also very difficult to answer the question about a trend due to the climate change. Although the trends during the last few decades are increasing, it can be seen in Fig. 6 that all partial series of a 5 decade period after 1800 produce increasing trends whereas the series over 3 decades yield 2 increasing, 3 decreasing and 2 almost constant trend lines. These differences are only caused by the mathematics despite using the same flow data.

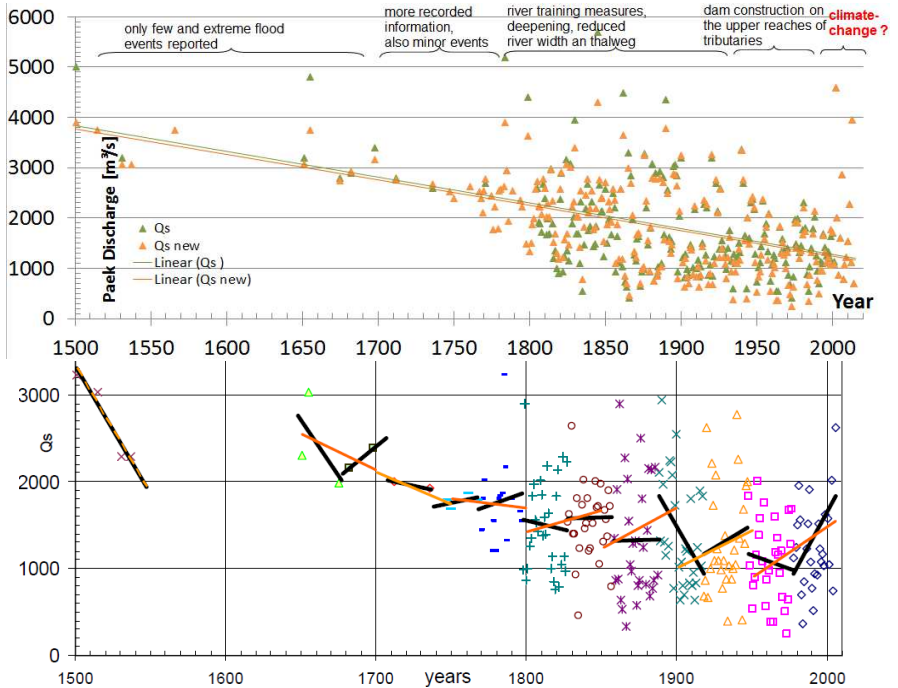


Fig. 6 Linear Trends of partial Series of annual Peak Discharges 30 Years (black line) 50 Years (orange line)

5. CHANGING FLOODS, CHANGING CITIES, CHANGING RESILIENCE

As long as the mankind can remember, people have built their settlements near rivers. Thus they could take advantage concerning water supply, hydropower generation, fertile soils, agricultural irrigation, transport of goods and navigation respectively. But settling near the river has also one main disadvantage: the hazard of inundation.

Although this cannot be proved for the Saxon Elbe with statistical significance an increasing of flood peaks or a decreasing of the return periods can't be excluded for the future. In the recent years, several research fields were established, which include the adaptation of societies to changing requirements due to natural events. This is also indicated by scientific events, to discuss these issues like "Urban Flood" (Paris 2009), "Resilient Cities" (Bonn 2010) or "UFRIM" (urban flood risk management Graz 2011). Central issues consider the development of vulnerability of communities due to natural disasters (vulnerability) and the resistance against these challenges (resilience).

A first estimation of corresponding values indicates mainly positive developments in the sample areas, also in very densely populated areas in South-East Asia [Jongman et al. 2015]. The upper part of Fig. 8 shows the qualitative history and trend of characteristic numbers related to flood resilience for the city of Dresden [Pohl 2011]. For Dresden the percentage of the inundated area is declining because the growth of the city stretches also on the higher terrain. Although the hazard potential in the possibly flooded area is increasing the hazard normalized with the Gross Domestic Product (GDP) in this area is decreasing. This is an estimation for Dresden but could be proved for Sion in Switzerland [Popp-Walser 2013], where the risk could be reduced considerably in the case of the 3rd Rhone correction (1850 – 2050). The period of only 20 years in the work by [Jongman et al. 2015] seems to be too short to prove a decreasing risk for large cities in developing countries too. For an exploding population, in a Megacity with comparable low GDP near a large river and only a few meters above sea level the trends of the absolute and normalized hazard potential might run like the dotted lines in the lower chart of Fig. 8.



Fig. 7 The Elbe River in Dresden, left: City and River during History; right: Situation in the City Centre. Top 1845 before River training Measures, bottom 2006.

Vulnerability and Resilience of communities against floods have changed during the centuries. Very often also the river banks and river beds in urban areas were reshaped in the past so that stage-discharge curves were and are valid only for certain periods. It has been shown above that these changes have to be considered when evaluating flood statistics.

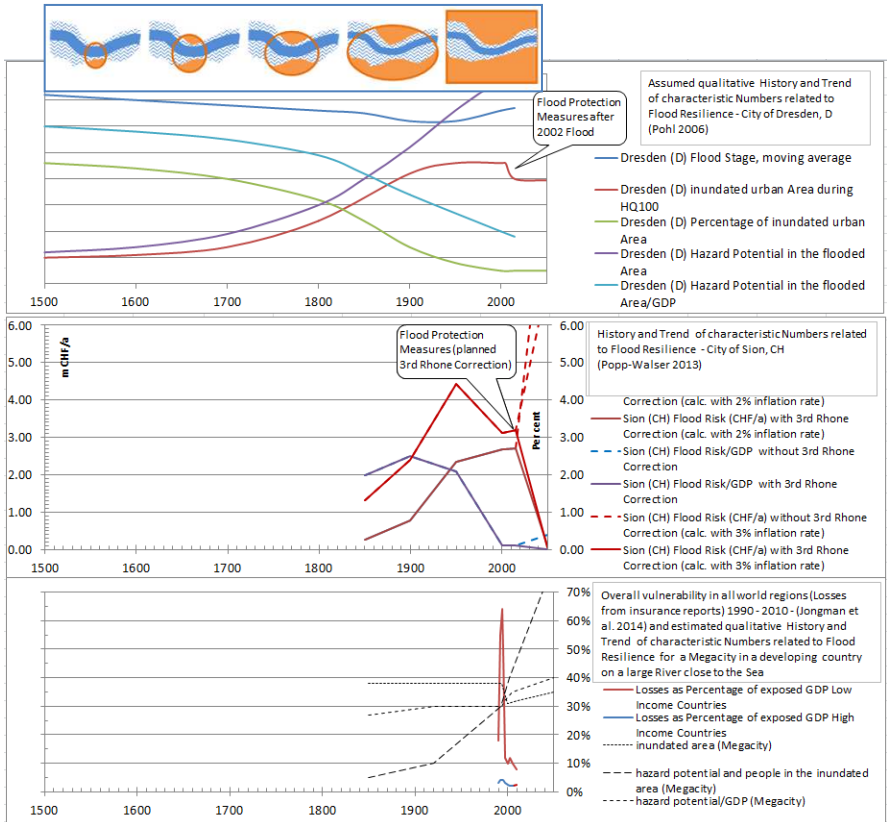


Fig. 8 Qualitative description of the estimated consequences of extreme floods with schematic map of the inundated area of the city.

Further research on the base of large data sets is needed to find out which tendency flood resilience will have at different places in the world in future. First steps were initiated to verify these presumed curves in Fig. 8.

6. DISCUSSION, CONCLUSION, OUTLOOK

The above considerations show that a check of the stage-discharge-curves of the past should be done by means of water level profile calculations with historical data if the availability of geographic and stage data allows it. The result is a stage-discharge-relation being valid for a certain period in time. After converting the peak stages to peak discharges a probability distribution function can be fitted to the values in order to extrapolate the new recurrence periods. The example of the Dresden gauge shows that as a result of this investigation the design floods can change.

The above investigations assume steady hydrologic conditions. At the Dresden gauge no significant long term tendency towards increasing peak discharges could be shown clearly. If such trends due to climate change or other causes should become evident the recurrence periods and the degree of protection will have to be adjusted.

Densely populated urban areas at rivers are often exposed to flood risk. In many cases they can be inundated from both sides: by the main river with the large catchment area which hydrograph can be forecasted for more than one day due to upstream gauging and on the other hand by the city-crossing streams from smaller watersheds which have a so short concentration time to peak that makes a reliable flood forecast impossible in most cases.

Flood analyses have shown that structural measures of flood protection are limited applicable, especially in urban areas, and that an absolute protection is not feasible.

To evaluate the flood resilience of communities the development of the hazard potential as an absolute value or normalized with the economic potential might be used.

For the case study area it seems that the general vulnerability has been decreasing as it could be found by means of characteristic indices. Also the relative values of inundation and hazard seem to become smaller. In other parts of the world (especially with a huge growth of population in coastal and fluvial areas) other tendencies than in Fig. 8 might to be expected and are worth to be investigated.

7. REFERENCES

- DWA 2012. Merkblatt DWA-M 552 Ermittlung von Hochwasserwahrscheinlichkeiten, DWA, Hennef 2012 ISBN 978-3-942964-25-8
- FAULHABER P. 2000. Veränderung hydraulisch-morphologischer Parameter der Elbe. In: Mitt.der Bundesanstalt für Wasserbau 82 (2000), Seite 97–117
- Karte des Elbstroms des Königreiches Sachsen in 15 Kartenblättern (Lithographie, Maßstab 1:12000 mit den Grenzen der Überschwemmung vom 31. März 1845). Sächsische Landes- und Universitätsbibliothek, Kartenforum Sachsen, Section IX Dresden von 1850-55 (SLUB/KS 3.gr.2.61, SLUB/DF DK 6) <http://fotothek.slub-dresden.de/karten/index.html?karten/slub-ks.html>.
- JONGMAN, B. et al. 2015. Declining Vulnerability to River Floods and the global benefits of Adaption.- PNAS Early Edition: April 2015
www.pnas.org/cgi/doi/10.1073/pnas.1414439112
- KIRSCH, F.; POHL, R. 2011. Modellierung historischer Abflussverhältnisse für die Hochwasserprognose.- In: Wasserwirtschaft 101(2011)3, S. 14-19
- LfUG 2002. Hochwasserschutz in Sachsen.- Materialien zu Wasserwirtschaft, Staatministerium für Umwelt und Landwirtschaft, Mai 2002 (ergänzende historische Wasserstandsangaben vom Sächsischen Landesamt für Umwelt und Geologie dankenswerter Weise zur Verfügung gestellt)
- MATZ, S.; POHL, C.; DHI Syke 2008. Erstellung eines hydraulischen Teilmodells für die deutsche Obere Elbe anhand historischer Daten für das Sommerhochwasser von 1890. DWA, 2008.
- NESTMANN, F., BÜCHELE, B. (Hrsg.) 2002. Morphodynamik der Elbe.- Schlussbericht des BMBF-Verbundprojektes, Karlsruhe 2002 (ISBN 3-00-008977-2)
- POHL, R. 2011. Changing City – Changing Flood.-In: Zenz, Hornich: Proc. of the intl. Symposium on Urban Flood Risk Management (UFRIM) Sept. 2011, Verl. d. TU Graz, ISBN 978-3-85125-173-9, pp. 521-526
- POHL, R. 2007. Auswertung von Wasserspiegellagen mit hist. Datensätzen für die Hochwasseranalyse.- In: Wasserwirtschaft (2007)5, S. 16-20
- PÖTZSCH, C.G. 1784. Chronologische Geschichte der großen Wasserfluthen des Elbstroms seit tausend und mehr Jahren.- Waltherische Hofbuchhandlung, Dresden, 1784. mit Nachtrag und Fortsetzung von 1786 und 1800
- POPP-WALSER, CH. 2013. Entwicklung von Hochwasserrisiken unter Berücksichtigung von Verletzlichkeit und Widerstandsfähigkeit (Development of flood Risks considering Vulnerability and Resilience – The Example of the Rhone in Valais from 1850 to 2050).- Diplomarbeit, TU Dresden, Fakultät BIW, Professur THM 2013
- SIGLOW, A. 2007. Auswertung von Wasserspiegellagenberechnungen mit historischen Datensätzen für die Hochwasseranalyse.- Diplomarbeit, TU Dresden, Fakultät für Forst-, Geo- und Hydrowissenschaften, 2007, 70 S.

Seepage Problems at Areas Protected against Floods

T. Julínek, J. Říha,

Brno University of Technology, Faculty of Civil Engineering, Institute of Water Structures, Veveří 95,
602 00 Brno, E-mail: julínek.t@fce.vutbr.cz, riha.j@fce.vutbr.cz

Abstract

The underground elements of flood protection structures such as levees or floodwalls may represent significant interventions into the groundwater regime if not treated. Seepage progressing during a flood from a river to an adjacent aquifer can endanger flood protection elements and may result in the internal erosion of the soils of the foundation. The increased piezometric head and water pressures at the area protected against flooding can harm the subsurface parts of buildings such as cellars, underground garages and also sewer mains. The paper deals with groundwater flow issues related to the flood protection of urban areas. Hydraulic modelling and risk mapping techniques used for the assessment of the impact of groundwater on flood protection facilities and on structures in protected areas are applied. Additionally, the effect of subsurface parts of floodwalls and levees on the groundwater regime in adjacent areas is discussed.

Keywords

Seepage, groundwater, reliability, limit state

1. INTRODUCTION

Changes in groundwater (GW) flow regime during floods and also due to flood-protection structures are affected by various factors. Excessive seepage may endanger both flood protection elements and structures in protected urbanized areas. Factors related to natural characteristics mostly include the vagueness of descriptions of the geomorphology and topology of the area of interest, the quality of the interpretation of the geological composition, hydrogeological conditions, etc. Anthropological factors usually comprise poor understanding of the historical development of towns and cities at river zones, the generation of anthropogenic geological layers, river training including flood protection structures, the drainage of ground water into the sewage system and others. These factors might influence the change in groundwater regime during floods and should be taken into account when modelling the effects of designed flood protection measures (FPM).

During periods when flooding is absent, channels and rivers usually drain adjacent aquifers. With the increasing water level in streams during flood events, the direction of groundwater flow changes. During a flood groundwater usually flows from the river and is accompanied by rising water level (piezometric head) in the aquifer in the protected area. The adjacent aquifer is then subject to GW flow from upper terraces, and also from the river. The rate of the flow depends on

the permeability of aquifer materials, the saturation rate of the soil, and the flow regime (confined, free flow). In Fig.1 a scheme of groundwater flow during flooding is shown for a river without (A) and with (B) flood protection measures [Levee Handbook 2013], [Říha 2010].

During the design and operation it is necessary to deal with the reliability of levees and floodwalls. It is the goal of design and assessment to involve all the important uncertainties in the solution. In current practice this is carried out using traditionally recommended safety factors published in the technical standards and guidelines. Another more comprehensive approach is the limit state method using partial reliability factors or fully probabilistic reliability assessment. In the paper the two latter procedures are described in the context of the initiation phase of internal erosion. Both methods are demonstrated in case studies of flood protection schemes of at the village of Troubky and the city of Prague.

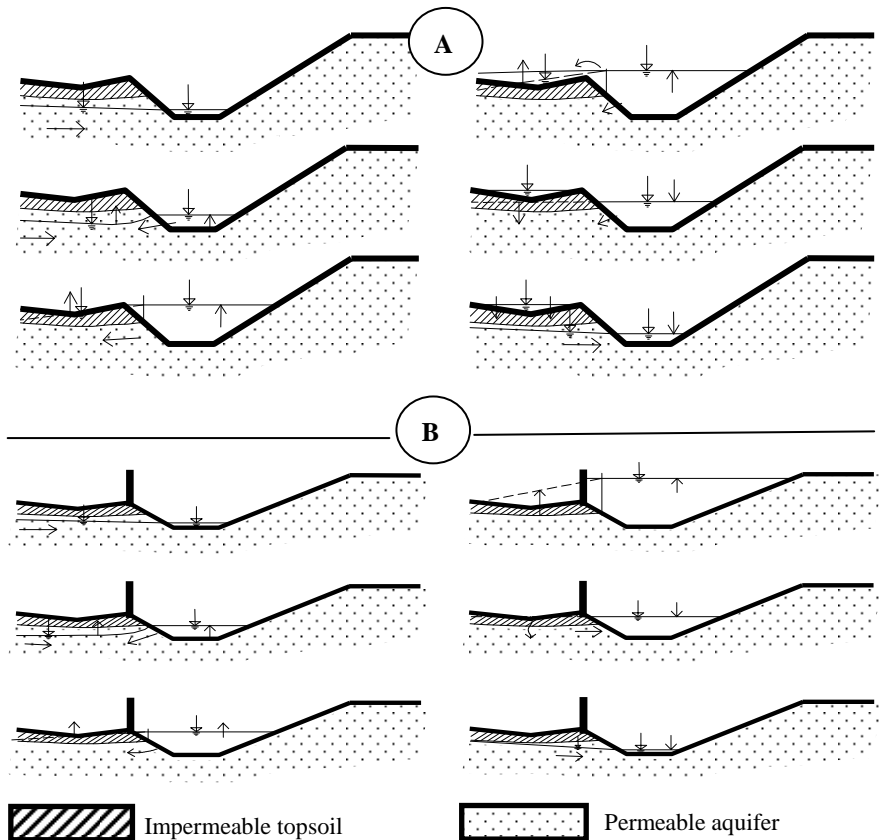


Fig. 1 Scheme of groundwater flow during flood
A) no flood protection measures, B) with flood protection measures

2. FLOOD PROTECTION STRUCTURES

Structural flood protection measures are built mainly in urbanized areas and their vicinity. Their primary function is to protect adjacent areas against surface flooding and to avoid losses in the case of more frequent floods (usually with the return period $N \leq 100$ years). Common structures are flood levees and floodwalls frequently combined with mobile elements designed according to aesthetic considerations or at places where roads cross the area.

During periods when flooding is absent streams usually drain adjacent aquifers. To avoid unexpected damming of natural groundwater flow it is important to consider the effects of the subsurface parts of flood protection measures. Such measures must not cause a significant rise in the ground water table behind the flood protection line and must not interrupt the natural drainage function of rivers. Such a requirement usually excludes slurry walls with their foundations in impermeable base soils. An important problem can arise in the case of the failure of any flood protection element. This can be caused due to structural instability or loss of filtration stability (internal erosion). Groundwater acts in this case as a surface load and also as a body load corresponding to the water pressure and hydraulic gradient in sub-base. The structural stability of buildings can be influenced by non-uniform increases in the water pressure below their foundations. Structures should be designed with respect to these types of loading and in combination with adequate measures (drainage, relief wells, etc.).

The basic characteristics of groundwater flow (seepage velocity, hydraulic gradient, water pressure) which represent load on the flood protection structures and their sub-base are usually obtained using groundwater flow modelling techniques (see below).

3. GROUNDWATER FLOW ISSUES

The objective of GW regime assessment is to avoid or reduce its negative impacts in the protected area behind flood protection structures. There are several aspects to consider when designing a flood protection measure. The relevant issues are as follows:

- Flood protection measures and their subsurface parts affect the groundwater regime during both flood events and periods without flooding. Designed measures should provide protection against the negative impact of GW during the flood and assure the safety of FPM, but on the other hand they must not cause significant changes to the natural regime of groundwater flow in the protected area in a flood-free period. Therefore, subsurface elements of FPM should not obstruct natural GW flow by completely penetrating slurry walls.
- GW pressure is one of the loads influencing the stability of FPMs and their foundations:
 - water pressure on subsurface parts of structures (e.g. uplift pressure),

- uplift pressure on less permeable topsoil layers behind FPMs,
- pressure gradients which can cause internal instability in levees and the subsoil of FPMs due to internal erosion.
- Considerable leakage into the protected area may occur in the case of permeable floodplain aquifers. If the water table rises up to the level of the terrain, it can cause:
 - the instability of subsurface parts of houses due to increased water pressure,
 - leakage into subsurface parts of buildings (cellars, subsurface garages, etc.),
 - waterlogging of the surface in the protected land area.

4. SOLUTION OF GROUNDWATER FLOW PROBLEMS

When designing a FPM one should take into account the above-mentioned issues (Chapter 3). The procedure is as follows:

1. First, the conceptual design of FPM layout and the definition of basic design parameters (design flood, freeboard, etc.) are carried out.
2. Second, it is necessary to assess the groundwater regime and discuss all of the issues mentioned above. This step is usually carried out using GW models and spatial mapping and enables the specification of:
 - loads to the FPM from GW,
 - the susceptibility of soils to internal erosion, in order to assess relevant criteria,
 - measures assuring the required safety of the FPM (structural and filtration stability),
 - the amount of leakage to the protected area,
 - the extent of waterlogging in the area behind the FPM,
 - the impact of subsurface parts of the FPM on the groundwater regime.
3. The final design of the FPM, the specification of land acquisition, the amount of pumping needed, etc. is based on the results of groundwater flow modelling.

In the following text we restrict our focus to item 2).

4.1 Groundwater flow modelling

For the quantification of GW flow parameters a wide variety of mathematical seepage flow models are used. These are one-dimensional (1D), two-dimensional (2D) horizontal and vertical and also three-dimensional (3D) steady or transient flow models. The mentioned models are sufficiently described in the available literature [Bear, Verruijt 1987].

The most frequent are 2D horizontal steady or unsteady state models used for the assessment of the impact of subsurface elements of FPM (e.g. slurry walls) on the natural groundwater table during a flood-free spell. Transient flow models are

applied when studying the progression of the flood wave to the aquifer. The results are expressed in terms of the piezometric head $h(x,y,t)$ and its maximum value $h_{MAX}(x,y)$ reached during the time interval - duration of the flood. The time dependent piezometric head $h(x,y,t)$ in the permeable aquifer has to be taken from the results of mathematical modelling of groundwater flow. The Dupuit assumptions are taken into account for the calculations. The governing equation is as follows:

$$\frac{\partial}{\partial x} \left[T \cdot \frac{\partial h}{\partial x} \right] + \frac{\partial}{\partial y} \left[T \cdot \frac{\partial h}{\partial y} \right] - S \frac{\partial h}{\partial t} - Q = 0 \quad (1)$$

where $T(x,y)$ is isotropic aquifer transmissivity, $S(x,y)$ is the storage coefficient, $h(x,y,t)$ is the piezometric head and Q is the point source/sink.

The boundary conditions are:

$$h(t) = \bar{h}(t), \quad (2)$$

where \bar{h} is the known water level in the river during a flood. At the boundary with the prescribed flux it holds:

$$k \cdot \frac{\partial h}{\partial x} n_x + k \cdot \frac{\partial h}{\partial y} n_y = q \quad (3)$$

where n_x, n_y are cosines related to the outer normal vector to the boundary with prescribed flux q (per unit width of the boundary).

The initial condition expresses the known piezometric head h_0 over the flow domain at the beginning of the flood ($t = 0$) taken from the calibrated steady state model:

$$h(x, y, 0) = h_0(x, y) \quad (4)$$

The maximum piezometric head h_{MAX} at the given point of the domain was taken from the results of the above described simulations:

$$h_{MAX}(x, y) = \max h(x, y, t) \quad (5)$$

4.2 Groundwater flow mapping

The modelling results in the case of 2D horizontal models are efficiently analysed, manipulated and displayed via GIS mapping techniques. The following maps are relevant in the case of GW flow in the flood protection context:

- maps of the terrain level (digital model of terrain - DMT),
- maps of the results of present state modelling - calibration scenarios,
- maps of groundwater levels for selected scenarios,
- maps of differences between the present state and the state influenced by subsurface elements of FPM,
- maps of the maximum water table (piezometric level) during flooding,
- maps of differences between the maximum ground water level and the terrain (Fig. 2),

- maps of waterlogged areas,
- maps displaying reliability factors (see below), etc.

As the first six mentioned map types are generated by standard GIS techniques, their processing is not described in more details.

5. RELIABILITY ASSESSMENT

For the reliability assessment it is desirable to classify the internal erosion process into 4 stages - initiation, continuation, progression and failure [Fell, Fry 2007]. For the reliability assessment and following risk analysis of the structure an event tree can be set up (Fig. 2). In the paper reliability assessment is only focused on the initiation phase, which is assumed to be the most important phase in dam safety assessment. Two possible approaches are mentioned, namely the application of the limit state method and the probabilistic assessment of internal erosion initiation due to rupture of the topsoil layer at the back side of a flood protection measure. This section focuses on “reliability maps” and the procedure for the assessment of the initiation of internal erosion (Fig. 2) [Čejda, Říha 2011]. In a situation corresponding to Fig. 3 the flood levee is founded on the relatively impermeable topsoil layer (fluvial loams) overlaying a highly permeable gravel-sand aquifer. The maximum piezometric head h_{MAX} in the aquifer behind the FPM has been determined by a transient 2D horizontal GW flow model. The levels of the terrain and base of the topsoil have been interpreted from land and geological survey data. The reliability assessment using limit state method and fully probabilistic assessment is described in more details in the following chapters together with examples of their application at case studies.

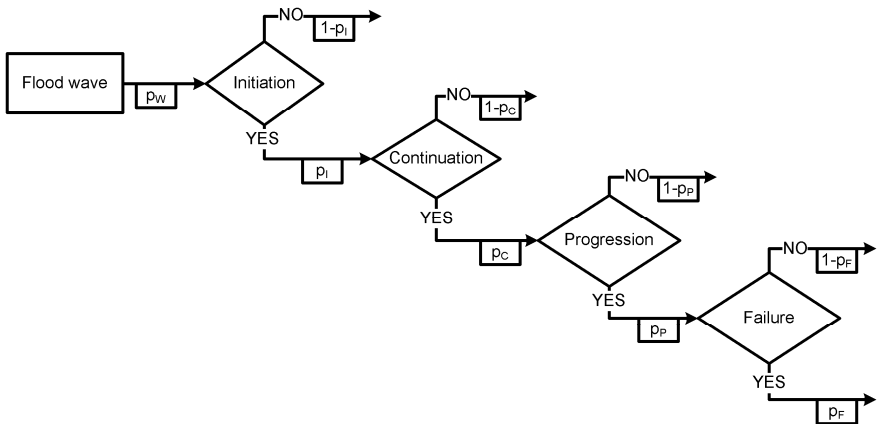


Fig. 2 Event tree for reliability assessment of levee failure due to internal erosion [Čejda, Říha 2011]

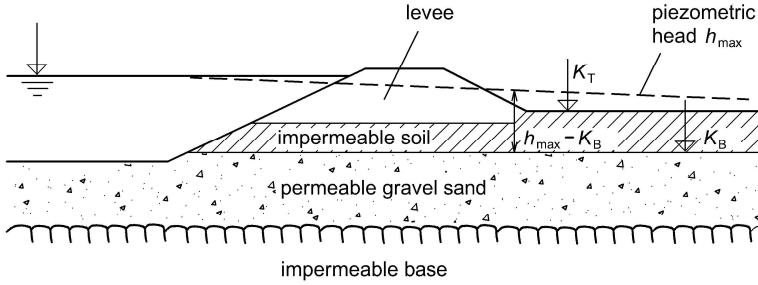


Fig. 3 Scheme for condition (6)

5.1 Limit state method

The following limit state condition may be used for safety assessment at the given location specified by the co-ordinates (x, y) :

$$\gamma_{sit} \gamma_n \gamma_{fv} \gamma_w (h_{MAX} - K_B) \leq \gamma_{fg} \gamma_s (K_T - K_B), \quad (6)$$

where γ_{sit} is the performance factor, γ_n is the importance factor, γ_{fv} is the load reliability factor (according to the method of determining h_{MAX} and K_B), γ_w is the unit weight of water, $h_{MAX}(x,y)$ is the maximum piezometric head $h(x,y,t)$, $K_B(x,y)$ is the level of the top stratum base, γ_{fg} is the resistance factor covering uncertainty in K_B and the soil's saturated unit weight γ_s , and $K_T(x,y)$ is the terrain level (Fig. 4). The values of particular reliability coefficients depend on the type of structure, the numerical method used, the description of geological conditions, etc.

For spatial processing the “reliability parameter” $RP(x, y)$ is proposed:

$$RP = \frac{\gamma_{fg} \gamma_s (K_T - K_B)}{\gamma_{sit} \gamma_n \gamma_{fv} \gamma_w (h_{MAX} - K_B)} \quad (7)$$

$RP(x, y)$ expresses the reserve/deficit towards condition (1). When spatially processed, the areas with $RP(x, y) \geq 1$ represent reliable conditions while the values $RP(x, y) < 1$ indicate areas susceptible to topsoil layer rupture and to the initiation of an internal erosion process. An example of a map showing the reliability parameter RP over the area of Olympia shopping centre close the city of Brno is in Fig. 4. In the areas where condition (6) is not satisfied ($RP < 1$) the rupture of the topsoil layer may be expected. According to Fig. 2, the continuation phase of internal erosion is assessed, e.g. using the condition related to the mean hydraulic gradient along the potential seepage path:

$$\gamma_{sit} \gamma_n \gamma_{fa} i \leq \gamma_{sf} \gamma_{fp} i_K \quad (8)$$

where i is the mean hydraulic gradient along the seepage path, i_K is the critical mean hydraulic gradient, γ_{fa} is the load reliability factor, γ_{sf} is the factor related to the given failure mode and γ_{fp} is the soil resistance factor. The factors mentioned can be found e.g. in [Istomina 1957], [DIN 19712].

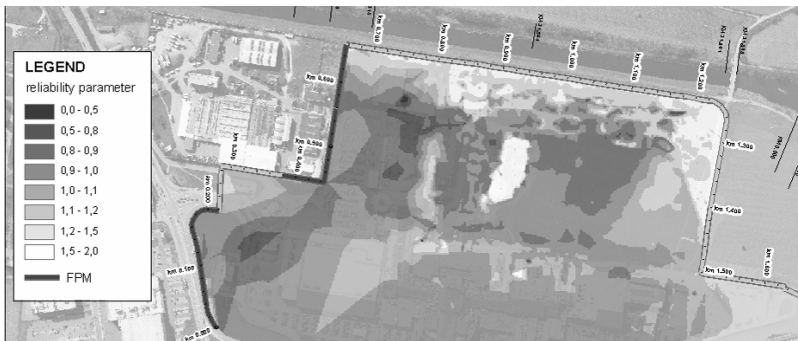


Fig. 4. Reliability map (flood protection of Olympia shopping centre)

An analysis with the application of the procedure mentioned was carried out at the flood protection design of the village of Troubky, where “reliable zones” were marked out in the area surrounded by a ring-system of flood levees (Fig. 5). It can be seen that in most of the protected area condition (6) is not satisfied ($RP < 1$).

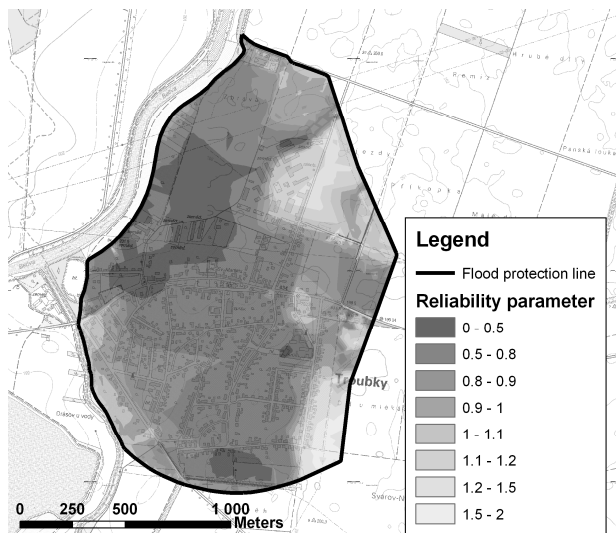


Fig. 5 Map with RP parameter - no relief wells

To decrease water pressure in the aquifer and to satisfy condition (6), namely in the area behind the levees, a system of relief wells and drainage ditches was proposed (Fig. 6). The effect of such measures on the reliability parameter RP can be seen from Fig. 7, where in most of the protected area condition (1) is already satisfied and only a small portion of the centre of Troubky is susceptible to topsoil layer uplift failure. These zones are rather far from the levee line and if rupture occurs it will definitely not lead to the continuation of internal erosion.

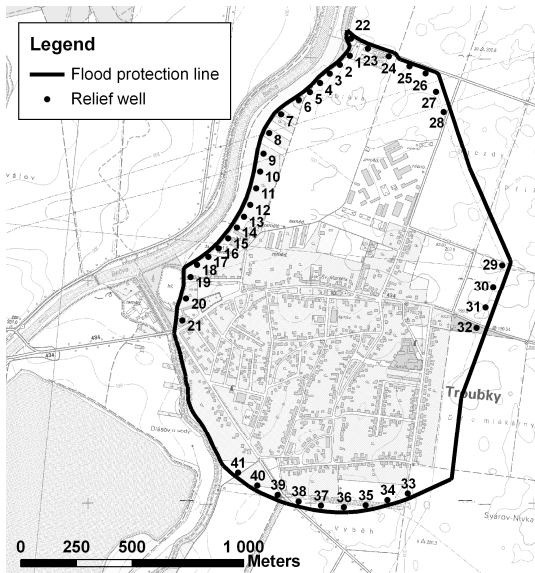


Fig. 6 Layout of relief wells

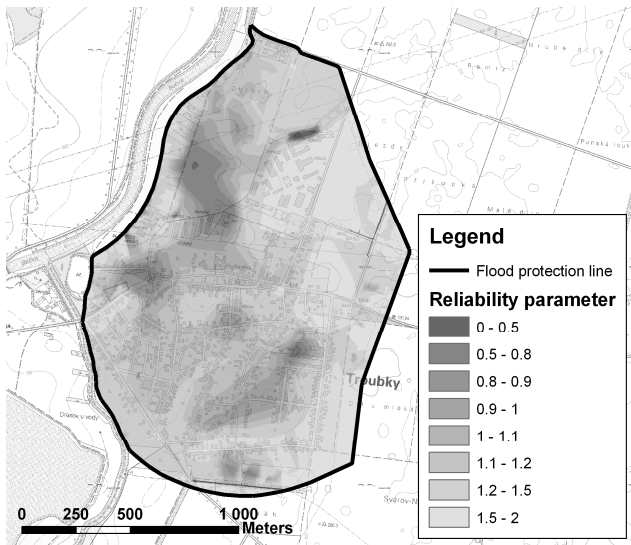


Fig. 7 Map with *RP* parameter - set of wells was applied

5.2 Probabilistic assessment of initiation phase of internal erosion

Another more sophisticated method is the probabilistic evaluation of the “dangerous” zones where the initiation phase of internal erosion can occur. This

technique was applied during optimisation of the flood protection system in several parts of the city of Prague: Zbraslav, Chuchle and Radotin.

The joint probability p_{JI} of failure initiation at a given point (x, y) is then defined as follows:

$$p_{JI}(x, y) = p_W \cdot p_I(x, y) \quad (9)$$

where p_W is the probability of a corresponding flood wave and p_I is the conditional probability of exceeding the limit state of the topsoil layer (Fig. 2). With this approach the relatively small probability p_W of an extreme flood event is included in the assessment. The partial reliability p_{RI} of the flood protection in terms of the initiation of internal erosion is as follows:

$$p_{RI} = 1 - p_W \cdot p_I \quad (10)$$

Estimation of the flood wave probability p_W is quite complicated and the relevant techniques still have not been proven worldwide. For our purpose the peak flood discharge exceedance probability is used as an approximation of p_W :

$$p_W = 1 - e^{-1/N} \quad (11)$$

where N is the peak flood discharge return period.

The initiation phase of internal erosion at a given point with co-ordinates (x, y) in the area behind the levees starts when the following condition (analogical with condition (6)) is satisfied:

$$\gamma_W [h_{MAX}(x, y, \Theta) - K_B(x, y, \Theta)] > \gamma_S(x, y, \Theta)[K_T(x, y, \Theta) - K_B(x, y, \Theta)] \quad (12)$$

where Θ is the parameter of randomness. Other variables in the formula (12) correspond to those explained above. γ_Z , h_{MAX} , K_B and K_T are assumed as uncertain (random) variables and are subject to statistical modelling.

The probability $p_I(x,y)$ of not satisfying the limit state condition (12) at a given point in the area behind the levee can be calculated from the formula:

$$p_I = P[\gamma_W(h_{MAX} - K_B) > \gamma_S(K_T - K_B)] = \frac{m}{n}, \quad (13)$$

where m is the number of simulations for which condition (12) was satisfied and n is the total number of simulations (in our case $n = 10^5$). The stochastic modelling method consisted in the following steps:

- The probability density function of random variables (γ_S , h_{MAX} , K_B , K_T , k , S_p) was assumed as uniform. The minimum and maximum values of individual variables were derived from the laboratory tests (γ_S), hydrogeological surveying and site tests (k , S_p , K_B), and a digital terrain model (K_T).
- Random sampling in terms of the Monte Carlo method was used for statistical simulations of the sets of input variables for model (1)

- Deterministic groundwater flow simulation was carried out using models (1) to (4). For each simulation the value of h_{MAX} was determined over the whole flow domain using the relation (5).
- Evaluating condition (12) for each simulation step, the probability p_I was assessed using frequency analysis (13).
- The probability p_{JI} of failure initiation was determined from eq. (8) assuming two flood scenarios with return periods of $N = 100$ and 500 years and corresponding probabilities $p_{W100} \approx 0.01$ and $p_{W500} \approx 0.002$.

Spatial analysis was carried out using GIS techniques. The final “probability map” for the area of Chuchle (district of Prague) is shown in Fig. 8.

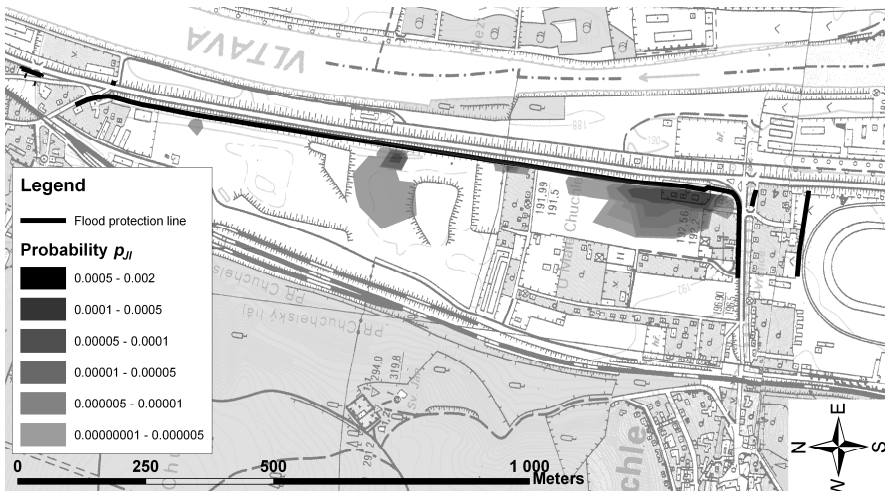


Fig. 8 Probability map - Prague, Chuchle

In this context, an acceptable probability has to be chosen as a political decision by the representatives of the local authorities. As an example Tab. 1 is attached, which can be a base for the assignment of such a probability threshold. The marked value $p_{JI} = 5 \cdot 10^{-6}$ has been chosen in our study.

Tab. 1 Threshold acceptable probability of failure

Expenses necessary for reliability increase	Low consequences	Medium consequences	High consequences
High	$1 \cdot 10^{-3}$	$5 \cdot 10^{-4}$	$1 \cdot 10^{-4}$
Medium	$1 \cdot 10^{-4}$	$1 \cdot 10^{-5}$	$5 \cdot 10^{-6}$
Low	$1 \cdot 10^{-5}$	$5 \cdot 10^{-6}$	$1 \cdot 10^{-6}$

6. CONCLUSIONS

In this paper the groundwater flow issues related to the flood protection of urban areas are addressed. For the hydraulic calculations of GW flow 2D horizontal mathematical model was used. The spatial interpretation of the results and data processing was carried out using GIS analysis and mapping techniques.

Two methods of the analysis of flood protection schemes are mentioned. The safety assessment is related to the initiation phase of internal erosion which consists in the evaluation of the limit state condition of rupture of the topsoil layer overlying the highly permeable aquifer. The first method is based on the evaluation of the limit state condition (6), where uncertainties in geometric, hydraulic and geotechnical parameters are expressed via reliability factors. The second method uses stochastic modelling, where all uncertain variables entering the assessment are regarded as random variables with a uniform probability density function. The uncertainty was expressed via the probability of the initiation phase of internal erosion. The probability was determined using Monte Carlo, seepage flow simulations and frequency analysis of the results. The techniques described were applied at the flood protection schemes of the Olympia shopping centre in Brno, the village of Troubky and the city of Prague.

The limit state method, employing reliability factors to express uncertainties in input data and modelling procedures, is strongly recommended by the authors.

7. REFERENCES

- BEAR, J., VERRUIJT, A. 1987. Modeling Groundwater Flow and Pollution, *Dordrecht*, Netherlands, 1987.
- ČEJDA, M., ŘÍHA, J. 2011. Reliability assessment of internal erosion initiation. *In Fry J.J., Julínek T., Říha, J. Internal Erosion in Embankment Dams and Their Foundations, Conference on Internal Erosion in Embankment Dams and Their Foundations*, Brno, Czech Republic, 4/2011.
- DIN 19712, Flussdeiche (1997).
- FELL, R., FRY, J.J. 2007. The state of the art of assessing the likelihood of internal erosion of embankment dams, water retaining structures and their foundations. *In: Internal Erosion of Dams and Their Foundations*. Taylor & Francis, London.
- ISTOMINA, V.C. 1957. Filtracionaja ustojcivost gruntov. *GILSA*, Moscow.
- LEEVEE HANDBOOK. 2013. The International Levee Handbook. *CIRIA C731*, London, UK, 1333 p.
- ŘÍHA, J. 2010. Flood levees. *Grada Publishing*. 223 p. ISBN 978-80-247-3570-2.

Acknowledgement

The paper is part of the projects TA-04020670 of the Technology Agency of the Czech Republic and FAST-S-13-2056 of the Internal Foundation Agency of Brno University of Technology.

Development of Automated Approaches for Hydropower Potential Estimations and Prospective Hydropower Plants Siting

N. V. Badenko², T. S. Ivanov², O. Nikonova¹, V. Oleshko²

¹Saint-Petersburg Polytechnical University, Civil Engineering Institute
Address: Polytechnicheskaya str., 29, Saint-Petersburg, 195251, Russia
E-mail: olgaoniks@hotmail.com

²JSC VNIIG, Laboratory of Geographic Information Systems and Technologies
Address: Gjatskaya str., 21, Saint-Petersburg, 195220, Russia

Abstract

Hydropower potential studies usually include estimation of hydropower resources and creating propositions for hydropower development on study area. The current paper describes authors' study, dedicated to development of methodological approaches and software designed for solving problems stated above. Process automation is achieved by using geographic information systems (GIS) and additional programs (Python language was used).

Hydropower potential estimation is the key element for understanding future prospects of hydropower development within the study area. The latest large-scale hydropower potential studies of Russian territories were held in 1940-1980. In those times, such researches were carried out almost without any automation, so calculation process was time-consuming. As a result, only hydropower potential of large and several medium-sized rivers was estimated; hydropower potential assessments of small rivers were conducted only using approximate approach.

Nowadays, implementation of technologies and software products, such as geographic information systems, contributes to development of methodologies, which can be used to automate business-processes in different scientific disciplines, including processes of hydropower potential estimation and prospective hydropower plants siting. In comparison with former studies, GIS allow to reduce labour work significantly and to perform analysis of large study areas and large number of streams (including small rivers) in relatively short time using up-to-date topographical, hydrological and hydrographical information.

Authors have developed and tested methodological approach and GIS-tools for automated hydropower potential estimation. Re-estimation of hydropower potential was fulfilled by the authors for the most part of Russia. The data for more than 10 000 river's was compared to the results of prior studies (data, such as river basin area, annual river flow, hydropower potential). The gross hydropower capacity of rivers and gross hydropower potential were estimated as 350 GW and 3.07-103 TWh respectively.

The next step in hydropower potential studies is prospective hydropower plants siting. Authors developed methodological approach and GIS-tools to automate this process. The GIS-tools provide comparison of site alternatives based on their

hydropower parameters; transport, infrastructure, electricity network proximity; topographic situation and other factors affecting site suitability. Algorithm of automation and results of the search siting are presented.

Keywords

Geographic information systems, Hydropower plants siting, Hydropower potential.

1. INTRODUCTION

1.1 Relevance of the research

Large-scale studies of Russian rivers hydropower potential are currently conducted in order to identify locations of prospective small hydropower plants [RusHydro web-site], [Shestopalov 2012].

Previous large-scale studies of hydropower potential of large and medium-sized rivers in Russia were conducted in 1940-1980. These studies were held by Grigoriev S.V. [Grigoriev et.al. 1946], Voznesensky A.N. [Voznesensky et.al. 1967], Feldman B.N. [Feldman et.al. 1985].

Due to insufficient amount of annual rivers flow data (especially in the eastern regions of the country) and poor precision of topographic data, assessment of hydropower potential in these studies was approximate and it was performed only for large and medium-sized rivers [Voznesenskiy et.al. 1967].

In addition, due to complexity of these researches and a large amount of rivers studied (for example, 4702 rivers in study [Voznesensky et.al. 1967]), estimations of hydropower potential performed in 1940-1980 have required a lot of time and labor.

Usage of modern computer technologies, such as geographic information systems (GIS), allows building tools which provide partial automation of hydropower potential calculations. However, analyzing of recent researches and developing methodology of automated hydropower potential calculations was needed to build these tools.

Present paper describes approaches of automated hydropower calculations, based on ESRI ArcGIS Desktop and modules for interactive data processing (GIS server ESRI technologies), developed and implemented by the authors. Comparisons of catchment areas, flow rates and gross hydropower potential values obtained in this research and the results of past years studies are given.

Presented approaches allow partially automated calculation of Russian rivers hydropower potential using updated hydrological data and relevant digital terrain models.

1.2 Analysis of other GIS-based studies of hydropower potential

Estimation of hydropower potential using GIS was lately performed for a set of countries (USA, France, Italy, Norway, Canada, Scotland and others) – examples are shown in [Punys et.al. 2011], [Douglas et.al. 2004], [Feizizadeh et.al. 2012], [Dante et al 2010], [Ballance et.al. 2000]. Brief review of these researches

was described in [Punys et.al. 2011]. Also, paper [Punys et.al. 2011] overviews some GIS-based tools for hydropower assessments.

The main difference between the GIS-based tools described in [Punys et.al. 2011] is in the initial data which was used for hydropower assessment. The key initial data that is necessary for hydropower potential calculations includes **hydrographic data, terrain data and hydrological data** (in particular, mean annual flow rates). The studies mentioned in [Punys et.al. 2011] use GIS-layers for hydrographic data, digital elevation models (DEM) as terrain data and annual river runoff or annual river runoff module (l/s, km²) values for flow rates calculation.

Paper [Douglas et.al. 2004] describes methodology of calculating gross, available and economic potential of the United States of America. National Hydrography Dataset (synthetic rivers network for territory of the entire country) was used as hydrographic data, SRTM was used as DEM and runoff data was derived from precipitation data.

1.3 Purpose of the research

The main purpose of this study was to develop and implement methodology and GIS-based tools to automate the calculation of the hydropower potential of rivers and stream reaches.

Based on the analysis of previous studies authors have performed the following tasks:

1. Methodology of partially automated hydropower calculation was proposed and requirements for initial data (terrain, hydrographic and hydrological) for calculation were described;
2. Terrain, hydrographic and hydrologic data was gathered and systemized;
3. ArcGIS Desktop based tools for calculating hydropower potential were developed;
4. Several Esri GIS-server technologies based applications were developed for automating calculations, for verification and presenting of the results;
5. Proposed approaches were implemented on a set of hydrological units in Russia, the results for a selected hydrological unit (Ket river watershed, basin of upper Ob) are presented in the paper;
6. Results of calculations (watershed areas, flow rates, gross potential values) were compared to the results of prior studies.

2. MATERIAL AND METHODS

2.1 Proposed approach for dividing territory into calculating zones

Hydropower potential estimations are usually performed for large areas, so there is a need in organizing data using hierarchical structures. Territory of Russian Federation is divided into hydrological units based on rivers' watersheds.

In present research basin-landscape approach was used for calculating of hydropower potential.

The advantage of this approach is that boundaries of hydrological units are coincident with natural watersheds, which is necessary for delineating catchments inside the study area.

Currently classification of water use zoning in Russia includes 4 levels of classification of hydrological units: regions, basins, sub-basins and the so called water management areas (Figure 1). Water management area is selected as the smallest area for calculation of hydropower potential.

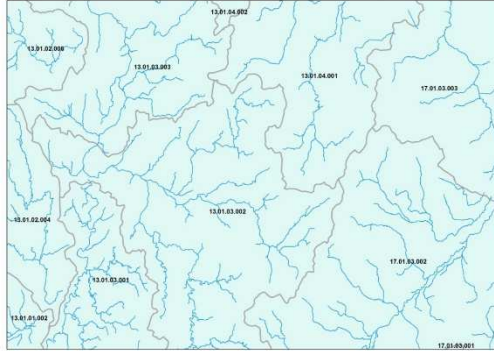


Fig. 1 Example of Russian water use zoning map (zones with identifiers)

2.2 Categories of hydropower potential

According to [Voznesensky et.al. 1967] there are 3 categories of hydropower potential:

Gross hydropower potential is the full theoretical sum of water flow energy.

Gross hydropower potential of a river can be calculated by summing potentials of its stream reaches:

$$P = \sum_{i=1}^n N_i * t = \sum_{i=1}^n [g * \frac{(Q_{1i} + Q_{2i})}{2} * H_i] * t \quad (1)$$

Where P is gross hydropower potential [kWh], N_i – gross capacity of a stream reach [kW], i is number of stream reach, g is the acceleration of gravity, Q_{1i} is flow rate in beginning point of stream reach, Q_{2i} is flow rate in ending point of stream reach, H is elevation difference on stream reach, $t = 8760$ hours is the number of hours per year.

In this study the same approach as in [Voznesensky et.al. 1967] was used: streams are divided by the sections (stream reaches) between the tributaries where the flow rate significantly increases.

Technical hydropower potential is a part of theoretical hydropower potential that can be technically used.

In most cases estimation of technical potential is based on analysis of empirical data of the studied rivers [Voznesensky et.al. 1967]. According to [Feldman et.al. 1985], rivers in Russia may be classified by annual mean power (N), which can be obtained from annual mean flow rate of stream reach:

- $N < 2$ MW – first group (Theoretical usage coefficient is set as 0,17);
- $2 \text{ MW} < N < 100$ MW – second group ($K_i = 0,35$);
- $N > 100$ MW – third group.

Theoretical usage coefficient for the third group in the current study was set to 0,4; 0,5; 0,6 for rivers with the slope of less than 1,0 m / 1,0 km; 1,0-2,5 m / 1 km; over 2,5 / 1,0 km respectively.

Economical hydropower potential is a part of technical hydropower potential that is feasible for usage. This study doesn't cover economical potential estimation. Traditionally estimation of economical potential is a complex work due to the necessity of analyzing many factors affecting the feasibility studies of HPP sites [Voznesensky et.al. 1967], [Feldman et.al. 1985], [International Hydropower Association, 2010].

In many studies researchers also estimate available hydropower potential, which is the gross hydropower potential for all the river sections (stream reaches) that are not situated in excluded areas [Douglas et.al. 2004]. Usually the stream reaches, where flooding territories is prohibited or where the potential is already used are excluded.

In the current study the following territories are excluded: ecologically protected areas; reservoir territories; territories that are classified as improper for creating HPPs due to geotechnical conditions.

2.3 Initial Data for gross hydropower potential calculation

In the current study authors used the following data to calculate gross hydropower potential:

1. Russian water register database.

Russian water register is a systemized information catalog of water objects, situated in Russia. The register holds information about the river basin areas, lengths, identifiers of water management areas and etc.

2. Terrain data

The study uses digital elevation models (DEM) as the terrain data. Authors used the following DEMs in the current study: SRTM; DEM based on digital maps (scale 1:100000).

3. River's flow rate.

For estimating hydropower potential using (1) a river flow rates at every tributary inflow site are needed. Two possibilities of flow rate calculation were taken into account:

- Usage of 1976's annual river runoff module (q , l/s, km²) map.
- Creating an up-to-date annual river runoff module (q , l/s, km²) map.

2.4 Algorithm for theoretical hydropower potential calculation

Algorithm implemented for gross hydropower potential calculation is as follows (Figure 2).

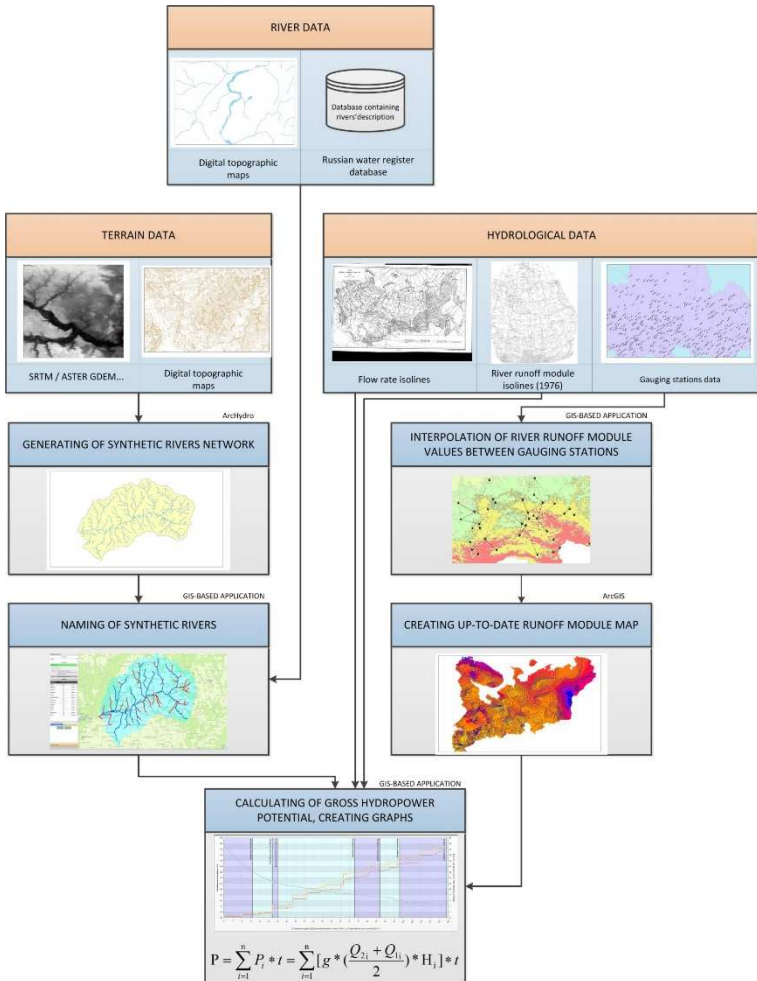


Fig. 2 Algorithm for gross hydropower potential calculating

1. Synthetic river creation. The latest studies of hydropower potential estimation deal with synthetic rivers, which are mathematical models of river flow networks, calculated from the terrain data using a set of algorithms. ArcHydro Toolset for ArcGIS Desktop was used and extended for the needs of this study.

Comparison of synthetic rivers and rivers obtained from digital maps showed that the tributary's sites match well, but the source of real rivers and synthetic rivers don't match. This is due to the fact, that finding a source of a real river always needs a complex study. At the same time source of a synthetic river placement (as well as synthetic rivers network density) depends on a set of thresholds in the algorithm [Djokic 2008].

2. In present study the partially automated algorithm for synthetic rivers naming was created to have the possibility for verifying current study results with the results obtained in previous researches. GIS-based application was created to match synthetic stream reaches with GIS-layers containing rivers. When all stream reaches which belong to the same river are selected, the name of this river is automatically assigned to them. Besides this, length and watershed area taken from Russian water register database are assigned to synthetic rivers.

3. For synthetic rivers' named stream reaches gross hydropower potential can be obtained using formula (1), where:

$$H_i = H_{2i} - H_{1i} \tag{2}$$

DEM is used to obtain beginning and ending point elevations of stream reach.

$$Q_{1i} = q_{1i} * F_{1i} \tag{3}$$

$$Q_{2i} = q_{2i} * F_{2i} \tag{4}$$

Where Q is annual flow rate, q is the average annual river runoff module inside a watershed area [$l/(s.km^2)$], F is watershed for a selected site at a river [km^2].

Runoff module in beginning and ending point of stream reach is a mean value of runoff module raster cells inside respective catchment area.

2.5 Approbation of proposed methodology for calculating the hydropower potential using GIS-technologies

For approbation of proposed methodology water management area with hydrologic unit code (HUC) 13.01.06.001 was chosen. This water management area belongs to Upper Ob basin and presents river Ket's watershed. This water management area was chosen because there is a possibility for comparing obtained in current study values of gross hydropower potential for river Ket with results obtained in the previous study [Voznesensky et.al 1967, p.89]. Also, flow rates and watershed areas for several Ket's tributaries are known.

Approbation of proposed methodology included following steps:

1. Creating synthetic river network (Figure 3)

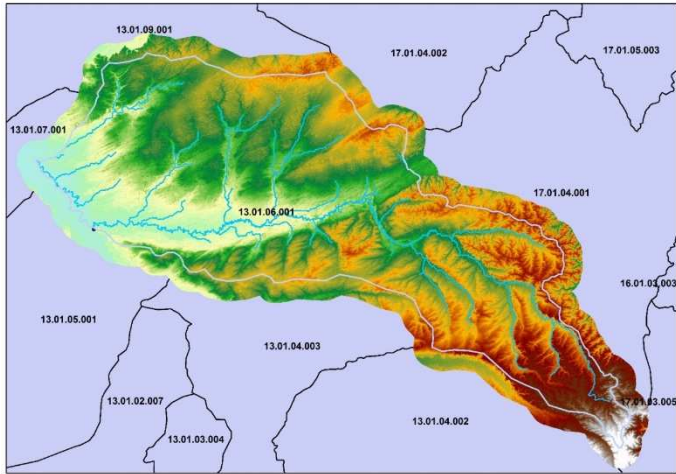


Fig. 3 Synthetic river network created for water management area 13.01.06.001

2. Naming of synthetic rivers according to digital map GIS-layer for “real” rivers. Real values of lengths and watershed areas were assigned to synthetic rivers using data from Russian water register database (Figure 5)

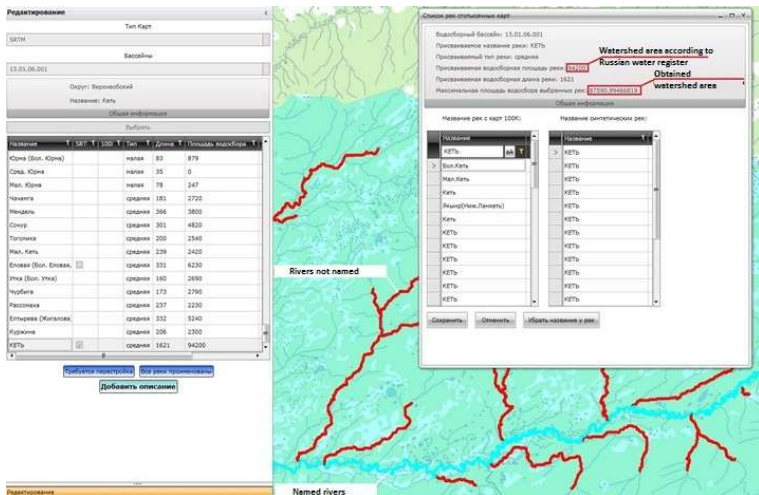


Fig. 4 Naming of synthetic rivers

3. Automated calculation of hydropower potential for all created synthetic rivers was performed.

Calculation results are presented on Figure 7. Process of calculation is rapid: 81 stream reaches were processed in 1,5 minutes (the study area is over 90 000 km²).

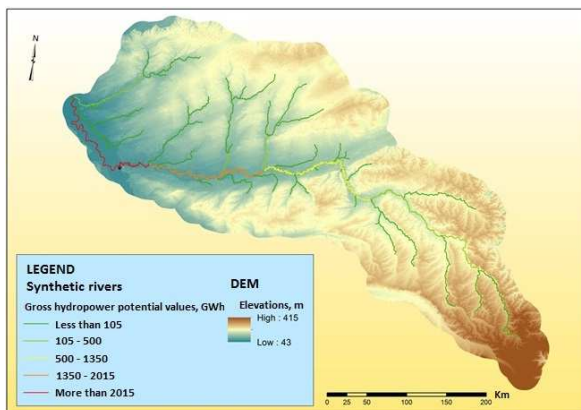


Fig. 5 Hydropower calculation results for water management area 13.01.06.001

Automated creation of graphs presenting longitudinal profile of rivers, increase of flow rate over the river and increase of hydropower potential over the river can be done using the GIS-based application, developed by the authors.

4. There were no excluded zones (ecologically protected areas or territories improper for creating HPPs due to geotechnical conditions) and existing reservoirs inside the study area, used for approbation. Hence, available potential is equal to gross hydropower potential of the rivers.

5. For each stream reach, theoretical usage coefficient was calculated automatically and technical hydropower potential was obtained.

6. Verification of obtained results was performed including:

- Verification of watershed areas.
- Obtained results were compared with Russian water register data (Table 1).
- Verification of flow rates in pour points.
- Verification of obtained based on up-to-date runoff module flow rate values was performed. These values were compared with relevant gauge stations data and collected from prior studies data (Table 2).
- Verification of gross hydropower potential.

Gross hydropower potential of river Ket obtained in this study was compared with [Voznesensky et.al 1967]. Calculation of hydropower potential in [Voznesensky et.al 1967] was made only for river trunk (river itself); tributaries were not included in calculations. Comparison of the results is shown in Table 3.

Tab 1. Verification of watershed areas

River name	Obtained watershed area [km²]	Watershed area according to Russian water register database [km²]	Discrepancy, %
Orlovka	8804	9010	2,3
Churbiga	2647	2790	5,1
Kelma	1347	1390	3,1
Sochur	5079	4820	5,1
Yelovaya	6067	6230	4,0
Ket	87591	94200	7,0

Tab 2. Verification of flow rates in pour points

River name	Obtained flow rate, [m³/s]	Flow rate according to relevant gauge stations data, [m³/s]	Flow rate according to [Voznesensky et.al 1967], 1967 year., [m³/s]	Discrepancy of obtained and relevant flow rates, %
Orlovka	62,0	63,5	-	2,3
Ket	572,5	560	531	2,1

Tab 3. Comparison of gross hydropower potential obtained in current study and in study [Voznesensky et.al 1967]

River name	Gross hydropower potential obtained in current study, GWh	Gross hydropower potential obtained in [Voznesensky et.al 1967], GWh	Discrepancy, %
Ket	2490	2129	14,5

Discrepancy in gross hydropower potential obtained in the present study and in [Voznesensky et.al 1967] is due to updating of hydrological data and using DEM that can cause some discrepancies in obtaining watershed areas as compared with traditional methods of delineating watersheds.

Also, the methodology used in the current study allows to automatically calculate the hydropower potential for a river itself and for the basin (the gross hydropower potential of a river and its tributaries are summed). Total Ket's river basin hydropower potential was estimated as 3387 GWh.

3. RESULTS

3.1 Applying proposed methodology for estimating hydropower potential of rivers in Russia

Authors created synthetic rivers networks for entire territory of Russia and hydropower potential calculations were performed. Density of synthetic rivers networks corresponds to second-third order tributaries. Russian rivers gross

hydropower capacity and gross hydropower potential were estimated as 350 GW and $3.07 \cdot 10^3$ TWh respectively.

Obtained results subsequently will be used for purposes of small hydropower plants siting. Generalized algorithm of this process is provided in Section 2.2.

3.2 Generalized algorithm for automated search of feasible small hydropower plants sites

This section includes only brief introduction to the methodology of economical hydropower potential estimation developed by the authors. The detailed methodology description will be presented after the verification of results of automated sites search.

The algorithm of entire process of prospective hydropower plants siting is shown on Figure 6.

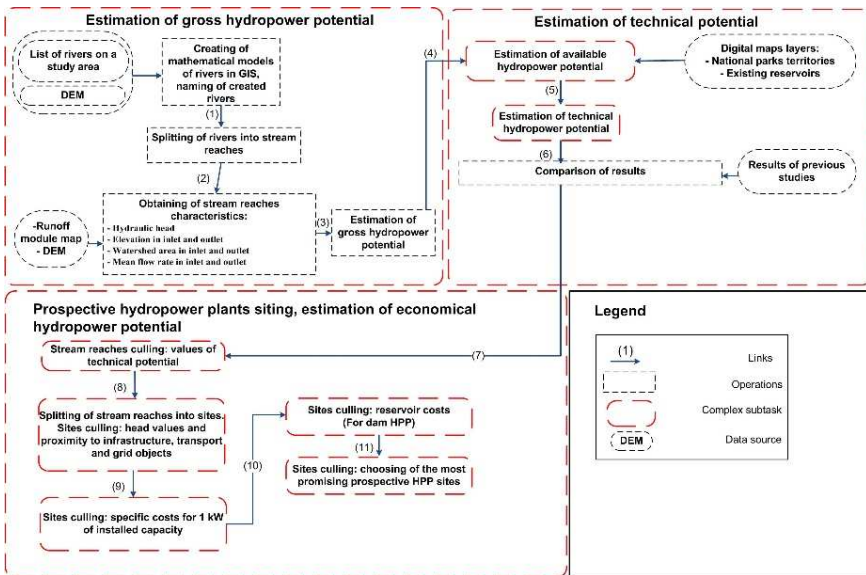


Fig.6 Generalized algorithm of entire process of prospective hydropower plants siting

To identify locations for prospective sites, first, stream reaches with low values of technical hydropower potential should be excluded.

After that, every remaining stream reach should be split into sites, and basic technical characteristics (installed capacity, discharge and head) of sites should be calculated.

Algorithm for small hydropower plants siting provides the way to identify suitable locations for dam HPPs and diversion HPPs. In case of dam HPP siting, at

every site a list of HPP variants with different installed capacity should be analyzed. For each variant, the HPP head might be obtained using equation:

$$H = \frac{N}{8Q} \quad (5)$$

Where H is HPP head, N is installed capacity [kW], Q is HPP discharge.

In case of diversion HPP, a penstock should be drawn from every site to every site inside the current stream reach. Elevation difference between inlet and outlet of penstock is the head of HPP, so, the installed capacity can be calculated using (6).

After obtaining basic HPP technical characteristics, a list of criteria can be used to exclude sites not matching the criteria:

- If obtained value of HPP head and discharge does not match the range of head and discharge values for HPP equipment, this site should be excluded.
- Proximity to infrastructure, transport and power grid objects affects site suitability. If site is located too far from settlements, roads, power grid, etc., this site should be excluded.
- Specific costs for 1 kW of installed capacity is the next criteria.
- For dam HPP, reservoir can be delineated. Using spatial intersection of reservoir GIS-layer and layers such as agricultural lands, roads, forests and other flooded objects, reservoir creating costs can be calculated, having statistics of reservoir costs for relative sites. If these costs exceed 30% of entire HPP investments, this site should be excluded.
- Remaining sites after all culling stages should be analyzed to identify the most promising sites. On this step, economic calculations should be performed. Rough estimations of costs of construction for each site can be obtained having the estimation of volumes of dam, length of diversion scheme, costs of units and other equipment. These estimations at the prefeasibility stage of the study are fulfilled only for the purpose of searching feasible sites according to preferable topographical and hydrological conditions. Geotechnical conditions should also be taken into account, but at this stage authors only exclude territories with unsuitable geotechnical conditions for hydropower development. After that, all the sites are treated as equal according to geotechnical conditions. According to obtained technical-and-economic indexes, sites can be filtered to find most feasible ones. The final selection of sites can be performed based on multi-criteria analysis to identify the most promising sites.

Figures showing the results of the main steps are shown on Fig.7 (example of dam small hydropower plants siting).

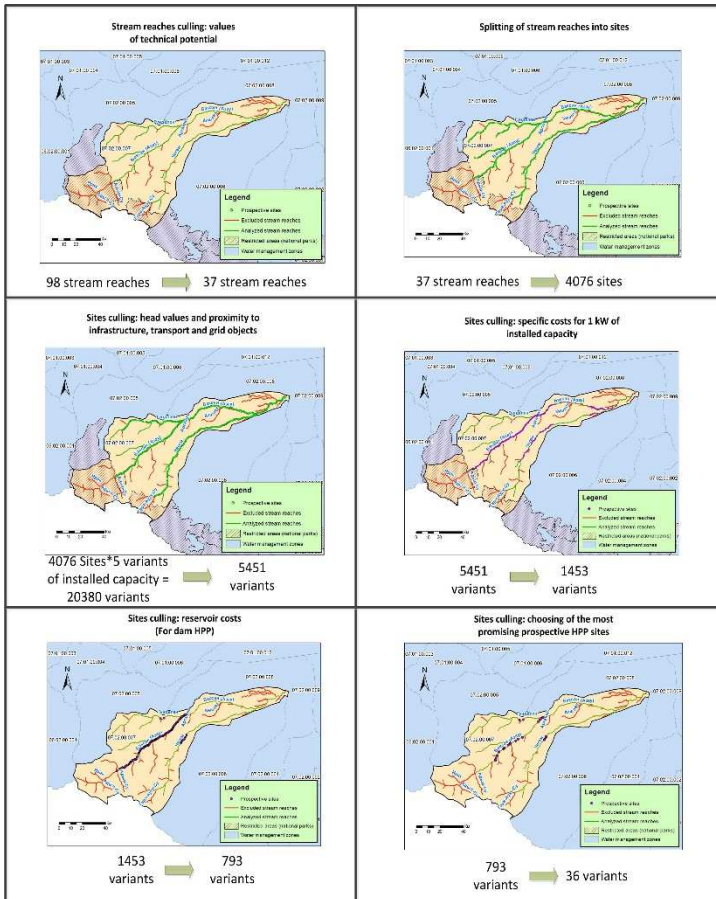


Fig. 7 Results of the main steps of small hydropower plants siting

4. DISCUSSION AND CONCLUSIONS

Authors have developed and tested methodological approach and GIS-tools for automated hydropower potential estimation. Created GIS-based tools and applications were used for calculation and re-assessment of the hydropower potential in Russia. Verification of obtained results proved their reliability. Currently verification performed for about 300 pour points and 100 gauge stations.

Assessment of hydropower potential can be performed not only for water management areas, but also for administrative regions. Process of calculating hydropower potential is largely automated, so this allows calculating hydropower potential on large areas in a relatively short time. The proposed methodology allowed to execute automated hydropower potential estimation for the territory of

Russia. Russian rivers gross hydropower capacity and gross hydropower potential were estimated as 350 GW and 3.07·10³ TWh respectively.

Generalized algorithm for identifying prospective hydropower sites is presented in the paper. Figures presenting the results of main steps of the algorithm are shown. Detailed algorithm with criteria used for each factor while comparing the sites will be presented in additional paper, after methodology of feasible sites search is verified and the results are compared with the previous studies.

5. REFERENCES

- BALLANCE, A., STEPHENSON, D., CHAPMAN, R. A., MULLER, J. 2000. A geographic information systems analysis of hydropower potential in South Africa. *Journal of Hydroinformatics* 2 (2000), pp.247-254.
- DJOKIC, D. Comprehensive Terrain Preprocessing Using Arc Hydro Tools. ESRI, 2008.
- FEIZIZADEH. B., HASLAUER, E. M., 2012, GIS-based procedures of hydropower potential for Tabriz basin, Iran, *GI_Forum* 2012, Salzburg, Austria, July 3-6, 2012, pp.492-502.
- FELDMAN B.N., MIKHAILOV L.P., MARKANOVA T.K., 1989. Small hydro. Moscow, «Energoizdat», 184 p.
- GRIGORIEV S.V. Potential water resources of small rivers in USSR. Leningrad, «Gidrometioizdat», 1946. – 115p.
- HALL, D.G., CHERRY, S.J. Reeves, K.S., LEE, R.D., CARROLL, G.R., SOMMERS, G.L., VERDIN, K.L., 2004. Water Energy Resources of the United States with Emphasis on Low Head/Low Power Resources, Idaho national engineering and environmental laboratory.
- Hydropower Sustainability Assessment Protocol, International Hydropower Association, November 2010, 220 p.
- LARENTIS, D. G., COLLISCHONN, W., OLIVERA, F., TUCCI, Carlos E.M. 2010. Gis-based procedures for hydropower potential spotting, *Energy* 35 (2010), pp.4237-4243.
- PUNYS, P., DUMBRAUSKAS, A., KVARACIEJUS, A., VYCIENE, G. 2011. Tools for small hydropower plant resource planning and development: A review of technology and applications. *Energies* 2011. 4(9), pp. 1258-1277
- RusHydro: Program of small hydropower development (rus). Available from: <http://www.rushydro.ru/industry/res/tidal/> (Accessed on 15.04.2013)
- SHESTOPALOV P.V. Why only third part of hydropower potential of Northern Caucasus is used?. *Energopolis*, July – August 2012, pp.36-37 (rus). Available from: <http://energypolis.ru/portal/2012/1484-pochemu-gidroyenergeticheskij-potencial-severnogo.html> (Accessed on 05.09.2013)
- VOZNESENSKIY A.N. Hydropower resources of USSR. Moscow, «Nauka», 1967. – 598p.

Braided river gravel reach hydrodynamics: a field example

A. Radecki-Pawlik¹, J. Bencal¹, M. Kowalski¹, B. Radecki-Pawlik²

(¹ University of Agriculture, Krakow, ² Statik-EkoBud Engineering Designing Office, Kraków

Corresponding author: Artur Radecki-Pawlik, Professor, Agricultural University of Cracow,
Department of Hydraulic Engineering and Geotechniques, 30-059 Krakow, Al. Mickiewicza 24-28,
Poland, phone: +48 (0)12 662 4089, e-meil: rmradeck@cyf-kr.edu.pl)

Abstract

The paper presents the results of examination of some basic hydraulic parameters such as shear velocity, shear stresses, Froude number, Reynolds number and flow resistance coefficient within the region of the braided middle gravel bar formation in the mountainous river. Hydrodynamics survey was done in the river channel just immediately after the spring flood when the bar formation has started. The number of observations was done which describe the braided process of the middle braided bar development. The study was undertaken in the Skawa River in Polish Carpathians.

Keywords

braided river, hydrodynamics, shear stresses, water velocity

1. INTRODUCTION

Different types of channel braiding can be observed. The first type consists of 'multiple-channel 'watercourses' separated by bare channel beds. In this type of pattern, the flow can be frequently diverted from one channel bed into other channels, as a function of local sediment deposition. This type of braiding is frequently observed, for instance, downstream of valley glaciers. The second major type of braiding consists of more stable multiple-channel pattern, even under high flow conditions, but with the sub-channels being separated by well defined vegetated islands. The third type can be defined as multi-thalweg rather than multiple channel, with the 'braids' being separated by submerged bars under peak flow conditions.

(Selby 1985). Alternating bars form in straight channel segments within curves of meandering thalweg. Point bars develop in areas of relatively low stream power at the inside of channel meander. Braid bars, mostly diamond-shaped, are often associated with coarse material. They are aligned to the flow and are called longitudinal bars. Braiding processes are highly dynamic, with rapid interactions between channel configuration, flow, and sediment transport (Fig.1). As specified before, braided rivers are associated with high-energy environments, high sediment loads, and unstable channel banks.

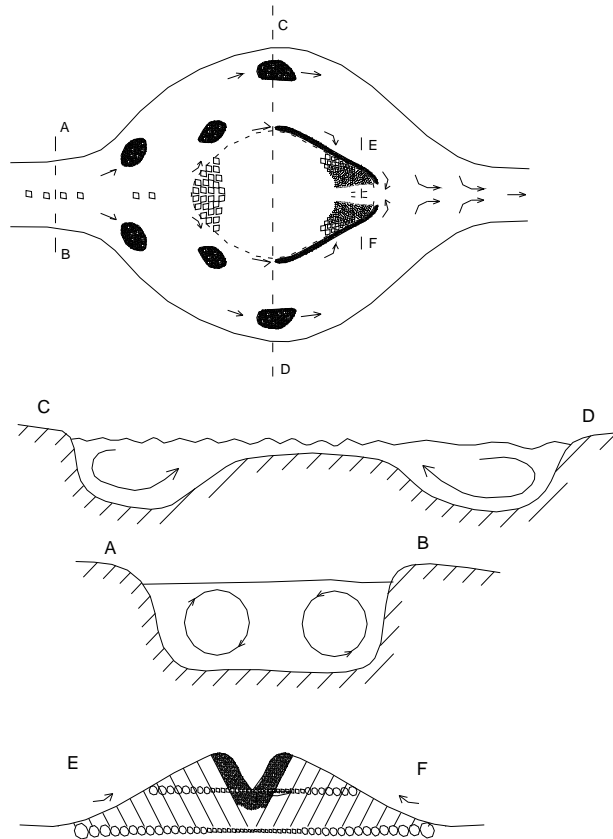


Fig. 1. Schematic model of secondary circulation, sediment sorting and downstream bar fining mechanism in a simple, idealized braided reach – modified after Robert (2003).

Under low water conditions such braids form middle gravel bars and developed as sort of islands sticking out of water (Robert 2003). In braided channels, three types of bars are commonly recognized: alternating bars, point bars and braid bars.

Although most braided rivers appear to adopt a braided pattern at all stages, the platform characteristics of braided channels can change radically with discharge (Bristow and Best 1993, Rowinski and Radecki-Pawlik 2015). The number of bars exposed may vary significantly with flow stage, and complex sequences of erosion and deposition may take place as the stage varies. Bar growth and channel erosion occur more or less simultaneously, and most exposed bars are the result of complex multiple erosional and depositional events

(Southard et al. 1984). Relatively few extensive field studies of channel morphology, flow, and sediment transport processes have been conducted on braided rivers (Bridge 1993). Also little is known about the hydraulic conditions within the region of braided bars. The purpose of the current paper is to identify differences in hydraulic conditions in the areas where the already-developed braided gravel bar is situated in a mountainous gravel river. Such conditions are responsible for braiding.

2. MATERIALS AND METHODS

2.1 Research catchment

The investigated Skawa River is situated in Polish Carpathians within the region called Beskidy (Fig. 2). The Skawa River catchment lies in the Carpathian flysch, where the streambed consists mainly of sandstone and mudstone bed-load pebbles and cobbles, which form a framework, where the interstices are filled by a matrix of finer sediment. The Skawa cuts through an alluvial bed, mainly consisting of Quaternary and Holocene river gravels, sands and mudstones. Strong bank erosion is evident, especially along the left bank at the tested reach. Many gravel river bed-forms were noticed within the investigated Skawa reach, such as point and middle bars (Radecki-Pawlik et al. 2004, 2005). These free bed-forms migrate downstream, but occasionally fixed bars occur, which are swept away during huge floods but tend to arise and recover in places where they were previously found. Mostly, gravel bed-forms grow behind and in front of obstacles and are durable only during over-bank floods, particularly those situated at riverbanks. Some basic physical characteristics of the streams investigated are presented in Tab. 1.

Table 1. Physical characteristics of investigated site

Variables	The Skawa River
Precipitation [mm]	850
Catchment Area [km ²]	835
River length [km]	31,0
Channel gradient	0.002
Max. Stream width [m]	67.0
Max. Stream depth [m]	2.3
Mean annual discharge [m ³ s ⁻¹]	12.7
Max annual discharge [m ³ s ⁻¹]	242.0
Two years flood Q _{50%} [m ³ s ⁻¹]	223.50
Ten years flood Q _{10%} [m ³ s ⁻¹]	473.20
D ₉₀ [mm]	46
D ₅₀ [mm]	144

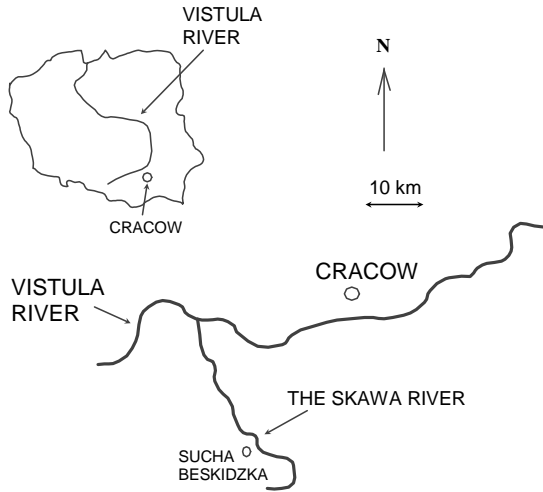


Fig. 2. General sketch of the research catchment area of the Skawa River

2.2 Methods

For the purpose of the study, a 100 meter-long research reach was selected within the Skawa River channel near Zembrzyce municipality. Identification and field measurements of bed-forms were carried out during early spring 2003 just after a year annual flood. The study was based on a hydraulic field survey of water velocity close to the streambed to calculate shear velocities, stresses and other hydraulic characteristics (Fig. 5). A well-developed streambed features was recognized in the form of braided bar. Research cross-sections were established within the region of the identified bar, and measuring points were chosen there. Wading velocity measurements were performed at all of chosen points (Fig. 3, Fig. 4).

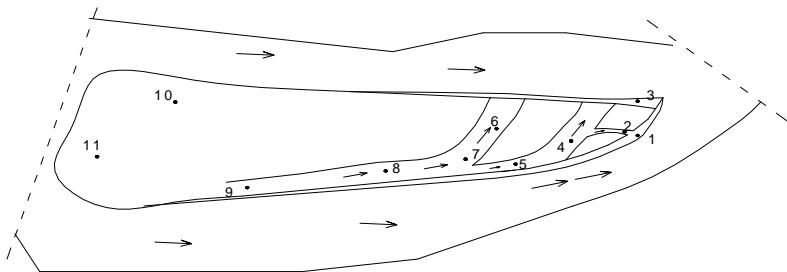


Fig. 3. Investigated braided bar with measuring points on the Skawica River



Fig. 4. Investigated braided bar.



Fig. 5. Field work during field campaign on the investigated braided bar on the Skawica River.

Water velocity measurements were based on Jarrett's (1990) findings regarding the taking of velocity profiles in mountain stream cross-sections. Gordon et al. (1992) and Bergeron & Abraham's (1992) methods were then

applied to the field data, and shear velocity V_* values were calculated from the velocity profiles obtained near-to-river-bed. Finally, shear stress τ values were calculated from: $\tau = V_*^2 \rho$ [N m^{-2}], where: ρ - water density [kg m^{-3}] and V_* - shear velocity [m s^{-1}]. Shear stress value (V_*) was obtained just directly from the equation $v = f(D)$ (Gordon et al. 1992): $V_* = a / 5,75$ where: a - slope coefficient $v = f(D)$, according to the general line equation: $v = aD + b$, where: D - log water depth above the stream bed [m], b - free coefficient. To calculate the flow resistance coefficient (f), the conclusions drawn by Ven Te Chow (1967) and Przedwojski et al. (1995) were applied. Flow resistance coefficient was obtained from: $f = 8 g J R / V_{mean}^2 = 8 (V_* / V_{mean})^2$, where: R - hydraulic radius [m], J - slope [-], V_{mean} - mean velocity [m s^{-1}]. The detailed methods used to obtain values for all of the above-mentioned parameters using classic hydraulics equations are shown in Radecki-Pawlik (2014).

2.3 Results, discussion and final conclusions

For reasons of clarity, all results obtained are presented in a table manner. Table 2 shows all hydraulics parameters measured and calculated above the research points within the regions of the investigated bar (Fig. 3). Measurements were taken just after the flood so the pattern of the falling flood along the bar was easily visible and analyzed. The braided formation has just formed thus the analysis of the investigated hydraulics parameters is relevant to its formation.

Generally bars which growth near the center of a wide and shallow channel lead to a concentration of flow in the narrower flanking channels, which leads to more active erosion of bed and banks and thus to the formation of an “island” (mid-channel bar). The feedback process is then repeated elsewhere along the channel, which leads eventually to the formation of a braided pattern. The observations on the Skawa river were done immediately just after the large flood when the water discharge was almost close to the bankfull, and the activity of flow forming the braided bar were visible even under lower water stage conditions since water was coming back in to the main channel of the Skawa river but still was covering the braided bar surface following flow patterns as it was under highest discharges when the braided bar has developed. Here in the particular example of the Skawa braided middle bar water approaching point 11 – the distal part of the bar - (Fig. 3) the Froude number is $Fr < 1$ (equal 0.725) and a flow here is subcritical (Chow 1959). Then is flowing over a bar is dividing into two streams/or branches or main braids. The flow is changing its character from subcritical to supercritical (point 10, $Fr=1.050$). The thalweg of one of the main braids is moving towards the right bank of the structure, also it was observed that the roughness has changed here.

Table 2. Hydraulics parameters for investigated points

Measuring point	1			2			3		
	A	b	c	a	b	C	A	b	c
V*[ms ⁻¹]	0.034	0.030	0.032	0.082	0.093	0.091	0.064	0.005	0.009
τ ₀ [Nm ⁻²]	1.140	0.877	0.997	6.650	8.638	8.286	0.039	0.030	0.073
h _{max} [cm]	19			6			14		
V _{sr} [ms ⁻¹]	1.171			0.667			0.08		
Fr [-]	0.736			0.756			0.005		
Re [-]	1 948 248.7			350 437.8			98 073.6		
f [-]	0.0060			0.0092			0.0126		
Measuring point	4			5			6		
Variable	A	b	c	A	b	c	a	b	C
V*[ms ⁻¹]	0.011	0.015	0.019	0.035	0.033	0.033	0.022	0.023	0.022
τ ₀ [Nm ⁻²]	0.112	0.233	0.374	1.222	1.118	1.068	0.505	0.539	0.482
h _{max} [cm]	9			11			7		
V _{sr} [ms ⁻¹]	1.188			1.692			0.722		
Fr [-]	1.599			2.653			0.759		
Re [-]	936 252.2			1 629 772.3			442 556.9		
f [-]	0.0072			0.0062			0.0086		
Measuring point	7			8			9		
Variable	A	b	c	A	B	c	A	B	c
V*[ms ⁻¹]	0.031	0.030	0.032	0.011	0.015	0.016	0.018	0.021	0.022
τ ₀ [Nm ⁻²]	0.938	0.934	0.980	0.126	0.229	0.261	0.317	0.425	0.498
h _{max} [cm]	11			12			6		
V _{sr} [ms ⁻¹]	1.261			0.636			0.428		
Fr [-]	1.474			0.344			0.311		
Re [-]	1 214 623.5			668 301.2			712 084.1		
f [-]	0.0067			0.0078			0.0077		
Measuring point	10			11					
Variable	a	b	C	A	b	c			
V*[ms ⁻¹]	0.017	0.018	0.020	0.007	0.007	0.006			
τ ₀ [Nm ⁻²]	0.283	0.320	0.417	0.046	0.054	0.031			
h _{max} [cm]	9			7					
V _{sr} [ms ⁻¹]	0.963			0.725					
Fr [-]	1.050			0.765					
Re [-]	758 931.7			444 395.8					
f [-]	0.0076			0.0086					

In points 1, 7, 5 and 4 water flow is supercritical and in point 5 water has the largest shear stress value equal to 1.20 N m^{-2} . The intensive linear erosion was noticed here caused by the secondary circulation which has place here under bigger stages (Fig.1). In the proximal part of the structure water again is dividing into two main channels (braids) firstly slowing widening its main braid a little in point 8 (here also shear stresses are not as big as earlier in point) to reach the biggest value of Fr in point 7 (flow is supercritical here) and shear stresses are reaching nearly 1 N m^{-2} . That way water separates along the middle bar into branches or braids and the small channels are formed splitting (when the next flooding will have place) the structure into smaller parts. The different situation has in the two points at the edge of the proximal part of the structure. In point 2 the highest shear stresses values were noticed since the structure here is very steep and avalanching like channels were observed. Here the finest particles were removed and flowing water is slowly demolishing that part of the bar. Here the main braid has its own channel-like stream and here also is going the main direction of the flow under flooding condition. On the other side of the bar, however, point 3, the different situation was noticed. Shear stresses here are smallest (less than 0.03) $Fr = 0.005$ and the deposition process of fine particles has started here in the shadow of the left bank of the bar. It is here where the finer taken out of the matrix of coarser gravel upstream of the structure is deposited.

The following conclusions could be drawn from the analysis above:

- when the braided bar is formed the huge difference in hydraulics parameters is noticed along the body of the structure,
- the braided bar is dividing slowly into many smaller bars which are separated by channel-like braids from where the fine particles are removed faster,
- since small particles are removed from braided channels of the structure under flooding conditions gravel sitting here is easier entrained thus more easily braids are formed,
- along the braided bar some places of low shear stresses were noticed where fine particles are deposited. In such shadows flow is subcritical with $FR \ll 1$,
- at the proximal part of the bar where water is flowing along the main braid the lee side of the structure is very steep with many avalanches with no fines and it is here where the braid is slowly disappearing into the main channel of the river under flooding conditions.

3. REFERENCES

- BERGERON, N. E. & ABRAHAMAS, A. D. 1992. Estimating shear velocity and roughness length from velocity profiles. *Wat. Resour. Res.*, 28 (8), p. 2155-2158.
- BRIDGE J. 1993. The interaction between channel geometry, water flow, sediment transport and deposition in braided rivers. Geological Society of London, 75, p. 13-71.
- BRISTOW C. AND BEST J. 1993. Braided rivers: perspectives and problems. Geological Society of London, 75, p. 1-11.
- CHOW, VEN TE, 1959, Open-Channel hydraulics. McGraww-Hill, NY, p. 108-114.
- GORDON D., MCMAHON T.A. & GINLAYSON B.L. 1992. Stream Hydrology. An Introduction for Ecologists. Wiley and Sons, London, p. 526.
- JARRETT, R. D. 1991. Wading measurements of vertical velocity profiles. *Geomorphology*, 4, p. 243-247.
- PRZEDWOJSKI B. BŁAŻEJEWSKI R. PILARCZYK K.W. 1995. River training techniques. Balkema, Rotterdam, Brookfield.
- ROBERT A. 2003. River processes. Arnold, London.
- RADECKI-PAWLIK A., BENCAL. J., KOWALSKI M. 2004. In stream hydraulics within a braided Ravel bar region formation. Materials of XXIV International School of Hydraulics: Hydraulic Problems In Environmental Engineering, editor: W. Majewski, p. 233-240.
- RADECKI-PAWLIK A., BENCAL J., KOWALSKI M., RADECKI-PAWLIK B. 2005. The variability of sediment and hydraulics parameters hen a braided bar is formed. In Polish: Zróżnicowanie warunków hydrodynamicznych i granulometrycznych podczas tworzenia się łachy środkowo-korytowej w potoku górskim o dnie zwirowym. Infrastruktura i Ekologia Terenów Wiejskich , Komis. Tech. Inf.. Wsi, PAN Oddz. w Krakowie, 3, p. 115-129.
- RADECKI-PAWLIK A. 2014. Hydromorphology of rivers and mountain streams. In Polish: Hydromorfologia rzek i potoków górskich – działy wybrane. Agriculture University of Krakow Publishing House, pp. 304.
- ROWINSKI P. , RADECKI-PAWLIK A. 2015. Rivers – Physical, Fluvial and Environmental Processes. Springer Int. Pub., ISBN 978-3-319-17718-2, Series - GeoPlanet: Earth and Planetary Sciences, pp. 450.
- SELBY M.J. 1985. Earth's changing surface, Clarendon Press, Oxford, p. 607.
- SOUTHARD J., SMITH N., KUHNLE R. 1984. Chutes and lobes: newly identified elements in braided streams. Canadian Society of Petroleum Geologists, 10, p. 51-59.

Parameters of wind driven waves on Nove Mlyny water reservoir

P. Pelikán, M. Šlezinger

Department of Landscape Management, Faculty of Forestry and Wood Technology, Mendel University in Brno, Zemědělská 3, 613 00 Brno, Czech Republic, phone: +420 545 134 009, e-mail: pelikanp@seznam.cz

Department of Landscape Management, Faculty of Forestry and Wood Technology, Mendel University in Brno, Zemědělská 3, 613 00 Brno, Czech Republic, phone: +420 541 147 758, e-mail: slezinger.m@fce.vutbr.cz

Abstract

The paper is focused on wind driven waves occurring inside inland water bodies. The wave parameters are usually considered during the design of dikes and stabilization measures around the water reservoir backwater zone adhering to the valid Czech standard specification 75 0255 (Calculation of wave effects on waterworks, 1987). Two main parameters are represented by wave period and characteristic wave height. These ones represent the basic input into the subsequent computations of hydrodynamic events occurring on the point of interaction between water table and shore for purposes of the proper altitudinal stabilization setup. The computational methods for the wave parameters estimation were verified on Nove Mlyny water reservoir (Czech Republic). The investigated methods include CSN 75 0255 and foreign practices developed in the conditions of sea.

Keywords

Offshore waves, shoreline stabilization, wave height, wave parameters, wave period.

1. INTRODUCTION

The primary research of wind-water interactions and wave mechanics had been accomplished in coastal areas along the shores of world oceans and seas because a basic understanding of coastal meteorology is an important component in coastal and offshore design and planning. Consequently the similar principles of water wave mechanics started to be considered in conditions of inland water bodies.

The problem of wind-driven was investigated worldwide by many specialists as published by [PHILLIPS and MILES 1957], [HSU 1988] in the sea conditions and [LUKÁČ 1972, 1980], [RESIO and VINCENT 1977], [KRATOCHVIL 1987], [ŠLEZINGER 2004, 2007, 2010], [OZEREN and WREN 2009] in the conditions of water reservoirs.

In the Czech Republic, the wave parameters and characteristics are usually considered during the design of dikes and stabilization measures around the water

reservoir backwater zone according to the valid Czech standard specification CSN 75 0255 Calculation of wave effects on waterworks (1987).

The simplest method describing water surface is called the first order theory (linear wave theory) – the original regular wave theory. The wave motion is represented by sinusoidal advancing wave (simple linear wave). Sinusoidal character means that the wave is steadily repeated in the form of constant smooth shape. The crests of particular waves have the same height, constant celerity and they collaterally proceed in the same mutual distance in perpendicular direction to the wave front without change of their shape. The theory was presented by English mathematician George Biddell Airy in 1845. The theory is simple and it is possible to relatively exactly determine number of wave characteristics with its aid. However the higher order theories were developed [CHEN et al. 2014]. They have been frequently used for modelling waves along sea coastlines [HSIEH et al. 2015], [JANNO and ŠELETSKI 2015].

The energy transferred to the water surface by wind generates a range of wave heights and periods that increase as the waves travel across the available fetch length (well describable by irregular wave theory). The process of wave generation by wind can be explained by combining the resonance model developed by Phillips in 1957 and the shear flow model developed by Miles in 1957 (see details in [CERC 1973–1984], [USACE 2002–2011]). Today, the irregular wave approach leads to derivation of wave characteristics of wave spectra – spectral analysis [KUMAR 2014].

Due to the complexity of the physical phenomena, most methods for wave prediction are based on semi-empirical relations. The methods have been modified as wind and wave data were accumulated over time, resulting in better predictions.

2. MATERIAL AND METHODS

Actual observed waves do not look as simple as the sinusoidal profile. With their irregular shapes, they appear as a confused and constantly changing water surface, since waves are continually being overtaken and crossed by others. As a result, waves are short-crested. The fact is particularly true for waves growing under the influence of the wind in conditions of deep water.

The irregular wave theory was used for purposes of the research. An irregular wave train is constructed by linear superposition of a number of linear wave components. Wave train analysis is based on statistical processing of observed data. The data are represented by record of water table motion in a given point. The individual wave is identified by local maxima (wave crest) and local minima (wave trough) of water table fluctuation.

The adopted engineering procedure is the zero-crossing technique, where a wave is defined when the surface elevation crosses the zero-line or the mean water level (MWL) upward and continues until the next crossing point. This is the zero-upcrossing method. When a wave is defined by the downward crossing of the zero-line by the surface elevation, the method is the zero-downcrossing. The zero-

crossing wave height is the difference in water surface elevation of the highest crest and lowest trough between successive zero-crossings. The definition of wave height depends on the choice of trough occurring before or after the crest. Here, a wave will be identified as an event between two successive zero-upcrossings and wave periods and heights are defined accordingly [USACE 2008]. There can be differences between the definitions of wave parameters obtained by the zero up- and down-crossing methods for description of irregular water surface. Both methods usually yield statistically similar mean values of wave parameters. There seems to be some preference for the zero-downcrossing method (therefore used for the research). The downcrossing method may be preferred due to the definition of wave height used in this method (the vertical distance from a wave trough to the following crest). It has been suggested that this definition of wave height may be better suited for extreme waves [IAHR 1986].

A measured wave record never repeats itself exactly, due to the random appearance of the water surface. But if the water surface state is “stationary”, the statistical properties of the distribution of periods and heights will be similar from one record to another. The most appropriate parameters to describe the water surface from a wave record are therefore statistical [WMO 1998].

Determination of wave statistics involves the actual processing of wave information using the principles of statistical theory. A highly desirable goal is to produce some statistical estimates from the analysed time-series data to describe an irregular water surface state in a simple parametric form. For engineering, it is necessary to have a few simple parameters that in some sense tell us how severe the water surface is and a way to estimate or predict what the statistical characteristics of a wave record might be had it been measured and saved. Fortunately, millions of wave records have been observed and a theoretical/empirical basis has evolved to describe the behaviour of the statistics of individual records [USACE 2008].

For parameterization, there are many short-term candidate parameters which may be used to define statistics of irregular water surface. Two of the most important parameters are characteristic height H and characteristic period T . Characteristic (significant) wave height ($H_{13\%}$) represents the mean height of one third of the highest waves in wave train, i.e. the wave with the height coming up to the 13% probability of occurrence. Period is the time during two consequent wave crests pass through a given point. The characteristic period could be designated as mean period \bar{T} , or average zero-crossing period. The terms are applied worldwide in wave estimation and related calculations (also in CSN 75 0255).

Data collection was accomplished in fetch limited deep water conditions in water reservoir Nove Mlyny – Dolni near Sakvice municipality. The data are represented by wave train record with simultaneous logging of wind speed and direction by means of anemometer. The record of water surface motion was realized with the aid of continuous fluid level sensor on the base of resistance anchored to the bottom.

3. RESULTS

The periods and heights of irregular waves are not constant with time, changing from wave to wave. Wave-by-wave analysis determines wave properties by finding statistical quantities (i.e., heights and periods) of the individual wave components present in the wave record. It is recommended the wave records must be of sufficient length to contain several hundred waves for the calculated statistics to be reliable. Continual data collection was realized during the time of 3 hours. The data set contained 145 000 records of elevation of water surface (about 13 records per second with time stamp).

Wave train analysis is essentially a manual process of identifying the heights and periods of the individual wave components followed by a simple counting of zero-crossings and wave crests in the wave record. The process begins by dissecting the entire record into a series of subsets for which individual wave heights and periods are then noted for every zero down-crossing or up-crossing, depending on the method selected. In the interest of reducing manual effort, it is customary to define wave height as the vertical distance between the highest and lowest points, while wave period is defined as the horizontal distance between two successive zero-crossing points [USACE 2008]. In this analysis, all local maxima and minima not crossing the zero-line were discarded (Fig. 1).

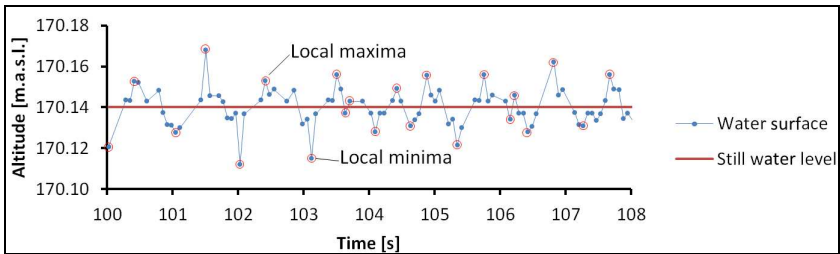


Fig. 1 Segment of water surface record and zero-crossing technique in detail

Approximately 12 000 waves were extracted by means of zero-crossing method in total. The value of height H and period T was calculated for each wave. Necessary to note the following results are related to the 4 179 waves originated by wind from SE direction and 4 wind speed categories from 1.9 to $2.9 \text{ m}\cdot\text{s}^{-1}$. Values of wind speed refer to the 10 m reference level above water surface (u_{10}). Conversion was worked out through the following equation, where u_z means velocity at the elevation z (i.e. elevation of anemometer):

$$u_{10} = u_z \left(\frac{10}{z} \right)^{\frac{1}{7}} \quad (1)$$

Detailed wind calculations and graphical solution available in [PELIKÁN and MARKOVÁ 2013]. Final values of wave parameters result from combination of

factor of fetch and wind. Fetch (F) is the length along the wind of a given speed and direction affects the water surface in reservoir. Experiment was realized in the fetch-limited conditions – wind blew sufficiently for a long time, thus the waving developed along the whole fetch. It stands to reason that lot of combinations may arise – irregular horizontal projection of reservoir, fluctuations of wind speed and direction, etc. If one wants to analyse and compare data gained from various factor combinations, dimensionless parameterization should be introduced. Wave heights were converted into the dimensionless parameter $g \cdot H \cdot u_{10}^{-2}$ and wave periods converted into the parameter $g \cdot T \cdot u_{10}^{-1}$. Analogous parameterization with little differences is usually used worldwide [USACE 2008], CSN 75 0255.

Subsequently, the obtained datasets of wave heights were statistically processed with emphasis on the verification of the hypothesis that various wind speed originates waves with various parameters (whether, if the wave parameters are directly dependent on wind).

It seems suitable method how to solve this task could be single-factor ANOVA (analysis of variance, analysis of simple sorting). Before performing the analysis, let's see whether the assumptions are met. These would be preferable to try e.g. on a pilot sample (at which we really only verify assumptions). However, usually the other data are not available, therefore the assumptions have to be verified on observed data. The first presumption is the normality of dependent variable (height and period) in all groups (4 wind speed categories). Right skewed distributions of observed data dimensionless parameters are depicted in Fig. 2 by means of categorized histograms.

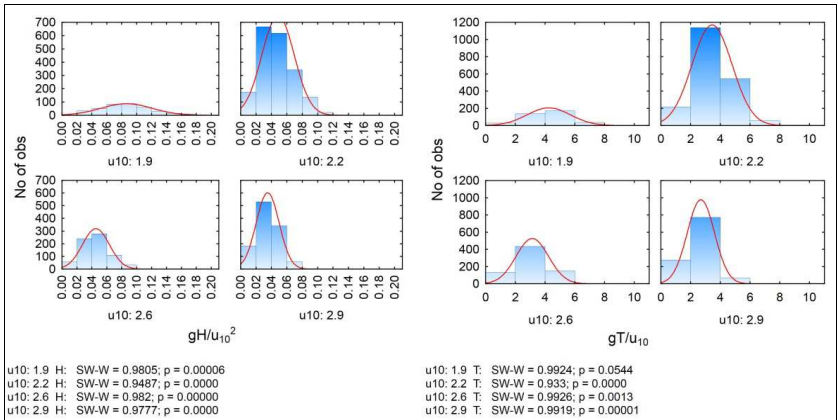


Fig. 2 Categorized histograms of dimensionless variables with Shapiro-Wilk test of normality

The normality of data was tested via Shapiro-Wilk test. The hypothesis of normality of wave heights and periods was rejected in all cases except the wave period originated by wind speed of $1.9 \text{ m} \cdot \text{s}^{-1}$. The values from the Shapiro-Wilk

test show that assumption of normality was violated. Additionally, the number of cases in each group is different. Instead ANOVA analysis, a nonparametric equivalent Kruskal-Wallis test was used. The test is based on the order and it is not expected that the data come from a normal distribution, but it is assumed that data follow the continuous distribution. The overall result of the test approved statistically significant difference of wave heights and period caused by various wind speed (Tab. 1).

Tab. 1 Kruskal-Wallis ANOVA (Statistica 12)

Depend.: gH/u_{10}^2	Multiple Comparisons z' values Independent (grouping) variable: u_{10} Kruskal-Wallis test: (3, $N= 4179$) =798.2925 $p =0.000$			
	1.9 (R:3443.2)	2.2 (R:2193.6)	2.6 (R:2092.1)	2.9 (R:1453.1)
1.9		18.38027	17.58022	27.64433
2.2	18.38027		1.92977	16.39014
2.6	17.58022	1.92977		11.08168
2.9	27.64433	16.39014	11.08168	
Depend.: gT/u_{10}	Multiple Comparisons z' values Independent (grouping) variable: u_{10} Kruskal-Wallis test: (3, $N= 4179$) =431.0235 $p =0.000$			
	1.9 (R:2932.8)	2.2 (R:2248.9)	2.6 (R:2033.9)	2.9 (R:1564.4)
1.9		10.05789	11.69613	19.00766
2.2	10.05789		4.09023	15.15185
2.6	11.69613	4.09023		8.14149
2.9	19.00766	15.15185	8.14149	

Multiple comparisons of average rank show us the differences among particular variables. We can see that statistically significant difference were approved among all variables except the case of wave heights between data sets related to the wind speed 2.2 and 2.6 $m \cdot s^{-1}$ (Tab. 1). The results could be represented in a graphical form – boxplots demonstrate the median, lower and upper quartiles and ranges (Fig. 3).

The observed values of characteristic wave height $H_{13\%}$ and mean period \bar{T} in real dimensions are scheduled in Tab. 2. Furthermore, the hindcast (retroactive modelling) of the characteristic wave parameters was accomplished with the aid of 4 models. The first one is derived from the Czech standard specification CSN 75 0255 Calculation of wave effects on waterworks. Other methods were developed in USA by USACE and ASABE in conditions of sea and large inland water bodies.

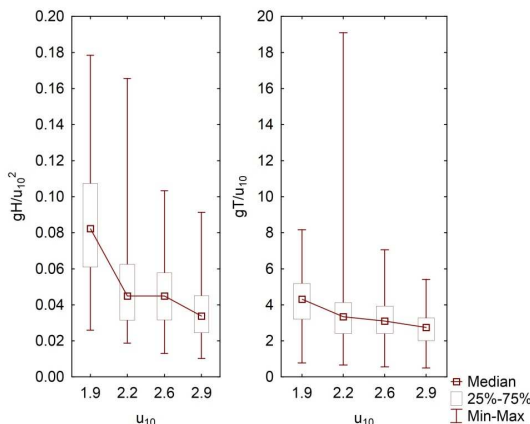


Fig. 3 Kruskal-Wallis ANOVA: boxplots of dimensionless variables

Tab. 2 Hindcast of wave parameters $H_{13\%}$, \bar{T}

	Observed	CSN	CEM	SPM	ASABE	
F [m]	–	1878	1878	1926	1926	
$H_{13\%}$ [m]						
u_{10} [m·s⁻¹]	1.9	0.045	0.052	0.036	0.034	0.031
	2.2	0.037	0.061	0.043	0.042	0.039
	2.6	0.046	0.074	0.052	0.052	0.050
	2.9	0.046	0.084	0.058	0.060	0.059
\bar{T} [s]						
u_{10} [m·s⁻¹]	1.9	0.817	4.033	0.806	0.893	0.801
	2.2	0.743	4.332	0.852	0.954	0.874
	2.6	0.827	4.694	0.908	1.028	0.965
	2.9	0.825	4.943	0.946	1.079	1.028

The input data for the computational models of characteristic wave height and periods are represented by measured average wind speed and direction related to the fetch length. However the data were collected during the same experiment, the input data of wind and fetch may differ in models (1 828 vs. 1 926 m). The fact is caused by different methodology of wind and fetch determination in the models that was fully respected (detailed practice and formulas available in [PELIKÁN, 2013]).

Although it may seem the American models provides better estimates of wave parameters in all cases, the deviations from measured data are practically negligible in connection with water reservoir extent. The Czech model provides probably overestimated results, especially in the case of period.

4. DISCUSSION AND CONCLUSIONS

The application of wave models is necessary for solution of coastal engineering studies and long-term prognostic tasks. The characteristic wave height represent the main input for consequent calculations – for example wave breaking, wave setup and run-up on the structures and reservoir banks. The knowledge of this wave parameter allows the determination of active part of shore due to the waving, proper altitudinal emplacement of shore-stabilization constructions and altitudinal dimensions of dikes due to the water table.

The important decision lies in the formulation of the protection degree of shoreline – setting up of the design wave height and design wind speed respectively. The dams and levees are protected from the waves with 1% probability of occurrence and the backwater zone is usually protected from characteristic wave with 13% probability of occurrence due to high expenses spent on stabilization measures (CSN 75 0255). The protective measures are determined right by the wave run-up height with same probability of occurrence. However the inputs into the calculations of wave run-up are represented mainly by wave parameters in deep water – characteristic wave height and period. Thus, calculation of the parameters in deep water is the first step in a process of determination of proper altitudinal design of protective measures in a given reservoir. Any degree of protection could be determined thanks to known statistical distribution (and estimation of statistical parameters) with the aid of presented models.

Knowledge of the characteristic wave height is essential for the design of coastal projects because it is the major factor that determines the geometry of beaches, the planning and design shore protection measures and hydraulic structures. Estimates of wave conditions form the basis of almost all coastal engineering studies.

The presented relationships are well applicable in combination with regular wave theory (Airy waves) leading to accurate estimates of wave parameters and characteristics on open water areas and inland water bodies.

The verification of models with real data is quite complex procedure involving data collection and statistical processing with emphasis on exploratory data analysis due to the special attributes (skewness, uncommon distribution). The overall results indicate the model used by USACE is applicable for wave estimations in inland water bodies as well however originally developed for sea conditions.

The characteristic wave height and period in deep water conditions represents basic input into the subsequent computations of hydrodynamic events occurring on the point of interaction between water table and shore, i.e. solution of engineering tasks generally in the field of coastline water management in transitional and shallow water conditions. For example, it is possible to compute proper altitude emplacement of particular design components of bank stabilization measures. The knowledge of probability distributions of some design parameters

allows us to compute waves with any level of probable exceeding. Thus, the models could be useful for calculations when designing the dam crest and its fortification where the probability of wave run-up occurrence is considered 1%.

The objectives of the research and given hypothesis were reached by means of statistical methods. The results approved statistically significant difference of wave heights and period caused by various wind speed. The gains of the research consist in verifying foreign state of the art computational methods and implementing new piece of knowledge into conditions of water reservoirs in the Czech Republic.

5. REFERENCES

- CERC. 1973, 1977, 1984. Shore protection manual. Waterways Experiment Station, U.S. Army Corps of Engineers, Washington, D.C.
- CHEN G.-Y., WU C.-L., WANG Y.-H. 2014. Interface depth used in a two-layer model of nonlinear internal waves. *Journal of Oceanography*, Vol. 70: 329–342. ISSN 1573-868X.
- HILLIPS O. M. 1957. On the generation of waves by a turbulent wind. *Journal of Fluid Mechanics*, 417–445.
- HSIEH C.-M., HWANG R. R., HSU J. R.-C., CHENG M.-H. 2015. Numerical modeling of flow evolution for an internal solitary wave propagating over a submerged ridge. *Wave Motion*, Vol. 55: 48–72. ISSN 0165-2125.
- IAHR. 1986. List of Sea State Parameters. Intl. Assoc. Hydr. Res., Suppl. to Bull. No. 52, Brussels.
- JANNO J., ŠELETSKI A. 2015. Reconstruction of coefficients of higher order nonlinear wave equations by measuring solitary waves. *Wave Motion*, Vol. 52: 15–25. ISSN 0165-2125.
- KUMAR V. S., DUBHASHI K. K., NAIR T. B. M. 2014. Spectral wave characteristics off Gangavaram, Bay of Bengal. *Journal of Oceanography*, Vol. 70: 307–321. ISSN 1573-868X.
- LUKÁČ M. 1972. Waves on the water reservoir and its effects on the reservoir bank. Bratislava, MS Katedra Geotechniky SVŠT. (in Slovak)
- LUKÁČ M., ABAFFY D. 1980. Waves on the water reservoirs, its effects and anti-abrasive measures. Ministerstvo lesného a vodného hospodárstva SSR, Bratislava. (in Slovak)
- MILES J.W. 1957. On the generation of surface waves by shear flows. *Journal of Fluid Mechanics*, Vol. 3: 185-204.
- OZEREN Y. WREN D.G. 2009. Predicting wind-driven waves in small reservoirs. *American Society of Agricultural and Biological Engineers*, Vol. 52(4): 1213–1221. ISSN 0001-2351.
- PELIKÁN P. 2013. The effect of shore abrasion on the transformation of the bank of water reservoirs. [Ph.D. Thesis.] Mendel University in Brno, Faculty of Forestry and Wood Technology, Brno, 147 p. (in Czech)

- PELIKÁN P., MARKOVÁ J. 2013. Wind effect on water surface of water reservoirs. *Acta Universitatis Agriculturae et Silviculturae Mendelianae Brunensis*, 2013, LXI, No. 6, pp. 1823–1828. ISSN 1211-8516.
- RESIO D. T., VINCENT, C. L. 1977. Estimation of winds over the Great Lakes. *Journal of the Waterways, Harbors, and Coastal Engineering Division, American Society of Civil Engineers*, Vol. 102: 263–282. ISSN 0044-8028.
- ŠLEZINGR M. 2004. Bank abrasion. CERM, Brno, pp 160. ISBN 80-7204-342-0. (in Czech)
- ŠLEZINGR M. 2007. Stabilisation of reservoir banks using an “armoured earth structure”. *Journal of Hydrology and Hydromechanics*, Vol. 55: 64–69. ISSN 0042-790X.
- U.S. ARMY CORPS OF ENGINEERS. 2002–2011. *Coastal Engineering Manual. Engineer Manual 1110-2-1100*, Vol. I-VI, Washington, D.C., 2923 p.
- VOTRUBA L., KRATOCHVIL S. 1987. CSN 75 0255 Calculation of wave effects on waterworks. Vydavatelství Úřadu pro normalizaci a měření, Praha. (in Czech)
- WORLD METEOROLOGICAL ORGANIZATION. 1998. *Guide to Wave Analysis and Forecasting*. 2nd edition, WMO No. 702, Geneva, Switzerland, 168 p., ISBN 92-63-12702-6.

Acknowledgement

The paper was worked out as a part of research project “Active anti-abrasion structures”, reg. no. LDF_VT_2015011, funded by IGA FFWT MENDELU Brno.

List of symbols

F [m] ... fetch length

g [$\text{m}\cdot\text{s}^{-2}$] ... gravitational constant

$H_{13\%}$ [m] ... characteristic wave height in deep water

\bar{T} [s] ... mean period in deep water

u_{10} [$\text{m}\cdot\text{s}^{-1}$] ... wind speed in 10m reference level above water surface

u_z [$\text{m}\cdot\text{s}^{-1}$] ... wind speed in elevation z above water surface

List of abbreviations

ASABE ... American Society of Agricultural Biological Engineers

CEM ... Coastal Engineering Manual

CSN ... Czech standard specification

SPM ... Shore Protection Manual

USACE ... United States Army Corps of Engineers

Physical and Mathematical Modelling for Canoe Slalom Whitewater and the 2016 Olympic Games in Rio de Janeiro

*J. Pollert¹ junn., J. Pollert¹ sen., J. Procházka¹, P. Chmátal¹, B. Campbell²,
J. Felton², D. Dungworth³*

(1 - České vysoké učení technické v Praze, Fakulta stavební, Katedra zdravotního a ekologického inženýrství, Thákurova 7, 166 29 Praha 6, Email for correspondence: pollertj@fsv.cvut.cz; 2, 3 - Whitewater Parks International, Glenwood Springs, Colorado, USA; Whitewater Parks International, Sydney, Australia; 4 - CUNDALL, Newcastle upon Tyne, U.K.)

Abstract

The article provides an analysis of hydraulic physical and mathematical (CFD) model investigations of the artificial slalom channels designed for the Rio de Janeiro 2016 Olympic Games. The main aim of the physical model investigations was to evaluate these channel designs from a hydraulic point of view - to validate technical performance objectives and to determine the optimal positioning for hydraulic features within the channels, with respect to design criteria which are: optimal water depth at prescribed flows, optimal current velocities, optimal Games-ready hydraulic configurations, safety criteria compliance, suitability for various Legacy uses (per IOC intent).

Keywords

Hydraulics, open channel flow, physical and mathematical modelling, water sport facilities, Olympic Games

1. INTRODUCTION

What makes canoeing so attractive to so many people? Perhaps it's a feeling of freedom and adventure that takes us back to a time when someone first sat in a hollowed-out log and floated down a previously unexplored stretch of river. Canoeing is an activity that can be enjoyed by people of all ages and physical abilities. From foaming whitewater to meandering rivers to flat water lakes, it affords opportunities for both excitement and relaxation. It's an outdoor aquatic sport that fully interacts with its surrounding environment and, in this sense, an ideal way of better understanding and respecting nature.

What does the term "artificial canoe slalom course" mean? It is an attempt to re-create the natural hydraulic phenomena found in open river basins in an artificial, purpose-built river basin. These artificial courses can often be constructed within a short period of time, as opposed to their natural counterparts built over millions of years, and be operated with unnaturally predictable and controlled conditions.

Relative to the success of other individual sport disciplines included in the Summer Olympic Games program, Canoe Slalom has always enjoyed one of the highest ratings among international TV viewers (third highest of all sports during the Sydney 2000 Games, POLLERT, J. 2001, with similar popularity during Athens 2004, Beijing 2008 and London 2012). The excitement of the sport has proven particularly attractive to youth and with participation and interest levels on the rise, new focus now turns to Rio de Janeiro and the 2016 Olympic Games.



Fig. 1 Map of Rio 2016 sport zones



Fig. 2 Basic description of whitewater courses

All Rio 2016 competition venues will be spread across four zones that were selected in accordance with development guidelines for the Olympic Games. Canoe Slalom will be held in Deodoro Sport Complex, which will be the second largest concentration of competition venues during the Rio 2016 Games. A sport legacy will remain after the Games in the form of the Deodoro X-Park, which will include the Olympic Whitewater Stadium and BMX Centre, along with a 500,000 m² of public recreation area, the second largest in Rio. Deodoro's nine venues will host 11 Olympic sports and four Paralympic sports in 2016.

2. WHITEWATER CANOEING – THE SCIENCE BEHIND THE SPORT

We could certainly wonder about the reasons for building artificial courses of this type for sport. Why do we invest huge funds in something that is available naturally for free? There are a few reasons and they could be summarized as follows: Create more spectacular sites for racing and training for canoe slalom, promote whitewater sport, increase the popular appeal of canoe slalom, protection of the environment; the creation of new facilities for water sport parks would eliminate the current tendency to hold slalom races in existing wildlife parks, create a focal point for civic pride and the legacy after top sport events like Olympic Games.

In terms of technical aspects, the specialist design team responsible for an Olympic canoe slalom course must observe the following considerations from early in the process: International canoe slalom rules of ICF (International Canoe

Federation), IOC requirements (International Olympic Committee) for organization of Olympic Games.

A majority of whitewater canoe slalom courses (the first one was built in Augsburg, Germany, for the Olympic Games in 1972) were traditionally copies of watercourses with a prevailing linear channel. This changed with the course for Sydney 2000 when the team of designers attempted opted for a more circular shape, addressing a desire to let viewers observe more of the course from the start to the finish.

3. OPEN CHANNEL FLOW AND WHITEWATER COURSES

Artificial whitewater canoe courses are typical examples of open channel flow, CHANSON, H. 2004. The main driving force is fluid weight and gravity forces driving the flow downhill.

Artificial canoe courses should meet several criteria – high velocities, big waves, etc. for top athletes, but also appropriate and safe for recreational users. From this point of view, well designed courses must include a number of different hydraulic features which make up a course's "whitewater". The course would be expected to contain the following hydraulic features which should remain consistent, not surging or changing shape with time, and they should be similar in form to the surface features found on natural rivers: Chutes. From a hydraulic point of view, the flow is supercritical and refers to the term "streaming flow". Stoppers, or Holes. The proper hydraulic term for these is "hydraulic jump". Stoppers may be at right angles or diagonal to the flow. Haystacks. The hydraulic term would be "standing waves". Eddies, or reverse flow. This can occur when the flow is constricted through a narrow section and then expands as a jet in the centre of the stream. Turbulence. This would be on a small scale (i.e. less than the canoe's length) and would consist of small eddies and local, random variations in water velocity. Surface waves. These would be similar to wind waves and travel along or across the stream, usually being small. Other important characteristics are consistency or steadiness, i.e. no surging or changing of hydraulic features with time.

Analysis shows important facts and reciprocal functions between Froude number Fr , bottom slope i_0 , and water level slope i_f :

- Bottom slope i_0 is possible to define:
 - Steep : $y_n < y_c$
 - Critical : $y_n = y_c$
 - Mild : $y_n > y_c$
 - Horizontal : $i_0 = 0$
 - Adverse : $i_0 < 0$
- Decisive depth for various flow is given by:
 - 1: $y > y_n$

- 2 : $y_n < y < y_c$
- 3 : $y < y_c$

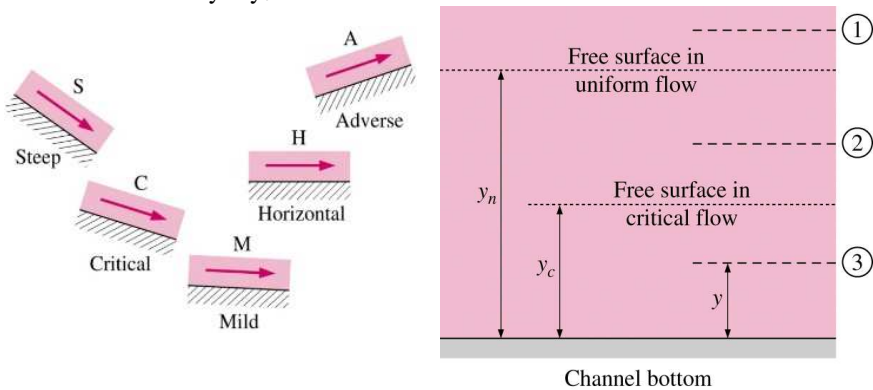


Fig. 3 Examples of the typical slopes and deepness

Slalom courses can be described by using a Froude number as the best characterization of the courses of different type and difficulty

$$Fr_{ch} = \frac{v_s}{\sqrt{g y_s}}$$

This describes the streaming in the course as a whole. It is thus defined by the mean value of depth, width, cross section, hydraulic radius and mean longitudinal slope $i_0 = H/l$ (where H is the difference between upper and lower elevation and l is the course length). The mean velocity of a turbulent flow can be expressed in the well known Manning formula, STREETER, V.L., WYLIE, E.B., BEDFORD, K.W. 1998.

$$v_s = \frac{1}{n} R_s^{2/3} i_0^{1/2}$$

The dependence of characteristic Froude number on the roughness coefficient is shown on Fig.4 with mean longitudinal slopes $i_0 = 0.01$ and $i_0 = 0.015$, discharges $Q = 10 \text{ m}^3/\text{s}$ and $20 \text{ m}^3/\text{s}$ and usual mean width $B_s = 10 \text{ m}$ were taken into account (these values correspond to the common ranges of longitudinal slopes, discharges and to the width of slalom courses). From Fig. 4 it is evident that the roughness is very important factor, having a strong influence on the course difficulty, BÉMOVÁ I., POLLERT, J. 1996.

Generally, the following ranges of characteristic Froude numbers are recommended for preliminary evaluation of any course design

Novices	$1.3 < Fr_{ch} < 1.7$
Elite athletes	$1.7 < Fr_{ch} < 2.4$

4. PHYSICAL HYDRAULIC MODELLING AND WHITEWATER COURSES

Many designers and engineers who have been involved with the development of artificial slalom courses believe that using hydraulic models to inform the design is particularly effective. The method of design by calculation alone can be challenging unless simple geometrical cross-sections are adopted.

The basic relevant parameters needed for any dimensional analysis may be grouped into the following classifications, STREETER, V.L. 1964:

- a. Fluid properties and physical constants. These consist of the density of water ρ (kg/m^3), the dynamic viscosity of water μ (N s/m^2), the acceleration of gravity g (m/s^2), etc.
- b. Channel (or flow) geometry. These may consist of the characteristic length(s) l (m).
- c. Flow properties. These consist of the velocity(ies) v (m/s) and the pressure difference(s) p (Pa).

In free-surface flows (e.g. rivers and wave motion), gravity effects are predominant. Model prototype similarity is performed usually with a Froude similitude

$$Fr = \frac{v^2}{g \cdot L} = idem$$

The most economical strategy for modelling of slalom course is:

1. To choose a geometric-scale ratio such as to keep the model dimensions small,
2. To ensure that the model Reynolds number is large enough to make the flow turbulent at the smallest test flows.

Based on previous experiences and considering the available space of the hydraulic laboratory at the Czech technical university, the scale for physical model of the Rio 2016 Olympic course was 1:13 and used the dynamical similitude (two phenomena are dynamically similar if the dimensionless form of each physical variable has the same value at corresponding points).

Open channel structures, such as artificial slalom courses, generally have gravity forces and inertial forces that far outweigh viscous and turbulent shear forces. Thus, geometric similitude and equivalency of Froude number for the model number and prototype produce a good approximation to dynamic similitude. Although the accuracy of Froude scale models is well established, their interpretation can be difficult. The main problem is that since all water levels, including heights of standing waves and other surface disturbances are reduced by the linear scale factor, this very fact makes observation difficult. A further difficulty arises in that the water surfaces of the full-size channel will have much more "whitewater" than the model. In fact, the model has very little "whitewater", whereas the full size channel will be very impressive with large areas of

whitewater. This is because the white colour is produced by entrained air in the water surface and the amount of air entrained depends to a great extent on the absolute water velocity. Therefore, there will be many regions in the model where the water surface looks smooth and black, that in full-size will appear white and turbulent. The model study for some whitewater courses with relatively small number of obstacles showed that in part with higher bottom slopes (1% and higher) would resolution high velocities and shallow depths. Tentatively, it was decided that large/higher number of obstacles would be needed on the flat concrete floor (low roughness) to control flow depths and velocities, and produce desirable current and eddy patterns.

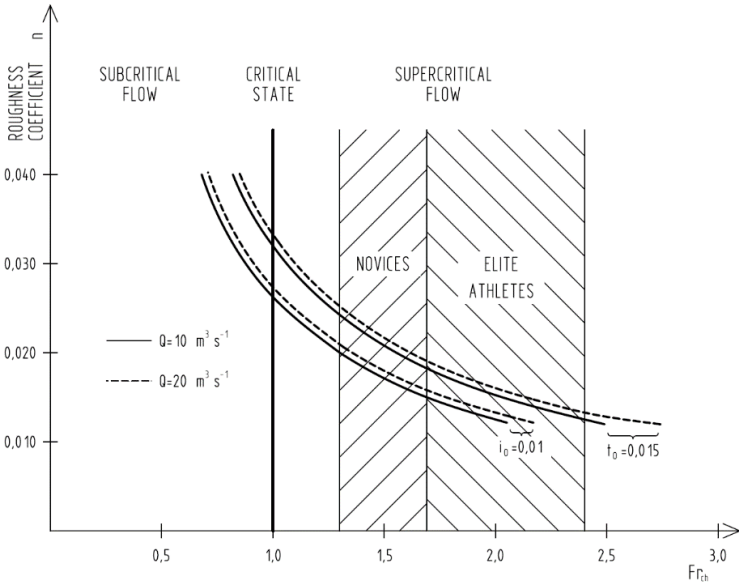


Fig. 4 Relationship between friction factor and characteristic Froude number (artificial slalom courses)

5. PHYSICAL AND MATHEMATICAL MODELLING OF RIO'S COURSES

Basic geometry - the length of an artificial slalom course should conform to the standards of International Canoe Federation (ICF) from 200 – 400 m, the width of 10 m or more is suggested for putting gates allowing manoeuvring among them, minimum depth of about 0.6 m is needed, since canoeists would have difficulty in paddling in shallower water; depth of 0.6 m of water is also so that paddlers can successfully perform an Eskimo roll; however, depths great enough should be minimized to reduce costs or necessary flow rate Q. The second group of parameters, which apparently influence the quality and difficulty of the course, includes the discharge through the course and the bottom slope. Both of

these are often limited; the discharge - by insufficient capacity of upstream reservoir or by low discharge in the river during the season; the bottom slope - by configuration of the ground.

There are three ways of forming hydraulic features in whitewater courses:

1. Permanent blocks, with rounded edges for safety, to constrict and divert the water flow. These should not be undercut, and their upstream surfaces should be sloped to allow the current to push boats to the surface.
2. Moveable blocks, temporarily secured in position so that the flow patterns within the course can be changed from time to time and for different standards of paddling skills. Rapids created by high velocity water falling into slow-moving water areas. They have no obstacles in them to obstruct boats or swimmers.

Two independent physical models were constructed at a scale of 1:13 for the Rio 2016 Olympic Competition and Training courses. The overall concept and design for the courses is the work of the USA based company Whitewater Parks International (WPI), who also designed the Canoe Slalom courses for London in 2012 Olympic Games. The UK engineering firm Cundall, who worked with WPI on the London 2012 facility, also assisted them with the Rio 2016 project. WPI commissioned Czech Technical University in Prague to conduct hydraulic experiments connected with these courses, including the construction and testing of these physical models. Each model was constructed and investigated separately. The main aim of all investigations concentrated on finding an optimal position and size of obstacles in each section and pool with respect to functionality of hydraulic features and safety (e.g. minimum water depth 0.6 m). Other criteria were: velocities in a usable range; no fluctuating water (stable stream flow and depth); creating different characteristics in each section and pool to address different uses (whitewater slalom, rafting, rodeo and others). In each section, investigated separately and in connection to each other, we tested at least 5 different scenarios from which an optimal configuration was chosen.

Tab. 1 Parameters of the full sized and modelled courses

Scale 1:13	Competition course Reality	Training course Reality	Competition course Model	Training course model
Length (m)	250	200	19,23	16,15
Flow rate	12,0 (m ³ /s)	10,5 (m ³ /s)	19,69 (l/s)	17,23 (l/s)
Max slope (%)	2	1	2	1
Head (m)	4,5	2,0	0,35	0,15

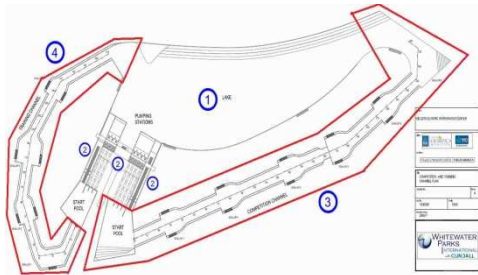


Fig. 5 Placement of models in the laboratory; Arrangement of Rio 2016 courses in Deodoro 1 – feeding lake, 2 – pumping stations and boat lifts, 3 – competition course; 4 - training course

Basic construction material for the each model was used:

- Water protected plywood with additional surface improvements with plastic folia extruded polystyrene for construction of banks and obstacles steel plates for channel bottom and quick changes of obstacle positions,
- Magnets – each obstacle for modelling flow in the courses was equipped with Nd magnets (size $D = 5$ mm) in the bottom. The system of mountable obstacles was recommended by WPI and was scaled 1:13. The system is like brick-box “LEGO” and thus very flexible in affecting formation of all types of hydraulic features for whitewater canoeing.

The experiments concentrated on velocities, creation of key hydraulic features in different sections of the courses (whitewater experience of investigators was particularly useful here), depths, directions of flow, and everything else that could be influenced by the configurations of obstacles. Each measured point in the model was characterized as follows:

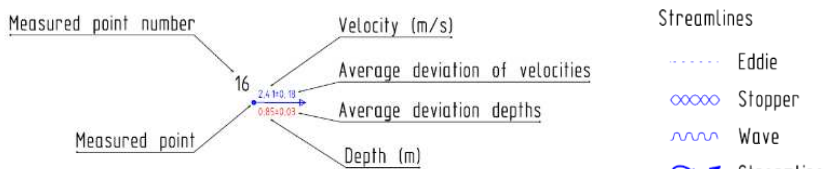


Fig. 6 Schematization of measurements with respect to recorded points

Discharge in the model was measured by magnetic-induction flowmeter KROHNE DN 200. Point velocities were recorded by micro propeller Greisinger Electronic GmbH, GMH 3350 (accuracy 0,01 m/s; frequency of measurement 1 s; range 0,05 – 5 m/s). Depths were measured using ultrasonic sensor Pepperl-Fuchs and thus flow was not influenced. Five different configurations of obstacles were tested in each section, from which an optimal configuration was recommended. During model construction, special attention was paid to control of model bottom roughness established by steel plates. Roughness of steel plates was measured in Carl Zeiss Metrology Centre Faculty of Mechanical Engineering, CTU in Prague. After scale recalculation roughness corresponded to Manning friction coefficient $n = 0.011 - 0.012$ (fair-face concrete). For mathematical modelling ANSYS – FLUENT CFD modelling was used.

The basic ground plan and placement of the courses in Deodoro Complex was designed by Whitewater Parks International, which while addressing all the technical requirements of IOC and ICF, also aimed to reduce construction and operating costs by +/- 30%, compared with earlier iterations. Both competition and training courses are fed from a storage lake by a single pumping station. Each course in the model includes a start pool, 11 whitewater sections or pools, and a feeding lake (reservoir). The competition course was divided into 11 sections. The following example of an investigation is section “4 – asymmetric”. This section could be characterized from a hydraulic point of view as a fast meandering flow created by a combination of bigger obstacles adjacent to the bank walls and smaller submerged obstacles closer to the main current. System of the obstacles create strong stoppers (hydraulic jumps) and high waves perpendicular to the linear profile. Near the end of the section is area of fast flowing water with high turbulence and eddies. Near the banks are strong reverse flows with sharp boundaries between the main downstream flow and reverse flow. Maximum velocities here reach 3.9 m/s and on average 1m depth is found nearly everywhere, while not lower than 0.9m.

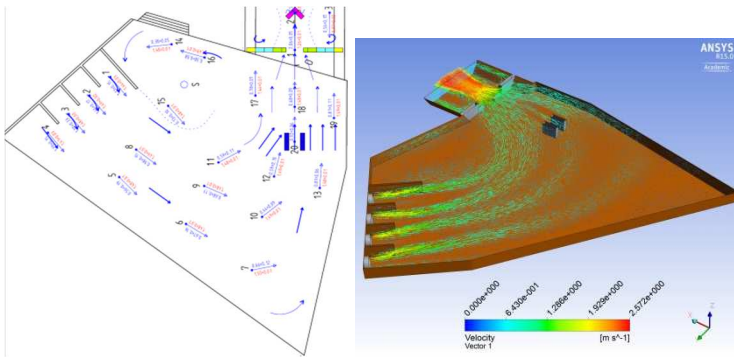


Fig. 7 Construction configuration of start pool – outlet from pumping station without water; Physical and mathematical modelling of flow in start pool

The main aim of the training course is to provide basic training, as well as a warm up area for the athletes during Olympic Games. Post-Games use (following IOC and ICF recommendations) will include basic instruction and training of novices and young athletes. For these purposes, the whitewater difficulty is only Grade II-III. The results from the physical modelling showed could be possible to decrease channel flow to $9.5 \text{ m}^3/\text{s}$ yet retain a similar sport difficulty and character of whitewater. This can lead to decreased pumping demands and reduced operating costs.

The training course was also divided into several sections: starting pool, 5 sections and finish pool (feeding lake). Section 3 – “wave section” was established by a series of submerged bottom obstacles which form stable waves in the middle of the channel. Such waves are useable for basic training of canoeists. The end of this section has obstacles adjacent to both banks, causing strong flow leading into the next section. Maximum velocities here are 1.5 m/s and depth is sufficient.

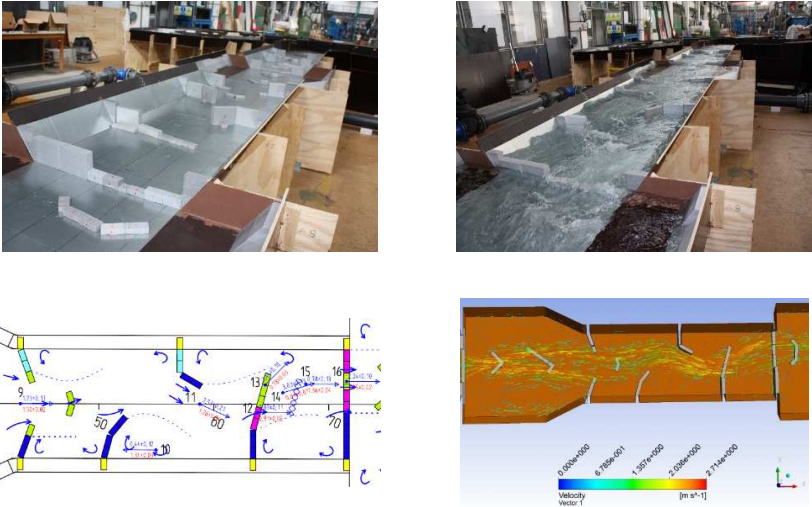


Fig. 8 Asymmetric section No. 4 without and with water, map of obstacle distribution (each colour represents a different size obstacle); mathematical modelling of flow

Where future users of the training course are concerned, the model showed areas of high velocities near the feeding lake. The 1.5 m/s velocities might be excessive for navigation by novices, so additional submerged obstacles were placed in the model channel to further restrict flow. This decreased velocities to lower than 1 m/s.

6. CONCLUSIONS

Physical and mathematical modelling of the competition and training courses for canoe slalom events in the 2016 Olympic Games in Rio de Janeiro was carried out within 5 weeks. The models in linear 1:13 scale fully addressed the main objectives: prepare a map of obstacles distribution and establish suitable whitewater characteristics according to IOC and ICF requirements. A moveable obstacle system will allow creation of all necessary hydraulic features, critical for good quality competition and safe recreation. The model demonstrated hydraulic features which can be stable while minimizing water level surging or other inconsistencies. Hydraulic model investigation results also support future collaboration between course designers, the IOC, the ICF and host organizers of the Games in attempting to minimize construction and operation costs (see Table 2– comparison with previous Olympic facilities) and the risks associated with future projects:

Tab. 2 Possible savings in construction of Olympic Games white water facilities

	Sydney 2000	London 2012	Rio 2016	Savings Sydney/Rio
Discharge	14 m ³ /s	15 m ³ /s	12 m ³ /s	15 %
Head	5.5 m	5.5 m	4.5 m	18 %
Length	320 m	300 m	280 m	13 %
Width	12 m	10 m	9.5 m	21 %

7. REFERENCES

- BÉMOVÁ I., POLLERT, J. 1996: Návrhové charakteristiky umělých drah pro vodní slalom. (Design characteristics for slalom artificial courses), In Czech, Stavební obzor, roč.5, č.1, str. 18-21, ISSN 1210-4027, Praha 1996
- CHANSON, H. 2004: The Hydraulics of Open Channel Flow: An Introduction. Elsevier Publishing, ISBN 0 7506 5978 5, 2004
- POLLERT, J. 2001: Vodní stavitelství a Olympijské hry v Sydney 2000 - Penrith Whitewater Stadium. (Water structures and Olympic Games 2000 - Penrith Whitewater Stadium), In Czech, -In: Vodní hospodářství. 2001, roč. 51, č. 4, s. 90-91. ISSN 1211-0760.
- STREETTER, V.L. 1964: Handbook of Fluid Dynamics. First Edition Mc Graw-Hill Book Company, Inc. , 1964
- STREETTER, V.L., WYLIE, E.B., BEDFORD, K.W. 1998: Fluid Dynamics. Nith Edition, Mc Graw-Hill Book Company, Inc, ISBN 0 07 062537 9, 1998

Acknowledgement

This works was supported by the Student grant Foundation SGS13/173/OHK1/3T/11 and TAČR TE02000077 Smart Regions – Buildings and Settlements Information Modelling, Technology and Infrastructure for sustainable Development.

Calculating erosion rates of river bank sediment by combining field measurements of erodibility parameters and small-scale topographic features – A case study at the Danube River

M. Pfemeter, M. Klösch, E.J. Langendoen, H. Habersack

(Christian Doppler Laboratory for Advanced Methods in River Monitoring, Modelling and Engineering; Institute of Water Management, Hydrology and Hydraulic Engineering, Department of Water - Atmosphere - Environment, University of Natural Resources and Life Sciences, Vienna, Muthgasse 18, 1190 Wien, Austria, phone: +431476545507, e-mail: martin.pfemeter@boku.ac.at.)

Abstract

This paper examines the application of a method for calculating fluvial erosion on river banks. In the investigated area the determination of potential erosion rates are essential to estimating the initiated river widening processes and their effect on navigation. A mini-jet device was employed, for in situ measuring of the erodibility of river bank sediments with respect to shear stresses induced through the jet-flow on the bank surface. The obtained data was then used to calculate the parameters of a commonly used excess shear stress equation to compute bank erosion rates, the critical shear stress and the erodibility coefficient, for a variety of Danube sediments. The actual shear stresses on the river banks were calculated according to the method of Kean & Smith (2006a). The method accounts for the effects of eddies in the lee of small scale topographic features in reducing the shear stress acting on the bank surface. This implies an accurate representation of the bank topography as well as its mathematically defined simplification. The law of the wall and the boundary layer theory are the bases for the calculation of the ‘skin drag,’ which is the part of the total shear stress responsible for fluvial erosion and is therefore used in the excess shear stress equation for determining erosion rates. Based on a natural discharge hydrograph potential erosion rates were calculated. While sands reached rates up to 6.5 cm/h, the critical shear stress of some sandy silts (higher than 12 N/m²) where never exceeded. Furthermore, relations between erodibility parameters as well as dependencies of the erodibility on the grain size distribution were found.

Keywords

Fluvial erosion, skin drag, form drag, mini jet test, river restoration

1. INTRODUCTION

In the wide-ranging scientific field of quantifying erosion rates, fluvial erosion of fine sediments still gives rise to many questions. Since fine-grained sediment is influenced by cohesive forces a simple approach based on the balance of gravitational and drag forces only leads to underestimation of the critical shear

stress for mobilization. In addition, the processes determining the rate of erosion above this threshold are different from those of coarse grains. To finally predict actual erosion rates at surfaces that are exposed to fluvial forces, one must be able to calculate the actual shear stress acting on the surface. A simple depth-slope approach for estimating the fluvial shear stress is misleading when topographic features are present, especially along river banks.

In this paper we concentrate on fluvial erosion along riverbanks. Inspired by the physically based model from Darby et al. [2010] we combine a method for calculating the fluvial shear stress with a method for measuring soil erodibility to finally estimate potential erosion rates of cohesive sediment layers. The acting forces are calculated using a model presented by Kean & Smith (2006) like in Darby et al. [2010], while the resisting parameters are derived from tests with the mini jet test apparatus [Simon & Thomas 2010]. This way we were able to directly calculate the erodibility coefficient of the tested sediment, while Darby et al. (2010) used the cohesive strength meter and therefore had to rely on literature values for the erodibility coefficient provided by Hanson and Simon (2001). For calculating the potential erosion rates of the sediment, the excess shear stress equation served as theoretical basis.

2. MATERIAL AND METHODS

The study site was located on a reach of the Danube River near Hainburg (fig. 1).

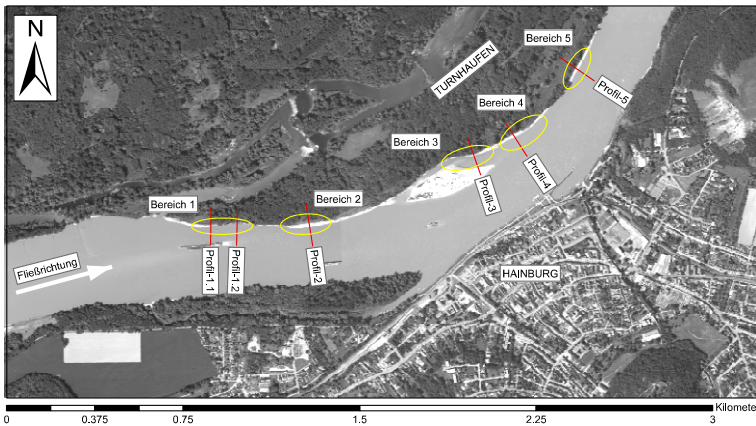


Fig. 1 Location of the study site and the test areas

The Danube's mean annual discharge in this area is 1930 m³/s and the one-year flood reaches 5300 m³/s.

At the five bank sections several sediments were tested using the Mini Jet device. In addition, their grain size distributions were determined. Hand-shoveled

pits at the bank face allowed determining the layering of the river bank and assigning erodibility parameters to layers that were not tested (e.g. layers that were too thin to produce an appropriate scour for test evaluation).

For the determination of the actual shear stress using the concept of Kean & Smith [2006] the riverbank topography has been recorded via photogrammetric survey. The necessary flow velocities adjacent to the bank were derived from simulations made by Liedermann et al. [2013] using the model RSim3d [Tritthart, 2005].

2.1 Measuring sediment erodibility parameters

The deployed Mini Jet test Apparatus is a smaller version of the original Jet tester by Hanson & Cook [2004]. Its advantages are mainly in its size making it more portable, nonetheless its results are comparable to the original one [Al-Madhhachi, et al. 2013].

Theoretical base of the test is the calculation of the erosion rate (ε_r , m s^{-1}) by the use of the excess shear stress equation (equation 1, [Smerdon & Beasley, 1961; Temple & Hanson, 1994]).

$$\varepsilon_r = k_d (\tau - \tau_c)^a \quad (1)$$

where τ [Pa] describes the exerted boundary shear stress, τ_c [Pa] denotes the critical shear stress or erosion threshold, and k_d represents the progress of the erosion that is called the erodibility coefficient [$\text{m s}^{-1} \text{Pa}^{-1}$]. The coefficient a is usually assumed to be 1 [Hanson, 1990; Hanson and Cook, 1997].

During the jet test procedure a submerged circular water jet impinges on the sediment surface. The jet obtains its energy from an overflow tank which delivers constant pressure to the jet. The resulting scour increases in depth until the critical shear stress between the diverted jet and the sediment surface is reached.

Based on the findings of Beltaos and Rajaratnum [1974], Poreh and Cermak [1959] and Hanson [1990] the shear stress along the surface could be calculated via equation 2 and 3.

$$\tau_0 = C_f \rho U^2 \quad H < H_p \quad (2)$$

$$\tau_0 = C_f \rho \left(C_d U_0 \frac{d_0}{H} \right)^2 \quad H > H_p \quad (3)$$

where τ_0 is maximum stress on the surface, C_f is the coefficient of friction (0.00416), ρ is the fluid density, U_0 is velocity at the jet nozzle, C_d is diffusion constant (6.3), d_0 is nozzle diameter, H is scour depth, and H_p is length of the jets potential core. In order to obtain the erosion parameters, the data points from the test are fitted to the time-scour depth function from Hanson (1997) based on the work of Stein et al. [1993] investigating free overfalls (equation 4).

$$t_m = T_r \left[0.5 \ln \left(\frac{1+J^*}{1-J^*} \right) - J^* - 0.5 \ln \left(\frac{1+J_i^*}{1-J_i^*} \right) + J_i^* \right] \quad (4)$$

where t_m is the measured time, $T_r = J_e/(k_d \tau_c)$ is the dimensionless time, $J^*=J/J_e$ is the dimensionless scour depth, J is the scour depth, J_i is the initial scour depth, and the equilibrium depth J_e is reached only after a long time past the duration of the test (Blaisdell encountered continued scouring near pipe outlets even after 14 months). Blaisdell et al. [1981] approximated J_e by describing the evolution of scour depth by a logarithmic hyperbolic function in equation 5.

$$(f - f_0)^2 - x^2 = A^2 \quad (5)$$

The parameter f_0 is linked to the equilibrium depth via equation 8. By iteratively varying A and f_0 an optimal value for J_e can be obtained via a least square fitting of the data points presented through equation 6 and 7.

$$f = \log \frac{J}{d_0} - \log \frac{U_0 t}{d_0}, \quad x = \log \frac{U_0 t}{d_0}, \quad f_0 = \log \frac{J_e}{d_0} \quad (6,7,8)$$

where t is time. Hanson and Cook [1997] presented two methods to determine the critical shear stress and the erodibility coefficient. Method 1 varies k_d and τ_c in equation 4 to obtain a best fit to the data points, however this leads to multiple answers. In Method 2 τ_c is calculated with the Blaisdell solution involving equation 5 to 8 and fitting the data points to the function of equation 4 only by varying k_d . Both Methods are used in this Study and are referred to as “iterative” for Method 1 and “Blaisdell” for Method 2.

2.2 Calculating actual shear stresses

In order to determine the effect of topographic roughness elements on the flow along the river bank, Kean & Smith [2009] adopted the model of Smith & McLean (1977) concerning spatially averaged flow over a wavy surface. partitioning the total shear stress on a boundary τ_T into a “skin friction” τ_{SF} and “drag” τ_D part:

$$\tau_T = \tau_{SF} + \tau_D \quad (9)$$

While the drag part acts on the topographic elements, the skin friction is responsible for fluvial erosion and thus of interest in this paper. They found, that the shape of a topographic element could be described mathematically through a Gaussian curve. The influence of Gaussian shaped features on the flow was investigated by Hopson [1999]. For determining the drag coefficient C_D , using the parameters of a Gaussian curve he derived:

$$C_D = 1.79 \exp \left(-0.77 \frac{\sigma}{H_G} \right) \quad (10)$$

where σ is the standard deviation and H_G the height of a Gaussian shaped feature. The drag related shear stress is given by:

$$\tau_D = \frac{1}{2} \rho C_D \frac{H_G}{\lambda} u_{ref}^2 \quad (11)$$

where λ is the distance between two features and u_{ref} is the reference velocity. The flow field in the lee of a Gaussian shaped feature can be separated into a turbulent internal boundary layer, a wake region which is modeled by using Schlichting's far field wake solution [Schlichting, 1979], and a logarithmic outer boundary layer. The intersection of the velocity profiles of these three layers at the layer boundaries give the velocity profile u as a function of z . The reference velocity u_{ref} then is the average velocity in the area A of a topographic feature that would arise in the absence of the feature and can be calculated by:

$$u_{ref}^2 = \frac{1}{A} \int_A u^2(x, z) dA \quad (12)$$

For closing the solution either the total shear stress or a velocity in the outer region has to be known. While on river beds τ_T could be derived from the depth slope product, on river banks a flow velocity is more appropriate. In our study this velocity is calculated via a numerical model RSim3d [Liedermann et al., 2013; Tritthart, 2005]. By expressing the spatial averaged skin friction stress in the internal boundary layer (IBL) as $\langle \tau_{IBL} \rangle = \rho \langle u_{*IBL} \rangle^2$, where u_* is shear velocity, the total shear stress is written as

$$\tau_T = \rho \left(\alpha_0 \langle u_{*IBL} \rangle^2 \right) + \frac{1}{2} \rho C_D \frac{H}{\lambda} u_{ref}^2 \quad (13)$$

In these calculations the ratio $\alpha_0 = u_{*SF} / \langle u_{*IBL} \rangle$ is taken to be one, the logarithmic velocity profile of the outer region is defined as

$$u = \frac{u_{*T}}{\kappa} \ln \left(\frac{z}{z_{0f}} \right) \quad (14)$$

and the spatial averaged skin friction based shear velocity is

$$\langle u_{*IBL} \rangle = \alpha_1 u_b \quad (15)$$

The coefficient α_1 depends on the shape of the topographic features and the height of the flow region boundaries.

Due to the natural variety of topographic features and the computational complications that arise from this heterogeneity, Kean & Smith [2006b] developed a statistical method to identify a regular sequence of one characteristic Gaussian shaped feature, characterized by the height H_{reg} , the standard deviation σ_{reg} and the wavelength λ_{reg} , which represents the irregular sequence found in the field.

The parameters of this characteristic topographic element can be calculated by:

$$H_{reg} = \exp(\mu_H + 1.2 \cdot v_H) = H_{88} \quad (16)$$

$$\sigma_{reg} = \exp(\mu_\sigma + 1.2 \cdot v_\sigma) = \sigma_{88} \quad (17)$$

$$\lambda_{reg} = 6H_{88} \quad (18)$$

H_{88} and σ_{88} are the 88th percentile of the normal distributed topographic feature parameters shown in figure 2 and can be calculated via the mean value μ and the standard deviation v of the the size distribution. The river bank topography in the area of investigation was recorded using terrestrial photogrammetry. From the obtained point clouds with a resolution of about 0.5 cm, horizontal cross sections along the bank in regular, vertical intervals of 0.25 m were extracted. Large-scale shapes with much bigger wavelengths than the investigated topographic features, like the channel curvature, were removed. Gaussian curves were fitted to the remaining graphs and their parameters were noted. After a statistical analysis of the data the representative Gaussian shaped feature was defined using equations 16 to 17.

2.3 Predicting erosion rates

The potential erosion rates of sediment layers were calculated for two riverbank sections which were exposed to a natural hydrograph of the Danube River from 2009. Based on the three-dimensional hydrodynamic-numerical model established by Liedermann et al. [2013] discharge-flow velocity curves were created for the two investigated riverbank sections. The points were placed in a distance of 10 m and 10.4 m from the bank, which – according to the model of Kean & Smith [2006a] – is in the outer sub layer of the flow velocity distribution. The hydrograph was then converted into a flow velocity time series for each bank section. Subsequently, the skin friction along both banks was estimated for the year 2009 using the equations of section 2.2. Finally, the erosion rates were calculated via equation 1.

3. RESULTS

The parameters computed from the results of the mini jet tests are listed in Table 1. The results show that with increasing grain size, k_d increases while τ_c decreases. This decrease of erodibility is probably related to the higher clay content in fine-grained sediment. The Blaisdell method was shown to generally produce smaller critical shear stresses than the iterative method. The highest values of k_d are reached by sediment number 0312-1, a low cohesive sand with 198.26 cm/sPa calculated with method 1 and 475.45 cm/sPa with method 2 and a τ_c of 0.8 Pa and 2.13 Pa respectively. Silty sediments show values of k_d down to 1.02 cm/sPa and τ_c up to 82 Pa computed by Method 2, and similar results in method 1.

Tab. 1 Results of the jet tests (i_n indicates the number of measured scour depths during one test)

Test	i_n^*	pressure head [m]	Blaisdell		iterative		Soil parameters			
			τ_c [Pa]	k_d [cm/sPa]	τ_c [Pa]	k_d [cm/sPa]	Texture	sand [%]	silt [%]	clay [%]
2611-1	15	1.27	1.14	7.41	3.64	23.74	S	72.6	26.9	0.5
0312-1	8	0.63	0.80	198.26	2.13	475.45	S	96.8	2.6	0.6
0312-2	15	0.58	0.34	53.34	2.01	187.95	S	96.8	2.6	0.6
1411-8	8	2.185	11.78	4.71	20.03	27.30	S	77.0	21.6	1.4
0312-3	12	3.59	28.59	1.01	37.21	11.15	S	80.1	18.4	1.5
2611-2	23	1.20	0.68	24.50	4.18	16.03	S	70.1	28.2	1.7
1411-7	7	1.13	8.10	3.34	12.84	11.90	S	75.0	23.0	2.0
1111-5	11	0.99	0.50	8.69	3.61	16.83	uS	52.8	42.9	4.3
1411-6	8	1.13	5.29	2.59	13.33	19.87	SU	49.6	45.8	4.6
0312-4	5	6.62	61.86	0.16	82.13	1.02	SU	43.3	51.8	4.9
1111-1	10	2.535	17.85	0.87	15.13	2.80	SU	45.9	46.5	7.6
1411-9	9	4.505	21.87	1.67	29.30	9.23	SU	n.a.	n.a.	n.a.
2711-3	9	2.39	11.26	1.29	22.06	12.71	sU	21.9	72.9	5.2
2711-4	13	4.22	4.65	0.48	19.54	1.55	sU	27.1	66.5	6.4
2711-5	15	4.65	0.42	1.82	7.76	4.50	sU	28.8	64.7	6.5
1111-3	5	3.52	37.66	0.47	46.55	6.61	sU	30.8	60.3	8.9

Across the studied bank section sites 3272 Gaussian shaped features were analyzed. Based on the 88th percentiles off all features a representative feature with an H_{rep} of 55.5 cm a σ_{rep} of 116.2 cm and a λ_{rep} of 332.9 cm was defined.

Figure 2 shows the parameter deviation of the located topographic elements. The combination of the computed topographic parameters and the hydrograph based flow velocities allowed producing time-series of total- and skin friction shear stresses for the year of 2009 (Figure 3.a). In figure 3,b the computed potential erosion rates for two sediments are presented. The non-continuous behavior of shear stresses in figure 3,a is caused by the fact that the investigated sediments are not submerged for some periods in a year. Sediment no. 11 represents a highly erodible sand, while sediment no. 14 consists of a more cohesive sandy silt. The highest skin friction based shear stresses occurred during a summer flood with 9.6 Pa while the total shear stress reached 25.9 Pa. These shear stresses lead to erosion rates up to 0.3 m/h in the sand. In the sandy silt, the erosion rate is – with 0.03 m/h – an order of magnitude smaller. According to the calculations, the sandy silt was subject to erosion only during the summer flood. Besides these two examples,

Table 1 presents seven sediments whose critical shear stresses were not exceeded at all and thus should not have been subject to fluvial erosion.

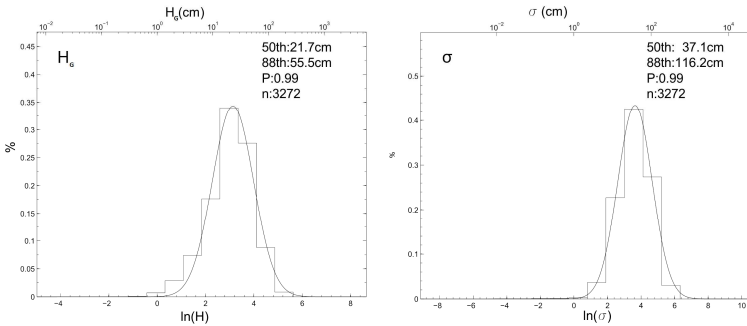


Fig. 2 Deviations of Gaussian shaped features

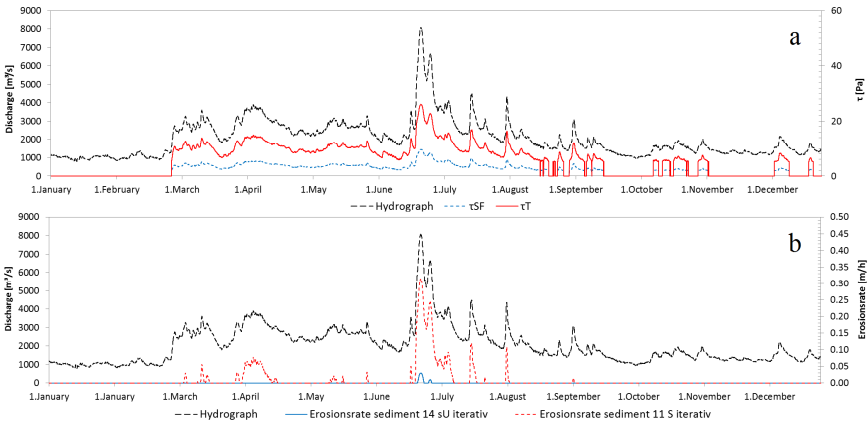


Fig. 3 Shear stresses (a) and erosion rates (b) in the tested area

4. DISCUSSION

Caution has to be taken when trying to estimate bank retreat rates from fluvial erosion rates, as performed by Darby et al. [2010]. It is recommended to additionally account for effects like oversteepening and subsequent mass failure, as well as the role of slump material in temporarily protecting the bank from undercutting. One may account for these effects by fully coupling fluvial erosion and mass failure, as it was implemented in the bank erosion module of the computer model CONCEPTS [Langendoen and Simon, 2008].

The studied bank section consisted of several layers with alternating erodibility, producing cantilevers as well as step-like bank geometries. Hence, for calculating retreat rates of the investigated bank sections, interactions between sediment layers through mass failure and interactions via the flow field are

important to be considered. Less erodible sediment layers may protrude into the channel (by forming cantilevers and/or steps) and reduce the shear stresses along the adjacent sediment layers (e.g. below the cantilever). Three-dimensional effects of topographic elements on the flow velocity distribution may be significant for the investigated bank, given features of small vertical extent.

5. CONCLUSIONS

A distinction between form and skin drag is essential in predicting erosion rates of surfaces with small scaled topographic features. Neglecting leads to substantial overestimation of erosion rates and their impact. The mini jet test apparatus proved to be a practical device for estimating the erodibility parameters.

6. REFERENCES

- AL-MADHHACHI, A. T., G. J. HANSON, G. A. FOX, A. K. TYAGI, R. BULUT, 2013. Measuring soil erodibility using a laboratory “mini” jet. *2013 American Society of Agricultural and Biological Engineers*, Vol. 56(3), 901-910
- BELTAOS, S. & N. RAJARATNAM, 1974. Impinging circular turbulent jets. *Journal of the Hydraulics Division*, 100, HY10, 1313-1328.
- BLAISDELL, F. W., G. G. HEBAUS & C. L. ANDERSON, 1981. Ultimate dimensions of local scour. *Journal of the Hydraulics Division*, ASCE, 107, HY3, 327-337.
- DARBY, S. E., H. Q. TRIEU, P. A. CARLING, J. SARKKULA, J. KOPONEN, M. KUMMU, I. CONLAN & J. LEYLAND, 2010. A physically based model to predict hydraulic erosion of fine grained riverbanks: The role of form roughness in limiting erosion. *Journal of Geophysical Research: Earth Surface* (2003–2012), 115, F4.
- HANSON, G., 1990a. Surface erodibility of earthen channels at high stresses. Part I-open channel testing. *Transactions of the ASAE*, 33, 1, 127-131.
- HANSON, G. J. & K. R. COOK, 1997. Development of excess shear stress parameters for circular jet testing. *ASAE Annual International Meeting*. Minneapolis, Minnesota: ASAE, 972227.
- HANSON, G. & A. SIMON, 2001. Erodibility of cohesive streambeds in the loess area of the midwestern USA. *Hydrological Processes*, 15, 1, 23-38.
- HANSON, G. & K. COOK, 2004. Apparatus, test procedures, and analytical methods to measure soil erodibility in situ. *Applied engineering in agriculture*, 20, 4, 455-462.
- HOPSON, T. M., 1999. The form drag of large natural vegetation along the banks of open channels. Boulder: University of Colorado, M. S. , 114.
- KEAN, J. W. & J. D. SMITH, 2006a. Form drag in rivers due to small scale natural topographic features: 1. Regular sequences. *Journal of Geophysical Research: Earth Surface* (2003–2012), 111, doi: 10.1029/2006JF000467.

- KEAN, J. W. & J. D. SMITH, 2006b. Form drag in rivers due to small scale natural topographic features: 2. Irregular sequences. *Journal of Geophysical Research: Earth Surface* (2003–2012), 111, doi: 10.1029/2006JF000490.
- LANGENDOEN, E.J & A. SIMON, 2008. Modeling the Evolution of Incised Streams. II: Streambank Erosion. *Journal of Hydraulic Engineering*, ASCE, 134, 905-915.
- LIEDERMANN, M., M. TRITTHART & H. HABERSACK, 2013. Particle path characteristics at the large gravel bed river Danube: results from a tracer study and numerical modelling. *Earth Surface Processes and Landforms*, 38, 5, 512-522.
- POREH, M. & J. E. CERMAK, 1995. Flow Characteristics of a Circular Submerged Jet Impinging Normally on a smooth Boundry. *Proceedings of the Sixth Midwest Conference on Fluid Mechanics*. University of Texas, Austin, 198-212.
- SCHLICHTING, H. & K. GERSTEN, 1979. Boundary-layer theory. McGraw-Hill, New York.
- SIMON, A. & R. THOMAS, 2010. Comparison and experiences with field techniques to measure critical shear stress and erodibility of cohesive deposits. *2nd Joint Federal Interagency Conference*. Las Vegas, Nevada.
- SMERDON, E. T. & B. R. P, 1961. Critical tractive forces in cohesive soils. *Agricultural Engineering*, 42, 1, 26-29.
- SMITH, J. D. & S. MCLEAN, 1977. Spatially averaged flow over a wavy surface. *Journal of Geophysical research*, 82, 12, 1735-1746.
- STEIN, O., P. JULIEN & C. ALONSO, 1993. Mechanics of jet scour downstream of a headcut. *Journal of Hydraulic Research*, 31, 6, 723-738.
- TEMPLE, D. & G. HANSON, 1994. Headcut development in vegetated earth spillways. *Applied Engineering in Agriculture*, 10, 5, 677-682.
- TRITTHART, M. (2005). Three-dimensional numerical modelling of turbulent river flow using polyhedral finite volumes. *Wiener Mitteilungen Wasser-Abwasser-Gewässer* 193, 1–179. Vienna University of Technology, Austria.

Acknowledgement

The financial support from the Federal Ministry of Economy, Family and Youth and the National Foundation for Research, Technology and Development is gratefully acknowledged, as well as the financial support of via donau. We would also like to thank the „Nationalpark Donau-Auen“ for the support and the permission to perform tests in the area. Finally we thank the Institute of Hydraulics and Rural Water Management for performing the grain size distribution analyses.

Modelling of open channel flow with FLOW-3D

D. Duchan, T. Julinek

Brno University of Technology, Faculty of Civil Engineering, Institute of Water Structures, Veveří 95,
602 00 Brno, E-mail: julinek.t@fce.vutbr.cz, duchan.d@fce.vutbr.cz

Abstract

The paper deal with application of FLOW-3D software for the simulation of flow in open channel. The simulated results were compared with values measured on laboratory model of channel bend. Simulation was carried out for several turbulent models. The verification of the model was based on simulation of three different flow scenarios. The verified model was applied for simulation of natural channel flow.

Keywords

CFD, open channel flow, Flow-3D, turbulent model

1. INTRODUCTION

Most rivers of open channels without any regulation or human intervention have the tendency to develop winding course of their channel. This cross-sectional pattern of the flow governs processes of erosion and sedimentation and therefore reshaping of the meander.

Presently available CFD tools involve numerous uncertainties. The paper deals with computational problems of an open channel flow. The results physical modelling of the river bend were used in order to get accurate description of the modelled area. This also offered data on the hydraulic phenomena.

Due to centrifugal forces in the natural winding channels the transversal flow is developed. It is important to notice that the transversal flow is developing from the start of the bend and after the end of the bend is progressively fading. It is generally assumed that the streamwise velocities are the highest in the outer half of the bend. This process has important consequences for the morphology of the river bed in the bends.

Application of the 3D CFD model in natural open channel flow evaluation is assumed to be helping tool for design of proposed specific measure to retain floating flood debris. In the first step the validation of CFD model was done based on the data measured in laboratory [Výbora 1980].

2. MODEL DESCRIPTION

For the simulation of the turbulent flow of water, a wide variety of approaches is available. Different techniques incorporate different extent of parameterizations incorporated. Numerical techniques usually rely on the equations of Navier-Stokes

(direct methods) or Reynolds (statistical approach). These equations form the basis of the model. The models are described in numerous publications. [Wilcox 1992, Flowscience 2010]

The software tool Flow-3D for three dimensional computations was used in the study. The geometry of the modelled area was set up according to physical model [Výbora 1980] in the scale 1:1. The solution was done with application of three different turbulent models in order to assess their sufficiency for the solved task.

2.1 Turbulence model

As long as the flow cannot be considered as laminar in the bend, the correct definition of turbulent models is essential. The numerical model was set up in FLOW-3D, which offers five turbulent models. These are the one-equation turbulence transport model, the Prandtl mixing length model, the two-equation model (k- ϵ), RNG model and a large eddy simulation model (LES).

For the simulation of the channel flow three models were applied:

- two equation k- ϵ model consists of two transport equations for the turbulent kinetic energy and its dissipation described in detail for example in [Kolmogorov 1942, Wilcox 1992],
- RNG model applies statistical approach to solution of equations for turbulent kinetic energy and its dissipation rate. The RNG model explicitly derives the equation constants that are empirically defined in the standard k- ϵ model [Yakhot et al. 1992],
- LES allows direct compute of turbulent flow structures that can be resolved by the computational grid and only approximate those features that are too small to be resolved by using a subgrid-scale model [Smagorinsky 1963].

Further description of governing equations of the turbulent models used within the software tool FLOW-3D can be found in [Flowscience 2010].

2.2 Boundary condition

The river bed and banks are treated as solid walls with the predefined roughness. As long as the physical model was constructed with uniform roughness the roughness coefficient was specified as uniform as well.

The boundary conditions in streamwise direction were defined with steady hydraulic parameter. At the outflow boundary a standard convective outflow boundary condition was applied.

The boundary at the side of free surface was treated as a horizontal, impermeable rigid lid at upper boundary of the model domain. As long as the gradient of the water surface was small enough, such a type of boundary is applicable (see chap. 3.1).

2.3 Initial conditions

Initial conditions was defined as state at time $t = 0$ with reasonable accuracy (e.g. horizontal water level). This is due to that the effect of inaccuracy in initial

condition is reduced with time progresses. The initial conditions for the purposes of solved model were defined at a global scale.

3. PARAMETER STUDY

The study was done in laboratory on trapezoidal profile of the channel with bottom width of 0.40 meters and slope of the banks 1:2. Channel was composed of three parts:

- straight inlet reach with length 6.85 m;
- channel bend with radius 3.00 meters and internal angle of 90 degrees;
- straight outlet reach with length 4.60 m.

The slope of the channel was 0.1% (see Fig. 1). The physical model of the channel bed and walls was made of wooden boards with very smooth varnished surface.

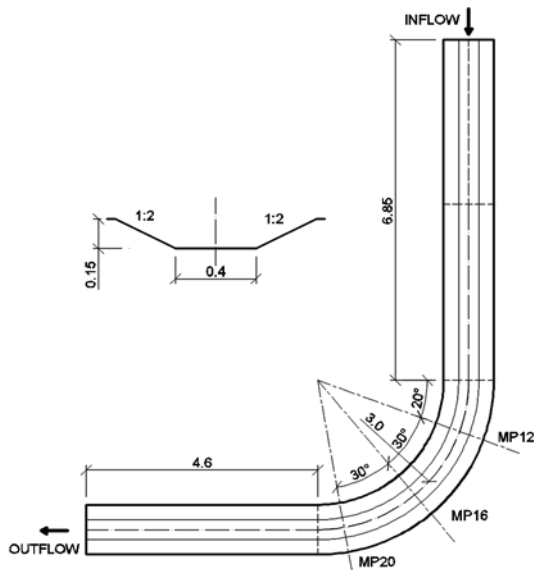


Fig. 1 Model situation

Laboratory measurements were performed on the above described model with two different surface roughness and three different flow rates. The roughness of the varnished boards representing the channel surface was according Maning $n = 0.0093$. Afterwards, sand grains with diameter $d = 1.0$ mm were glued to the surface, which modified surface roughness to $n = 0.0129$. Uniform steady flow regime was simulated on the model for all modelled scenarios. In selected measured profiles (MP), which were marked as MP 12, MP 16, MP 20, the hydraulic parameters (water depth h and point velocities in verticals v) were measured.

3.1 Pre-processing

The representation of the modelled channel bend for the numerical simulation was created as 3D model with geometry of laboratory model. First, wireframe was created using Autodesk Autocad. Created wireframe was imported into the program Blender, where the final 3D model of the channel was created (Fig. 2) in stereolithographic format *.stl.

The next step was import of 3D model to FLOW-3D. The applied computational grid consisted of cubic elements with resolution 0.0075 to 0.01 m. In case of lower flow rate the computational mesh was generated with smaller elements with resolution of 0.0075 m.

Computational grid consisted of 3 blocks that described inflow, curve and outflow. The number of cells in all blocks was about 3.8 million.

Boundary conditions in Flow-3D was set for 3 blocks as follows (Fig .2):

- The bottom of the computational grid for all blocks was defined by embedded 3D model, which created a solid surface (wall);
- The upper part of the computational grid for all blocks has been set to “symmetry” [Flowsience 2011];
- Inflow and outflow in the model was set up to hold the whole time calculation constant level corresponding to the uniform steady flow for a given geometry, the inclination, surface roughness and discharge.

The initial condition of simulation has been set a horizontal surface at depths predicted at the outflow of the model.

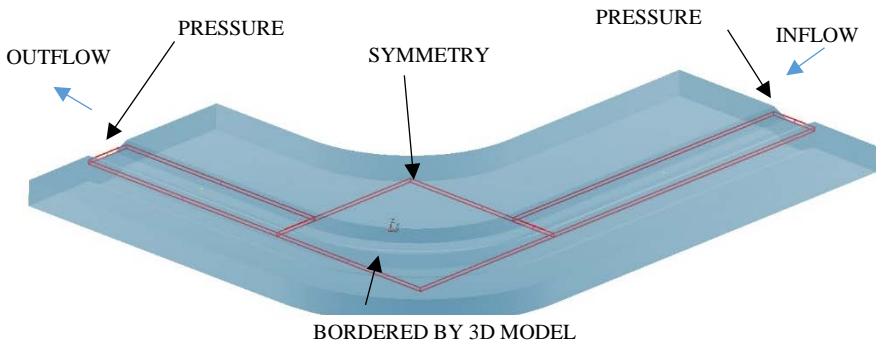


Fig. 2 Boundary condition of model (red lines are boundary of blocks)

3.2 Simulation

Numerical simulations were performed for the roughness $n = 0.0093$ for three different discharges in the program FLOW-3D. For each flow scenario with lower roughness three mentioned different turbulent models were applied. All computed scenarios of numerical simulation are shown in Tab. 1.

Tab. 1 Scenarios of numerical simulation

Scenario	Discharge Q [l/s]	Applied turbulent model
11A	5.0	Two equation k- ϵ model
11B	5.0	RNG model
11C	5.0	LES model
21A	15.0	Two equation k- ϵ model
21B	15.0	RNG model
21C	15.0	LES model
31A	37.0	Two equation k- ϵ model
31B	37.0	RNG model
31C	37.0	LES model

The simulation time for each scenario was chosen 200 s in order to get state of steady flow. Computer time for one simulation was approximately 3 days (CPU with 6 cores, 32 GB RAM).

3.3 Results

The comparison of measured and computed velocity field in selected cross section profiles was done for each flow scenario and for each turbulent model (Fig. 4 and 5). Longitudinal, transversal and depth-averaged velocity vectors were compared to measured ones. Longitudinal and transversal velocity was computed from angle of cross section and velocity vectors v_x , v_y and v_z . Velocity v_z was very small in comparison with velocities v_x , v_y . Depth-averaged velocities were computed by FLOW-3D. For physical model velocity measuring the anemometer and Prandtl probe was used [Výbora 1980]. The accuracy of used devices depends on the calibration, however the comparison of obtained values by each device showed good accordance.

Accuracy of the used turbulent model was derived by comparison of the measured and calculated values. Two equation k- ϵ and RNG turbulent models fitted better the results of physical modelling. The average difference of measured and calculated values of averaged depth velocity was up to 15.0%.

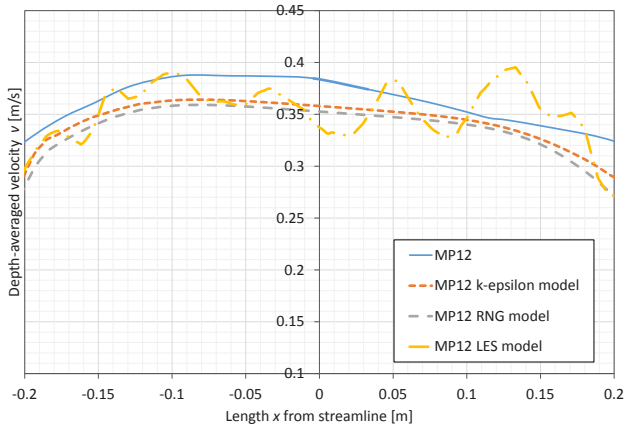


Fig. 3 Comparison of velocity field in profile MP12, $Q = 5$ l/s

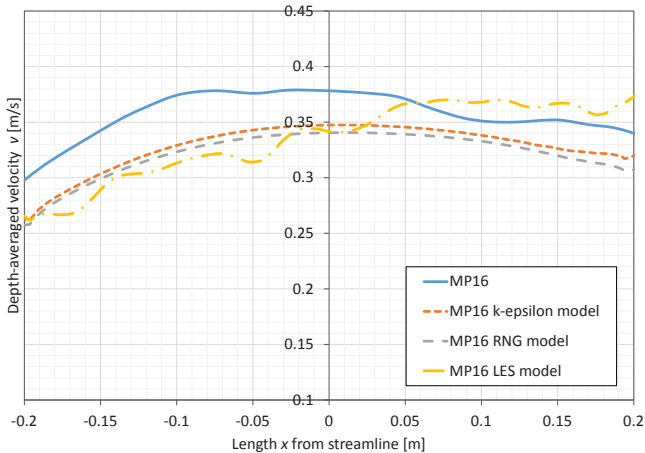


Fig. 4 Comparison of velocity field in profile MP16, $Q = 5$ l/s

The comparison of total discharges used at laboratory model and these obtained from numerical model is shown in table 2. The difference between measured and calculated values is about 10% for the lower discharges. With increasing discharge the differences between measured and calculated values rises up to 23 % (fig. 3 and 4).

Calculated water depths in selected profiles differed with the measured values by less than 4%. The difference increased close to concave bank of the channel bend. For lower discharges the measured values did not describe the slope of the water level in the bend (see fig.5).

Tab. 2 Comparison of discharge rate in measured profiles

Variant	Q from laboratory model [m ³ /s]	Q from numerical model [m ³ /s]	Diff. [%]
11A	5.00E-03	4.52E-03	9.58
11B	5.00E-03	4.43E-03	11.43
11C	5.00E-03	4.59E-03	8.13
21A	1.50E-02	1.33E-02	11.60
21B	1.50E-02	1.27E-02	15.47
21C	1.50E-02	1.32E-02	12.18
31A	3.70E-02	2.84E-02	23.24
31B	3.70E-02	2.97E-02	19.77
31C	3.70E-02	2.87E-02	22.51

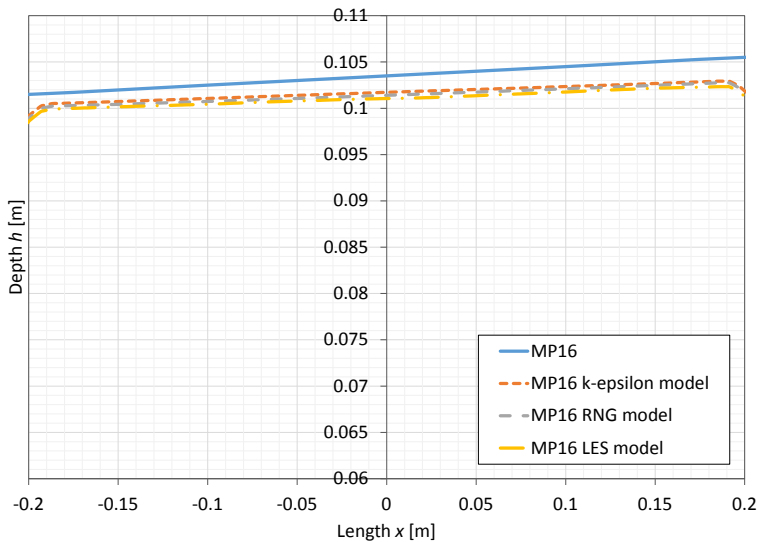


Fig. 5 Comparison of water depth in profile MP16, $Q = 37$ l/s

4. CONCLUSIONS

From the laboratory measurements the velocity fields and water levels were available for the measured profiles. The numerical simulations provided water levels, water depth and velocity vectors in specified profiles in the channel. The results obtained from numerical simulations and laboratory measurements were compared in order to assess the applicability of different turbulent models for the tasks of 3D simulation of open channel flow.

With specified boundary conditions similar resulting hydraulic parameters of the numerical solution and laboratory measurements were obtained. For this reason, the boundary conditions were used in the form of known pressures.

Differences were found in the flow rates of the order of 10-20 %. Water depths in the numerical simulations at the same conditions (slope, geometry, surface, roughness) were on about 4 %.

The accuracy of the CFD model and selected turbulent model was done by comparing the resulting values of three different turbulent models with results of laboratory research. The resulting average difference was 15 %. This value corresponds to average computed value of velocity in MP20 compared to the physical model. Regarding the depth h or surface level some values specified in physical research are arguable. However the lowest value of difference between calculated and measured value were obtained for water level 4.2 %. In this case the correlation between physical and mathematical research is acceptable also when taking into the consideration the precision ± 1 mm in measurement of the water level with applied equipment.

Considering the comparison of the simulations with different turbulence models and physical model measurements, the k- ϵ and RNG turbulence model appeared to be more accurate than the LES model for the task of open winding channel flow. The significant influence has the definition of computational grid and boundary conditions.

5. REFERENCES

- FLOWSCIENCE, INC. 2011. Flow 3D v10 User's manual. Santa Fe : Flow Science Inc, 2011.
- KOLMOGOROV, A.N. 1942. Equations of turbulent motion of an incompressible field, *Izv. Akad. Nauk SSSR, Seria fizicheska* VI. 1942, pp. 55-58. Original in Russian language.
- ŘÍHA, J. 2010. Flood levees. Grada Publishing. 223 p. ISBN 978-80-247-3570-2.
- SMAGORINSKY, J. 1963 General circulation experiments with the primitive equations. 1. The basic experiment. *Mon. Weather Rev.* 91, 99.
- VÝBORA P. 1980. Struktura proudění v obloucích otevřených koryt s pevným dnem. VUT v Brně, FAST.
- WILCOX, David C. 1998. Turbulence Modeling for CFD. Second edition. Anaheim: DCW Industries, 1998.
- YAKHOT, V., ORSZAG, S.A., THANGAM, S., GATSKI, T.B., SPEZIALE, C.G. 1992. Development of turbulence models for shear flows by a double expansion technique, *Physics of Fluids A*, Vol. 4, No. 7, pp1510-1520.

Acknowledgement

The paper is part of the projects TA-04020670 of the Technology Agency of the Czech Republic and FAST-S-13-2056 of the Internal Foundation Agency of Brno University of Technology.

Quantification of hydrodynamic load on the bridge deck using numerical simulations

M. Špano, A. Dráb

Institute of water structures, Faculty of civil engineering, University of Technology Brno, Veveří 95, 602 00 Brno, Czech republic, phone: +420 541 147 756, fax: +420 541 147 752, e-mail: spano.m@fce.vutbr.cz

Abstract

The article summarises results of research aimed at determination of hydrodynamic load using numerical simulations and their verification on physical model. The practical application was performed on a simple rectangular bridge with adjacent sidewalks. Hydrodynamic load on the bridge deck was separated into three actions. Those are the drag force, lift force, and bedding moment at the centre of gravity of the bridge deck. Hydrodynamic load was expressed via dimensionless resistance coefficients that correspond to combination of the flow properties and determined (measured and calculated) forces. Results of the research show quite good agreement in case of mean value of drag and lift force. In case of bedding moment the agreement was found in absolute value of the moment but not in direction.

Keywords

hydrodynamic load, bridge, drag force, lift force, bedding moment, resistance coefficients.

1. INTRODUCTION

Total action on the bridge deck is represented by a series of loads caused by self weight and by external factors. Those were usually considered as loads caused by traffic, wind, and snow. The experiences from recent floods and especially application of new enhanced standards for bridge proposals made the question of hydrodynamic loads on the bridge deck caused by flooding topical. This is related particularly to the existing bridges situated on small and regional roads and railways where the application of new demands for higher freeboard between the design water level the bridge deck leads to high investments into both the existing bridge construction and connected ways. There are locations where designers have to take the possibility of flooding into account. Mainly in case of bridges that have already been seriously damaged or destroyed by flood and have to be quickly reconstructed there is a current deal to consider relatively cheap alternative of modification of the deck bearing to sustain finite hydrodynamic load. Proposal of flood resistant bridge includes also an adjustment of the embankment construction and slopes by meaning of protection against erosion (both surface and internal) and in relevant cases also protection against impact from floating objects and

clogging of the bridge cross-section. However, this article is focused on determination of hydrodynamic load on bridge deck only.

According to [Boor et al. 1963] the hydrodynamic load is caused by both shear stress along the obstacle surface and by the change of the normal stress (i.e. pressure) along it. For practical purposes the hydrodynamic load is expressed as force acting on the bridge deck. This force is proportional to dynamic pressure of the flow [Boor et al. 1963]. In case of bridge deck the effect of submergence also plays role [Picek et al. 2006]. Hydraulic aspects of bridge flooding focused on the bridge cross-section capacity and flow patterns are introduced and closely discussed in [Picek et al. 2004], [Picek 2006] and [Picek and Havlík 2008].

2. METHODS

For purposes of this study the hydrodynamic force is described by three components expressed with respect to the centre of gravity of the bridge deck. Those are horizontal force F_D (hereinafter the drag force), vertical force F_L (hereinafter the lift force) and the bedding moment M , see Fig. 1.

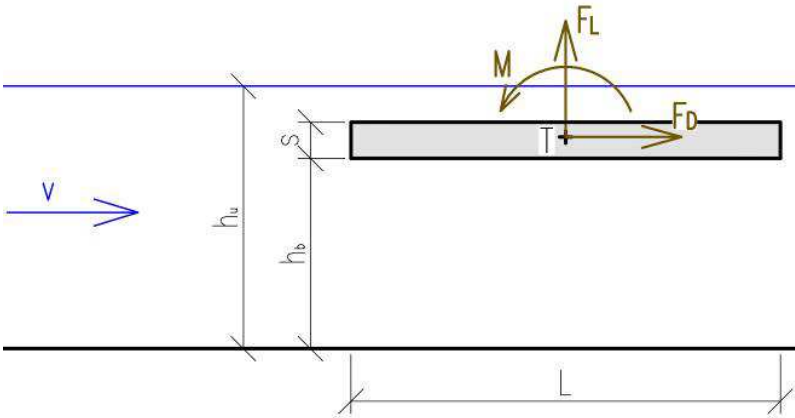


Fig. 1 Scheme of hydrodynamic load with marked convention

The magnitude of each force component is dependent on flow conditions (mainly the depth, density of fluid and velocity), projection of the bridge deck dimensions into the direction of flow and the shape and friction of the bridge deck which is expressed by load coefficients, see [Kerenyi et al. 2009] and [Guo et al. 2010]. Each load coefficient corresponds to specific component of the hydrodynamic force, i.e. drag coefficient corresponds to drag force, lift coefficient corresponds to lift force, and moment coefficient corresponds to bedding moment.

Flow conditions upstream of the bridge are described by two dimensionless characteristics. Those are Froude's number Fr and relative submergence of the bridge deck h^* .

$$Fr = \frac{v}{\sqrt{gh_u}}, \quad (1)$$

$$h^* = \frac{h_u - h_b}{s}, \quad (2)$$

where Fr is Froude's number upstream of the bridge, h^* is relative flooding of the bridge deck, h_u is water depth upstream of the bridge deck, h_b is height of the lower face of the bridge deck above the channel bottom, s is thickness of the bridge deck, v is mean velocity upstream of the bridge.

Components of the hydrodynamic force are expressed as [Kerenyi et al. 2009]:

$$F_D = C_D \frac{1}{2} \rho_w v^2 b s \text{ for } h^* \geq 1 \text{ and } F_D = C_D \frac{1}{2} \rho_w v^2 b (h_u - h_b) \text{ for } h^* < 1, \quad (3)$$

$$F_L = C_L \frac{1}{2} \rho_w v^2 b L, \quad (4)$$

$$M = C_M \frac{1}{2} \rho_w v^2 b L^2, \quad (5)$$

where F_D is drag force, F_L is lift force, M is bedding moment, C_D is drag coefficient, C_L is lift coefficient, C_M is moment coefficient, ρ_w is water density considered as $998,2 \text{ kg.m}^{-3}$, v is mean flow velocity upstream of the bridge, h_u is water depth upstream of the bridge, h_b is distance e between channel bottom and lower face of the bridge deck, s is thickness of the bridge deck, b is length of the bridge, L is width of the bridge deck, h^* is relative flooding of the bridge deck, see equation (5).

The hydrodynamic load was determined using both numerical simulations and measurement on physical model. The comparison of calculated and measured hydrodynamic loads was performed through values of dimensionless load coefficients.

3. PRACTICAL APPLICATION

Practical application was made on a simple rectangular shape of the bridge deck with connected sidewalks which is shown in Fig. 2. The bridge deck is considered as prefabricated and interlocked so the bridge act together with sidewalks as one piece. Relative dimensions of the bridge are summarized within the Tab. 1. Presented shape is typical for smaller bridges on regional ways.

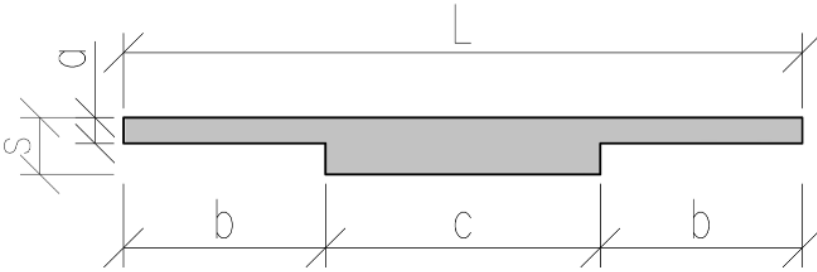


Fig. 2 Cross-section of examined bridge deck

Tab. 1 Proposed relative dimensions of the bridge deck

L/s	c/s	a/s	b/s
11,909	4,818	0,455	4,545

Within this study a small bridge of thickness $s = 0.55$ m and $L = 6.55$ m was assumed (foot bridge capable to sustain passage of medium weight vehicle). A subcritical flow with a Froude number $Fr = 0.22$ was simulated together with three levels of submergence $h^* = \{0.5, 1.0, 2.0\}$. These conditions were chosen as typical for possible flood event combined with representative range of relative submergence h^* .

Numerical simulations were performed with the ANSYS Fluent software. A 2D model of real fluid flow was used together with standard $k-\varepsilon$ model of turbulence and standard wall function. The water level was traced using the volume of fluid method. All model parameters were set up according to recommendations in ser manual [Fluent Inc. 2006]. Closer description of the model is available in [Spano, Stara 2010]. View on basic computational domain is shown in Fig. 3. The hydrodynamic load was calculated by integration of pressure field along the bridge deck while shear force was neglected since the bridge surface is considered as smooth.

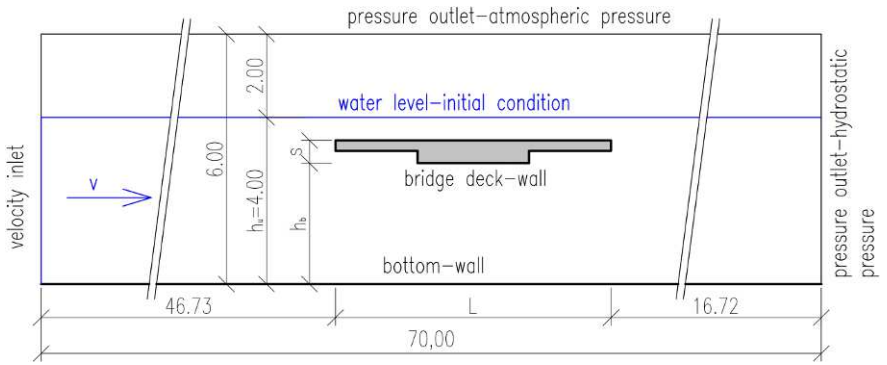


Fig. 3 Computational domain used for numerical simulations

Physical model was built in the testing flume at the Laboratory of hydraulic research. The hydrodynamic load was measured directly by four pressure sensors. Resulting force is considered as time averaged value. The view on the physical model is shown in Fig. 4.

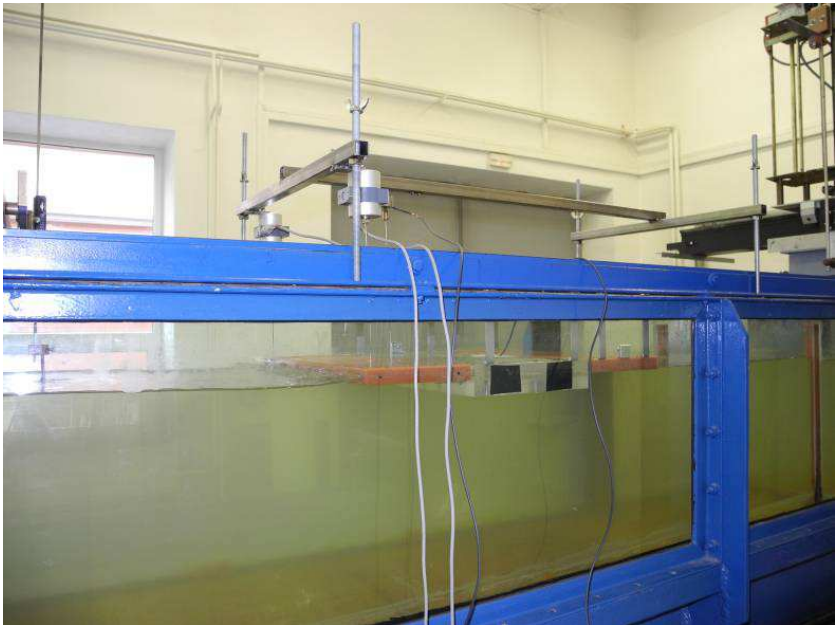


Fig. 4 View on physical model of the bridge

4. RESULTS

Results of simulation and measurements are shown in Fig. 5, 6 and 7.

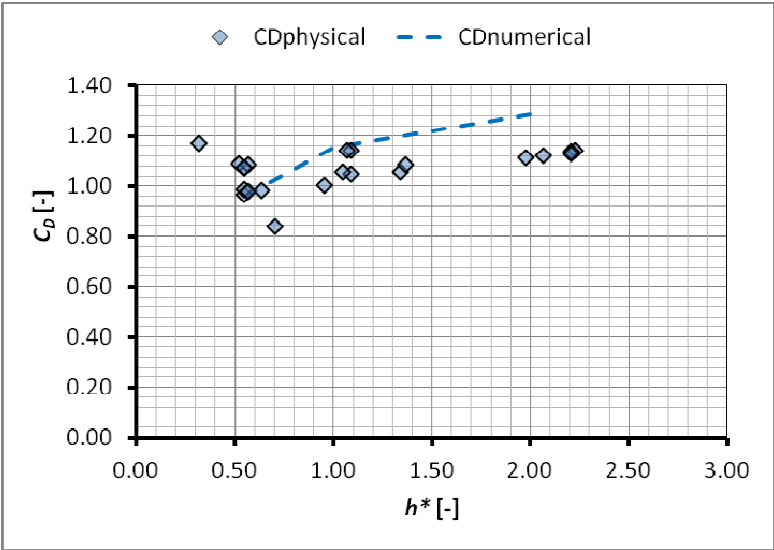


Fig. 5 Drag coefficients as a function of relative submergence

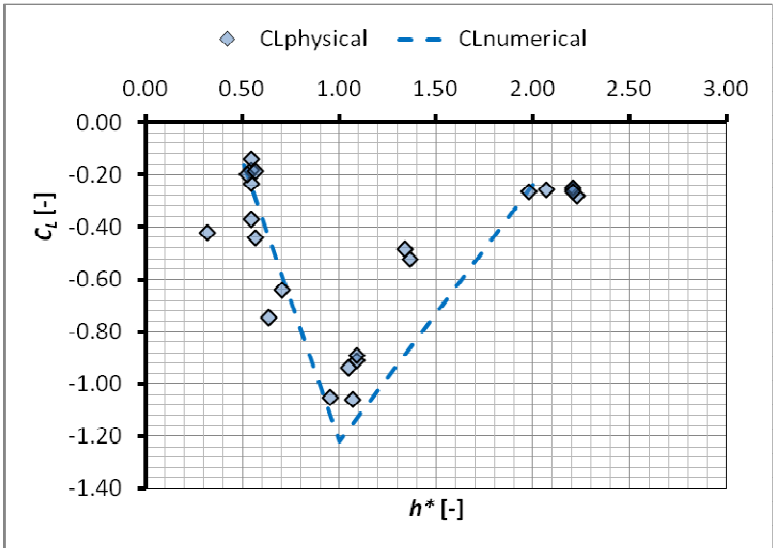


Fig. 6 Lift coefficients as a function of relative submergence

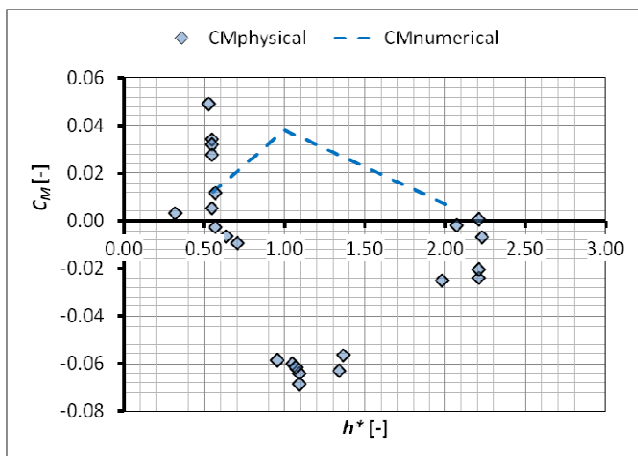


Fig. 6 Moment coefficients as a function of relative submergence

Results in Fig. 5 show a good agreement between measured and calculated values of drag coefficient C_D . Some difference can be seen at submergence level $h^* = 2.0$ where the difference in drag coefficient between measured and calculated values is about 0.1. A good agreement can be also seen if compared with values published by [Boor et al. 1963] for similar shape of obstacle who recommends values of C_D around 1.0. Based on measurements performed on physical model it can be concluded that the highest drag force should be expected at any level of submergence.

A very good agreement between measured and calculated values of the lift coefficient C_L can be seen in Fig. 6. Here, the lift force represents a supplement to the hydrostatic buoyancy force. The flowing water causes decrease of the buoyancy and therefore the value of lift coefficient is negative. Also it can be seen that the maximum lift force can be expected if the submergence level is $h^* = 1.0$.

As shown in Fig. 6 the results reached in case of the moment coefficient C_M are significantly different if compare measured and calculated values. Measured moments have opposite direction than calculated. However, the absolute value of the coefficient is similar. Also it can be concluded that the highest moments should be expected at submergence level $h^* = 1.0$.

5. DISCUSSION AND CONCLUSIONS

Presented results show a good agreement of both drag and lift coefficient but quite a poor agreement of moment coefficient. The highest hydrodynamic load on a bridge should be expected at submergence level $h^* = 1.0$. Measurements on physical model showed that there is also quite strong effect of fluctuation which should be also considered during design process. For example in case of bedding moments both positive and negative values were indicated.

Numerical simulations seem to be a good tool for calculation of hydrodynamic load. However, further research has to be performed to be able to set the model parameters and boundary conditions properly. Also the effect of fluctuations should be involved here.

Further research should be also aimed to different shapes of the bridge decks and also to special parts of a bridge like change of flow around piers and railing.

6. REFERENCES

- BOOR, B., KUNŠTÁČKÝ, J., PATOČKA, C. 1968. *Hydraulika pro vodohospodářské stavby*. SNTL Praha, 1968.
- FLUENT INC. 2006. *FLUENT 6.3 User guide*, Fluent Inc., Centerra Resource Park, 10 Cavendish Court, Lebanon, NH 03766, 2006.
- GUO, J., ADMIRAL, D., ZHANG, T. 2010. Computational design tool for brige hydrodynamic loading in inundated flows of midwest rivers. Report No. 25-1121-0001-227. 2010.
- KERENYI, K., SOFU, T., GUO, J., BUSHRA, A. 2009. Hydrodynamic Foreces on inundated bridge decks. Report No. FHWA-HRT-09-028. 2009.
- PICEK, T. 2006. Ovlivnění průchodu velkých vod mostními objekty na malých vodních tocích (Influence of bridge structures on a course of floodwaters on small rivers). *Disertation thesis*. Prague, 2006. p. 108.
- PICEK, T., HAVLÍK, A. 2008. Výpočet průtoku vody nad přelévanou konstrukcí mostovky – aplikace rovnice přepadu (Calculation of discharge above entirely submerged bridge deck – application of weir equation). *Journal of Hydrology and Hydromechanics*, 2008, Vol. 56, No. 2, p. 82-87, 7 fig., 1 tab., ref. 6.
- PICEK, T., HAVLÍK, A., MATTAS, D. 2004. Tlakové proudění mostním otvorem a přelévané mosty (Pressure flow and overflow bridges). *Journal of Hydrology and Hydromechanics*, 2004, Vol. 52, No. 3, p. 185-192, 10 fig., 1 tab., ref. 5.
- PICEK, T., HAVLÍK, A., MATTAS, D., MAREŠ, K. 2007. Hydraulic Calculation of Bridges at High Water Stages. *Journal of Hydraulic Research* 45 (3): 400-406 2007, Publisher: Int Assn Hydraulic Research (IAHR), Paseo Bajo Virgen Del Puert o, 3, 28005 Madrid, Spain, IDS Number: 186UV, ISSN: 0022-1686
- ŠPANO, M.; STARA, V. 2010. Model turbulence pro stanovení přepadového součinitele přelivu s kruhovou přelivnou plochou. *Stavební obzor*, 2010, roč. 19, č. 6, s. 170-174. ISSN: 1210- 4027.

Acknowledgement

This work was performed within the project of Specific Research at Brno University of Technology No. FAST-S-15-2843 “Hydrodynamické zatížení mostních konstrukcí při povodňových průtocích”

Water hammer analysis-impact of the pipe material in water supply system

G. Taseski, C. Popovska,

(Faculty of Civil Engineering, University of Ss Cyril and Methodius, Skopje, Macedonia,
e-mail: taseski@gf.ukim.edu.mk; popovska@gf.ukim.edu.mk; pelivanoski@gf.ukim.edu.mk)

Abstract

Water supply systems are complex systems where often appears non stationary flow regime known as water hammer. The water hammer characteristics in water supply systems depend on several factors, including water consumption, network density, length of the pipes, material of the pipes and others. This paper deals with modelling the water hammer and hydraulic analysis of the water supply system. The case study is gravitational water supply system with zoned network supplied with the valve before the tank in lower zone.

The presented mathematical model enables to simulate different pipes material, such as asbestos cement, cast iron, PVC, PE pipes and steel pipes. The hydraulic analysis of the obtained results will be presented graphically and recommendations will be proposed.

Keywords

Water supply system, mathematical model, water hammer, pipe material

1. INTRODUCTION

Water supply systems are complex systems that can be composed of objects which are capturing the water, objects that are used for improvement of water quality, water intakes that may be gravity or pump, objects for changing the pressure, valves, reservoirs and home plumbing. Such complexity of the water supply systems leads to water flow under pressure where the speed and pressure change over time –unsteady flow of water.

In practice more applicable are number of new ecological materials on the base of polyethylene for producing pipes for water supply. The pipes on the basis of polyethylene are more widely used in water supply systems during the performance of new or reconstruction of the existing systems. Therefore, often in practice when reconstruction or during the design of new water supply systems, a combination of two or more materials of pipes is used, one of which is a base material of polyethylene while the other material may be of asbestos cement, ductile iron, steel, etc.

In this paper subject of analysis is the influence of the pipe material on the characteristics of the water hammer in the water networks.

2. BASIC EQUATIONS FOR WATER HAMMER

According Wylie (1993), the water hammer is defined as the hydraulic variable occurrence of flow, which causes an increase of overpressure in a pipeline system. The water hammer can be generated by certain operational measures such as: opening or closing of the valve, turning the pumps on or off, abrupt cracking of the pipe etc.

Starting points in the mathematical description of the water hammer are the basic laws in the mechanics of fluids:

- Law of maintaining the amount of movement and
- Law of maintaining weight.

Satisfying these basic principles for conservation/maintenance comes to the dynamic equation and the equation of continuity.

The final form of the dynamic equation for unsteady flow in closed systems under pressure:

$$\frac{\partial V}{\partial t} + V \frac{\partial V}{\partial x} + g \frac{\partial H}{\partial x} + \frac{\lambda}{2D} V |V| = 0 \quad (1)$$

And the final form of the equation of continuity gets the following form:

$$V \frac{\partial H}{\partial x} + \frac{\partial H}{\partial t} - V \sin \alpha + \frac{a^2}{g} \frac{\partial V}{\partial x} = 0 \quad (2)$$

Where a is the speed of propagation of the pressure wave and it is determined by the ratio of compression of the fluid and the module of elasticity of the pipe.

3. METHOD OF CHARACTERISTICS FOR SOLVING BASIC EQUATIONS OF WATER HAMMER

With the method of characteristics the basic partial differential equations which are not integrable in closed form, are transformed into ordinary differential equations which have a solution in a closed form. The basic equations, the equation of continuity and the dynamic equation can be designated with L_1 and L_2 :

$$L_1 = g \frac{\partial H}{\partial x} + \frac{\partial V}{\partial t} + V \frac{\partial V}{\partial x} + \frac{\lambda}{2D} V |V| = 0 \quad (3)$$

$$L_2 = \frac{\partial H}{\partial t} + V \frac{\partial H}{\partial x} + \frac{a^2}{g} \frac{\partial V}{\partial x} - g \sin \alpha = 0 \quad (4)$$

These linear equations can be combined as follows:

$$L = L_1 + \chi L_2 \quad (5)$$

From the previous equation it can be concluded that it's about two families of curves that are practically straight lines, where the speed of propagation is constant and many times faster than the basic flow, so the system of two partial

differential equations are transformed into system of ordinary four differential equations which are marked with a C+ and C- and determine straight lines:

$$\left. \begin{aligned} \frac{d\Pi}{dt} + \frac{a}{g} \frac{dV}{dt} + \frac{\lambda}{2D} V|V| - V \sin \alpha &= 0 \\ \frac{dx}{dt} &= V + a \end{aligned} \right\} C^+ \quad (6)$$

$$\left. \begin{aligned} -\frac{d\Pi}{dt} + \frac{a}{g} \frac{dV}{dt} + \frac{\lambda}{2D} V|V| + V \sin \alpha &= 0 \\ \frac{dx}{dt} &= V - a \end{aligned} \right\} C^- \quad (7)$$

3.1 Numerical model

Figure 1 shows discretization of the physical system in a numerical network with computing steps Δx and Δt where the solutions are obtained at the intersection of the positive and negative lines of characteristics.

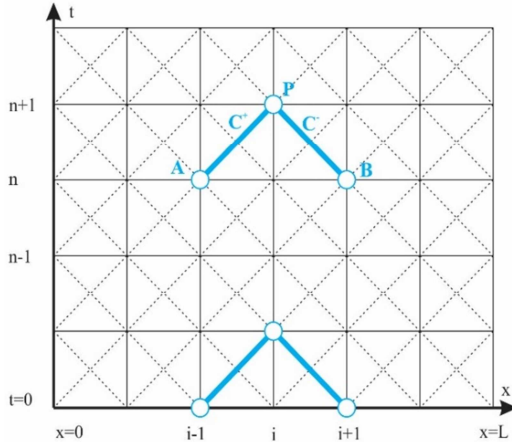


Figure 1. Numerical network for the method of characteristics.

According to the given numerical network, equations (6) and (7) can be written as follows:

$$\frac{d}{dt} \left(\Pi \pm \frac{a}{g} V \right) + \lambda \frac{a}{D} \frac{V|V|}{2g} \mp V \sin \alpha = 0 \quad (8)$$

After integration, equation of positive characteristic are written:

$$\frac{\Pi_P - \Pi_A}{\Delta t} + \frac{a}{g} \frac{V_P - V_A}{\Delta t} + \frac{\lambda a}{2gD} V_A |V_A| - V_A \sin \alpha = 0 \quad (9)$$

If it is known that the hydraulic analysis is important to determine the change in the flow and height position of the hydrodynamic line in any section along the pipe and at a specified interval, additional approximating is introduced that the cross-section of the pipe throughout its length is constant and if it is known that the average speed can be determined by the equation $V=Q/A$, the previous equations knowing the numerical network can be written in the following final form:

$$CP = \Pi_{i-1}^n + BQ_{i-1}^n - MQ_{i-1}^n \left| Q_{i-1}^n \right| \quad (10)$$

$$CM = \Pi_{i+1}^n - BQ_{i+1}^n + MQ_{i+1}^n \left| Q_{i+1}^n \right| \quad (11)$$

For: $B = \frac{a}{gA}$ and $M = \frac{\lambda \Delta x}{2gDA^2}$

3.2 Boundary conditions

The conditions of the flow that govern within the boundary of the system under pressure – the water supply system are defined as boundary conditions. Their definition is of crucial importance for getting the solution at the points in the system. Follow-on are the most common cases of boundary conditions encountered in the water supply systems.

- Connection of more pipes in a junction

$$\text{Pressure: } \Pi^{n+1} = \frac{CP_1/B_1 + CM_2/B_2 + CM_3/B_3 + CM_4/B_4}{1/B_1 + 1/B_2 + 1/B_3 + 1/B_4}$$

$$\text{Flow: } -Q_{I,N}^{n+1} = \frac{\Pi^{n+1}}{B_1} - \frac{CP_1}{B_1}; Q_{2,I}^{n+1} = \frac{\Pi^{n+1}}{B_2} - \frac{CM_2}{B_2}; Q_{3,I}^{n+1} = \frac{\Pi^{n+1}}{B_3} - \frac{CM_3}{B_3};$$

- Reservoir at the end of pipeline

$$\text{Pressure: } \Pi_I^{n+1} = \Pi_R$$

$$\text{Flow: } Q_I^{n+1} = \frac{(\Pi_I^{n+1} - CM)}{B}$$

- Valve at the end of the pipeline

$$\text{Pressure: } \Pi_I^{n+1} = CP - BQ_N^{n+1}$$

$$\text{Flow: } Q_N^{n+1} = -B \cdot C_1 + \sqrt{(B \cdot C_1)^2 + 2C_1(CP - Z_Z)}$$

- Valve at the middle of the pipeline

$$\text{Pressure: } \Pi_{I,N}^{n+1} = CP_I - B_I Q_{I,N}^{n+1}; \Pi_{2,I}^{n+1} = CM_2 - B_2 Q_{2,I}^{n+1}$$

$$CP_I - B_I Q_{I,N}^{n+1} - CM_2 - B_2 Q_{2,I}^{n+1} - C_I Q^{n+1} \left| Q^{n+1} \right| = 0$$

$$\text{Flow: } Q^{n+1} = \frac{-(B_1 + B_2) + \sqrt{(B_1 + B_2)^2 + 4C_1(CP_1 - CM_2)}}{2C_1}$$

4. DEFINITION THE IMPACT OF THE PIPE MATERIAL IN WATER SUPPLY SYSTEM

In order to determine the influence of the pipe material to the characteristics of the water hammer an accrual scheme of zoned gravity water supply system is used with branch water system, where the water from the source of water - piping first is distributed in the upper altitude zone while the excess of water i.e. the needs of water for the lower zone are filling the reservoir for the lower zone. According to the previous one can conclude that for the upper zone there is no reservoir space, and it can be said that the projected reservoir except for leveling the supply amount of water with the needs of water for the lower zone, represents an interrupted chamber, figure 2.

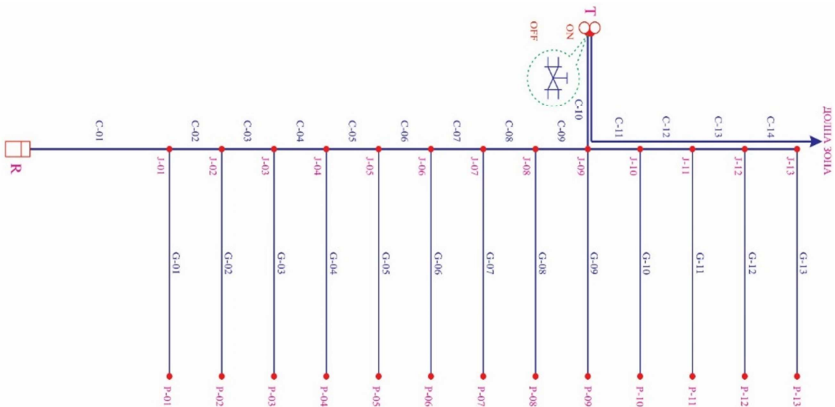


Figure 2. Calculation scheme for determining the influence of the material at the characteristics of the water hammer

In the reservoir for the lower zone hydro-mechanical equipment is provided for proper functioning of the entire water supply system. Namely, in front of the reservoir a pressure regulator is mounted which maintains the inlet pressure in the reservoir (Pressure sustaining valve) in order not to reduce the pressure of the water supply network of the upper zone i.e not to cause drop of the hydro-dynamic line to the reservoir height. After the pressure regulator a float valve is set that regulates the level in the reservoir. The float valve in this calculation scheme practically is the initiator to cause unsteady flow, namely at the time when the reservoir will reach its maximum elevation, the float valve currently closes and vice versa, at the time when the level in the reservoir descends to a certain limit, the float valve sharply opens. It should be mentioned that the regulator pressure is

continuously in function and does not allow drop of the hydro-dynamic line for the upper zone.

The choice of such a calculation scheme is made to analyze the phenomenon of the water hammer in a complex system with a gravity pipe and cover at the end of the primary pipeline. This calculation scheme is practically equivalent to the model of a simple system - reservoir and pipeline which at the end has cover.

In order to determine the impact of the pipe material on the characteristics of the water hammer two scenarios are made:

One of the operational criteria of the new plant in Popolzhani is that it should run only when all the needs of water for water supply are covered for the settlements and potable water for the Thermal plant Oslomej. During the hydraulic analysis in stationary and non-stationary regimes of flowing the following alternative scenarios are made:

I. First scenario: The plugs on the branches of the secondary network at a distance of 200 m, and all pipes from water supply of the same material - ductile pipes.

II. Second scenario. The plugs of the branches of the secondary network are at distance of 200 m, while the primary pipeline is provided by ductile pipes and the pipes of the secondary network of polyethylene HDPE.

5. RESULTS OF THE ANALYSIS

In addition to figures 3, 4, 5 and 6 are shown the analysis of the water supply system from the mathematical model during abrupt closure of the float valve in case of maximum and minimum water consumption. The system is composed of two materials, the main pipeline is derived from steel, while the branches are derived from polyethylene pipes (HDPE).

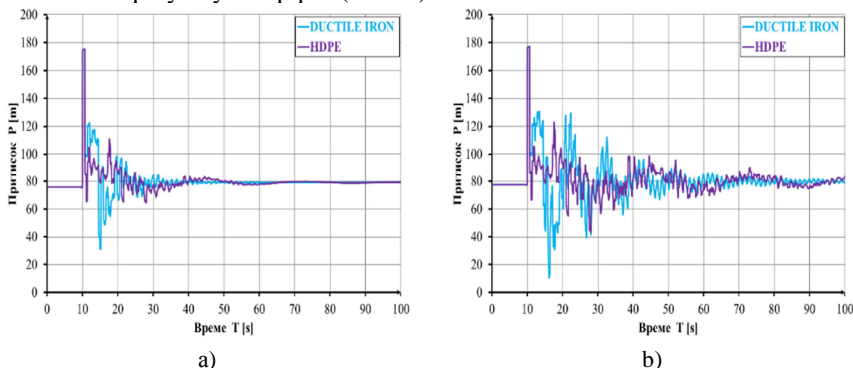
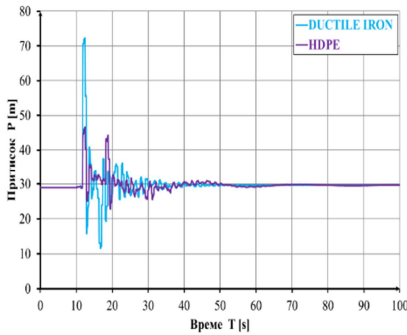
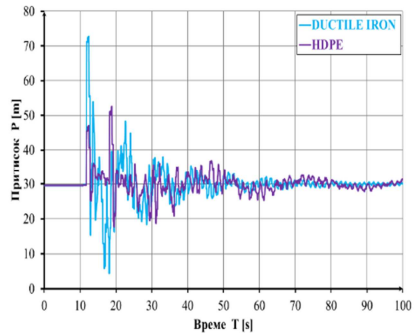


Figure 3. Impact of material characteristics on the pipes of the water hammer q_{max} / h (a) and q_{min} / h (b) in the nodal point T-2

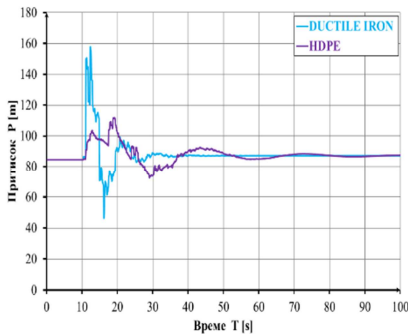


a)

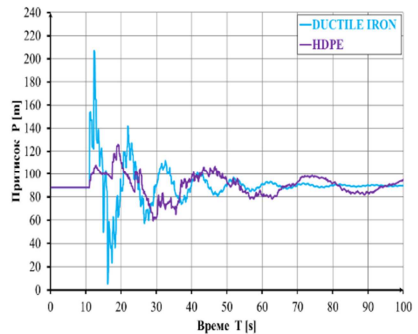


b)

Figure 4. Impact of material characteristics on the pipes of the water hammer q_{max} / h (a) and q_{min} / h (b) in the nodal point J1

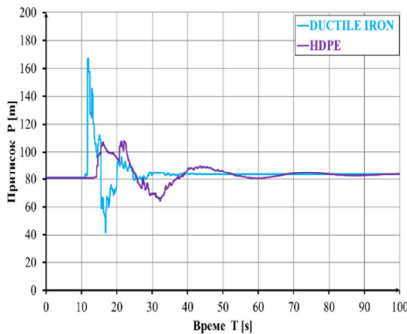


a)

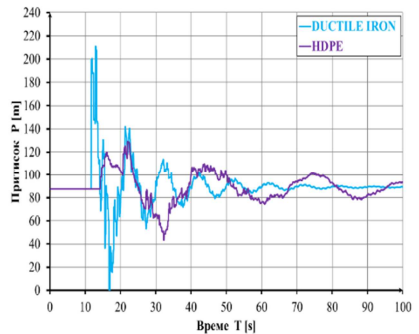


b)

Figure 5. Impact of material characteristics on the pipes of the water hammer q_{max} / h (a) and q_{min} / h (b) in the nodal point J13



a)



b)

Figure 6. Influence of material characteristics on the pipes of the water hammer q_{max} / h (a) and q_{min} / h (b) the nodal point P13

6. CONCLUSION

From previous graphics schemes it is notable that the choice of the pipe material has an impact on the pressure increase in the pipeline as well as in the branches of the water supply network. That is, if analyzed what impact has the pipe material, a comprehensive conclusion as follows can be given: if the speed of propagation of the wave of pressure has less value then the increasing of the pressure is lower, i.e. how much the pipe material is resilient that better the water hammer amortizes in the water supply network.

7. REFERENCES

- BETAMINO DE ALMEIDA, E. 1992. Fluid transient in Pipe Networks, Publisher: WIT Press, ISBN-13: 978-1853121678.
- IZQUIERDO, J., INGLESIAS, L.P. 2004. *Mathematical modelling of hydraulic transients in complex systems*. Mathematical and Computer Modelling, 39,529-540.
- KAVEH HARIRI ASLI. 2013. Water Hammer Research: Advances in Nonlinear Dynamics Modeling”, Publisher: Apple Academic Press, ISBN 9781926895314 - CAT# N10708.
- LOHRASBI, A.R, ATTARNEJAD, R.. 2008. *Water Hammer Analysis by Characteristic Method* American J. of Engineering and Applied Sciences 1 (4): 287-294.
- PARMAKIAN, J. 1995 Water hammer Analysis. Publisher: Prentice Hall, Inc.; 1st edition, ASIN: B0000CJ5U0.
- PELIVANOSKI, P., TASESKI, G. 2012. Study for Innovation the Regime of Water Use by Regional Water Supply System "Studencica".
- POPOSKA, C. 2000. *Hydraulics*. Publisher Civil Engineering Faculty, University Ss. Cyril and Methodius, ISBN 9989-43-100-0.
- STREETER, V. L., WYLIE, E.B. 1967. Hydraulic Transient, McGraw Hill Book Company, New York.
- TASESKI, G. 2015. *Characteristics of water hammers in water supply networks*. Doctorate dissertation, Skopje, Macedonia.
- THOMAS REPP, T. 2011. *Fluid Dynamic Water Hammer Simulations with Consideration of Fluid-Structure Interaction*, <https://www.hzdr.de/FWS/publikat/JB98/jb08.pdf>.
- ZARUBA, J. 1993. Water hammer in pipe-line systems. Publisher: Elsevier Science, ISBN-13: 978-0444987228.

Numerical analysis of the impact of breakwater culvert to the sea exchange in the Adriatic marinas

G. Loncar, H. Mostecak, T. Polak

(University of Zagreb Faculty of Civil Engineering, Fra Andrije Kacica-Miocica,
e-mail: hmostecak@grad.hr)

Abstract

3D numerical model analyses the impact of the breakwater culvert on the exchange between the sea waters of the marina and the open sea of the northern and southern Adriatic. The breakwater in the model analysis was treated as a vertical impervious barrier. In the analysis the hypothetical layout configuration of the marina (position inputs and width of the entrance to the marina, proportion of the length and width of the marina) varied. Sea currents in the model domain was generated by using non-stationary boundary conditions in the form of time series of sea levels based on seven constituents of the tidal signal. Wind-driven forcing is not taken into analysis.

The research results show that the breakwater culvert in the analysed conditions reduces the e-folding time for exchange between the sea waters of the marina and the open sea average to 88%. The construction of breakwater culvert increases exchange between the sea waters when three breakwater culverts are positioned in the marina with an entrance in the side breakwater.

Keywords

breakwater culvert, marina, numerical analysis, sea exchange

1 INTRODUCTION

The primary role of marinas, harbors and ports is the protection of vessels of the unwanted effects caused by sea waves. The functionality of a marina / harbor / port in a wider context, is gained by applying a marine construction (protective structures) which reduces the intensity of waves in the protected waters [USEPAS, 1993]. Regardless of the manner of performance of protective structures (pontoons, breakwaters, partially submerged breakwaters, etc.), the desired reduction of the intensity of waves is achieved by an embankment construction with the final length and depth. With this intervention the intensity of the currents in the port basin is decreases, and it hinders the natural environmental conditions [USACE, 2002]. In order to avoid or minimize unwanted effects of construction grips on the aquatic biocenosis in the "newer" project, for example, is a realisation of the breakwater in the form of construction of the pilots with the partially immersed vertical screen to the appropriate depth (examples in Umag and Dubrovnik - Gruz) [Goda, 2000; Carevic at all, 2011]. Those solutions are acceptable in terms of mild wave climate and the great depths at which it is

necessary to use breakwaters. On the other hand, Croatia has the largest number of marinas, harbor and small craft harbours protected by the rubble mound breakwaters or gravitational breakwaters that continuously interrupt communication over the entire depth of the external seawater with the sea port basin.

The problem of the decreased circulation of the seawater in port aquatoria results with the design practices and performance of pipe culverts through the body of the rubble mound and gravitational breakwaters. The purpose of the performance of pipe culverts is forcing changes between the ports protected waters and the "open" sea waters. However, according to our knowledge, any fundamental research on the contribution of pipe culverts in the exchange sea has not yet been carried out. This paper presents the results of a numerical simulation of circulation sea and flow of tracer solution, particularly with the aim of quantifying the contribution of pipe culverts in the exchange of "old" sea waters of the marina with the "external" sea waters. As a comparative parameter for determining the quality of the decision of pipe culverts, so-called "e-folding" time has been used. Cucco and Umgiesser [2006] in their work extensively described how to determine the approach with the "e-folding" time. The concentration tracer (non-reactive) solution for the entire area protected port basin is initially set, followed by the zero concentration value for the rest of the spatial model domains. Due to the sea changes, a dilution of the initial concentration through the convective dispersion mechanism takes place, together with the falling of the mean concentrations tracer solutions in the area of the port basin.

The adoption of this methodology allows the detection of areas with longer residence time, so-called "dead zones" (areas of increased concentrations of tracer solution). Areas with longer residence time, so-called "dead zones" (areas of increased concentrations of tracer solution) have been obtained by running the numerical simulations in the protected area of the marina. The analysis of the results of each numerical simulations gives us the "e-folding" time representing the time required for tracer solution concentration to drop to 37% of its initial value.

2 NUMERICAL MODEL

The used numerical model MIKE 3 (www.dhigroup.com) simulated three-dimensional flow of Newtonian fluid through a system of momentum equations and continuity equation for mass. The used mathematical formulation of the equation of continuity and momentum equation is based on the Reynolds averaging Navier-Stokes equations. The analysed liquid in the model is assumed to be incompressible with the accepting of assumptions about the distribution of hydrostatic pressure in the vertical water column. In the analysis of convective-dispersive contaminant transport processes, dispersion coefficients are divided into horizontal and vertical components, and are proportional to the kinematic coefficient of turbulent viscosity. As a part of the model simulation the standard k-

ε turbulence model has been used. The numerical model is based on the method of finite differences.

1.1 Model spatial domain

The spatial step $\Delta x = \Delta y = 10$ m horizontally and $\Delta z = 1$ m in vertical direction has been used for the spatial discretization. The minimum depth of the sea in the marina is 2 m. Furthermore, the slope of the bottom of the port basin is variable and is 1:10 of the distance of 100 m away from the coast, then the 1:15 and 1:20 of the distance to the open sea. Breakwater culverts are defined as opening width of 10 m, with the bottom elevation at a depth of 1.5 m (15 m^2).

A total of 48 of numerical experiments were completed which simulated hypothetical marinas located in the area of the northern Adriatic (Umag position) and the southern Adriatic (Dubrovnik position). The following features were taken into consideration (Figure 1):

- Two widths of entrance to the port B (30 and 50 m);
- Two positions of the entrance to the marina (in the direction of the direction of alongshore currents and perpendicular to it);
- Three length L and port width D ratio ($L/D=1; 2; 3$);
- Marinas without and with breakwater culverts.

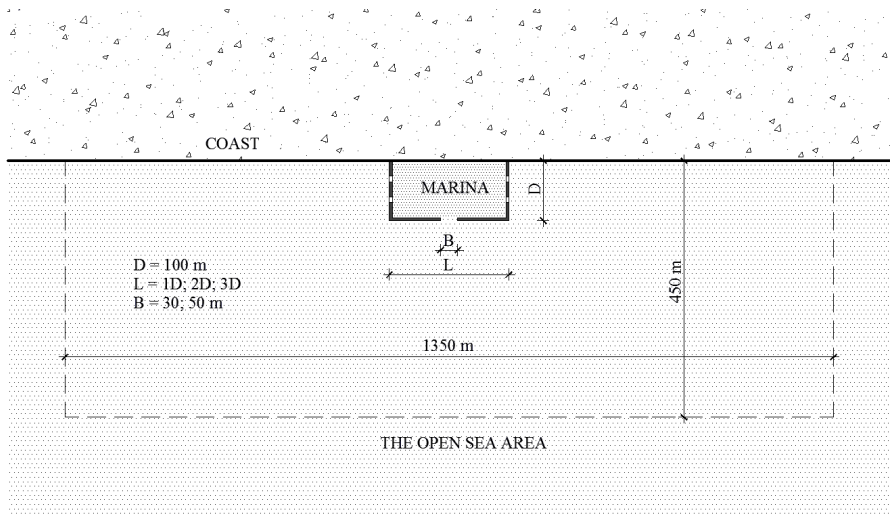


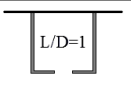
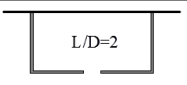
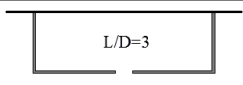
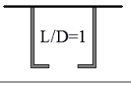
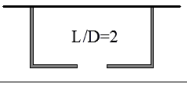
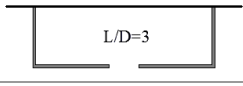
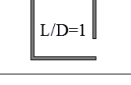
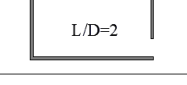
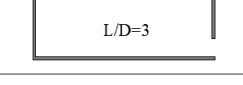
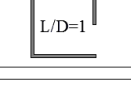
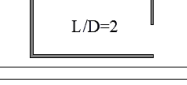
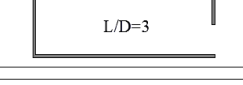
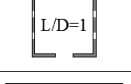
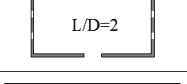
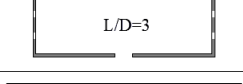
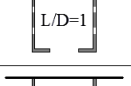
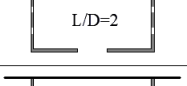
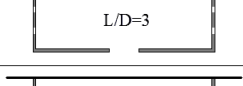
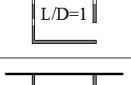
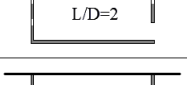
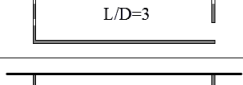
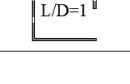
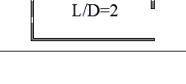
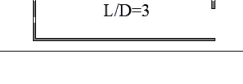
Fig. 1 Schematic demonstration of the marina with varied features in different experiments

1.2 Initial and boundary conditions

Generating flow was achieved by the time series of sea surface level differences along transects of the open borders. Hourly dynamics of sea levels,

based on seven basic constituents of tidal signal, has been used, [Janekovic et al., 2003; and Janekovic Kuzmic 2005 Janekovic and Sikiric-Dutour, 2007]. Time period simulations of sea levels are from 01/08/2014 to 06/08/2014 (total 120 hours).

Tab 1. Demonstration of implemented experiments with analysed characteristics of marinas

Entrance to the marina: in the direction of the alongshore currents Width of the entrance: 30 m Length L and width D ratio: 1, 2, 3			
Entrance to the marina: in the direction of the alongshore currents Width of the entrance: 50 m Length L and width D ratio: 1, 2, 3			
Entrance to the marina: perpendicular to the direction of alongshore currents Width of the entrance: 30 m Length L and width D ratio: 1, 2, 3			
Entrance to the marina: perpendicular to the direction of alongshore currents Width of the entrance: 50 m Length L and width D ratio: 1, 2, 3			
Entrance to the marina: in the direction of the alongshore currents Width of the entrance: 30 m Length L and width D ratio: 1, 2, 3			
Entrance to the marina: in the direction of the alongshore currents Width of the entrance: 50 m Length L and width D ratio: 1, 2, 3			
Entrance to the marina: perpendicular to the direction of alongshore currents Width of the entrance: 30 m Length L and width D ratio: 1, 2, 3			
Entrance to the marina: perpendicular to the direction of alongshore currents Width of the entrance: 50 m Length L and width D ratio: 1, 2, 3			

3 NUMERICAL MODEL RESULTS

The results of the numerical simulations in this paper are presented as the fields of vertically averaged concentration tracer solution, the currents fields for the two time-frames, the graphical demonstration of lowering the concentration of tracer solution, and the tabular presentation of e-folding time required for the dilution of the initial solution to $1/e = 36,8\%$.

Figure 2 shows the fields of the vertically averaged concentration of the tracer solution for marina in northern Adriatic in which the ratio of length to width ratio is $L/D = 2$, and the entrance to the marina is 50 m wide and located on the front breakwater.

The results of the simulations with and without the usage of pipe culverts are shown. The initial tracer solution concentration in the protected waters of the marina was 100 (the dimensionless value of tracer solution concentrations).

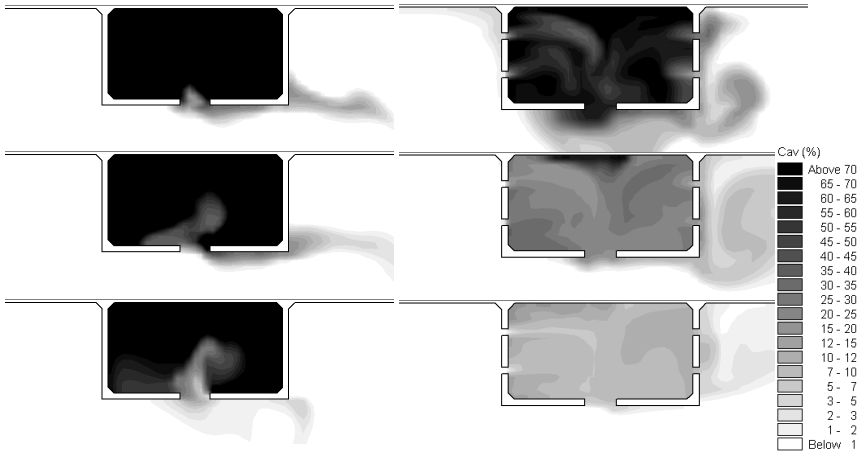


Fig. 2 Fields of vertically averaged concentration tracer solution for northern Adriatic marina (left: marina without pipe culverts, right: marina with pipe culverts); entrance to the marina is on the frontal breakwater

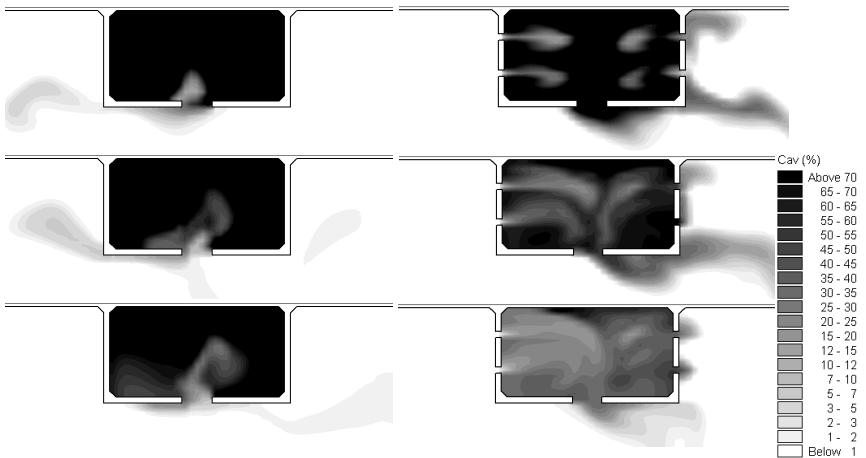


Fig. 3 Fields of vertically averaged concentration tracer solution for southern Adriatic marina (left: marina without pipe culverts, right: marina with pipe culverts); entrance to the marina is on the frontal breakwater

Figure 3 shows the fields of vertically averaged concentration for the same layout variation of the marina located in the southern Adriatic.

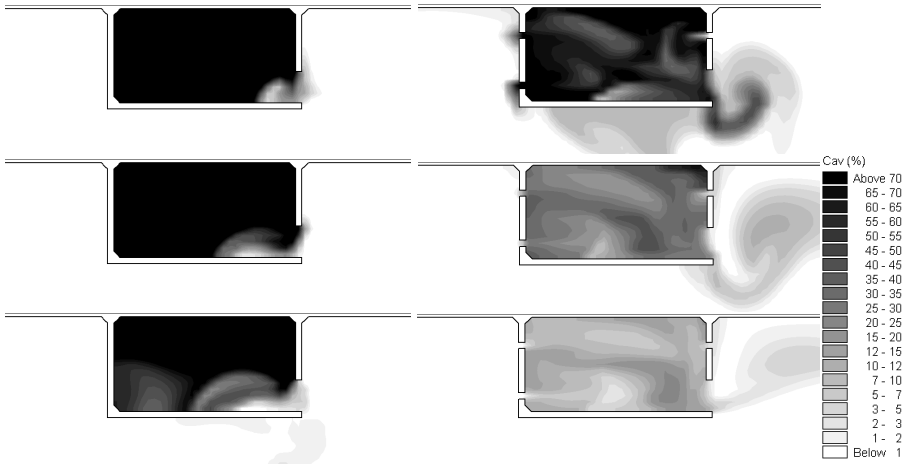


Fig. 4 Fields of vertically averaged concentration tracer solution for northern Adriatic marina (left: marina without pipe culverts, right: marina with pipe culverts); entrance to the marina is on the side breakwater

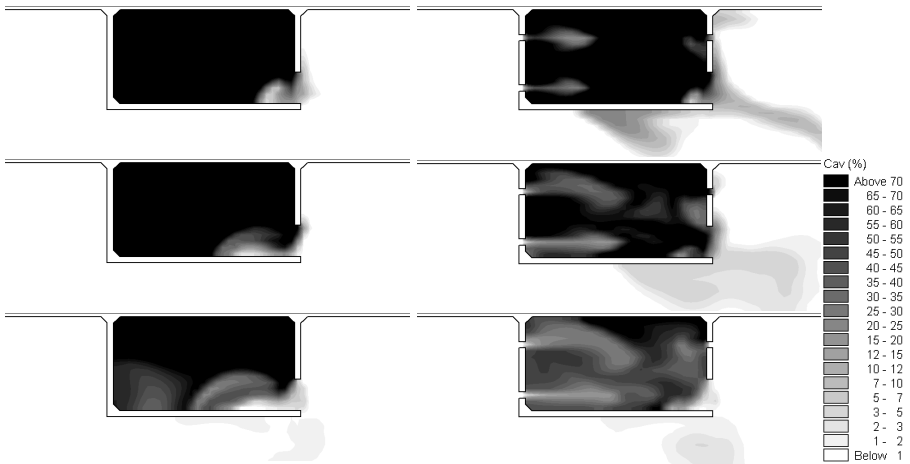


Fig. 5 Fields of vertically averaged concentration tracer solution for southern Adriatic marina (left: marina without pipe culverts, right: marina with pipe culverts); entrance to the marina is on the side breakwater

In order to compare the results of simulations, figures 4 and 5 shows the fields with the averaged concentration for the marine of the northern and southern Adriatic with entrance set on the side of the breakwater, with and without the usage of pipe culverts. All simulated situations are presented after 24, 72 and 120 hours from the initial moment.

Figures 6 illustrate a comparison of current fields in two different moments for the northern and southern Adriatic marina with the front positioned entrance. Shown fields are related to the currents in the east-west and west-east direction. The intensity of the currents between the northern and southern Adriatic are clearly different for the two current fields (in the east-west and west-east), as a result of the extensive tidal fluctuations between the northern and southern Adriatic.

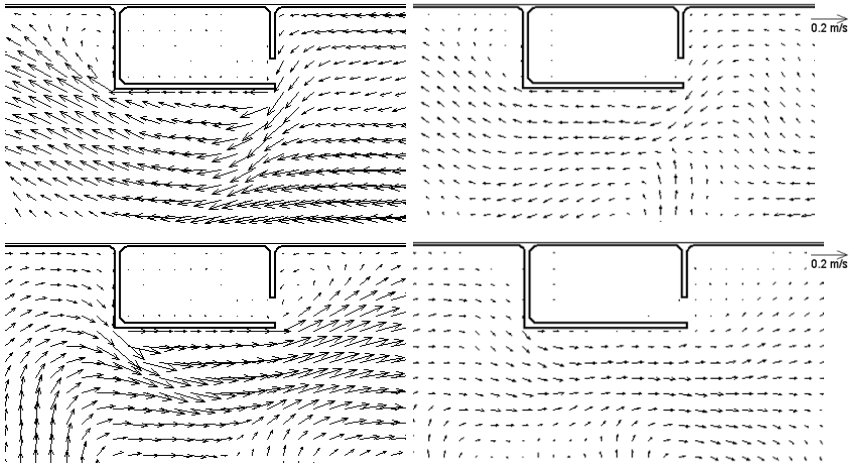


Fig. 6 Comparison of current fields for two different moments for northern and southern Adriatic marina with front positioned entrance

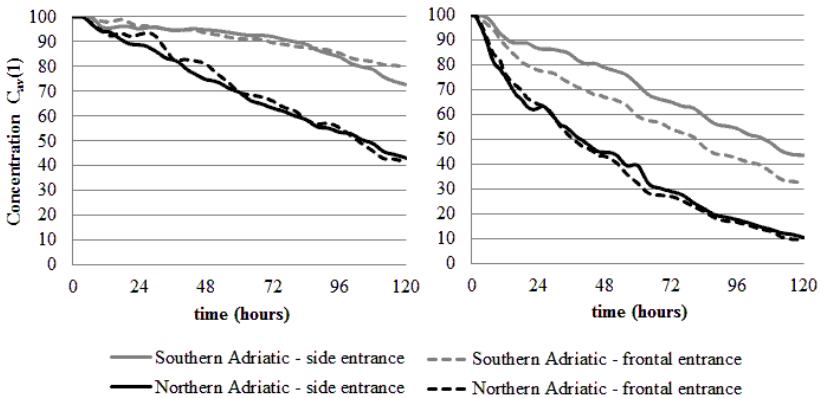


Fig. 7 Time series of mean values of concentration tracer solution for protected marine waters

A comparison of vertically averaged concentration tracer solution for the analysed variant of the marina with its length and width ratio $L/D = 2$ is shown in the graph in Figure 7. The shown values are valid for the marina with and without

pipe culverts. The x -axis presents the simulation time of five days (120 hours), whereas the average value of the concentration of the tracer solution (C_{av}) for the whole area of the protected marine waters is shown on the y -axis. The left side of the picture shows the results of the simulations without using pipe culverts, while the right side shows the results with included pipe culverts in the breakwater.

The graphs shows a decrease of averaged concentration solution for the marine with side and frontal entrance which is 50 m wide. On the northern Adriatic, due to more prominent tidal oscillations, the process of dilution of the initial concentration was markedly faster.

After 120 hours the average value of the concentration on the northern Adriatic is 42.9 for the side position of the entrance, and 41.0 for the front entrance to the marina. On the southern Adriatic concentration values after 120 hours are much higher, and for the side position of the entrance to the marina is 72.5 and 79.7 for the frontal position. The value of the solution concentration using pipe culverts for the northern Adriatic is 10.3 for side position of entrance and 9.5 for the front entrance to the marina. For the southern Adriatic the mean value for side entrance is 43.6, and for the frontal entrance 32.5.

The results of the carried numerical 3D simulations in Table 2 show the values of the concentration of the tracer solution for all varied positions and entrance sizes to the marina aquatoria, 120 hours after the initial moment when the concentration level was 100.

Tab 2. The results of 3D numerical simulations for all analysed situations

Variant of marina	Northern Adriatic marina				Southern Adriatic marina			
	without pipe culverts		with pipe culverts		without pipe culverts		with pipe culverts	
	frontal entrance	side entrance	frontal entrance	side entrance	frontal entrance	side entrance	frontal entrance	side entrance
$L/D=1, B=30$ m	57.3	33.8	1.4	1.7	83.4	62.4	11.7	29.9
$L/D=1, B=50$ m	19.8	16.7	0.2	0.8	62.7	42.2	2.4	26.2
$L/D=2, B=30$ m	75.1	60.0	11.6	12.8	89.2	85.9	34.4	46.3
$L/D=2, B=50$ m	41.0	42.9	9.5	10.3	79.7	72.5	32.5	43.6
$L/D=3, B=30$ m	75.8	66.5	22.4	27.0	79.1	77.5	42.0	59.0
$L/D=3, B=50$ m	54.0	61.4	18.0	25.5	76.0	74.5	39.9	54.5

Table 3 shows e-folding time for all simulated variants of northern and southern marina.

Tab 3. E-folding times (hours) for all analysed situations

Variant of marina	Northern Adriatic marina				Southern Adriatic marina			
	without pipe culverts		with pipe culverts		without pipe culverts		with pipe culverts	
	frontal entrance	side entrance	frontal entrance	side entrance	frontal entrance	side entrance	frontal entrance	side entrance
$L/D=1$, $B=30$ m	209	112	32	36	407	176	66	104
$L/D=1$, $B=50$ m	80	74	3	31	223	125	3	99
$L/D=2$, $B=30$ m	248	194	60	66	450	297	110	164
$L/D=2$, $B=50$ m	129	136	54	61	260	206	108	148
$L/D=3$, $B=30$ m	297	256	84	95	467	330	128	218
$L/D=3$, $B=50$ m	196	205	72	89	470	281	125	185

4 DISCUSSION AND CONCLUSIONS

By the performed numerical simulations of the analysed 3D geometric size, the position of the entrance to the protected waters of the marina with impermeable vertical breakwaters, and the position and the number of the built pipe culverts in the body of the breakwater, a series of results that quantify the contribution of the size and position of the marina on the exchange between the sea waters of the marina and the open sea have been obtained. The results of the analysis without using the pipe culverts shows that the geometric relationship of the length and width of the marina 1:1 has the strongest contribution to the sea exchange between the marina and external, open sea waters. The analysis of the results of the position of the entrance to the marina shows that the optimum position of the entrance to the exchange between the internal and the open sea waters is on the side breakwater, and when the entrance to the marina is placed perpendicular to the direction of alongshore currents. In the mentioned position the decrease in the concentration of the solution tracer 120 hours after the initial moment is an average of 53% for the northern Adriatic marina, and of 30% for the southern Adriatic marina.

The analysis of the results obtained by using the pipe culverts indicates a significantly decrease in the concentration of tracer solution. Thus, the average value of the concentration after 120 hours in the marina with the frontal entrance is 18.8 % (66.1 % without culverts), while in the marina with the side position of the entrance the concentration is 28.1 % (58.0 % without culverts). In the analysis of the results the fact that the frontal entrance to the marina used four positions of

pipe culverts, and in case of a side entrance just three of them, should be taken in account.

The analyses indicate that the least favourable situation for the sea exchange is if marina's relationship between length and width is 3:1, thus making the situation in the northern Adriatic more favourable in comparison to the southern Adriatic, due to the influence of the tidal signal.

The results of the simulations can be used as guidelines for future research that would in their analyses include the influence of wind contribution to the time of initial dilution of the concentration of tracer solution in the marina.

5 REFERENCES

- CUCCO, A., UMGIESSER, G., 2006, Modelling the Venice lagoon residence time, *Ecological modelling*, Volume 193, p. 34-51.
- CAREVIC, D., OCVIRK, E., PRSIC, M. 2011. Reduction of Wave Load on the Perforated Seawall Defended by the Submerged Breakwater, *Current Events in Hydraulic Engineering* (Sawicki, Jerzy M.; Zima, Piotr), Elsevier, New York, p. 32-41.
- DHI, WATER & ENVIRONMENT 2001. Estuarine and Coastal Hydraulics and Oceanography, DHI, Hørsholm, Danska.
- GODA, Y., 2000. Random seas and design of maritime structures, *Advanced Series on Ocean Engineering* (World Scientific Publishing Co. Pte. Ltd.), World Scientific, Singapore, vol. 15, p. 356–361.
- JANEKOVIC, I., BOBANOVIC, J., KUZMIC, M. 2003. The Adriatic Sea M2 and K1 tides by 3D model and data assimilation, *Geophysical Research Abstracts*, 9, p. 203-217.
- JANEKOVIC, I., KUZMIC, M. 2005. Numerical simulation of the Adriatic Sea principal tidal constituents, *Annales Geophysicae*, 23, p. 3207–3218.
- JANEKOVIC, I., SIKIRIC-DUTOUR. M. 2007. Improving tidal open boundary conditions for the Adriatic Sea numerical model, *Geophysical Research Abstracts*, 9, p. 203-217.
- MALA INTERNET ŠKOLA OCEANOLOGIJE, Plimne oscilacije u Jadranu, <http://skola.gfz.hr/> (11.02.2015.)
- US ARMY CORPS OF ENGINEERS 2002. Coastal Engineering Manual (CEM), EM 1110-2-1100, Vicksburg.
- US ENVIRONMENTAL PROTECTION AGENCY STAFF 1993. Environmental Engineering for Small Boat Basins, Engineering Manual, EMP 10-2-1206, New York.

The CFD analyses of the lateral spillway using different turbulence models

M. Orfánus, A. Šoltész

Department of Hydraulic Engineering, Faculty of Civil Engineering, University of Technology in Bratislava, Radlinského 11, 810 05 Bratislava, Slovak Republic , e-mail: martin.orfanus@stuba.sk.

Abstract

Submitted article is aimed on the several aspects of dynamic water behaviour using the three-dimensional numerical model CFD supported by physical research. The calibration of the model is important procedure to obtain the results close to real conditions. In terms of CFD modelling, one of the most important calibration parameters, except the roughness, is the turbulence model. Submitted article shows the result differences between several turbulence models and physical model measurements.

Keywords

Fluid Dynamics, three dimensional mathematical model CFD, lateral spillway

1. INTRODUCTION

By the damming of a continual stream of free surface flow by the obstacle reaching from bottom to defined level an overflow effect will occur. The flow on the upper side of such an obstacle is backwatering and its water level will justify at the level corresponding to condition when volume discharge overflowing through the obstacle is equal to the inflowing discharge [Mäsiar, et al., 1986].

Overflow is a physical phenomenon of water overflowing the spillway. If the spillway is placed on the parallel to channel centreline, it is a lateral spillway. The lateral spillway is constructed on the bank of channel and is removing the part of discharge from the channel (Dvořák, 2012). The overflowing edge should be placed as parallel or sharp angled to channel streamline. Lateral spillway should be used as flood protecting object as well as to transform the flood wave passing the object [Mays, 1999].

The flow near the lateral spillway is complicated with large flow deformation in all the three dimensions. The discharge along the spillway is decreasing from the value Q_1 at the beginning to the value of Q_2 at the end of the spillway. Generally should be the downstream discharge defined as $Q_2 = Q_1 - Q_b$ where Q_b is defined as discharge overflowing trough the lateral spillway (Fig. 1).

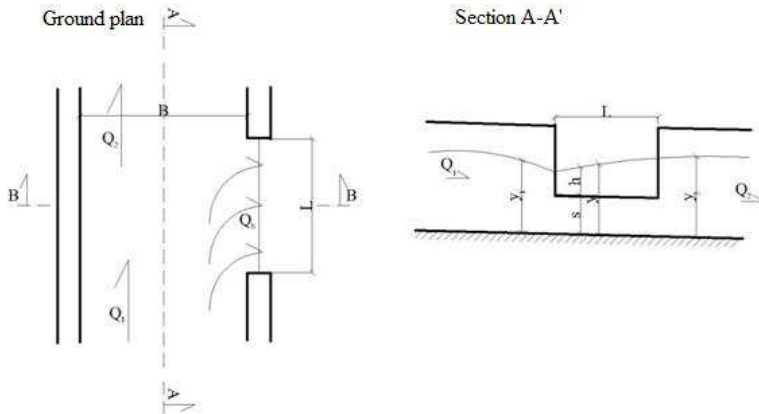


Fig. 1: The lateral spillway scheme

2. PHYSICAL MODELLING

Lateral spillway physical research was performed in hydraulic laboratory of Department of hydraulics at Faculty of Civil Engineering, Slovak University of Technology in Bratislava under the supervision of prof. Mäsiar, DrSc. and realized by Ing. Miškay, CSc. The overall concept of the research were set on the basis of previous works analyzes in the field of water dynamics near the lateral spillway (Fig. 2).

The goal of experimental research was the performance of 225 experiment divided in two series of lateral spillway with sharp crested overflow (series I.) and broad crested overflow (series II). Both series had experiments with systematically changed geometric parameters (Tab. 1).

Tab 1 Main parameters description of physical model

Channel width	Length of overflowed edge „L“	Height of overflowed edge „s“	Discharge Q_1	Bottom slope
[cm]	[cm]	[cm]	[$l \cdot s^{-1}$]	[‰]
40	20, 60, 100	5, 10, 15, 20	10, 15, 20, 25	0,5

The overall dynamics were monitored and post processed in:

- Measuring the water level y_1 and y_2 in two cross section placed $(3 \div 5)h$ above and under the lateral spillway location
- Determination of the cross sectional velocity v_1 and v_2 depended on known discharge and measured velocity in cross section placed $(3 \div 5)h$ above and under the lateral spillway location

Detail analyzes were done for experiment 177 of series I, which was submitted except standard measuring also to measuring of velocity field for selected cross

sections. By photogrammetric methods were also generated the streamlines near the lateral spillway.

3. MATHEMATICAL MODELLING

The project primary method for obtaining the results is the three dimensional mathematical CFD model supported by physical research performed in hydraulic laboratory of Department of hydraulics at Faculty of Civil Engineering, Slovak University of Technology in Bratislava.

All knowledge of fluid dynamics is summarized in fluid mechanics. Classical fluid mechanics is subdivided into statics, kinematics and dynamics of fluids. Modern Applied fluid mechanics is built on three pillars:

- Theoretical fluid mechanics and thermodynamics
- Experimental Fluid Mechanics
- Computer fluid dynamics CFD and numerical mathematics

The geometry was created in CAD ("Computer added engineering") application on the basis of hydraulic collapsible canal with rectangular cross section (Tab. 1) in full three dimensional space in SI units. The geometry format used for program was stereolithographic (*.stl).

The computational mesh for simulations series is structured mesh with characteristically element resolution of 0.01 m in orthogonal coordinates. For numerical stability of the simulations and good convergence the element resolution ratio in X-Y direction was 1.99964, X-Z direction 1.00008 and Y-Z direction 1.99961. Total number of active and passive cells was 1 931 700 where active number of cells was 1 407 274.

Unlike the physical model where the discharge was set at the inlet of canal, the boundary conditions for CFD model were different. Discharge as boundary condition was replaced by specified velocity for the better simulations unification.

The verifying series boundary conditions were set according the physical model experiments. Simulations were set as specified velocity of $0.280 \text{ m}\cdot\text{s}^{-1}$ and water elevation of 0.089 m.

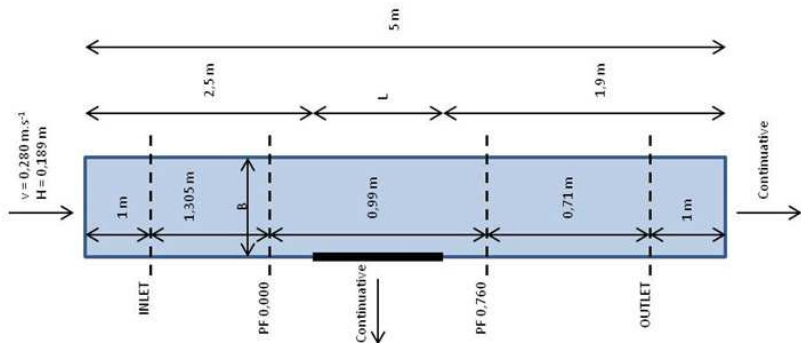


Fig. 2 Basic setup of the model

The general CFD model numeric setup was set as steady flow analyses of two fluids with sharp interface. The fluid was set as water with temperature of 20 degrees in incompressible mode and with dynamic behaviour of viscous flow defined by turbulence model (Chapter 4.)

4. TURBULENCE

A considerable attention is devoted to the correct turbulence simulation. If the simulated problem is not that of the laminar flow, the selection of an appropriate turbulent model is very important . Every turbulence model has been developed for different needs and there is no universal model, which would be sufficient for all aspects of three-dimensional modelling using CFD (Huber, 2010).

For the purposes of modelling turbulence in incompressible fluid flow with low velocities and free surface the two equation models are the mostly used. They belong to a group known as RANS models ("Reynolds averaged Navier-Stokes equations"). The most used and one of the most robust models is k-ε model. The k-ε model is a solution of two equations semi-empirical simulation method based on the turbulent kinetic energy dissipation "k" and specific energy per unit time "ε" (Ansys, 2009).

In this equations are the velocities and density averaged through the time.

Another well-known turbulence model suitable for the simulation of hydraulic problems is the RNG model. In principle, it is a modification of the standard model of k-ε, described in detail above, but using statistical theory known as renormalization group ("renormalization group theory"). Renormalization method of statistical physics is utilized primarily in the area of quantum physics, cosmology, and fluid dynamics. The method was developed to remove divergences arising from solutions in theoretical physics complex problems. In mathematics point of view is the method criticized by many, but in the experimental testing is very accurate and efficient. Introduction the Renormalization group calculation to turbulence modelling resulted in:

- efficiency and stability in simulations of a sudden increase in voltage flowing liquids
- well describes the creation of vortices
- RNG model incorporates analytical formulation for the determination of Prandtl numbers, while the standard k-ε model contains only a constant, user-specified value
- standard k-ε model is developed primarily for high flow Reynolds number, but the RNG model has an analytical formulation to determine the effective viscosity of the flow-to-use and low Reynolds number (Flowscience, 2011).

For the purpose of such a simulation can be used the model with spatial filter known as a simulation of large eddies (LES - Large Eddy Simulation). Concept LES is based on the fact that the swirl motion of large scales is calculated and

swirling motion of small scales is modelled. The bid eddies are the main carriers of turbulent energy.

With regarding to genesis of turbulent models development and their purposes, two main groups should be considered as potential for such a project. First group are RANS ("Reynolds Averaged Navier-Stokes equations") turbulent models and the second one are models with space filter. From these groups were chosen k-ε, RNG and LES models. All three turbulent models were tested on validating series A, simulation A1.

The accuracy comparison of each turbulent model was compared to experiment of physical research (experiment 177, series I) in two ways:

- Comparison of cross sectional parameters
- Comparison of velocity field

The comparison of cross sectional parameters $Q_1, Q_2, Q_b, v_1, v_2, y_1, y_2, h_1, h_2$ is arranged in Tab 2.

The velocity field comparison for identical cross section profiles with physical model was performed for each turbulent model as well. Both v_x and v_y velocity vectors were compared to measured ones. For physical model velocity measuring the micro wing was used. This method was used for both velocity vectors but such a method is accurate just for longitudinal velocity vector because of micro wing calibration. Here, at the cross velocity vector had just an informative character.

At the both aspects of turbulent model accuracy comparison the best fitted turbulent model to physical model is RNG model overall. The total average deviation of monitored hydraulic parameters is 9.4%.

Tab 2 Cross sectional parameters comparison

	Parameters					Deviations							
	Physical model - experiment 177, series I	Model k-ε	Model RNG	Model LES		Physical model - experiment 177, series I	Model k-ε	model RNG	Model LES		Average	max	min
$Q_1 =$	0.01	0.01	0.01	0.01	$m^3 \cdot s^{-1}$	-	10.6	10.5	10.8	%	10.6	10.8	10.5
$Q_2 =$	0.00	0.00	0.00	0.00	$m^3 \cdot s^{-1}$	-	21.6	21.1	21.9	%	21.5	21.9	21.1
$Q_b =$	0.01	0.01	0.01	0.01	$m^3 \cdot s^{-1}$	-	6.9	7.0	7.1	%	7.0	7.1	6.9
$v_1 =$	0.28	0.27	0.27	0.27	$m \cdot s^{-1}$	-	1.9	1.8	2.5	%	2.1	2.5	1.8
$v_2 =$	0.07	0.06	0.06	0.05	$m \cdot s^{-1}$	-	19.9	19.3	20.3	%	19.8	20.3	19.3
$y_1 =$	0.09	0.08	0.08	0.08	m	-	8.6	8.6	8.2	%	8.5	8.6	8.2
$y_2 =$	0.09	0.09	0.09	0.09	m	-	1.6	1.6	1.5	%	1.6	1.6	1.5
$h_1 =$	0.04	0.03	0.04	0.03	m	-	20.5	6.4	20.5	%	15.8	20.5	6.4
$h_2 =$	0.04	0.04	0.04	0.04	m	-	8.6	8.6	8.6	%	8.6	8.6	8.6

Overall
Average: 11.1 9.4 11.3

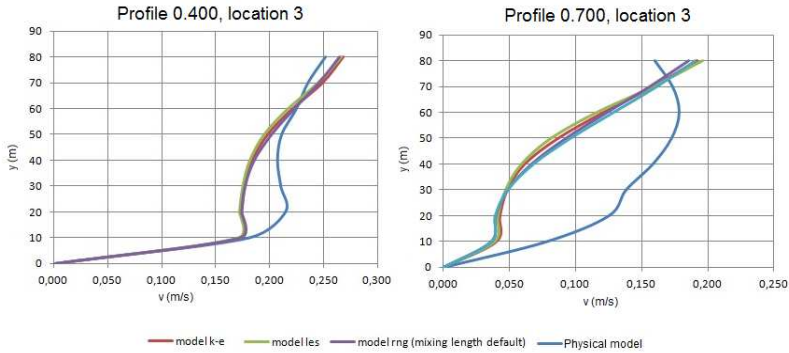


Fig. 3 Velocity field comparison for various turbulent models - selection

5. QUANTIFICATION OF RNG K- ϵ MODEL ACCURACY

The goal of the model verification procedure was to quantify the mathematical model accuracy, compare it to the physical research and decide if the CFD modelling is an accurate enough to be used as relevant scientific method. Basically it is a process of accuracy quantification and representativeness of mathematical model compared to real world from possible utilization perspective [Molnár, 2010].

Main verifying were A series simulations A1 and A2. Because the back control with physical model was impossible, some of the mathematical model parameters had to be adapted to physical model.

The verification of A1 and A2 simulations were monitored in four categories:

- The profile parameters comparison (discharge $\text{m}^3 \cdot \text{s}^{-1}$)
- Comparison of velocity fields
- Visual comparison
- Convergence quality

The profile parameters comparison was made for two profiles which location was identical for mathematical and physical model. The localization of profiles was $(3 \div 5)h$ above (upstream) and under (downstream) the lateral spillway. Other profiles (baffles) were set for mathematical model to avoid the volume error as well as comparison to boundary condition discharge output in result file.

Depending on discharge Q_1 , Q_2 in profiles above the lateral spillway (upstream) and under the spillway (downstream) the Q_b was specified according to $Q_1 = Q_2 - Q_b$.

Velocity fields were post processed and compared in priority locations near the lateral spillway identically to physical model experiment 177, series I.

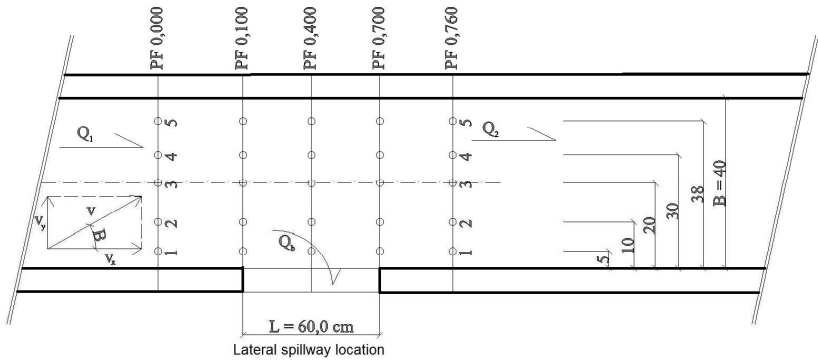


Fig. 4 Compared velocity fields

Visual comparison was made with photogrammetric method and streamline visualization generated by CFD software.

Even if quality convergence is not the guarantee of relevant results compared to real world or physical model it is an important indicator of stability and numerical setting correctness. The simulations were set as steady state simulation with maximum 1% variation threshold of total mass, average mean kinetic energy, average mean turbulent energy and average mean turbulent dissipation.

The simulation A1 was compared with experiment 177, series I of physical research of sharp crested lateral spillway as follows:

Most markedly deviation is velocity v_2 value. The deviation of discharge Q_2 is just a result of calculation depended on v_2 in profile 0.700. In this case is the relevance of physical model not so clear because the v_2 measurements in physical research show itself as problematic overall (Tab 4).

Tab 3: Model verification

Parameter	Physical model Experiment 177, series I	CFD	Unit	Deviation [%]
Q_1	0,010	0,009	$\text{m}^3 \cdot \text{s}^{-1}$	10,53
Q_2	0,003	0,002	$\text{m}^3 \cdot \text{s}^{-1}$	21,06
Q_b	0,007	0,007	$\text{m}^3 \cdot \text{s}^{-1}$	6,99
v_1	0,280	0,275	$\text{m} \cdot \text{s}^{-1}$	1,81
v_2	0,069	0,056	$\text{m} \cdot \text{s}^{-1}$	19,31
y_1	0,089	0,081	$\text{m} \cdot \text{s}^{-1}$	8,59
y_2	0,091	0,089	m	1,62
h_1	0,039	0,031	m	20,50
h_2	0,041	0,037	m	8,64

Tab 4: Experiments with same settings in physical model, series I with large v_2 deviations

Experiment	L [mm]	s [mm]	Q_1 [l/s]	Q_b [l/s]	Q_2 [l/s]	v_1 [mm/s]	v_2 [mm/s]	h_1 [mm]	h_2 [mm]	v_1 [m/s]	v_2 [m/s]
176	600	50	10	9,927	0,073	97,000	98,000	47	47	0,257	0,002
177				7,488	2,512	89,000	90,500	39	40,5	0,28	0,069
178				5,071	4,926	81,000	83,000	31	33	0,308	0,148
179				2,934	7,066	72,500	74,500	22,5	24,5	0,345	0,237

Another difference compared to physical model was the specification of depths h_1 and h_2 of lateral spillway (Fig. 5). In the mathematical simulation post processing, the depths were extracted from result file directly but in the physical model the depths were calculated according to $h = y - s$, which is not representative value compared to reality because after the upstream edge of lateral spillway (beginning of overflow edge) a critical depth will occur according to

$$\frac{dy}{dx} = \frac{d}{dx} \left(y + \frac{\alpha Q^2}{2 g S^2} \right) = 0 \quad (1)$$

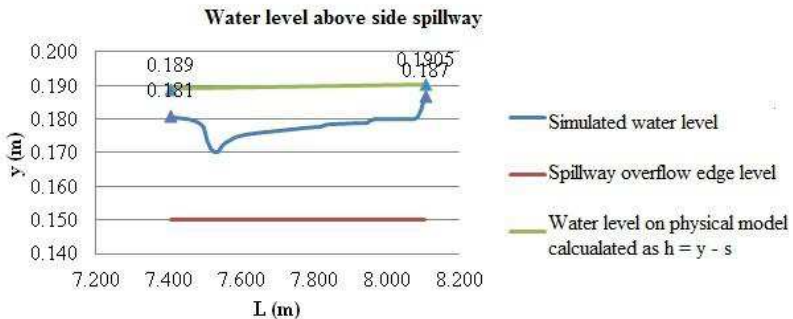


Fig. 5 Water level above lateral spillway edge

Simulated states also approved the water level rising postulate above the lateral spillway edge which is correct.

Comparison of velocity fields was carried out in terms of profile location of physical model measurements (Fig. 6).

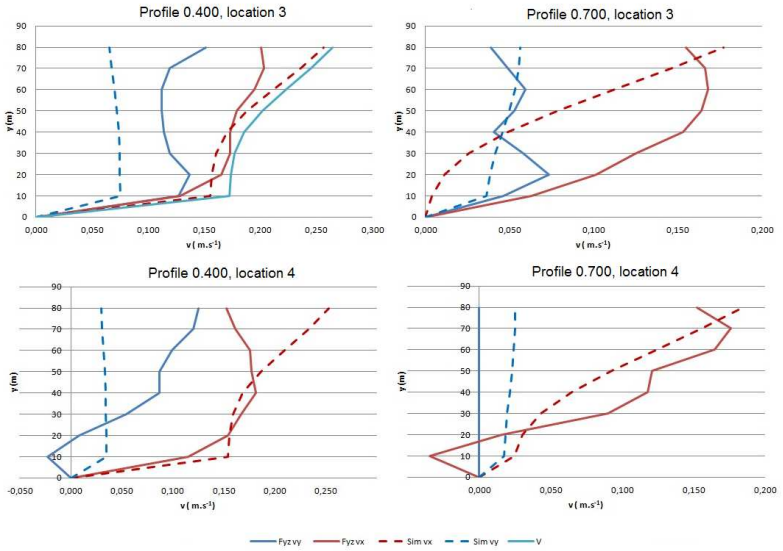


Fig. 6 Velocity field comparison of CFD model, series A, simulation A1 and physical model series I, experiment 177 - selection

For visual comparison the streamlines were used to get overview about discharge distribution and vortices. The photogrammetric method was used to obtain the streamlines in physical model. The mathematical model is able to generate streamlines automatically (Fig. 7).

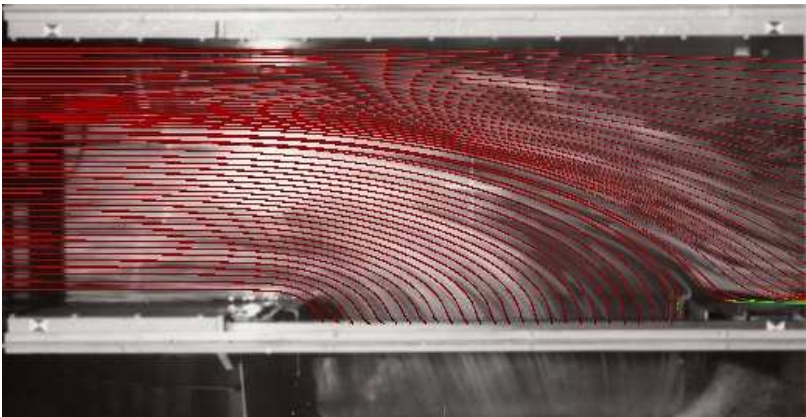


Fig. 7 Visual comparison trough the streamlines (plan view) - red are simulated and white made by photogrammetric method in lab

6. CONCLUSION

The comparison of accuracy and relevancy of CFD model was done for two different models with average deviation of 11.3 %. This deviation includes also the biggest deviation compared to physical model v_2 and h_1 which should be considered as wrong specified in physical research. Most lowest deviation are values of water level which were simulated with average deviation of 3.1 %. In this case the correlation between physical and mathematical research is well also when taking into the consideration the possibilities of used equipment to measure the water level with precision ± 1 mm. E contra the velocity measuring shows that the used method is affected by large number of factors which should be taken into consideration.

Based on the comparison of the simulations with different turbulence models and physical model measurements, the k- ϵ RNG turbulence model was shown as the most accurate turbulence model for tasks such as lateral spillway flow analyses.

From the CFD code accuracy point of view there should be also considered other calculating methods where the average CFD deviation is adequate.

In the context of hydraulic parameters post processing on physical model experiments it should be noted that from all 255 measured experiments, almost 25 % had to be excluded with deviation over 31 % [Miškay, 1976].

7. REFERENCES

- ANSYS, INC. 2009. Ansys Fluent 12.0 Theory guide. Canonsburg : Ansys, 2009.
- DVOŘÁK, L. 2012. Hydraulické poměry v předpolí hrázového přelivu. Brno : Vysoké učení technické v Brně, 2012.
- FLOWSCIENCE, INC. 2011. Flow 3D v10 Users manual. Santa Fe : Flow Science Inc, 2011.
- HUBER, BORIS. 2010. Prevention of air-entrainment at the outlet of a pumped storage plant – large scale model tests. Wien : IAHR 2011, 2010.
- MÄSIAR, E., KAMENSKÝ, J. 2001. 1986. Hydraulika pre stavebných inžinierov I. Bratislava : ALFA, 1986.
- MAYS, L. W. 1999. Hydraulic design handbook. New York : MacGraw-Hill, 1999.
- MIŠKAY, V. 1976. Hydraulický výpočet bočného prepadu. Bratislava : STU v Bratislave, 1976.
- MOLNÁR, V. 2010. Počítačová dynamika tekutín. Bratislava : STU v Bratislave, 2010.

Analysis and visualization of irrigation distribution systems

M. Cisty, Z. Bajtek, L. Celar

(Faculty of Civil Engineering, STU Bratislava, Slovak Republic - Radlinskeho 11 810 05 Bratislava, milan.cisty@stuba.sk)

Abstract

At the time of its design and during its life cycle an irrigation system must fulfill the purpose for which it was designed and must also comply with the requirements of its users. Users' needs may change over time; they may change over the course of the irrigation season, and the equipment they require may also vary. These changes may alter the conditions of the irrigation system's operations. These changes also call for an assessment or analysis of already designed irrigation systems especially, under different conditions of its operation, i.e. for example, the various demands. Over the years many tools and programs have been developed for the purpose of hydraulic analyses of pressurized water distribution networks. Among the best known and most widely used EPANET can be included, not only because of its graphical user interface (GUI) version, but also because its functions can be used in a variety of programming environments such as Visual Basic, Matlab, C++, etc. In order to briefly describe the many possible operating conditions, we need some tools, the design, development and testing of which is the main task of this paper. Such an analysis has many applications in the design and operation of irrigation networks.

Keywords

Irrigation networks, Epanet, R-package, simulation model, demand-driven analysis, pressure-driven analysis

1. INTRODUCTION

A hydraulic assessment of an irrigation network is particularly important when optimizing its operation, as well as in the context of a proposal for this modernization and reconstruction. In the case of a pressurized water distribution system, pressure fluctuations in the system have a negative impact on the proper functioning of irrigation details, such as traveling gun sprinklers, pivot sprinklers or micro-sprinklers. Such a hydraulic analysis is particularly important for the verification of the optimal pressure conditions during the operation of the system, which in the case of irrigation systems, significantly varies over in time. Hydraulic models are used to simulate network performance under diverse management alternatives and water demand scenarios [Rodríguez Díaz et al. 2009]. Thus, the integration of these hydraulic models in a decision support system (DSS) allows the evaluation of actions and the introduction of different factors in the simulation

process to assess unforeseen events [Le Bars & Le Grusse 2008]. [Lamaddalena 1997] and [Lamaddalena and Pereira, 1998] have proved that even in cases where the flows in a network comply with the original dimensioning flows, states may occur during operations with very low pressures in the system, for example, due to inappropriate irrigation detail placements during operations. Therefore, it is evident that it is necessary to address the performance analysis of an irrigation system, because of the significant spatial variability of flow situations [Calejo et al. 2005]. This variability is particularly important, because the node demands are relatively large (for example, in comparison with demands in drinking water distribution systems). In view of these facts, several models have been developed to improve the analysis and functionality of irrigation systems while one is accomplishing their design or for purposes of their operation and management [Lamaddalena and Sagardoy, 2000]. They are very helpful in irrigation network management for detecting critical points or identifying malfunctions. The disadvantage of these simulation models is that they cannot be easily adapted to situations where the behavior of the network is significantly affected by pressure conditions. In order to perform an analysis of irrigation networks, [Lamaddalena and Pereira 2007] developed the FLUCS model. It is necessary to link the data acquisition system with the analysis tool. Hence, another dimension of the integration is based on the use of GIS not only as a common framework and reference point but also as the primary display paradigm. This integration effectively transforms the system into a spatial decision support system (SDSS) [Ochola & Kerkides 2004]. SIMIS is an FAO conceptual DSS used in irrigation districts for planning, maintenance and administrative tasks [Mateos et al. 2002].

Nowadays irrigation managers require several tools to assess the performance of irrigation networks, such as hydraulic models, geographic information systems (GIS) or decision support systems (DSS) which are available but used as independent elements. The objective of this work is to provide a new tool to assess the performance of distribution networks and the quality of the service provided. The results can be spatially identified and managed in an incorporated visualization. The aim was to provide a complex overview of a hydraulic evaluation of water distribution systems in irrigation, mainly from the point of view of its variable operation.

2. MATERIAL AND METHODS

2.1 Generator

For the purpose of this work, a generator of the demand situations was created, because as has already been emphasized, an irrigation system can be characterized by significantly variable demand situations. It is not possible to assess and properly evaluate a system by taking only a single demand situation into consideration. The authors have created a tool for generating realistic demand situations, the task of which is to place the selected irrigation detail (user-defined types of sprinklers and eventually groups of sprinklers) in various places in an

irrigation network according to pre-set rules. This is done alternatively, as the placement of the sprinkler changes, which reflects the actual operation of an irrigation system. Such alternative placements of irrigators leads to a high amount of demands and hydraulic situations, which have to be assessed and evaluated by the simulation model. In general, we can conclude that during an operation, hydraulic situations in which there is a demand concentrated on some parts of the network (irrigators are close to each other in some places) are usually more problematic with regard to ensuring there is necessary pressure in hydrants. The number of irrigators in a group, together with a minimal number of free hydrants between the groups (hydrants without a demand), is the main input parameter for the proposed generator to create demand situations. Because of this strategy, prior to calculating the demand situation of the irrigation system, a realistic deployment of groups of sprinklers is established together with the time schedule of the operational status. This plan also considers various facts, such as the requirements from the operator of the network and pump station and the agricultural requirements (water requirements of crops, etc.).

2.2 Evaluation of the demand scenarios from the generator

The EPANET computer model was used for the hydraulic analysis. Its GUI version served for the development of the hydraulic model of the network studied. Furthermore, its Toolkit version (basically a DLL file) was incorporated in the R program interface, thus allowing the creation of various demand scenarios by the generator. The calculation of the pressures follows and then the demands in the demand scenarios generated by the Generator. An older irrigation system, “Trhove Myto II” (Figure 1) was used the case study. This system is located in southern Slovakia. It is approaching the end of its useful life and is suitable for demonstrating reconstruction design procedures. It was originally designed as a branched network with two main branches. A hydraulic model was created for the purpose of the system analysis; it contains 188 pipes and 189 nodes. As with most of the systems designed in the former Czechoslovakia, the pipe material is a combination of asbestos cement and cast iron pipes.

Two alternatives were generated, i.e., one with four and another with five sprinklers in a group. Considering the arrangement of the proposed system and taking into account its technical parameters there was, a total of 28 groups with four sprinklers and 23 groups with five sprinklers. These represent potential placements the irrigators; not all of these groups work at the same time. A scheme of simultaneously working groups was created by the generator. In the case of a group of 4-sprinklers 23 simultaneously operating groups an 18 in the case of a 5-sprinklers, working at the same time in group. The number of groups depended on the maximum delivery rate of the pump station.

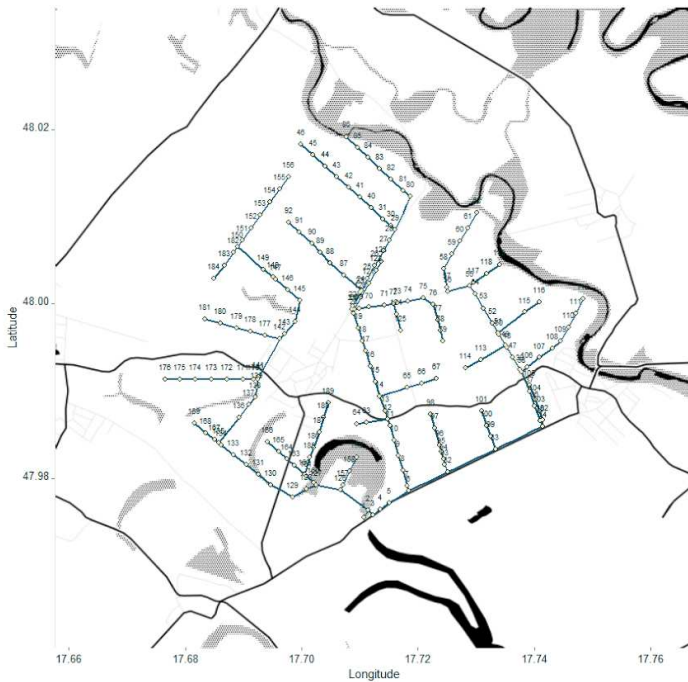


Fig. 1 Situation of the "Trhove Myto II" irrigation network

The number of irrigators in a group, together with a minimal number of free hydrants between the groups (hydrants without a demand), are the main input parameters in the proposed generator to create demand situations. In this paper the authors investigated the operation of the system when the system is fully loaded, e.g., the total number of irrigators was considered for a situation when the maximum possible flow is taken from the pumping station. The combination (without any repetition) of these values represents the amount of possible hydraulic situations (placement of the possible irrigators). A total of 98280 possible situations was enumerated by the generator for the group of 4 irrigators; in case of 5 irrigators in a group, the total number was 33649 situations. This value represents the total number of hydraulic situations which were evaluated.

Furthermore, the generator allows two alternative demands – pressure analysis. In the first case the demand driven-analysis (DDA) is a demand from the node constant and does not depend on pressure (7.5 l.s^{-1}). In the second case a pressure-driven analysis (PDA), was accomplished; at first it was necessary to determine the parameters of the irrigator used according to its pressure/flow curve, which is usually provided by the manufacturer. The "emitter coefficient" and "emitter exponent" parameters serve in EPANET for a definition of this function. It is

defined as the dependence between the pressure and the pressure in the node using the following form:

$$Q = C \cdot P^y \quad (1)$$

Where Q is the flow through a sprinkler (demand); C is the emitter coefficient; P is the pressure in the sprinkler; and y is the emitter exponent.

2.3 Evaluation of the operation's variability

The evaluation of the operation generator was focused on two main areas. The first was the mean pressures for both alternatives (DDA, PDA). The second evaluation represents the probability of satisfying the required demands in the nodes in the PDA. Due to the significant amount of the output data, it was decided that these data would be aggregated into the results by each group to the mean pressure in a group for the demand situation. Box plot graphs were chosen for the data visualization. They offer a simple possibility for the evaluation and also provide a better overview of the large amounts of given data.

3. RESULTS

The results can be seen in the first figure, (Fig. 2) represents a histogram for the frequency of the pressure in a demand situation for both the DDA and PDA. In the next figures (Fig. 3, 4, 5 and 6) the values for the DDA and PDA for each evaluated alternative separately are presented. The horizontal axis in these figures represents the individual demand group. The vertical axis shows the mean pressure head in the demand group. As we can see, the minimum pressures in the PDA (Fig. 4 and 6) are at least 10-15 meters higher than in the case of the DDA (Fig. 3 and 5). It can also be noted that the dispersion of the values in the PDA is smaller than in the case of the demand-driven analysis. This can be logically inferred from the fact of using the fixed demand, which is greater — this demand does not exist in a real situation, because of the insufficient pressure in the network, which limits this value.

For all the cases, we can briefly identify the groups with the largest variances of the values, for example in Fig. 3 it is group 13. These figures illustrate the degree to which these groups are affected by changes in the demand situations in other parts of the network. This information can in both cases help us to identify a potentially problematic group; this was subsequently addressed in a more detailed further analysis. Eventually, it is possible to propose for this part of an irrigation system another way to operate the irrigation or sprinklers or chose other irrigators which need different pressures at the inlet to the machine. Better pressure is characteristic of the PDA, which is a consequence of a reduction in demand in the node in the case of the lower pressure.

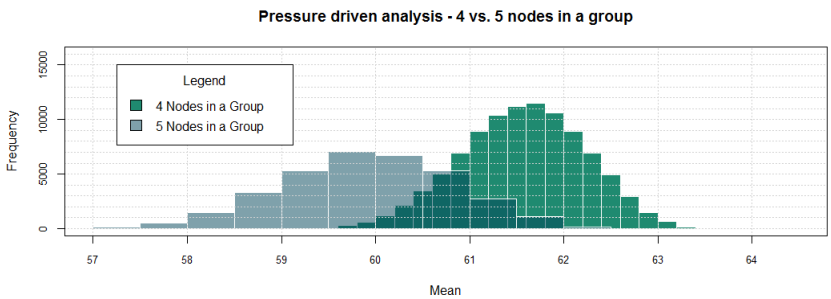
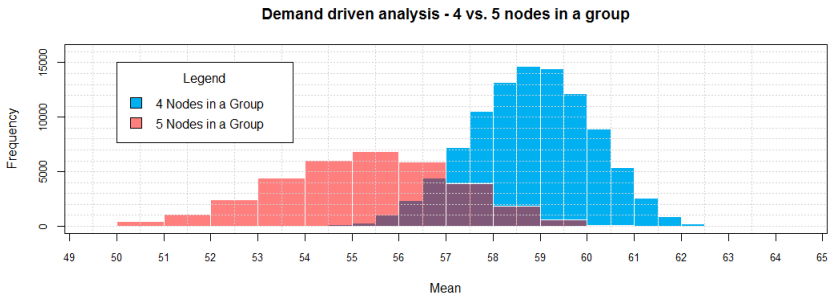


Fig. 2 Comparison of two types of analysis using histograms.

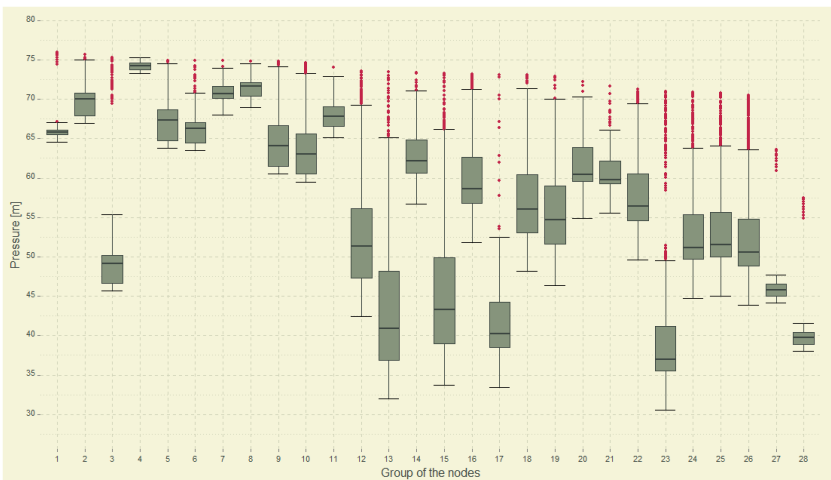


Fig. 3 Demand-driven analysis, Boxplots of mean pressures in a group (4 hydrants in a group)

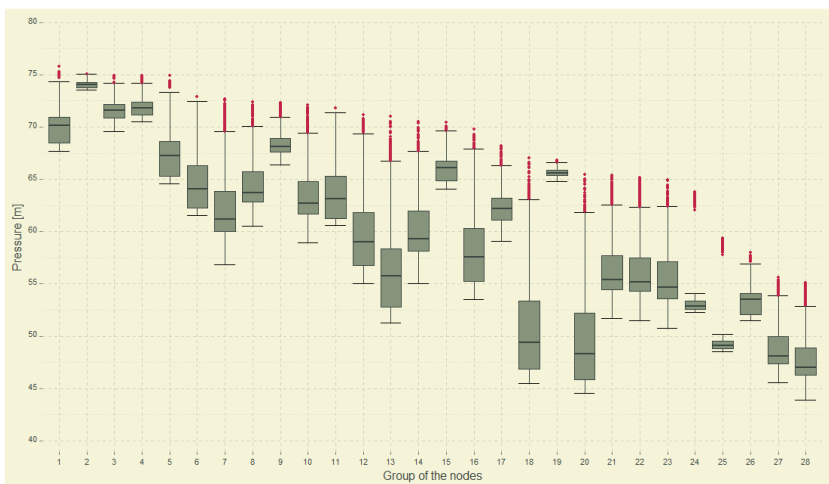


Fig. 4 Pressure-driven analysis, Boxplots of mean pressures in a group (4 hydrants in a group)

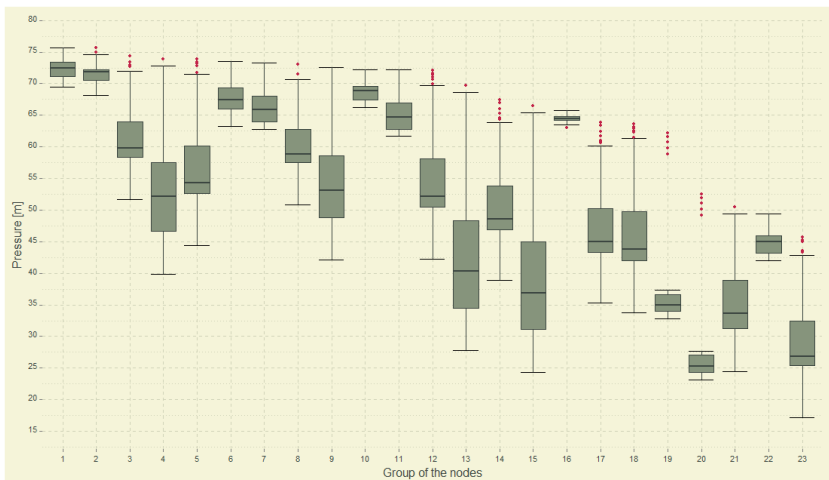


Fig. 5 Demand-driven analysis, Boxplots of mean pressures in a group (5 hydrants in a group)

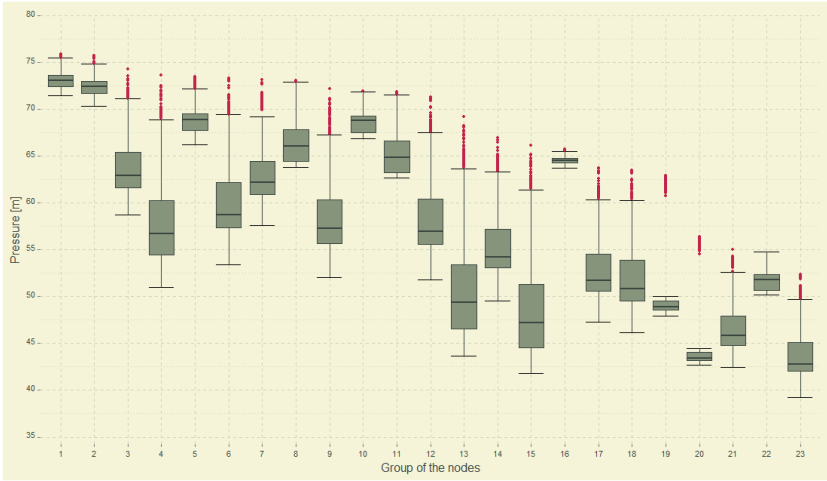


Fig. 6 Pressure-driven analysis, Boxplots of mean pressures in a group (5 hydrants in a group)

By these means we can obtain a tool for identification of the hydrant groups, in which the most commonly insufficient demand appears; respectively, it is also possible to identify a possible critical group for which the required nodal demand is not achieved, which is important information with regard to irrigation requirements. A further evaluation has aimed at an analysis of demands at the hydrants during the PDA. The aim was to analyze at what level the demand in the demand nodes is influenced by the pressure, which could be evaluated in this type of analysis. Logically, the DDA does not offer this type of assessment. The mean deficits of the demand in the nodes were calculated according to the following formula:

$$\bar{Q}_c = \frac{\sum_{i=1}^n (Q_{ci} - Q_p)}{Q_p} \quad (2)$$

Where \bar{Q}_c is the average deviation from the required demand at the node; Q_{ci} is the nodal demand calculated by the simulation model; Q_p is the required (design) flow through the sprinkler.

The obtained values of the deficit in the amount of the water supplied, which is based on the previous equation, is interpreted in Fig. 7. The figure shows the relative average deficit in the demand nodes in the form of a boxplot, when running all the demand situations as in the case of the PDA. Thanks to this, they

can provide a better understanding of the pressure behavior as well as the performance of the whole network within the demand situation.

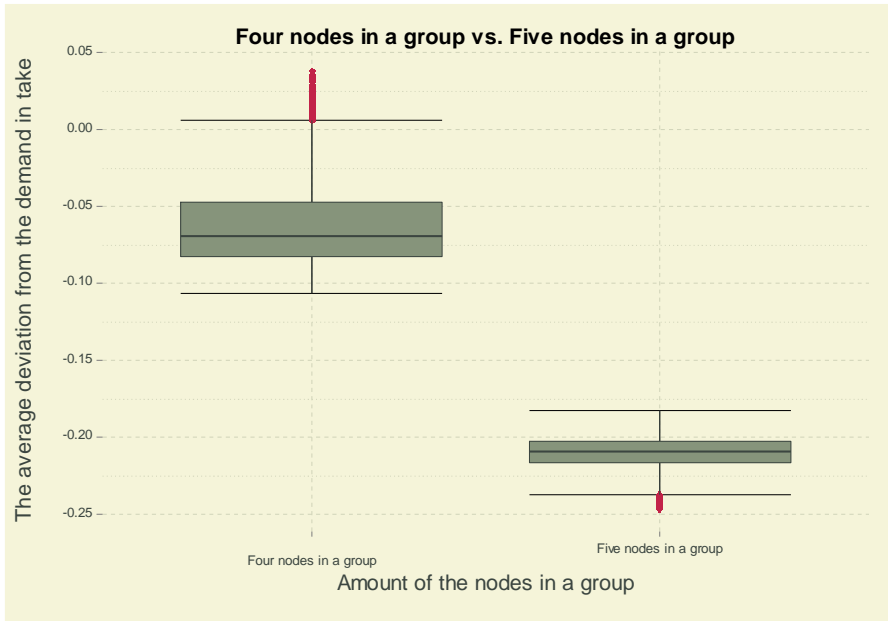


Fig. 7 The average deviation from the demand intake during the pressure-driven analysis

4. DISCUSSION AND CONCLUSIONS

The use of the R - environment for statistical computing for a water distribution system can be justified by taking into account the variability of an operation characterized by an amount of data from a number of operational and demand situations (pressures, flow rates, etc.) which have to be evaluated or, respectively, visualized by statistical methods. With the aim of providing a complex tool for evaluating and analysis of irrigation network. The result would be the creation of a package for such an analysis, which would provide a better overall picture of the system as well as the quantity of water supplied. The final tool will be composed in the R environment and will be produced as a package (library) in the language of R. The GUI version can still serve for the formation of the actual hydraulic model, and its DLL library can serve to detect the actual pressure or demands in hydrants for a potentially large number of demand situations (variable spread sprinklers) generated by the afore mentioned generator.

5. REFERENCES

- CALEJO, M.J., LAMADDALENA, N., and PEREIRA, L.S. 2005. Pressurized irrigation network modelling: a flow driven analysis approach. In: Boaventura Cunha, J., Morais, R., Proceedings of the EFITA/WCCA 2005 Joint Conference on Information Technologies in Agriculture. EFITA and Univ. Trás-os-Montes e Alto Douro, Vila Real, pp. 260–265.
- LAMADDALENA, N. 1997. Integrated simulation model for design and performance analysis of on-demand pressurized irrigation systems. Ph.D. Thesis. Instituto Superior de Agronomia, Universidade Técnico de Lisboa.
- LAMADDALENA, N. and PEREIRA, L.S. (1998): Performance analysis of on-demand pressurised irrigation systems. In: Pereira, L.S., Gowing J.W.(Eds.), Water and the Environment: Innovation Issues in Irrigation and Drainage (1st. Inter- Regional Conf. Environment-Water, Lisbon), E and FN spon, London, pp 247-255
- LAMADDALENA, N., & PEREIRA, L. S., 2007. Pressure - driven modeling for performance analysis of irrigation systems operating on demand. *Agricultural water management*, 90(1), 36-44.
- LAMADDALENA, N., SAGARDOY, J.A. 2000. Performance analysis of on-demand pressurized irrigation systems. Irrigation and Drainage Paper No. 59. FAO, Rome.
- LE BARS, M. & LE GRUSSE, P. 2008 Use of a decision support system and a simulation game to help collective decision-making in water management. *Comput. Electron. Agric.* 62, 182–189.
- MATEOS, L., LÓPEZ-CORTIJO, I. & SAGARDOY, J. A. 2002. SIMIS: the FAO decision support system for irrigation scheme management. *Agric. Wat. Mngmnt.* 56, 139–206
- OCHOLA, W. O. & KERKIDES, P. 2004 An integrated indicator-based spatial decision support system for land quality assessment in Kenya. *Comput. Electron. Agric.* 45, 3–26.
- PEZZINGA, G. 1999. Quasi-2D model for unsteady flow in pipe networks. *J. Hydrogen Energy* 125 (7), 676–685.
- PLAYÁN, E. & MATEOS, L. 2002 Modernization and optimization of irrigation systems to increase water productivity. *Agric. Wat. Mngmnt.* 80 (1–3), 100–116.
- RODRÍGUEZ DÍAZ, J. A., PÉREZ Urrestarazu, L., Camacho Poyato, E. & López Luque, R. 2009 IGRA: a tool for applying the benchmarking initiative to irrigated areas. *Irrig. Drainage* 54, 307–319.

Acknowledgement

This work was supported by the Scientific Grant Agency of the Ministry of Education of the Slovak Republic and the Slovak Academy of Sciences, Grant No. 1/0665/15.

Stormwater and snowmelt runoff storage control and flash flood hazard forecasting in the urbanized coastal basin

M. Szydłowski, P. Zima, K. Weinerowska-Bords, P. Mikos- Studnicka, J. Hakiel, D. Szawurska

(Department of Hydraulic Engineering, Faculty of Civil and Environmental Engineering Gdańsk University of Technology ul. Narutowicza 11/12 80-233 Gdańsk, Poland, coresponding author tel. +48 0 58 347 21 12 email: patstudn@pg.gda.pl)

Abstract

City of Gdańsk is located in a coastal region where changing climatic conditions increase the frequency of extreme weather events. Developing urbanization affects the hydrology of natural basins by simplification of the drainage system and reduction of infiltration and base flow. Consequently greater runoff rates flow into storm water collection systems, reservoirs and surrounding water bodies. Not only infrastructures of urban areas but also citizens are exposed to the effects of heavier rainfalls or sudden snowmelts, resulting in flash floods, damages of hydro-technical systems, as well as environmental risks. Development of integrated solutions including precipitation, stream flow and reservoirs storage monitoring and management can reduce flood risk and help to protect the public health. In years 2011-2013 Department of Hydraulic Engineering (Faculty of Civil and Environmental Engineering of Gdańsk University of Technology) in collaboration with The Provincial Fund For Environmental Protection and Water Management in Gdańsk and Gdańskie Melioracje Sp. z o.o undertook the implementation of storm water monitoring system in the Strzyża River basin in Gdańsk. The results of measurements allowed performing the HEC-HMS hydrological model for one of the most flood prone areas of Gdańsk. Research on the development of the technical and non-technical methods of flood control, numerical modeling for build-up area inundation prediction, expansion of the existing rainfall-runoff and storage monitoring system, integrated water quantity and quality analysis are continued in frame of ongoing research project (2015-2017). The aims, objectives and preliminary results of the project will be discussed in the proposed paper on WMHE 2015 International Symposium in Brno.

Keywords

flash floods, urbanized basin, stormwater management, surface runoff, numerical modeling

1. INTRODUCTION

Urbanized regions of Gdańsk very often suffer from flash floods as a result of high precipitation. This type of spatial flood is caused mainly by creeks and

streams overflowing during torrential rains and storms. In the urbanized catchment, with many impervious areas, a large volume of surface runoff gets into drainage network in a very short time. The velocity of water is high so streams rise quickly and more rapidly with higher peak discharge, than those in undeveloped areas [BARBOSA A.E., et.al., 2013]. In the last decades the natural cover of the Strzyża Creek basin has been replaced with impermeable surfaces such as huge parking lots, residential and industrial areas, shopping centers and driveways. An intensive expansion of the urban infrastructure in the direction of the surrounding moraine hills can be observed in south and east districts of Gdańsk. All those transformation caused not only reduction of the temporary surface storage, limitation of the infiltration and base flow, but also completely changed natural drainage patterns. Land use modifications strongly affected primary hydrological cycle that resulted with higher flood risk in Gdańsk according to Strzyża Creek conveyance and reservoirs capacity [SZYDŁOWSKI M. and ZIMA P., 2011]. In light of the growing threat of flood preventive integrated solutions, developed with the collaboration of the representatives of engineering, environmental science and city authorities should be taken.

1.1 The Strzyża Creek catchment characteristics

The Strzyża Creek is one of the most important storm and snowmelt water receivers in Gdańsk. It starts in the upland region of Gdańsk's moraine hills, flows through the green suburbs and then crosses the strongly developed areas of the city (Fig.1). The stream finally supplies the Dead Vistula and consequently the Baltic Sea. The denivelation of the Strzyża Creek basin is significant and reaches 60 meters with highest hills rising up to 170 m ASL. The total catchment area is about 35 km² and the total length of the stream is 13 km. The most important tributaries of the watercourse are Królewski Creek, Matarnicki Creek and Jasioń Creek. The river flows in a combined natural and artificial channel with slope varying from 0.5% to 5%. The value of Manning's roughness coefficient in well-maintained concrete channel is 0.013, while in a streambed with vegetated banks 0.06 [CHOW, V.T., 1959]. Along the stream flow there are eight reservoirs varying in size of a surface area from 0.3 to 2.7 hectares, of a total capacity of approx. 80 thousand m³.

In the upper basin the natural streambed is carved in clay- rich glacial sediments with sand and gravel. On the hills of the western part of the catchment forest management is conducted. The upper section of the watercourse lies in the Nature Reserve Forests in the Strzyża Valley where sediment transport and strong erosion of the riverbed take place.

In the lower catchment, bottom of the stream lies on alluvial sediments, sand, gravels and silts [HYDROPROJEKT 1994]. After leaving the reserve, brook flows in artificial channel through reservoirs: Nowiec II, Górne Młyny, Ogrodowa, Srebrzysko. The lower catchment is covered with dense urban, residential and industrial areas.

2. THE STORM WATER MONITORING SYSTEM IN THE STRZYŻA CREEK BASIN IN GDAŃSK

In last decades the Strzyża Creek catchment was strongly transformed that caused a significant acceleration of surface runoff and increase of discharge in the channel. The change of hydrological cycle of the basin resulted with rising flood risk in the city due to limits of stream conveyance and reservoirs capacity. Moreover during heavy storms in 2001 and 2010 great catastrophes of the Strzyża Creek reservoirs dams took place.

In years 2011-2013 Department of Hydraulic Engineering, Faculty of Civil and Environmental Engineering of Gdańsk University of Technology, in collaboration with The Provincial Fund For Environmental Protection and Water Management in Gdańsk and Gdańskie Melioracje Sp. z o.o started the implementation of storm water monitoring system in the Strzyża Creek basin in Gdańsk [SZYDŁOWSKI M., 2011].

The objective of the project was to develop the water stage and precipitation monitoring network in discussed basin. All gauges were connected to a single data acquisition system. Starting from 2013 records can be view and download easily via a web interface <http://anywhere.hydranet.pl/>. Till that time, observed stages can be converted into discharges and compared with those resulting from numerical simulations. Consequently previously prepared hydrological model of upper Strzyża Creek basin has been supplemented by the lower part of the catchment (Fig. 2). The verified model in the future can be used as a prognostic tool for flood prone areas of Gdańsk.

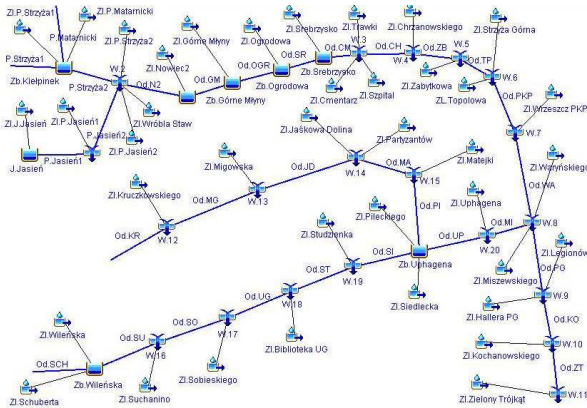


Fig. 2 The structure of the HEC-HMS hydrological model of the entire Strzyża Creek basin

2.1 Monitoring network- stage 1

Localization of the monitoring gauges was based on complex analysis of the Strzyża Creek catchment area and hydrographic network of the region (Fig. 3).

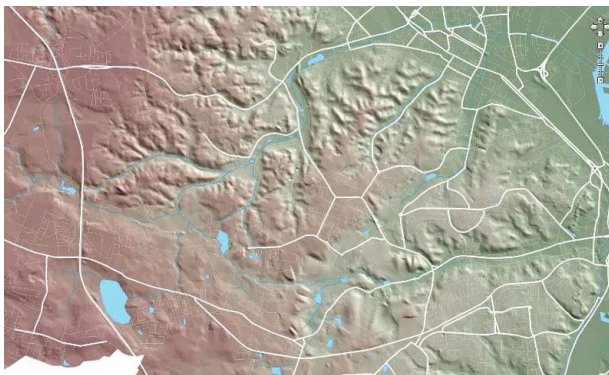


Fig. 3 Digital terrain model (DTM) of the Strzyża Creek catchment area with hydrographic network, roads marked with white color (source: Geographical Information System (GIS) city of Gdańsk, <http://www.gis.Gdańsk.pl>)

Installation of the elements of the system was a compromise between the needs associated with the diagnosis of spatial parameters of the catchment and the possibility of purchasing measuring equipment. The on-site investigation and verification of data on land cover, basin shape and drainage network were done for entire area of the Strzyża Creek catchment and its tributaries like the Królewski Creek, Jaśkowy Creek and Matarnicki Creek. New stations included water stage monitoring in open channels, the hydrostatic pressure and flow in the storm sewer collector and precipitation gauges. Additionally measurement stations owned by Gdańskie Melioracje and Gdańsk University of Technology have been added to the system. The localization of the measurement points and cross-sections for the monitoring system are presented in Fig. 4.

The historical and current precipitation values and water stages at chosen cross-section of the Strzyża Creek channel can be view by the web interface <http://anywhere.hydranet.pl/> (Fig. 5).

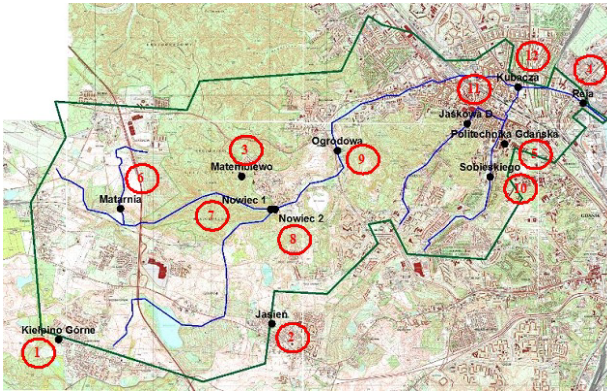


Fig. 4 Location of measuring gauges in the Strzyża Creek catchment

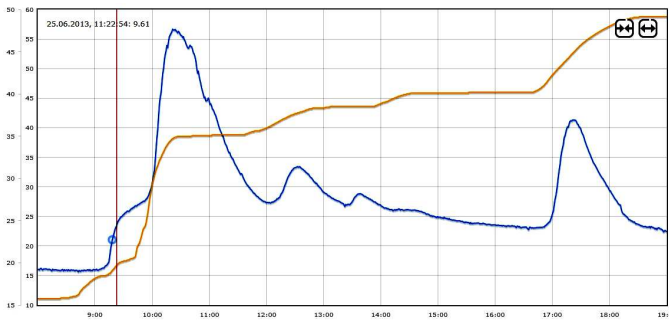


Fig. 5 Exemplary cross-section, water stage marked with blue color, precipitation marked with yellow color, date 25.06.2013
[\(http://anywhere.hydranet.pl/\)](http://anywhere.hydranet.pl/)

2.2 Monitoring network- stage 2

According to limited found the first stage of monitoring network did not include the reservoirs control stations. Thus in 2015-2017 authors are going to continue research on the development of the technical and non-technical methods of flood control including storage monitoring system. What is more the integrated water quantity and quality analysis [MIKOS-STUDNICKA P. and SZYDŁOWSKI M., 2015] is also the purpose of ongoing research project “Stormwater and snowmelt runoff storage control and flash flood hazard forecasting in the urbanized coastal basin”. The project duration is planned for 2 years. Collected data will be used to the Strzyża Creek rainfall-runoff hydrological model assessment and calibration. Optimization of short and long-term operation of single and multi-reservoir systems could also be achieved. Furthermore for assumed catchment simulation of outflow based on actual measurements of precipitation and analysis of potential flood risks will be able. New water level

gauges will be placed on 8 reservoirs and help to estimate their level-elevation-area functions. The example of water level station installed over the reservoir is shown in Fig. 5.

Additionally hydrodynamic model of interaction between surface runoff and storm sewer system will be constructed. The model will be based on the two-dimensional equations. As a result, it will be possible to simulate the drainage system overload including local flooding from the storm sewers.

Finally the meteorological data on the amount of precipitation will be used as input information to developed model of hydrological forecast. As a result it will become achievable to predict extreme stormwater outflows from all sub-catchments and undertake some preventive actions to secure the city and its inhabitants.



Fig. 5 Water level gauge on Wileńska reservoir in the Królewski Creek catchment

3. RESULTS OF HYDROLOGICAL MODELLING

The developed hydrological model of the Strzyża Creek catchment is being verified at the moment of studies. Only by comparing the measurements from the monitoring system with simulations carried out with model it can be proved that prepared numerical solution can be reliable tool in avoiding and predicting floods over the urbanized areas of the city of Gdańsk. However the urban basin has very complex nature and can react differently to identical precipitation. The reason among others can be antecedent moisture conditions of the catchment or failure of stormwater drainage systems. Therefore, checking the numerical model should be carried out very carefully considering not only parameters of the model but also external influences.

As an example of the verification process, stormwater outflow from the Królewski Creek catchment analysis can be presented.

The run-off from the Królewski Creek catchment was computed using HEC-HMS software and compared with the flow observed in analyzed cross-section, where the measuring weir is located in the stream channel (Fig. 6).



Fig. 6 Cross- section chosen for stormwater outflow analysis in the Królewski Creek catchment

For the identification procedure there have been chosen seven heavy and torrential rainfall events observed and recorded by the monitoring system in years 2013- 2014. Cumulative curves of precipitation were introduced to the model as an input data. After running the simulation seven outflow hydrographs have been calculated. To make the comparison of the flows possible, the discharge curve for the cross- section had been established. Stage-discharge function was developed by field measurements of water velocity at a wide range of stages and resulted in measuring overflow characteristic curve. In the next step, observed water stages resulting from particular rainfall events were recalculated into discharges. The exemplary comparison of the simulated outflow from the catchment and the real outflow observed in the analyzed cross section is shown in Fig. 7. Presented outflow was computed for the rainfall event that occurred on 01 March 2014. Calculations were preceded on the basis of two rainfall gauges measurements. The total observed amount of rainfall registered by the weather station of Gdańsk University of Technology was 11.8 mm while the rainfall amount registered by precipitation gauge Ogrodowa was 10.29 mm.

As it can be observed the results of modeling were not satisfactory and do not corresponded with field observations in the cross-section. The total volume of the simulated outflow was 10 422 m³ for gauge Ogrodowa and 7 812 m³ for gauge Gdańsk University of Technology since the observed outflow volume equaled 1 391 m³. As far as hydrological model simulations are driven by different parameter the senility analysis should improve correlation between model output and observation.

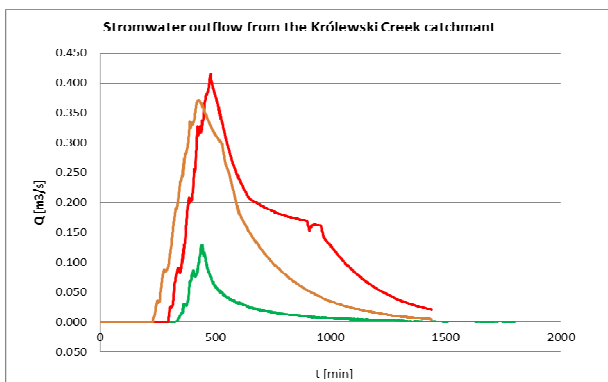


Fig. 7 Stormwater outflow from the Królewski Creek catchment; green line corresponds to observed discharge, brown line corresponds to HEC-HMS computed discharge and Gdańsk University of Technology precipitation gauge, red line corresponds to HEC-HMS computed discharge and Ogrodowa precipitation gauge

In order to hydrological model calibration the percentage of the impervious area of the Królewski Creek catchment was reconsidered and estimated with detailed topographic maps and field investigations. The results are presented in Fig. 8.

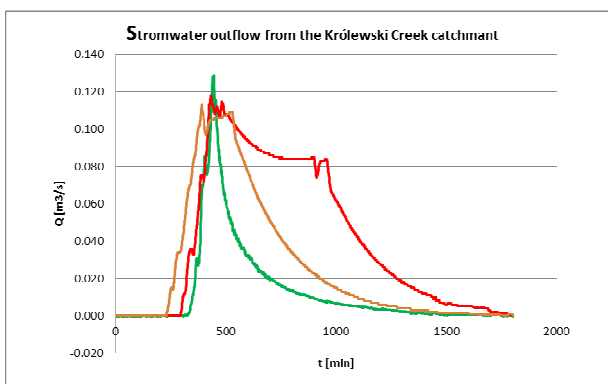


Fig. 8 Stormwater outflow from the Królewski Creek catchment after model calibration; green line corresponds to observed discharge, brown line corresponds to HEC-HMS computed discharge and Gdańsk University of Technology precipitation gauge, red line corresponds to HEC-HMS computed discharge and Ogrodowa precipitation gauge

The manual calibration improved the accuracy of the numerical model. The total volume of the simulated outflow was 4 342 m³ for gauge Ogrodowa and

2 866 m³ for gauge Gdańsk University of Technology. Also the results were better proposed model still could not be used as a reliable prognostic tool for Króleski Creek basin. Authors believe that the fact of the matter is not inappropriate model construction or parameters failure but the difference between expected and real surface drainage patterns resulted from complex surface development.

4. CONCLUSIONS

Full information about flood risk and hazard should consist of time of the wave arrival to characteristic cross sections of the analyzed basin, extreme water levels and its range on inundated areas, duration of flooding and water depth and velocity. Thanks to storage control flood peak delays or advances with flood wave travel times can be achieved to reduce damage at the most flood prone areas. That is why integrated solutions including precipitation, stream flow and reservoirs storage monitoring and management should be undertaken to reduce flood risk and to help to protect the public health and property in Gdańsk.

5. REFERENCES

- BARBOSA A.E., FERNANDES J.N., DAVID L.M., 2013, Understanding, management and modelling of urban hydrology and its consequences for receiving waters: A state of the art, *Advances in Water Resources*, Vol 51, No. 261–279 p.
- CHOW, V.T., 1959, *Open channel hydraulics: New York*, McGraw-Hill, 680 p.
- HYDROPROJEKT 1994, *Kompleksowa koncepcja regulacji Potoku Bystrzec I*.
- MIKOS-STUDNICKA P., SZYDŁOWSKI M. 2015: Analizy ilości i jakości odpływu wód deszczowych i roztopowych z kontrolowanej zlewni zurbanizowanej// *Technologia Wody*. -Vol. 39., nr. 152-59 p.
- SCHILLING W., 1991, Rainfall data for urban hydrology, what do we need? *Atmospheric Research*, Vol 27, No 5-21 p.
- SZYDŁOWSKI M., ZIMA P., 2011 Application of Rainfall - Runoff Model for the Analysis of Extreme Outflow from the Upper Strzyża Basin, *Current events in hydraulic engineering WMHE 2011 Gdańsk University of Technology*, 247p.
- SZYDŁOWSKI M. 2011, Monitorowanie, modelowanie i analiza zagrożenia powodziowego w małej zlewni miejskiej na przykładzie zlewni Potoku Strzyża w Gdańsku. *Umowa dotacji nr WFOS/D/201/162/2011*, 10 p.

Acknowledgement

Paper presents some results of urban basin modeling as well as purpose and scope of work of ongoing research project “Stormwater and snowmelt runoff storage control and flash flood hazard forecasting in the urbanized coastal basin” RX-09/01/2014.

Determining Czech Republic's minimum residual discharges

P. Balvín, A. Vizina, M. Nesládková, L. Kašpárek

T. G. Masaryk Water Management Research Institute - Podbabská 30, Prague 6, Czech Republic, e-mail: pavel_balvin@vuv.cz

Abstract

The revision of the Water Act No. 254/2001 Coll. Implemented by the act No. 150/2010 Coll. has implied a need for review of the methodology of minimum residual flow (MRF) setting. MRF is defined as a stream flow, which still allows for general surface water use and for ecological functions of the watercourse. The water authorities are responsible for setting the value of MRF according to the local conditions, type of water use and with consideration of measures identified in River Basin Management Plans to achieve the environmental goal of affected surface water body. The paper describes a proposal of reviewed methodology for MRF setting in conditions of the Czech Republic.

Keywords

Hydrology, minimum residual flows, methodology, ecology, e-flows, czech legislation

1. INTRODUCTION

Based on the amendment to Act no. 254/2001 Coll. pursuant to the wording of Act no. 150/2010 Coll., the Ministry of Environment has been charged with the task of drafting a Government regulation on the method and criteria for determining the minimum residual discharge values. During the course of 2011 and 2012, the TGM Water Management Research Institute received a subsidy in this connection toward elaborating the methodology for determining the minimum residual discharge (MRD) and the methodology of measuring its values. The paper outlines the proposed MRD measuring methodology which serves as a basis for the Ministry of Environment drawing up the Government regulation proper.

Pursuant to Section 36 of the Water Management Act, the minimum residual discharge shall be understood as the flow rate of surface waters barely adequate for a general water management and for supporting the environment-shaping functions of the watercourse. The amendment to the Water Management Act makes it mandatory for the water management authorities to establish the values of the minimum residual discharge, bearing in mind the conditions prevailing at the watercourse under scrutiny, the character of water management, and the measures conducive to attaining the objectives of water protection adopted in the catchment management plan. The requirements spelled out by law had to be taken

account of in the draft methodology specification. The novel concept issues from the hitherto valid methodology guidance document of the Ministry of Environment concerned with the principles of determining the values of the minimum residual discharge for water streams dating from 1998 [MEnviro, 1998]. Out of consideration to a better implementation of the requirements imposed on aquatic ecosystems and on ecosystems dependent on the aquatic environment, the specification of the original guidance document has been modified by adopting a regional approach to determining the MRD value; the MRD value is variable during the year and its determination ought to take both the character of water management and also the objective of water protection associated with the body of water under scrutiny.

The value of the minimum residual discharge exerts a considerable influence on the ecological as well as chemical state of the body of water affected by the water management procedures adopted, inasmuch as it ensures the survival of aquatic and water-dependent ecosystems during periods of drought and provides for an adequate dilution of effluents. In this context, the term of ecological (environmental) discharge or ecological (environmental) flow can be encountered in literature. As a rule the value of ecological discharge is determined based on information about the specifics of the locality under consideration which include, e.g., the structure of the ecosystem (the prevalent, protected species of organisms and plants), the hydromorphology of the stream leg under scrutiny, the occurrence of habitats, etc. For determining the value of ecological discharge there is a number of expert methods available which however, in any case, require that the specific locality be scrutinized professionally; frequently, these methods are time consuming and cost intensive. This is why these methods cannot be recommended for routine determinations of the MRD values by the water management authority so as to cover all the management procedures being approved. When deriving the new methodology of determining the minimum residual discharge, efforts were made to accommodate the ecological discharge concept to the maximum possible extent while, at the same time, elaborating a methodology that would find practical application; hence the approaches to MRD determination actually adopted had to be distinguished depending on the potential impact of the various types of water management.

2. DATA AND METHODS

The data available for the purpose of drafting the MRD methodology included the statistical characteristics of the discharge values obtained at 185 hydrometric stations from all over the Czech Republic during the 1981–2010 period, which were acquired from the Czech Hydrometeorological Institute [Czech abbreviation, ČHMÚ]. The characteristics examined included the value of long-term annual mean flow, the p-percent and M-days discharges, the variation coefficient and the asymmetry of the daily discharge series, the mean flow rate values in different months of the year, and the values of the probability field of the mean monthly

discharges. The mean surface area of the catchments covered by selected hydrometric stations constitutes 222 km².

The Czech Hydrometeorological Institute determines the M-days discharges from observation values corresponding to natural or to more or less impacted hydrological conditions. In the case of the impacted modem the institute has been providing the M-days discharges from 2013 onwards, either impacted or corrected for impact, obtained by subtracting the effects of documented management; thus they represent the mode which corresponds to the „natural“ hydrological routine. Even though the recommendation for computing the MRD has been to source precisely these values of hydrological characteristics that have been corrected for impact, it has been found expedient to adopt a pragmatic solution, so that the sole hydrological characteristics that will be used in the finalized Government regulation will be those deriving from the observed, i.e., often impacted discharges.

2.1 The proposed partitioning of the Czech Republic by regions

The necessity of taking the natural conditions of flow into account when preparing to regionalize the CR was based primarily on taking into consideration of the key processes that take part in determining the over-all discharge from a catchment. Regions had to be delimited where for most of the year, the values of total discharge conform to a well-balanced character so that no marked reduction in the water availability of the stream takes place during summertime or at the outset of the fall period. These are mainly those regions of which the total discharge is being subsidized for most of the year from the groundwater reserves, or regions having their total discharge constituted mostly of surface flow resulting from heavy rainfall/precipitation. On the other hand, regions had to be delimited which might become potentially vulnerable by drought; those have their total discharge rather unbalanced during the course of the year. For the proposed partitioning, the parameter K_{99} was selected giving the ratio of the mean daily discharge having a 99 % probability of being exceeded during the reference period to the value of the long-term mean discharge Q_a . The higher the value of this parameter, the more balanced i.e., the more stable discharges can be expected to occur during the course of the year.

The values of the parameter K_{99} as established at the tested hydrometric stations were plotted in the hydrogeological districts map. Based on the relationships concerning the values of the parameter K_{99} , the hydrogeological conditions, and the elevation above sea level the partitioning of the CR territory was proposed to consist of four types of regions or ‘districts’. A class of its own is represented by the regions of Cretaceous sediments which represent the drainage bases and where the basic discharge, i.e., the runoff depleting the groundwater reserves, constitutes a substantial part of the total runoff. This includes the right-hand tributaries of Labe River, Upper Metuje, Loučná, the upper reaches of Svitava and Třebůvka Rivers, Říčka Brook. In these regions the value of the parameter K_{99} usually is greater than 0.18. The second class comprises

mountainous areas which also have a relatively high hydraulicity. Here the well-balanced character of runoff is given mainly by the high level of precipitation. In these regions the value of the parameter K_{99} usually is greater than 0.15. Classified in this class are above all the areas of Krkonoše (Giant Mountains) and Jizerské Mountains, of Šumava, Jeseníky Mountains, the hilltop areas of Krušné Hory (Ore Mountains), and also a part of the catchment of Tichá Orlice River which also has a similarly uniform character. The third class comprises regions formed predominantly of crystalline structures such as are encountered in the foothill areas of the borderland mountain ranges and in the area of the Bohemian-Moravian Highlands. These regions exhibit discharge excess lines rather similar to those of Class 2 regions. Owing to their height above sea level which is lower than that of the Class 2 regions the springtime thaw sets in at an earlier date here. Precipitation is lower than in Class 2 regions, too. In these regions the value of the parameter K_{99} will as a rule vary within the limits of 0.1 and 0.15. Classified in Class 4 are regions exhibiting discharge routines which are markedly unbalanced during the course of the year, with values of the parameter K_{99} lower than 0.1. The map of the regions is shown in Fig. 1.

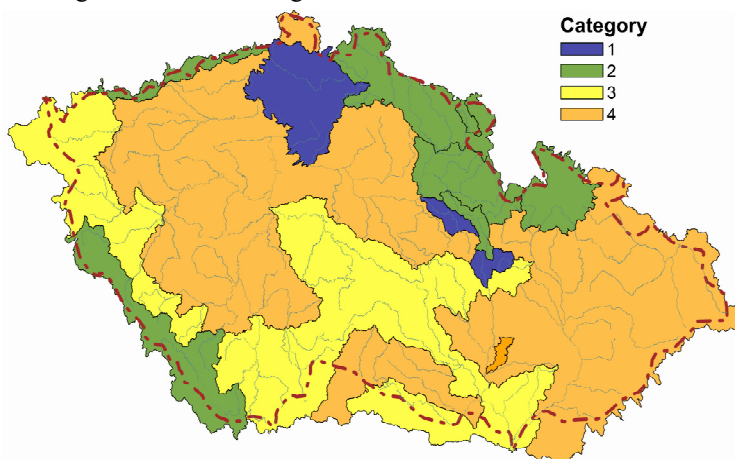


Fig. 1 – Partitioning of the CR to four categories depending on the K_{99} value

2.2 Proposed method of MRD determination

In order that the proposed method of determining the MRD should adequately respect the needs of the aquatic and water-dependent ecosystems, the first step taken was conducting an analysis of existing studies focused on the MRD determination using the expert method referred to as „Instream Flow Incremental Methodology“ [IFIM, Bovee, et al. 1998] and the modeling instrument „Physical Habitat Simulation Software“ [PHABSIM, Milhous, et al., 1989] under the conditions of the Czech Republic. This is a method of MRD determination making use of the results of a reconnaissance of the watercourse section under scrutiny

from the standpoints of its hydraulic parameters, the character of its habitat, and the animal and plant species occurring thereon. The method incorporates a simulation of the weighted usable surface area of the habitat under different discharge conditions. Further on, the results of this simulation modeling are put to use when discussing the choices for a compromise level of the MRD that would allow the existing ecosystems to be preserved, while at the same time allowing for a reasonable degree of water management [Balvín, Mrkvičková, 2011]. It usually takes 1.5 to 2 years to derive the MRD value by applying the IFIM method, also requiring a repetitive collection of biological data from the watercourse section that would be influenced by the proposed water management procedures. The data search covered 15 localities in the CR, yielding the conclusion that the resultant compromise level of the MRD varied at the level of a discharge having a probability of being exceeded in 330 days of the year in most cases.

Tab. 1 The ratio of the M-days discharge value having a given exceedance time to the mean long-term discharge value—averages for pilot hydrometric stations classified by regions.

Region	M-days Q/Q_a [-]						
	Q_{210d}	Q_{240d}	Q_{270d}	Q_{300d}	Q_{330d}	Q_{355d}	Q_{364d}
1	0.72	0.65	0.59	0.53	0.46	0.38	0.29
2	0.57	0.50	0.43	0.37	0.31	0.24	0.17
3	0.54	0.46	0.39	0.33	0.26	0.18	0.11
4	0.44	0.35	0.28	0.22	0.15	0.08	0.04

The studies conducted on the basis of the IFIM method were elaborated for the most part for localities classified as belonging to Class 2 and 3 regions. For these regions it holds that the value of Q_{330d} is approximately 26–31 % of Q_a (cf. Table 1). It also transpires from the Table that for Region 1 the value corresponding to the streamflow of 30 % of Q_a is a M-days discharge with an exceedance reached in 364 days of the year, while for stations classified as located in Region 4 this would be a discharge with an approximately 300-day to 270-day flow exceedance in the year. For the draft specification of the method of MRD determination, an orientational requirement has also been considered that the MRD value should amount to approximately 20–30 % of Q_a . This is a requirement which is in line with the conclusions drawn in the document „Environmental Flows as a tool to achieve the WFD Objectives – discussion paper“ [EC, 2012]. According to the recommendation suggested in the said document, an ecological discharge within the range of 25–50% of Q_a should be maintained in order to ensure a healthy ecological situation; thus the proposed level of 20–30 % represents the lower limit of the range specified. The computation of the MRD also derived from the value of the discharge having an exceedance probability of 330 days in a year.

The original methodology guidance document concerned with MRD determination, dating from 1998, operates with the fact that the flow conditions become more uniform as the size of the watercourse becomes bigger, and it

recommends that MRD determination for the higher-hydraulicity watercourses should implement the discharge values having higher exceedance probabilities. A similar approach has also been adopted e.g., in the water management act of Switzerland (FASC, 1991) where the value of the minimum residual discharge („residual water flow“) grows higher as an exponential function of the 347-days exceedance probability discharge in a year, the exponent being less than 1. In order that the proposed new MRD determination methodology would also adhere to the principle described above, the first thing done was conducting an evaluation of the dependence of the ratio of the 330-days exceedance discharge in a year to the long-term mean discharge Q_a as a function of the volume of flow Q_{330d} . For the purpose of deriving a relationship that would be well-suited for determining the MRD values for the various regions, a plot of the function values of the proposed MRD/Q_{330d} ratio against the values of Q_{330d} was separately produced for each of the regions. It has nevertheless been decided that the degree of reduction of the MRD value as a function of the control flow Q_{330d} will be the same for the whole of the CR territory, while the parameter defining the multiple in the equation will be different. The effect of the proposed value of the exponent occurring in the equation upon the resultant MRD value was compared with the effect of the MRD concept deriving from the original methodology guidance document dating from 1998. Eventually, the exponent of the equation was modified to the value of 0.85. This mitigates the level of reduction of the MRD value as a function of Q_{330d} . Again, the resultant equations to be used for determining the MRD values for the different regions were derived from the requirement of attaining MZP/Q_a ratios at the level of approximately 25 %. The resultant equations are listed in Table 2.

Tab. 2 Proposed computational method for determining the MRD values for the different categories, for two seasons in the year

Category	Main season		Springtime season	
1	May - January	$0.65 \times Q_{330d}^{0.85}$	February - April	$0.85 \times Q_{330d}^{0.85}$
2	May - January	$0.8 \times Q_{330d}^{0.85}$	February - April	$Q_{330d}^{0.85}$
3	May - January	$0.85 \times Q_{330d}^{0.85}$	February - April	$Q_{330d}^{0.85}$
4	May - January	$0.9 \times Q_{330d}^{0.85}$	February - April	$Q_{330d}^{0.85}$

It was a part of the assignment handed down by the Ministry of Environment that the MRD value be split between at least two periods, so as to more closely approximate the flow distribution during the course of the year. This would ensure that, as opposed to the original methodology guidance document, the MRD value would not remain constant throughout the year but would be ‘improved’ during springtime. The resultant split was that the so-called main season was defined to be May through January, and the springtime season extending from February through to April.

To adopt an optimal treatment of the MRD values for $Q_{330} < 1 \text{ m}^3 \cdot \text{s}^{-1}$, the formula used to cover these cases was additionally modified, assuming the form: coefficient $\times (Q_{330d}^{0.85})^{1.09}$.

2.3 Proposed implementation of the seasonal concept of the MRD

To implement seasonality in the MRD concept, it has been necessary first to perform an analysis of the effect of diverse types of water management upon the over-all hydrological routine, inasmuch as the differentiation of the MRD depending on season makes sense mainly in the case of such water management procedures which could induce a principal change to the hydrological routine. Such interventions that affect the flow rates of the watercourse to an extent that, regarded from the standpoint of the long-term averages, would induce a hydraulicity reduction of less than 20 % of the Q_a , have been evaluated as water management procedures producing no significant impact on changing the over-all hydrological routine of the watercourse under scrutiny. Changes of this kind may be, for example, water withdrawals and transferences not exceeding the limit of 20 % of Q_a in volume. To safeguard the water protection aspect with water management procedures of this kind, measures have to be adopted that such measures be constrained, or even suspended during periods of low flow, so as not to endanger the survival of the aquatic ecosystems. Basically, the natural variability of flow along the watercourse section under consideration will be preserved as long as the MRD requirement is respected.

3. RESULTS

The results are presented in this chapter, and the proposed values of minimum residual discharge are compared with the currently applicable values. The analysis was performed using some 200 catchments on Czech Republic territory, having average flow rates of up to $20 \text{ m}^3 \cdot \text{s}^{-1}$. Most of the profiles however have an average flow rate of up to $2 \text{ m}^3 \cdot \text{s}^{-1}$. Once the proposal was made, the catchments under scrutiny were subjected to a sensitivity analysis aiming to assess whether the proposed MRD values are realistic for the various months of the year and whether these values can actually be reached in the months of reduced water availability. For the purpose of this assessment, the deficit volumes (under a threshold level) with a constant and a variable limiting value have been computed. These deficit volumes were compared with those deficit volumes computed based on assigning a constant limiting value of the applicable MRD. The assessment was contingent upon the condition that each individual event should be of a duration of at least 5 days, with at least two days elapsing in-between successive events.

Figure 2a renders the proposed MRD values for the summer (red) and winter (blue) seasons, alongside the currently applicable (orange) MRD values, subdivided into categories. The scale for the Q_{330} values is on the x-axis and that for the MRD values is on the y-axis. All the catchments that have been taken into consideration are shown in this plot. On the other hand, Fig. 2b renders information only on those catchments of which the Q_{330} values are less than or

equal to $2 \text{ m}^3 \cdot \text{s}^{-1}$, in order to make the plotted results more synoptic. This graph presents a summarization for all the categories. It can be observed that all the proposed values lie below the Q_{330} value and that, in the case of low flow rates, the differences are miniscule and the question arises whether they are measurable at all. However, this problem occurs with all watercourses experiencing low flow rates (of the order of dozens of liters/s).

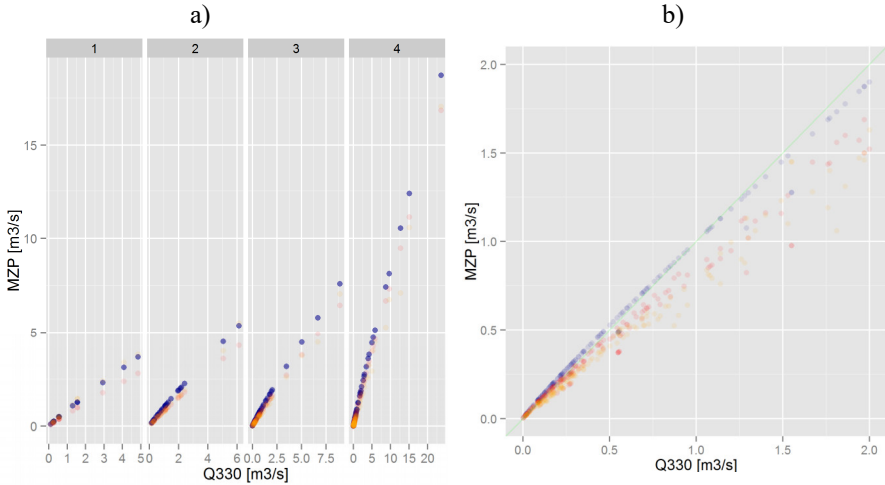


Fig. 2 Comparison of the currently applicable MRD values (in orange color) with the proposed values for the summer (red) and winter (blue) seasons

Figure 3 depicts the ratios of MRD values for summertime (red) and wintertime (blue) to the $Q_{50\%}$ values. It can be seen in the graph that these ratios vary around 35% for the summer season (38.6% for Category 1, 38.6% for Category 2, 35.7% for Category 3, and 32.8% for Category 4), and 41% for the winter season (48.3% for Category 1, 42% for Category 2, 51.1% for Category 3, and 36.5% for Category 4). Then these ratios for the main season are represented in Fig. 4 showing their incidence and spread over Czech Republic territory. The higher values encountered during the secondary season are to no detriment to this, owing to the fact that water is abundant during this period so there will be no problem meeting these values.

In Fig. 5 the changes of the MRD values proposed for the two seasons, referenced to the current value, are represented by a boxplot type graph where the rectangle signifies the 25 and 75% quantiles, the line in the middle of the box represents the median, and the lines issuing from the box correspond to 5 and 95%.

Then these changes for the main season are represented in Fig. 6 showing their distribution over Czech Republic territory. It can be observed that on the average, the changes pertaining to the main season (in red) vary from -25% per cent for

Category 1 to ca. 20% for Category 2. For the secondary season these changes are ca. 20% higher.

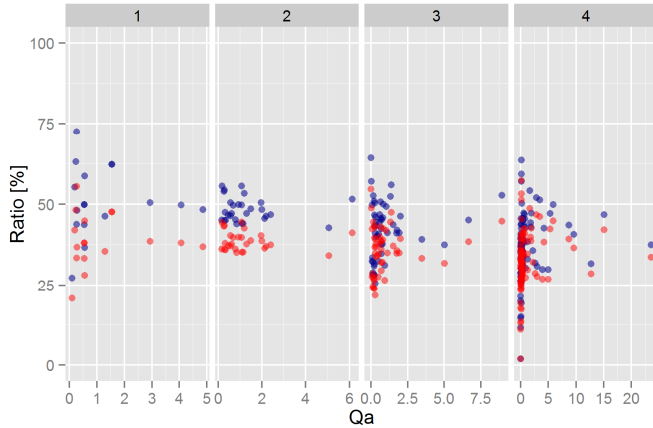


Fig. 3 Ratio of the MRD value to the flow $Q_{50\%}$ – main season shown in red, secondary season shown in blue

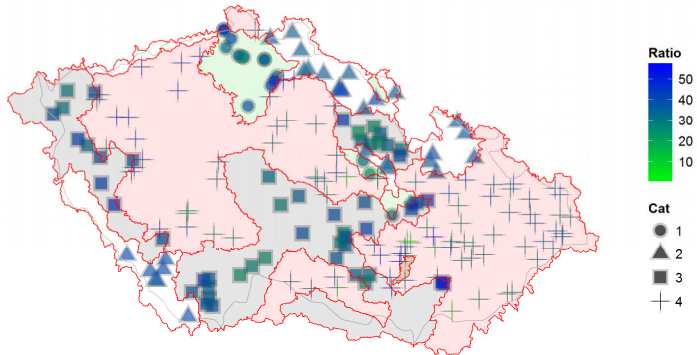


Fig. 4 Dislocation of the MRD to flow $Q_{50\%}$ ratio in terms of surface area coverage (main season)

4. CONCLUSION AND DISCUSSION

Inasmuch as this is a novel approach to the task of determining the minimum residual discharges, and owing to the circumstance that the specification of the proposed methodology serves as supporting documentation for drafting the CR Government regulation, this new approach has provoked a broadly based discussion. The original methodology guidance document of the MEnviro possessed certain degrees of freedom as it had the form of a recommendation and the computed values were indicative only. Thus the resultant residual discharges

could be both lower and higher. It has to be noted that the original methodology guidance document already contained the recommendation that the residual discharge be split by seasons during the course of the year, also underlining the links to biology, especially to fish and zoobenthos.

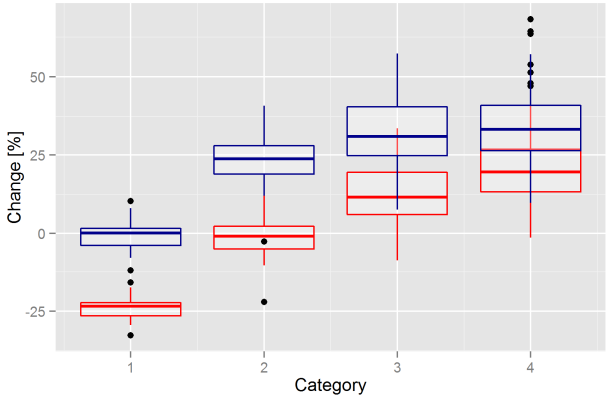


Fig. 5 Changes in the MRD value (proposed/currently applicable value) – main season shown in red, secondary season shown in blue

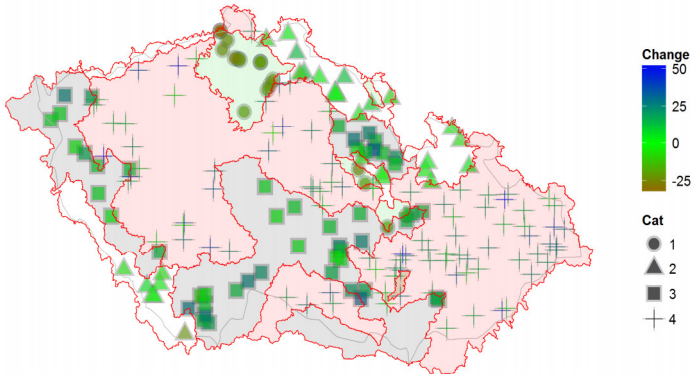


Fig. 6 Distribution of the changes in the MRD value (proposed/currently applicable value) in terms of surface area coverage - (main season)

Owing to the fact that the Government regulation now is being drafted in its articulated wording, the possibilities of setting analogous criteria in the form of a recommendation are very limited. For the authors of the draft this meant that they had to thoroughly verify the approach adopted and to interlink the values of the m-days discharges with the biological components present in the watercourse at the very outset of preparations of the draft. The justifiability of this approach has unequivocally been also strengthened by the pressures issuing from the EU, where it will be necessary to explain to the European Commission the relationship

between the ecological discharge as defined within the framework of EU documents [CIC GD31 E-flows] and the residual discharge as defined in Section 36 of the Water Management Act.

In most cases, the adopted approach brings about a strengthening of the requirements imposed on the MEnviro as against the indicative values which correspond to the requirements spelled out in the original methodology guidance document dating from 1998. The more stringent regulations apply primarily to Region 4 watercourses having fluctuating conditions of flow, which is the type that prevails, in terms of surface area coverage, on the CR territory.

An intra-sectoral round of consultations is currently underway at the CR Ministry of Environment, and the novel approach is being presented to watershed administrators, water management authorities, but also to associations representing the operators of small-sized hydro power stations as well as to naturalist protectors and guardians.

5. REFERENCES

- ACKERMAN, M. et al. 2008. *Developing environmental standards for abstractions from UK rivers to implement the EU Water Framework Directive*. Hydrological Science Journal, 2008, Vol. 53, 6, p. 1105–1120
- BALVÍN, P., MRKVIČKOVÁ, M. 2011. *Determination of the minimum residual discharges (in Czech)*. Water Management Technical and Economic Information J., VTEI, Vol. 53, no. 4, p. 1-3; available online at: http://www.vuv.cz/fileadmin/user_upload/pdf/vtei/2011/vtei_4-2011.pdf
- BOVEE, K.D., LAMB, B.L., BARTHOLOW, J.M., STALNAKER, C.B., TAYLOR, J. and HENRIKSEN, J., 1998. *Stream habitat analysis using the instream flow incremental methodology*: U.S. Geological Survey Information and Technology Report 1998-0004. 130 p., available online at: <http://www.fort.usgs.gov/Products/Publications/3910/preface.html>
- FASC (1991) Federal Law on the Protection of Water 814.20, 1991, The Federal Assembly of the Swiss Confederation, available online at: http://www.admin.ch/ch/e/rs/814_20/index.html
- EK (2012) Environmental Flows as a Tool to Achieve the WFD Objectives – discussion paper, <https://circabc.europa.eu/sd/d/0898cf3d-657a-4018-b53d-b34ac3460997/55171-Eflows-Discpap-Ed2-20120613.pdf>
- Ministry of Environment 1998. Ministry of Environment's water protection methodology guidance document for determining the minimum residual discharges in watercourses, ref. no. ZP16/98, [http://www.mzp.cz/osv/edice.nsf/BB978B5BAEDF46C0C1256FC8003F1EB8/\\$file/metod.html](http://www.mzp.cz/osv/edice.nsf/BB978B5BAEDF46C0C1256FC8003F1EB8/$file/metod.html)
- MILHOUS, R. T., UPDIKE, M. A., SCHNEIDER, D. M. 1989. *Physical Habitat Simulation system. Reference Manual Version II*. Instream Flow Information Paper 26. National Ecology Research Center, Fish and Wildlife Service. Ft Collins, CO, <http://www.fort.usgs.gov/Products/Publications/3912/3912.pdf>

Predicting output flood wave on the section of the Drava River

M. Šperac, T. Mijušković- Svetinović, A. Rabi

Faculty of Civil Engineering Osijek, Drinska 16a, 31 000 Osijek, Croatia, phone +385 31 274 377, fax +385 31 274 444, e-mail: msperac@gfos.hr, tatjanam@gfos.hr, anamarija.rabi@gfos.A.

Abstract

The movement of the flood wave along the river bed is a complex process, not only because of this that the flow varies in time, but because the watercourse hydraulic and geometric characteristics of the river bed is very variable. Propagation of water waves is the process that defines the characteristics of flood waves on a downstream section of the river flow on the basis of known flood waves in the upstream section. The main problem with the forecasts of flood wave output is in the mathematical description of the transformation input flood wave. The wave propagation can be illustrated by the space and time functions of discharge and depth. Flood routing is the determination of flow conditions in a river, given its initial state, the stream morphology and an inflow hydrograph. Flood-routing procedures may be classified as either hydrological or hydraulic. Hydrological methods use the principle of continuity and a relationship between discharge and the temporary storage of excess volumes of water during the flood period. Hydraulic methods of routing involve the numerical solutions of either the convective diffusion equations or the one-dimensional Saint-Venant equations of gradually varied unsteady flow in open channels. An example of a simple hydrological flood-routing technique used in natural channels is the Muskingum flood-routing method. In this paper for predicting output flood wave on the section of the Drava River (in the lower reaches) two methods are applied: Muskingum methods and a modified Kalinin-Milyukov method. The Muskingum method belongs to the class of hydrologic routing methods. Hydrologic routing models involve only storage and flow rates of floodwater and aim to capture the wave dynamics through their parameters. The Kalinin and Milyukov method is especially appealing for flow routing, because both model parameters, the number of linear reservoirs in the series and the time constant (or storage coefficient of the linear storage-outflow relationship of each reservoir in the cascade) are related to the channel's characteristics and hydraulic conditions.

Keywords

Flood wave, propagation, Muskingum method, Kalinin-Milyukov method, Drava River

1. INTRODUCTION

Water wave propagation along the river course is the process that defines the characteristics of the flood wave in the downstream of a profile section of river flow on the basis of the known water wave on the upstream profile and shares.

Thus, the term model flood waves propagation, involves the procedures and methods used in hydrology for the calculation "advancement" water wave along the course, or through the accumulation of calculate in terms of the time of its occurrence and form of flood wave. In natural watercourses and channels, as well as reservoirs, while passing flood waves, a certain amount of water is temporarily retained, which results in the deformation of the water wave. The area in which water reserves have the effect of retention which affects the shape of the flood wave that travels downstream. The degree of accumulation of water depends on hydraulics and topographical characteristics of the shares. The effect of this holding at a certain section of the river is a function of the size of volume of space where the water reserves. The greater the volume of the space between the input and output profile river stocks are higher and differences in the form of input and output hydrograph. This impact is reflected in the fact that the peak flow of the wave decreases and at the same time prolongs the time base [Hrelja, 2007].

The wave propagation can be illustrated by the space and time functions of discharge and depth. Flood routing is the determination of flow conditions in a river, given its initial state, the stream morphology and an inflow hydrograph.

Many methods have been sought for predict the characteristic features of the movement of a flood wave along a river in order to determine the actions necessary for protecting life and property from the effect of flooding and improve the management of water related systems along natural or manmade watercourses [Balaž et al. 2010].

1.1 Study area

For prediction of output flood wave the area of the lower course of the river Drava was selected. The area is part of a basin in Croatia. Two water level gauging stations that measure flow rates which are selected are: Donji Miholjac (upstream river km 77 + 000) and Belišće (downstream river km 55 + 450) (Fig. 1). Distance between the two profiles is 21.55 km.

The maximum flow measured at the gauging station in Donji Miholjac is 2 020 m³/s. The most frequent floods in this area occur in late spring and early summer. They come as a result of melting snow in the Alps and at the same time as the appearance of large amounts of rainfall in the observed area. Fig. 2 shows the recorded wave of high water at the stations Donji Miholjac and Belišće. It is evident that the downstream station peak water wave decreased. It clearly means that the water wave transformed on the observed section.

2. METHODS

In this paper for predicting output flood wave on the section of the Drava River (in the lower reaches) two methods are applied: Muskingum method and a modified Kalinin-Milyukov method.

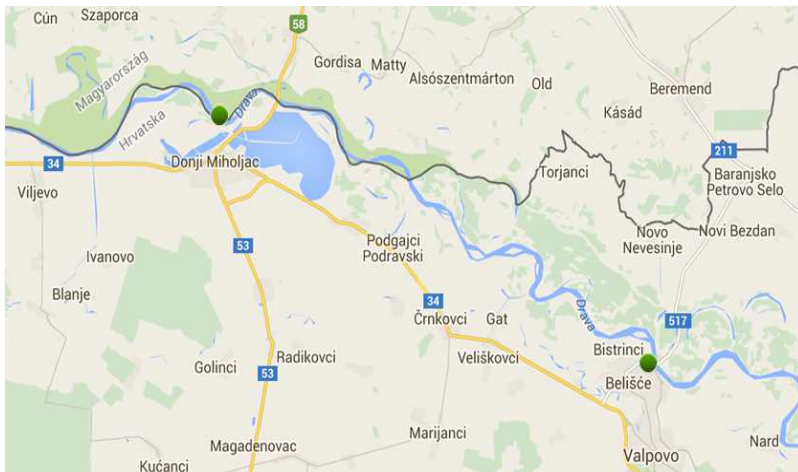


Fig. 1: Selected water gauging stations on the Drava River

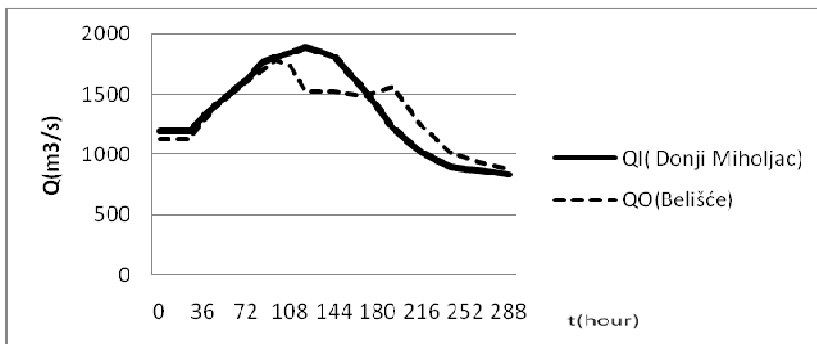


Fig. 2: Transformation water wave on analysed section

2.1 Muskingum method

The Muskingum method belongs to the class of hydrologic routing methods. Hydrologic routing models involve only storage and flow rates of floodwater and aim to capture the wave dynamics through their parameters [Koussis et al. 2012]. The key parameters in Muskingum routing are K (travel time) and X (weighting coefficient). The value of X depends on the shape of the wedge storage which is modelled, and the value of X ranges from 0 for reservoir-type storage to 0.5 for a full wedge. In natural streams, X is between 0 and 0.3 with a main value near 0.2. K is the time required for an incremental flood wave to traverse its reach, and it may be estimated as the observed time of travel of peak flow through the reach.

Equation for calculating the propagation:

$$O_i = C_0 I_1 + C_1 I_{i-1} + C_2 O_{i-1}, \quad (1)$$

where

$$C_0 = \frac{0.5\Delta t - KX}{K(1-X) + 0.5\Delta t}, \quad (2)$$

$$C_1 = \frac{KX + 0.5\Delta t}{K(1-X) + 0.5\Delta t}, \quad (3)$$

$$C_2 = \frac{K(1-X) - 0.5\Delta t}{K(1-X) + 0.5\Delta t}. \quad (4)$$

The coefficients C_0 , C_1 and C_2 are computed from K , X and t , input values. The sum of these coefficients will always equal 1.0:

$$C_0 + C_1 + C_2 = 1.0. \quad (5)$$

Limits of parameter values are:

$$\Delta t \geq 2KX. \quad (6)$$

2.2 Modified Kalinin-Milyukov method (MKM)

Kalinin and Milyukov's (1957) flow routing method assumes that a river section, with no lateral inflow, can be conceptualized as a series of characteristic reaches where the outflow (Q_o) is a linear function of water stored within the reach [Szilagy 2006].

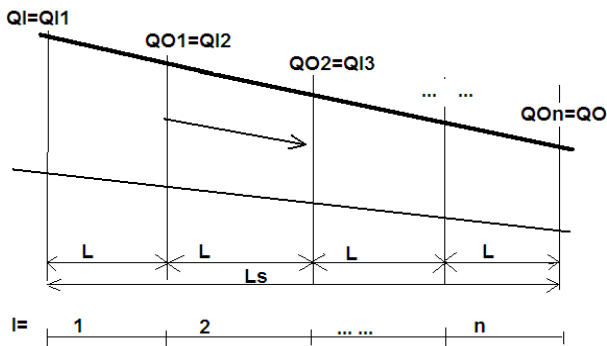


Fig. 3: Characteristic shares

The Kalinin and Milyukov method is especially appealing for flow routing, because both model parameters, the number of linear reservoirs in the series and the time constant (or storage coefficient of the linear storage-outflow relationship of each reservoir in the cascade) are related to the channel's characteristics and hydraulic conditions.

Calculation of propagation of input hydrograph (Q_i) along the sector of the river to the output profile Q_o (output hydrograph) are made successively by characteristic shares [Prohaska et al. 2002]. Characteristic shares is part of the river course with length there is an unambiguous link between the water level in the middle of the characteristic length of the section ($L / 2$) and the flow at the exit of the characteristic section. Schematic diagram of the basic assumptions of the method is shown in Fig. 3.

The symbols in the figure mark:

- Q_i - input hydrograph on the observed river section
- Q_o - output hydrograph on the observed river section
- Q_i' - input hydrograph on the i -th characteristic share
- Q_o' - output hydrograph on the i -th characteristic share
- L - length of the characteristic shares
- L_s - length of the observed river section
- I - ordinal number of the characteristic shares
- N - the total number of the characteristic shares

Important assumption:

$$Q_o^{i-1} = Q_i^1 \tag{7}$$

The equation for calculating the propagation along a characteristic shares:

$$Q_o'(t) = Q_i'(t-1)C_1 + (Q_i'(t) - Q_i'(t-1))C_2 + Q_o'(t-1)C_3, \tag{8}$$

where:

$$C_1 = \left(1 - \exp\left(-\frac{\Delta t}{\tau(Q_i)}\right) \right), \tag{9}$$

$$C_2 = 1 - \left(\frac{\tau(Q_i)}{\Delta t} \right) \left(1 - \exp\left(-\frac{\Delta t}{\tau(Q_i)}\right) \right) = 1 - \left(\frac{\tau(Q_i)}{\Delta t} \right) C_1, \tag{10}$$

$$C_3 = \exp\left(-\frac{\Delta t}{\tau(Q_i)}\right), \tag{11}$$

Model parameters:

$\tau(Q_i)$ - function of the propagation time,

n – number of the characteristic shares.

3. RESULTS

3.1 Muskingum method

The value of the parameter K was obtained by calculation shown in Table 1. For different values of the parameter X calculated consecutive increase in the volume and at the same time the weighted increase rate.

$$K = \frac{\frac{\Delta t}{2} \left[(Q_{I(j)} + Q_{I(j-1)}) - (Q_{O(j)} + Q_{O(j-1)}) \right]}{X(Q_{I(j)} - Q_{I(j-1)}) + (1-X)(Q_{O(j)} - Q_{O(j-1)})} \quad (12)$$

Dependence of the numerator and denominator of the equation 12 is represented by a loop (Fig. 4). Booms are closed loop maximum value for $X = 0.20$, and $K = 7000/1000 = 7$

Tab 1: Calculation of the parameter K

T (hours)	Q_I (m ³ /s)	Q_o (m ³ /s)	Summary volume increase	Summary the weighted increase flow		
				$X=0.15$	$X=0.20$	$X=0.10$
0	1193	1133	12050			
12	1193	1133	12050	2284	2290	2278
24	1193	1133	12593	2284	2290	2278
36	1307	1274	13685	2420.95	2425.6	2416.3
48	1422	1415	14749	2695	2697	2693
60	1524	1512	15785	2929.85	2930.8	2928.9
72	1627	1609	17031	3125.5	3127	3124
84	1762	1694	17929	3315.9	3320.2	3311.6
96	1805	1779	18405	3487.1	3491.8	3482.4
108	1848	1734	19176	3534	3541	3527
120	1891	1524	19404	3330.15	3354.2	3306.1
132	1851	1524	18924	3152.1	3186.8	3117.4
144	1811	1524	17903	3140.1	3170.8	3109.4
156	1678	1507	16341	3099.7	3122.6	3076.8
168	1545	1490	14548	3030.9	3042.2	3019.6
180	1382	1524	12523	3000.95	2996.6	3005.3

T (hours)	Q_I (m ³ /s)	Q_o (m ³ /s)	Summary volume increase	Summary the weighted increase flow		
				$X=0.15$	$X=0.20$	$X=0.10$
192	1219	1559	11086	3010.7	2986.6	3034.8
204	1122	1401	10159	2867.15	2836.2	2898.1
216	1012	1244	9430	2568.35	2542.8	2593.9
228	955	1128	8977	2311.25	2291	2331.5
240	898	1013	8693	2097.8	2083.4	2112.2
252	882	974	8578	1955.95	1945.6	1966.3
264	866	936	8444	1885.7	1877.6	1893.8
276	849	910	8292	1826.35	1819.8	1832.9
288	832	884	4108	1777.05	1771.4	1782.7

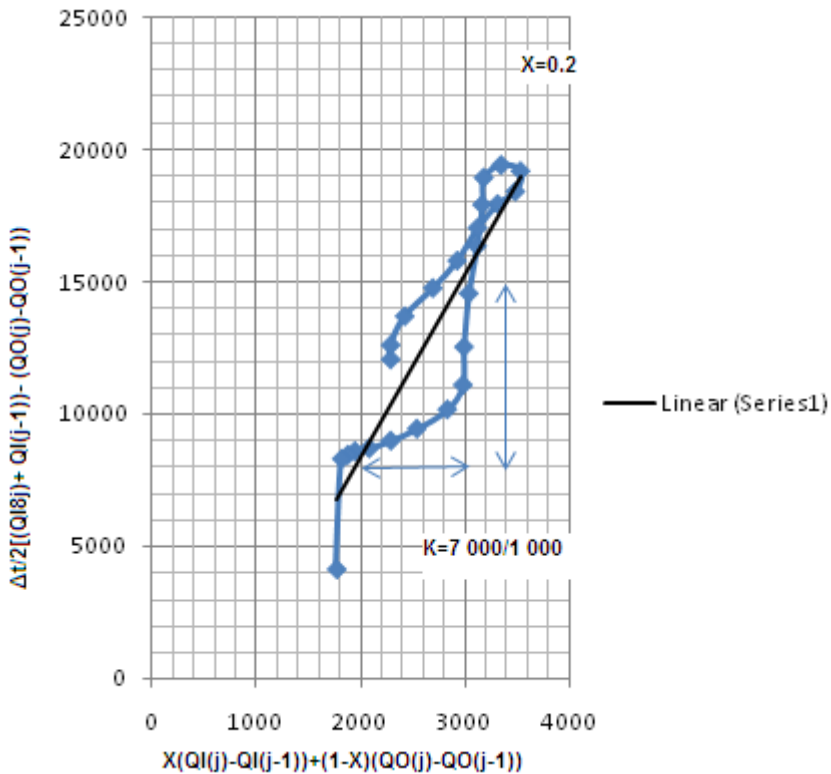


Fig. 4: Determining parameter K.

For adopted value of $K = 7$ hours; $X = 0.2$, and $\Delta t = 12$ hours , on the basis of equation (1), (2), (3) and (4) was performed calculation of transformations of the input hydrograph Q_I . The results are shown in Fig. 5.

3.2 Modified Kalinin-Milyukov method (MKM)

On the section of the Drava River , from Donji Miholjac to Belišće, total length $L = 22$ km, modified Kalinin Milyukov method define 15 characteristic shares. Calculation of function the propagation time τ flood waves on the considered section is shown in Tab. 2, and the transformation of flood wave in Fig. 5.

Tab. 2: Calculation of the function of the propagation time flood wave on the analysed section

Q_{AV}	$\Sigma \Delta W / \Delta t$	Q_{AVi}	$\Delta \Sigma \Delta W / \Delta t$	$\tau \times \Delta t$	τ	$T(Q)$
800	138	section				Charact . share
		900	605	6.05	3.025	0.202
1000	743	1100	551	5.51	2.755	0.184
1200	1294	1300	456	4.56	2.28	0.152
1400	1750	1500	308	3.08	1.54	0.103
1600	2058	1700	107	1.07	0.535	0.036
1800	2165					

4. CONCLUSIONS

Results of calculating forecasting flood wave on the analysed section of the Drava River showed that achieved very good matching phrase of actual and calculated hydrograph at the output by using both methods of propagation - modified Kalinin-Milyukov (MKM) and Muskingum methods. This means that the parameters of the methods well-defined and that they can be applied to analysed section; for any other river, or share it is necessary to redefine the parameters.

Flood routing is important in the design of flood protection measures in order to estimate how the proposed measures will affect the behaviour of flood waves in rivers so that adequate protection and economic solutions can be found.

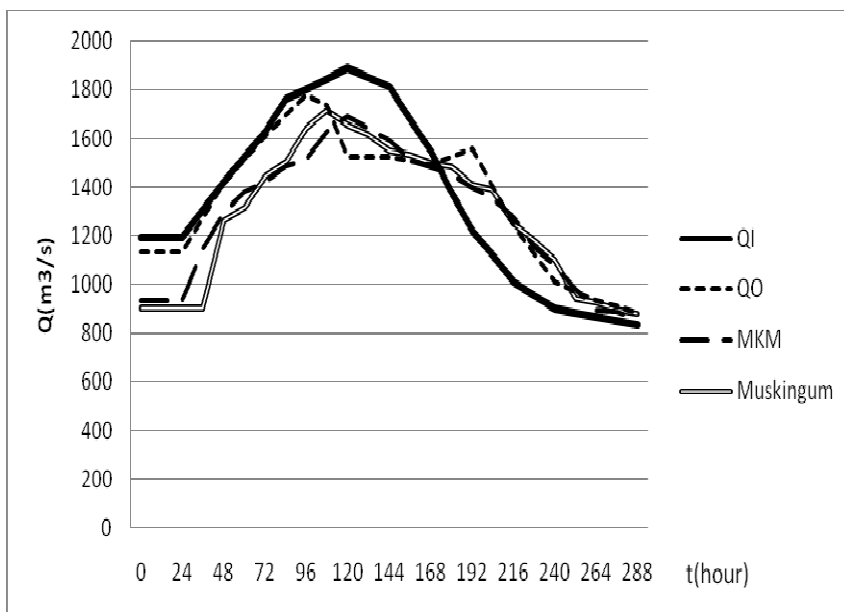


Fig. 5: The transformation of water wave on the section of the Drava River

5. REFERENCES

- BALAŽ, M., DANAČOVA, M., SZOLGAY, J. 2010. *On The Use Of The Muskingum Method For The Simulation Of Flood Wave Movement*. Slovak Journal of Civil Engineering 14-20 p.
- HRELJA, H. 2007. *Inženjerska hidrologija*. (Engineering Hydrology). Univerzitet u Sarajevu, Građevinski fakultet. 1065-1112 p.
- KOUSSIS, A.D., MAZI, K., LYKOU DIS, S., ARGIRIOU, A.A. 2012. *Reverse flood routing with the inverted Muskingum storage routing scheme*. Nat. Hazards Earth Syst. Sci., 12, 217–227 p.
- PROHASKA, S, RISTIĆ, V. 2002. *Hidrologija kroz teoriju i praksu*. (Hydrology through theory and practice). Univerzitet u Beogradu Rudarsko geološki fakultet. 527 p.
- SZILAGY, J. 2006. *Discrete state-space approximation of the continuous Kalinin-Milyukov-Nash cascade of noninteger storage elements*. Journal of Hydrology 328. 132-140 p.

Climate and land use changes impacts on small catchment areas

T. Dadic, L. Tadic

Assistant, Faculty of Civil Engineering Osijek, University of Osijek, Crkvena 21, 31 000 Osijek, Croatia, phone: +38531540087, e-mail: tamaradadic@gfos.hr
Associate Professor, Faculty of Civil Engineering Osijek, University of Osijek, Crkvena 21, 31 000 Osijek, Croatia, phone: +38531540086, e-mail: ltadic@gfos.hr

Abstract

Considering hydrological and environmental processes, small catchment areas are very vulnerable. Their size, shape and land use characteristics as well as topographical features have strong influence on hydrological regime. This paper deals with these problems on one smaller catchment area in Croatia: Karašica-Vučica catchment, part of the Danube water basin. The total catchment area is 234.000 ha, the hilly part has 70.000 ha and the lowland part has 164.000 ha which is basically agricultural area. The altitude is between 85 and 953 m a.s.l. The watercourse network consists of natural rivers and artificial canals as part of surface drainage system. In the last hundred years, drainage system has been developing for flood protection. The natural watercourses have maximum discharges in spring and winter time and minimum in vegetation period. This hydrological regime is very unsuitable for irrigation implementation which becomes necessity for stable agricultural production. The annual precipitation in the period between 1981 and 2014 is 797 mm, without significant change, but its distribution has been changing. The mean annual air temperature in the same period is 11,25mm but it shows more significant change of +0.31 °C/10 years. Analysis of catchment water balance and its change in the last thirty years will be presented, together with pressures on it. River discharges, ground water fluctuation, precipitation and meteorological data will be analysed for the period between 1980 and 2013. In this period few extreme droughts have occurred, in 2000 and 2003, causing damages in agriculture and the environment as well. The climate and anthropogenic influences on the water balance of the small catchment area are present and this paper will show how significant they are.

Keywords

Hydrological regime, climate change, land use

1. INTRODUCTION

Small catchments are very vulnerable from hydrological point of view. Their size is main characteristic which generate its hydrological features and water balance in general. Large catchments have well definable relationship between the actual discharge in the closing profile and the precipitation total for a given antecedent period. Gradually it became evident that models conceived in this way

are unable to describe the reality of runoff formation from small catchments (Tesar et al.,2002).

Their topographical characteristics, vegetation cover, shape and slope of the catchment and density of watercourse network have a strong influence on hydrological and geochemical processes. Especially in mountainous region, water balance is strongly influenced by land use, climatic, and topographic conditions. As a result, soil moisture and water balance patterns are very patchy, leading to large spatial variations in evapotranspiration and stream discharge (Ruch and Harum, 2002). Human activities in the forms of settlements, infrastructures and hydraulic structures have also significant impacts in a small scale (Moldan, 1994), and as a climate change driving forces in a large scale.

In the catchment area of Karašica and Vučica rivers all these characteristics can be recognized. It has been situated in Danube River basin, part of the Drava River catchment area (Fig. 1). Fig. 1 also presents meteorological and hydrological stations and groundwater observation wells.

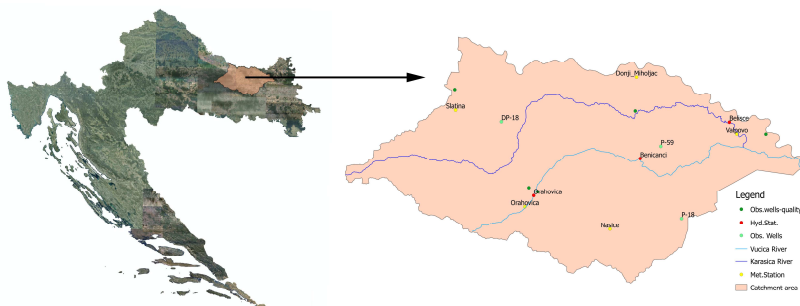


Fig. 1 Study area

It is small catchment with two different parts. The bigger part is typical lowland with altitude between 85 and 125 m a.s.l. The lowest point is at the mouth of Vučica River to the Drava River. The most of the terrain is higher than maximum water level of the Drava River, so the area is not endangered by high Drava River water levels. The vegetation cover mostly consists of agricultural land, pastures and forests. Hilly part of the catchment is situated on the southern part, with the altitudes between 125 and 953 m a.s.l. Hilly part is covered by forest, orchards and vineyards and takes about one third of the total area. There are many smaller brooks that during high water periods convey a significant discharge to the lower part and cause floods. The main flood protection system consists of three big canals constructed in order to convey water directly to the Drava River and reduce flood peaks in lower part of the catchment. The whole catchment area has very dense network of natural and artificial watercourses constructed in last 150 years. Its main purpose was, and still it is, flood protection and land drainage (Tadić, 2002). Frequent prevalence of extreme hydrological events is also

characteristics of small catchments without possibilities of high water retention or drought mitigation.

2. METHODS AND DATA

In this chapter, land use and changes which occurred between 1980 and 2012 will be analysed as well as temperature and precipitation from meteorological stations on catchment area. Data series from five stations were observed. Hydrological analysis was based on discharges and water levels data for Karašica and Vučica River. Extreme events such as drought and floods were calculated from above mentioned data series. Drought indices will be compared with groundwater levels for three different stations. Besides levels, short inside will be given in some groundwater quality parameters.

2.1 Land use change

Changes in land use on catchment area were analysed based on Corine Land Cover which is digital database of changes in land cover and land use for Republic of Croatia in period from year 1980 to 2012. This database is consistent and homogenized with the data of land cover for the entire European Union (Croatian Environment Agency). There are five different covers, for years 1980, 1990, 2000, 2006 and 2012. For Karašica-Vučica catchment, the biggest change appeared between 1980 and 1990 when 6673 ha were altered in its purpose. Most common changes were from deciduous forest, unirrigated arable land and predominantly agricultural land with larger areas of natural vegetation to transition area of forest, unirrigated arable land and complex of cultivated plots. Between 1990 and 2000, 4554 ha were altered from deciduous forest to transition area of forest and the vice versa. Smaller parts of land cover, 1078 and 1161 ha, for period 2000-2006 and 2006-2012 respectively, went through similar changes. Land use for year 2006 is shown on Fig. 2.

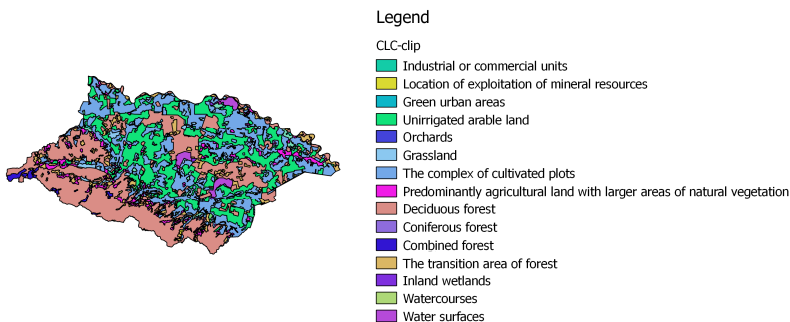


Fig. 2 Land use for year 2006 on catchment area

It is evident from Fig. 2 that the biggest part of catchment area is covered with forest and agriculture land. Even though agriculture is considered significant source of water pollutions, available data shows that there is no significant pollution on catchment area. Several groundwater samples were analysed from five different locations (Fig. 1) in period from 2006 to 2012. The highest concentration of nitrates, which are anthropogenic contaminant from agricultural activities, is 3.5 mgN/l (Fig. 3). Some of the most common heavy metals which can be found in groundwater are lead and mercury. Obtained concentrations of mercury are less than 0.3 $\mu\text{gHg/l}$ for entire period, and only four samples showed concentrations of lead greater than maximum permissible concentration.

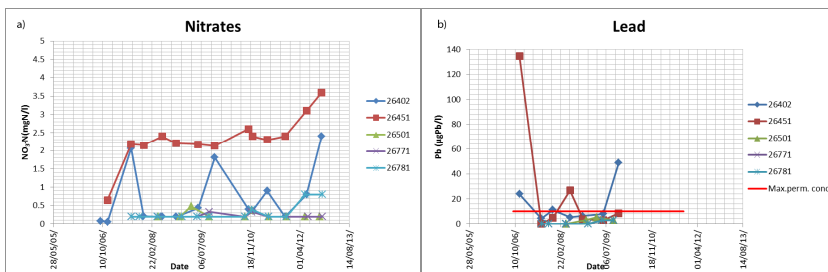


Fig. 3 Concentrations of nitrates and lead for five locations

2.2 Meteorological and hydrological features

Precipitation data series are available for five meteorological stations (Fig. 1) for the period between 1981 and 2014. Annual precipitation analysis did not show any significant change, but its fluctuations have been increasing which is evident from Fig. 4.

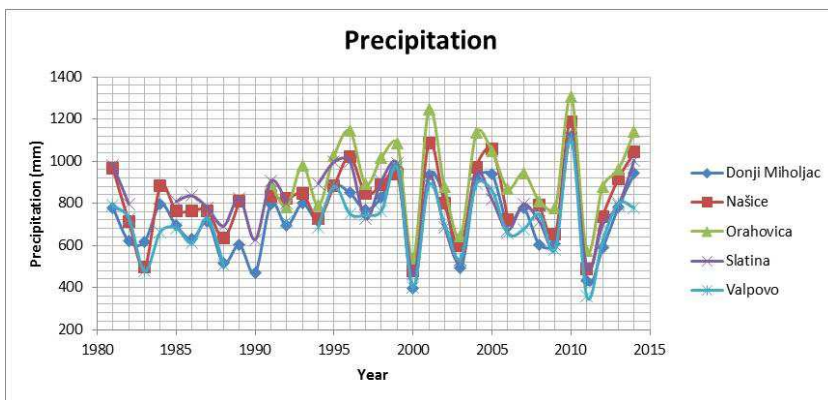


Fig. 4 Mean annual precipitation for five meteorological stations

The mean annual air temperature in the same period is 11.25 mm but it shows more significant change of $+0.31\text{ }^{\circ}\text{C}/10\text{ years}$ (Fig 5).

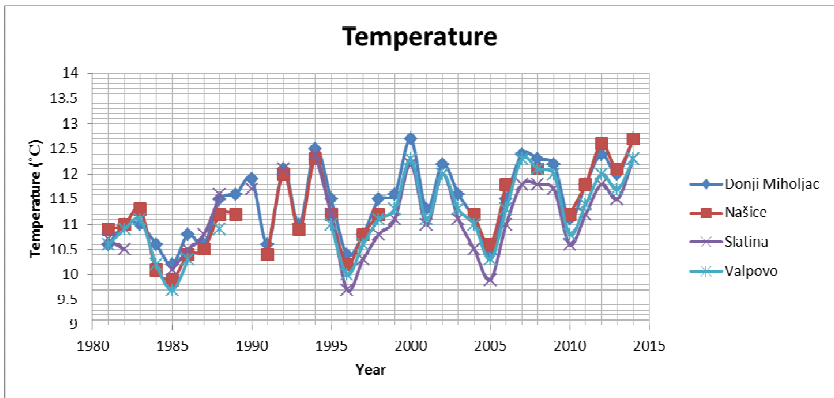


Fig. 5 The mean annual air temperature in the period between 1981 and 2014

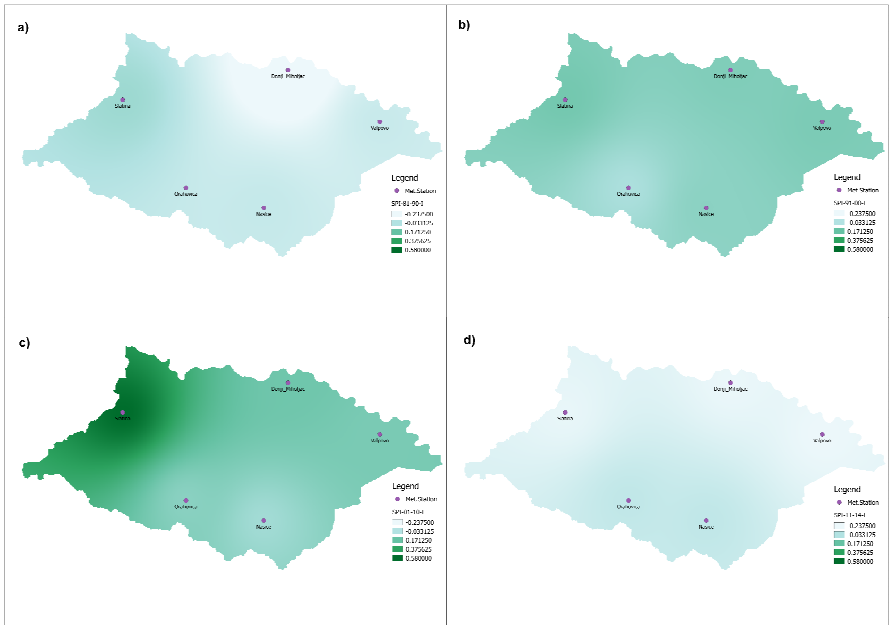


Fig. 6 Distribution of SPI for analysed area for different periods (a) 1981-1990; b) 1991-2000; c) 2001-2010; d) 2011-2015)

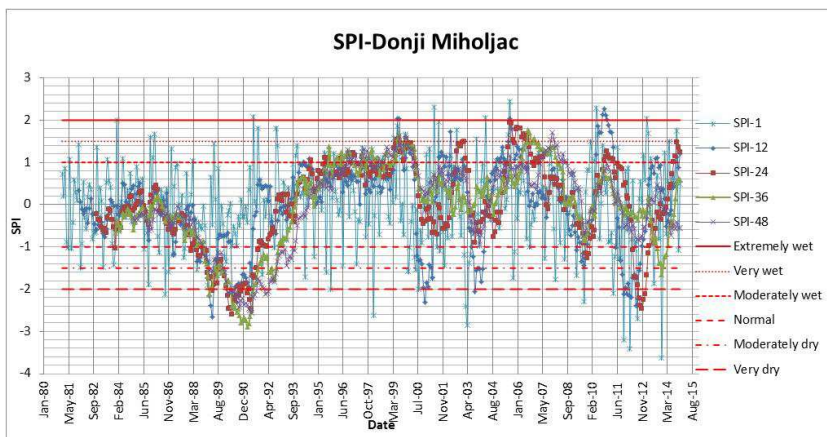


Fig. 7 SPI values for station Donji Miholjac

Drought was analysed based on standardized precipitation index (SPI). The SPI is based on normalised gamma distribution of precipitation and presents a number of standard deviations with regard to an average value. The basic advantage of this method lies in the fact that it necessitates only a set of precipitation for a longer period of time (30 or more years), and that it can be used for various time scales, the most frequent ones being 1, 3, 6, 12, and 24 months. Thus the same index can be used for the evaluation of precipitation deficit in various water resources (groundwater, open watercourses, soil moisture) depending on the purpose for which the drought analysis is made (McKee, 1995, Tadić et al., 2015). The computer program "spi_si_6" (National Drought Mitigation Centre, USA) was used for calculating monthly indices of standardised precipitation. Obtained results are shown in Fig. 6 and Fig 7. Occurrence of drought was more expressed in periods 1981-1990 and 2011-2014. For meteorological station Donji Miholjac, based on SPI-1, 28 months are categorized as very or extremely dry and 22 as very or extremely wet. The dries months occurred in period between 2011 and 2013 and in year 2003.

Besides, another extreme hydrological event, flood occurs also frequently. These floods are convective storm floods characterised by short duration on relatively small catchments (Tadić et al., 2002). Croatian flood protection system consists of three stages of warning. Each of them is related to specific water level. Fig. 8 presents annual frequency of flood episodes on the Karašica River (station Kapelna, 1981-2013) and Vučica River (station Beničanci, 1975-2013).

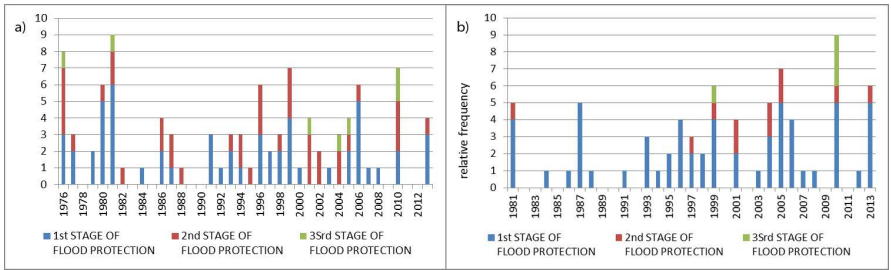


Fig. 8 Frequency of flood events on the for the a) Karašica and b) Vučica rivers

Hydrological characteristics of Karašica and Vučica rivers are presented in Figure 9 and Figure 10. It is important to notice extreme fluctuations of daily discharges which is significant characteristic of small catchments in general.

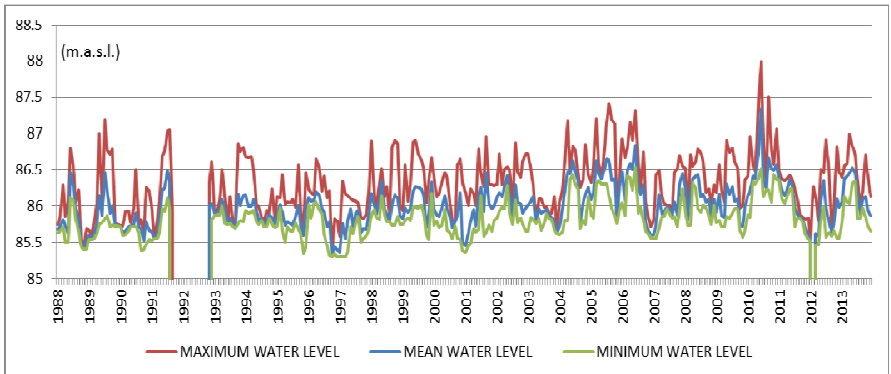


Fig. 9 Characteristic water levels of Karašica River (station Beliše) of the period between 1988 and 2014

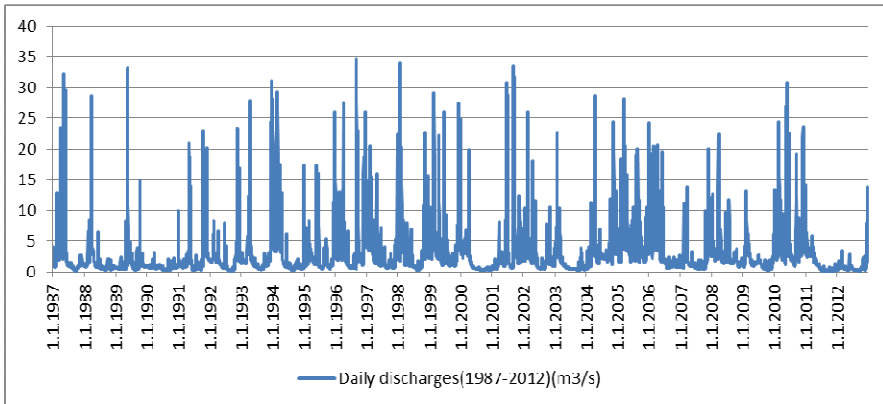


Fig. 10 Daily discharges of Vučica River (station Beničanci) of the period between 1987 and 2012

2.3 Groundwater

In the Pannonian Valley Problem of ground water depletion was recognized few decades ago. The scientists 25 years ago pointed out that intensive water abstraction, drainage systems and disturbance of the water balance caused by increasing of evapotranspiration in some parts of the Danube River Basin (Drava, Tisza, Sava river catchments) can have extreme impacts on groundwater recharge. The problem of depletion of shallow groundwater table was recognized in the Karašica and Vučica catchment area (Tadić, 1997).

Occurrence of drought has a negative impact on groundwater also. This impact is evident by decreasing of groundwater recharge, levels and discharge on time scale of months to years (Mishra et al, 2010).

Impact of drought on groundwater of catchment area is assessed by testing correlation between SPI indices and groundwater levels for three locations (Orehova, 2014).

Obtained coefficients of correlation are shown in Tab 1. Low, mean and high groundwater levels are tested with SPI indices calculated on basis of 1, 12, 24, 36 and 48 months. For two locations highest correlation is observed for SPI-12 and for third location SPI-36 is significantly correlated with low groundwater levels (0.768). For medium and high levels SPI-24 showed the highest correlation (0.762 and 0.730 respectively) for third location.

Tab 1. Coefficient of correlation of the SPI indices and groundwater levels

Station	Period	GWL	GWL _{ave} r	GWL _s t.dev.	SPI-1	SPI-12	SPI-24	SPI-36	SPI-48
P-59	1980 - 2012	GWT _{low}	90.959	0.789	0.156	0.599	0.500	0.473	0.413
		GWT _{mean}	91.218	0.760	0.239	0.607	0.481	0.463	0.411
		GWT _{high}	91.526	0.768	0.325	0.566	0.430	0.407	0.369
P-57	1980 - 2012	GWT _{low}	86.221	0.357	0.039	0.612	0.764	0.768	0.745
		GWT _{mean}	86.275	0.391	0.054	0.652	0.762	0.746	0.722
		GWT _{high}	86.331	0.417	0.068	0.634	0.730	0.718	0.691
DP-18	1988 - 2012	GWT _{low}	94.960	1.109	0.065	0.605	0.423	0.459	0.507
		GWT _{mean}	95.218	1.145	0.115	0.623	0.409	0.461	0.501
		GWT _{high}	95.487	1.185	0.166	0.621	0.385	0.450	0.481

The existence of connection between groundwater levels and SPI indices for longer time scale is confirmed with results of this analysis. This is in concordance with literature and statement that SPI of longer time scales are tied to stream flows, reservoir and groundwater levels (Orehova, 2014).

3. CONCLUSIONS

Small catchments are vulnerable areas where climate change has significant impact on all catchment's components. Analysis of data series of precipitation and temperature for catchment area Karašica-Vučica led to two different conclusions. Mean annual temperatures are increasing for all stations on catchment area. Increase is between 0.15 and 0.45 °C/10 years. However, observing mean annual precipitation, no significant trend can be detected, except for increased fluctuations in the last 15 years. Due to those fluctuations, extreme hydrological events such as droughts and floods are frequent in catchment area.

Occurrence of drought has a negative impact on entire hydrological system, including groundwater. This impact was demonstrated by correlating SPI indices and groundwater levels. Significant correlation coefficients were obtained with SPI of longer time scales and groundwater levels.

Fluctuations in precipitations cause fluctuations in stream flows which have impact on biodiversity and on water use for irrigation because of its instability.

4. REFERENCES

- CROATIAN ENVIRONMENT AGENCY. URL: <http://www.azo.hr/>.
- MCKEE, T.B., DOESKIN, N.J., KLEIST J. 1995. Drought Monitoring with Multiple Time Scales. *Conference of Applied Climatology*, American Meteorological Society, Boston, pp. 179-184,
- MISHRA, A.K., SINGH, V.P. 2010. A review of drought concept. *Journal of Hydrology*. 391, pp. 202-216.
- MOLDAN, B., ČERNÝ, J. 1994. Biogeochemistry of Small Catchments: A Tool for Environmental Research. *Environmental Science and Pollution Research*, Volume 1, Issue 4, pp 284-285.
- NATIONAL DROUGHT MITIGATION CENTRE, USA. URL: <http://drought.unl.edu/MonitoringTools/DownloadableSPIProgram.aspx>.
- OREHOVA, T., PAVLOVA, V. 2014. Groundwater drought in Northeast Bulgaria and SPI index. *Proceedings of XXVI Danube Conference*, 22-24 September 2014, Deggendorf, Germany. 335-338.
- RUCH, C.A., HARUM, T. 2002. Water balance components for forest and meadow land use systems in a crystalline catchment. *Proceedings of the 9th Conference of the European Network of Experimental and Representative Basins (ERB)*, Demänovská dolina (Slovakia), 25 – 28 September 2002, pp 26-32.
- TADIĆ, L. 1997. Groundwater Problems of the Agricultural Region in Drava River Basin. *Proceedings of the Workshop on Groundwater Depletion in Basin regions: problems arising in the area between the rivers Danube and Tisza*. Budapest, pp 107-108.
- TADIĆ, L. 2002. Analiza indikatora relevantnih za održivo gospodarenje vodama sliva Karašice i Vučice, Dissertation, Faculty of Civil Engineering Zagreb.
- TADIĆ, L., DADIĆ, T., BOSAK, M. 2015. Comparison of different drought assessment methods in continental Croatia. *Građevinar* 67, pp 11-22.
- TADIĆ, L., TADIĆ, Z., CRNČAN, I., KOROV, J. 2002. Analysis of Flood Frequency on the Area of Drava River Basin. *21st Conference of Danube Countries*. (Proceedings on CD), Bucharest, Romania.
- TESAŘ, M., ŠÍR, M., LICHNER, L. 2002. Runoff formation in a small catchment. *Proceedings of the 9th Conference of the European Network of Experimental and Representative Basins (ERB)*, Demänovská dolina (Slovakia), 25 – 28 September 2002, pp 7-12.

The influence of the synthetic rainfall hyetograph on runoff from urban catchment

K. Mazurkiewicz, M. Sowiński

The Institute of Environmental Engineering, Poznan University of Technology
M. Skłodowskiej-Curie 5, 60-965 Poznań, Poland,
e-mail: karolina.mazurkiewicz@put.poznan.pl; marek.sowinski@put.poznan.pl

Abstract

The purpose of the analysis presented in the paper was to examine the influence of the synthetic hyetograph pattern on characteristics of runoff hydrograph from urban catchment. The storm water outflow simulations were made with the use of rainfall-runoff model implemented for use as EPA SWMM5 package. The model was built on basis of real catchment of area 6.7 km², which was located in the city of Poznan, Poland. The model consisted of 82 conduits with the total length of 14 km. On basis of the regional IDF Curves, the Euler rainfall hyetographs of II type were developed for the frequencies of the rainfall recommended by PN-EN 752 for typical catchment development (i.e. 2 years, 5 years and 10 years). The simulations were made for five rainfall durations: 15 min, 30 min, 45 min, 60 min and 90 min. For different rainfall durations and frequencies of the rainfall the simulations were made for three locations of rainfall peak: at 0,3 of the rainfall duration (according to ATV118) and two neighbouring locations: at 0,2 and 0,4 of the rainfall duration. The outflow hydrographs at the outlet of main sewer for each simulation were compared. The following characteristics of outflow hydrograph were compared: maximum flow (peak), time to peak and maximum flow depth. Obtained conclusions can be useful for design of storm sewers.

Keywords

Rainfall-runoff model, runoff hydrograph, SWMM5, synthetic hyetograph, urban catchment

1. SYNTHETIC STORM HYETOGRAPH

The correct design of an efficient and economic drainage system basis on the knowledge of drainage system hydrograph. The estimation of inflows at all drainage inlets is then required. In Poland for any specific frequency the customary rainfall-duration formula is used (i.e. IMGW formula). This formula gives an information only about the average rainfall intensity during a specific

rainfall duration, but the temporal changes of the rainfall intensity during this duration period is unknown. The usual situation is when the rainfall intensity is changing during a specific rainfall duration. In most cases in Poland there are no reliable records of intense rains that can be used in hydrodynamic modelling of sewer design. The synthetic storm hyetograph presenting the temporal variation of rainfall intensity (or rainfall depth) during a specific rainfall duration of sewer design is an option that can be used in hydrodynamic modelling of storm sewer system.

According to available literature reviews two types of synthetic storm pattern for runoff study are used: the block rainfall intensity (the same intensity during whole rainfall duration, used e.g. in construction of IDF curves) and an intermediate type (the rainfall intensity is changing during rainfall duration, the peak occurs inside the borders of the interval). Using a block rainfall intensity can result in a lower values of runoff peak [Sieker et al. 1980], thus the intermediate type of synthetic storm pattern should be used in hydrodynamic modelling in sewer design.

The purpose of the presented research was to examine the influence of the rainfall peak location in the synthetic hyetograph (represented by time to peak for rainfall hyetograph t_{pr}) on characteristics of runoff hydrograph from urban catchment, i.e. maximum flow depth, peak flow and time to peak flow.

The Euler rainfall hyetographs of II type were chosen for presented research due to the several reasons. First, this type of rainfall hyetograph is recommended by ATV-A 118, which has a rich experience in rainfall- runoff modelling. Second, the method of developing synthetic storm pattern presented in ATV is the most recent method among others like recommended by the SCS [US SCS 1964] and DVWK [DVWK 1984]. The final argument for selection ATV method is that the climatic and geographic conditions in Germany and Poland are similar.

2. EULER HYETOGRAPH AND ITS MODIFICATION FOR PURPOSE OF AN ANALYSIS

The construction method of Euler II type hyetograph according to ATV-A 118 is based on the following procedure. On the basis of IDF curves, the rainfall depths for the consecutive rainfall intervals are calculated. The beginning of rainfall peak is located at the 0,3 of the rainfall duration. The next lower intervals are joined on to the left of the rainfall peak until the point in time $t = 0$ is reached. Further rainfall intervals of lower rainfall depth are attached on the right side of peak period until the end of considered rainfall duration. In Figure 1 a synthetic storm pattern of Euler II type for rainfall duration $t_d=15$ min and frequency $c=5$ years is shown. This storm pattern was developed from IDF curve which was evaluated using recommended in Poland formula of Bogdanowicz and Stachy [Bogdanowicz, Stachy 1998].

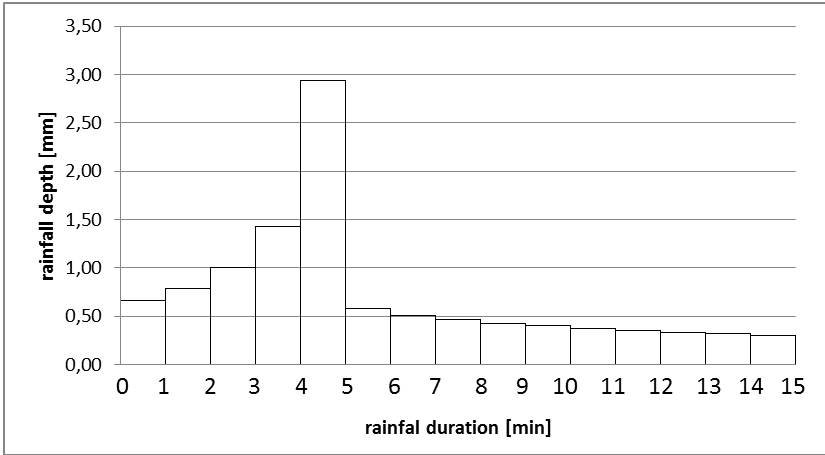


Fig. 1 A synthetic hyetograph of Euler II type for Poznan city based on Bogdanowicz-Stachy formula; c= 5 years

Computer simulations were performed for three synthetic hyetographs with different peak locations characterized by the ratio of time to peak t_{pr} to rainfall duration t_d :

$$r = \frac{t_{pr}}{t_d} \quad (1)$$

The locations of rainfall peak were assumed for Euler type hyetograph as a basic on $t_{pr}^{bas}=0,3t_d$ ($r=0,3$), $t_{pr} = t_{pr}^{bas} - 0,1t_d$ ($r=0,2$) and $t_{pr} = t_{pr}^{bas} + 0,1t_d$ ($r=0,4$). It means decrease and increase of t_{pr}^{bas} by 10%, respectively.

The rainfall peak location was examined for different rainfall durations ($t_d= 15; 30; 45; 60; 90$ min) and rainfall frequencies ($c= 2; 5; 10$ years).

The maximum rainfall duration was determined by the concentration time—the time needed for water to flow from the farthest point in the catchment to the considered cross section. For the concerned experimental catchment this time was evaluated as about 60 min.

Considered rainfall frequencies were recommended by the PN-EN-752 for typical kinds of land development.

The rainfall time step recommended by ATV is 5 minutes. The time step in this research was assumed as $\Delta t= 1$ min in order to enable precisely location a peak of the hyetograph. For larger time step recommended by ATV-A118 and short rain durations the rainfall peak location would not have changed in the considered hyetograph. For example for rainfall duration of 15 min and time step of 5 min for time to peak t_{pr} equal to $0,2 t_d$ and $0,3 t_d$ the rainfall peak would occur in first five minutes period, so the research purpose would not be achieved.

3. THE EXPERIMENTAL URBAN CATCHMENT AND ITS MODEL

An experimental catchment is located in Poznan, Poland. Its surface is 6.7 km² and is mainly covered by dwelling houses built in the second half of the last century.

Evaluated separately for each subcatchment an average percentage of impervious surface was assessed as about 30%. A slope of the catchment was computed as an average slope of the terrain determined along its main collector.

The runoff from the surface is directed to storm sewer system. Model of the catchment consisted of 55 subcatchments. Only larger conduits with diameter of 500 mm and above were taken into consideration in the model. Therefore number of sewer stretches was limited to 82.

The computation of storm sewers roughness based on depth and flowrate measurements [Skotnicki, Sowiński 2008]. The evaluated roughness was $n=0,018$.

In order to ensure flow with a free surface in each storm sewer a slight modification of existing conduits was required. It was realized by enlarging the diameters of certain conduits by 1 or 2 normalized sizes.

4. TRANSFORMATION OF RAINFALL INTO RUNOFF FROM EXPERIMENTAL CATCHMENT

The transformation of rainfall into runoff was performed applying package SWMM5 to the model of catchment described above. As a result of simulations an outflow hydrographs were computed which were later used for evaluation such characteristics as:

- Maximum depth: h_{\max} [m];
- Maximum flow (peak flow): Q_{\max} [dm³/s];
- Time to peak flow: t_p [min].

Exceeding full flow conditions causes pressurized flow. To avoid this situation the maximum depth and maximum flow in the main sewer were considered. Time to peak flow was examined due to overlapping the peak flow rates in further sewerage conduits. This overlapping depends on specific storm sewer system-time to peak flow in individual main sewers may be at the same range which may cause exceeding full flow conditions in the main sewer.

5. THE RESULTS OF COMPUTER SIMULATIONS

To examine the influence of the rainfall peak location on maximum depth h_{\max} the following terms were defined:

- A difference between depths h_{\max}^{bas} evaluated in main sewer outlet for Euler II type synthetic hyetograph ($r=0,3$) assumed as a basic and its

modified variants h_{\max}^r (for $r=0,2$ and $0,4$) for given rainfall duration t_d and frequency c :

$$\Delta h_{\max}^r = h_{\max}^r - h_{\max}^{\text{bas}} \quad [\text{m}] \quad (2)$$

- A relative difference defined as a ratio of Δh_{\max}^r with respect to the peak flow evaluated for basic (Euler II type) variant of synthetic hyetograph h_{\max}^{bas} :

$$\delta h_{\max}^r = \frac{\Delta h_{\max}^r}{h_{\max}^{\text{bas}}} \cdot 100 \quad [\%] \quad (3)$$

Similar investigation of the influence of rainfall peak location on Q_{\max} and t_p was based on following terms:

- For peak flow Q_{\max} :

$$\Delta Q_{\max}^r = Q_{\max}^r - Q_{\max}^{\text{bas}} \quad [\text{dm}^3/\text{s}] \quad (4)$$

$$\delta Q_{\max}^r = \frac{\Delta Q_{\max}^r}{Q_{\max}^{\text{bas}}} \cdot 100 \quad [\%] \quad (5)$$

- For time to peak flow t_p :

$$\Delta t_p^r = t_p^r - t_p^{\text{bas}} \quad [\text{min}] \quad (6)$$

$$\delta t_p^r = \frac{\Delta t_p^r}{t_p^{\text{bas}}} \cdot 100 \quad [\%] \quad (7)$$

In order to analyze the influence of rainfall peak location on maximum depth h_{\max} Figure 2 was made. It presents three pencils of curves, each consisted of three individual curves. They show the relation between maximum depth h_{\max} and rainfall duration t_d for three different rainfall frequencies c (the lowest, the middle and the highest pencil respectively for $c=2, 5$ and 10 years) and three variants of synthetic hyetograph (according to equation 1: $r=0,2; 0,3$ and $0,4$) represented by individual curve from each pencil.

The middle situated curves in each pencil on Figure 2 represents values approximated for basic variants of synthetic hyetographs (for $r=0,3$), the lower and upper curves represent modified variants evaluated respectively for $r=0,2$ and $0,4$.

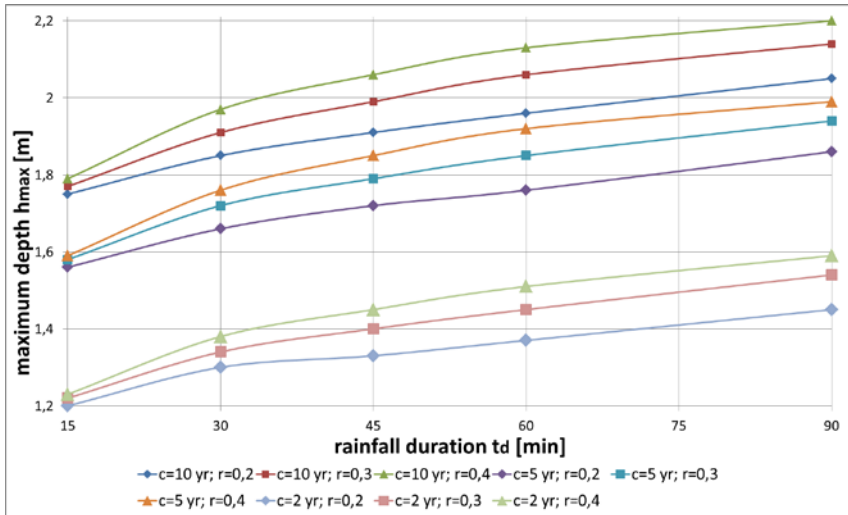


Fig. 2 Maximum depths for different rainfall durations t_d , rainfall frequencies c and r values

According to the equation (2) and (3) the differences between maximum depths determined for lower values of time to peak t_{pr} (for $r=0,2$) had negative values. It means that the maximum depths were lower than for basic variant ($r=0,3$). Respectively mentioned above differences between maximum depths for upper values of t_{pr} (for $r=0,4$) had a positive values, which means that they were greater than for basic variant. The variability of differences δh_{max}^r is presented in Table 1.

Tab 1. Variability of differences δh_{max}^r and δQ_{max}^r

Rainfall duration t_d [min]	Rainfall frequency c [years]	$r=0,2$		$r=0,4$	
		δh_{max}^r [%]	δQ_{max}^r [%]	δh_{max}^r [%]	δQ_{max}^r [%]
15÷45	2	-(1,6÷5,0)	-(2,1÷9,3)	0,8÷3,6	1,5÷6,4
	5	-(1,3÷3,9)	-(2,6÷7,7)	0,6÷3,4	1,2÷6,5
	10	-(1,1÷4,0)	-(2,8÷7,9)	1,1÷3,5	1,4÷6,9
60÷90	2	-(5,5÷5,8)	-(9,7÷10,9)	3,2÷4,1	7,1÷8,3
	5	-(4,1÷4,9)	-(7,8÷9,1)	2,6÷3,8	5,8÷7,2
	10	-(4,2÷4,9)	-(7,8÷9,2)	2,8÷3,4	5,2÷5,8

The analyze of the influence of rainfall peak location on maximum flow Q_{max} based on Figure 3, which construction was similar to Figure 2. The variability of differences between δQ_{max}^r is presented also in Table 1.

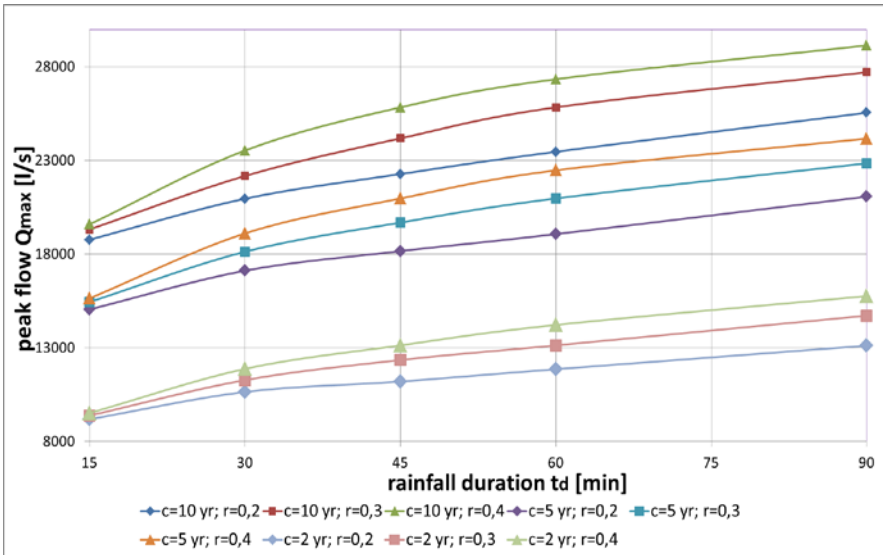


Fig. 3 Maximum flows for different rainfall durations t_d , rainfall frequencies c and r values

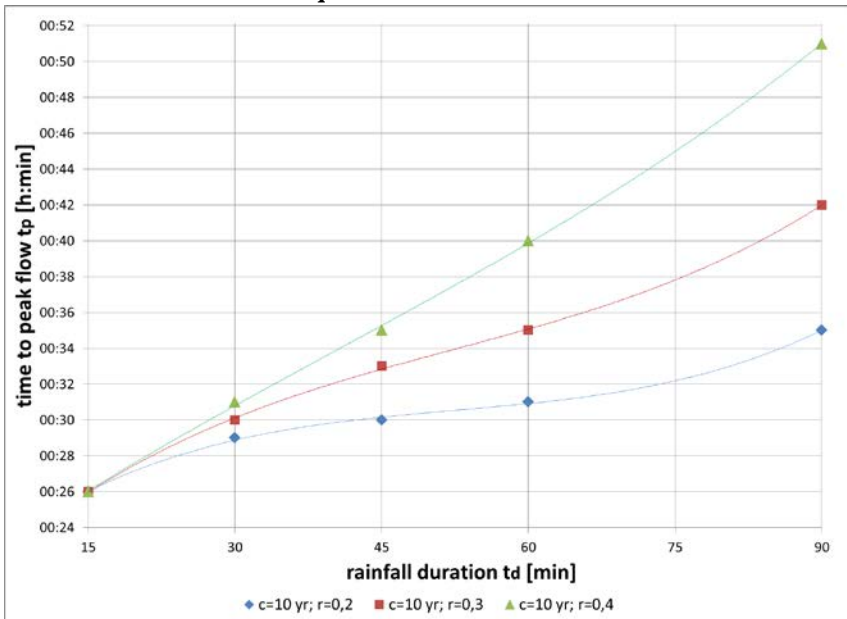


Fig. 4 Times to peak and regression lines for rainfall frequencies $c=10$ years and different rainfall durations t_d and r values

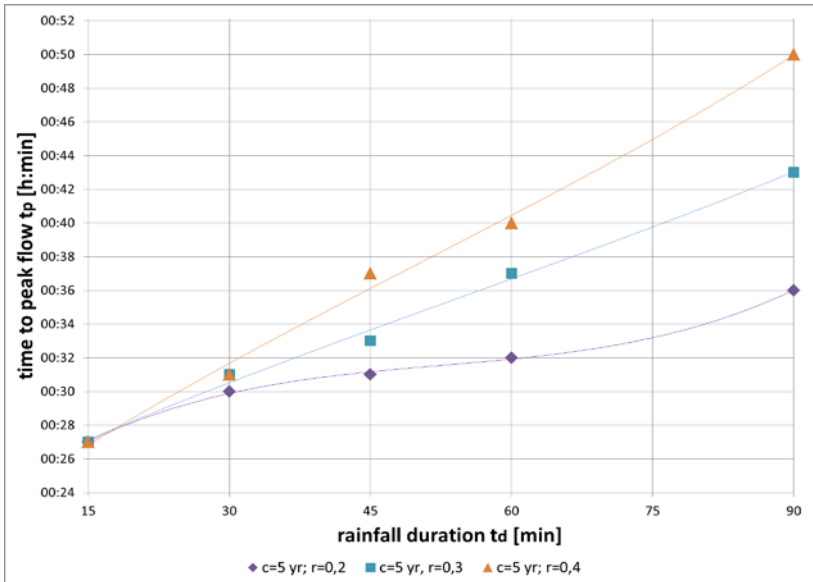


Fig. 5 Times to peak and regression lines for rainfall frequencies $c=5$ years and different rainfall durations t_d and r values

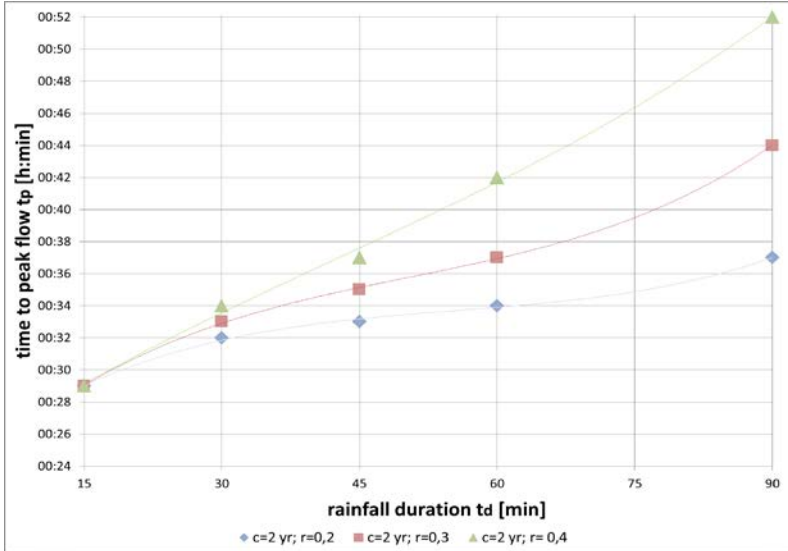


Fig. 6 Times to peak and regression lines for rainfall frequencies $c=2$ years and different rainfall durations t_d and r values

To analyze the influence of rainfall peak location on time to peak t_p Figures 4,5 and 6 were made. On each Figure the middle situated curve represents values approximated for basic variants of synthetic hyetographs (for $r=0,3$), the lower and upper curve represent modified variants evaluated respectively for $r=0,2$ and $0,4$. Due to irregular location of points outlining curves a regression analysis was applied to generate the regression line. They were described by polynomial of the third degree with the coefficient of determination R^2 higher than $0,998$.

The variability of differences Δt_p^r and δt_p^r is presented in Table 2. According to the equations (6) and (7) the differences between times to peak flow determined for lower values of time to peak t_{pr} (for $r=0,2$) had negative values, which means that the maximum flows occurred earlier than for basic variant ($r=0,3$). Respectively mentioned above differences between times to peak flow for upper values of t_{pr} (for $r=0,4$) had a positive values, which means that the maximum flow occurred later.

Tab 2. Variability of differences Δt_p^r and δt_p^r

Rainfall frequency c [years]	r=0,2		r=0,4	
	Δt_p^r [min]	δt_p^r [%]	Δt_p^r [min]	δt_p^r [%]
2	0÷(-6)	0÷(-14)	0÷9	0÷20,9
5	0÷(-6)	0÷(-14,3)	0÷7	0÷16,7
10	0÷(-7)	0÷(-16,7)	0÷9	0÷21,4

6. CONCLUSIONS

A decrease of time to peak of synthetic hyetograph by 10% of rainfall duration in comparison with Euler type hyetograph (for $r=0,2$) results in:

- decrease of maximum depth in the range $\delta h_{\max}^r = -(1,1 \div 5,0)\%$ for $t_d=(15 \div 45)\text{min}$ and $\delta h_{\max}^r = -(4,1 \div 5,8)$ for $t_d= (60 \div 90)\text{min}$;
- decrease of peak flow in the range $\delta Q_{\max}^r = -(2,1 \div 9,3)\%$ for $t_d=(15 \div 45)\text{min}$ and $\delta Q_{\max}^r = -(7,8 \div 10,9)\%$ for $t_d= (60 \div 90)\text{min}$;
- decrease of time to peak flow of outflow hydrograph by $\delta t_p^r = 0 \div (-16,7) \div \%$.

An increase of time to peak of synthetic hyetograph by 10% of rainfall duration in comparison with Euler type hyetograph (for $r=0,4$) results in:

- increase of maximum depth in the range $\delta h_{\max}^r = (0,6 \div 3,6)\%$ for $t_d=(15 \div 45)\text{min}$ and $\delta h_{\max}^r = (2,6 \div 4,1)$ for $t_d= (60 \div 90)\text{min}$;

- increase of peak flow in the range $\delta Q_{\max}^r = (1,2 \div 6,9)\%$ for $t_d = (15 \div 45)\text{min}$ and $\delta Q_{\max}^r = (5,2 \div 8,3)\%$ for $t_d = (60 \div 90)\text{min}$;
- increase of time to peak flow of outflow hydrograph by $\delta t_p^r = 0 \div 21,4\%$.

Changes of flow Q_{\max} and depth h_{\max} characteristics, as an effect of changing rainfall peak location in synthetic hyetograph, can result in overloading in storm sewers. According to European regulations (e.g. ATV A118, PN-EN 752), designers should check on the model a behavior of the system in a case of its overloading in order to evaluate consequences of potential overflows.

An influence of third considered characteristic- time to peak outflow- can be important in case of well-developed network, when flows from individual conduits can overlap in main sewer. Similar to mentioned above situation, flows overlapping can result in main sewer overflow.

7. REFERENCES

- ATV A118 2006. Hydraulische Bemessung und Nachweis von Entwässerungssystem. *ATV Regelwerk Abwasser – Abfall*. ATV GFA, Hennef
- BOGDANOWICZ E., STACHY J. 1998. Maksymalne opady deszczu w Polsce. Charakterystyki projektowe. Materiały badawcze, seria: Oceanologia i Hydrologia, IMGW, Warszawa
- DVWK 1984. Arbeitsanleitung zur Anwendung Niederschlag-Abflub-Modellen in kleinen Einzugsgebieten. Regeln 113, Teil II: Synthese, Verlag Paul Parey, Hamburg
- SIEKER, F.; VERWORN H.R. 1980. Wird der Blockregen als Bemessungsregen dem Postulat "Regenhäufigkeit= Abflusshäufigkeit" gerecht? *Wasser und Boden*, 32, H.2, p. 52-55
- SKOTNICKI M., SOWIŃSKI M. 2008. Badanie zmienności współczynnika szorstkości kanału deszczowego na podstawie pomiarów przepływu, materiały I Ogólnopolskiej Konferencji Naukowo-Technicznej INFRAEKO 2008, Rzeszów - Paczółtowice, p. 193-204
- US SCS (Soil Conservation Service) 1964. National engineering handbook. Section 16. Drainage of Agricultural Land. US Dept. of Agric., Washington D.C.

Acknowledgement

This research was made under the project dedicated for young researches DSMK 806 in 2015 year.

Evaluation of reservoir degradation state by Autonomous Underwater Vehicle (AUV)

V. Sočuvka, Y. Velísková

(Institute of Hydrology, Slovak Academy of Sciences, Racianska 75, 831 02 Bratislava, Slovak Republic, e-mail: socuvka@uh.savba.sk.)

Abstract

Understanding the interactions of ecological condition in water reservoir system and how they vary over time and space is necessary for evaluation, modeling and predicting various types of productivity for a given water body. Therefore repetitive surveying of inland water areas has become more essential to evaluate reservoir sedimentation, river degradation, water flow or water quality monitoring. Traditional techniques of observation are generally expensive and non effective. They also do not offer a comprehensive coverage, especially nowadays, when the requirements for environmental field studies become more and more demanding. AUVs represent the newest trend in hydrographic survey which makes the research of water environment more accessible to scientific study. This contribution present first results of using an AUV, in Central Europe, to collect high-resolution spatial data and water quality parameters which have been obtained in 2014 at location Water Dam Veľké Kozmálovce.

Keywords

AUV, EcoMapper, bathymetry, water quality, water reservoir

1. INTRODUCTION

Erosion, transport and deposition of bottom sediments in water bodies represent a significant impact on river system and its environment. As a result of erosion, within the terms of the Slovak Republic, is every year created nearly 40 million cubic meters of sediments. This causes a gradually clogging of water dams and the related reduction of surface and groundwater quality. Between the most intensive erosion-sedimentation processes affected water dams (WD) in Slovakia belongs WD Veľké Kozmálovce. Since the start of operations in 1990, enormous sedimentation of bottom sediments is monitored in WD Veľké Kozmálovce. The result is relatively fast and permanent loss of the disposal volume of the reservoir (Sočuvka & Velísková, 2014). The reservoir sedimentation has a significant negative impact on water quality and hydraulic continuity between surface and underground water. On this basis, the site has been identified as potentially suitable for monitoring spatial and qualitative changes in the short as well as in the long term. Recent developments in research and development of AUVs equipment allows us to obtain detailed data information on the state of the water environment. AUVs now represent one of the most modern and complex ways of

hydrographic survey. The aim of this paper is to provide introductory information on AUVs, describe their basic functions, create overview of their applications and the creation of bathymetric model of the bottom of the reservoir in the area WD Velké Kozmálovce.

2. A BRIEF HISTORY OF AUV VEHICLE

AUVs represent devices which are currently used in a wide range of hydrographic research, marine geoscience, military, commercial, and policy sectors. In general, they have shape of a torpedo and originally they were developed for military purposes. The first AUV was developed at the Applied Physics Laboratory at the University of Washington as early as 1957 by Stan Murphy and Bob Francois. Vehicle was used to study diffusion, acoustic transmission, and submarine wakes (Vijay, 2011). During the eighties of last century AUVs have been applied also for the water exploration and hydrographic survey. As one of the most significant instrument is considered IFREMER L'Epaulard, which has been built by ECA in association with the French oceanology research institute in the eighties of last century. IFREMER L'Epaulard was used for oceanographic survey with a depth range up to 6000 m. In the following years research and development of new AUV devices allows their use in inland conditions and also increases the area of the measurement about biological and geochemical parameters. Currently there are about 10 companies which develop and sell AUVs on the international market, including company like Kongsberg Maritime, Yellow Spring Instrument, Bluefin Robotics, International Submarine Engineering or Hafmynd.

3. YSI ECOMAPPER

Ecomapper represents a device, which is capable to move on the surface and subsurface water level independently and perform data logging. This device is ideal for coastal and shallow water applications such as hydrographic surveys and spatial environmental monitoring. Survey mission can be performed in water with depth more than one meter and EcoMapper is fully capable of subsurface operations down to 100 m. EcoMapper has been development by YSI Company (USA) and it's designed for a quick and easy collection of bathymetry, sonar and water quality data.

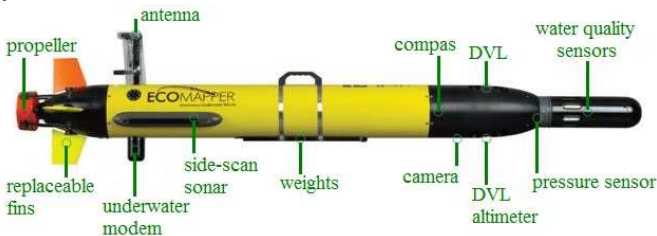


Fig.1. YSI EcoMapper side view (YSI, 2009)

EcoMapper device consists of a hardware part (Fig.1) and software program Vector Maps, which is designed for mission planning and for partial analysis of measured data (Fig.2). Physically, the vehicle can be divided in 3 distinct parts. The bow section contains water quality sensors that interact with the aquatic environment and Dopler Velocity Log (DVL) for navigation under water. The middle section includes on-board computer, the electronic components, batteries and weights for balance of vehicle. The tail section contains a propulsion system and GPS antennas for navigation on water surface. The physical design allows an easy deployment from shore by one person. All external components on the vehicle can be easily replaced. The external replaceable components include the water quality sensor, handle and balance assembly, vehicle antennae, control planes, propeller and cowling (YSI, 2009).

Tab.1. System Technical Specifications of AUV EcoMapper (YSI, 2012)

Dimensions	Diameter: 14.73cm, Length: 160.8cm
Weight (air)	Weight: 20.41kg
Depth	1 - 100 meters
Endurance	8 hours at speeds of 4.5 km/h;
Speed Range	2 – 6 km/h
Communication	Data: wireless 802.11g Ethernet 2.4 GHz radio link when on the surface
Navigation	Surface: GPS Subsurface: Bottom tracking or DVL
Onboard Electronics	Intel ATOM processor with Windows XP; 80 GB drive for data collection
Software	VectorMap: Mission planning Sonar Mosaic: Processing of sonar records UVC: Underwater Vehicle Control,
Depth Sonar	500kHz SBES within 5°, accuracy 0.003m
Doppler Velocity Log	10-beam DVL for navigation, bathymetry and current profiling
Water Quality Sensors	Conductivity, Temperature, Dissolved Oxygen, Turbidity, pH/ORP, Chlorophyll, Blue-green Algae, Rhodamine Dye, Salinity

During the measurement (mission) Ecomapper collects every second predetermined parameters, which are automatically associated with Geographic Coordinates (latitude, longitude). Water quality measurements include information's such as water temperature, dissolved oxygen, turbidity, pH, chlorophyll, salinity, etc. Measuring of the depth of the bottom (bathymetry) is

carried out by integrated single beam echo-sounder. Device uses a frequency of 500 kHz, a range of measurement from 1 to 100 m depth, and measurement accuracy ± 0.003 m.

3.1 Mission planning

The EcoMapper follows a predefined mission plan created by the user. This mission plan is created in the graphical user environment of Vector Map Software. Mission planning starts by downloading available geo-referenced charts, maps or satellite images into the Vector Maps planning software and then clicking position of way points for vehicle navigation (Fig.2.). Mission planning includes set points for each leg to a way point, speed, depth or undulate for data collection. Additionally, operators can click and drag any way points to edit a mission. This simple but powerful tool lets you program the vehicle and sensor parameters for each leg or for a complete survey.

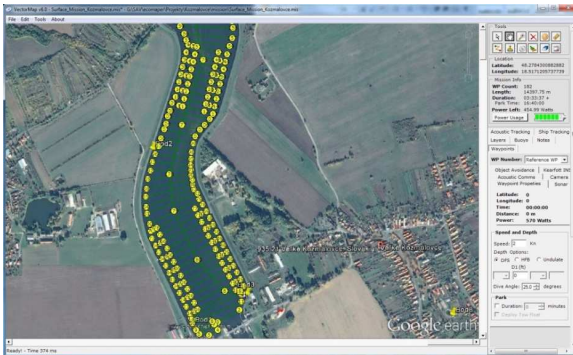


Fig.2. Mission planning in software program VectorMap

The programme output is an ASCII mission file that is uploaded to the EcoMapper via a wireless interface prior to mission start. Once the vehicle has started its mission, it operates independently and uses GPS waypoints and DVL navigation to complete its programmed course. Throughout the course, the vehicle constantly steers toward the line drawn in the mission planning software (VectorMap), essentially following a more accurate course of coordinates instead of transversing waypoint-to-waypoint. Upon completing its mission, the vehicle uses Windows® Remote Desktop to relay the collected data via WiFi connection, facilitated by the Communications Box, to the user's computer (YSI, 2012).

4. CHARACTERISTICS OF THE STUDY AREA

Water Dam Veľké Kozmálovce is located in the Hron River basin, which is characteristic by 284 km river system with mainly short tributaries. The catchment of the area has an elongated shape due to the narrow valleys with high

mountains on both sides of the river. The mean slope of the river varies from about 7.6 ‰ in the upper part to 0.9 ‰ in the lowlands. The Hron River drains 11.2% of Slovakia. From the geological point of view the catchment area of the river Hron is formed by rocks of the Neogene - Quaternary pools, Neogene-Quaternary volcanics, Mesozoic and Crystalline. Geographically, the selected area is the north-eastern part of the Danube Lowland, which is bordered from the north by Štiavnicke Vrchy Mountains. The location of the river within the territory of Slovakia is shown in Figure 3.

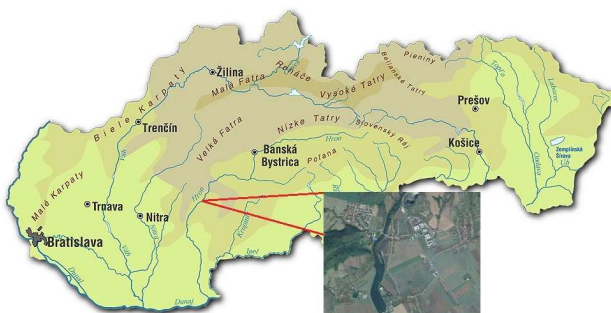


Fig.3 Locations of the Water Dam Veľké Kozmálovce

The climatic conditions of the Hron River basin correspond to the European-continental climatic region of the mild zone, with oceanic air masses transforming into continental ones. The selected location is geomorphologically part of Hron basin, which represent comparatively monotonous flat land splitted by locally deeper erosion furrows and distributary channels of Hron river. Groundwater around the selected area is formed by quaternary alluvial deposits of floodplain river, which are characteristic by a high degree of saturation. Quaternary sediments mainly consist of sandy gravel, which are covered by a layer of flood clay loam. Surface water regime is influenced by rivers flowing through the territory and is in hydraulic continuity with ground water. Ground water level is free, respectively very slightly tense with a depth of 2 - 4 meters below the ground. The average ground water level on the basis of engineering-geological survey is on the elevation of 171.8 m asl. WD Veľké Kozmálovce is designed for short term balance of the flow on Hron River and for irrigation withdrawals to channel Perec. However the main purpose of WD is to provide cooling water for nuclear power plant in Mochovce, which has a strategic importance in the energy field.

5. DATA COLLECTION AND DATA PROCESSING

Hydrographic survey of the WD Veľké Kozmálovce took place in October, 2014. The aim of the survey was create, respectively update 2D topography of the reservoir. For data collection has been utilized previously described AUV

EcoMapper, which gather data about depth and water quality in one second intervals.

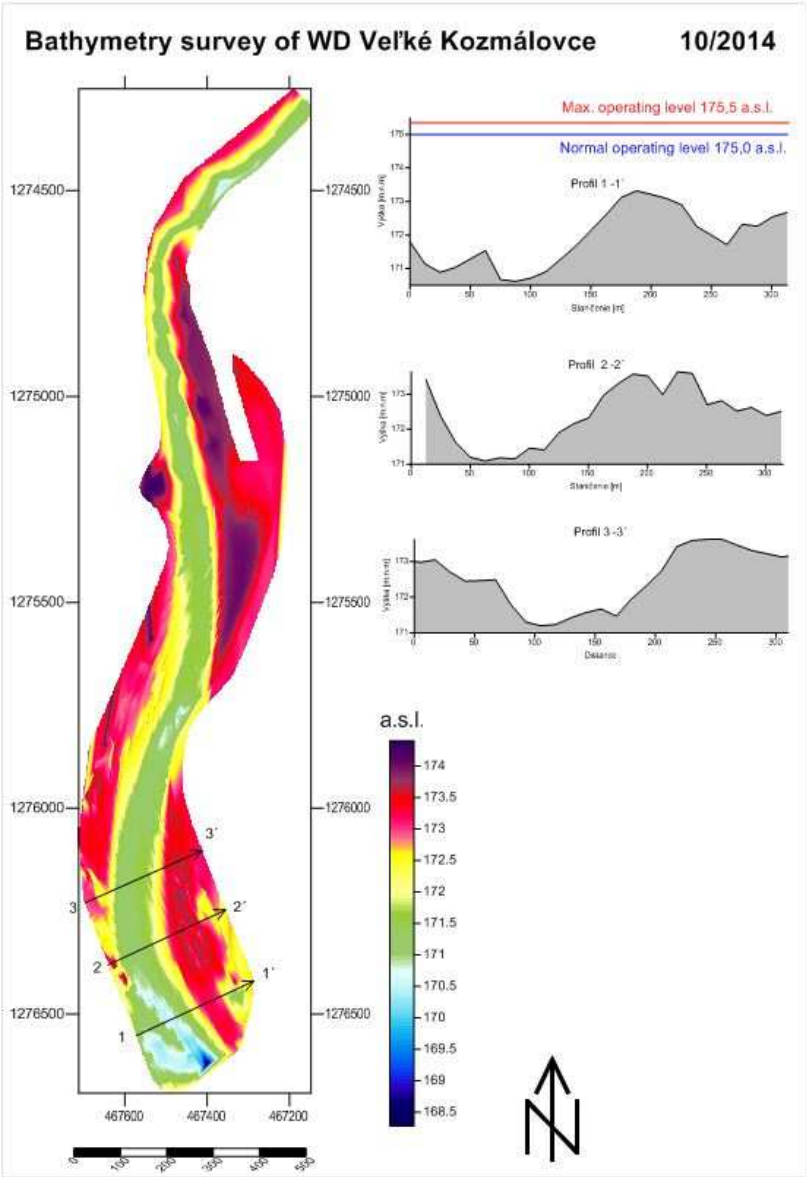


Fig. 4 Bathymetry of WD Velké Kozmálovce and curve of the bottom in selected profiles

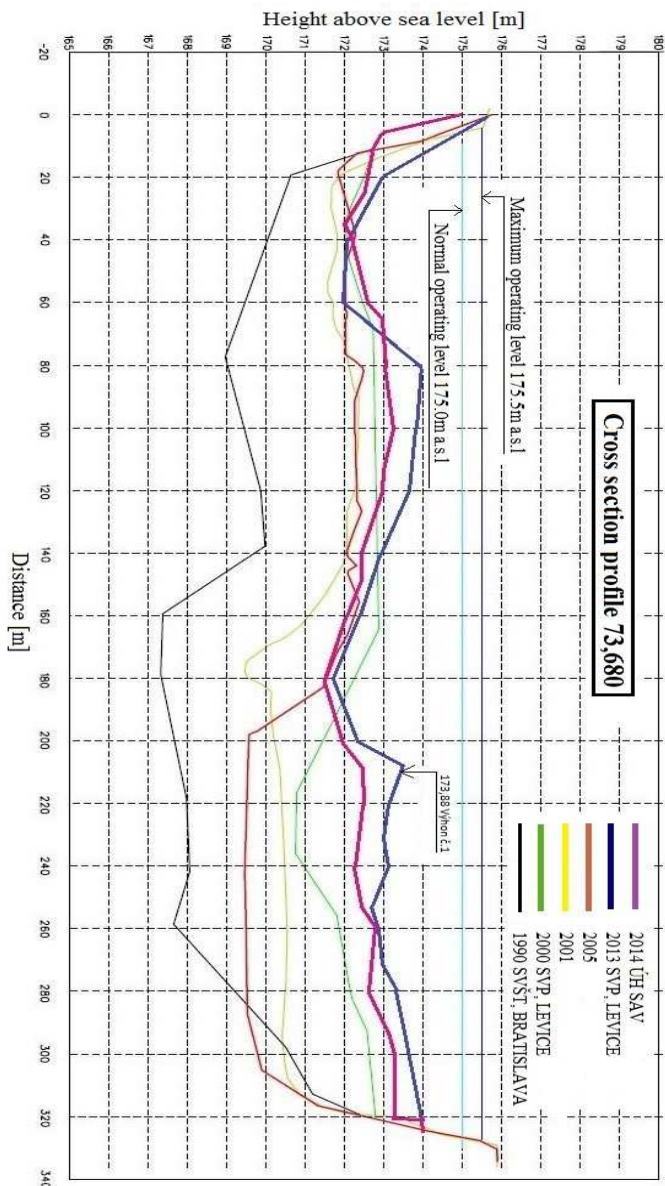


Fig. 5 Comparison of colmatage of WD Veľké Kozmáľovce between years 1990 - 2014

Simultaneously, these data were automatically supplemented to geo-referenced data, which combine qualitative parameters and depth to the exact position in the

coordinate system of the World Geodetic System 1984. The total number of collected data is 14499 for each measured parameter. As the previous measurements and the results of measurements on VD Veľké Kozmálovce were presented in a coordinate system S-JTSK, the first step in the processing of measured data was the conversion of measured data. To the data conversion program was used Univcol 3.6 (Universal Column Calculator), which is oriented to work with geo data, which have specified coordinates. In addition to mathematical operations with columns, allows sorting data shows basic statistics for the columns, calculates the coordinate systems, filters data, calculates the correlation between the columns and formats output (Marušiak, 2014). Simultaneously to the coordinate system conversion, the depth data conversion was performed. The depth figure was subtracted from the actual water level H level, which had value of 174.9 m during the measurement. Followed by importing and processing measured points in the software Surfer 9 (Golden Software), where were generated with cell dimensions of 2 x 2 meter (Fig.4). To display the relief of the bottom was also used software ArcMap 10.1.

6. DISCUSSION AND CONCLUSIONS

Based on the current status of the bottom bathymetry the current status of clogging the reservoir was evaluated. Subsequently, comparison of reservoir clogging over the years was created, respectively updated. Figure 5 shows one profile on the 73.68 river kilometer and comparison of clogging between years 1990-2014. According to project documentation of WD, storage capacity has been considered before starting acceptance run in 1990 on 3 230 155 m³. Based on operating instructions of WD Veľké Kozmálovce and newest bathymetry storage capacity is only 1 989 450 m³. It entails a reduction of reservoir storage about 38,41 %. It therefore follows that role of bathymetry and recent sedimentation in water reservoir management is very important. Innovation and development of new hydrographic equipments increased the range of their potential applications and effectiveness of their use. Their application allows us to obtain these informations more efficiently, faster and with relatively high precision.

7. REFERENCES

- SOČUVKA, V., VELISKOVÁ, Y. 2014. Possibilities of determining the thickness and volume of the bottom sediments in water reservoirs. Acta Hydrologica Slovaca 2014, Vol., 15., 370-378 p.
- MARUŠIAK, I., 2014. Universal Column Calculator 3.6 manuál. G-trend, 25p.
- VIJAY .S, 2011, AUTONOMOUS UNDERWATER VEHICLES ,PESCE Mandya, <http://www.scribd.com/doc/55826714/Autonomous-Underwater-Vehicles>
- YSI Ecomapper operation manual, 2009, YSI (Yellow Springs Instruments)
- YSI Hydrodata Limited,2012, Messingham Sands Bathymetry and Water Quality Survey, Report Number 5219032012

Reasons why Onsite Wastewater Treatment Systems are not Systematically Used in the Republic of Croatia

D. Malus, D. Vouk

Water Research Department, Faculty of Civil Engineering, University of Zagreb, Kaciceva 26,
1000 Zagreb, Croatia, phone: +38514639359, fax: +38514639238, e-mail: malus@grad.hr,
dvouk@grad.hr

Abstract

Onsite wastewater systems (OWTS) are practically not used at all in Croatia. All old sewerage systems, new ones and planned ones are classical. The fact is that some countries use OWTS very intensively, improve them in terms of safety and technical efficiency and prove their advantages in use in many situations. The question is why such systems do not pass in Croatia although 40% of Croatian population lives in villages and settlements up to 2,000 inhabitants.

When treated wastewater is discharged underground, limitations in use of OWTS are primarily related to soils permeability, groundwater table and terrain slope. Likewise family home lots are often too small for the implementation of some basic OWTS technologies. On the other hand the utility companies in Croatia are not organizationally and technically competent to manage such systems, and resist implementation. Among citizens and some professional circles OWTS are inferior in every way and cannot meet sanitary and environmental standards.

The national agency for water management has not made the necessary steps in the professional and legal regulations, so the basic requirements for the wider application are not satisfied.

The paper studies the objective and subjective reasons why OWTS systems are not used. It analyzes briefly the situation in the world and then in Croatia. The reasons for lack of OWTS implementation are searched at local and national level through traditional and new urban solutions, soil type and hydro-geological realities, the attitude of the profession and policy, traditional heritage, cultural habits. The paper also draws attention to the fact that uncontrolled implementation of OWTS by the enthusiastic citizens can result in dangerous sanitary and environmental impacts.

Keywords

onsite wastewater treatment systems, implementation, Croatia

1. INTRODUCTION

What are Onsite Wastewater Treatment systems (OWTS)? There are several definitions, out of which three are mentioned herein. The first one is: Onsite/decentralized wastewater treatment systems, commonly called septic systems, treat sewage from homes and businesses that are not connected to a centralized wastewater treatment plant (EPA, 2000); the second (Boulder County, Colorado, 2014): "Onsite wastewater treatment system," or "OWTS," and, where

the context so indicates, the term "system" means an absorption system of any size or flow or a system or facility for treating, neutralizing, stabilizing, or dispersing sewage generated in the vicinity, which system is not a part of or connected to a sewage treatment work, and third (Boulder County, Colorado, 2014): Onsite wastewater treatment system (OWTS) is a broad term referring to any system for collection, storage, treatment, neutralization, or stabilization of sewage that occurs on the property.

The most important starting points in the definition is that these are systems not connected to a centralized wastewater treatment plant (WWTP), located at or close to the source of wastewater, most frequently on private property, consisting of the septic tank and the absorption unit, and treating sewage from households and business premises (not from industry).

In developed countries the largest number of OWTS, or decentralized systems was built in USA. Onsite wastewater treatment systems collect, treat, and release about 15.14 million cubic meters of treated effluent per day from an estimated 26 million homes, businesses, and recreational facilities nationwide (U.S. Census Bureau, 1999). These systems, that serve fewer than 20 people, include treatment units for both individual buildings and small clusters of buildings connected to a common treatment system (EPA, 2000).

By 2001, it was estimated that more than 1 million OWTS were installed in Australia, with the greatest distribution in New South Wales (300,000), followed by Victoria (250,000) and Queensland (250,000) (Gunday, et.al. 2015).

In Europe, OWTS are not used in such great numbers, but are realized through sewerage plans for all settlements under 2,000 PE that have not been included in priority construction programs in EU member countries.

In Germany, 1.8 million plants (up to 50 PE) are installed, despite the fact that 96% of households are connected to public sewer systems and slightly less than 4% of the population treat their wastewater in small scale sewage facilities (Baltic Sea Region Programme, 2011).

The basic unit of OWTS is one household. Around the house there is enough space to accommodate OWTS consisting of a treatment unit and the absorption unit. Treated wastewater is often used within the household as well as sludge from the treatment process.

Connecting of several households, larger residential buildings and minor settlements unavoidably imposes the need of construction of sewerage network with specific plants, and the sewerage systems begin to look like conventional public sewerage systems; however, these systems show their decentralized nature, first of all due to their size and maintaining of other properties of OWTS, such as reuse of treated wastewater and nutrients from sludge. Final capacities of OWTS/decentralized systems are not strictly defined. Sometimes they are divided into larger and smaller, individual and cluster or joint ones. In EU there are guidelines for systems up to 50 PE (EN 12566-3, 2006) and in USA OWTS

include systems with inflow less than 2000 gallons per day (7600 l/day) (EPA, 2000).

According to the IWA Specialist Group for Small Water and Wastewater Systems the limit for small systems was arbitrarily set to less than 100,000 L/day. Depending on per capita water use within the house this is equivalent to wastewater produced by about 500-1000 persons. A decentralized system can of course consist of many individual onsite systems or a series of larger clusters or one decentralized system. The most important thing is not how large the system is, but whether it meets the prerequisite of the fundamental definition, i.e. that it is not connected to a centralized sewerage system, and even more important that treated wastewater and nutrients from sludge are used at their source. Decentralized sewerage systems often use unconventional systems for transport of wastewater (vacuum and pressure sewerage, small profile gravity sewerage), treatment of wastewater and discharging of treated wastewater. Likewise, ready-made package WWTPs are often used as well. Where OWTS are used in the framework of strategic approach, and not only as one of technical solutions of sewerage, usually other operations are carried out as well, as drainage of rain water and separation of gray and black wastewater, or even separation of urine from feces.

2. CENTRALIZED VS DECENTRALIZED SYSTEMS

There is a long tradition of dispute which system is cheaper, centralized or decentralized? If we believe the authors (ORTH, 2007; HO, 2004) the costs of construction, operation and maintenance are approximately the same, provided that centralized systems do not involve a lot of re-pumping and deep excavation. A certain approach or strategy of using of decentralized systems may be conceived on their other advantages such as higher ecological sustainability due to recycling of water and nutrients, and higher level of social sensitivity. This means that decentralized systems are not only a supplement to centralized systems in the areas where their use would be economically unfeasible, but that it is a matter of approach which takes into account a larger number of relevant standpoints.

Table 1 gives the comparison of environmental impacts of centralized and OWTS, demonstrating that OWTS show better properties due to the use of treated wastewater and nutrients which are returned into soil. Controlling the use of toxic agents allows obtaining of sludge and treated wastewater free of toxic substances, while in centralized systems avoiding of toxic substances from industry is hardly possible. It should be kept in mind that many centralized systems suffer from considerable infiltration of ground water and rainfall which cause adverse influence on operation of WWTP and costs of pumping. Higher sustainability of decentralized sewage systems is supported by the fact that such solutions are frequently connected with more efficient drainage of rain water and use of gray waters from households.

Table 1 Comparison between environmental impacts of centralized and onsite systems (HO, 2004)

Centralized systems	Onsite systems
Safe disposal of treated wastewater is primary objective. Removal of nutrients and other pollutants have been increasingly required, to prevent eutrophication of receiving water bodies. Reuse of treated wastewater will require an additional piping and pumping system.	Onsite reuse of treated wastewater is usually an objective of onsite systems. Nutrients are recycled back onto land.
Wastewater may be contaminated with industrial wastewater discharged to sewerage system.	Contamination with toxic substances can be minimized by householder. Treated wastewater and sludge can be applied onto land onsite.
Ingress of stormwater into sewerage system is common, resulting in combined sewerage overflow.	Stormwater can be permeated to groundwater.

Likewise, social aspects should not be omitted from the analysis for selecting of the system of public sewerage. Table 2 shows the comparison of social aspects for centralized and decentralized systems which is valid in Australia and other countries having similar legal solutions and sources of financing regarding sewerage. The need is stressed for central management of decentralized systems, as otherwise the desired effects might be lost, with adverse impact on ground water and health risks.

The project of the sustainable city strives towards the optimum organization of space and functions in traffic, management of air pollution, energy for heating and cooling, forming of structures and properties, and social aspects of personal security and general welfare of the community. The idea is that towns should consist of more densely populated urban villages separated by free open space, interconnected by quick public transport (Newman et al., 1999). In the urban village all places are accessible by maximum 15 minute walk. This limits the size of the settlement to 5,000-10,000 inhabitants. Such settlement is serviced by OWTS at lower population density either with one decentralized system, or more decentralized systems at greater population density. Treated wastewater is used within the settlement and on areas between urban villages, as well as the nutrients from sludge, all in dependence on population density. Water supply and rainwater drainage are based on local sources (use of rainwater), avoiding of channeling and recharging of the aquifer.

In this concept of the sustainable city decentralized sewage reaches its full sense, showing that it is not only the matter of which solution is less expensive regarding construction, operation and maintenance.

**Table 2 Comparison of social aspects of centralized and onsite systems
(HO, 2004)**

Centralized system	Decentralized system
<p>Taken for granted as the standard of wastewater management. Well established government policy, regulatory framework, government agencies or corporation responsible for its management.</p>	<p>Fragmented management of septic tanks. Local government responsible for approval of installation. Householders are responsible for management with poor environmental outcome. Rapid development of onsite and decentralized system technology meeting same standard of performance as centralized system, but still with unsatisfactory management. Centralized management is essential.</p>
<p>Considerable investment by governments, and requirement to connect to recoup investment costs.</p>	<p>Investment by householder, and expectation to forego investment when sewerage reaches property.</p>
<p>Community expectation for water reuse in arid regions may force governments to consider decentralized systems.</p>	<p>Environmental sustainability features of onsite and decentralized systems may make communities consider installing them.</p>

3. SITUATION IN REPUBLIC OF CROATIA

In Croatia there is a number of installed smaller package WWTPs operating on the principle of activated sludge, SBR process or rotating biological contactors. Most of them are related to service facilities in remote locations out of towns (hotels, gas stations, tourist camps, small industrial plants), and only a negligible number serve households. The OWTS concept has not been incorporated in any of the sewerage projects for a settlement as a whole.

In the Republic of Croatia about 40% of population live in settlements smaller than 2000 inhabitants. There are about 2500 settlements of up to 100 inhabitants and about 1800 settlements with 100 to 500 inhabitants (Croatian Bureau of Statistics, 2011). One could conclude on the basis of the above data that Croatia is an ideal country for application of OWTS and decentralized sewerage systems in general.

It must be mentioned that houses in small rural settlements are situated on the average on small individual plots and properties, condensed in historic centers and dispersed in the periphery, which often renders full application of OWTS impossible. A large part of the country is the karst area, and there are areas with frequently high ground water tables, where aquifer pollution is highly probable if conventional methods of subsurface infiltration are applied.

Table 3 Number of settlements according to size from 1-2000 (Croatian Bureau of Statistics, 2011)

Number of inhabitants	Settlements	Population	Share (%)	
			Settlements	Population
Total in CRO	6,759	4,437,460	100.0	100.0
up to 100	2,489	108,186	36.82	2.44
101-200	1,337	194,230	19.78	4.38
201-500	1,561	496,824	23.10	11.20
501-1,000	719	505,860	10.64	11.40
1,001-1500	218	253,192	3.08	5.71
1501-2,000	113	194,253	1.67	4.38
Total		1,752,545	95.09	39.51

The social and economic picture of the Croatian village is considerably poorer than the EU average, and the average age of the population is high, with constant depopulation. In such social environments, which frequently do not have the solution of wastewater management in a sanitarly acceptable way, it is hard to introduce technologies that require more intensive participation of the population and a high level of ecological consciousness. Some households still use old solutions of joint collecting of wastewater from domestic animals and the people, a great number use so-called “black pits” which are in fact primitive septic tanks without bottoms, and some of them which are closer to urban centers are connected to centralized sewage systems.

On the other hand, through realization of the Implementation Plan for Water Utility Directives (Gov. R.C., 2010) as the commitments taken over from pre-accession negotiations with EU, projects are in progress in which a large number of small settlements is connected to agglomerations with centralized sewerage systems. This is the choice of the national agency for water protection, with strong pressure of local communities to be included in agglomerations larger than 10,000 PE in the first wave of priority investments. Huge sewerage systems were constructed, with a large number of re-pumping stations, long pressure pipelines and unreasonably high unit costs of construction for small rural settlements.

According to everything that has been done so far, in Croatia the question is not centralized or decentralized public sewerage systems but is there any room left for decentralized systems? What could look like a decentralized system are the subsystems of centralized systems. Analyzing of alternative solutions of public sewerage, only economic criteria are evaluated, related to the scope of agglomeration, where often the data are produced that speak in favor of a centralized sewerage system.

As regards the criteria of reuse of treated wastewater, nothing has been done so far, but there are possibilities to do this on centralized systems with MBR technology which still remain to be constructed in Istria (2 WWTP with total 120.000 PE). Even for these plants there is only a declaration of intention to use

treated water in agriculture, although nothing has been done regarding technical prerequisites and contracts with possibly interested users.

3.1 Science-profession

In Croatia, science is trying to follow developments in the world of OWTS, and the students of hydro-engineering in civil engineering colleges are taught about the subject. Scientific papers are published, courses and workshops are organized. The Faculty of civil engineering, University of Zagreb, has developed a program package primarily meant for finding of optimum solution of public sewerage for one or more minor settlements (Vouk, 2009). On the basis of the data on the number and type of users, topographic, hydrogeological and other data the program will, through a sequence of simulations, determine the optimum configuration of the public sewerage system for a number of technical and technological solutions of collecting, transport, treatment and releasing of wastewater, through multicriteria analysis procedures.

The professional community, in its major part, does not possess adequate knowledge in this sector, and generally takes a negative attitude towards such solutions. The reason may be that such solutions are simple and based most frequently on onsite preparatory works for installation of ready-made equipment, and such projects are not so lucrative as those for centralized systems. It is interesting that multicriteria analysis is often misused in selecting of optimum sewerage systems to prove that centralized systems are a better choice than the decentralized ones.

3.2 Legislation and government administration

The European Council Directive 91/271/EEC concerning urban wastewater treatment states that “Treated wastewater shall be reused whenever appropriate”. The problem is that the term ‘appropriateness’ remains legally undefined and left to each country to define it independently.

In application of decentralized sewerage and OWTS, very often the classic recipient of treated wastewater is not close at hand, and treated water is released into the ground by means of various infiltration units. Releasing into soil, and further into ground water is restricted in legislation. The Regulations on Limit Values of Wastewater Emissions (Croatian Legislative, 2015) in the first article state that the Regulations “prescribe the limit values of emissions in wastewater prior to release into sewerage facilities or recipients, and exceptionally permitted release into ground water”. The last amendment to the same Regulation of 2015 announces passing of the following documents within one year:

- criteria for elaboration of analyses of impact on the status of water related to exceptional indirect release of wastewater into ground water, and
- criteria for indirect release into ground water (limit values of emissions, degree of treatment, etc.).

So far it is not known whether these criteria are going to be on the existing restrictive line, or will be adjusted to the practice of the countries that exercise

releasing of treated wastewater into the soil. This of course does not mean that any release should be permitted without limitations.

There are no documents on the national and local level that would regulate OWTS from the legal and technical standpoint. Also, there is no extension service to help the users by qualified advice, nor registered contractors capable of constructing OWTS in accordance with the rules of profession.

3.3 Users

The authors believe that final users feel uneasy and reject decentralized systems for various reasons:

- they are not educated enough to know what it is all about,
- they are familiar with the conventional centralized system which does not require almost any personal engagement in use.
- some of them are secretly afraid of potential health problems,
- general climate in the society from political and professional standpoints is not ready for alternative solutions.

In the present trend of rapid growth of coverage by public sewerage systems, authorities in local communities do not want, for instance, a constructed wetland in their settlement, because they believe, due to its simplicity, that it cannot compete with activated sludge process requiring a large number of concrete tanks and a lot of various electromechanical equipment.

According to various sources, some house owners (mostly owners of weekend cottages) build their own OWTS. Although these are mainly educated people, they often, due to the lack of professional assistance, threaten their own health, and also the environment, in particular ground water.

4. CONCLUSION

Sustainability of decentralized systems should be considered in the context of sustainable management of urban water supply, wastewater treatment, solving of rainwater drainage, and planning of settlements, making the cities more sustainable in other sectors as well (power, transport, food, construction, biodiversity).

Environmental considerations indicate that small (onsite and decentralized) systems are more conducive to achieving environmental sustainability. These include water reuse, recycling of nutrients (nitrogen and phosphorus) contained in the wastewater, separating domestic wastewater from stormwater runoff, and excluding industrial wastewater thus preventing contamination of domestic wastewater (and the sludge) designed for reuse.

There is economy of scale to be realized with centralized systems. This is particularly true with the cost of treatment. The investment, operation and maintenance costs of centralized systems are, however, largely tied to the

sewerage system. There can therefore be diseconomy of scale if pumping is required to move wastewater through the sewerage system, and if ingress of stormwater or ground water is excessive when we try to collect and transport wastewater from a large urban area (hence long distances).

The Republic of Croatia, due to a large number of small rural settlements, is suitable for application of OWTS. Unfortunately, for several reasons they are not applied, while at the same time huge central systems are built, with many connected small settlements through a large number of repumping stations and long pressure pipelines.

OWTS certainly bring some risks if used without predetermined criteria. Drawbacks and risks are elaborated in the experience of the countries that use them and that have undertaken all necessary legal and technical measures in the field of planning, construction, operation and maintenance of the systems in order to make them environmentally effective and safe from the sanitary point of view. In this respect, the Republic of Croatia is lagging in all relevant fields. There is no political will, existing legislative solutions are very restrictive regarding releasing of treated water into the soil, reuse of treated wastewater and sludge generated in the treatment process. The profession shows no affinity to OWTS, municipal utilities are not ready from the staff, technical and organizational point of view, and the local population and administration is skeptical and uneducated.

With all pros and cons regarding the use of OWTS in Croatia, the fact remains that there is a large number of cases where they may be utilized, especially if modern solutions are applied that guarantee high efficient treatment (at tertiary level) and high sanitary safety.

It may be expected that in future the use of OWTS will become more intensive, mainly at the level of conscious individuals and local communities, but some decisive steps have already been taken which will never give OWTS the chance they deserve.

5. REFERENCES

- BOULDER COUNTY, COLORADO, 2014. Onsite Wastewater Treatment System (OWTS) Regulations, Onsite wastewater treatment system act, 25-10-101, et seq. C.R.S. (i.e. Colorado Revised Statutes),76 p.
- BALTIC SEA REGION PROGRAMME, 2011. Decentralized Wastewater Treatment, 2007-2013. *SPIN Newsletter #4 - May 2011*, <http://spin-project.eu/>
- COUNCIL DIRECTIVE 91/271/EEC, 1991 concerning urban waste-water treatment.
- CROATIAN BUREAU OF STATISTICS, 2011, Census of population, households and dwellings.
- CROATIAN LEGISLATIVE, 2015. Pravilnik o graničnim vrijednostima emisija otpadnih voda (Regulations on limit values of wastewater emissions), Narodne novine, br. 80/13, 43/14, 27/15.

- EPA, 2000. Guidelines for Management of Onsite /Decentralized Wastewater Systems, EPA-832-F-00-012, 2 p.
- EUROPEAN STANDARD EN 12566-3, 2006. Small wastewater treatment systems for up to 50 PT - Part 3: Packaged and/or site assembled domestic wastewater treatment plants, 34p
- GOVERNMENT OF THE REPUBLIC OF CROATIA, 2010. Implementation Plan For Water Utility Directives, 46p
- GUNADY, M., SHISHKINA, N., TAN, H. and RODRIGUEZ C. 2015. A Review of On-Site Wastewater Treatment Systems in Western Australia from 1997 to 2011, *Journal of Environmental and Public Health*, Vol. 2015, 12p
- HO, G., ANDA, M. 2004. Centralized versus decentralized wastewater systems in an urban context: the sustainability dimension, In: Beck, M. and Speers, A. (eds) (2006), 2nd IWA leading-edge conference on sustainability, Sydney, November 2004. IWA Publishing, pp 80-89.
- NEWMAN, P.W.G. AND KENWORTHY J.R. 1999. Sustainability and cities: overcoming automobile dependence. Island Press, Washington D.C., 442p
- ORTH, H. 2007. Centralized Versus Decentralized Wastewater Systems? *Gewässerschutz wasser abwasser*. pp 42/1-42/8
- U.S. CENSUS BUREAU. 1999. 1997 National Dana Chart for Total Occupied HousingUnits. <<http://www.census.gov/hhes/www/housing/ahs/97dtchrt/tab2-6.html>>.
- VOUK, D., 2009. Ekspertni sustav podrške pri odabiru optimalnog sustava odvodnje u ruralnim naseljima, Disertacija, (Expert support system in selection of optimum sewerage system in rural settlements: Thesis) Građevinski fakultet, Sveučilište u Zagrebu.

Membrane Technology in Surface Water Treatment for Drinking Purposes

D. Barloková¹, J. Ilavský¹, M. Kunštek¹, J. Buchlovičová²

¹Department of Sanitary and Environmental Engineering, Faculty of Civil Engineering, Slovak University of Technology, Bratislava, Radlinského 11, 810 05 Bratislava, Slovakia, danka.barlokova@stuba.sk

²Vodatím s.r.o., Zvolenská 27, 821 09 Bratislava, Slovakia

Abstract

At this article are presented membrane separate processes – microfiltration, ultrafiltration, nanofiltration in water treatment and materials and modules used in application of various membrane technologies. Theoretical part is completed with results from pilot plant experiments realised in water treatment plant Klenovec, where was compared present technology of water treatment and microfiltration with ceramic membranes. Over the last years water quality has deteriorated in water-supply reservoir Klenovec and this technology was tested for the purposes of modernization of the inefficient technology in water treatment plant. The results obtained from pilot plant experiments in WTP Klenovec supported theory, that this process with high efficiency of treatment surface water is suitable for this kind quality of water to obtain water for drinking purposes.

Keywords

drinking water, membrane processes, microfiltration, ultrafiltration, surface water

1. INTRODUCTION

Membrane separation processes are increasingly being used not only for water treatment of sea water during last years, but in the treatment of underground, surface and waste water as well. In consideration with a classic treatment (such as coagulation and classic filtration) the reason of increasing popularity of use of membrane processes in a treatment of drinking water is mainly in a perfect water quality of a treated water that is being achieved by using membrane technologies. Alike achieving a good water quality the other aspects of using membrane processes are beneficial such as decreasing the sludge production, reduction in energy consumption, making possible the easy expansibility by modular system. Moreover, for being realised these processes do not demand a large built up area.

Membrane processes solve a lot of requirements connected to tighter specifications for a various ineligible substances. These substances are presented in water which makes them a reasonable issue in obtaining a quality drinking water. The biggest advantage of these processes represents their ability to remove

completely the pathogenic organisms resistible to the disinfection based on using chlorine. Membrane technologies are very efficient also in combination with a proper pre-treatment of water in removal of presented natural organic matter (NOM) whose presence is responsible for an ineligious colouring of the water, the stink and taste of the water. These substances mainly act as the pre-cursors for formation of the disinfection by-products.

1.1 Membrane processes

A thin, semipermeable membranes in water separation into two separate flows caused by the action of pressure are used in membrane processes.

Microfiltration (MF), Ultrafiltration (UF), Nanofiltration (NF) and Reverse Osmosis (RO) are among the membrane processes based on separation of particles of a certain size from water by using the impact of pressure difference. A typical feature common for all these methods is a semipermeable membrane (0.05 – 2.0 mm), which catches/holds or passes required components. Towards the classic mechanical filtration, these processes are able to separate the particles of the size of microns above all. The macromolecules and particles up to the size of the ions may be separated eventually by these processes.

1.2 Membranes

Membrane has to be as so much thin as possible, because of its resistance to pass-by of the components would be as low as possible. The membrane has to resist the effect of big pressure differences. Therefore it is being usually manufactured as a thin layer on a porous solid base making a low resistance against the passing-by component – so called asymmetry membrane or the membrane may consist of more than a one layer – a composite membrane formed by a combination of several inorganic and organic layers in order to improve its mechanic attributes.

The requirements given to a membrane are these:

1. high selectivity,
2. high permeability,
3. long lifetime.

Selectivity influences the separation efficiency, the regeneration of membrane and purity of the product. The selectivity is inversely proportional to the dimension of membrane area. It is the most important factor in assessment of membrane quality, since an insufficient selectivity requires a multistage equipment which is usually less economically profitable than a conventional separation processes.

Permeability has an impact on the velocity of filtration process and also it affects the dimension of membrane area necessary for a proper separation and therefore it increases the capital costs to the process.

Lifetime of the membrane depends on its stability to the mechanical, thermal and chemical impacts and has an impact on maintenance costs or on eventual membrane exchange.

Membranes are being manufactured from a modified natural polymers (acetate, acetylbutyrate and a nitrate of cellulose), from synthetic polymers (polyamides, polyethylene, polypropylene) and from other various materials (ceramic, metal membranes).

There is a disadvantage in using these materials:

- a natural affinity to the organic substances,
- sensibility towards the strong oxidizers,
- sensibility towards the formation of microbial biofilms.

These factors are decreasing the lifetime of polymeric membranes and it is necessary to perform the membrane exchange after some time.

The ceramic membranes whose pores are regular (equidistant), with a good thermal and mechanical properties are perspective. These membranes are manufactured by laying a ceramic layer containing pores of a diameter of 0.05 μm on the bearing stratum consisting of SiC or Al_2O_3 with pores of a diameter of 8-10 μm .

In consideration to polymeric membranes, the advantage in using the ceramic membranes rests in:

- almost no (or minimal at least) affinity towards the organic substances
- the endurance towards the aggressive chemical substances (strong oxidizers, strong acid solutions)
- a short time of washing (by compressed air or power water)

Based on the factors that are mentioned above, the opinion on the lifetime of ceramic membranes is much longer than it is in case of polymeric. Therefore the operation costs are decreasing in the process of water treatment.

1.3 Membrane modules

In a membrane technology, the membranes are used in a form of membrane modules, so called structural elements containing a proper arrangement of the membranes for a certain process. The requirements on the module are: a large surface of the membrane on the unit volume of the module, a cheap production, an easy access during the treatment and an easy exchange of the membrane.

In terms of shape and arrangement the modules are:

- | | |
|-------------------------|--------------------|
| a) tubular | d) plate-and-frame |
| b) capillary | e) spiral wound |
| c) with a hollow fibres | |

1.4 Comparison of the membrane processes

Microfiltration

In contrary to the classic filtration, when the smaller particles that are being removed from water are about the dimension of micrometres, the particles of the size of 10^4 to 10^2 nm of an order are being retained when using the microfiltration. The pressure requirement on microfiltration is up to 2 bars. This process is being used in removal of particularly suspended substances, bacteria, algae and protozoa such as *Gardia* and *Cryptosporidium* from the water. Most frequent is the application of microfiltration in a treatment of drinking water. Microfiltration membrane modules are usually plate-and-frame or with a hollow fibres made from polymers and tubular or capillary, unless the material which are they made from is ceramic. Microfiltration can be carried out in two ways, the dead-end-filtration (DEF) and cross-flow-filtration (CFF). The DEF method represents a parallel to the classic filtration while the filtration mixture is flowing upright towards the membrane and the filtrate is passing through the membrane. But other much more method of filtration is getting more popular currently – the much more effective method of filtration with a cross-arrangement of the permeate and retentate flow (cross flow filtration) **Figure 1**.

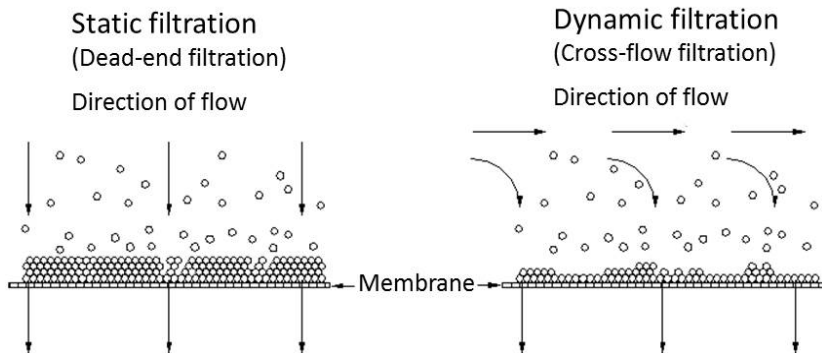


Fig. 1 Mode of flow onto the membrane

Ultrafiltration

Macromolecules may be separated by using the Ultrafiltration (molecular weight range 2-200 kDa). So as the particles of $0.002 \mu\text{m}$ diameter about and bigger particles of a diameter about 10^2 up to 10^0 nm, such are viruses, proteins, polysaccharides or colloid particles may be separated. A required difference in pressure in front of the membrane and behind the membrane is just a bit higher than the difference at MF. But still we deal with the units of several bars. Ultrafiltration modules are similar to the microfiltration, mostly used are the spiral-wound membrane modules.

Nanofiltration

Organic substances of low molecular weight are separated by this type of membrane process. The size of separated substances is rather being mentioned in units of molecular weight than in size units. Nanofiltration is capable to separate the substances up to 20 kDa approx., which corresponds to the molecules of pesticides and herbicides. The pressures are higher than as it is for Ultrafiltration and they ranged in a tenths of bars. Most frequent are the applications of water softening and pesticides removing from the water. Only the spiral-wound modules are used and the hollow fibres are rare. But the material they are made from is always the same, the polymeric material.

Tab. 1 Comparison of membrane processes

	Microfiltration	Ultrafiltration	Nanofiltration
pore size	0,1-10 μm	1-100 nm	< 2 nm
applied pressure [bar]	0,2-2	1 - 5	5 - 20
membrane thickness [μm]	10-150	150	carrier layer about 150 μm active layer about 1 μm
Transmembrane pressure [bar]	< 4	1-10	10-25
membrane material	polymer, ceramic	polymer, ceramic	polyamide

2. MATERIAL AND METHODS

At the WTP Klenovec, the pilot-plant tests for membrane filtration examination were carried out by using the microfiltration unit AMAYA 5 with a performance of 5 m³/hod. Microfiltration unit consists of two main parts: coagulation / flocculation part and membrane module with equipment for backwash.

Coagulation and flocculation run in two stages. At the first stage, the coagulant is dosing into a static mixer, which led the mixture to the second stage from. The second stage represents the tubular flocculator. In the membrane module, there is placed one ceramic element with a membrane surface of 25 m², pores size of 0.1 μm , and consisting of 2000 tubules with a diameter of 2.5 mm.

At first, the reverse washing (physical washing) is carried out by filtered water from the reverse washing reservoir at the pressure of 5 bars. Then the aeration follows at the pressure of 2 bars. The time needed for a washing and aeration is very short, just 20 seconds. Sludge is led into the reservoir of waste water. We performed membrane washing each 2 hours in the beginning of the tests and each 4 hours later over the tests.

The equipment itself performs the chemical washing (CEB) automatically within the above mentioned time intervals. The CEB can be oxidative or acidic. Sulphur acid concentrate is used in ACID CEB which was performed once a day. Sodium hypochlorite is used in OXID CEB, once a day in the beginning and 3 times a day in the later period of experiments. This interval we prolonged in order

to avoid the increase in transmembrane pressure – TMP and therefore it would not had been necessary to perform the oxidative washing so often.

Basic parameters of microfiltration during pilot plant experiments are illustrated in Table 2.

Tab. 2 Basic parameters of microfiltration during pilot plant experiments

Source of water	surface water from water reservoir Klenovec
Flow	2,5; 3,6 and 4,0 m ³ /hod
Filtration cycle	2 hours and 4 hours
ACID CEB	once a day
OXID CEB	at the beginning once a day, later three times per a week
Applied coagulant	PIX 113, PAX XL 19

3. RESULTS AND DUSCUSSION

The aim of the performed tests was the evaluation of the possibility of using the microfiltration technology on ceramic membranes with preliminary coagulation in one-step water treatment process at the WTP Klenovec during the seasons when the water is tolerably pure in terms of physical-chemical properties of the water. But a relatively high activation (biological) is typical for the water over that season as well. In Figure 2 is shown the progress of activation and insoluble substances (expressed by a number of particles) in a raw after at the influx to the WTP Klenovec during the whole testing period.

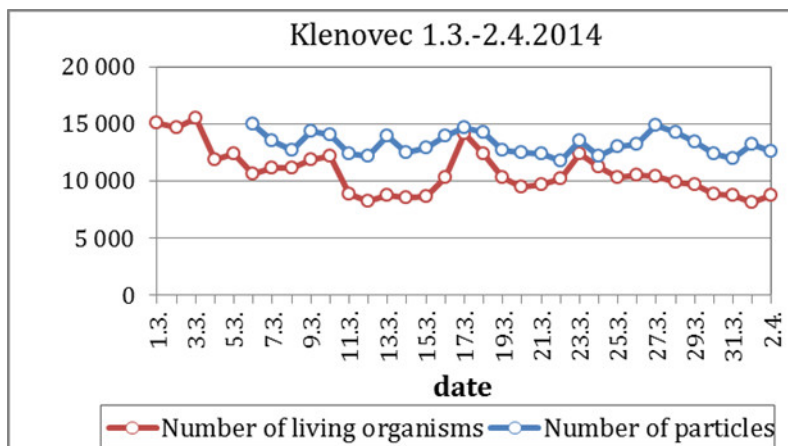


Fig. 2 Number of living organisms and insoluble substances particles in a raw water at the influx to WTP Klenovec during a testing period.

There was no activation, after using the microfiltration with a ferric sulphate PIX113 as a coagulant or polyaluminium chloride PAX-XL19. This is illustrated in Figure 3 regarding the different performances of the equipment.

The results of water after the treatment testing show that the water met the criteria of Government Regulation no. 496/2010 Coll. of the Slovak Republic (Figures 3, 4) whether that the coagulant (on the basis of iron or aluminium) was used or not within the tests. In case we did not use the coagulant, plugging of the pores was more quick and by that the transmembrane pressure was increasing – TMP. Thereby the general consequence in a filtration process shortening and therefore the need for more frequent membrane washing occurred as well. Applying this into the operation would mean a moderate increasing of the operational costs.

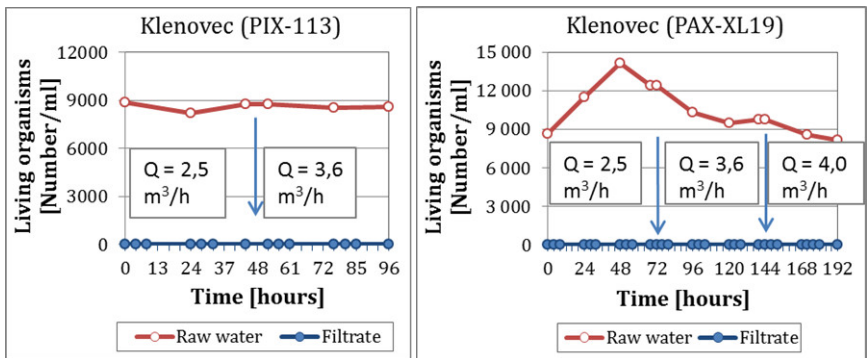


Fig. 3 Number of living organisms before and after microfiltration with preliminary coagulation

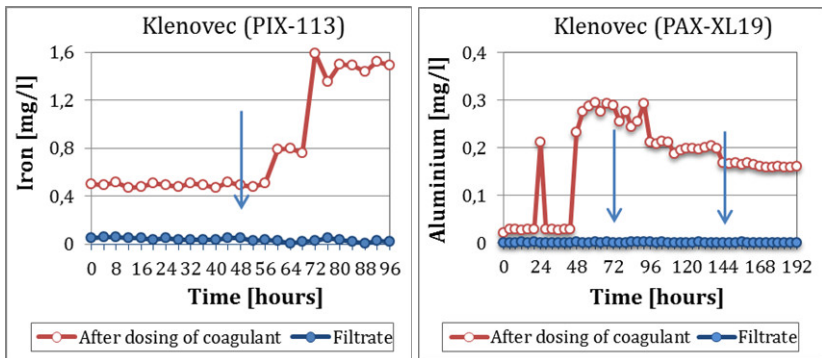


Fig. 4 Fe content (in the left) and Al content (in the right) in raw water and water after microfiltration

In **Figure 4** there is shown the plot describing the coagulant Fe PIX 113 traces which was dosing during the first four days and AL PAX-XL19 which was dosing during the next 8 days. After dosing of coagulant Fe PIX the values for Fe ranged between 0.47-1.59 mg/l, in case of coagulant Al PAL-XL19 the values of Al ranged between 0.02-0.294 mg/l and were close to 0 after the filtration.

Figure 5 (left) shows the values of turbidity in raw water (ranged between 2.14-3.89 NTU) and values of turbidity after dosing of coagulant Fe PIX and after microfiltration (ranged between 0.09-0.16 NTU). In case of second experiment with coagulant Al PAL-XL19, the values of turbidity in raw water ranged between 2.36-5.16 NTU, after dosing of coagulant and after microfiltration values were between 0.08-0.19 NTU (Figure 5 right).

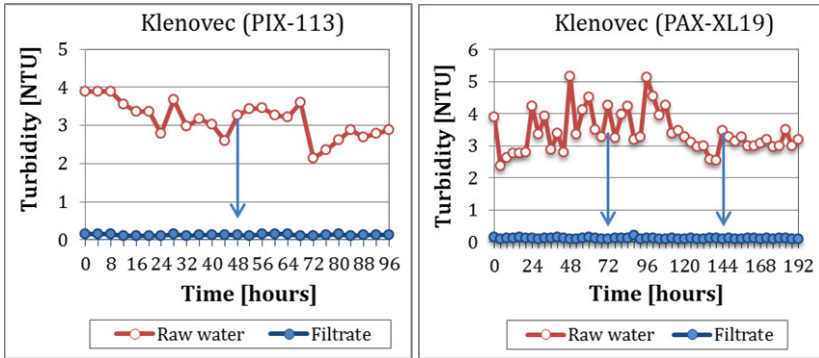


Fig. 5 Turbidity progress in a raw water and in filtrate during the microfiltration tests

Limit value for COD_{Mn} of a treated water originating from a surface reservoirs is 3.0 mg/l at the outflow from the WTP. COD_{Mn} ranged between 2.3-3.6 mg/l during the tests at the WTP Klenovec and was 1.5 mg/l after the treatment.

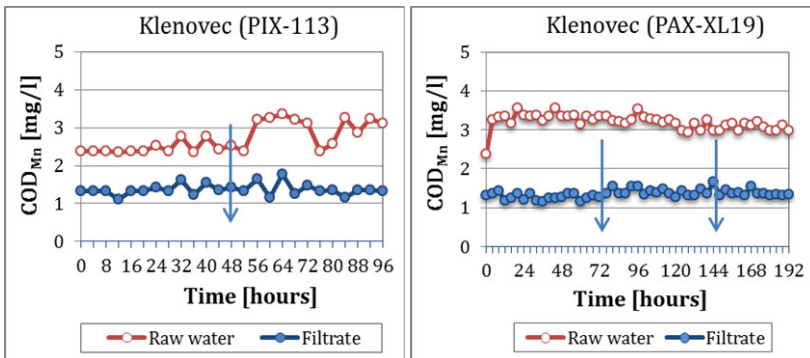


Fig. 6 COD_{Mn} progress in a raw water and in filtrate during the microfiltration tests

4. CONCLUSIONS

All obtained results from pilot-plant tests at the WTP Klenovec confirm the possibility of ceramic microfiltration membrane to treat surface water excellently and to make it a drinking water. Several factors refer this technology is a prospective treating technology and for obtaining a drinking water of high quality. These processes are among the low-pressure membrane processes and are highly chemically durable. In every WTP using where these processes were installed, the processes are designed of ceramic microfiltration elements. The oldest WTP with microfiltration is in Kyoto and it comes from 1998.

5. REFERENCES

- BAKER, R.W. 2012. *Membrane Technology and Applications*, 3rd ed.; Published by John Wiley & Sons: Hoboken, New Jersey, 575 p.
- BINNIE, C., KIMBER, M. 2013. *Basic water treatment*. 5th ed.; Published by ICE Publishing, One Great George Street, Westminster, London SW1P 3AA, 316 p.
- CRITTENDEN, J.C., TRUSSELL, R.R., HAND, D.W., HOWE, K.J., TCHOBANOGLOUS, G. 2012. Chapter 12. Membrane Filtration. *MWH's Water Treatment: Principles and Design*, 3rd ed.; Published by John Wiley & Sons: Hoboken, New Jersey, 1907 p.
- DOBIÁŠ, P., DOLEJŠ, P., DRDA, M., SVOBODA, M.: *Poloprovozní ověřování membránové mikrofiltrace pro úpravu huminových vod. Pilot Plant Verification of Membrane Microfiltration for Treatment of Humic Water*. In: Proceeding of International Conference of Drinking Water 2004, Tábor, Czech Republic, pp. 95–100.
- DOLEJŠ, P., DOBIÁŠ P., KALOUSKOVÁ N. (2003): Poloprovozní experimenty s membránovou mikrofiltrací v reálných podmínkách provozu úpravny vody. *Pilot Plant Experiments with Membrane Microfiltration in Real Conditions of Water Treatment Plant Operation*. In: Proceedings of 7th International Conference on Water Zlín 2003, Czech Republic, pp. 91-96.
- DOLEJŠ, P., KALOUSKOVÁ, N., NOGOVÁ, Z. 2002. Využití membránových procesů při úpravě pitné vody. *The Utilization of the Membrane Processes in Water Treatment*. In: Proceedings of 6th International Conference on Water Zlín 2002, Czech Republic pp. 109-114.
- DRDA, M., ČERVENKA J. 2009. *Použití keramických mikrofiltračních membrán pro úpravu pitné vody. The Use of the Ceramic Microfiltration in Water Treatment*. In: Proceedings of 13th International Conference on Water Zlín 2009, Czech Republic, pp. 143-148.
- DURANCEAU, S. J. 2000. The future of membranes, J. AWWA 92(2), pp. 70-71.
- EDZWALD, J.K. 2011. *Water Quality and Treatment. A Handbook of Drinking Water*, 6th ed.; AWWA, McGraw-Hill Companies, New York, 1696 p.

- HOEK, E.M.V., TARABARA, V.V. 2013. *Encyclopedia of Membrane Science and Technology*. Published by John Wiley & Sons: Hoboken, New Jersey, 2329 p.
- HOWE, K.J., HAND, D.W., CRITTENDEN, J.C., TRUSSELL R.R., TCHOBANOGLOUS, G.: *Principles of water treatment*. Published by John Wiley & Sons, Inc., Hoboken, New Jersey 2012, 654 p.
- LI, N.N., FANE, A.G., HO W.S.W., MATSUURA T. 2008. *Advanced Membrane Technology and Applications*. Published by John Wiley & Sons: Hoboken, New Jersey. 994 p.
- MOHANTY, K., PURKAIT, M.K. 2012. *Membrane Technologies and Applications*, 2nd ed.; Published by CRS Press, Taylor&Francis Group, 2012, 503 p.
- TARIČ, J. 2004. *Membránové procesy v úprave vody. Membrane Processes in Water Treatment*. Faculty of Civil Engineering, The Slovak University of Technology Bratislava, Diploma Thesis, 2004.
- VONDŘYSOVÁ, J., ČERVENKA, J., DRDA, M., BEYBLOVÁ, S., LÍBAL, A. 2011. *Provozní zkušenosti úpravy vody pomocí membránové mikrofiltrace na keramických membránách s předřazenou koagulací/flokulací. Operating experience of Water Treatment with Membrane Microfiltration Preliminary with Coagulation/Flocculation*. In: Proceedings of 15th International Conference on Water Zlín 2011, Czech Republic, pp. 91-98.

Acknowledgement

The results of pilot-plant tests which are a part of this paper were published with a consent of company Stredoslovenská vodárenská spoločnosť, a.s., Banská Bystrica.

Possibilities for recycling of sewage sludge

D. Vouk, D. Nakić, N. Štirmer, D. Malus

University of Zagreb, Faculty of Civil Engineering, Water Research Department, Kaciceva 26, 10000 Zagreb, Croatia, phone: +385 1 4639 213, dvouk@grad.hr, dnacic@grad.hr, ninab@grad.hr, malus@grad.hr

Abstract

Each wastewater treatment plant (WWTP), whether it treats sanitary or industrial wastewater, generates certain quantities of sewage sludge, primarily through the settling process in primary and secondary sedimentation tanks. Generated sludge needs to be adequately treated at WWTP and disposed of in the environment in accordance with certain regulations and laws. In most EU countries, the problem of adequate disposal of sewage sludge has not been solved, nor is determined by the rules, instructions or guidelines. Due to the different technological possibilities of wastewater and sludge treatment as well as sludge disposal and possible negative social and environmental impacts, scientific and professional community of each country should achieve a consensus at the national level on which solutions are acceptable and at what level.

Among the solutions that seem reasonable recycling of sewage sludge and its by-products reaches the top recommendation. Determining the optimum way of sludge disposal is important not only in terms of meeting the regulations, but the aspect of selecting optimal concept of wastewater treatment, including the selection of optimum technology for sludge treatment. Within the framework of sustainable development, recycling of sludge almost completely closes the cycle of wastewater treatment in which only negligible amounts of waste products that need to be disposed in the environment are generated. In most EU countries, significant amounts of stabilized and dehydrated sludge are incinerated. Current proposal of sewage sludge management strategy in Croatia is also oriented towards the construction of four to five sludge incineration plants. In the process of sewage sludge incineration special form of ash is generated – incinerated sewage sludge ash (ISSA), which is three to five times less in volume compared to stabilized and dehydrated sludge. ISSA also need to be disposed of in accordance with certain legislation. In this paper special emphasis is given on the possibility of recycling the ISSA in concrete industry. Up to date results on a worldwide basis will be described in the paper.

Keywords

sludge, wastewater, treatment plant, sludge disposal, ISSA, concrete

1. INTRODUCTION

Treatment of wastewater and management of byproducts generated in the process is an important problem at the global level, in particular in the past 20-30

years. The same problem is becoming increasingly important in Croatia as well, with regard to the fact that the commitments towards EU have resulted in intensive designing and construction of a great number of wastewater treatment plants (WWTP) larger than 10,000 PE.

Construction of WWTP represents a favorable effect on the environment, but simultaneously it causes new problems related to generating of considerable quantities of sludge which must be adequately managed. In the wastewater treatment procedure, certain quantities of sludge are generated as a byproduct of any technology applied (mainly through separation of sludge from primary and secondary sedimentation tanks). Generated primary and biological sludge must be adequately processed within the plant perimeter and disposed into the environment in accordance with legislation and regulations. In Croatia, sludge is still disposed on landfills or in other inadequate or forbidden ways. For example, according to available data from existing WWTP in Croatia unit production of sludge is about 50 to 55 g DM/PE·day.

The sludge is of complex texture, a mixture of organic and non-organic substances dispersed in water and contains also pathogenic microorganisms, parasites, viruses and numerous potentially hazardous elements and compounds (heavy metals, etc.).

According to European guidelines for final disposal of sewage sludge, conventional disposal of sludge on landfills is not permissible. Designs and construction of WWTP without solved final sludge management cannot be regarded complete. The price of water services related to wastewater treatment should not be based only on costs arising within the WWTP perimeter, but should include all costs, including sludge management. The costs of sludge processing and management in most WWTP planned to be built in Croatia by 2018 will amount to about 50% of total operating costs [Nowak et al., 2003], and in certain conditions, with transport and disposal at larger distances they may be even higher. Some study analyses indicate that at WWTP of larger capacities the sludge incineration process might be the acceptable concept related to terminal sludge management. Incineration of sludge generates ash, which has a considerably smaller mass and volume in comparison with stabilized and dehydrated sludge. However, if the sludge incineration concept is accepted, 4 or 5 regional incinerators would generate considerable quantities of ash which has to be disposed at the final stage. In accordance with principles of sustainable development, at present there is a growing tendency of recycling of various materials. In this context, the possibility is emphasized of reusing of ash, first of all in construction industry, in particular in production of concrete and concrete elements, production of bricks and for soil improvement [Al Sayed et al., 1995; Anderson and Skerratt, 1999; Monzo et al., 2003; Weng et al., 2003; Cheeseman and Virdi, 2005; Merino et al., 2005; Chiou et al., 2006; Lin et al., 2007; Dunster, 2007; Garcés et al., 2008; Jamshidi et al., 2011; Kosior-Kazberuk, 2011; Yusuf et al., 2012; Donatello and Cheeseman, 2013; Al-Sharif and Attom, 2013; Husillos Rodriguez et al., 2013; Chen et al., 2013; Agrawal et al., 2014; Baeza-Brotons et

al., 2014]. In the framework of sustainable development, recycling of sludge completes the wastewater treatment cycle, generating negligible quantities of waste matter to be disposed into the environment.

The paper reviews various possibilities of reuse of ash resulting from incineration of sewage sludge. Particular importance is attributed to the use of ash in concrete industry. Some of the results of investigations at the global level are given and compared with results obtained in Croatia.

2. GENERATING OF SLUDGE AT WWTP

In the process of wastewater treatment at WWTP, waste substances are removed from water, and treated water is released into the environment without disturbing the natural balance in recipients (surface and ground water bodies). In the treatment process, as a byproduct of any technology applied, certain quantities of sludge are generated (mainly through sludge separation from primary and secondary sedimentation tanks). Along with mechanical pretreatment (coarse and fine grid, aerated sand-fat trap), three basic stages of treatment are applied:

- I stage – sedimentation or micro-filtration, with removal of total dispersed matter (min. 50%) and minor part of organic pollution (min. 20%)
- II stage – biological treatment with removal of organic pollution
- III stage – biological and chemical treatment with removal of N and P.

3. SLUDGE TREATMENT AT WWTP

The method of sludge treatment should be determined in dependence of the way of final sludge disposal. There is no universal method of terminal sludge disposal, and in relation to relevant factors (properties of wastewater, treatment stage and technology, properties and quantity of sludge, WWTP capacity, legal requirements, local conditions, construction and maintenance costs, etc.) it is necessary to determine for each plant the way how the sludge will be finally disposed. The choice of the optimum technological solution of sludge treatment in WWTP should be the result of detailed analysis of different solutions and their multicriteria ranking, respecting the economic, technical-technological and social criteria, as well as the sustainability criterion.

Sludge treatment at WWTP usually follows three basic phases: thickening, stabilization and dewatering. If necessary, other phases may be applied: homogenization, conditioning, drying, incineration, disinfection. In many European countries considerable quantities of stabilized and dehydrated sludge are incinerated. Sludge incineration generates ash whose volume is three to five times smaller than fresh sludge, which is reflected in reduction of costs of its final disposal, with additional possibility of ash recycling.

4. INCINERATION OF SEWAGE SLUDGE

Stabilized and dehydrated sludge containing 18 – 35% of dry matter is usually dried prior to incineration, first of all in order to increase its energetic efficiency. Sludge containing 75 – 95% of DM is then introduced in incineration furnaces, producing ash (ISSA), finely granulated waste material.

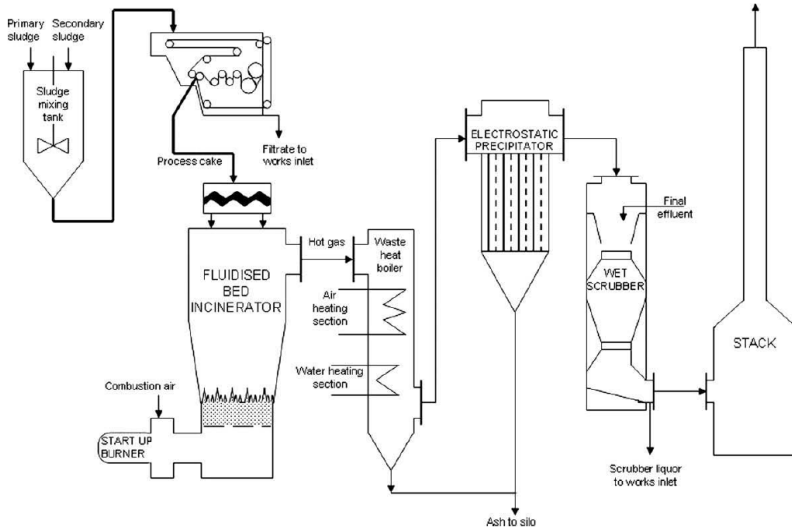


Fig. 1 Sewage sludge incineration system using a fluidised bed furnace [Donatello and Cheeseman, 2013]

Calorific value of sludge is close to that of brown coal, but it should be kept in mind that this refers to the calorific value of the organic component of sludge, while the non-organic part has no calorific value whatsoever. Therefore it is usually necessary to bring sludge at least to the level of 28 – 33% DM to enable auto-thermal combustion without adding of external fuel to maintain the process [Donatello and Cheeseman, 2013]. In stabilized and dehydrated condition the calorific value of sludge is within the range 12 – 20 MJ/kg. Various types of furnaces are used for incineration of stabilized and dehydrated sludge. The most frequently used type is fluidized bed furnaces. Ash generated in sludge incineration is separated from exhaust fumes in filter bags or by electrostatic sedimentation before fume treatment [Yusuf et al., 2012]. In incineration of sewage sludge, in addition to generation of ash that may be used for various purposes, the process also includes complete thermal destruction of organic, as well as the major part of non-organic pollutants [Al-Sharif and Attom, 2013].

5. POSSIBILITIES OF SLUDGE REUSE

Successful management of sewage sludge is a challenge for all utilities involved in sewerage and wastewater treatment and waste management. Terminal

disposal of sewage sludge is a costly and environmentally sensitive process which is the actual challenge for almost all developed countries of the world. It is important to keep in mind that various possibilities of sludge reuse are limited by treatment technologies, and consequently by resulting properties of processed sludge. According to results of worldwide practice, there are several possible ways of reuse of sludge and byproducts of its processing (e.g. ash), as follows:

1. Use in agriculture
2. Extraction of phosphorus
3. Use in civil engineering
 - a. For soil improvement
 - b. In road construction
 - c. In brick industry
 - d. In concrete industry.

This paper particularly stresses the basic aspects related to the possibility of the use of ash, produced by incineration of sewage sludge, in concrete industry.

5.1 Use of sludge/ash in concrete industry

There are three basic principles of using of waste material in cement industry: as raw material for formation of clinker, as alternative fuel in the production process, or as alternative material replacing a part of Portland cement. The fundamental chemical elements present in Portland cement are Ca, Si, Al and Fe. These elements are also present a great deal in ash generated by incineration of sludge [Donatello and Cheeseman, 2013]. The largest potential reuse of sludge/ash in concrete industry refers to the possibility of use as replacement of a part of original raw materials in concrete. Ash may be used in concrete as pozzolanic active material, partly replacing cement, or as inert filler replacing sand and/or fine aggregate. A number of authors [Monzo et al., 1997; Donatello and Cheeseman, 2013; Monzo et al., 2003; Pan et al., 2003; Cyr et al., 2007; Jamshidi et al., 2011; Garces et al., 2008] reported that partial replacement of Portland cement by ISSA influenced the workability and development of strength of cement mortars and/or concrete.

In cases of replacement of a part of cement by ash in cement pastes and concrete, longer setting times have been recorded [Lin et al., 2009; Donatello and Cheeseman, 2013; Cyr et al., 2007] reduced setting time and increased total porosity [Yusuf et al., 2012], reduced workability [Monzo et al., 2003; Donatello and Cheeseman, 2013], and increased water demand [Monzo et al., 2003; Donatello and Cheeseman, 2013]. Monzo et al. (2003) concluded that the decrease of workability of mortars with addition of ash is non-linear, and that lower workability with higher portion of ash is less significant. These defects may be partly compensated by means of alternative chemical additives such as plasticizers and super-plasticizers [Monzo et al. 2003], finer ash particles [Pan et al., 2003], and even by adding flying ash [Paya et al., 2002]. As regards the strength of resulting concretes, two important trends may be noted: increasing of the portion

of ash to replace cement, concrete strength is decreased, and with finer ash particles the concrete strength increases. Comparing of results by different authors, significant differences of absolute values may be noticed.

Hereafter, the paper presents some of the results of investigations carried out on cement mortars with adding of certain portions of ash (5 – 30% as replacement for cement) obtained by incineration of ash from WWTP Karlovac, and comparison of these results with the results of worldwide investigations.

5.1.1 Setting time and workability

Analysis of the results reveals a general trend of delay of initial and final setting time with increase of the v/c ratio, but also with increasing of temperature of sludge incineration. The longest setting times were those of mixtures containing 10 and 20% of ash. The results prove increased water demand and reduced workability with increasing of the portion of ash in cement mortar.

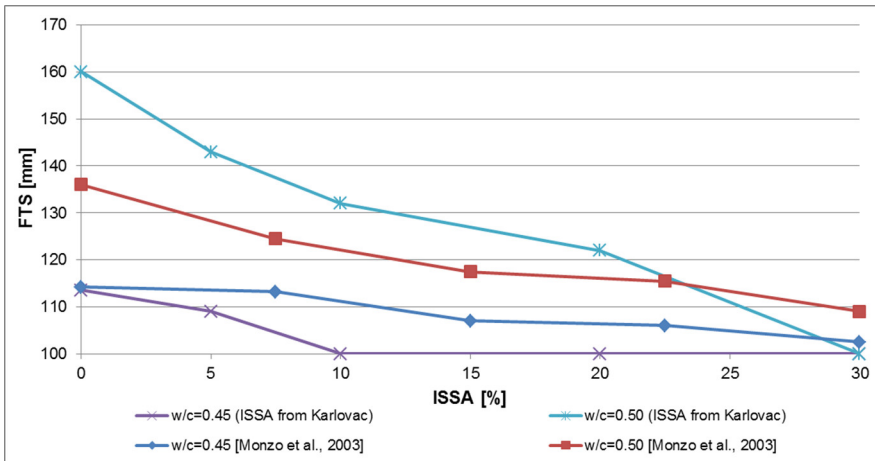


Fig. 2 FTS for ISSA-cement mortars [Monzo et al., 2003]

5.1.1 Mechanical properties

To determine the mechanical properties of cement mortar, standard samples 4x4x16 cm were used. The samples were prepared by mechanical mixing, and after 1, 7 and 28 day curing, respectively, used for compressive and flexural strength tests. In researches done so far, the general trend may be noticed of reduction of compressive and flexural strength with increased proportion of ash. It is important to note that adverse effect of adding ISSA to cement mortars becomes less important in later phases of hydration (influence in reduction of 28-day strengths is considerably less in relation to strengths after 7 days) [Cyr et al., 2007].

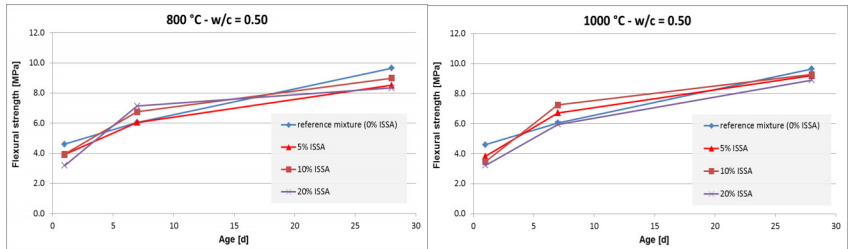


Fig. 3 Flexural strength as a function of curing age for cement mortars containing ISSA form Karlovac WWTP

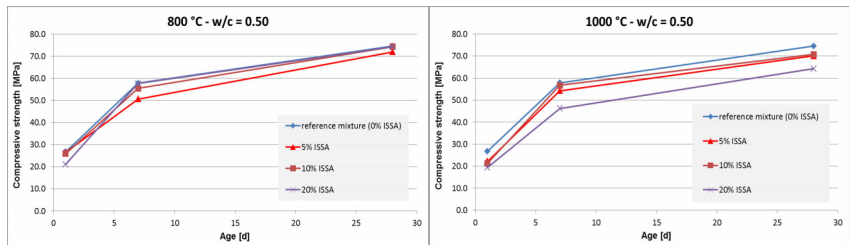


Fig. 4 Compressive strength as a function of curing age for cement mortars containing ISSA form Karlovac WWTP

As regards both compressive and flexural strength, there is a notable trend of strength increase with longer curing time, which is in favor of the mentioned remark about pozzolanic activity of ISSA. Early strengths have proven particularly sensitive to adding of ISSA.

It is also important to note that all analyzed samples for values of late compressive strengths (28 days) have met the strength requirements according to the class of cement used (CEM II/B-M(S-V) 42.5N) of minimum 42.5 MPa.

5.2 Possible problems with use of sludge/ash in concrete industry

Problems encountered in use of sludge/ash in concrete industry may be divided into several groups:

- sociological impact reflected through negative perception of plants for thermal processing of sludge, as well as inadequate information of the public about sanitary and ecological acceptability of final products containing ash
- readiness of the market to accept ash as ingredient in products of concrete industry
- environmental impact of incineration (modern technological solutions make it possible to maintain emission of harmful fumes during incineration below legally permissible limits), but also in the use of products containing ash (tests of heavy metals leaching from concrete samples on global level show that excessive leaching does not occur)
- lack of universal regulations and guidelines.

6. CONCLUSION

Judging according to present global trends, it may be expected that in near future reuse of sewage sludge will gain more importance in Croatia as well, both as regards scientific research and the aspect of final application.

Solutions that seem acceptable include reuse of sludge and its byproducts for various purposes, i.e. all solutions giving optimum multicriteria results. According to the principles of sustainable development, reuse of sludge almost completely closes the wastewater treatment cycle, generating negligible quantities of waste that has to be disposed in the environment,

Results of investigations carried out on cement mortars show that samples in which cement is partly replaced by incinerated sewage sludge ash have mechanical properties similar to those of reference samples. Workability of cement mortars with ash content is considerably reduced with higher proportions of ash content, but the possibility of overcoming such adverse effects should be sought in application of additives (plasticizers and super-plasticizers).

The process of incineration of sewage sludge and the use of resulting ash in concrete industry naturally requires a high degree of control and application of environment protection measures in all parts.

Looking upon technical requirements, management of incinerated sewage sludge ash and its use in production of construction materials seems practical and justified.

7. REFERENCES

- AGRAWAL, D., HINGE, P., WAGHE, U.P., RAUT, S.P., 2014. Utilization of industrial waste in construction material – A review. *International Journal of Innovative Research in Science, Engineering and Technology*. 3 (1).
- AL SAYED, M.H., MADANY, I.M., BUALI, A.R.M., 1995. Use of sewage sludge ash in asphaltic paving mixes in hot regions. *Constr. Build. Mater.* 9 (1), pp 19-23.
- AL-SHARIF, M.M., ATTOM, M.F., 2013. A geo-environmental application of burned wastewater sludge ash in soil stabilization. *Environ. Earth Sci.*, DOI 10.1007/s12665-013-2645-z.
- ANDERSON, M., SKERRATT, G., 1999. The use of sewage sludge incinerator ash in brick making. *Wastes Management*. Aug. 1999, page 36.
- BAEZA-BROTOS, F., GARCES, P., PAYA, J., SAVAL, J.M., 2014. Portland cement systems with addition of sewage sludge ash. Application in concretes for the manufacture of blocks., *Journal of Cleaner Production*, <http://dx.doi.org/10.1016/j.clerpo.2014.06.072>.
- CHEESEMAN, C.R., VIRDI, G.S., 2005. Properties and microstructure of lightweight aggregate produced from sintered sewage sludge ash. *Resour. Conserv. Recy.* 45 (1), pp 18-30.

- CHEN, M., BLANC, D., GAUTIER, M., MEHU, J., GOURDON, R., 2013. Environmental and technical assessments of the potential utilization of sewage sludge ashes (SSAs) as secondary raw materials in construction. *Waste Manage.* 33, pp 1268-1275.
- CHIOU, I.J., WANG, K.S., CHEN, C.H., LIN, Y.T., 2006. Lightweight aggregate made from sewage sludge and incinerated ash. *Waste Manage.* 26, pp 1453-1461.
- CYR, M., COUTAND, M., CLASTRES, P., 2007. Technological and environmental behaviour of sewage sludge ash (SSA) in cement-based materials. *Cem. Concr. Res.* 37, pp 1278-1289.
- DONATELLO, S., CHEESEMAN, C.R., 2013. Recycling and recovery routes for incinerated sewage sludge ash (ISSA): A review. *Waste Manage.* 33, pp 2328-2340.
- DUNSTER, A., BRE, 2007. Incinerated sewage sludge ash (ISSA) in autoclaved aerated concrete (AAC). WRT 177 / WR0115.
- GARCÉS P., PEREZ-CARRION, M., GARCIA-ALCOCEL, E., PAYA, J., MONZO, J., BORRACHERO, M.V., 2008. Mechanical and physical properties of cement blended with sewage sludge ash. *Waste Manage.* 28, pp 2495-2502.
- HUSILLOS RODRIGUEZ, N., MARTINEZ-RAMIREZ, S., BLANCO-VARELA M.T., DONATELO, S., GUILLEM, M., PUIG, J., FOS, C., LARROTCHA, E., FLORES, J., 2013. The effect of using thermally dried sewage sludge as an alternative fuel on Portland cement clinker production. *Journal of Cleaner Production.* 52, 94-102.
- JAMSHIDI, A., MEHRDADI, N., JAMSHIDI, M., 2011. Application of sewage dry sludge as fine aggregate in concrete. *J. Envir. Stud.* Vol. 37, No. 59.
- KOSIOR-KAZBERUK, M., 2011. Application of SSA as Partial Replacement of Aggregate in Concrete. *Polish J. of Environ.* Vol. 20, No. 2, 365-370.
- LIN, D.F., LIN, K.L., HUNG, M.J., LUO, H.L., 2007. Sludge ash/hydrated lime on the geotechnical properties of soft soil. *J. Hazard. Mater.* 145 (1-2), pp 58-64.
- LIN, K.L., LIN, D.F., LUO, H.L., 2009. Influence of phosphate of the waste sludge on the hydration characteristics of eco-cement. *J. Hazard. Mater.* 168, 1105-1110.
- MERINO I., AREVALO, L.F., ROMERO, F., 2005. Characterization and possible uses of ashes from wastewater treatment plants. *Waste Manage.* 25, 1046-1054.
- MONZO, J., PAYA, J., BORRACHERO, M.V., BELLVER, A. PERIS-MORA, E., 1997. Study of cement-based mortars containing Spanish ground sewage sludge ash. *Stud. Environ. Sci.* 71, 349-354
- MONZO, J., PAYA, J., BORRACHERO, M.V., GIRBES, I., 2003. Reuse of sewage sludge ashes (SSA) in cement mixtures: the effect of SSA on the workability of cement mortars. *Waste Manage.* 23, 373-381.

- NOWAK, O.; KUEHN, V.; ZESSNER, M., 2003, Sludge management of small water and wastewater treatment plants, *Water Science and Technology*, Vol 48, 11-12, 33-41.
- PAN, S.C., TSENG, D.H., LEE, C.C., LEE, C., 2003. Influence of the fineness of sewage sludge ash on the mortar properties. *Waste Manage.* 33, 1749-1754.
- PAYA, J., MONZO, J., BORRACHERO, M.V., AMAHJOUR, F., GIRBES, I., VELAZQUEZ, S., ORDONEZ, L.M., 2002. Advantages in the use of fly ashes in cements containing pozzolanic combustion residues: silica fume, sewage sludge ash, spent fluidized bed catalyst and rice husk ash. *Journal of Chemical Technology and Biotechnology.* 77, 331-335.
- WENG, C.-H., LIN, D.-F., CHIANG, P.-C., 2003. Utilization of sludge as brick materials. *Advances in Environmental Research.* 7, 679-685.
- YUSUF, R.O., MOH'D FADHIL, M.D., AHMAD, H.A., 2012. Use of sewage sludge ash (SSA) in the production of cement and concrete – a review. *Int. J. Global Environmental Issues*, Vol. 12, Nos. 2/3/4. 214-228.

Acknowledgement

This work has been fully supported by Croatian Science Foundation under the project "7927 - Reuse of sewage sludge in concrete industry – from infrastructure to innovative construction products".

The Greenhouse Gas Emissions for Several Water Utility Companies in Croatia

I. Halkijevic, Z. Vukovic, D. Vouk

(Faculty of Civil Engineering, University of Zagreb, e-mail: halkijevic@grad.hr, vukovic@grad.hr, vouk@grad.hr)

Abstract

In recent years the impact of physical processes within an urban water system to a global climate change has gained an increasing attention. As a measure of this impact a greenhouse gas (GHG) emissions are primarily considered. Totality of all greenhouse gas contributions (without the influence of water vapour) is expressed as the CO₂ equivalent. This express the potential impact on global warming of various greenhouse gases as an equivalent value of CO₂ emissions. GHG emissions are taken into account as a by-product of the electricity production that is consumed in the process of water abstraction, water conditioning, water distribution and wastewater treatment. Also, GHG emissions in urban water system are sometimes associated with GHG emissions caused by the end user. The resulting emissions are considered in terms of the energy used in the mentioned processes while the emissions as a result of the process itself (for example, the formation of various gases in the purification process) are usually not taken into account. Procedures for quantifying the contributing emissions have been developed over the last years for sewerage systems and wastewater treatment processes, while the same are lacking for water supply systems. This paper deals with determining a unit value of greenhouse gas emissions in the form of CO_{2e} for 14 water supply systems in the Republic of Croatia.

Keywords

Greenhouse gas emissions, CO₂ equivalent, water supply systems

1. INTRODUCTION

The processes of water abstraction, conveyance and treatment can be very energy demanding depending on the used technological process. Since electrical energy is normally used, all of these activities thus result in greenhouse gas emissions coming from burning of coal, natural gas or petroleum for electricity production.

Nowadays the energy demand for water related processes is even increasing due to more stringent water quality requirements. In the United States water and wastewater systems account for approximately 3-4 percent of energy use annually [EPA, 2015].

The water industry in UK contributes 0.8 per cent of annual UK greenhouse gas emissions while the emissions resulting from heating water by the end user increases this figure to 5.5 per cent [Environment Agency, 2008].

Some studies indicate that in the US approximately 5 per cent of all greenhouse gas emissions are related to the processes in urban waste water systems, while in the UK about 6 per cent is related to the same processes [Rothausen and Conway, 2011].

Totality of all greenhouse gas contributions (without the influence of water vapour) is expressed as the CO₂ equivalent. Different greenhouse gases (GHGs) have a different atmospheric lifetime and heat-trapping potential thus the concept of a Global Warming Potential (GWP) has been developed to compare the ability of different GHGs to trap heat in the atmosphere relative to CO₂ over a specified time horizon. The GHG emissions are calculated in order to show of how much CO₂ would be required to produce a similar warming effect.

GWP is defined as the ratio of the time-integrated radiative forcing from the instantaneous release of 1 kg of a trace substance relative to that of 1 kg of a reference gas [IPCC, 1990]. It is calculated for a specified period mostly for 100 years [Solomon et al., 2007].

GWPs are based on the heat-absorbing ability of each gas relative to that of carbon dioxide (CO₂) as well as the decay rate of each gas (the amount removed from the atmosphere over a given number of years).

This express the potential impact on global warming of various greenhouse gases as an equivalent value of CO₂ emissions. Thus CO₂e is the multiplication of the mass of each greenhouse gas and global warming potential (GWP).

The annual volume of CO₂e which is associated with the processes of abstraction, preparation and distribution of water in the US is between 70 and 85 million tonnes of CO₂e (70 and 85 [Mt CO₂e]) while for the United Kingdom data indicate 41 [Mt CO₂e]. If the processes at the location of end users are taken into account then the amount of emissions rises up to 290 [Mt CO₂e] [Rothausen and Conway, 2011].

On average about 27 per cent CO₂e emissions of the urban water system originate from the treatment and the distribution of drinking water, about 5 per cent emissions are the result of administrative and transport needs of water utilities, while the rest of the emissions are realized through the wastewater treatment and pumping (about 40 per cent), and the disposal of the sludge (about 28 per cent) [SWOCFR, 2011]. About 70 per cent of all generated emissions is the result of the use of electricity in these processes.

2. METHODOLOGY

There are numerous choices in methodologies for GHG accounting and energy assessment and it can be challenging for a utility or a country to understand which of these may be most applicable [Water Research Foundation, 2013].

In most of the studies the calculation of the emission amount is based on the life cycle methodology and as main characteristic the lack of a uniform methodology is underlined.

Studies differ in spatial coverage analysis with some taking into account the end-user, while others do not account it within the scope of the urban water system. Nevertheless it is usually stated that 70 - 90 per cent of the total energy consumption associated with drinking water, and therefore with CO₂ emissions, is related to the end-user water heating.

This paper determines a unit value of greenhouse gas emissions in the form of CO₂e for 14 water supply systems in Croatia. The amount of the emitted greenhouse gases in the form of CO₂e [kg] is calculated regarding to the amount of electrical energy [kWh] used to perform the abstraction, preparation and the distribution of water to the end user, also taking into account the electrical energy consumed by utility alone (buildings, offices, warehouses and etc.), and the total amount of oil products (gasoline and diesel fuel) used for administrative needs of the company and the maintenance the water supply system.

For these processes, considering the amount of the used energy, the emission values are calculated through conversion coefficients which represent a value of CO₂e emissions in kg per unit of used electrical energy.

Conversion coefficients vary both from country to country and on an annual basis within the same country. The above is a result of changes in the share of energy sources used by electric power stations and the increase of the proportion of electrical energy obtained from renewable sources.

Thus, CO₂ emissions related to electricity production depends on the energy mix that is used in the production process.

Tab 1. CO₂e conversion coefficients

ENERGY SOURCE	CONVERSION COEFFICIENT
Electrical Energy	$k_1 = 0.445$ [kg CO ₂ e/kWh]
Gasoline Fuel	$k_2 = 2.214$ [kg CO ₂ e/l]
Diesel Fuel	$k_3 = 2.601$ [kg CO ₂ e/l]
Natural Gas	$k_4 = 0.184$ [kg CO ₂ e/kWh]

Since there are no relevant researches related to Croatia, for the purpose of emissions calculation the conversion coefficients published by the UK Department for Environment, Food and Rural Affairs (DEFRA) from 2013 were used. The same department in cooperation with Water UK continuously monitors and publishes relevant information regarding greenhouse gas emissions in the UK water sector since 2006.

Also, similar values of emissions per unit of consumed electrical energy can be found in data published by the US Electric Power Research Institute (EPRI), while studies in Japan indicate much lower value [Shimizu, 2012].

Conversion coefficients are the average annual values representing the total direct emissions per used unit of electrical energy or fuel. These direct emissions are emissions created at the place of the electricity production (power plant). The conversion coefficients used in this paper are given in Table 1.

In order to take into the account the size of the water supply system the emissions of greenhouse gases is considered as the emissions per cubic meter of the abstracted, treated and transported water.

The unit amount of the emission is obtained according to the expression:

$$GHG = \frac{E_{tot}}{Q_a} \cdot k_1 + \sum_i \frac{G_i}{Q_a} \cdot k_i \quad (1)$$

where E_{tot} [kWh] is the total annual consumption of electricity for the system or company, Q_a [m³] the total annual amount of water abstracted / introduced into and distributed in the system and G_i [l] the total annual consumption of certain types of fuel for the system or company needs.

The impact of natural gas consumption is not taken into account since data regarding gas consumption were not available.

3. WATER UTILITY GHG PRODUCTION INDEX

In order to compare between different systems and to evaluate relative environment performance a GHG production index is defined. This index can provide a comparison between systems that are different in size or have different operating characteristics.

From an environmental point of view the target value of the unit amount of the emission certainly aims towards zero. This can be achieved solely by using electricity obtained from renewable resources where GHG emissions are absent and do not come as a by-product of electricity production. In this case, there are still GHG emissions that are inherent consequences of the processes inside the system itself (fuel usage for the maintenance, etc.).

Since this target value is not realistically achievable for Croatian water utilities and there are no GHG reporting requirements or emissions limitations at the level of the urban water system, the emission index is defined regarding to the possibly achievable minimum value of unit emissions for the drinking water treatment and distribution that can be found in the relevant literature.

The value of 0.17 [kg CO₂e/m³] was chosen. This value corresponds to the values of emissions in Scotland and Canada while the average for the UK is 0.36 [kg CO₂e/m³] for the year 2012. It should be noted that for some countries, like Norway, GHG emissions related to the water sector are not an issue since almost all electricity production is realized from renewable resources (hydropower). This however is not applicable for Croatia since electricity production from renewable resources accounts for approximately 50 %.

Therefore, the index of CO₂e production, k_{GHG} , is defined as:

$$k_{GHG} = \frac{0.17}{GHG} \quad (2)$$

Thus target unit emission values are equal to or less than 0.17 [kg CO₂e/m³] and for them, the index value is equal to the number one. For greater unit emissions values greenhouse gases index production will have a value less than one.

4. DATA COLLECTION

For the purpose of data gathering a survey questionnaire was made and distributed to utility companies in digital form. The questionnaire is formed such that only numerical values are entered for the years 2011 and 2012.

The questionnaire was designed so that certain information is requested a few times in slightly modified form in order to determine the consistency and reliability of the collected data. Data were also collected from the databases of official agencies and organizations.

The required data included information regarding to the annual volume of abstracted and treated water, the consumption of electric energy for pumping stations (at the water intake, treatment plant and distribution network), the consumption of electric energy for the rest of the system and the company itself as well as the overall fuel consumption by fuel type.

5. RESULTS AND CONCLUSION

In total, relevant data were collected for 14 water utilities for which the unit amount of the emission and introduced CO₂e production index were calculated in Table 2.

For some water utilities data regarding fuel consumption were not available and for one utility only data for the year 2012 were available.

As it can be seen there is no significant relationship between the size of the system or distributed water volume and GHG emissions. Some small systems have very high or very low emission values while larger systems tend to have similar values. This indicates that the energy consumption and the associated GHG emission depends on the raw water quality and drinkable water quality demands, water losses and some inherent properties of the supply system such as topological characteristics, etc.

GHG emissions can present a significant indicator for evaluating the performance of the system, especially in terms of environmental impact and it can measure its progress towards sustainability. Thus water utilities should assess and publish their carbon footprint related to water supply on a regular basis (yearly) and develop a strategy for GHG emission reduction.

Tab 2. GHG emissions for 14 water utilities in Croatia

Water Supply System	Volume of distributed water		The overall electric energy consumption		The overall fuel consumption		Unit amount of the GHG emission		GHG production index k_{GHG}	
	[m ³]	[m ³]	[kWh]	[kWh]	[l]	[l]	[kg CO ₂ e/m ³]	[kg CO ₂ e/m ³]	[1]	[1]
	2011	2012	2011	2012	2011	2012	2011	2012	2011	2012
1	3,230,466	3,433,390	2,473,015	2,563,035	184,386	195,115	0.478	0.469	0.36	0.36
2	7,062,444	6,583,000	1,431,854	1,511,648	582,449	602,873	0.289	0.323	0.59	0.53
3	-	998,620	-	609,517	-	10,070	-	0.296	-	0.57
4	3,069,325	3,003,399	2,986,719	3,235,504	133,633	143,415	0.538	0.594	0.32	0.29
5	717,000	764,300	340,798	360,135	90,115	121,916	0.514	0.594	0.33	0.29
6	873,824	892,636	710,350	696,942	213,841	205,717	0.952	0.903	0.18	0.19
7	957,000	1,015,000	67,732	80,655	67,732	80,655	0.202	0.227	0.84	0.75
8	570,206	546,809	323,358	355,420	223,281	234,562	1.196	1.323	0.14	0.13
9	14,397,989	14,154,773	11,400,000	11,458,000	59,800	50,500	0.362	0.369	0.47	0.46
10	881,869	979,212	384,423	387,423	-	-	0.194	0.176	0.88	0.97
11	965,595	970,829	441,488	510,986	6,497	9,197	0.220	0.257	0.77	0.66
12	23,299,500	22,729,100	16,247,497	14,821,132	83,362	84,135	0.319	0.299	0.53	0.57
13	8,355,407	8,010,583	3,812,362	3,399,960	87,334	55,356	0.228	0.206	0.74	0.83
14	3,303,839	3,246,250	3,080,934	3,043,362	-	-	0.415	0.417	0.41	0.41

6. REFERENCES

- Defra / DECC's GHG Conversion Factors for Company Reporting: Methodology Paper for Emission Factors; Department for Environment, Food and Rural Affairs; London; United Kingdom; 2013.
- Energy-Water Nexus: The Water Sector's Energy Use, Claudia Copeland, Congressional Research Service, CRS report, USA, 2014
- Energy Efficiency for Water and Wastewater Utilities, Retrieved June 15, 2015, from EPA webpage:
<http://water.epa.gov/infrastructure/sustain/energyefficiency.cfm>
- Greenhouse gas emissions of water supply and demand management options, Science Report – SC070010, Environment Agency, England, 2008
- IPCC First Assessment Report on Climate Change; IPCC Working Group, 1990.
- ROTHAUSEN, S. G. S. A.; CONWAY, D. Greenhouse-gas emissions from energy use in the water sector; Nature Climate Change; Macmillian Publishers Limited; doi: 10.1038; 1 - 10; 2011.
- Scottish Water Operational Carbon Footprint Report (SWOCFR); Scottish Water; 2011.
- SHIMIZU, Y.; DEJIMA, S.; TOYOSADA, K.; The CO₂ Emission Factor of Water in Japan; Water; 4; 759-769; 2012.
- SOLOMON, S.; QIN, D; MANNING, M.; CHEN, Z. et al.; IPCC Fourth Assessment Report: Climate Change 2007; Cambridge University Press; 2007.
- Toolbox for Water Utility Energy and Greenhouse Gas Emission Management, Water Research Foundation, England, 2013.

The Comparison of Green and Conventional Stormwater Management – Zagreb Case Study

I. Halkijevic, M. Kuspilic, Z. Vukovic

(Faculty of Civil Engineering, University of Zagreb, e-mail: halkijevic@grad.hr, mkuspilic@grad.hr, vukovic@grad.hr)

Abstract

Stormwater management continues to evolve as a result of increased regulatory requirements and a desire to create sustainable solutions that attempt to bring urban water cycle closer to the natural hydrologic cycle. There is also the intention for increasing the use of stormwater for various purposes and improving energy efficiency in the urban water cycle. Such management approaches are known as Low Impact Development (LID), Green Infrastructure (Blue-Green Infrastructure), or Sustainable Urban Drainage Systems (SUDS). These attempts are reflected in the efforts addressing both water quality and quantity thus creating processes such as infiltration and bioretention as well as treating urban stormwater runoff apart from centralized wastewater treatment plant. Such actions often differ from conventional stormwater management that is primarily oriented to be in the service of stormwater runoff quantity thus reducing the possibility of storm floods. In order to choose between these different management approaches it is necessary to be able to compare them. This paper analyses the application of different stormwater drainage scenarios. One comprising of conventional drainage infrastructure and other that includes a use of sustainable drainage infrastructure on one small urbanized area and one undeveloped urban area in the city of Zagreb in Croatia.

Keywords

energy efficiency, low impact development, stormwater management

1. INTRODUCTION

Conventional sewage systems are usually designed in a way to convey water as quickly as possible while low impact development (LID) infrastructure typically store surface water aiming to infiltrate it into the ground.

Water and wastewater facilities frequently represent the largest and most energy-intensive burden for water utilities, representing up to 35% of municipal energy use (Bueno et. al., 2014).

Different approach in stormwater management can help in reducing the overall energy consumption in the urban water cycle. Through stormwater harvesting a reduction in potable water use can provide an energy reduction for acquiring and treating drinking water. Also reducing stormwater quantity entering the sewage system and improving stormwater runoff quality a reduction in energy used for pumping and wastewater treatment can be achieved, (Pérez-Navarro et al., 2014).

This article compares and evaluates two stormwater management scenarios for energy saving in one developed (urbanized) area in the city of Zagreb. First scenario considers the improvement of the existing sewage system by using new, additional conventional sewage structures, while in the second scenario the improvement case is based on retrofitting the existing sewage system with LID structures.

2. INITIAL CONSIDERATIONS

The improvement of the existing sewage system, in both cases, is designed in a way to meet next criteria:

- the same initial construction costs;
- reduction of stormwater runoff peaks entering the existing sewage system;
- reduction of annual volume of wastewater leaving analysed area and entering the existing sewage system;
- enhancement of the social and ecosystem benefits;
- improvement of the stormwater runoff quality.

The same initial construction costs are taken into account in order to make a fair comparison. The reduction of stormwater runoff peaks will reduce the frequency of combined wastewater overflowing events, reduce the ability of flooding in downstream areas and reduce the required pipe diameters.

The reduction of annual volume of wastewater leaving analysed area will reduce the energy needed for pumping and wastewater treatment and will result in lower water treatment costs at the WWTP. This will also have a positive effect on the equivalent CO₂ emissions produced by consumed electricity.

Environment and social criteria are also taken into account as a contribution to the quality of urban environment as well as the social acceptance of different types of infrastructure.

The flood protection benefits resulting from an improved sewage conditions are also analysed. For the analysed area the possibility of flooding occurs in the case of heavy precipitation accompanied with high water level of the Sava River causing high groundwater table and saturated soil. In this case the excess of precipitation is retained on the surface due to less infiltration capacity and sewer inability to absorb the excess water.

Therefore, rainfall events with a return period of 20 years have been chosen for the flooding analysis since the preliminary analysis showed that events with lower return periods will not cause the occurrence of water on the terrain surface due to the additional detention storage provided by sewage network.

The hydrologic and hydraulic analysis for each scenario was performed using EPA's (Environmental Protection Agency) Storm Water Management Model (SWMM) software since it has the possibility to model the performance of

specific types of low impact development controls. Dynamic wave rainfall-runoff routing simulation was used for a single-event with a 5-year return period and 20-year return period needed for the flooding examination.

Horton's infiltration model was selected and soil characteristics are defined according to the experience from similar analysis and data from the literature values. For some of the parameters a sensitivity analysis was performed in order to obtain relevant values. Surface permeability was assessed based on detail digital area images.

The initial analysis showed that the time of concentration for the surfaces that generate most of the runoff was 35 minutes. For this rainfall duration a constant rainfall value (hyetograph) of 54 [mm/h] was used for 5-year design storm and 72 [mm/h] for 20-year design storm. The values were obtained from the intensity-duration-frequency curves for Zagreb.

2.1 Conventional drainage scenario

The analysed developed area is located on the left bank and directly by the Sava River and it is one of the newly built parts of the city located southwest of the city center, Figure 1. The area of the analysis covers a total area of 115.000 [m²] (11.5 [ha]).

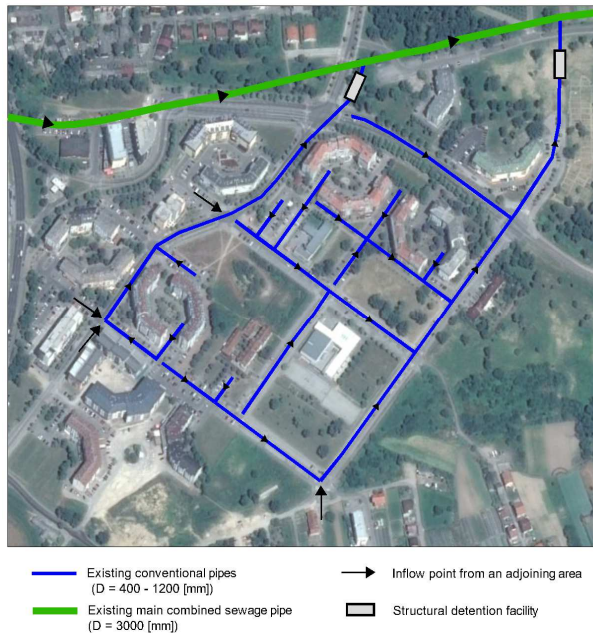


Fig. 1 Conventional drainage scenario solution

Existing sewage system in the analysed area is a combined sewer system designed to remove rainfall from the urban area as quickly as possible. It consists of a conventional pipe network with pipe diameters ranging from 400 to 1200 [mm], with two connections to the main combined sewage pipe (D = 3000 [mm]) located north of the area, Figure 1.

The main combined sewage pipe transports the combined wastewater to the WWTP solely by gravity; there are no pumping stations located between the analysed area and the WWTP. Prior to the WWTP a combined sewer overflow is located which allows the wastewater to overflow directly into the Sava River if the hydraulic load is too large for the WWTP. Total length of sewage network is 2.690 [m].

Taking into consideration the previously determined goals, an improvement of the existing system is made by adding two storage tanks (detention structures) whose total volume is 300 [m³] (50 [m³] and 250 [m³]).

Stormwater storage tanks are located at the point where sewer network exits the study area. They reduce runoff peaks and provide a temporary accumulation of sediment thus have a limiting potential for water quality control.

Proposed conventional solution does not provide rainwater reuse.

For the existing drainage conditions (without detention structures) maximum runoff occurring for 5-year design storm is 695 [l/s]. By using stormwater detention structure a peak runoff from a subcatchment is reduced to 450 [l/s], Figure 2.

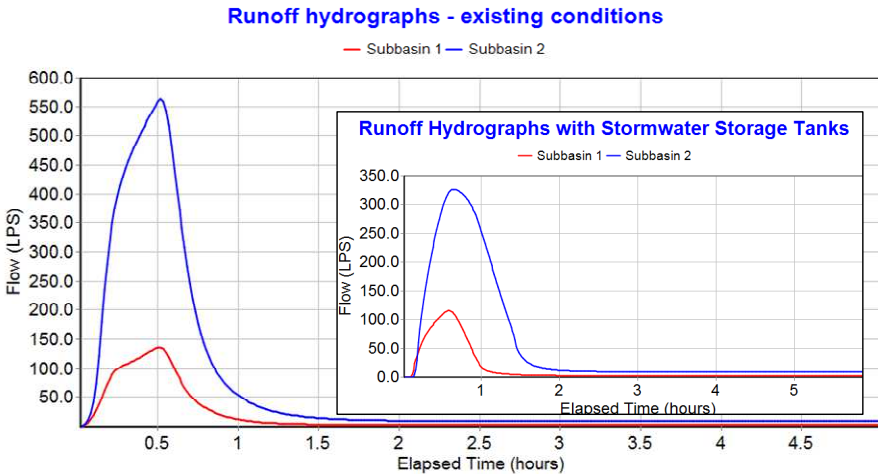


Fig. 2 Runoff hydrographs for the existing drainage conditions and the conventional drainage scenario

For each subcatchment a runoff coefficient is obtained from SWMM model resulting with an average runoff coefficient of the analyzed area in the value of 0.59 [1]. Since there is an average of 1.060 [mm] of rainfall per year, runoff volume from the area of analysis per year is approximately 71 930 [m³].

With the existing drainage condition some local flooding occurs in parts where the drainage network has a minimum diameters and is close to the terrain surface. Flooding occurs since there is no possibility of quick soil infiltration and the sewer network capacity does not meet the need for the excess of rainfall volume that occurs. Potential areas affected by flooding were estimated with a SWMM hydraulic model, Figure 3.

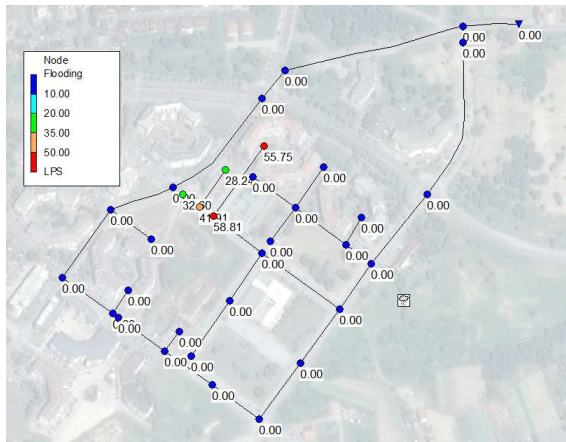


Fig. 3 Local flooding occurs after fully meeting the sewer system capacity

Maximum runoff occurring for 20-year design storm is 1225 [l/s]. In total, 12180 [m²] are affected by surface flooding with an average height of 17 [mm].

In the case with a conventional development with two stormwater detention structures a maximum runoff of 1150 [l/s] is realized. This lower value realizes due to a partial attenuation of the runoff at the bottom of the stormwater detention structure. When the water in the detention structure reaches the weir height the rest of the runoff overflows through weir. In this way overflow increases the downstream flow and the drainage system acts as a system without detention structures, thus as in the existing drainage conditions.

This conventional development with a detention structures has a very small effect on the flooding if the return period of rainfall is much greater than the detention structure design period. There are no major changes compared to the existing conditions; about 15 households would be affected on the same flooding area with an average of 17 [mm] of rain water height.

2.2 Conventional drainage scenario

In this scenario the existing conventional drainage network is improved with LID structures in a way to achieve previously defined goals, thus bioretention areas, water butts, soakaways and one green roof were used.

Since a high portion of the analysed area is covered with standard pavement, construction of bioretention areas will allow higher infiltration of the rainwater into the ground. Bioretention areas are placed next to parking areas and pedestrian pathways, and apart from reducing the annual runoff they also provide additional benefits to the local ecosystem.

Total area of 220 [m²] of bioretention areas were chosen for this scenario, and around 100 trees would be planted as an integral part of this structure providing carbon dioxide reduction and other environmental benefits.

In general it is estimated that by fixing carbon during photosynthesis and storing excess carbon as biomass a tree annually reduce carbon dioxide by 10 [kg CO₂e/year/tree]. Also an average annual quantity of carbon dioxide reduced in green roofs per square meter is 0.068 [kg CO₂e/year/m²], (Bueno et. al., 2015).

Total of 65 rain barrels (water butts) are placed next to existing buildings in order to collect rainwater. This water can be useful in providing a part of the water needed for irrigation of the nearby gardens.

Rainwater draining from the existing roofs will be collected by water butts and the excess water will overflow into soakaways, allowing the rainwater to infiltrate into the ground more effectively, Figure 4.

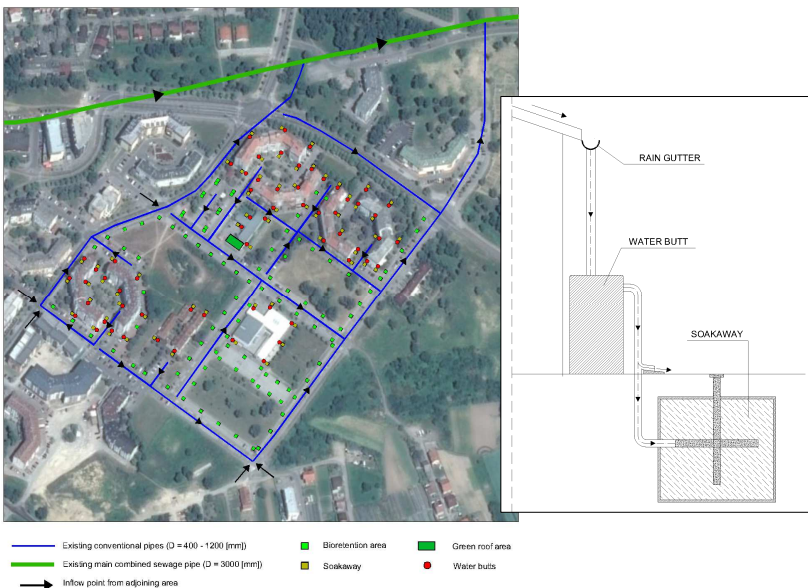


Fig. 4 LID drainage scenario solution

Hydraulic effects of LID structures and flooding areas were examined using SWMM model. Water quality and the production of pollutant loads associated with stormwater runoff were not analyzed due to insufficient data.

5-year design storm results with a maximum runoff peak of 485 [l/s] which represents a decrease of 30 [%] respectively, regarding the existing sewer network. However, this runoff value is 7 [%] higher than the runoff peak achieved with the conventional drainage scenario.

An average runoff coefficient for the LID scenario model provided by SWMM mode is 0.50 and it is smaller than the one for the conventional scenario. Since there is an average of 1060 [mm] of rainfall per year estimated runoff volume per year is 61.250 [m³].

In the case of flooding the excess of the precipitation is retained on the surface due to small retention capacity of the water butts and zero infiltration capability of the soakaways and bioretention areas (due to the saturated soil). It was determined that about the same surface area is covered by flood as in the case with conventional drainage scenario. This is due to the LID scenario design that is primarily focused on improving the downstream effects than the reduction of the flooding effects in the analyzed area. Approximately the same 15 households together with some parking areas would be flooded by 17 [mm] of water.

Two types of LID structures would have a noticeable effect on the ecosystem: bioretention areas and the green roof. Green roofs provide multiple ecological, social and aesthetical benefits such as air quality improvement, habitat provision for various species, reduction of greenhouse emissions, noise reduction etc.

Since around 100 trees would be planted, carbon dioxide reduction gained from the planting of additional trees and green roof implementation was calculated as 1013 [kg CO₂e/year] resulting in a significant positive effect on the local ecosystem.

3. RESULTS

The period of 20 years was chosen for the analysis in order to determine long scale effects (total costs of different scenarios, environmental impacts etc.) of proposed solutions. Longer periods would result in very unreliable results of the analysis, due to many uncertainties (discount rate, change in weather patterns etc.).

The results obtained from conventional and LID scenario are evaluated in regards to economic, environmental and social criteria. All these criteria are used in a multi-criteria evaluation (weighted sum model) for which following weights were used:

Criteria	Weight
Net cost of stormwater management	35 %
Peak outflow reduction	20 %
Net energy consumed by stormwater management	20 %
Net emissions of stormwater management	5 %
Global evaluation of ecosystem services	10 %
Social acceptance	10 %

Net cost of stormwater management includes cost of stormwater management minus benefits achieved by water reuse and flood protection. Net energy consumed by stormwater management takes into account total energy used for construction, maintenance and treatment minus energy saved by water volume reduction and water reuse. Net emissions are total CO₂ equivalent emissions obtained by adding the emissions from infrastructure construction and maintenance, runoff treatment and conveyance minus emissions avoided due to water reuse and water volume reduction.

Global evaluation of ecosystem services and social acceptance have been defined as qualitative decision criteria whose values range from very low to high. Ecosystem services include different possibilities for enhancements of quality of life such as aesthetics, landscape benefits, recreational use, regulation of urban microclimates, reduction of greenhouse gas emissions, etc. Qualitative evaluation is rated with linear distribution as: none (numerical value equal to 0), very low (25), low (50), medium (75) or high (numerical value equal to 100).

According to the ecosystem services provided by the structures used in scenarios global evaluation of ecosystem services were rated as very low for conventional scenario and medium for LID scenario.

Social acceptance presents an equally valued qualitative criteria which should show how residents accept the implementation of stormwater management structures.

For both scenarios cost of construction and maintenance, used energy and CO₂ emissions together with achieved benefits were calculated, Table 1.

Tab 1. Quantitative criteria calculation for the period of the analysis

Year	Net cost of stormwater management (€)		Net energy consumption (kWh)		Net CO ₂ emissions (kg CO ₂)	
	Conventional solution scenario	LID solution scenario	Conventional solution scenario	LID solution scenario	Conventional solution scenario	LID solution scenario
0	81.000,00	80.275,00	254.787,00	76.014,00	80.706,00	23.657,80
5	112.496,76	114.146,12	313.168,56	124.614,58	94.523,05	26.087,92
10	136.596,02	140.062,09	371.550,12	173.215,15	108.340,10	29.733,12
15	155.035,19	159.891,28	429.931,68	221.815,73	122.157,16	32.770,72
20	169.143,63	175.063,27	488.313,24	270.416,31	135.974,21	35.808,42

Relative scenarios comparison is given in Figure 5, for which maximum and minimum values were chosen in a way to give the better scenario a score of 100 and the worse scenario a score which is a ratio of better and worse criteria values.

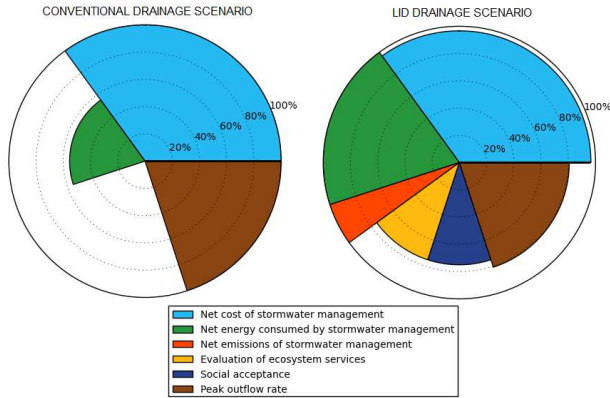


Fig. 5 Relative criteria results for two drainage scenarios

The overall result was calculated as a weighted sum for which conventional scenario was rated with 66 % in total and LID scenario with 90 %, Figure 6.

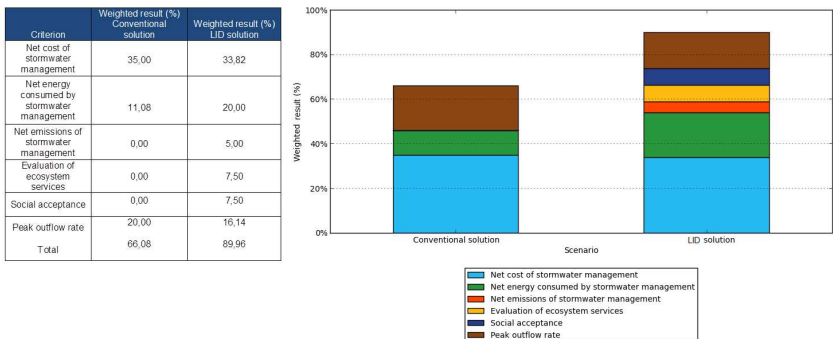


Fig. 6 Scenario evaluation - the overall result

4. CONCLUSION

For the same initial investment (or almost the same) each scenario yields different benefits during the period of analysis.

Total net costs of stormwater management during the analysis period are very similar for both scenarios, although at the end of the period of analysis they are

slightly higher for the LID scenario due to higher costs of maintenance of LID infrastructure.

Cumulative energy consumption is much higher in the conventional scenario; at the end of the period of analysis it is almost twice the value achieved in the LID scenario. Over half of the energy consumed in the conventional scenario is attributed to the construction of detention facilities. It accounts for 52 [%] of the net energy consumed by stormwater management during the period of analysis, and is the main cause for such a high difference in energy consumption of analysed scenarios.

Net CO₂e emission values of both scenarios follow different patterns. Conventional scenario has higher initial values of CO₂e emissions, caused by the construction of detention facilities and emissions generated by infrastructure maintenance and water treatment energy use. LID scenario has lower initial emissions and very slow growth trend. This positive ecological effect is caused by the vegetation which is an integral part of some of the chosen LID infrastructure (bioretention areas and green roof).

Designed improvement using conventional infrastructure was able to provide a fairly significant reduction in stormwater runoff peaks. This was made possible due to structural detention facilities. Reduction of annual volume of wastewater entering the system was not achieved since a conventional structures capable of reducing the runoff volume (by infiltration or evapotranspiration) were not used. LID structures were able to fulfill this goal to a certain degree due to the ability of the infrastructure to increase stormwater soil infiltration as well as to provide some water reuse.

Conventional scenario proved to be a cheaper alternative than the LID, but only slightly. Its maintenance costs proved to be drastically lower than the ones in the LID scenario, but the benefits achieved from reduction in wastewater treatment costs due to lower energy use and water reuse managed to balance out the high maintenance costs.

5. REFERENCES

- BUENO, I. E., DOMÉNECH, I. A., MOMPARDLER, S. P., TORRES, A. M., E2STORMED Decision Support Tool Guidelines, E2STORMED PROJECT; Work Package 3.E: Compilation of information; Improvement and Adaptation to MED Regions of integrated management tools for energy efficiency and incorporation of pilot actions results, 2014.
- PÉREZ-NAVARRO, A., LÓPEZ, E. P., SOLAR, D. A., BENITO, S. C.; Report on Energy in the Urban Water Cycle; E2STORMED PROJECT; Work Package 3.A: State of the art, analysis and proposed indicators and adaptation measures: Energy consumption in the water cycle, 2014.

Technical Audit of Water Supply Systems

L. Tuhovčák, T. Kučera, M. Tauš

(Institute of Municipal Water Management, Brno University of Technology – Veveří 331/95, 602 00 Brno, Czech Republic, tuhovcak.l@fce.vutbr.cz)

Abstract

The paper deals with auditing the technical condition of the Water Supply Systems (WSS) and its elements. Ageing of the water infrastructure is a worldwide problem. It is estimated that upgrading water mains in the United States would cost US \$ 77 billion over 20 years. In the Czech Republic, for example, the estimated need of rehabilitating the water systems totals \$0.9 billion/year but the actually invested amount is less than a half. The knowledge of the technical condition of the WSS is a key point in predicting the performance of the WSS and in optimising maintenance and rehabilitation of the WSS in the future.

The paper presents the methodology of determining the operating and technical indicators (TI) for a preliminary assessment of the elements of WSS such as pumping stations, water tanks, transmission mains, water distribution networks and pipe sections. The necessary data and system of TI evaluation using the multi-objective optimisation and FMEA method are defined. The proposed methodology allows the selection and ranking of WSS critical elements for more detailed analyses and suggestions of the type of renewal, including the estimated financial costs. The results and experience from the implementation of this methodology in real transmission mains, water tanks, pumping stations and distribution networks including the TEA Water web tool will be presented in this paper, too.

Keywords

Water supply system, technical audit, ageing of infrastructure

1. INTRODUCTION

Sustainable condition of the water infrastructure focus primarily on continuous planned rehabilitation. It should be the interest of every water mains owner to know the technical condition of the system owned by him. The information may then be used in decision-making on investment projects and in planning water mains renewal. Knowing the technical condition is crucial in predicting the performance of the WSS and optimising its maintenance and renewal.

In the Czech Republic (CR) there are over 5,000 owners (26 of which owning 61 % of the water supply assets value) and more than 2,000 operators (50 of which supply 90 % of billed water) of the water infrastructure. There is also a large number of small owners and operators who may face restricted possibilities in terms of renewal – in particular planning and available funds. As indicated by a questionnaire survey (Tuhovčák, Tauš 2013) even larger companies are sometimes not familiar with the technical condition of the infrastructure. The Czech law

imposes a duty to develop and implement the water supply and sewerage system renewal financial plan; however, this is only a plan of funds allocated for the renewal and determined based on the assets deterioration percentage. Furthermore, the law does not define the procedure for defining the deterioration percentage and leaves this determination method up to the WSS owner.

The common practice is to use only practical experience to assess the WSS condition as there is no standardised evaluation scale to measure the technical condition of the water mains (Al-Barqawi, Zayed 2006). Efficient assessment of the technical condition calls for the engagement of a large number of specialists, reliable databases, substantial period of time and equipment. Therefore it is advisable to make fast efficient assessment of the technical condition first and then take a decision whether it is necessary to make another, more detailed assessment (Rahman, Zayed 2009). The proposed methodology presented in this paper should serve as a tool for such a preliminary audit of the technical condition.

2. PROPOSED TECHNICAL AUDIT METHODOLOGY

2.1 Description of the methodology

The proposed uniform concept of the methodology dealing with preliminary assessment of the technical condition of the on WSS elements is based on the FMEA method. The FMEA (Failure Mode and Effects Analysis) is a method analysing reliability which allows for the identification of defects with major impacts on the function of the system and its elements. To assess the WSS using this method, sets of **Technical Indicators** are identified for the specific sections or structures of the water supply system in question. Necessary input data, physical dimensions and the method of determining the resulting point score on a scale of 1 – 5 are set for each of the defined TI. Determined values of the relevant technical indicators are then used to classify the assessed sections or structures in the WSS into specific categories based on the weighted average method:

- **A** (very good) – optimal condition of the relevant part of the WSS, no immediate measures are needed
- **B** (good) – good technical condition of the relevant structure, no immediate measures are needed;
- **C** (average) – average condition of the relevant structure or the audited part where certain measures may be needed in the near future;
- **D** (critical) – critical condition of the structure. Potential planned measures should be taken to deal with the situation;
- **E** (poor) – undesirable condition calling for an immediate solution based on the operator’s options resulting in the improvement of the technical condition of the audited section or structure.

Compared to the FMEA method, this approach was extended by another level - **Factors**. The technical indicators are currently not assessed directly but to ensure their more precise assessment use is made of the specific indicator factors. The assessment of each element based on the determined technical indicators is carried

out on the basis of the tabulated limits of the relevant factors. A table is defined for each factor setting the limits of the individual categories. Aggregation is performed sequentially from the lowest level using the weighted sum method. The assessment of the individual WSS sections and structures is performed in the following three steps:

- 1st step: Scoring of the technical indicator factors by the evaluator;
- 2nd step: Calculation of the assessment (1 - 5) of the individual technical indicators;
- 3rd step: Determination of the assessment category (A - E) of the relevant WSS section or structure.

If the technical condition of the individual basic defined sections or structures of the public WSS are taken into account, it is a semi-quantitative multi-criteria approach. The proposed methodology for assessing the individual TI and determining the category for the assessed sections (structures) is based on the weighted sum method.

As part of the proposed methodology a total of 7 basic sections and structures of the public water supply system have been defined. For each assessment of each of these sections (structures) separate modules with sets of technical indicators have been designed. The modules are the following:

- Module TEAR: water intake structures;
- Module TEAT: water treatment plants;
- Module TEAM: water transmission mains;
- Module TEAA: water tanks;
- Module TEAP: pumping stations;
- Module TEAN: water distribution networks;
- Module TEAS: water mains.

2.2 TEAR MODULE– water resources

To assess the technical condition of water resources, the TEAR module is developed while taking into account both the surface water resources and groundwater resources. The structure of the assessing technical indicators is designed with regard to the structural condition of the civil structures, condition and composition of technical equipment, method of operation, including the water resource protection. Naturally, the individual TIs take into account the binding standards and legislative requirements.

From the structural point of view we have included indicators such as the condition of the civil structures (e.g. concrete), water tightness of the structure, and condition of the ventilation equipment. Some of these indicators monitor mainly protection of the raw water intake structures against contamination caused by surface water and air.

In technical terms, the water abstraction pipe condition is primarily assessed. If the pipe is laid in the underground environment, attention is paid to the degree of perforation, clogging, ingrowing roots, etc.

A part of the technical indicators related to the operation compares the water yield with water demand both in physical as well as legal terms (permitted extraction). It also monitors drought threats.

The last but not least important part is concerned with the functionality and the presence of water protection as such.

2.3 TEAT MODULE – water treatment plants

Water treatment plants can be assessed by means of the TEAT module. With respect to the water treatment plants the authors of the methodology realise that it is hard to generalise the entire audit since there are many types of water treatment plants as well as technological elements used.

The proposed set of assessment indicators is based on the water treatment plant function, i.e. production of drinking water in the required quantity and quality. When assessing the technical condition of the water treatment plant this facility may not be viewed simply in structural and technical terms but it is absolutely necessary and much more important to assess it in technological terms. It is obvious that the resulting product - drinking water - must meet the prescribed indicator values but the production process efficiency may differ.

The indicators and factors related to the structural condition of water treatment plants are designed similarly to the water intake structures. The assessment of these indicators focuses on the condition of the tank and wall surfaces (concrete and masonry structures), the condition of windows and doors, ventilation and thermal insulation, etc.

Technically speaking, it is recommended that the proposed assessment indicators should be used to monitor the individual pipelines (e.g. progress of corrosion), functionality of closing and control elements as well as the age of pumps and other machinery. What is difficult is to determine the service life of these components. In general, the described methodology considers a limit service life works of 10-15 years for the machinery.

In the technological part of the assessment we focus mainly on the efficiency of drinking water production, the technical condition is then evaluated both in terms of the water treatment plant as a whole, and specifically for the crucial process units. These indicators include the treatment plant performance usability examining the ratio between the actual average treatment plant output and the projected output. The favourable ratio is considered at 90-100%. If the plant capacity is not fully utilised or if the plant is overloaded in hydraulic terms, the efficiency of technological processes is adversely impacted (design flow rate values, surface load and retention time are not followed). An indicator monitoring internal water consumption is used to follow the volume of water used to operate the process units (flushing water, sludge extraction, rinsing, etc.). A good situation

in terms of internal water consumption is in the range of 3-5%, a value above 10% is considered unsatisfactory.

In addition to quantitative indicators, qualitative indicators have also been proposed to monitor compliance with the requirements for drinking water quality and the number of exceeded limit values, as well as the standard of the measurement and monitoring equipment at the plant and the degree of automation.

As regards the indicators assigned to the individual technological stages, removal efficiency is evaluated along with the retention time in the clarifiers, filtration rate and net unit production.

With respect to the efficiency, it is quite difficult to give an assessment verdict and some of the decisions must be left to be made by each individual assessor. However, the proposed methodology generally recommends to consider as a very good condition if the efficiency of removing suspended solids during sedimentation is over 80%. Similarly, with respect to filtration it is recommended as a very good efficiency if the turbidity values in the effluent reach 1.0 NTU.

2.4 TEAN MODULE – water distribution networks

The TEAN module is designed to assess the technical condition of the individual pressure zones and metering districts. The currently proposed indicator structure is shown in table 1.

Tab 1. Proposed technical indicators of the TEAN module

TEAN – technical indicators
Average pipe material age
Burst rate
Water losses
Pressure conditions
Impacts on water quality
Valve vaults
Valves in the network

The indicator of pipe material average age is divided into two factors that are not evaluated at the same time. The age determination by calculation calls for a detailed database of the pipe material and age of the individual water mains. If such a detailed database of the age of water mains made of various pipe materials is not available, the assessment uses the second factor - expert estimate.

The burst rate assessment is one of the basic indicators assessing the technical condition. If database exists with separate records of burst water mains, valves and service pipes, it is advisable to evaluate each of this group of bursts separately.

To assess water losses, the developed module uses the most common indicators applied in the CR: the percentage of non-revenue water, unit leakage of non-revenue water, minimum night water demand, economic water loss index.

For the assessment of the pressure conditions we recommend to make the assessment in terms of the maximum hydrostatic pressure, mean hydrodynamic pressure and hydrodynamic pressure fluctuations during the day in the assessed water supply network.

Assessment of the direct influence of the water supply network on the quality of water is very difficult. For the purposes of assessing the technical condition we recommend the use of derived parameters: influence of the pipe material, quality of conveyed water, pipe incrustation, water retention time in the mains.

The assessment of the valve vaults and the valves in the network is designed to be made by means of visual inspections and assessment of the average age.

3. CASE STUDIES

The presented methodology was tested in actual water-related structures operated in the CR. For most of the modules the methodology requires both visual inspections as well as data from the operations and the dispatching. The methodology was tested in cooperation with selected water utilities. As an example, the assessment results of selected structures in water treatment plants and water mains are presented.

3.1 TEAT MODULE

The TEAT module and, in particular, the proposed set of TI have so far been tested mainly in separation structures, i.e. sedimentation and filtration stages at three real water treatment plants. The findings from the ongoing testing are still being used to modify the technological indicators, factors and the scoring scale.

One of the treatment plants where the technical condition assessment using the proposed methodology was tested was built in 1959 with a designed outflow of 200 l.s^{-1} . The sources of raw water were both ground and surface water sources - bored wells in combination with a water tank. During its operation, the water treatment plant has been extended several times, technological elements have been added, the building has been reconstructed and the control room upgraded.

Raw water is mainly characterised by increased iron and manganese concentrations if water is extracted from boreholes, sometimes it is characterised by aggressiveness and ammonia content. Water coming from surface resources is mainly characterised by increased content of organic matter and microbial growth in the spring and autumn. Suitable mixing results in mixed raw water which is treated by ozone oxidation followed by two-stage filtration and final treatment on filters with granulated activated carbon. Water is disinfected with chlorine gas.

The designed daily capacity of the water treatment plant is 210 l.s^{-1} and the actual average daily output is 160 l.s^{-1} . At this plant, a total of 13 TI were assessed, with 3 being given 5 points - unsatisfactory condition, 3 indicators scoring 3 points – average conditions and the others scoring 1 point - very good condition. One of these indicators is the indicator of internal consumption, which was assessed as slightly over 10%.

Tab 2. Selected indicators of the technical condition of the water treatment plant

Total assessment	B
Usability of the plant output given its design values	2
Internal water consumption	3
Filtration efficiency determined by reduced water turbidity	1
Automated operation of the specific separation structures	1

During the assessment of the indicators in tab. 2, it was determined that the average output was 76% of the design output, internal water consumption at the plant amounted to 10.2%, the turbidity value at the outlet of the second filtration stage did not exceed 0.3 NTU for a period longer than 10 minutes and the separation structures were fully automated in performing the technological tasks.

3.2 TEAN MODULE

The tested pressure zone (PZ) supplies water mainly to real estates built in the 1980s. The dominant pipe material is gray cast iron, which accounts for close to 80% of the total length of the pipeline in the zone. The total length of pipes in the PZ is 16.06 km. The average age of the cast iron pipes is 40 years. The occurrence of bursts in the PZ is up 10 bursts per year (mains only). The network operator states that no significant increase in the number of bursts has been recorded in recent years. The size of the water mains ranges from DN80 to DN400. The largest pipe clearance is that of the supply main which leads directly from the water tank.

Most technical indicators are included in the first two categories. The worst assessed technical indicator was TI4 – Pressure conditions - two of the three factors received three points. Based on the score, the pressure zone is categorised as “**B - good condition**“. The resulting assessment of the individual technical indicators for the tested pressure zone is shown in table 2.

Tab 3. Resulting assessment of the pressure zone

Total assessment	B
Average pipe material age	1
Burst rate	2
Water losses	1
Pressure conditions	4
Impacts on water quality	3
Valve vaults	1
Valves in the network	3

4. TEA WATER SOFTWARE TOOL

The web application TEA Water (Technical and Energy Audit) is an interface which enables WSS audits using a uniform methodology for the assessment of the technical condition. The software tool is available at <http://tea.fce.vutbr.cz>, at the time of this paper it is, however, still intended for development and testing only. It is expected that the application will be released for commercial use at near future.

The working environment of the application is accessible from any Internet browser. This indicates minimum hardware and software requirements. However, the user needs Internet connection to be able to use the application. After starting up the application the user must first sign up and then log in with a user account and password. In the next step, the user creates a new project and fills in project details. This enables new structures to be created in the active project in the specific modules, make assessments and review the assessment results. Current working design of the application without the graphical interface is shown in Fig. 1.

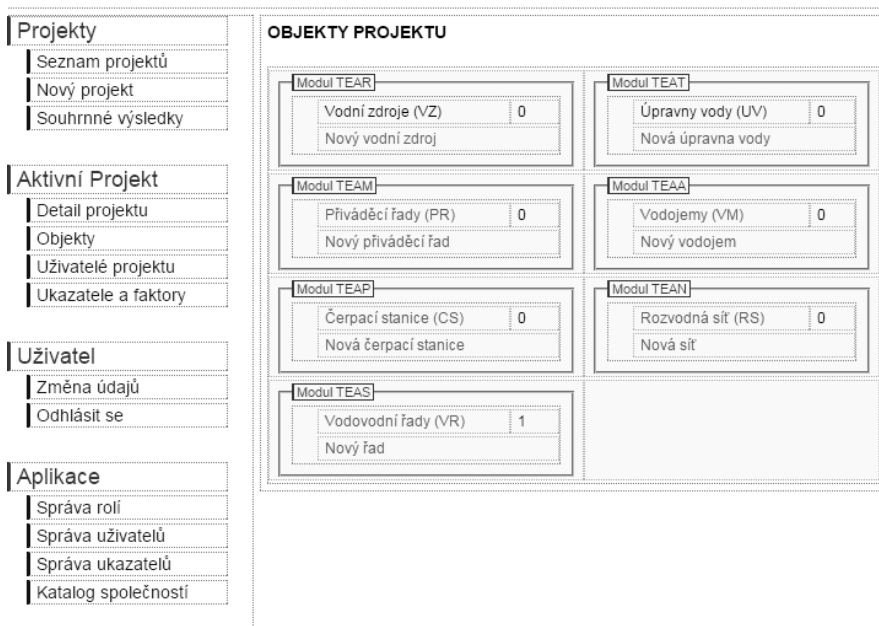


Fig. 1 Interface of TEA Water software tool (techn. and energetical audit)

5. CONCLUSION

The presented methodology is the outcome of the efforts made to design a simple yet effective methodology for auditing the technical condition of public water supply systems. The proposed methodology is designed to categorise the

technical condition assessment concerning the basic parts of the public water supply system. The outcomes of this methodology can serve as a basis for comparative analysis, repairs planning, renewal planning, repairs funding planning required by the act on water supply and sewerage systems, as a basis for further detailed structural and technological surveys etc. The proposed methodology is able to interpret the technical condition of the individual parts or structures, present critical points through various technical indicators and perform comparative analyses of the considered water infrastructure. The disadvantage may be the apparent difficulty in obtaining and processing input data and certain subjectivity in assessing the individual factors.

6. REFERENCES

- AL-BARQAWI, H. and ZAYED, T., 2006. Assessment Model of Water Main Conditions. American Society of Civil Engineers, pp. 1-8.
- RAHMAN, S. and ZAYED, T., 2009. Condition Assessment of Water Treatment Plant Components. Journal of Performance of Constructed Facilities, 23(4), pp. 276-287.
- TUHOVČÁK, L. and TAUŠ, M. 2013 Hodnocení technického stavu vodovodů, in Proc. Voda Zlín 2013, pp.26-32, in Czech

Acknowledgement

This paper was created as part of the specific research project BUT in 2015 BD12500000 "Sensitivity analysis of technical indicators and their weights in the evaluation of the technical state of public water" and project AdMaS UP.

Defining the time of closing the valve at small hydro power plant on the main pipeline of the water supply system

G. Taseski, C. Popovska, P. Pelivanoski

(Faculty of Civil Engineering, University of Ss Cyril and Methodius, Skopje, Macedonia,
e-mail: taseski@gf.ukim.edu.mk; popovska@gf.ukim.edu.mk; pelivanoski@gf.ukim.edu.mk)

Abstract

Very often water supply systems are used not only for water supply but also for energy production. This paper deals with hydrodynamic analysis of a small hydropower plant constructed on the main pipeline of the regional water supply system "Studenchica". The water supply system "Studenchica" is located in northwest part of the Republic of Macedonia. It provides technological water for TE Oslomej and drinking water for cities Kichevo, Prilep, Makedonski Brod, Krushevo and many villages in the region. Knowing that the main pipeline has been designed and constructed on hydrodynamic conditions, then the operational regime at the closing valve must be limited. To obtain the desired closing time a water hammer model has been applied for the entire system and to check whether nowhere in the system the maximum allowed pressure has not been exceeded. Abstract should summarize the most important points of the paper.

Keywords

Small hydropower plant, closing valve, mathematical model, water hammer

1. INTRODUCTION

The regional water supply system "Studenchica" is used to provide potable water for the Thermal plant Oslomej in Kichevo and water supply of the cities: Kichevo, Prilep, Makedonski Brod, Krushevo as many villages in the region, Figure 1 [Pelivanoski, Taseski 2012].

The water supply system "Studenchica" was launched in 1980 with provided - designed service period of 30 years and a maximum installed capacity of 1.500 l/s. The water from the regional water supply system "Studenchica" covers from the source "Studenchica" located at an elevation of 966.38 m above sea level and is characterized by large fluctuations in its capacity of 490 to 5.495 l/s [Pelivanoski, Taseski 2012].

With the General solution for the regional water supply system Studenchica that is prepared in 1975, that does not plan construction of power plants on the pipeline, it is probably because in that period the implementation of this kind of power plants-on pipe was rarely present that one can say that there isn't one at all [Pelivanoski, Taseski 2012].

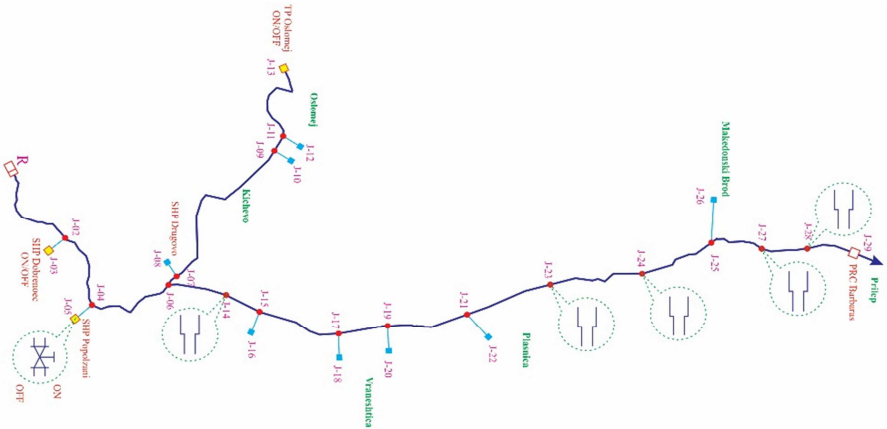


Figure 1. Schematic presentation of the part of the Regional water supply system Studenčica for which the mathematical model HTM is applied

According to the project documentation *Study for innovation of the regime of using the regional water supply system "Studenčica"* prepared by the Civil Engineering Faculty where they analyze the current needs of water supply of the settlements and the future needs of water supply by 2040, it can be concluded that the capacity of the source in great part of the year is greater than the current and future needs of water for water supply of settlements, Thermal plant Oslomej and from the installed capacity of small hydro-plant Dobrovo. Therefore with the *Study for optimal utilization of the hydropower potential of the regional water supply system Studenčica by innovative water supply regime*, which is made by Aquawatt from Skopje, plans construction of a small hydro power plant near the settlement Popolzhani with installed flow of 450 l/s. This plant is considered to operate only on the excess water from the regional water supply system Studenčica [Pelivanoski, Taseski 2012].

Regardless of the type of the turbine always when setting the hydro-mechanical equipment for these plants before the turbine usually a butterfly valve is placed that in the stage of exploitation of the system may require closure. The closing of the valve can cause a sharp increase in the pressure as close to the valve and along the pipeline depending on the speed of propagation of the wave, i.e. with the sudden closure of the valve a water hammer is caused [Pelivanoski, Taseski 2012].

On the other hand, typical for the regional water supply system Studenčica is that during the preparation of the General project the thickness of the pipe is dimensioned for hydrodynamic pressure, and knowing that the pipeline is currently at the end of its service period, it is possible with even a small increase in the pressure, at a part or the entire pipeline significant damage of the same to appear [Pelivanoski, Taseski 2012].

Due to the foregoing, the regional water supply system Studenchica with built small hydro-plant in Popolzhani, during a sharp opening and closing of the valve before the plant is the subject of analysis in this paper [Pelivanoski, Taseski 2012].

The geometric characteristics of the pipeline and the high land elevations of the nod points are shown in the following Table 1 [Taseski 2015], [Pelivanoski, Taseski 2012].

Table 1. Geometric characteristics of the pipeline from the regional water supply system Studenchica

Area		Elevation		L m	Material	Diameter, mm		Thick. δ , mm	a m/s
						OD	ID		
1	2	966	758	4,500	Steel	1,016.0	992.0	12.0	1,104
2	3	758	758	500	Steel	323.9	307.9	8.0	1,194
2	4	758	654	4,000	Steel	1,016.0	992.0	12.0	1,104
4	5	654	654	500	Steel	711.2	691.2	10.0	1,146
4	6	654	619	4,000	Steel	1,016.0	992.0	12.0	1,104
6	7	619	621	500	Steel	457.2	441.2	6.0	1,196
7	8	621	722	500	Steel	508.0	492.0	8.0	1,165
7	9	621	640	9,500	Steel	355.6	343.6	6.0	1,189
9	11	640	648	500	Steel	355.6	343.6	6.0	1,189
11	13	648	721	4,000	Steel	355.6	343.6	6.0	1,189
6	14	619	613	2,000	Steel	914.4	890.4	12.0	1,130
14	15	613	598	2,500	Steel	914.4	889.0	13.0	1,149
15	17	598	586	3,500	Steel	914.4	889.0	13.0	1,149
17	19	586	581	2,000	Steel	914.4	889.0	13.0	1,149
19	21	581	576	3,500	Steel	914.4	889.0	12.0	1,130
21	23	576	590	5,500	Steel	914.4	889.0	13.0	1,149
23	24	590	574	5,500	Steel	914.4	890.4	12.0	1,130
24	25	574	546	1,000	Steel	863.6	839.6	12.0	1,143
25	26	546	546	500	Steel	244.5	224.5	10.0	1,201
25	27	546	681	1,500	Steel	863.6	839.6	12.0	1,143
27	28	681	785	1,000	Steel	863.6	841.6	11.0	1,123
28	29	785	863	4,500	Steel	863.6	847.6	8.0	1,041

2. BASIC EQUATIONS FOR WATER HAMMER

According Wylie (1993), the water hammer is defined as the hydraulic variable occurrence of flow, which causes an increase of overpressure in a pipeline system. The water hammer can be generated by certain operational measures such as: opening or closing of the valve, turning the pumps on or off, abrupt cracking of the pipe etc [Popocska 2000], [Streeter, Wylie 1967], [Betamino De Almeida 1992], [Zaruba 1993], [Parmakian 1995].

Starting points in the mathematical description of the water hammer are the basic laws in the mechanics of fluids:

- Law of maintaining the amount of movement and

- Law of maintaining weight.

Satisfying these basic principles for conservation/maintenance comes to the dynamic equation and the equation of continuity.

The final form of the dynamic equation for unsteady flow in closed systems under pressure:

$$\frac{\partial V}{\partial t} + V \frac{\partial V}{\partial x} + g \frac{\partial \Pi}{\partial x} + \frac{\lambda}{2D} V|V| = 0 \quad (1)$$

And the final form of the equation of continuity gets the following form:

$$V \frac{\partial \Pi}{\partial x} + \frac{\partial \Pi}{\partial t} - V \sin \alpha + \frac{a^2}{g} \frac{\partial V}{\partial x} = 0 \quad (2)$$

Where:

- V – velocity of fluid,
- Π – piezometric head,
- $\sin \alpha$ – angle of the pipe axis with horizontal,
- a – pressure wave celerity,
- g – acceleration due gravity,
- t – time,
- x – distance along the pipe axis,
- λ – friction factor.

3. METHOD OF CHARACTERISTICS FOR SOLVING BASIC EQUATIONS OF WATER HAMMER

With the method of characteristics the basic partial differential equations which are not integrable in closed form, are transformed into ordinary differential equations which have a solution in a closed form. The basic equations, the equation of continuity and the dynamic equation can be designated with L_1 and L_2 [Kaveh Hariri Asli 2013], [Izquierdo, Inglesias 2004]:

$$L_1 = g \frac{\partial \Pi}{\partial x} + \frac{\partial V}{\partial t} + V \frac{\partial V}{\partial x} + \frac{\lambda}{2D} V|V| = 0 \quad (3)$$

$$L_2 = \frac{\partial \Pi}{\partial t} + V \frac{\partial \Pi}{\partial x} + \frac{a^2}{g} \frac{\partial V}{\partial x} - g \sin \alpha = 0 \quad (4)$$

These linear equations can be combined as follows:

$$L = L_1 + \chi L_2 \quad (5)$$

From the previous equation it can be concluded that it's about two families of curves that are practically straight lines, where the speed of propagation is constant and many times faster than the basic flow, so the system of two partial differential equations are transformed into system of ordinary four differential

equations which are marked with a C+ and C- and determine straight lines [Streeter, Wylie 1967], [Izquierdo, Inglesias 2004]:

$$\left. \begin{aligned} \frac{d\Pi}{dt} + \frac{a}{g} \frac{dV}{dt} + \frac{\lambda}{2D} V|V| - V \sin \alpha &= 0 \\ \frac{dx}{dt} &= V + a \end{aligned} \right\} C^+ \quad (6)$$

$$\left. \begin{aligned} -\frac{d\Pi}{dt} + \frac{a}{g} \frac{dV}{dt} + \frac{\lambda}{2D} V|V| + V \sin \alpha &= 0 \\ \frac{dx}{dt} &= V - a \end{aligned} \right\} C^- \quad (7)$$

3.1 Numerical model

Figure 2 shows discretization of the physical system in a numerical network with computing steps Δx and Δt where the solutions are obtained at the intersection of the positive and negative lines of characteristics [Popocska 2000], [Streeter, Wylie 1967], [Betamino De Almeida 1992], [Zaruba 1993], [Parmakian 1995].

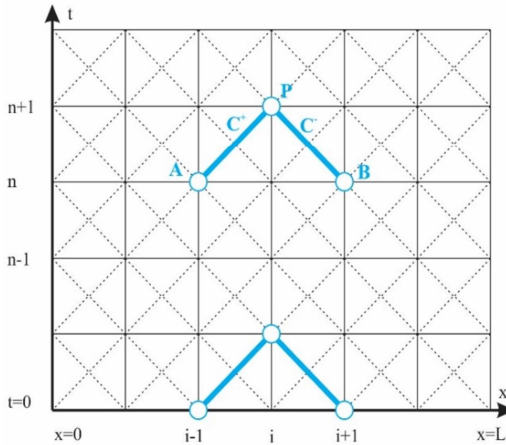


Figure 2. Numerical network for the method of characteristics.

According the given numerical network, equations (6) and (7) can be written as follows:

$$\frac{d}{dt} \left(\Pi \pm \frac{a}{g} V \right) + \lambda \frac{a}{D} \frac{V|V|}{2g} \mp V \sin \alpha = 0 \quad (8)$$

After integration, equation of positive characteristic are written:

$$\frac{\Pi_P - \Pi_A}{\Delta t} + \frac{a}{g} \frac{V_P - V_A}{\Delta t} + \frac{\lambda a}{2gD} V_A |V_A| - V_A \sin \alpha = 0 \quad (9)$$

If it is known that the hydraulic analysis is important to determine the change in the flow and height position of the hydrodynamic line in any section along the pipe and at a specified interval, additional approximating is introduced that the cross-section of the pipe throughout its length is constant and if it is known that the average speed can be determined by the equation $V=Q/A$, the previous equations knowing the numerical network can be written in the following final form:

$$CP = \Pi_{i-1}^n + BQ_{i-1}^n - MQ_{i-1}^n \left| Q_{i-1}^n \right| \quad (10)$$

$$CM = \Pi_{i+1}^n - BQ_{i+1}^n + MQ_{i+1}^n \left| Q_{i+1}^n \right| \quad (11)$$

$$\text{For:} \quad B = \frac{a}{gA} \quad \text{and} \quad M = \frac{\lambda \Delta x}{2gDA^2}$$

3.2 Boundary conditions

The conditions of the flow that govern within the boundary of the system under pressure – the water supply system are defined as boundary conditions. Their definition is of crucial importance for getting the solution at the points in the system. Follow-on are the most common cases of boundary conditions encountered in the water supply systems [Popocska 2000], [Kaveh Hariri Asli 2013], [Zaruba 1993], [Parmakian 1995], [Izquierdo, Inglesias 2004].

- Connection of more pipes in a junction

$$\text{Pressure: } \Pi^{n+1} = \frac{CP_1 / B_1 + CM_2 / B_2 + CM_3 / B_3 + CM_4 / B_4}{1 / B_1 + 1 / B_2 + 1 / B_3 + 1 / B_4} \quad (12)$$

$$\text{Flow: } -Q_{1,N}^{n+1} = \frac{\Pi^{n+1}}{B_1} - \frac{CP_1}{B_1}; \quad Q_{2,I}^{n+1} = \frac{\Pi^{n+1}}{B_2} - \frac{CM_2}{B_2}; \quad Q_{3,I}^{n+1} = \frac{\Pi^{n+1}}{B_3} - \frac{CM_3}{B_3} \quad (13)$$

- Reservoir at the end of pipeline

$$\text{Pressure: } \Pi_I^{n+1} = \Pi_R \quad (14)$$

$$\text{Flow: } Q_I^{n+1} = \frac{(\Pi_I^{n+1} - CM)}{B} \quad (15)$$

- Valve at the end of the pipeline

$$\text{Pressure: } \Pi_I^{n+1} = CP - BQ_N^{n+1} \quad (16)$$

$$\text{Flow: } Q_N^{n+1} = -B \cdot C_I + \sqrt{(B \cdot C_I)^2 + 2C_I(CP - Z_Z)} \quad (17)$$

- Valve at the middle of the pipeline

$$\text{Pressure: } \Pi_{1,N}^{n+1} = CP_1 - B_I Q_{1,N}^{n+1}; \quad \Pi_{2,I}^{n+1} = CM_2 - B_2 Q_{2,I}^{n+1} \quad (18)$$

$$CP_1 - B_I Q^{n+1} - CM_2 - B_2 Q^{n+1} - C_I Q^{n+1} \left| Q^{n+1} \right| = 0 \quad (19)$$

$$\text{Flow: } Q^{n+1} = \frac{-(B_1 + B_2) + \sqrt{(B_1 + B_2)^2 + 4C_1(CP_1 - CM_2)}}{2C_1} \quad (20)$$

4. IMPLEMENTATION OF THE MATHEMATICAL MODEL TO DETERMINE THE TIME OF CLOSING THE VALVE BY THE SMALL HYDRO-PLANT POPOLZHANI

As starting conditions for analysis of the water hammer that are used by the HTM model are the hydraulic characteristics in a stationary regime that in this case are made with the software package WaterGEMS. Given that it is about realistic systems the model is previously calibrated with measured data from the systems [Taseski 2015].

During the hydraulic analysis of the water supply systems, the process of calibration consists in adjusting the results of the hydraulic simulation with the actual measured values. According to the recommendation in the literature and from previous experiences with modeling of such systems, during calibrating the model should be calibrated - compared to the real system with two key parameters, namely: with the measured water flow and the measured pressures that occur during this flow, at the same time the flow and change of pressure should be measured in at least three points. From the obtained measurements of the flow and the pressure with hydraulic analysis, the real coefficient of the friction of the pipeline is obtained and the same is compared with the ratio of the friction in the model. The allowed deviations of measurements and calculations with the model during calibration for this type of piping is recommended not to exceed from 15% [Taseski 2015].

For the water supply system Studenchica the mathematical model HTM is calibrated with a series of systematic measurements of flows and pressures conducted on 09.11.2011. The values for the measured flows and pressures suggest that they were made in circumstances where the capacity of the source Studenchica is greater than the needs of water for the water supply. However, the data from a series of measurements, as in this case, was enough to make the calibration of the model [Taseski 2015].

One of the operational criteria of the new plant in Popolzhani is that it should run only when all the needs of water for water supply are covered for the settlements and potable water for the Thermal plant Oslomej. During the hydraulic analysis in stationary and non-stationary regimes of flowing the following alternative scenarios are made:

- I. Thermal plant Oslomej and Small hydro plant Dobrenoec are in function.
- II. Small hydro plant Dobrenoec is in function and Thermal plant Oslomej is not in function.

III. Thermal plant Oslomej and Small hydro plant Dobrenoec are not in function.

5. RESULTS OF THE ANALYSIS

In addition to the figures 3 and 4, that show the results of the analysis of the characteristics of the hydraulic hammer in the regional water supply system Studenchica during the abrupt closing of the valve in the intended Small hydro plant Popolzhani.

From the presented results it may be noted that with the sharp closing of the valve by the new projected Small hydro plant Popolzhani the pressure is sharply increasing as near the plant and in the entire system which exceeds the projected performances and operational criteria. The conclusion is that in the entire system the pressure is greater than the maximum allowable pressure according to the project.

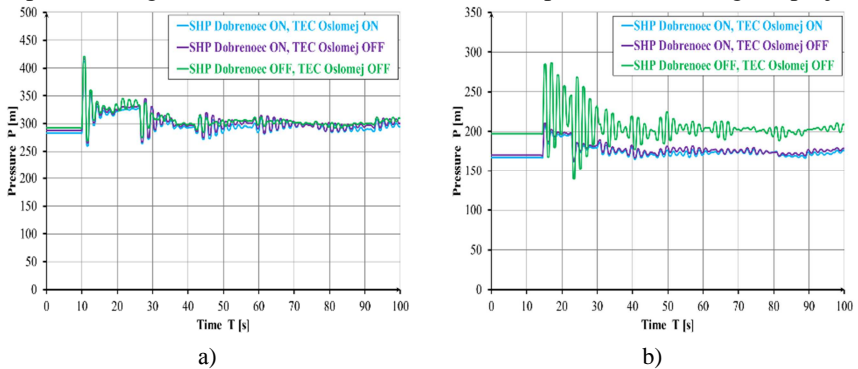


Figure 3. Increasing of the pressure during abrupt closing of the valve in the new Small hydro plant Popolzhani (a) and in Small hydro plant Dobrenoec (b)

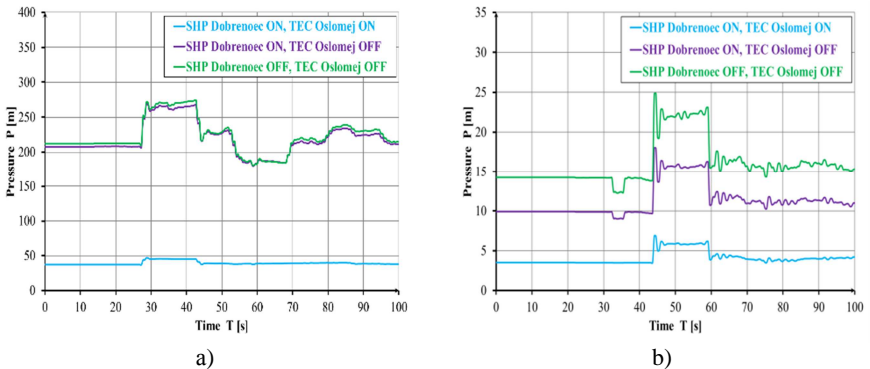


Figure 4. Increasing of pressure during abrupt closing of the valve in Thermal plant Oslomej (a) and in PRC Barbaras (b)

With the mathematical model HTM further analysis is made which determines the time of closing the valve as it doesn't allow increasing of the pressure over the maximum permitted in the entire system. In this analysis it is assumed that the closing of the valve is linearly in function of time. According this analysis the total time required for the gradual closing of the valve is 180 s. Figures 5 and 6 show the results of this analysis.

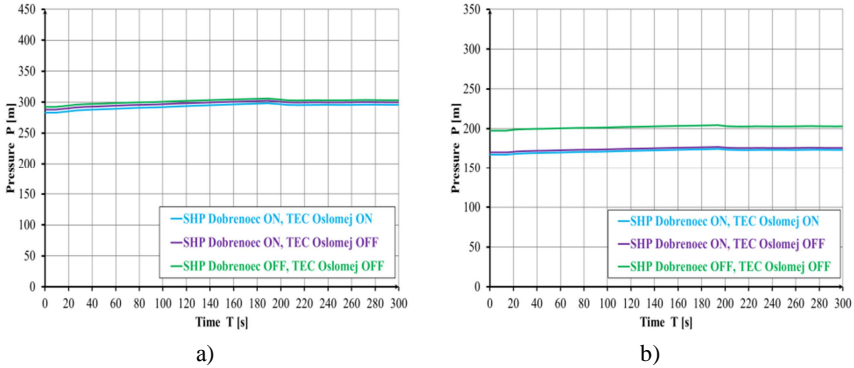


Figure 5. Increasing of pressure during regular closing of the valve in the new Small hydro power Popolzhani (a) and in Small hydro plant Dobrenoec (b)

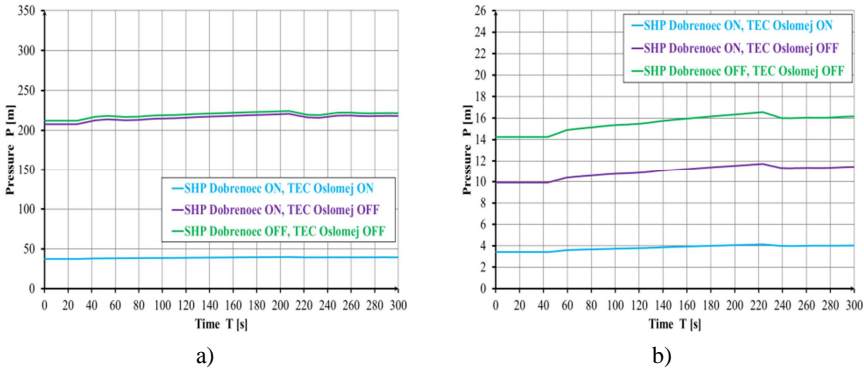


Figure 6. Increasing of pressure during regular closing of the valve in the Thermal plant Oslomej (a) and in PRC Barbaras (b)

6. CONCLUSION

From the performed analyzes the following can be found:

- The characteristics of the water hammer that would occur near the valve by Small hydro plant Popolzhani does not depend of the flowing amounts of water in the pipeline.

- Abrupt increase of the pressure above the allowable operating pressure of the system occurs in all branches of the regional water supply system Studenchica only during the abrupt closing of the valve.
- During the valve opening in Small hydro plant Popolzhani occurs only abrupt reduction of the pressure in the whole system.
- When the Thermal plant Oslomej does not work, a sharp increase in pressure compared only when Thermal plant Oslomej is operating occurs at the point of connection of the Thermal plant Oslomej.
- Also in a situation when Small hydro plant Dobrenoec is not in function according to the analysis made by the mathematical model HTM, sharp increase in pressure appears near Small hydro plant Dobrenoec.
- From the previous conclusions it can be stated that when sudden closure of the valve in Small hydro plant Popolzhani in all branches of the Regional water supply system Studenchica it comes to pressure increasing that is greater than the pressure for which the pipeline is dimensioned. Therefore, as a measure that is recommended to eliminate the pressure increasing, with the mathematical model HTM is the determined time of closing the valve, which in this case is 180 s.

7. REFERENCES

- BETAMINO DE ALMEIDA, E. 1992. Fluid transient in Pipe Networks, Publisher: WIT Press, ISBN-13: 978-1853121678.
- IZQUIERDO, J., INGLESIAS, L.P. 2004. *Mathematical modelling of hydraulic transients in complex systems*. Mathematical and Computer Modelling, 39,529-540.
- KAVEH HARIRI ASLI. 2013. Water Hammer Research: Advances in Nonlinear Dynamics Modeling”, Publisher: Apple Academic Press, ISBN 9781926895314 - CAT# N10708.
- PARMAKIAN, J. 1995 Water hammer Analysis. Publisher: Prentice Hall, Inc.; 1st edition, ASIN: B0000CJ5U0.
- PELIVANOSKI, P., TASESKI, G. 2012. Study for Innovation the Regime of Water Use by Regional Water Supply System "Studenchica".
- POPOSKA, C. 2000. *Hydraulics*. Publisher Civil Engineering Faculty, University Ss. Cyril and Methodius, ISBN 9989-43-100-0.
- STREETER, V. L., WYLIE, E.B. 1967. Hydraulic Transient, McGraw Hill Book Company, New York.
- TASESKI, G. 2015. *Characteristics of water hammers in water supply networks*. Doctorate dissertation, Skopje, Macedonia.
- ZARUBA, J. 1993. Water hammer in pipe-line systems. Publisher: Elsevier Science, ISBN-13: 978-0444987228.

Runoff quality from green roofs

M. Sokáč

Department of Sanitary and Environmental Engineering, Faculty of Civil Engineering, Slovak University of Technology Bratislava, Radlinského 11, 810 05 Bratislava, Slovak Republic, e-mail: marek.sokac@stuba.sk

Abstract

Green roofs have many advantages: improving the roof thermal insulation, noise absorption, temperature and humidity control in cities (urban microclimate), fire resistance and protection of roof structural surface layers against UV- radiation. The most important green roof ability, which appears as a key feature in terms of rainwater management in urban catchments is the ability of rainwater detention and retention. To increase the retention capacity of green roofs are being used in addition to the drainage layer and the storage layer, which in hydrological terms significantly change the properties of these roofs.

Paper describes preliminary results of a scientific project VEGA 1/0691/13, focused on experimental research of the hydrological function of green roofs in urban areas with regard to the reduction and the detention of rainfall runoff, which may be one of the crucial factors for sustainable urban development. Another objective of the research is to test the filtration ability of green roofs, rainwater runoff quality and possible use of green roofs as a supplementary source of service water in urban areas. We assume that runoff water collected from green roofs can be in some cases a valuable source of service water and can be used in many private or commercial applications.

Keywords

Green roofs, water resource, water quality, runoff

1. INTRODUCTION

Big expansion of sewer systems construction currently raises several conceptual questions, which have not always simple or clear answer. They are mainly basic conceptual issues of cities (sewer agglomerations) drainage strategy [Krejčí et al., 2002].

Current trends in most cities in Slovak republic can be described that the trend and the overall concept for the cities development is to keep the combined sewerage network type in a wider urban centres, but in all developing outskirts outside urban centres is the tendency to separate the waste water types. This creates multiple sewerage systems in complex urbanized area.

Foul wastewater (dry weather flows) does not represent in terms of capacity of the existing sewer network bigger problem. As in previous years there was a decrease in production of foul wastewater, it is also the capacity of wastewater

treatment plants (WWTP) generally satisfactory, problems occurs rather with requirements for advanced treatment technology - nitrogen and phosphorus removal.

However, the problem may be to change the ratio of the discharges of foul sewage water relative to the discharges of surface runoff, i.e. change the mixing ratio. There are however, two conflicting tendencies: on the one hand reduce the volume of industrial waste waters from a collecting system (to exclude problematic industries outside city centres) and on the other hand increase the volume of sewage from households (new residential areas, office, shopping centres, etc.). These volume changes may change the mixing ratio of combined sewer overflows (CSO's) and thus negatively affect the legislative possibility of wastewater overflows in CSO's.

As mentioned earlier, the problem of new urban outskirt areas is mainly water from surface runoff. Sewer network operators in most cases do not agree with the entry of surface runoff waters to the public combined sewer systems, as capacity main collectors is in most cases exhausted. Surface runoff from large development areas would require considerable and extensive reconstruction of sewer network and increase of its capacity. So the question is how to deal with waste water from surface runoff?

In principle, there are several ways of dealing with water from surface runoff. In principle, there are according the Slovak legislation two possible ways:

1. The disposal of water in places of their origin (infiltration, evaporation)
2. Accumulation and subsequent controlled discharge into water bodies or sewage systems

Accumulation and subsequent controlled discharge into water bodies or sewage systems face very often very strict and excessive requirements of authorities or sewer network operator. Regulation is generally limited to the requirement that the amount of surface runoff water must not be higher than the natural outflow of the catchment [7/2010 Coll.]. The solution of this situation is to the infiltrate the maximal possible extent of rainwater, while it should be noted that only lightly contaminated rainwater (e.g. from roofs, pedestrians sidewalks) can be infiltrated into the ground (with appropriate filtration through soil layer). More contaminated rainwater (e.g. from car parking lots, roads) can be infiltrated only after removing the harmful substances (e.g. oil separators, etc., see [364/2004 Coll.], [269/2010 Coll.]).

If infiltration is impossible due to local conditions (e.g. soil with low permeability) or if the infiltration restricted or prohibited for some reason (e.g. water resource protection zones), consideration should be given to draining rainwater into the local recipients. In this case there are also restrictions and requirements regarding the removal of polluting substances [364/2004 Coll.].

Therefore, we believe that in the future mainly the methods of spatial decentralized runoff retention and detention will be used.

From this point of view, we consider to be very promising and important the detention and retention decentralized methods using the green roof technology, which is not very common and widespread in Slovakia yet. However, we consider the green roof technology as very important tool for the surface runoff disposal together with the local infiltration. Green roofs hydrological characteristics are very close to the natural catchment, permitting evaporation of significant rainwater volumes.

2. GREEN ROOFS

Green roofs are already known for quite a while, but only in last decade come this idea back to life, mainly due to the development of building materials and technologies that permit the construction of such roofs on a new level of excellence. Green roofs have many advantages: improving the roof thermal insulation, noise absorption, temperature and humidity control in cities (urban microclimate), fire resistance and protection of roof structural surface layers against UV- radiation. The most important green roof ability, which appears as a key feature in terms of rainwater management in urban catchments is the ability of rainwater detention and retention.

To increase the retention capacity of green roofs are being used in addition to the drainage layer and the storage layer, which in hydrological terms significantly change the properties of these roofs. Green roofs retain a portion of rainwater that would otherwise flow out from the roof into the sewer system; this can significantly reduce the hydraulic load of sewer network.

Property that seems to be crucial in terms of rainwater management in urban catchments is the ability of runoff regulation and reduction.

Retained rainwater evaporates slowly, resulting in cooling and humidification of ambient air. It is also possible to accumulate the effluent water from the green roof and subsequently use it as service water, for irrigation or for other purposes. In addition to the impact on hydrology runoff (regulation and reduction) an important is also the effect of green roofs on runoff water quality. Some publications [Stausloff, S., 1998] pointed out on very high heavy metals removal efficiency (Cu, Zn, Cd, Pb, 92-99 %), as well as a significant buffering capacity with respect to acid rain [Teemusk et al., 2007].

3. FIELD EXPERIMENTS

For these reasons the project VEGA 1-0691-13 started experimental research aimed besides basic examining hydrological characteristics of green roofs also to the possibility of using waste materials as substrate layer for green roofs plants. Such suitable material can be the sewage sludge from municipal wastewater treatment plants, but should not be excessively polluted (e.g. heavy metals). The second option is to add filter materials directly into the roof structure, or their inclusion in the outflow area. Therefore, another objective of the project is to explore the possibility of using the filtration material - natural zeolite, whose relatively large resources are located in east Slovakia. This material has excellent

absorbent abilities and in combination with activated carbon filter could form an effective system for runoff pollution reduction from green roofs. Such approach might create additional sources of urban service water.

For further examination of the green roofs properties in terms of the runoff quality, we construct within the research work on the above mentioned project the experimental device, which consists of four boxes - green roof models, representing different types of roofs. Models are located on the roof of the "A" building of the Faculty of Civil Engineering in Bratislava in order to ensure model exposure in realistic conditions. Models are placed in a 2% slope. The in the bottom of the boxes are drilled holes to enable the outflow of the rainwater and sampling collection. The green roof model was constructed as intensive green roof type according rules and recommendations [EN 12056, 2001], [FLL, 2008], [ÖNORM L 1131, 2010].

In the first year of the project the experimental roof was filled with organic soil (humus layer), which is commonly used for the green roof construction. The construction type of the experimental green roof was an intensive green roof with a substrate layer with a 100 mm thickness. Half of the total experimental green roof area was filled with the organic soil, slightly mixed with the sludge from a wastewater treatment plant (from WWTP Bratislava - Petržalka). Surface of the experimental green roofs is covered with vegetation - standard seed mixtures, which are used in practice for the construction of green roofs (see Fig. 1). To increase the storage capacity of a green roof model we added in the model a storage layer consisting of a standard non-perforated drainage hard plastic foil, used in practice for the green roofs construction. For the first two models we used a drainage foil with 25 mm storage layer, in two models is used a storage layer 50 mm thickness.

The use of the common commercial organic soil proved to be a wrong choice; the runoff from the experimental green roof was extremely polluted. There could be two reasons for it: the first one is probably the high contents of pollution substances in the organic soil itself, the second one is the ability of the organic soil (humus layer) to keep the water and thus allow the extraction of large amounts of pollution from the incorporated sludge.

Despite the zeolite filters used (attached on the outflow pipe form the experimental green roof models) the runoff water quality was extremely poor. The runoff water contained high amounts of organic matters, this is reflected in the extremely high values of the BOD (over 1600 mg.l⁻¹, similar situation was with the COD indicator). A simple - visual comparison of the rainwater and the runoff from the green roof model can be seen on Fig. 1.

Pollution extraction will probably decrease over time, but we were afraid, it will stay very high for long time. Due to this reasons, in the second year we changed the soil type, used for the green roof model construction to the soft sandy soil with a small proportion of organic compounds (can be characterized as sandy, sandy-loam soil, regosol from the west- Slovak region Záhorie).



Fig. 1 Visual comparison of the rainwater (right) and the runoff from the green roof model (model with sludge incorporation – two samples most left, without the sludge – two samples in the middle)

4. RESULTS AND DISCUSSION

Results of chemical analyses from the year 2014 are listed in the Tab. 1. In this table we present the concentrations of the rain water, as well as the concentrations of the runoff water from the green roof model, which was based on “pure” soil without sludge addition.

Tab. 1 Results of chemical analyses

Substance	Unit	Rain water	Green roof runoff
Total organic carbon (TOC)	mg.l ⁻¹	2.265	30.85
Absorbable organic halides (AOX)	µg/l	20	30
Polycyclic aromatic hydrocarbons (PAH)	µg/l	0.335	0.055
Benzene	µg/l	<0.1	<0.1
Organochlorinated pesticides	µg/l	<0.01	<0.01
Silver (Ag)	mg.l ⁻¹	<0.0010	<0.0010
Aluminum (Al)	mg.l ⁻¹	0.345	0.099
Total alkalinity	mmol/l	<0.20	2.025
Arsenic (As)	mg.l ⁻¹	<0.0010	0.00498
Barium (Ba)	mg/l	0.0054	0.013
Boron (B)	mg/l	<0.030	<0.030
BOD ₅ with nitrification suppression	mg/l	1.2	1.225
Calcium (Ca)	mg/l	1.155	56.45
Cadmium (Cd)	mg/l	<0.00030	<0.00030
The total substance at 105 ° C	mg/l	84	297
Chlorides (Cl)	mg/l	0.3055	2.95
Cobalt (Co)	mg/l	<0.0020	<0.0020
Chrome (Cr)	mg/l	0.0012	0.0064
Copper (Cu)	mg/l	0.0037	0.0158

Substance	Unit	Rain water	Green roof runoff
Nitrate nitrogen N-NO ₃	mg/l	0.2875	8.8
Nitrite nitrogen N-NO ₂	mg/l	0.0052	0.065
Fluoride	mg/l	<0.024	0.312
Iron (Fe)	mg/l	0.1715	0.056
Total phosphorus (P)	mg/l	<0.40	0.84
Phosphate phosphorus P-PO ₄	mg/l	0.035	0.615
Mercury (Hg)	mg/l	<0.00010	<0.00010
COD (test with permanganate)	mg/l	1.125	22.1
total cyanide	mg/l	<0.010	<0.010
Magnesium (Mg)	mg/l	0.185	3.025
Manganese (Mn)	mg/l	0.0062	0.039
Molybdenum (Mo)	mg/l	<0.0040	<0.0040
Organic nitrogen	mg/l	<2.5	<2.5
Sodium (Na)	mg/l	0.575	7.25
Ammonia nitrogen N-NH ₄	mg/l	0.21	3.175
Suspended solids at 105 ° C	mg/l	<10.0	<10.0
Nickel (Ni)	mg/l	<0.0050	0.0053
Lead (Pb)	mg/l	<0.010	<0.010
Dissolved solids at 105° C	mg/l	81	293.5
Antimony (Sb)	mg/l	<0.0010	0.00198
Selenium (Se)	mg/l	<0.0010	<0.0010
Tin (Sn)	mg/l	<0.010	<0.010
Sulphates	mg/l	2.0315	38.38
Free hydrogen sulphide (H ₂ S)	mg/l	<0.020	<0.020
Sulphides	mg/l	<0.020	<0.020
Vanadium (V)	mg/l	<0.0020	<0.0020
Turbidity	ZF	2.5	<1.0
Zinc (Zn)	mg/l	0.059	0.0215
Conductivity at 20 ° C	mS/m	1.5	23.88
Extractable non-polar substances (ENP- IR)	mg/l	<0.05	<0.05

Note: the sign “<” means, that the concentration was below the indicated detection limit

5. CONCLUSION

Use the classic commercial organic substrate layer (with as well as without the sludge addition) has proved out to be inappropriate for cases, where the water from green roof surface runoff intended to be used as service water. The substantial change of the green roof model (the vegetation layer change from organic humus layer to the sandy – loam soil, regosol) has of course serious effect on the results. The major change is that it has considerably increased the runoff water quality (see Tab. 1) and conclusion is that the water from the experimental green roof with the substrate layer used can be fully utilised as service water.

On the other hand, the vegetation is not as lively and proliferous as with the humus soil layer in the first year, so the vegetation cover is not so effective and the evaporation is smaller. This can also be regarded as an advantage, as it is not necessary to take very often part of the roof horticultural maintenance.

The second disadvantage is the relative high weight of the sandy soil, so the green roof vegetation layer shall be thinner, or with use of the same layer thickness there will be higher weight of the green roof construction.

Future research within the project framework will be focused on determination of the sludge amount, which can be added to the soil without deterioration of the runoff water quality, eventually with the use of improved zeolite filters. Also runoff water quality from green roofs with other soil types could be examined (in other locations buildings).

6. REFERENCES

- 269/2010 Coll. Governmental decree: Requirements for achieving good water status. Collection of laws, Slovak republic, Nr. 269, year 2010.
- 364/2004 Coll. The Water law. Collection of laws, Slovak republic, Nr. 364, year 2004.
- 7/2010 Coll. The Act on Flood Protection. Collection of laws, Slovak republic, Nr. 7, year 2010.
- EN 12056-3. 2001. Schwerkraftentwässerungsanlagen innerhalb von Gebäuden - Teil 3: Dachentwässerung, Planung und Bemessung. 2001.
- FLL. 2008. Dachbegrünungsrichtlinie. Bonn: Forschungsgesellschaft Landschaftsentwicklung Landschaftsbau e.V. (FLL), 2008. ISBN 978-3-940122-08-7.
- KREJČÍ, V., et al.. . 2002. Urban drainage – conceptual approach. Petr Hlavínek and Evžen Zeman (editors). Brno : NOEL 2000 s r.o., 2002. ISBN: 80-86020-39-8. (in Czech)
- ÖNORM L 1131. 2010. Gartengestaltung und Landschaftsbau - Begrünung von Dächern und Decken auf Bauwerken - Anforderungen an Planung, Ausführung und Erhaltung. 2010.
- STAUSLOFF, S. 1998. Input and output of airborne aggressive substances on green roofs in Karlsruhe. Urban ecology. 1998.
- TEEMUSK, A., MANDER, U. 2007. Rainwater runoff quantity and quality performance from a green roof: the effects of short-term events. Ecological Engineering. 2007, Vol. 30.

Acknowledgement

This paper was prepared with the support of the Scientific Grant Agency VEGA within the scientific project Nr. VEGA 1/0691/13 “Increase of stormwater runoff retention and detention in urban catchments” and VEGA 1/0400/15 “Optimization of water treatment processes of small surface water treatment plants to ensure availability of safe drinking water supply”.

Efficacy of sorption materials for metals removal from water

R. Biela, T. Kučera

(Brno University of Technology, Faculty of Civil Engineering, Institute of Municipal Water Management, Žižkova 17, 602 00 Brno, Czech Republic, biela.r@fce.vutbr.cz)

Abstract

Some uncommon elements can sometimes be present in groundwater and surface water. Metals belong to such elements. Increased concentrations of iron and manganese can be expected in groundwater but higher concentrations of metals such as nickel or arsenic are not typical of such water. Nevertheless, water sources exceeding prescribed limits for drinking water in arsenic and nickel concentrations can also be found. Because of the toxicity of these metals, we started to make a research into the possibilities of removing these elements from water. Our research is funded by a grant from the Brno University of Technology.

There is a number of ways to remove heavy metals from water. Sorption on granular media based on iron oxides and hydroxides is currently the most used option. Our experiment was carried out using sorption materials GEH, CFH 0818, CFH 12 and Bayoxide, which are primarily designed to remove arsenic from water. We prepared four columns of an inner diameter of 4.4 cm for the purpose of the experiment. The thickness of the filtration media was 0.62 cm on average. Nickel, iron and manganese pollution was simulated in a laboratory. The efficacy of metals removal by four selected sorption materials was compared. During the experiment, the flow rate was set to reach the required retention time of 2.5, 7 and 15 minutes.

We have found out that the nickel concentration was reduced according to Regulation No. 252/2004 setting the limit value even after the shortest retention time (2.5 mins). Longer retention time had no significant effect on nickel removal. Our measurements also proved that all sorption materials have the ability to remove iron and manganese from water. Bayoxide sorption material achieved the best results in nickel, iron and manganese removal from water.

Keywords

Iron, manganese, metals removal, nickel, sorption materials

1. INTRODUCTION

Groundwater and surface water sometimes contain substances that do not occur frequently in such water. Such substances include some of the metals. Increased iron and manganese content is expected in groundwater; however, metals such as nickel and arsenic in high quantities are not typical of such water. Still, there are sources where the occurrence of nickel, arsenic and other metals is in concentrations exceeding the prescribed values for drinking water.

Nickel can be found in minerals usually with sulphur, arsenic and potentially with antimony. These are, for example, gersdorffite (NiAsS), pentlandite [(Fe,Ni)₉S₈], nickeline (NiAs), millerite (NiS) and garnierite and pyrrhotite. It is also included in some of the aluminosilicates (serpentine). Anthropogenic sources of nickel include mainly wastewater from metal surface treatment where it is predominantly complexly bound, and wastewater from colour metallurgy. It is also used in ceramic and glass making industries and for some chemical syntheses as a catalyser. Another potential sources are nickel-plated parts of equipment that can in touch with water. [Pitter 2009]

Besides simple Ni²⁺ ions, water in alkaline environment contains also hydroxo-complexes [NiOH]⁺ - [Ni(OH)₄]²⁻, then carbonato-complex [NiCO₃(aq)]⁰ and sulphato-complex [NiSO₄(aq)]⁰. Wastewater coming from galvanisation includes nickel usually in the form of cyano-complexes [NiCN]⁺ - [Ni(CN)₄]²⁻ and ammino-complexes [NiNH₃]²⁺ - [Ni(NH₃)₆]²⁺.

Nickel solubility in water is restricted either by carbonate NiCO₃(s) or hydroxide Ni(OH)₂(s). Sulphides are present, NiS(s) may also be considered.

Natural nickel background in groundwater is considered as concentrations that are not above ca. 20 µg.l⁻¹. Average nickel concentrations in public drinking water systems in the CR are usually ca. 4.7 µg.l⁻¹. Bottled mineral water in the CR contain Ni concentrations usually ranging between 0.3 - 10 µg.l⁻¹. In sea water, the Ni concentrations reach between 0.1 - 2 µg.l⁻¹. Flush water from metal surface treatment reaches nickel concentrations of tens up to hundreds of mg.l⁻¹. [Pitter 2009]

Nickel is not significantly toxic to human beings but it is one of the potential carcinogens. Toxicity for some of the aquatic organisms is quite high and, for this reason, the permissible concentrations in water supply courses is limited more strictly than in drinking water.

For the quality of drinking water and the quality of table water and baby water the limit value is set at 0.02 mg.l⁻¹. For water intended for fish breeding it is recommended that the Ni concentration should not exceed the value of 0.1 mg.l⁻¹. The same concentration is recommended for water used for irrigation purposes. The general pollution standard of permissible surface water pollution for nickel is 0.04 mg.l⁻¹. Industrial wastewater discharged into municipal sewerage systems is subject to the concentration limit of 0.1 mg.l⁻¹, when discharged into surface, water from electro-technical operations have a permissible nickel concentration set at 0.5 mg.l⁻¹ and for water discharged from metal surface treatment it is 0.8 mg.l⁻¹. [Pitter 2009]

2. EXPERIMENTAL REMOVAL OF NICKEL FROM WATER

Some drinking water natural resources contain nickel concentrations that sometimes exceed several times the limit concentrations in drinking water as defined by Regulation No. 252/2004 Sb. For this reason, we focused on removing

Ni from water and during the experimental measurement we assessed the efficiency of its removal from water during filtration using various sorption materials. The measurement was carried out at the Faculty of Civil Engineering of the BUT in the laboratory of the Institute of Municipal Water Management.

For the experiment we used four filtration materials primarily designed to remove arsenic from water. These are materials CFH 0818, CFH 12, GEH and Bayoxide E33. At the same time, iron and manganese removal efficiency was examined during the filtration.

2.1 Sorption material description

Materials CFH 0818 and CFH 12 that are based on iron oxide hydroxide are used to remove mainly As, Se, P, Ag, Ni, Pb, Mo, Si, V, Cu and other metals from water. Sorbents have the shape of granules, whose properties are very similar and they mainly differ in terms of granularity (tab.1). They are manufactured by Lemura based in Finland. The distributor of the material in the CR is Kemwater ProChemie s.r.o. based in Bakov nad Jizerou.

Tab 1. Granularity of filtration materials CFH [Kemira 2013]

CFH 0818		CFH 12	
Dispersion	Presence	Dispersion	Presence
[mm]	[%]	[mm]	[%]
2 - 0,5	97,6	2 - 0,85	92,7
< 0,5	2,4	< 0,85	5,9
> 2	0	> 2	1,4



Fig. 1 Sorption material CFH 0818



Fig. 2 Sorption material CFH 12

Sorption material GEH based on granulated iron hydroxide is suitable for economical and efficient removal of arsenic and antimony from water. The material was developed by Berlin University, Department of Water Quality. It is manufactured by the German company GEH-Wasserchemie GmbH. It is imported to the CR by Inform-Consult Aqua s.r.o. Přeborn. The treatment technology consists in the adsorption of the contaminant on granulated iron hydroxide (GEH sorbent) in a reactor through which the treated water flow flows. The adsorption capacity of the material depends on operating conditions. [Biela 2012, GEH 2013]



Fig. 3 Sorption material GEH

Bayoxide is a dry crystalline granulated sorbent based on iron oxide. It was developed by Severn Trent in cooperation with Bayer AG and produced by LANXESS Deutschland GmbH, Leverkusen in Germany. It is produced in two variants, Bayoxide E33 and Bayoxide E33P. The difference is that Bayoxide E33

is granulated whereas Bayoxide E33P is produced in the form of tablets. The material was designed to remove arsenic and its advantage is the removal of As^{III} and As^{V} along with the removal of iron and manganese. The producer gives water treatment capacity at the arsenic content of $11 - 5\,000\ \mu\text{g}\cdot\text{l}^{-1}$ and iron content of $50 - 10\,000\ \mu\text{g}\cdot\text{l}^{-1}$. [Biela 2012, Bayoxide 2013]



Fig. 4 Sorption material Bayoxide E33

Tab 2. Sorption materials properties overview [Pěkný 2013]

Parameter	Unit	GEH	CFH	Bayoxide E33
Chemical composition	-	$\text{Fe}(\text{OH})_3 + \beta\ \text{Fe-O-OH}$	Fe-O-OH	$\text{Fe}_2\text{O}_3 + \alpha\ \text{Fe-O-OH}$
Particle size	mm	0,2 - 2	1 - 2	0,5 - 2
Density	$\frac{\text{g}}{\text{cm}^3}$	1,25	1,12	0,45
Specific surface	m^2/g	250 - 300	120	120 - 200
Working pH content	-	5,5 - 6,5	6,5 - 7,5	6,0 - 8,0
Porosity of the grains	%	72 - 77	72 - 80	85
Colour	-	dark brown to black	brown to brown-red	amber
Description	-	moist granular	dry granular	dry granular

2.2 Measuring procedure

Each sorption material was poured into a glass tube with an inner diameter of 4.4 cm, with a drainage layer at the bottom made of stones, diameter of 1 - 2 cm,

followed a layer of glass beads, diameter of 4 mm and then a layer of beads, diameter of 2 mm. This prevented from the escape of loose material from the column during filtration. The height of the filtration medium was 62 cm on average. The filtration columns were fixed to the wall next to each other.

The entire filtration system consisted of a vessel with raw water, pump, flow meter, set of filtration columns and vessels for the filtrate. The filtration system scheme for one column is shown in Fig. 5.

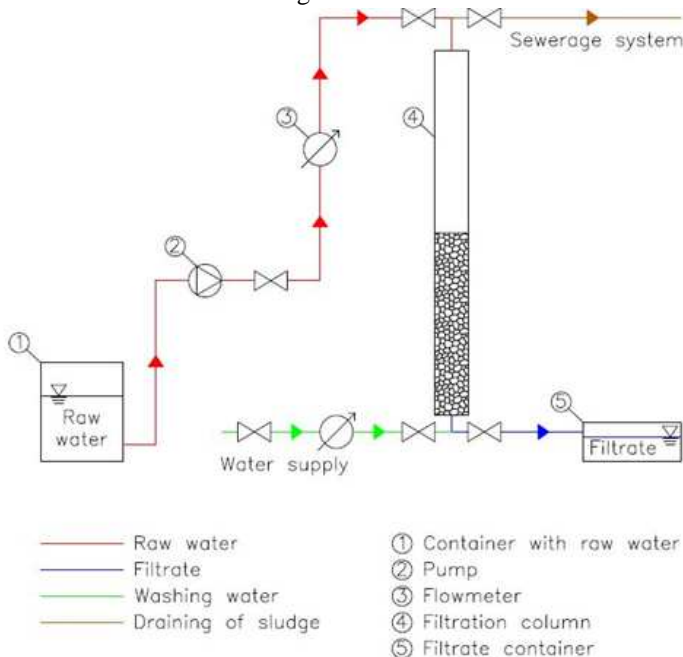


Fig. 5 Diagram of the filtration system

Before starting the filtration, the filtration material was processed as instructed by the producer. After that, the filters were flushed with tap water, in a reverse direction from filtration, i.e. bottom up, where the flush water was discharges into sewerage. During the flushing, the flow-rate through the column was selected so as to avoid the filtration material in suspension being flushed out. The filter flushing usually lasted until clear water started flowing out of the column.

Raw water with increased concentration of nickel, iron and manganese (tab. 3), this was simulated in a laboratory by adding chemical concentrates of these metals into drinking water from the Brno public water supply system. During the measurement, the raw water was pumped via a flow meter with flow rate values set in a way achieving the required retention time in the columns of 2.5 minutes, 7 and 15 minutes. Water filtered through the sorption materials had the following set concentrations of iron, manganese and nickel (see tables 4 - 7).

Tab 3. Analysis of raw water

t	pH	Turbidity	c Fe	c Mn	c Ni
[min]	-	[FNU]	[mg/l]	[mg/l]	[µg/l]
0	7,0	5,76	1,500	0,609	720,0

Tab 4. Analysis after filtration through the sorption material CFH 0818

t	Turbidity	c Fe	c Mn	c Ni
[min]	[FNU]	[mg/l]	[mg/l]	[µg/l]
2,5	1,43	0,111	0,052	2,0
7	0,66	0,116	0,034	2,0
15	0,41	0,021	0,037	5,0

Tab 5. Analysis after filtration through the sorption material CFH 12

t	Turbidity	c Fe	c Mn	c Ni
[min]	[FNU]	[mg/l]	[mg/l]	[µg/l]
2,5	2,54	0,400	0,057	4,0
7	1,45	0,363	0,056	5,0
15	1,21	0,332	0,044	4,0

Tab 6. Analysis after filtration through the sorption material GEH

t	Turbidity	c Fe	c Mn	c Ni
[min]	[FNU]	[mg/l]	[mg/l]	[µg/l]
2,5	1,63	0,153	0,155	10,0
7	0,70	0,142	0,153	9,0
15	0,67	0,133	0,150	9,0

Tab 7. Analysis after filtration through the sorption material Bayoxide

t	Turbidity	c Fe	c Mn	c Ni
[min]	[FNU]	[mg/l]	[mg/l]	[µg/l]
2,5	0,97	0,122	0,055	1,0
7	0,45	0,179	0,047	1,0
15	0,49	0,086	0,038	1,0

3. RESULTS EVALUATION

The analyses indicate that all sorption materials achieve excellent results in nickel removal thanks to its concentrations in raw water. Even the shortest retention time (2.5 min) ensures lower nickel concentration in raw water than the highest limit value in drinking water as per Regulation No. 252/2004 Sb. If the retention time was longer, there was no major increase in the nickel concentration reduction (see Fig. 6).

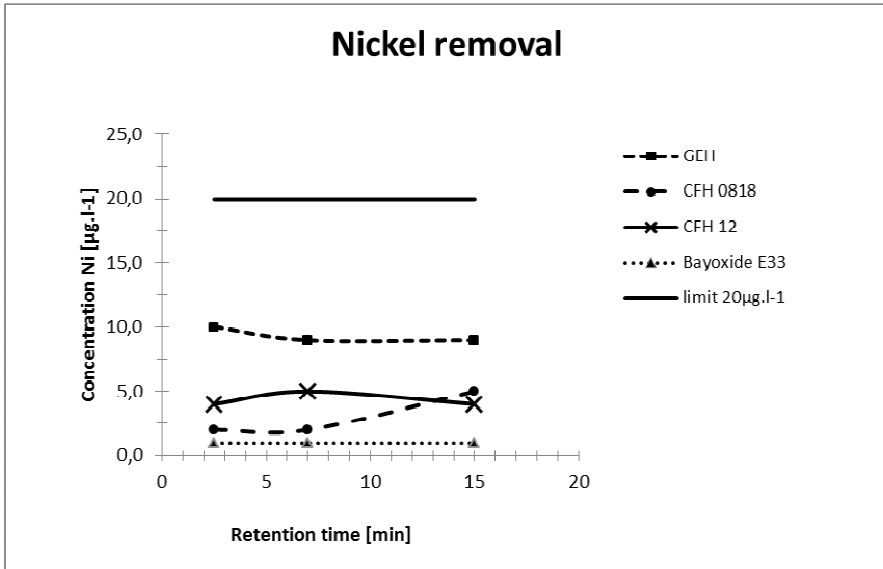


Fig. 6 Comparison of the efficiency of sorption materials with respect to Ni removal from water

The best results of nickel removal from water was achieved by Bayoxide E33, which managed to reduce Ni content during the shortest retention time and such good results were achieved constantly throughout the measurement period. When adsorbent CFH 0818 was used, Ni concentration increased if longer retention time was used, but this might be caused by measurement inaccuracy. Given the velocity of nickel removal from water, this is contact filtration with respect to all sorption materials.

The measurement also detected that the applied filtration materials also remove iron and manganese from water. Except CFH 12, other sorbents removed iron below the limit concentration for drinking water of 0.2 mg.l⁻¹. The most efficient material for iron removal seems to be sorption material CFH 0818. Manganese removal required a longer retention time than for nickel and iron to ensure the drop below the limit concentration for drinking water (0.05 mg.l⁻¹).

With the increasing retention time, the manganese removal efficiency increased. With the material GEH, the manganese concentration did not drop even after a contact period of 15 minutes to reach the limit prescribed value, which was probably caused by inaccurate measurement.

4. CONCLUSION

Laboratory tests of nickel removal from water were carried out at the Institute of Municipal Water Management as part of the specific university research project. The results show that by using sorption materials CFH 0818, CFH 12, GEH and Bayoxide E33 it is possible to reduce the nickel content from the over-limit value in just 2.5 minutes below a value set by the Regulation of the Ministry of Health 252/2004 Sb. In total, the best results of nickel removal from water were achieved by Bayoxide E33. It was also proved that the applied sorption materials have an effect on iron and manganese removal from water.

5. REFERENCES

- Bayoxide E33, 2013. *Arsenic Removal Media*. Dostupné z: <http://www.environmental-expert.com/products/bayoxide-e33-arsenic-removal-media-15343/view-comments#down>
- BIELA, R., KUČERA, T., VOSÁHLO, J. 2012. Odstraňování arsenu z vody sorpčními materiály. *TZB- info*, 2012, roč. 14., č. 11, s. 1-6. ISSN: 1801-4399.
- GEH, 2013. *Arsenentfernung*. Dostupné z: http://www.geh-wasserchemie.de/files/datenblatt_geh102_de_web.pdf
- KEMIRA, 2013. *Kemira CFH12, CFH0818*. Dostupné z: http://www.proximbio.eu/custom/media/TL_CFH.pdf
- PĚKNÝ, M. *Odstraňování vybraných kovů z vody*. Brno, 2013. 65 s. Diplomová práce. Vysoké učení technické v Brně, Fakulta stavební, Ústav vodního hospodářství obcí.
- PITTER, P. 2009. *Hydrochemie*. 4. vydání. Praha: VŠCHT Praha, 2009. 568 s. ISBN 978-80-7080-701-9.

Acknowledgement

The paper was prepared as part of the grant project on special research at BUT in Brno titled "Efficiency monitoring of water treatment processes in microcontamination elimination" (FAST-S-15-2701).

Flood Warning System for Valašsko – Horní Vsacko

V. Kolečkář, J. Kubík, R. Řihová

AQUA PROCON s.r.o., Palackého třída 12, 612 00 Brno, Czech Republic, e-mail:
vlastislav.kolecakar@aquaprocon.cz, jiri.kubik@aquaprocon.cz, renata.rihova@aquaprocon.cz

Abstract

The paper describes the creation of a Digital Flood Plan (DFP) for an association of 9 municipalities of the microregion of Valašsko-Horní Vsacko. The DFP is part of a project implemented under the Operational Programme Environment aiming at reducing flood risks and improving the system of flood services in the municipalities of Valašsko-Horní Vsacko. The main objective of the DFP was a direct connection with the newly created local warning system in the locality. The DFP newly uses data available on the Internet within the developed flood information system of the Czech Republic and enhances the awareness of all citizens in these municipalities.

Keywords

Digital Flood Plan, system of flood services, flood information system for the Czech Republic (POVIS)

1. INTRODUCTION

Over the past two decades, increased attention has been paid in the Czech Republic to flood protection also in relation to the transposition of the European Directive on the assessment and management of flood risks [ES: Directive 2007], [Dráb, Říha 2010]. Great attention is also paid to the so-called “flash floods” caused by heavy rains entailing significant damage to property as well as human casualties [Kocman et al. 2011]. The most severe damage occurs in montane and sub-montane zones experiencing very fast onsets of floods mainly in small streams. In relation to these frequent events, the Ministry of Environment (MoE) provided grant schemes [MoE - POVIS 2009 – 2011] whose main objective was to develop a Local Warning System (LWS) related to the development of the Digital Flood Plan. The reason behind was to ensure early and good-quality information to restrict flood risks caused by heavy rains. The MoE issued a uniform methodology [MoE 2009 – 2015] for the development of the Digital flood plans so that every DFP could be linked to a higher-level Flood Plan (FP) and the flood information system.

In the past, the region of Valašsko-Horní Vsacko was repeatedly affected by flood events of local and regional importance. Therefore, the association of 9 municipalities in the microregion of Valašsko-Horní Vsacko took a decision on the necessity to establish the Flood Warning System that can assess the potential

flood onset in a qualified manner. At the same time, measures could be taken in time to minimise potential flood damage. The project output had a form of the Digital Flood Plan for the aforesaid region. However, the development of the Digital Flood Plan was closely related to the development of the Local Warning Systems and its tasks were implemented in cooperation with the DFP development. The proposed Local Warning System and the Digital Flood Plan are interconnected and can provide early warnings against the onset of flood risk while enabling available on-time information to be received by all inhabitants of the endangered region.

2. PROCESS OF DEVELOPING THE DFP

The region of interest consists of a group of 9 municipalities in the microregion of Valašsko-Horní Vsacko and these municipalities are situated in two separate localities of the Vsetínská Bečva river basin. These are the following two separate areas.

1. Area upstream Vsetín with the following municipalities: Halenkov, Hovězí, Huslenky, Janová, Karolinka, Nový Hrozenkov, Velké Karlovice and Zděchov with the total catchment area of 294 km².
2. Area downstream Vsetín with the municipality of Bystřička with the total catchment area of 85 km².

The task of the project was to include the relevant data in the POVIS environment and to develop a well-functioning DFP of the comprehensive area formed using the DFPs of the individual municipalities. The DFP was elaborated according to the methodology for the DFP development [MoE 2009 – 2015] issued by the MoE meeting the conditions defined in [TNV 75 2931], i.e. it was divided into the following areas:

1. Factual part containing the data necessary to protect property or municipalities.
2. Organisational part containing lists of names, type of communication and tasks for the individual entities engaged in the flood protection process.
3. Graphic part containing maps showing the flood plains, evacuation routes, gauging stations and information points.

The DFP uses direct links to the geographical information system (GIS), which results in a great benefit having the digital form of the flood plan and its graphic attachments. The project precondition was also to develop a Local Warning System including the establishment of new auxiliary gauging stations, category C (rain gauges and level indicators) and determination of Degrees of Flood Protection Activities (DFPA) in these stations. The auxiliary gauging stations are operated by the municipalities and their DFPA are defined in the Digital Flood Plan.

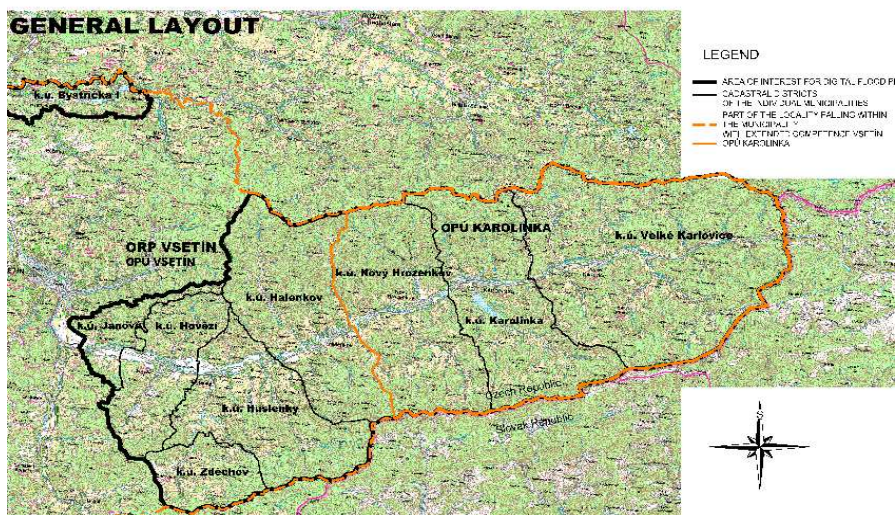


Fig. 1 General layout of the region in question

2.1 Supporting data for the DFP development

The DFP was based on the updated flood plans of the municipalities of Velké Karlovice, Karolinka, Halenkov, Huslenky, Hovězí, Zdechov and Bystřička. The municipality of Janová and the township of Nový Hrozenkov had no such plans in place and so they had to be developed. The updates and the development of new flood plans including surveys consisted of local surveys and terrain reconnaissance. The project team examined the most important watercourses in the project area. Based on the site visits and information provided by local inhabitants, watercourses important in terms of flood risks were defined. These were the following:

- The Janovský brook in the municipality of Janová, length - 320 m,
- The Hořanský brook in the municipality of Hovězí, length – 854 m,
- The Zdechovka – 1st section, in the municipality of Huslenky, length – 296m,
- The Zdechovka in the municipality of Zdechov, length – 137 m,
- The Kychová in the municipality of Huslenky, length – 341 m,
- The Brodská in the township of Nový Hrozenkov, length – 1445 m,
- The Miloňský brook, municipality of Velké Karlovice, length – 266 m.

Geodetic survey was conducted at the small watercourses used as the basis for the hydraulic calculation of the water levels for the design discharges Q_5 - Q_{20} . Based on these calculations localities with a potential flooding risk and localities affecting run-off conditions were determined. Civil structures on the watercourses

most endangered by flood and houses used by inhabitants for permanent or recreational dwelling were mapped out. The information was then entered into the DFP.

Furthermore, the validity of already declared Degrees of Flood Protection Activities (DFPA) in category C was validated. The DFPA in categories A and B for this locality were taken over from available supporting data and from the applicable flood protection plans.

The Degrees of Flood Protection Activities (DFPA) are in most cases related to the guiding water level limits in the gauging stations in the water courses that are specified in the flood protection plans.

The gauging stations are divided into three groups:

- basic gauging stations category A,
- additional gauging stations category B,
- auxiliary gauging stations category C.

Gauging stations category A cover important water courses evenly. Water gauging stations located here are automated (automatic data transfer) and operated by the Czech Hydrometeorological Institute (CHMI) or river basin authorities. Results of these meterings are available to the public on the website of the CHMI [CHMI].

Gauging stations category B complement gauging stations category A and they are also fitted with automatic data transfer. They are usually operated by river basin administrators with the data transfers available on the websites of these administrators but they can also be operated by other entities, mostly municipalities.

For the main streams in the study area, the Vsetínská Bečva and Bystřice rivers, flood plain maps and risk maps have been developed as they had not been elaborated yet for this locality and therefore they were not developed as the main data for the DFP.

Map data to collect information and to print out graphic outputs come from the ZABAGED vector data provided by the State Administration of Land Surveying and Cadastre (ČÚZK). The data was provided to each municipality free of charge. A map server was used to develop graphic attachments. The map design was developed in the ArcGIS software based on which customised raster maps have been generated.

Other information necessary for production of/implementation of the Digital Flood Plan have been collected from public servers such as [DIBAVOD], [WMIP] and [POVIS].

2.2 POVIS database data entering and preparation

Before the DFP development data was input into the POVIS database providing integration of information from various data sources. POVIS creates comprehensive information bases showing flood event progress, allows data

coordination and updates and publishes data in the DFP. The POVIS data entering was a compulsory part of the DFP and this was carried out for each municipality separately. The data is entered into POVIS by means of a flood plan data Editor, flood protection measure data Editor and flood plain data Editor. The data in POVIS may be divided as follows:

- central data that the user has no access to, maintained centrally and the user uses them in its DFP as a source of information concerning, for example, gauging stations categories A and B,
- user data entered and updated by the user based on the access password.

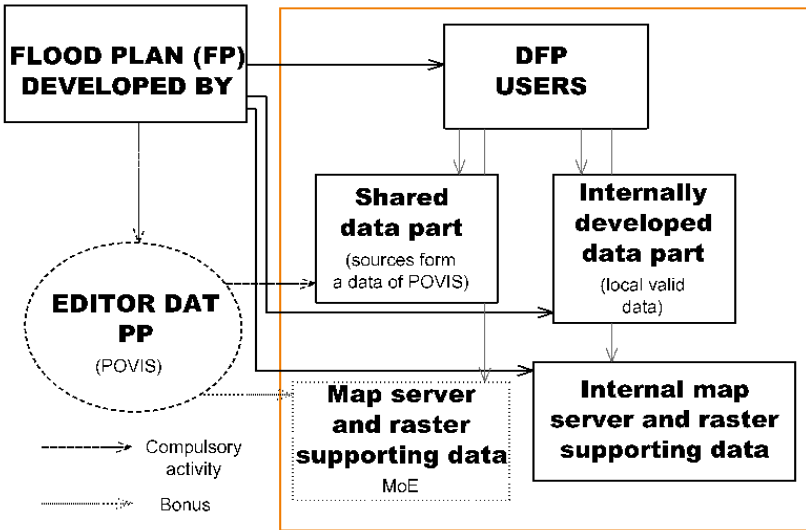


Fig. 2 Development of the DFP in the POVIS system

The data Editor is accessible for public and a logged-in user may use the central data storage to create or update flood plan by supporting data in a coordinated manner. Each user has an immediate access to the data of the other participants, the data are distributed to be accessible to everyone. Non-public data is accessible inly to authorised users. Current data may be exported from POVIS at any time in a relevant format into the DFP. The development of the Digital Flood Plan in the POVIS system is shown in Fig. 2.

To access the flood plan Editor application and POVIS, access data was provided by the system operator and given to the municipal council. The access data consists of a user name and password and allows the access to public and

non-public information stored in the application. It also enables to edit data in the municipal flood plans.

The preparation of data entered in the POVIS database and then into the DFP consisted of the creation of MS Excel spreadsheets used to assemble data to be entered into the DFP via the flood plan Editor application in the POVIS system. The spreadsheet structure was created on the basis of a data model of the flood plan Editor application. These spreadsheets were filled in by the author along with the municipal authorities. For all relevant information, the localisation information was added – i.e. coordinates of points representing its position. All the entered localisation information was then validated in the graphic form of the flood plan used by the graphic attachments to the DFP.

2.3 System description – Local Warning System (LWS)

The LWS was developed in parallel with the DFP and it is another important element of flood protection. A part of the LWS related to the Digital flood plan consisted of the establishment of auxiliary gauging stations category C. These were purpose-established gauging stations used for the purposes of local flood protection. The auxiliary gauging stations of the category C are proposed on the basis of terrain reconnaissance in cooperation with the municipal councillors. Their location depends on the position of the existing gauging stations category A and B that should be adequately complemented by the newly proposed gauging stations. In the project area and in its surroundings there were the following gauging stations listed in Tab. 1.

Tab 1. Gauging profiles in the area of interest and in its surroundings

Name	Watercourse	Category	Administrator	Data transfer
Vsetín	Vsetínská Bečva	A	CHMI	Automatic
Velké Karlovice	Vsetínská Bečva	B	CHMI	Automatic
VD Karolinka	Stanovnice	B	Povodí Moravy, s.p.	Automatic
VD Bystřička	Bystřice	B	Povodí Moravy,s.p.	Automatic

To improve the flood service and preventive protection system in the project area, the installation of 5 new level gauges and 12 new rain gauges was proposed. The system of deploying new auxiliary gauging stations category C is shown in Fig.3.

The LWS is designed as a two-stage, semi-automatic transfer of alert information:

- a) At the first stage, if the limit values are exceeded (rainfall, levels), alarm text messages are immediately sent to appointed people
- b) At the second stage, the relevant person in charge must assess received information and take the necessary measures.

The measuring system was launched after installing the specific instruments and their registration via GSM/GPRS to the target central server. The outcomes of the continuous measurements in the auxiliary gauging stations are available in the DFP and on the selected server.

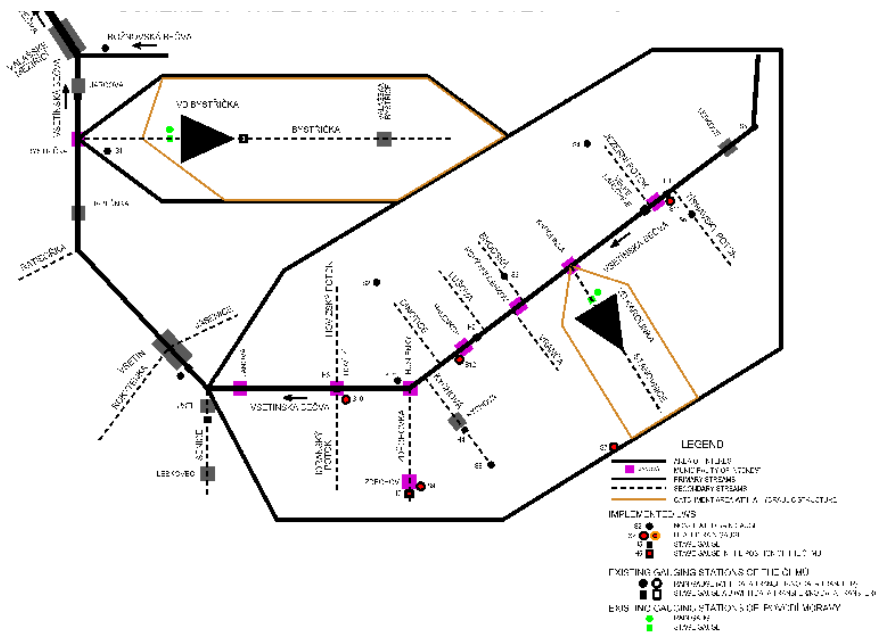


Fig. 3 The scheme of LWS location

2.4 Flood plan digitalisation and the DFP development

Based on the collected supporting data and data entering in the POVIS database, the flood plan has been made public in the form of a web-based application for the public. The texts and data available formats for websites in the HTML form and printed outputs in the *.pdf format.

The DFP are posted on the websites of the municipalities and are accessible to inhabitants with the Internet access. The DFPs have been also provided to all municipalities on a portable disk in the off-line version in case the Internet is not accessible during a flood event.

Based on a contractual relationship, the DFP is also stored on the central server administered by AQUA PROCON, s.r.o on the website: <http://www.aqp-dpp.cz>. The DFP as well as the POVIS data must be regularly updated, at least once a year.

Digitální povodňové plány

The screenshot displays the Aqua Procon website interface for the Digital Flood Plan (DFP) of Halenkov. On the left, a map shows the geographical area with various flood risk zones indicated by colored markers. On the right, a table provides detailed information about the flood risk units. The table has the following structure:

Místní územní jednotka	Kód	Název	Rozsah	Stupeň nebezpečnosti	Stupeň ohrožení
Halenský náhon	001	Halenský náhon	0,000000 - 0,000000	1	1
Halenský náhon	002	Halenský náhon	0,000000 - 0,000000	1	1
Halenský náhon	003	Halenský náhon	0,000000 - 0,000000	1	1
Halenský náhon	004	Halenský náhon	0,000000 - 0,000000	1	1
Halenský náhon	005	Halenský náhon	0,000000 - 0,000000	1	1
Halenský náhon	006	Halenský náhon	0,000000 - 0,000000	1	1
Halenský náhon	007	Halenský náhon	0,000000 - 0,000000	1	1
Halenský náhon	008	Halenský náhon	0,000000 - 0,000000	1	1
Halenský náhon	009	Halenský náhon	0,000000 - 0,000000	1	1
Halenský náhon	010	Halenský náhon	0,000000 - 0,000000	1	1

Fig. 4 Presentation of the website with the DFP for the municipality of Halenkov

3. LAUNCHING OF THE DFP

Before finishing the project, the representatives of the municipalities and all DFP users were made familiar with its contents and they were duly trained for its use. Likewise, data entering and updating training in the POVIS system using the flood plan data Editor took place.

The LWS was put into service in the following stages:

- first, the individual instruments were installed and logged in the target central server with process data collection starting,
- second, critical values were set for the specific types of instruments and their functionality was tested,
- subsequently, a 1 year testing operation took place during which the limit values were set according to the flood situation, i.e. extreme rainfalls occurring in the region.

4. CONCLUSION

The text part of the DFP was produced in accordance with [TNV 75 2931] and [MoE 2009 – 2015]. Compared to classic publishing, the digital processing of the text part enables a much larger scope of linking the contents via links both between the text part and the map views and the central database in the POVIS system. The graphical part follows the scope of the prescribed thematic maps. The map server fully complies with the requirements for working with maps via

remote connection (Internet), if installed locally it can also run via a portable medium without the need for the Internet installation. The flood plan information presentation in the digital form is most important as it enables the following:

- during a flood event, a well-arranged access to the necessary information offering analytical tools for decision-making processes,
- visual overview of the recorded information,
- easier distribution of the information before a flood event when the public can be informed via the Internet about the potential progress of the flood event situation.
- after the flood event, comprehensive mapping of the flood damage.

The DFP must be regularly updated immediately after any data change, however at least once a year in accordance with [Act No. 254/2001 Col]. The most important issue is to update the databases of flood committees and organisations, which is crucial in terms of emergency communication in flood situations.

5. REFERENCES

ACT NO. 254/2001 Col. on water and amending certain acts (Water Act) as amended.

CHMI Czech hydrometeorological institute: <http://www.chmi.cz/>.

DIBAVOD Digital base of water management data: <http://www.dibavod.cz/>.

DRÁB, A., ŘÍHA, J. An approach to the implementation of European Directive 2007/60/EC on flood risk management in the Czech Republic. Nat. Hazards Earth Syst. Sci., 10, 1977–1987, 2010.

ES: Directive 2007/60/EC of the European Parliament and of the Council of 23 October 2007 on the assessment and management of flood risks, European Parliament, Council, 2007.

KOCMAN, T., KUBÁT, J. A MUSIL, P., 2011. Local flood protection warning and alert systems – handbook, MoE Prague.

MoE - POVIS 2009 – 2011. Flood plan data Editor, user handbook.

MoE 2009 – 2015. Methodology for the development of digital flood plans - digital handbook: http://www.povis.cz/met_dpp/.

OPENV 2010. Operational Programme Environment. Support 1.3 Flood risk reduction, Sub-field of support 1.3.1 Improvement of the flood service system and preventive flood protection, MoE Prague.

POVIS. Flood information system : <http://www.povis.cz/html/povis.htm>.

TNV 75 2931 Flood Plans, technical standard.

WMIP Water management information portal: <http://voda.gov.cz/portal/cz/>.

The Adriatic Sea Wave Energy Analysis

E. Ocvirk, K. Duvnjak, M. Kaciga

(Faculty of civil engineering, University of Zagreb - Andrije Kačića Miošića 26, 10000 Zagreb,
ocvirk@grad.hr, kduvnjak@grad.hr, mkaciga@grad.hr)

Abstract

Nowadays we are witnesses of renewable energy becoming more popular in Croatia. According to the Annual Energy Report in Croatia, in 2013 the total electricity production in the Republic of Croatia amounted to 13 431.1 GWh, of which 65.2 % was produced from renewable energy sources, including large hydro power plants. In this, large hydro power plants had a share of 60.3 %, whereas 4.9 % of electricity was produced from other renewable sources, such as small hydro power plants, wind energy, solar energy, biomass, biogas and photovoltaic systems. Electricity produced from renewable energy sources had a share of 48.2 % in the gross electricity consumption in Croatia. In that, electricity produced in large hydro power plants had a share of 44.6 %, whereas the electricity produced from other renewable sources had a share of 3.6 %. As a member of European Union and in the spirit of sustainable development, Croatia is obligated to increase current total energy production achieved by renewable sources of energy from today's production of 4.9 % and reach the production of 20 % by the year 2020. On the other hand, Croatia is famous as a Mediterranean country with the length of the Adriatic coastline of 1777 km. If we include the additional 1246 islands it reaches the length of 6000 km. The average day amplitude of tides are not remarkable: In Dubrovnik amplitude is 22 cm, in Rovinj it is 47 cm, and is therefore not interesting from an energy viewpoint. According to some authors, the Adriatic Sea belong to seas with energy potential below 5kW/m which is not economically acceptable to use. In this paper, the analysis of wave parameters across the Adriatic coastline was made on the base of a 10 years simulation. According wave analysis energy potential is determined.

Keywords

Adriatic Sea, energy potential, renewable energy, renewable energy sources, wave energy

1. INTRODUCTION

The subject of this paper is an analysis of the Adriatic sea energy. The analysis is based on a model of generating waves designed in doctoral thesis Optimization of the rubble mound protective structures in the terms of extreme wave climate of the Adriatic Sea [Ocvirk 2010]. As a result, this model of generating waves at the Adriatic Sea gives the significant wave height, which with wave period make the basis for calculating the power of waves, subsequently the possible annual production of electricity. Referring to the World wave energy resource map, the

potential of the Adriatic sea waves is lower than 5 kW/m. In this paper the wave potential on the Adriatic sea is precisely defined in 30 points along the Croatian coast, with the final goal of defining the most interesting areas from the energetic aspect for exploiting the wave energy on the Adriatic sea.

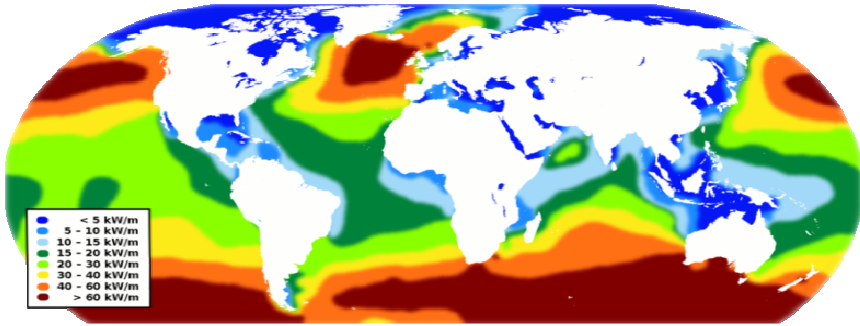


Fig. 1 World wave energy resource map (Resource: www.en.wikipedia.org/wiki/Wave_power)

2. SEA ENERGY

Sea waves are the typical example of accumulated solar energy transformed into the energy of water masses. The main cause of phenomena of sea waves is wind. Wind is caused by the differences in the atmospheric pressure and those differences are caused by the temperature differences depending on solar energy. The areas where permanent winds blow, areas of constantly generated sea waves, are favourable for exploiting sea energy.

Wave energy is consisted of potential and kinetic energy. It can be calculated when the wave parameters are known. Kinetic energy is most intensive just below the sea surface. Its value reduces with the increment of depth. Total wave energy E , for one wavelength and width of 1 m, is sum of kinetic energy E_k and potential energy E_p :

$$E = E_k + E_p = \frac{\rho g H^2 L}{16} + \frac{\rho g H^2 L}{16} = \frac{\rho g H^2 L}{8} \quad (1)$$

The potential part of energy and kinetic are defined by the same value. Specific wave energy is total average wave energy per unit surface area:

$$E_s = \frac{E}{L} = \frac{\rho g H^2}{8} \left[\frac{J}{m^2} \right] \quad (2)$$

In this equation ρ stands for the fluid density [kg/m^3], g gravitational acceleration [m/s^2], H wave height [m], L wave length [m] [Pršić 2007].

The value of total average wave energy per unit surface area perpendicular to the direction of wave propagation decreases rapidly with increasing depth below the surface. Some research show that at the depth of 20 m the value of energy is just 20 % of the energy on the surface.

3. OVERVIEW OF TYPES OF WAVE ENERGY CONVERTERS

Wave energy plants are energy plants which capture and exploit the wave energy, and than transform it into electricity. They are consisted of one or more wave energy converters.

Wave energy converters are devices for extracting the energy of waves and converting it into an energy suitable for transportation and use- electricity. In over 30 countries, there are over a hundred different concepts. The majority of them belongs to one of 8 groups. (Fig. 2)

The main part of the plant converters can be divided into two groups based on their position: off-shore environment converters and the near-shore environment converters. Within the group of the offshore environment converters belong attenuator, point absorber, oscillating wave surge converter, oscillating water column, over-topping/terminator, bulge wave and rotating mass. The converters of the second group are some types of oscillating water column and over-topping/terminator. Different types of converters vary from developer to developer, but all the common systems include structure and prime mover, foundations and moorings, power take off (PTO), control, installation, connection and operation and maintenance.

Electrical connection between the generating device and the local grid network goes through two stages. The first stage is to connect the device to an export cable, bringing electricity to shore. The second stage includes voltage step-up to the applicable level and connection to the distribution and transmission grid network.

The classification of wave energy plants based on location distinguishes wave energy plants into the two group: offshore and near-shore.

There are many advantages to near-shore wave energy plants. Near-shore wave energy plants encompass simplified building process as it is possible to use classical construction machines and building from the mainland. It is easier to maintain near-shore plants, as there is no need for divers or ships, there is easier and faster control and fixing of broken parts of machines, and there is a possibility of realization of multipurpose system because one structure can be a breakwater and wave energy plant at the same time.

On the other hand, the disadvantages include the noise they produce, the change in natural cost face, further disadvantages are related to wave characteristics. It is a challenge to choose a suitable location, respecting the mentioned disadvantages, that will realize the condition of economical exploiting despite the fact that the waves of intensive energy potential are offshore.

Efficiency of those turbines are because of the stochastic nature of wave quite low (50 – 60 %).

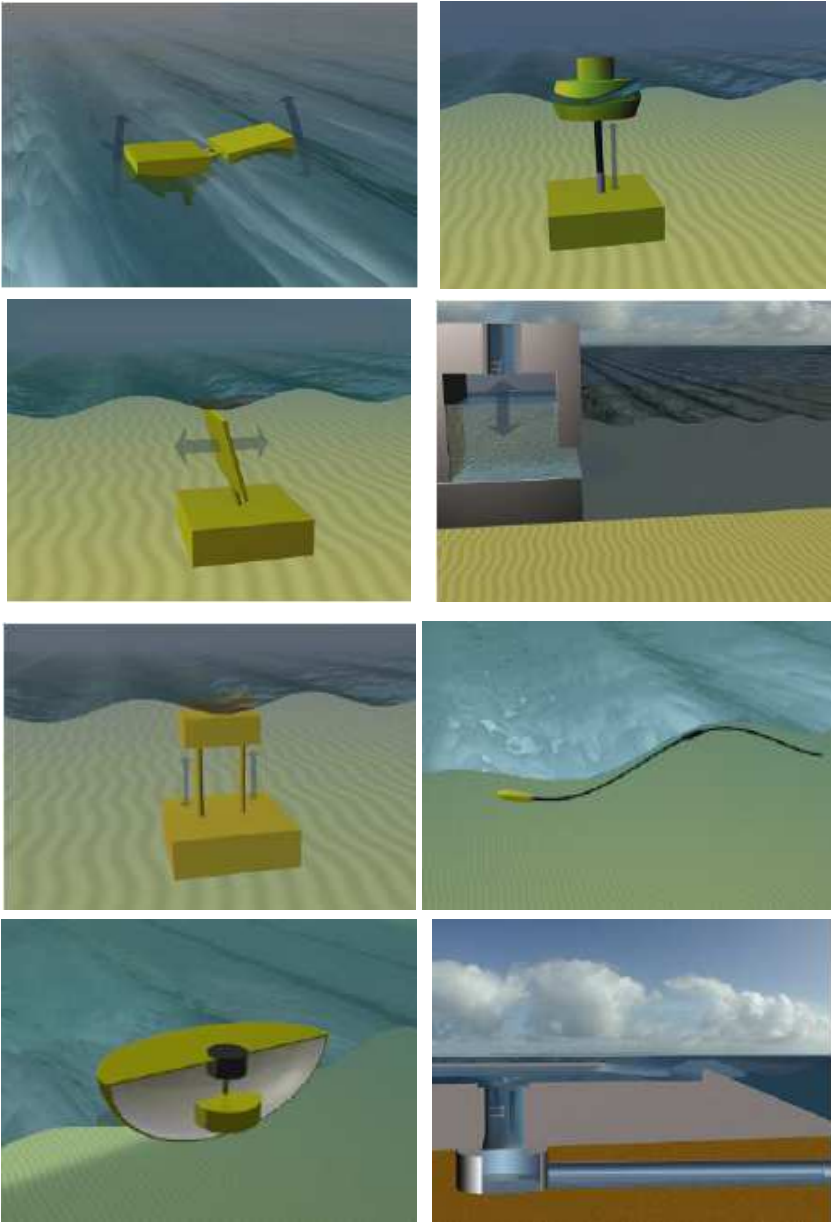


Fig. 3 Basic types of converters [Aqua – Ret 2015]

Advantages of offshore plants are firstly the possibility of exploiting the waves of higher energy potential. Offshore plants resolve the problem of electricity supply of offshore devices. A significant challenge is demonstrating the survivability of a device to extreme loads and connection to the local grid network. [Aqua – Ret]

4. ANALYSES OF WAVE CLIMATE ON THE ADRIATIC SEA

The analysis is based on the model of generating waves for short time wave prognosis designed in the doctoral thesis Optimization of the rubble mound protective structures in the terms of extreme wave climate of the Adriatic Sea [Ocvirk 2010], that as a final result gives the distribution of significant wave height H_s in the domain of the Adriatic sea. Because of the lack of data from valographs, short time wave climate is prognosed using the wind data in the numerical program for modelling wave generation MIKE 21/SW. Basic wind information are the wind velocity, direction, duration and the length of fetch. The wind data from prognostic model ALADIN, with grid resolution of 4 km and time step of 3 h, are analysed for the 10 years long time period (01.01.1992 to 31.12.2001). Prognostic model ALADIN (Aire Limitée Adaption dynamique et Development InterNational) is developed as a hydrostatic version and its base is a simple equation [Ocvirk 2010]. This model is used by the State hydrometeorological Institute of Croatia. Used in the model are the wave field from the prognostic model ALADIN in time period from 1.1.1992 to 31.12.2001. As a situation is considered constantly wind blowing in one direction during since 3 h with average velocity of more than 4.5 m/s. The numerical program MIKE 21/SW can be used for making simulations of growth, decay and transformation of wind-generated waves and swell including the processes of wave generating with wind, nonlinear wave interactions, refraction and shoaling, interaction of waves and drift, tides, disipational processes caused by friction with seabed and wave breaks. The model is based on a grid and spectral discretization made by method of finite volumes. Grid discretization is designed as unstructural mesh made of non-overlapping triangular cells. In frequent domain is used logarithmic distribution. Distances between centres of gravity of the triangular cells are from 160 m to 9500 m.

Dominant winds at the Adriatic Sea are Bora (NE) and Sirocco (SE). Bora is a strong wind caused by continental cold air. It is the strongest wind of the Adriatic sea. It is more often during the winter. The main characteristic of the Bora is that it blows in gusts. The strength of blows is usually two times more powerful than the average velocity. The area where some of the strongest Bora winds occur is Podvelebtski kanal and on the cost under the mountain Biokovo with the velocity more than 50 m/s. Strong Bora (with a velocity of more than 17 m/s) normally occurs along the Adriatic coast. The tendency of decreasing duration and

frequency of it is from north to south. Whereas Bora wind blows from NE, for the analysed area it does not have a big fetch, so it does not cause the high waves.

The Sirocco winds blow from the southeast. It is a relatively warm and wet wind blowing from the constant direction. Its average and quite constant velocity is 10 m/s, but often it reaches the velocity of 30 m/s. Its development is gradual than that of the Boras. Highly developed Sirocco winds blow at the whole area of the Adriatic Sea. It blows during the whole year, but the most during the spring and autumn seasons. The average duration of the strong Sirocco is 10-12 hours. The waves caused by the Sirocco winds have regular form and quite large height. It is stronger and more often present on the coast exposed to the effect of the open sea and the Southern coastline of the islands. It causes the larger waves on every part of the Adriatic Sea: Northern, Middle and Southern Adriatic because of the big fetch. It is more often on the Southern Adriatic. Negligible fetch on the Northern Adriatic causes the wind from northwest-Maestral. It blows during the warmer part of the year during the months of May to September. It is the result of the global drift and daily circulation between the mainland and the sea. It starts to blow in the forenoon, early in the afternoon it is the strongest, and during the evening it calms. It is the wind of stable weather.

Calculation of wave power

The power of waves in deepwater area, area with the depth bigger than a half of wave length, can be described by the following equation:

$$P = \frac{\rho g H^2}{8} \cdot c_g = \frac{\rho g H^2}{8} \cdot \frac{gT}{4\pi} = \frac{\rho g^2 H^2 T}{32\pi} \approx 0,57 H^2 T \left[\frac{kW}{m} \right] \quad (3).$$

In this equation ρ stands for the fluid density [kg/m³], g gravitational acceleration [m/s²], L wave length [m], H_s significant wave height [m], T wave period [s] and c_g velocity of the a group of waves [m/s]. [Dexawave]

Period can be read from the Groen-Dorrensteinovog diagram when the size of effective fetch [km] and significant wave height H_s [m] are known. In Groen-Dorrenstein diagramm the relation between period and significant wave height is not clearly determined for wave hights smaller than 0.6 m. From energy point of view those waves are not interesting so they were ignored.

The area of the Adriatic sea that was analysed and determined as promising for possible exploiting wave energy is the line parallel to the coastline on the distance of 2 km. The line goes through 30 points, for which the average power for the 30 min long time interval during the period of 10 years (1992 - 2011) is calculated by the described equation using the data of significant wave height from numerical model and the rest of defined input information.

5. RESULTS

Table 1 shows the results of the analysis presented as potential average annual power and estimated potential production per 1 m for the time period from 1992 to 2001.

Tab. 1 Potential average annual power and estimated potential production per 1 m for the time period from 1992 to 2001.

POINT	[kW/m]	[MWh]	POINT	[kW/m]	[MWh]
	$P_{\text{average10g}}$	W		$P_{\text{average10g}}$	W
Savudrija	1,064	9,325	Rogoznica-Hvar_2	1,201	10,520
Savudrija-Rovinj	0,512	4,481	Hvar	1,395	12,221
Rovinj	0,936	8,198	Hvar-Korčula	1,537	13,460
Rovinj-Medulin	0,940	8,233	Korčula	1,652	14,473
Medulin	1,235	10,820	Korčula_Mljet_1	0,380	3,328
Medulin-Susak	1,662	14,555	Korčula-Mljet_2	1,638	14,352
Susak	1,625	14,238	Mljet	1,512	13,246
Susak-Dugi Otok_1	1,560	13,665	Mljet-Cavtat	1,475	12,921
Susak-Dugi Otok_2	1,515	13,275	Cavtat	1,008	8,833
Dugi Otok	1,464	12,825	Cavtat-Prevlaka	0,977	8,557
Dugi Otok-Kornati	1,457	12,761	Prevlaka	0,939	8,221
Kornati	1,450	12,702	Lastovo zapad	1,826	15,994
Kornati-Rogoznica	1,677	14,688	Lastovo jugozapad	1,944	17,032
Rogoznica	1,446	12,666	Lastovo jug	2,042	17,887
Rogoznica-Hvar_1	1,198	10,491	Vis	1,966	17,222

6. CONCLUSION

The result of this paper is the distribution of wave energy potential, average wave power per 1 m in the Adriatic Sea, in 30 points from Savudrija to Prevlaka, 2 km away from the coast based on data for 10 years long period (1992.-2001.). Those results confirm the hypothesis known from the literature and enrich it with calculated values.

Ten years average power [kW/m'] for Northern, Middle and Southern Adriatic are compared, based on the results defined in 30 different points, and conferred to the point (42°18'41 N, 17°24'9 E) 50 km away from Mljet as the nearest island, totally offshore, exposed to waves of maximum energy potential reachable on the Adriatic sea. This assumption is based on the size of the fetch (Tab. 1).

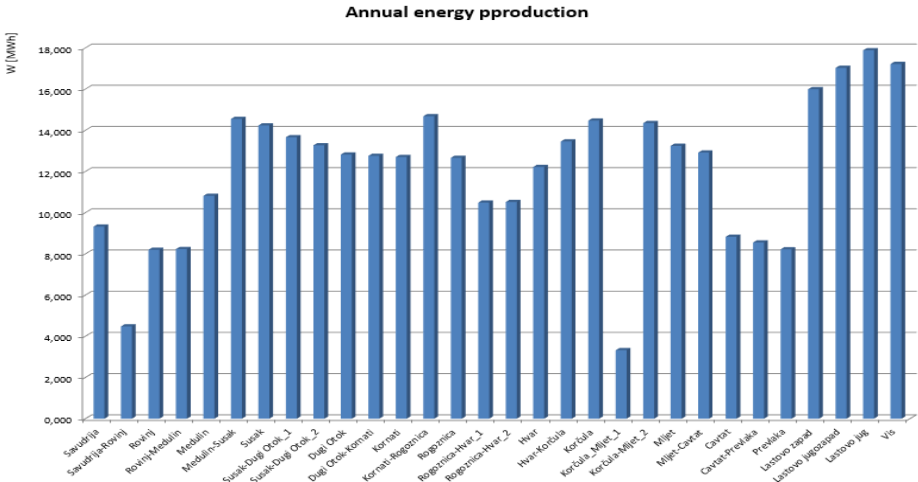


Fig. 6 Annual energy pproduction

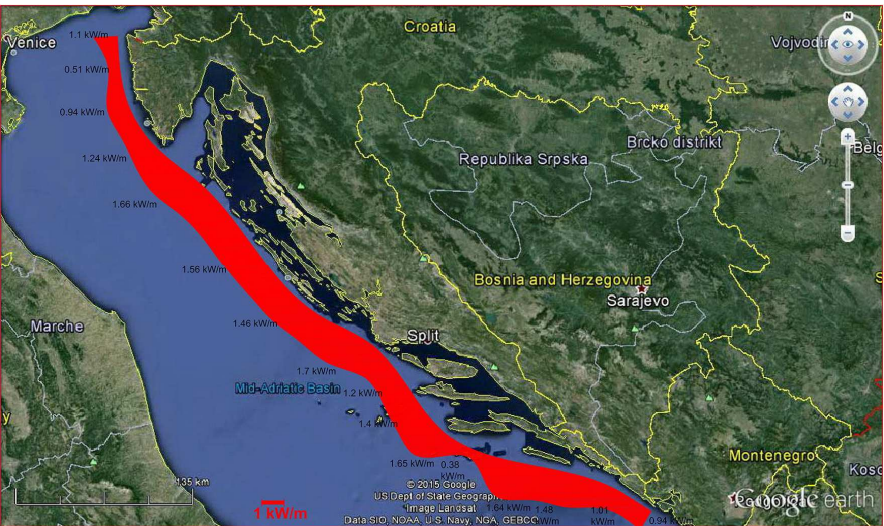


Fig. 6 Distribution of wave energy along the Adriatic Sea

Comparison of wave energy potential between the Northern, Middle and Southern Adriatic shows that waves of Southern Adriatic have the highest wave power. That was expected because the size of the fetch of the Southern Adriatic enables development of higher waves. Getting more offshore, wave power

increased, until the maximum average annual of 3,056 kW/m. Even the highest value is lower than 5 kW/m. The results of the analysis lead to the conclusion that Croatia is not one of the most favourable areas for wave energy exploiting, however this idea should not be rejected. Technology of wave energy converters has just recently started to develop and is already a quite popular topic. There are many existing interesting projects taking place globally and as the popularity of sea energy exploiting grows, there will be improved state of the art technologies, new ideas and further developed concepts. With this, it is realistic to expect the development of a wave energy converter suitable for seas of lower wave potential, such as the Adriatic Sea.

7. REFERENCES

AQUA – RET: www.aquaret.com. Last access: 15 April 2015.

DEXAWAVE. *Wave energy converter*. www.dexawave.com/energy-content.html. Last access: 14 April 2015.

OCVIRK, E. 2010. *Optimizacija nasipnih zaštitnih građevina u uvjetima ekstremne jadranske valne klime*. Zagreb.

PRŠIĆ, M. 2007. *Hidrotehnički Sustavi*. Građevinski fakultet Hidrotehnički sustavi - pomorske gradnje, Sveučilište u Zagrebu.

www.grad.hr/nastava/hidrotehnika/gf/hidrotehnicki_sustavi/predavanja/pomorske_gradnje.pdf. Last access: 19 April 2015

WIKIPEDIA.

www.en.wikipedia.org/wiki/Wave_power#/media/File:World_wave_energy_resource_map.png. Last access 20 April 2015.

Dispersion tracking experiments in different streams types

M. Sokáč

Department of sanitary and environmental engineering, Faculty of civil engineering, Slovak University of Technology Bratislava, Radlinského 11, 810 05 Bratislava, Slovak Republic, e-mail: marek.sokac@stuba.sk

Abstract

Water quality modelling is currently very effective and important tool in context of the task to ensure the required quality of water resources, respectively, to achieve (maintain) good water status according the Water Framework Directive (2000/60/EC). Mathematical models of water quality are an important tool for integrated water management, planning and protection. Integral part of such models is the modelling of fundamental physical processes affecting water quality - advection and dispersion.

This paper documents results of measurements of the dispersion coefficient within the scientific project APVV 0274-10. Measurements in this project have been performed in various surface water bodies in Slovakia - lowland streams with low turbulence (drainage, irrigation channels), as well as in mountain streams with a high degree of turbulence. Within the field experiments both longitudinal, so as the transverse dispersion coefficients were measured.

Keywords

Dispersion coefficient, case study, flow turbulence

1. INTRODUCTION

Surface flows are often used as a transport medium for diverse pollution, e.g. waste water or during ecological disasters can water transport different pollution that threatens the biota in the stream or in the stream surrounding. Ability of surface water to transport pollution is influenced by several factors, like morphological conditions, the flow rate in the stream, current status of water quality in the stream, etc. One important factor (characteristics) affecting transport processes in streams is dispersion, which can be characterised by dispersion coefficient. The significance of these coefficients increases with computer technology use for solutions of water management problems. Simulation models of dispersion in surface flows based on hydrodynamic principle cannot work without these coefficients.

Simulation models can describe the pollution transport three-dimensionally, what is very time consuming for the input data preparation, the calculation scheme

and computational time. However, deep reservoirs with thermal stratification can be simulated three-dimensionally only. Two-dimensional description of dispersion and transport processes could be applied in the case of shallow reservoirs without significant thermal stratification, eventually for detailed solutions of contamination spreading in surface streams before reaching the total transverse mixing of transported substances (the so-called mixing length). After this time it is usually sufficient to apply a one-dimensional model of water quality.

As already mentioned in [Vešíšková et al. 2013], models simulating pollution transport in surface flows based on hydrodynamic principles needed (among other input data) the value of dispersion coefficient. The most accurate values of these coefficients can be obtained by direct field measurements in specific conditions of investigated stream. This is not always possible because of financial, material or staffing reasons. Empirical relationship for the dispersion coefficient determination, especially for longitudinal dispersion coefficient, with a wider applicability was developed by several authors [Bansal, 1971, Elder, 1959, Fischer 1979, Jolánkai, 1992, Karcher, 2004, Kosorin, 1995, Říha et al., 2002 and Swamee et al. 2000]. Any such relationship has its limitations, based on the conditions during measurements, in this way the determined value of dispersion coefficient should be regarded as approximate.

The aim of this paper is to describe methods of dispersion coefficient determination in surface streams with different flow characteristics by field measurements. Obtained values can be used for numerical modelling of various alternatives of pollution spreading in streams with similar flow conditions.

2. THEORETICAL BASIS

The pollution transport in surface streams is affected by advection-dispersion processes occurring in it. Dispersion of the substances in the stream together with the advection represents basic mechanism of dissolved particles movement in an aqueous medium. These processes cause the reduction of the maximum pollution concentration values in the flow. The main characteristics of dispersion process are dispersion coefficients in the corresponding directions. Determination of the dispersion coefficients is therefore a key task in solving of pollutants transport in streams and in water quality modelling.

Models based on hydrodynamic approach describe and quantify the phenomenon of dispersion in flowing water in the form of equations, based on the elementary laws of fluid flow - conservation of mass and energy. Usage of these models is universal, but their major limitation is the difficulty of input data collection. Hydrodynamic dispersion models are based on the numerical solution of one - or multi-dimensional form of advection - dispersion equation (ADR), which is based on the above-mentioned laws of hydrodynamics. Most of the previously assembled models are one-dimensional. Relating to their one-dimensionality are these models relatively simple. Their disadvantage is the inability to simulate dispersion processes in river section, which has not yet

pollution spread across the width of the river. The length of this section varies depending on the hydraulic parameters of the flow [Fischer et al., 1979, Říha et al. 2002 and Yotsukura et al, 1976]. Two-dimensional models do not have this limitation. However, they are more complex and even more difficult to gain input data. They are based on two-dimensional numerical solution of ADR in the form:

$$\frac{\partial(hc)}{\partial t} + \frac{\partial(huc)}{\partial x} + \frac{\partial(hwc)}{\partial y} = \frac{\partial}{\partial x} \left(hD_L \frac{\partial c}{\partial x} \right) + \frac{\partial}{\partial y} \left(hD_T \frac{\partial c}{\partial y} \right) +$$

+ influence of local sources, non-conservative pollution and dead zones (1)

where c is the concentration of the pollutant substance [$\text{kg}\cdot\text{m}^{-3}$]; D_L is the longitudinal dispersion coefficient and D_T is the transverse dispersion coefficient [$\text{m}^2\cdot\text{s}^{-1}$], h is the depth [m], t is time [s], x, y are coordinates in the longitudinal and transverse direction [m], u, w longitudinal and transverse components of velocity [$\text{m}\cdot\text{s}^{-1}$].

The key characteristics in this equation, which determines the degree of dispersion in the flow, are the dispersion coefficients. Determination of their values suffers in practice from several limitations. The most accurate values are obtained using field experiments, which directly include the conditions present at the section of the river. It is not always possible to determine the values such way, because of limited time or financial reasons. In addition to this option, there is a way of determining these technical characteristics through empirical relationships derived by different authors for different flow conditions, or based on tabular values obtained from experimental research [Bansal, 1971, Elder, 1959, Fischer 1979, Karcher et al. 2004, Kosorin, 1995, Pekárová et al. 1998, Říha et al. 2002 and Swamee et al. 2000].

Finally, at the end of this theoretical introduction, it should be noted that the dispersion coefficient values are often also referred to in its dimensionless form:

$$p = \frac{D}{h \cdot u_*} \quad (2)$$

where p is the dimensionless dispersion coefficient, u_* is the friction velocity [$\text{m}\cdot\text{s}^{-1}$] and D is longitudinal or transverse dispersion coefficient [$\text{m}^2\cdot\text{s}^{-1}$]. This form is very useful especially when applied to different flow conditions.

3. FIELD MEASUREMENTS

As mentioned before, measurements were performed in various surface water bodies in Slovakia. In this paper we would like to present two typical cases of stream types in Slovakia. The first one (further marked as “case A”) is typical lowland stream (Malá Nitra stream), used for irrigation or drainage purposes, where the water velocity and turbulence are very low. Opposite, in the second case

(“case B”) we describe a typical mountain stream (Hron river) with a high degree of turbulence.

3.1 Case study A, Malá Nitra stream

Field measurements were performed at approximately 400 m long section of the stream Mala Nitra, close to the village Veľký Kýr. This stream is situated at the southwest part of Slovakia; measurements were done in Veľký Kýr settlement region (N+48° 10' 50.02", E+18° 9' 19.60"). Regime of the stream discharges is affected by flow regulation by the weir located 15 km upstream in bifurcation point with the Nitra River. Cross sections had originally trapezoidal shape with bed width $b = 4$ m, height 2,5 m and slope 1:2, but discharge area along the stream has been slightly changed by natural morphological processes during the years. Longitudinal bed slope was 1.5 ‰. Measured discharge values during field experiments were within the interval $(0,138 - 0,553) \text{ m}^3 \cdot \text{s}^{-1}$.

3.2 Case study B, Hron river

The main stream flowing thru the town Brezno is the river Hron. This river has a partially alpine runoff regime with maximum flows in April and minimal flows in January. The average water temperature is quite low, only 6.2 ° C. In the Hron (profile Brezno, river km. 243.200) is the average yearly flow of about $8 \text{ m}^3 \cdot \text{s}^{-1}$.

Adjusted river bed has a trapezoid cross section shape with a bottom width of 16 - 20 m, slope of banks 1:2, banks and river bed are partially stabilized with stone backfill. Over the years, the shape of cross section profile was partially modified by natural morphological processes (including stone backfill). Depth of flow ranged from 0.29 up to 0.52 m. The average cross- sectional velocity was $0.64 \text{ m} \cdot \text{s}^{-1}$, but the velocity reached locally values up to $1 \text{ m} \cdot \text{s}^{-1}$. This causes difficulties during walk in the river, or during placement of the equipment and tracer dosage. Measured flows during the field works ranged from 4.2 to $5.3 \text{ m}^3 \cdot \text{s}^{-1}$.

To determine the longitudinal dispersion coefficient the tracer with a known quantity and concentration was dosed into the geometric centre of the stream width at the beginning of measured section instantaneously. As a tracer was used salt (NaCl) – its solution, which caused a change of flowing water conductivity.

To determine the coefficient of transverse dispersion, a slightly different approach was used: a tracer was not dosed once - instantaneously, but continually (by pump) with a known discharge and concentration of the tracer. In some experiments we placed the tracer outlet at the beginning of measured section to the centre of the measured cross-section width, in other cases we put it at surface water levels near the right or left bank at the beginning of measured section. The velocity distribution and discharge were measured in each cross-section for all tracer experiments.

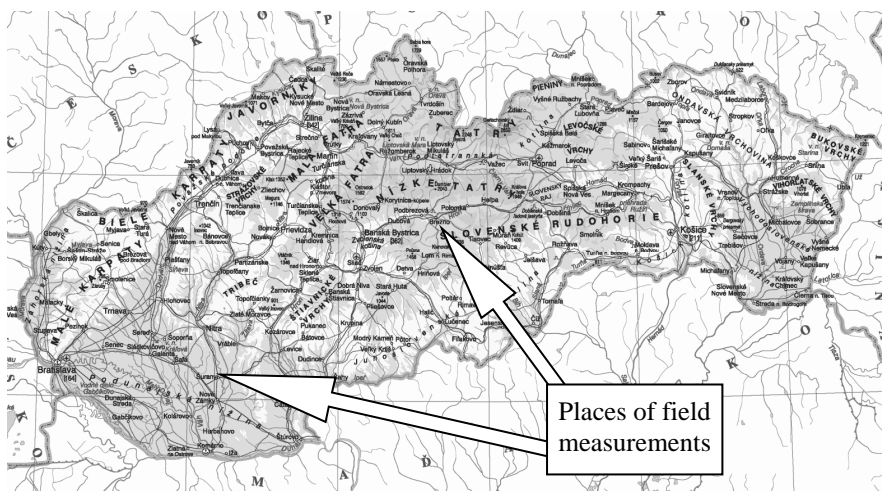


Fig. 1: Map of Slovakia, with the places of field measurements (case study A and B)

Subsequently, the time courses of tracer concentration were monitored in each measured cross-section of the stream. Measured cross-sections were distributed evenly along the length of the examined section. Conductivity measurements were completed with portable conductivity meters, located in the centre or evenly across the cross-section width. Measurements were always carried out from the beginning of conductivity values increase (front of tracer wave) until achieving of the original (background) conductivity values in each cross-section. Each kind of tracer experiment was repeated minimally two times.

4. LONGITUDINAL DISPERSION COEFFICIENT

Field measurements were evaluated using various methods for dispersion coefficients determination: based on analytical solutions of ADE, based on statistical evaluation and by using numerical models. The last method (numeric models) is not described in this paper.

The determination of longitudinal dispersion coefficient by analytical solutions of ADE was based on equation applicable for instantaneous injection of tracer [Cunge et al. 1985]:

$$c(x,t) = \frac{G}{2A\sqrt{\pi D_L t}} \cdot \exp\left[-\frac{(x - u_p t)^2}{4 D_L t}\right] \quad (3)$$

where A is a discharge area in a stream cross-section (m²), G is the mass of a tracer, u_p is a mean cross-section velocity (m.s⁻¹).

Equation (3) was used for simulation of tracer experiment (concentration distribution) for various values of longitudinal dispersion coefficient. The difference between the measured and simulated values is evaluated. The minimal difference determines the value of the longitudinal dispersion coefficient for each one of experiments (see Fig. 2).

The second way for evaluation of the longitudinal dispersion coefficient is based on direct determination of the statistical parameters (σ - standard deviation, t_{median} – median of time) of the acquired conductivity time courses. Principle of this method is to find the time, corresponding with the 15.87 and 84.13 percentile of the cumulative concentration curve [Socolofsky et al. 2005]. Distance of these two points is equal to 2σ and dispersion coefficient can be determined as

$$D_L = \frac{u_p^2 \sigma^2}{2t_{\text{median}}} \quad (4)$$

5. TRANSVERSAL DISPERSION COEFFICIENT

The method used for determining the transverse dispersion coefficient was the application of analytical solution of ADR - Eq. (5) derived for a continuous source of pollution - tracer [Demetracopoulos et al. 1983]:

$$c(x, y) = \frac{q_t \cdot c_t}{h \sqrt{4\pi D_T x u}} \exp\left(-\frac{y^2 \bar{u}}{4x D_T}\right) \quad (5)$$

where q_t is the tracer discharge ($\text{m}^3 \cdot \text{s}^{-1}$), c_t is the concentration of emitted tracer ($\text{kg} \cdot \text{m}^{-3}$), y is the distance from bank (m), D_T is the transverse dispersion coefficient [$\text{m}^2 \cdot \text{s}^{-1}$], h is depth [m], t is time [s], x, y are coordinates in the longitudinal and transverse direction [m], u is the longitudinal component of the velocity [$\text{m} \cdot \text{s}^{-1}$].

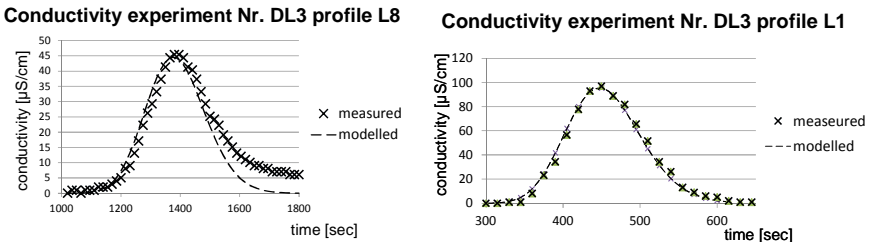


Fig. 2: Comparison of measured values from field experiments and results from analytical solution of advection-dispersion equation (Eq. 3) both case study A

The principle of the evaluation of the measured data was simulation of tracer experiments for different values of the transverse dispersion coefficient using analytical solution ADR (Eq. 5) Results of the simulations were compared with measured values. Minimum difference of squares between measured and simulated values determine the value of the measured transverse dispersion coefficient for each experiment.

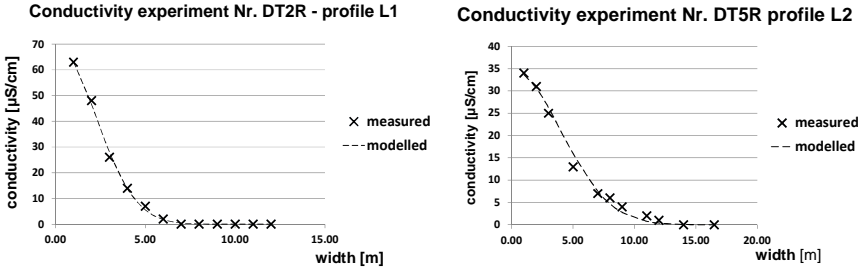


Fig. 3: Comparison of measured values from field experiments and results from analytical solution of advection-dispersion equation (Eq. 5) both case study B

6. RESULTS AND DISCUSSION

Data obtained from field experiments and measurements were processed by described methods. Values of the longitudinal and dimensionless dispersion coefficient are summarised in Tab. 1 and 2. Analytical solutions (for D_L only) can't be used in case study B, because of high velocity of the flowing water and high discharge in the river.

It should be noted that despite a careful selection of the investigated river section in both cases the hydraulic conditions does not meet ideal flow conditions and that investigated parts are not such prismatic channels as we supposed - numerical simulations showed it, too. In case study A the reasons are sediments, zones with relatively thick silts or other objects deforming velocity field and retention in so-called "dead zones" which causes deformation of tracer cloud (see Fig. 2 left).

In the case study B the reason is the irregular distribution of large rocks (boulders) in the river bed, which forms areas with significantly different flow velocities. Such area with different flow velocities generates "meandering" streamline and its deformation. All this results shows that the spread of tracer was not optimal, preferential flows were established, and thus distortions of tracer cloud occurred. It can be concluded that the transverse dispersion (and values of transversal dispersion coefficients) in flows of this nature is significantly affected by the arrangement of areas with different flow velocities and the resulting velocity field deformation.

The values of the transverse dispersion coefficient are summarised in Tab. 2.

Tab. 1: Values of longitudinal (DL) and dimensionless (pL) dispersion coefficient.

Longitudinal (DL) and dimensionless longitudinal (pL) dispersion coefficient		Case study	
		A (Malá Nitra)	B (Hron river)
Analytical solution (eq. 3)	DL ($m^2.s^{-1}$)	0,12 – 0,18	-
	PL (-)	4,98-11,18	-
Statistical evaluation	DL ($m^2.s^{-1}$)	0,13 – 0,22	1,047-1,443
	PL (-)	4,79-12,04	21,2-53,3

Tab. 2: Values of transversal (DT) and dimensionless (pT) dispersion coefficient.

Transversal (DT) and dimensionless transversal (pT) dispersion coefficient		Case study	
		A (Malá Nitra)	B (Hron river)
Analytical solution (eq. 5)	DT ($m^2.s^{-1}$)	0,011-0,032	0,06-0,017
	PT (-)	0,06-0,17	0,2-0,4

7. CONCLUSION

The paper described the longitudinal and transverse dispersion coefficient values, obtained from field tracer experiments performed in two different locations: Malá Nitra stream (case study A) and Hron river (case study B). The Malá Nitra stream is a typical lowland stream, with low velocities and turbulence, whereas the Hron river is a mountain stream with high velocities and turbulence. Both streams are typical for specific regions in Slovakia.

The range of obtained dispersion coefficient values is shown in Tab. 1 and Tab. 2. As expected, values of dispersion coefficients were higher in case study B.

The results can be used for next numerical simulation of water quality in the investigated streams or similar type one, but in spite of that it is necessary to perform further experiments and analysis to verify, validate or refute existing results, make clear obscurities and eliminate uncertainties.

8. REFERENCES:

BANSAL, M. K. (1971). Dispersion in natural streams. J. Hyd. Division, HY11, Nov., 1867-1886.

- CUNGE, J. A., HOLLY, F. M., VERWEY, A. (1985). Practical aspects of computational river hydraulics. Moskva, Energoatomizdat (in Russian)
- DEMETRACOPOULOS, A. C., STEFAN, H. G. (1983). Transverse mixing in wide and shallow river. Case study. *J. Environ. Engineering ASCE*, 109, No. 3, 685- 699.
- ELDER, J.W. (1959). Dispersion of marked fluid in turbulent shear flow. *J. Fluid Mech.*, vol. 5, Part 4, pp. 544-560.
- FISCHER, H. B. et al. (1979). *Mixing in inland and coastal waters*. Academic press, New York.
- JOLÁNKAI, G. (1992). Hydrological, chemical and biological processes of contaminant transformation and transport in river and lake systems. A state of the art report, UNESCO, Paris, 147pp.
- KARCHER, M.J., GERLAND, S., HARMS, I. H., IOSJPE, M., HELDAL, H.E., KERSHAW, P. J., SICKEL, M. (2004). The dispersion of 99Tc in the Nordic Seas and the Arctic Ocean: A comparison of model results and observations, *Journal of Environmental Radioactivity* 74 (1-3), pp. 185-198.
- KOSORIN, K. (1995). Dispersion coefficient for natural cross – sections of rivers. (in Slovak) *J. Hydrol. Hydromech.*, 43, 1-2, 93-101.
- PEKÁROVÁ, P., VELÍSKOVÁ, Y. (1998). Water quality modelling in Ondava catchment. VEDA, Bratislava, Slovakia. (in Slovak).
- ŘÍHA, J. et al. (2002). Water quality and its mathematical modelling. NOEL 2000, Brno, 269 p. (in Czech)
- SOCOLOFSKY S. A., JIRKA G. H. (2005). Cven 489-501: Special Topics in Mixing and Transport Processes in the Environment. Engineering – Lectures. 5th Edition, Coastal and Ocean Engineering Division, Texas A&M University, M.S. 3136, College Station, TX 77843-3136.
- SWAMEE, P. K., PATHAK, S. K., SOHRAB, M. (2000). Empirical relations for longitudinal dispersion in streams *Journal of Environmental Engineering* 126 (11), pp. 1056-1062.
- VELÍSKOVÁ, Y. SOKÁČ. M., KOCZKA BARA, M., DULOVIČOVÁ R. (2013): Hydrodynamic approach to the water quality modelling. In: *Acta hydrologica Slovaca*, Vol. 14, Nr. 1, s. 145 – 153. (in Slovak)
- YOTSUKURA, N.- SAYRE, W.W. (1976): Transverse mixing in natural channels, *Wat. Resour. Res.*, vol. 12, No. 4.

Acknowledgement:

This work was supported by the and Slovak Research and Development Agency No. APVV-0274-10.

Cross border water resources and water supply management – DRINKADRIA project

B. Karleuša¹, P. Banovec², I. Radman¹, J. Rubinić¹

¹Faculty of Civil Engineering University of Rijeka – Radmile Matejčić 3, Rijeka, Croatia,
barbara.karleusa@uniri.hr, ivana.radman@uniri.hr, jrubic@uniri.hr,

²Faculty of Civil Engineering and Geodesy, Jamova 2, Ljubljana, Slovenia
primoz.banovec@fgg.uni-lj.si)

Abstract

The strategic project Networking for Drinking Water Supply in Adriatic Region (acronym DRINKADRIA) is co-financed by the European Union within the program IPA Adriatic Cross Border Cooperation 2007 – 2013. It started on November 1st 2013, and it will last for 29 months. The total value of the Project is 6.600.000 EUR. The Project aim is to develop a base for strategies and procedures for secure cross-border water supply with specific emphasis on water resources management in trans-boundary context, climate change and specific socio-economic aspects of the Adriatic region. Significant financial resources will be invested in improvement of existing water supply systems in the region, and possibilities of cross-border connection of existing water supply systems will be analysed. Seventeen partner institutions from Adriatic region countries are involved in the Project: Italy, Slovenia, Croatia, Bosnia and Herzegovina, Montenegro, Serbia, Albania and Greece. This paper provides an overview of the project activities with emphasis on two work packages (WP): WP4 cross-border water resources management and WP5 cross-border water supply.

Keywords

cross-border, DRINKADRIA, water resources management, water supply management

1. INTRODUCTION

While management of water supply systems (WSS) is a broad domain well addressed by professionals and researchers the issue of cross-border water supply systems (CBWSS) is not so recognized. Cross-border water supply systems by the definition provide the water from a water resource in one county through a WSS in this country to another WSS and its users in another country. The management of drinking water supply in a cross-border context is much more complex and should be investigated [Altran et al., 2014].

Most of countries rely on the national territory based water supply defining it in some way as a national priority, even if it would be related to excessive costs. Several WSS turned to be a cross-border water supply system with a development of new borders, defining new countries. In these cases water supply systems which

were once conceptualized to operate in one administrative unit, start to operate within two national administrative systems. In the EU such development could be observed especially in the countries of former Yugoslavia.

The protection and management of cross-border water resources used for drinking purpose is also very complex. There are resources that are used for water supply in one country with a part of aquifer / catchment in another country. The EU Water Framework Directive (EU 2000/60) defines the need for a common definition and protection of water resources that are used for supplying population with drinking water. This is implemented by the water management plans. But the drinking water protection areas are still defined for each country separately, with no consensus with the neighbouring country.

In this paper an overview of the Project DRINKADRIA that encompasses the above explained complex problems regarding cross-border water supply systems and water resources management is given.

2. DRINKADRIA PROJECT STRUCTURE

The strategic project Networking for Drinking Water Supply in Adriatic Region (acronym DRINKADRIA) is co-financed by the European Union within the program IPA Adriatic Cross Border Cooperation 2007 – 2013. It started on November 1st 2013, and it will last for 29 months. The total value of the Project is 6.600.000 EUR. The Project aim is to develop a base for strategies and procedures for secure cross-border water supply with specific emphasis on water resources management in trans-boundary context, climate change and specific socio-economic aspects of the Adriatic region. Significant financial resources will be invested in improvement of existing water supply systems in the region, and possibilities of cross-border connection of existing water supply systems will be analysed. Seventeen partner institutions from Adriatic region countries are involved in the Project: Italy, Slovenia, Croatia, Bosnia and Herzegovina, Montenegro, Serbia, Albania and Greece [Karleusa et al., 2014a].

DRINKADRIA project is being implemented through six work packages (WPs).

Work package 1 (WP1) covers project management and coordination. It includes coordination of activities between the partners during various meetings of project partners, by on-line communication etc.

Work package 2 (WP2) includes communication with the general public and dissemination of project results. Communication and dissemination activities include production of promotional materials and publication of results to all interested stakeholders through the project website (www.drinkadria.eu) and media.

Work package 3 (WP3) covers capitalization and sustainability of the project, which also includes the period after its completion. Within this work package national workshops are held in all countries that participate in the project. It is important to include bilateral commissions, local and regional government units,

utility companies, educational institutions and others in the project, in order to inform them about the project activities so that they could contribute to project results.

Work package 4 (WP4) includes cross-border water resources management while work package 5 (WP5) is dealing with cross-border water supply systems management. More details about WP4 and WP5 are given in the next two chapters.

Within the work package 6 (WP6) pilot actions will be carried out, i.e. investments which should result in more effective water supply and water resources management. This work package consists of three activities: development of common analytical framework, individual pilot actions/investments, and development of rules and documentation of experiences.

3. CROSS-BORDER WATER RESOURCES MANAGEMENT

Within work package 4 which is led by FB8 Faculty of Civil Engineering University of Rijeka cross-border water resources management issues are analysed. Regulations of the countries involved in the Project related to water resources management will be analysed, in order to develop a common basis for the protection of transboundary water resources which are used in water supply. Drinking water protection areas are defined for each country separately, with no consensus with the neighbouring country. For example, Slovenia defined drinking water protection areas only to the Slovene-Croatian border and vice versa. Unified approach to protection of transboundary aquifers is crucial for ensuring safe water supply [Altran et al., 2014].

Partners will also apply common methodologies for analysing the impact of climate change/variations on water resources availability, different scenarios of changes in water demand and water resources quality on chosen test areas [Karleuša et al., 2014b].

In the Project, nine (9) test areas were selected. In Italy three test areas are analysed. The first is Isonzo Plain, located in the north-eastern side of the Friuli Venezia Giulia Region (NE Italy) at the border with Slovenia. Although this area has a significant water quantity in the alluvial deposits, there is also a need for careful withdrawal planning because of increasing demand. The water quality is good now. However, the herbicide atrazine degradation products are still present in the aquifers of the plains and in the groundwater, especially in the wells on the north of the Isonzo High Plain. Those wells are more vulnerable to the pollutants. Research on this area is done by project lead partner (LP) Area Council for Eastern Integrated Water Service of Trieste – CATO. The second is the ATO 3 test area which is located in the central part of Marche Region, stretching from the Apennines to the Adriatic coast. It has two hydrogeological domains - Calcareous ridges and Alluvial plains. In this test area there is a growing demand for water due to the population increase, and in the last decade, the increase in frequency of

the drought seasons was also observed. Regarding the water quality, an increase of pollution by nitrates of agricultural origin has been observed in some pumping wells. Research on this area is done by final beneficiary (FB) 2 Optimal Territorial Area Authority N.3 Marche Centro – Macerata. The third test area in Italy is Ostuni in Apulia Region, which includes the territories belonging to the Municipality of Ostuni and the surrounding 23 municipalities which span from the Adriatic to the Ionian coast. In this test area the agricultural irrigation has caused a massive exploitation of groundwater resources, and it resulted with a large decrease of the groundwater level and sea water intrusion in most of the coastal areas. An increasing trend in water demand was also observed in the touristic sector on the coast. Research on this area is done by FB3 Italian National Council - Water Research Institute, CNR-IRSA.

In Slovenia FB5 University of Ljubljana analyses the test area that covers the Kobariški stol, Mija and Matajur aquifers, which are cross-border aquifers on Slovenia-Italy border. In this test area settlements are scattered. Some of the inhabitants have public water supply, and some have their own water supply, so there is poor control of the amount of abstracted water and poor water quality monitoring on own water sources. Contamination may occur locally due to agriculture and grazing. Although there are several water sources, only for two of them the water protection areas are determined.

In Croatia two test areas are analysed. First is the test area in Northern Istria, which includes catchments of karst springs Sv.Ivan, Bulaž and Gradole in Mirna river basin. In this test area there are problems during extremely dry years (e.g. 2012), when spring capacities significantly decrease. Problems with water quality occur during high precipitation events after long-term drought periods, what causes increase of spring abundance, but also turbidity, bacteriological load and chemical quality parameters. There is also a risk of accidental pollution. The research on this area is done by FB8 Faculty of civil engineering University of Rijeka in collaboration with FB6 Region of Istria and FB7 Water Utility of Istria. The second test area is in Dalmatia, which includes Prud spring catchment and Blatsko polje on the island of Korčula. Possible pollution of Prud is connected with poor determination of catchment boundaries, lack of sanitary protection zones in Bosnia and Herzegovina, settlements within the catchment, roads and small industry. Most of the catchment area of the spring Prud is in Bosnia and Herzegovina, and there are no regulations for the protection of springs in Croatia with catchment in Bosnia and Herzegovina and vice versa. Pollutants in Blatsko polje originate from agricultural production, and there is also a problem with seawater intrusion which usually occurs when there are several dry years in a row. Most of the research on this area is done by FB9 Croatian Geological Survey also in collaboration with FB8 and FB12 Hydro-Engineering Institute of Sarajevo Faculty of Civil Engineering.

In Albania the test area Drini river basin, which is located in the Western Balkans is analysed by FB11 Water Supply and Sewerage Association of Albania. The total area of the basin includes the Black Drin, White Drin and Buna River, as

well as the Shkodra, Ohrid and Prespa lakes. Phosphate has relatively high values in river Drini. In river Buna pollution increases during periods of high water levels in its tributaries, and especially in summer during the tourist season. Regarding groundwater pollution, there is a high nitrite concentration in the Trush zone and surrounding areas.

The test area of the city of Nikšić in Montenegro is analysed by FB14 Public Utility "Vodovod i kanalizacija" Nikšić. Three springs - Gornji Vidrovan, Donji Vidrovan and Poklonci are included in the water supply system of the city. On the springs Gornji Vidrovan and Donji Vidrovan, during high intensity rainfalls in spring and autumn, there is an increased turbidity and mild microbiological contamination.

In Greece the test area is the island of Corfu located in the Region of Ionian Islands. The research is done by FB15 the Region of Ionian Islands and FB16 Civil Engineering Department, University of Thessaly – Greece. On this test area, the natural background (gypsum presence) in the aquifers causes high concentrations of sulfates. Point and diffuse sources of pollution cause increased nitrates and ammonium concentrations. High concentrations of chlorides occur locally in the coastal zones due to sea intrusion caused by excessive pumping and due to natural causes.

As an example of part of conducted analyses the possible impacts of foreseen climate changes/variations on water resources within the selected test areas, spring Gradole in Northern Istria (Croatia) is taken. Gradole is the most significant spring and groundwater intake in Istria whose catchment is not in the cross-border impacts domain, but its water balance has a pronounced cross-border impact given that it also supplies water to a part of Slovenian coast. Considering the already present negative trends of increase in air temperature and discharge on that spring from the middle of the last century until today, and the expected continuation and intensification of negative climate changes/variations, it is clear that the risks of unfulfilled possibilities of assuring the expected water supply needs from that spring also grow. The reduction of 1st degree in water supply which was introduced on the area of Istrian Region during summer in 2012, has further intensified the beliefs about the risks in the future. Within the DRINKADRIA project Croatian Meteorological and hydrological service and experts have carried out the climate conditions assessment (precipitation and air temperatures) until year 2050 with several climate models (RegCM3, Promes, Aladin), which have given different estimates of the intensity of those impacts (Güttler et al., 2014). It was found that more negative scenarios than those observed until now are also possible in the future. On the level of 30-year averages, it is expected that there will be no significant differences in precipitation, but their greater variability in terms of occurrence of extremely dry years is foreseen. Average annual air temperatures should increase significantly according to all models, whereby model results are quite different. Average mean 30-year air temperature increase for model Aladin is 1,6 °C, 1,2 °C for RegCM3 and even 2,2 °C (+19%) for Promes, also with increased maximum and minimum air temperatures. An overview of air

temperature and precipitation in period 1951-2050 is given on Fig.1 and 2, generated by model RegCM3. After generating the impact of those changes on characteristic parameters of spring Gradole water balance (mean annual discharge and minimum mean monthly discharge), model RegCM3 has given the lowest intensity of change.

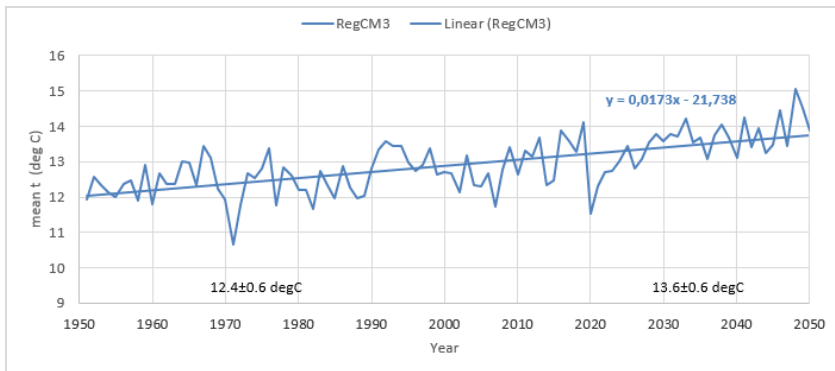


Fig. 1 Pazin station: mean annual temperature and associated linear trend in RegCM3 for the period 1951-2050. The numbers at the bottom of the panel are mean values and standard deviations for the periods P0 (1961-1990) and P1 (2021-2050). The model time series are for RCMcorr (Güttler et al., 2014)

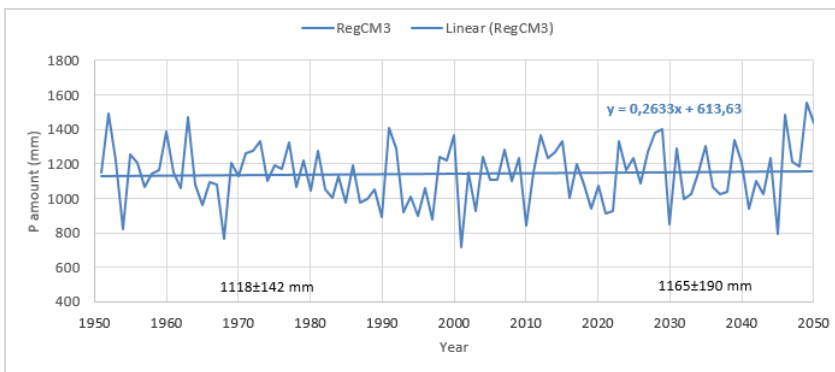


Fig. 2 Pazin station: annual precipitation amount and associated linear trend in RegCM3 for the period 1951-2050. The numbers at the bottom of the panel are mean values and standard deviations for the periods P0 (1961-1990) and P1 (2021-2050). The model time series are for RCMcorr (Güttler et al., 2014)

Generating of discharges was conducted on the basis of mentioned mean annual air temperatures and annual precipitation amounts which were generated

with climate models, and runoff estimation conducted based on them - effective infiltration of precipitation from catchments into karst aquifers [Rubinić and Katalinić, 2014]. Fig. 3 shows the results of modelling of the minimum mean monthly discharges based on climatological data generated by model RegCM3. They are selected as representative because of the highest homogeneity of historical and generated discharge data series.

The results of the assessments show that the average value of minimum mean monthly discharges in period 2021-2050 in relation to a reference period 1961-1990 could be reduced for 7,2%, the maximum value of mean monthly discharge could increase for 12,2%, and the minimum value of mean monthly discharge could decrease even for 30,7%.

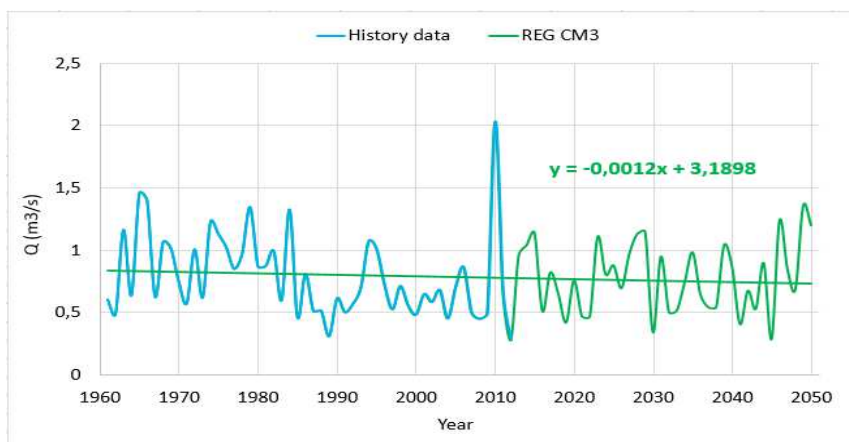


Fig. 3 Historical and generated synthetic series of minimum mean monthly discharges of spring Gradole (1961-2050) with associated trend by model REGCM3

4. CROSS-BORDER WATER SUPPLY SYSTEMS MANAGEMENT

Within the work package 5, which is led by the University of Ljubljana, following activities are under implementation: historical overview of cross-border water supply, analysis of existing and potential cross-border cooperation, development of protocols and procedures for effective cross-border water supply and the development of economic model. They are necessary for the analysis of current status of CBWSS and long-term planning of cross-border and regional water supply systems.

The analysis of currently active CBWSS show that the legal framework differs from one CBWSS to another in extreme range – from the water supply system

delivering water to another country based upon very simple two-page contract, to CBWSS which are based upon the international peace agreement.

More challenging is the analysis of the current pricing mechanisms upon which the actual water prices are determined. Our aim is to make them more transparent and standardized within the DRINKADRIA project. Fig. 4 shows the corresponding prices per m³ of delivered water in existing CBWSS, which could be compared to the retail prices (standardized per 10 m³/month consumption) in the observed non-cross-border water delivery (Fig. 5).

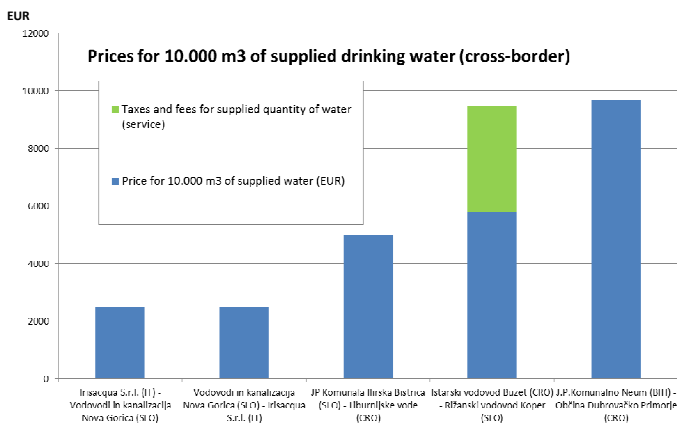


Fig. 4 Prices for standard 10.000 m³ of supplied drinking water – cross-border water delivery (cross-border wholesale prices 2014, 2015).

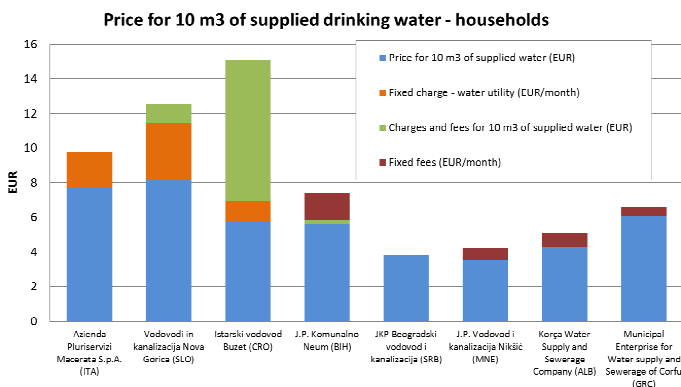


Fig. 5 Comparison of the retail prices for the delivery of 10 m³/month for the user category – households not cross-border (retail price 2014).

One can clearly observe noticeable variation in the prices per m³ (all prices are without VAT). Research shows that differences in prices could be explained with following arguments:

1. Resource taxes and levees – differences in the applied resource taxes, which usually mirror the costs related to the protection and development of water resources differ extremely from one country to another. Clear explanation and methodology on which the resource tax is charged is usually not available, or simply defined by a decree. It could be identified that the taxes and levees in the case of specific WSS in Croatia are by far higher than comparable taxes and levees in other countries.
2. Wholesale prices for the cross-border water delivery defined on the basis of retail prices – in some cases the wholesale prices for cross-border water delivery is defined to be the same as retail prices. Usually they are related to relative high prices of cross-border water delivery (Croatia-Slovenia and Band Herzegovina-Croatia).
3. Wholesale prices for the cross-border water delivery defined on the basis of actual water supply costs and opportunity benefits – some pricing approaches could be explained with this approach as well.

The described structure on the basis of which current CBWSS are operating is quite simplified, because one should consider also several other elements, which affect the price formation, above all:

1. Limitation or abundance of the water resources.
2. Minimum and maximum consumption requirements set by the contract.
3. Seasonal changes in water requirements and emergency water requirements.
4. Alternative water supply on the consumption side.

Beside these elements which define the pricing mechanism for the cross-border water delivery one can always consider also the negotiation skills and positions, where sometimes also other impact factors might influence the final outcome and resulting water price.

5. CONCLUSION

The aim of this paper was to present DRINKADRIA project and provide an overview of the project activities with emphasis on two work packages (WP): WP4 cross-border water resources management and WP5 cross-border water supply. In each WP one activity was presented more in more detail.

In WP4: cross-border water resources management, the joint activities of the partners were shortly presented and test areas in Adriatic region, on which more detailed research is done, shortly explained. The analyses of climate change on water resources availability was explained more in detail on just one test area of Gradole spring in Croatia. The results of the assessments on Gradole spring show that the average value of minimum mean monthly discharges in period 2021-2050 in relation to a reference period 1961-1990 could be reduced for 7,2%, the

maximum value of mean monthly discharge could increase for 12,2%, and the minimum value of mean monthly discharge could decrease even for 30,7%. These data are very useful for the future water supply management.

In WP5 an overview of planned activities was given and the analysis of the current pricing mechanisms upon which the actual water prices are determined is shown. The aim of the DRINKADRIA project is to make them more transparent and standardized.

Results from implementation of DRINKADRIA project are available on Project web page www.drinkadria.eu and drinkadria.fgg.uni-lj.si.

6. REFERENCES

- ALTRAN, E.; BANOVEC, P.; TOSCANO, P.; KARLEUŠA, B. 2014. Challenges in the Management of Cross - Border Water Supply Systems - the DRINKADRIA Project, *Water IDEAS 2014 Conference proceedings*, Bologna, Italy, 22-24.10.2014.
- GÜTTLER, I., GAJIĆ-ČAPKA, M.; CINDRIĆ, K. 2014. Report: Climate and climate change data for pilot areas in Croatia, published on www.drinkadria.eu
- KARLEUŠA, B.; BRAJKOVIĆ, M.; DRAVEC, LJ. TERZIĆ, J. 2014. Iskustva u prijavi i provedbi međunarodnog projekta DRINKADRIA / Experience in Application and Implementation of International Project DRINKADRIA, *Zbornik stručno-poslovnog skupa s međunarodnim sudjelovanjem: Aktualna problematika u vodoopskrbi i odvodnji*, Velika Gorica, Revelin d.o.o., 57-66.
- KARLEUŠA, B.; OŽANIĆ, N.; RUBINIĆ, J.; RADMAN, I.; DRAGIČEVIĆ, N.; VOLF, G.; SUŠANJ, I.; KRVAVICA, N.; RUŽIĆ, I.; CRNKO, T. 2014. Istraživanje mogućnosti unaprjeđenja opskrbe pitkom vodom u Jadranskoj regiji kroz projekt DRINKADRIA/ Analysing the Possibilities of Drinking Water Supply Improvement in Adriatic Region Through the DRINKADRIA Project, *Zbornik radova Građevinskog fakulteta Sveučilišta u Rijeci*.
- RUBINIĆ, J.; KATALINIĆ, A. 2014. Water Regime of Vrana Lake in Dalmatia (Croatia) – Changes, Risks and Problems. // *Hydrological Sciences Journal*. 59, 10; 1908-1924.

Acknowledgement

The authors would like to thank University of Rijeka for financially supporting the publication of this paper (research project 13.05.1.3.08 - Development of new methodologies in water and soil management in karstic, sensitive and protected areas). The authors would like to express acknowledgement to the EU IPA Adriatic Cross-Border Cooperation Programme, which provided the financial assistance necessary for the implementation of the DRINKADRIA project.

The operational water consumption of energy production: Czech Republic case study

L. Ansorge, M. Zeman

(T. G. Masaryk Water Research Institute p.r.i., Podbabská 30, 160 00 Prague, Czech Republic, phone: +420 220 197 385, e-mail: labor_ansorge@vuv.cz, martin_zeman@vuv.cz)

Abstract

Thermoelectric power plants require large amounts of cooling water. The energy sector is responsible for the largest annual volume of water withdrawals in the Czech Republic. It is a similar situation as in other countries in the world. Many reports have identified the water consumption of various energy production technologies around the world. This study is aimed at determining water withdrawals and water consumption per 1 MWh of energy produced in thermoelectric power plants in the Czech Republic. For the study 33 operational units were selected and considered individually. Real data on electricity and heat production and on water use were available for these operational units. The study included plants with a wide range of installed capacity of the order from tens of MW (MWe + MWt) up to units of GW. Most assessed plants use water recirculation cooling (closed cycle cooling). The individually assessed plants had flow (once-through) system, a combination of flow system with circulation system, and plants with a combination of flow with dry cooling system.

Keywords

energy production, water consumption, water-energy nexus, water withdrawals,

1. INTRODUCTION

Water is needed for energy and energy is needed for water. Energy production is generally water-intensive. Meeting ever-growing demands for energy will generate increasing stress on freshwater resources with repercussions for other users, such as agriculture and industry. Since these sectors also require energy, there is room to create synergies as they develop together [WWAP 2015]. The largest water users in the energy sector are thermoelectric power plants and hydropower plants which generally require large quantities of water. Thermoelectric power generation is a broad category of power plants consisting of coal, nuclear, oil, natural gas, and the steam portion of gas-fired combined cycles [Feeley III et al. 2008]. Approximately 90 % of global power generation is water intensive. Water is used directly for hydropower generation as well as for all forms of thermal power generation schemes [WWAP 2014]. Water is required not only in thermoelectric power plants but also to produce nearly all forms of energy.

For primary fuels, water is used in resource extraction, irrigation of biofuels feedstock crops, fuel refining and processing, and transport. In power generation, water provides cooling and other process-related needs at thermoelectric power plants; hydropower facilities harness its movement for electricity production [IEA 2012].

Globally, a little more than 4 000 km³ of fresh water is withdrawn each year for human use. Of that, about 70 % is withdrawn for agriculture and around 10% for the power industry [Williams and Simmons 2013]. There is a completely different situation in the Czech Republic. As shown in the annual report on water management in the Czech Republic in the period 2004-2013, the energy sector withdrew an average of 44.98% of all withdrawals from water resources in the Czech Republic and 56.07% if observing only surface waters.

The issues related to water demand and its determinants were considered in several earlier studies of thermoelectric water use. Examples of these studies can be found for example in [Dziegielewski and Bik [2006]. The group of operational conditions can include, in particular, technology of boilers, type of cooling systems and the way of dealing with fly ash and its transport. Because in conventional power plants half or more of the produced heat gets lost as waste heat [WWAP 2014], most power plants operate in a combined heat and power mode in the Czech Republic. And, conversely, most heating plants use power generation to maintain optimal operating conditions of boilers in periods of reduced heat demand. For this paper we use the term “power plant” for a classic power plant and also for a heating plant with power generation.

The design of a cooling system and its operational condition is the most important factor for water withdrawals and water consumption in thermoelectric power generation. Generally, higher withdrawals and lower consumptions of water per produced energy unit are typical for power plants with once-through (open loop) cooling systems. Conversely, lower withdrawals with higher consumption per energy unit are typical for recirculating (close loop) cooling systems [Macknick et al. 2012].

In the group of natural condition we can include water availability, temperature, air humidity, etc.

Social and economic conditions are very important in a longer perspective because they are the basis for investment decisions about improvement of technology of current plants, design of new plants, etc. The influence of indirect factors cannot be expressed exactly, but we can use econometrics tools to answer “how much” questions using theory and data from economics, business, statistics, as well as social and natural sciences [Hill et al. 2012]. Econometrics come into play either when we have an economic theory to test or when we have a relationship in mind that has some importance for policy decisions or analyses [Wooldridge 2009].

2. MATERIAL AND METHODS

2.1 Water usage and energy production

In our study we focused on the operational phase of power generation, thus excluding water usage in other stages of the life cycle [Fthenakis and Kim 2010; Williams and Simmons 2013].

For the study presented within this paper we collected data from evidence of water balance under Decree no. 431/2001 Coll. In most cases we examined permitted withdrawals and discharges in the IPPC licence. For the next solution we selected plants for which there were data on withdrawals and discharges. Some power plants must be grouped into the operational units because only data about withdrawals and discharges for operational units are available. For these power plants we obtained data on the production of electricity (MWe) and heat energy (MWt) and additional data from individual operators of these power plants. For the study 33 operational units were selected (see Table 1) and considered individually. The study included power plants with a wide range of installed capacity of the order from tens of MW (MWe + MWt) up to units of GW. The data availability determined the time period of the study to the decade 2004-2013.

For operational units for which data are only available on net electricity production, gross electricity generation was calculated by using average ratio gross and net electricity generation from records with both data.

Records which are not used for direct production of energy were excluded from the withdrawals and discharges data. Typically they are remediation pumping, cases of watercourse flowing through ash landfills, water supply to other users, etc.

2.2 Factors determining water needs for energy production

We assumed that water demand per energy unit is a function of direct and indirect determinants. As determinants describing natural conditions we selected average annual temperature and average temperature from June to September representing of the period with most intensive demand on cooling. As the determinants describing operational conditions we selected the amount of produced energy, heat energy to total energy production ratio, capacity factor - electricity, capacity factor - heat, and type of cooling equipment. The amount of produced energy includes both electrical and heat energy. The capacity factor - electricity (resp. heat) of an operation is the ratio of its actual electricity (resp. heat) output over a period of time, to its potential electrical (resp. heat) output if it were possible for it to operate at full electric (resp. heat) generation capacity (also known as nameplate capacity) continuously over the same period of time. As determinants describing socio-economic condition we selected payments for water withdrawals. For these determinants we collected data from the Czech Statistical Office and other sources. The type of cooling equipment was the only (purely) qualitative determinant and we divided the operations into groups accordingly.

The remaining seven determinants are quantitative and served as explanatory variables in the regression analysis described below.

As the main target of the study is the connection between thermoelectric sector as a whole and water withdrawal, we also took into account the relative energy production of individual operations. That means that each operation received the weight equal to its share on the sum of energy produced by all operations included in the relevant model. This approach contributes to reduce the (total) error of prediction when trying to predict the total amount of water withdrawn in a certain future year. In practice, a possible expected error of, for example, 0.1 m³/MWh gets more weight concerning large operations than 0.1 m³/MWh concerning small operations. However, we also tried to estimate the influence of the determinants without weighting the individual cases. This approach can be useful for predicting the withdrawals of smaller operations, either individually or when grouped. The determinant amount of produced energy, mentioned in the previous paragraph as an explanatory variable, may be useful for more accurate prediction of individual withdrawals and serves rather as a feature of an individual operation. Using the size of an operation as an explanatory variable does not interfere with weighting the cases by practically the same variable.

The operations listed in Table 1 were divided into three groups. The first group represents operations with once-through cooling system. The second group represents operations with recirculating cooling system, and the third represents hybrid cooling systems. This study focuses only on the first two groups because there were only two operation units with a hybrid system. So we got a group of 28 records in annual steps for operations with once-through cooling systems and 5 records for recirculating cooling system. These two groups of records were analysed with SPSS statistical software. For each group we tried to find the best model using weighted least squares regression and the best model using least squares regression without weighting. Therefore we searched for four models, each of them suitable for a different purpose or type of cooling.

Besides (not-) weighting the cases the process of searching for the best model was the same for all four segments. The dependent variable was water withdrawal per energy produced and the examined explanatory variables were always the seven quantitative variables mentioned in the first paragraph of section 2.2. We used the classical linear regression model in the form:

$$Y = \beta_0 + \beta_1 X_1 + \beta_2 X_2 + \dots + \beta_n X_n + \varepsilon \quad (1)$$

Where Y is the dependent variable (water withdrawals), β_i are regression coefficients, X_i are independent variables and ε is a random component (white noise). The models (i.e. sets of one to n explanatory variables, their regression parameters and other statistics) were generated with the procedures known as forward selection, backward selection and stepwise selection. For each model we estimated the Akaike information criterion (AIC) of the model and in the next step only examined models with the lowest AIC in the particular segment and with

appropriate signs of the regression parameters. We require positive dependence for both temperatures and negative dependence for energy production, heat energy to total energy and for price of withdrawals. We are not sure about the required signs of the regression parameters of the variables capacity factor - electricity and capacity factor - heat. Both signs were therefore acceptable for us. The proposed models had the lowest AIC of the models which we examined in each segment and which fulfilled the signs requirement.

Tab 1. Summary of operations -average data for period 2004-2013

Operation	Gross energy generation per year [MWh]	Ratio between power and heat generation	Water withdrawals per energy unit [m³/MWh]	Water consumption per energy unit [m³/MWh]
HPs Brno Sever+Špitálka*	825510	0.168	1.337	0.798
HP České Budějovice	1024075	0.193	1.321	1.175
HP Dvůr Králové	154163	0.132	21.584	2.399
HPs Energetika Třinec	2166807	0.449	4.983	2.622
HP Kolín	415099	0.135	18.443	0.616
HP Liberec	280130	0.101	1.181	0.992
HP Olomouc	832410	0.319	0.539	0.388
HP Ostrov	123615	0.105	3.105	2.086
HP Otrokovice	780256	0.36	1.207	0.914
HP Písek	155836	0.099	0.437	0.372
HP Planá nad Lužnicí	337921	0.871	2.873	2.486
HP Plzeň	1576252	0.634	1.658	1.402
HP Přerov	672558	0.687	3.643	3.031
HP Strakonice	365548	0.483	13.915	0.625
HP Trmice	1439117	0.407	3.626	1.411
HP Varnsdorf	74440	0.079	5.37	2.156
HP Zlín	683066	0.411	1.004	0.918
PPs Alpiq Kladno	2188569	2.675	2.163	1.011
PP Dětmárovice	2646007	14.048	2.043	1.346
PP Hodonín	607782	1.793	114.772	0.424
PP Chvaletice	3125041	60.779	3.082	2.104
PP Ledvice	2338291	6.091	3.281	1.352
PP Mělník	7637173	1.887	53.242	1.602
PP Opatovice	3514978	1.529	50.719	0.503
PP Počeradý	6699537	143.422	2.475	1.934
PP Poříčí	1098995	1.323	2.066	0.93

Operation	Gross energy generation per year [MWh]	Ratio between power and heat generation	Water withdrawals per energy unit [m ³ /MWh]	Water consumption per energy unit [m ³ /MWh]
PPs Prunéřov	8803992	20.03	2.341	1.841
PP Tisová	1869319	4.533	2.342	0.841
PP Tušimice	4021132	19.425	2.032	1.674
PP&HP Komofány	1520382	1.122	1.778	1.106
PP&HP Vřesová	7057527	1.043	1.805	0.581
NP Dukovany	14426350	108.981	3.376	2.079
NP Temelín	13295602	86.429	2.553	1.979

*Abbreviation: HP -heat power, NP - nuclear power plant, PP -fossil power plants

The first group included 10 cases (each case for the particular year of the period 2004-2013) for each of the 28 operations with recirculating cooling. Therefore the regression parameters related to the already mentioned determinants were estimated from 280 cases during the regression analysis. The second group included 10 cases for each of the 5 operations, making the size of the sample 50 cases.

3. RESULTS

The results of analyses operational water withdrawals and consumption for energy generation shown in Table 1 are similar to the published results of other studies [Macknick et al. 2012].

3.1 Operations with recirculation cooling

The Table 2 shows the estimated regression parameters, standard error of the estimation, standardized coefficients, t value of the relevant variable and its statistical significance and collinearity statistics VIF. The bottom part of the table shows the statistics of the models as a whole. In all tables the models are ordered according to the values of their AIC.

The first three best models (using the AIC) in the recirculating cooling category contained the variable price for withdrawal and its parameter's sign was positive according to the regression analysis. The model with the lowest AIC in the category exhibits AIC equal to 1776,8 which is close to the AIC of the models 3re,w,f and 5re,w,b that are the models with fourth and fifth lowest AIC. These models contained three explanatory variables each and none of their regression parameters interferes with its expected sign. The values of R^2_{adj} indicate that the models 3re,w,f and 5re,w,b could have slight to moderate predictive power.

The Table 3 shows the best three models and their parameters if the operations receive equal weight. We can see that the models include the capacity factor of electricity production and also of heat production again. The signs of the regression parameters are the same as in the weighted regression case. On the

other hand the R^2_{adj} of the models are low. As a result, the values of R^2_{adj} and F Significance are empirical evidence why (for the whole sector prediction) the models mentioned in the Tab 3 (i.e. models which take into account the size of individual operations) should be preferred. This may be confirmed by the lower values of AIC in weighted regression models however it is a question whether AIC is the best criterion for comparison of model estimated from equally weighted cases with model estimated from differently weighted cases.

3.2 Operations with once-through cooling

All of the three models for once-through cooling systems by energy production of individual operational units with the lowest AIC had the signs of their regression coefficients in accordance with our expectation (without considering the capacity factors). Apparently the values of the regression parameters of the same variables are in the models 3ot,w,b and 6ot,w,f very similar, which suggests that the explanatory variables, at least in the 3ot,w,b, could be very significant in once-through cooling segment. The Table 4 indicates that both models exhibit very high R^2_{adj} . According to the values of AIC we recommend the model 3ot,w,b. The Table 5 shows the first and the third best models and their parameters in case the operations receive equal weight. The regression parameter of the variable avg. annual temperature of the second best model exhibited minus sign, however in the next step this variable was eliminated because of its low significance (0,922). The elimination of average annual temperature resulted in the model 2ot,b. The model 2ot,b is the model with the lowest AIC in this segment and the signs of its regression parameters are in accordance with the expectations.

4. DISCUSSION AND CONCLUSIONS

For circulation plants it is not possible to recognize from the available water balance data what was actually used for energy production. If there are no data on technological or hot water delivery to other water consumers, then the processed data can be significantly overstated. For example at the heating plant Planá nad Lužnicí unadjusted sampling of water supplies to third parties causes the increase in demand for water per 1 MWh by 68.7 % and water consumption by 79.4 % !!! Collecting information about the hot water supplies to third parties is unfortunately very complicated.

The results of the regression analysis suggests that the created models seem to be rather partially successful for the recirculation cooling category of operation and much more successful for the once-through cooling category. For most models with optimal or close to optimum values of AIC the expected signs of the estimated coefficients of explanatory variables were in accordance with the apriori expected signs.

Possible reasons of the relatively low prediction power of the models for recirculation cooling category include:

- more heterogeneous category (while once-through cooling uses the water just once, the number how many times the water is used in the

recirculation system is not the same for all operations with recirculation system);

- not enough complex statistical model;
- the data availability only in annual step (while the electricity and heat production and temperature exhibits more variance during changing seasons or months rather than years).

Tab 2. Summary of analysis for best two models in category recirculating cooling – weighted by energy production of individual operational units

Model	Explanatory var.	Unstandardized Coeff.		Stand. Coeff.	<i>t</i>	Sig.	VIF
		β_i	Std. Error				
3re,w,f	(Constant)	-0,657	1,00		-0,66	0,511	
	capacity factor–electr. avg. temp.:June-Sept.	1,553	0,28	0,369	5,49	0,000	1,6
	capacity factor–heat	0,141	0,06	0,135	2,46	0,015	1,0
		-0,786	0,47	-0,111	-1,67	0,097	1,5
5re,w,b	(Constant)	1,713	0,22		7,71	0,000	
	capacity factor–electr.	1,990	0,37	0,473	5,42	0,000	2,6
	capacity factor–heat	-1,662	0,55	-0,235	-3,03	0,003	2,1
	total energy prod.	-3,7E-08	0,00	-0,245	-2,39	0,018	3,6
Model	no. of explanat. variables	R^2_{adj}	Std. Error of the Estimate	RSS	<i>F</i>	<i>F</i> Sig.	AIC
3re,w,f	3	0,195	0,042	0,483	23,5	0,000	- 1775,4
5re,w,b	3	0,194	0,042	0,484	23,4	0,000	- 1775,1

Tab 3. Summary of analysis for best two models in category recirculating cooling – equal weight assigned to each of the operations

Model	Explanatory var.	Unstandardized Coeff.		Stand. Coeff.	<i>t</i>	Sig.	VIF
		β_i	Std. Error				
1re,f	(Constant) capacity factor– electr.	1,935	0,18		10,77	0,000	
		0,927	0,33	0,164	2,78	0,006	1,0
2re,f	(Constant) capacity factor– electr.	2,169	0,28		7,79	0,000	
		0,760	0,37	0,135	2,07	0,039	1,2
	capacity factor– heat	-0,881	0,80	-0,072	-1,10	0,271	1,2
3re,f	(Constant) capacity factor– electr.	2,512	0,43		5,91	0,000	
		0,695	0,37	0,123	1,87	0,063	1,2
	capacity factor– heat	-1,113	0,83	-0,090	-1,34	0,180	1,3
	price for withdr.	-0,082	0,08	-0,065	-1,07	0,287	1,1
Model	no. of explanat. variables	R^2_{adj}	Std. Error of the Estimate	RSS	<i>F</i>	<i>F</i> Sig.	AIC
1re,f	1	0,023	1,181	387,7	7,7	0,006	93,1
2re,f	2	0,024	1,181	386,0	4,5	0,012	93,9
3re,f	3	0,025	1,180	384,4	3,4	0,019	94,8

Tab 4. Summary of analysis for best two models in category once-through cooling – weighted by energy production of individual operational units

Model	Explanatory var.	Unstandardized Coeff.		Stand. Coeff.	<i>t</i>	Sig.	VIF
		β_i	Std. Error				
3ot,w,b	(Constant)	160,74	42,32		3,80	0,000	
	price for withdr.	-41,02	7,65	-0,253	-5,36	0,000	1,9
	avg. temp.:June-Sept.	5,741	1,88	0,142	3,05	0,004	1,9
	heat e. to total energy	-216,48	11,07	-1,323	-19,6	0,000	4,0
	capacity factor–electr.	-87,11	21,45	-0,429	-4,06	0,000	9,7
	-	0,0000					
	total energy prod.	12	0,00	-0,614	-6,05	0,000	9,0
6ot,w,f	(Constant)	163,38	43,83		3,73	0,001	
	capacity factor–heat	24,90	90,84	0,028	0,27	0,785	9,2
	price for withdr.	-39,73	9,04	-0,245	-4,40	0,000	2,7
	heat e. to total energy	-221,95	22,88	-1,356	-9,70	0,000	16,7
	-	0,0000					
		total energy prod.	12	0,00	-0,630	-5,34	0,000
	capacity factor–electr.	-90,69	25,30	-0,446	-3,59	0,001	13,3
	avg. temp.:June-Sept.	5,618	1,96	0,139	2,87	0,006	2,0
Model	no. of explanat. variables	R^2_{adj}	Std. Error of the Estimate	RSS	<i>F</i>	<i>F</i> Sig.	AIC
3ot,w,b	5	0,944	0,931	38,2	166,0	0,000	-3,5
6ot,w,f	6	0,943	0,941	38,1	135,4	0,000	-1,6

Tab 5. Summary of analysis for best two models in category once-through cooling – equal weight assigned to each of the operations

Model	Explanatory var.	Unstandardized Coeff.		Stand. Coeff.	<i>t</i>	Sig.	VIF
		β_i	Std. Error				
2ot,b	(Constant)	124,24	47,23		2,63	0,012	
	price for withdr.	-51,46	7,54	-0,306	-6,82	0,000	2,7
	avg. temp.:June-Sept.	7,492	2,14	0,157	3,50	0,001	2,7
	heat e. to total energy	-185,40	18,85	-1,092	-9,83	0,000	16,6
	capacity factor–electr.	-54,23	23,84	-0,225	-2,27	0,028	13,2
	capacity factor–heat	-130,83	59,60	-0,146	-2,20	0,034	5,9
	total energy prod.	-0,000011	0,00	-0,369	-5,99	0,000	5,1
3ot,b	(Constant)	172,64	43,55		3,96	0,000	
	price for withdr.	-44,59	7,15	-0,265	-6,23	0,000	2,2
	avg. temp.:June-Sept.	5,530	2,03	0,116	2,73	0,009	2,2
	heat e. to total energy	-220,76	10,21	-1,300	-21,6	0,000	4,5
	capacity factor–electr.	-94,61	15,82	-0,392	-5,98	0,000	5,3
	total energy prod.	-0,000012	0,00	-0,390	-6,15	0,000	5,0
Model	no. of explanat. variables	R^2_{adj}	Std. Error of the Estimate	RSS	<i>F</i>	<i>F</i> Sig.	AIC
2ot,b	6	0,964	7,448	2385,5	217,2	0,000	205,3
3ot,b	5	0,960	7,765	2652,8	238,9	0,000	208,6

5. REFERENCES

- DZIEGIELEWSKI, B. & BIK, T. 2006. Water Use Benchmarks for Thermoelectric Power Generation (Project completion report). Southern Illinois University Carbondale, Carbondale, 213 p.
- FEELEY III, T. J., SKONE, T. J., STIEGEL JR., G. J., MCNEMAR, A., NEMETH, M., SCHIMMOLLER, B., MURPHY, J. T. & MANFREDO, L. 2008. Water: A critical resource in the thermoelectric power industry. *Energy* 33, p. 1–11.
- FTHENAKIS, V. & KIM, H. C. 2010. Life-cycle uses of water in U.S. electricity generation. *Renewable and Sustainable Energy Reviews* 14, p. 2039–2048.
- HILL, R. C., GRIFFITHS, W. E. & LIM, G. C. 2012. Principles of econometrics, 4. ed., international student version. ed. John Wiley & Sons, Hoboken, NJ.
- IEA 2012. World Energy Outlook 2012. International Energy Agency, Paris.
- MACKNICK, J., NEWMARK, R., HEATH, G. & HALLETT, K. C. 2012. Operational water consumption and withdrawal factors for electricity generating technologies: a review of existing literature. *Environmental Research Letters* 7, p. 045802+10.
- WILLIAMS, E. D. & SIMMONS, J. E. 2013. Water in the energy industry. An introduction. BP International.
- WOOLDRIDGE, J. M. 2009. Introductory econometrics: a modern approach, 4th ed. ed. South Western, Cengage Learning, Mason, OH.
- WWAP 2014. The United Nations world water development report 2014: Water and Energy. Unesco, Paris.
- WWAP 2015. The United Nations World Water Development Report 2015: Water for a Sustainable World. Unesco, Paris.

Acknowledgements

The study presented within this paper was carried out as part of the project TD020113 funded by the Technological Agency of the Czech Republic. The authors would like to thank the staff of the Energy Regulatory Office, Czech Statistical Office, United Energy and ČEZ for sharing their knowledge and for providing the necessary data for this study. We would like thank all unnamed colleagues from TGM WRI for their inspiring suggestions and comments.

Concept of Restoration and Preservation of River Odra's Biodiversity and Eco-system Services (BIO - ODRA)

D. Kunštek

(Water Research Department, Faculty of civil engineering, University of Zagreb, Kačićeva 26, 10000 Zagreb, Croatia, phone: 00 385 98 359468, fax: 00 385 1 4639 238, e-mail: kduska@grad.h)

Abstract

The river Odra has been heavily modified as a result of flood protection measures, its use as a watercourse for a water treatment plant and by an increased riverside population. Odra as urban source account for significant quantities of important diffuse pollutants, and is typically badly polluted with toxic metals, hydrocarbons including PAHs, and suspended matter, faecal pathogens and nutrients. The Restoration Odra concept (BIO - ODRA) engages 79 120.76 ha of Odra River Basin and it's the first environmental assessment of the river towards the European and international river restoration principles. Concrete restoration actions will be taken on upper reach of river Odra, i.e. from its source to the Sava-Odra Channel including Odra's tributaries (streams Želin, Siget, Kosnica, Ribnica, Lomnica), but project engages bigger area because of the referent monitoring stations on lower reach of river Odra. Hydro-morphological, habitat and physicochemical data collection and monitoring will be done with permits by private landowners and "Hrvatske Vode". Concrete actions which are planned will be on the State property. The objective is to establish self-sustaining stream functions and return an ecosystem to a former natural condition. This project also aims to help create a community that is more connected to the environment, with a real appreciation of the critical role of water systems and biodiversity in their lives and lifestyles. In Croatia, we need the community to be completely up to speed and mirroring the WFD overall directions through imaginative, comprehensive and persistent education and awareness programs, and through involvement of community at every step of the way.

Keywords:

River Odra, river restoration, environment, measure, monitoring

1. INTRODUCTION

BIO – ODRA project area engages 79 120.76 ha of Odra River Basin. The long term vision for the river Odra is to have fully wild river and to secure their health and productivity for all time. The aim is to ensure a variety of river dynamics, natural habitats and species while also producing greater benefits in natural goods and services for local people. This should be achieved through the

establishment of ecological management of the riverine area as well as the restoration of degraded river and floodplain areas.

The objective is to establish self-sustaining stream functions and return an ecosystem to a former natural condition. The goal is to secure a future for the river Odra and its wetlands as a healthy, productive and resilient wetland system.

Concrete restoration actions will be taken on upper reach of river Odra, i.e. from its source to the Sava-Odra Channel including Odra's tributaries (streams Želin, Siget, Kosnica, Ribnica, Lomnica), but project engages area bigger area because of the referent monitoring stations on lower reach of river Odra. They will improve conditions for flora and fauna, and ensure high water quality in the river and surroundings system. Proper applying of vegetation for sustainable river management requires: precise calculation of water movement parameters; an understanding of channel hydraulics; and knowledge about biomass distribution and ecology of dominant plant species.

This project involves mapping and assessment ecosystems and their services in vicinity of river Odra. Although, EU guidelines about mapping and assessment of ecosystem and their services exist, in Croatia is lack applying them. Also, river restoration is not a novelty in EU and it is at the forefront of applied hydrologic science, but in Croatia there is no example of restored river and associated floodplains implementing ecological and biological engineering. While many projects, supported through EU programmes, have already successfully finished or are still in progress, in Croatia, river revitalization and restoration is an innovative approach of river management.

Hydro-morphological, habitat and physicochemical data collection and monitoring will be done with permits by private landowners and "Hrvatske Vode". Concrete actions which are planned will be on the State property.

The hydromorphological monitoring and assessment will be done according to the "Meander - Guideline for Hydromorphological Monitoring and Assessment of Rivers in Croatia" which fully meets the EU Water Framework Directive requirements.

Hrvatske Vode (CV) has ample experience in flood protection, however mostly by technical (structural) measures that often adversely affect the ecological status. Experience is lacking in the assessment and mitigation of adverse effects of hydromorphological modifications and pressures on habitats and biota. To enhance sustainability, Croatia is therefore keen to develop its capacity to monitor and assess hydromorphological features in rivers and to design and implement measures in the River Basin Management Plans (RBMP's) and Management Plans to improve the ecological status. Integrated river restoration is also seen as a promising tool to reduce hydromorphological pressures, in order to meet the objectives of the WFD, Birds, Habitat and Floods Directives.

So, in fact, dissemination of the project results will be achieved according to recommendations in „Meander - Guideline for River Restoration Plans in Croatia“

2. GENERAL DESCRIPTION OF THE AREA TARGETED BY BIO – ODRÁ PROJECT

River Odra is flowing through field called „Odransko polje“, parallel to the river Sava and near town Sisak flows into the river Kupa. River Odra and its floodplain ranges from 95 to 110 m altitude. The Odra is connected to the River Sava by the Sava-Odra Relief Channel (built in 1965), which serves to deliver excessive water from the Sava to prevent it from flooding upstream urban areas (especially Zagreb) and it provides transportation of burdened waters from river Sava to retention area of the Odransko polje. Sava-Odra Relief canal artificially divided the Odra River in two parts; 6 km of strongly anthropogenically affected upper reach (river source area) and more preserved middle and lower reach. The catchment area of the Odra covers 604 km² and total length of the course is about 80 km. Due to the low slope (0.13%) the river meanders significantly. Water level of Odra is closely related to the water level of the Sava River. The largest part of its water volume is groundwater of the Sava River. Odra is the left tributary of the Kupa River and during high flows of the Sava and Kupa rivers, the Odra basin provides a retention area of about 30,000 ha along 30 km of its course. During dry periods, the Odra-Sava canal drains the basin to some extent. Thus, since 1965 the water table has dropped by 60 to 90 cm, with negative consequences for hydrology of streams in headwater area and for the ash and partly for the oak forests. Average riverbed width is about 25 - 30 m, and the maximal depth reaches 4 - 5 m.

Odra floodplain is important area for birds, among which corncrake (*Crex crex*) and white-tail eagle (*Haliaeetus albicilla*) are indicators of good condition of flooded meadows and forests along the Odra River. The vegetation composition and structure is strongly determined by the flood dynamics and groundwater level correlating the lowland topography.

For the purpose of this concept, we have divided the river Odra in two main sections (Fig. 1.): UPPER REACH is river section from its source downstream to the crossing of river and channel Sava-Odra. At this crossing is one of the main issues/problems: malfunctioning siphon. This object was intended to lead river Odra's flow beneath the channel Sava-Odra, but it was never finished.

MIDDLE and LOWER reach is the section of the river Odra from siphon downstream to the river mouth (into river Kupa).

Main issues addressed within this concept of the project are concentrated in the upper reach of the River Odra, with lesser negative effects in the middle and lower reach. Upper reach of the river is situated in the area with significant proportion of agricultural land. Floodplain along the middle and lower reach is dominated by lowland floodplain forests, especially along the right bank of the river.



Fig. 1. River Odra divided in two main sections: Upper and Lower Reach

3. BASIC IMPACTS

In the last few decades in the Odra catchment, but also in the wider area, there was a significantly increased urbanization and settlements expansion, which represents one of the greatest pressures on the environment. At the same time, there have been significant changes in the groundwater regime in the area of the Sava alluvium, or their reduction due to increased exploitation of drinking water and lowering the water level of small and medium-sized water of river Sava. River Odra has no classical source, but is formed from groundwater, these changes have led to a reduction of flow in the river and its tributaries (Figure 2.).

It is also a major problem of the river Odra sewage and industrial wastewater, especially from nearby farms, businesses and households, whose drainage systems have not yet been adequately solved. It was also determined the deterioration of water and it is now in a lower category, primarily by the amount of organic compounds. Odra and channel Sava-Odra are moderately polluted water and belong to the second degree of solvency.

Potentially large source of pollution of surface and groundwater is nitrate leaching from manure, settlements and agricultural fields. In the lower reach, there is also a Waste water treatment plant from Sisak, which also releases the treated water into the river Odra.



Fig. 2. Drought in stream Želin during dry period (left) and pollution from wastewater treatment plant in Velika Gorica by discharge of treated and untreated wastewater (right)



Fig. 3. Eutrophication and sedimentation caused by the “Syphon” (left) and Eutrophication impact in Stream Želin (right)

At the start of the flow of Kosnica and Ribnica, the bed is filled just in the rainy season, and during high groundwater level and water level of the river Sava. However, due to the continued trend of lowering of groundwater levels, these streams especially Kosnica, are drying up on the upstream side of its course. Very small slope and congestion of stream Želin caused water stagnation and eutrophication (Figure 3.). Due to the drought at the middle of the channel, it is assumed that the water in the end of channel and in stream Želin is backwater of river Odra.

One of the most negative impact on biodiversity is located in Poljana Čička, i.e. River Odra is interrupted by Sava – Odra Relief channel, where, through the siphon, part of the water of the river Odra engages in channel Sava – Odra (due to unfinished syphon) and part of the water leads through amelioration channel GA2, which is parallel with channel Sava – Odra. After approximately 12km from the

siphon, amelioration channel GA2, again, flows into the Odra River. The siphon causes slowing the flow which causes sedimentation and eutrophication.

4. ANALYSIS OF GROUNDWATER REGIME IN VELIKA GORICA AND ODRANSKO POLJE

The thickness of the aquifer is on average 40 m a. s. l. on the South and according to existing knowledge, it can range up to a 100 m a. s. l. in the North, but thickness distribution is spatially poorly known. Location of piezometers and previous studies are mainly related to the water supply. Water level analyses with piezometers were made for the time period from 1988 to 2005. Groundwater quality assessment and classification based on the allowable limit values of certain groups of indicators that characterize the sources and causes of water pollution is given in (Tab. 1.) for year 2004.

Tab 1. Classification of groundwater – Velika Gorica area [Glasnik, 2006]

VELIKA GORICA - classification of groundwater for year 2004.			53016-VG-9			
Groups of indicators	Indicator	Unit of Measure	n	Relevant value	type	Rating
A -physical and chemical	pH value		2	7.225	I	
	electro conductivity	µS/cm	2	675	II	
B- oxygen balance	KPK - Mn	mgO ₂ /l	2	0.35	I	I
C -nutrients	ammonium	mgN/l	2	0	I	I
	nitrites	mgN/l	2	0	I	
D - Microbiological	Number of kolif. bacteria	UK in 100mL	2	18	I	I
	Number of faecal bacteria	in 100mL	1	0	I	
	Aero bacteria number 37 °C	in 1mL	2	22	I	
F- total metals	copper	µg/l	2	1	I	
	zinc	µg/l	2	0.5	I	
	cadmium	µg/l	2	0	I	
	chrome	µg/l	2	0.5	I	
	nickel	µg/l	2	0.5	I	
	lead	µg/l	2	0.5	II	
	Hydrargyrum (Hg)	µg/l	2	0	I	
G - organic compounds	mineral oil	µg/l	2	4.45	I	
	phenols	mg/l	2	0	I	
	lindane	µg/l	2	0	I	
	ppDDT	µg/l	2	0	I	

5. CONSERVATION / BIODIVERSITY PROBLEMS AND THREATS

The upper reach of Odra River is anthropologically highly impacted river stretch. It is exposed to water pollution due to combination of the occurrence of untreated (from 1974 -1988) and poorly treated wastewater from the town of Velika Gorica, farming, butchery and meat industry (and other point pollution sources), illegal waste water load from private houses and pollution load from intensive agriculture. Substrates for benthic communities have been markedly changed due to deposition of fine mud and sludge. According to recent study [Filipović et al, 2013] the sludge from wastewater treatment plant in Velika Gorica is being considered as a hazardous waste and a subject of discussion regarding disposal due to high total metal concentration in sludge samples. There is no metal concentration analysis in riverbed of stream Želin and upper Odra River reach, but probably could be real threat due to food web heavy metal accumulation. In the upper reach aquatic communities are markedly changed, i.e. limnophilic organisms prevail instead of rheophilic ones. This trend has been observed in various organisms, e.g. in macrophytes, macroinvertebrates and fish [Duplić et al., 2011], [Mihaljević et al., 2011], [Mihaljević unpublished data]. Thus, according to available data, the middle reach of the Odra River could be considered as a reference site.

6. PROPOSED RESTORATION TECHNIQUES

River restoration techniques involve using only raw natural materials as river bed stabilization or improving river bed morphology for spawning, covering river bed with specific and native plant species as water regime stabilization. By smart applying of the river restoration techniques, we can help to river Odra ecosystem to regenerate itself and to help the nature to get into a balance again by improving biological diversity. Proposed restoration techniques on BIO – ODRA are given in Tab. 2.

7. CONCLUSION

The best way to restore the river environment of BIO – ODRA is not to reengineer it, but for the river to restore itself through natural processes: ‘self healing’ is best done by removing or reducing human interventions. One important issue is to restore connectivity within the hydrologic system as a base for a recovery of the biological function. New initiative for managing and restoring BIO - ODRA is interdisciplinary, integrative, and need to plan for different spatial and temporal scales and to develop sustainable flood risk management as part of an integrated and holistic approach to river Odra basin management. For the long-term sustainability of the project’s results, especially with regard to birdlife, it is essential that the wetland and meadow area are grazed.

This project aims to help create a community that is more connected to the environment, with a real appreciation of the critical role of water systems and

biodiversity in their lives and lifestyles. In Croatia, we need the community to be completely up to speed and mirroring the WFD overall directions through imaginative, comprehensive and persistent education and awareness programs, and through involvement of community at every step of the way.

Tab 2. Proposed restoration techniques on BIO – ODRA

Threat/ Problem	Reduced stream discharge in Odra River
Description/Drivers	hydrological, drop of the groundwater level in alluvial plain of the Sava River
Location	Odra River Upper reach
Impact on biodiversity	<ul style="list-style-type: none"> - Considerable changes in aquatic community composition and structure: - Communities characterised by taxa typical for lentic habitats and stagnant waterbodies (limnophilic instead of rheophilic); benthic macroinvertebrates, fish, macrophytes, phytobenthos - Reduction in overall diversity specific for natural flowing water condition (flora & fauna) - Changes in population densities and functional feeding guilds of aquatic organisms
Proposed measures	<p>Revitalization measures recharge Želin stream (which flows into the Odra River), refers to the Intake structures of water from two lakes that are close by (Lake Novo Čiče and Omladinsko Lake and flow into Želin. It is important to establish a monitoring water quality at both locations, in order to control the entry pollutants in Želin, and thus the Odra River. If monitoring shows that water quality in lakes is not environmentally acceptable, then the water diversion should be linked to a measure of water purification through the Recipient channel established construction self-purification lagoon, directly behind the discharge from the treatment of Velika Gorica, ca 1 km upstream.</p> <p>If, however monitoring showed satisfactory water quality, engaging water from the lake would then be applied for 1 km downstream of the treatment plant</p>
Threat/ Problem	Water pollution in Odra River due to
Description/Drivers	<ol style="list-style-type: none"> 1) malfunctioning and insufficient capacity waste-water treatment plant in the city of Velika Gorica 2) other sources of pollution (illegal outlets into Odra) 3) agriculture
Location	especially expressed in the Upper reach, but also present downstream in the Middle and Lower reach
Impact on biodiversity	<ul style="list-style-type: none"> - Development of toxic cyanobacteria due to increased level of phosphates and nitrates from waste water treatment plant and agriculture - Development of nitrophilous and toxin resistant plants - Considerable changes in aquatic community composition and structure
Proposed measures	Revitalization measures of removing contaminants from water streams of developing constructed wetland (CW). This self-cleaning solution is

	predicted for: Urban Waste Water (small settlements, individual homes, tourist and organic farms, tourist facilities, • non-point source pollution (urban, agricultural and roadway runoff); Method is based on extensive research of the application of various plant species, sand substrates and water flow modes, enabling efficient removal of pollutants from water through physical and chemical processes, microbial activity and plant uptake	
Threat/ Problem	Deposition of fine organic particles in the riverbed	River fragmentation due to malfunctioning siphon
Descriptor/Drivers	Hydrological (river impoundment) and organic pollution (waste-water treatment plant)	hydrological, uncompleted siphon
Location	upper reach	point between Upper and Middle reach
Impact on biodiversity	- Anoxia appearance, development of anaerobic bacteria in sludge;- toxic metal accumulation in the riverbed;- Considerable changes in aquatic communities due to changes in substrate composition	- Population fragmentation and alteration of migration patterns of aquatic species (fish, aquatic macroinvertebrates, aquatic mammals, etc.) - Lower genetic diversity in local populations and appearance of genetic drift
Proposed measures	Silt / sludge removal measure a consequence of the discharge of untreated water from treatment plants in Velika Gorica	Revitalization measures reconnection of the Upper and Middle reach of the river Oder, which would flow upstream part of the River Odra has increased significantly. Solution reconnection riverbed implies microtunnelling below flood control channel Sava - Odra of ameliorative channel GA2 by the middle reach of the Odra.

8. REFERENCES

- BAČANI, A., POSAVEC, K., PARLOV, J. 2010. Groundwater quantity in the Zagreb aquifer.-In: ZUBER, A., KANIA, J. & KMIĘCIK, E. (eds.): *XXXVIII IAH Congress Groundwater Quality Sustainability*, Krakow, September 12–17, 2010, 87-92.
- BARTOLEC, M. 2012. Izvješće o provedenom istraživanju (monitoringu) štekavca (*Haliaeetus albicilla*) na području Sisačko-moslavačke županije. Izvješće za Državni zavod za zaštitu prirode, Zagreb.
- BARTOLIĆ, G. 2005. Aktivnost šišmiša u različitim tipovima staništa u šumi Turopoljski lug. Magistarski rad. Biološki odsjek, Prirodoslovno-matematički fakultet Sveučilišta u Zagrebu.
- DRVODELIĆ, D. 1999. Ekološki prostorni značaj Turopoljskog luga. Diplomski rad. Šumarski fakultet Zagreb.

- DRŽAVNI ZAVOD ZA ZAŠTITU PRIRODE 2011. Provođenje edukacije i osposobljavanje za provođenje Akcijskog plana za očuvanje ptice kosac (*Crex crex*) u Odranskom polju u Zagrebačkoj županiji. Završno izvješće za Javnu ustanovu za upravljanje zaštićenim područjima i drugim zaštićenim prirodnim vrijednostima Zagrebačke županije.
- DRŽAVNI ZAVOD ZA ZAŠTITU PRIRODE, 2005. Značajni krajobraz Odransko polje. Stručna podloga za zaštitu.
- DUMBOVIĆ, V. 2008. Praćenje brojnosti kosaca (*Crex crex*) na području Odranskog polja i Sunjske Grede (Gredskim sinokošama). Izvješće za 2008. Godinu. Izvješće za Javnu ustanovu za upravljanje zaštićenim prirodnim vrijednostima Sisačko-moslavačke županije.
- DUPLIĆ, A., BORŠIĆ, I., KATUŠIĆ, L. 2011. Ocjena stanja biološke raznolikosti rijeke Odre i prijedlog mjera za poboljšanje stanja očuvanosti područja ekološke mreže "Odra HR 2000631". Studija, DZZP, Zagreb.
- EKOLOŠKA UDRUGA EMYS 2009. Istraživanje rasprostranjenosti vidre (*Lutra lutra* L.) na području kontinentalne Hrvatske.
- FILIPOVIĆ, J., GRČIĆ, I., BERMANEC, V., KNIEWALD, G. Monitoring of total metal concentration in sludge samples: Case study for the mechanical-biological wastewater treatment plant in Velika Gorica, Croatia, *Science of the Total Environment* 447 (2013), 17-24;
- GLASNIK, 2006. Glasnik Zagrebačke Županije, Broj 21, Godina XI., 4. Listopada 2006 Zagreb, ISSN 1845-8602.
- GRBAC, I. 2009. Znanstvena analiza vrsta vodozemaca i gmazova (*Eurotestudo hermanni*, *Emys orbicularis*, *Bombina bombina* i *Bombina variegata*) s dodatka II Direktive o zaštiti prirodnih staništa i divlje flore i faune. Hrvatski prirodoslovni muzej, Zagreb.
- GRUBEŠIĆ, M. 2008. Dabar u Hrvatskoj. Šumarski fakultet sveučilišta u Zagrebu.
- GRUBEŠIĆ, M., TOMLJANOVIĆ, K., KOVAČ, I. 2008. Znanstvena analiza dabra (*Castor fiber* L.) na području Hrvatske. Državni zavod za zaštitu prirode.
- IVKOVIĆ, M. & HORVAT, B. 2007. *Hemerodromia raptor* (Meigen) a newly recorded species of aquatic dance flies (Diptera, Empididae) in Croatia and its distribution on Balkan Peninsula. *Natura Croatica*, 16, 79–82.
- JAVNA USTANOVA ZA UPRAVLJANJE ZAŠTIĆENIM PRIRODNIM VRIJEDNOSTIMA SISAČKO-MOSLAVAČKE ŽUPANIJE 2011. Rezultati prebrojavanja kosaca (*Crex crex*) za 2010, 2011. I 2012.
- MIHALJEVIĆ, Z. ET AL. 2011. Testiranje bioloških metoda ocjene ekološkog stanja (Okvirna direktiva o vodama, 2000/60/EC) u reprezentativnim slivovima Panonske i Dinaridske ekoregije, Studija, Prirodoslovno-matematički fakultet Sveučilišta u Zagrebu, Biološki odsjek, Zagreb.

Environmental damage due to floods assessment

M. Zeleňáková¹, L. Gaňová²

¹Institute of Environmental Engineering, Faculty of Civil Engineering, Technical University of Košice, Vysokoškolská 4, 042 00 Košice, Slovak republic, e-mail: martina.zelenakova@tuke.sk

²Slovak Water Management Enterprise, branch office Košice, Ďumbierska 14, 041 59 Košice, Slovak republic, e-mail: lenka.ganova@svp.sk

Abstract

Flood damage assessment is an essential part of flood risk management. Risk assessment is the overall process of risk identification, risk analysis and risk evaluation. Risk itself is defined as probability that a substance or situation will produce harm under specified conditions. An accurate estimation of negative flood effects on environment is important in order to be able to determine the environmental flood risk level in a system and the effects of risk reducing measures. The objective of the paper is to show how to environmental flood risk for such flood-prone areas can be determined and evaluated. This methodology can be presented to decision makers to support decisions regarding environmental flood risk reduction measures. We introduce the methodology for environmental flood risk assessment based on point and diffuse sources of pollution classification, as main environmental damages during the floods are caused because of pollution in the flooded area.

Keywords

diffuse sources of pollution, floods, point sources of pollution,

1. INTRODUCTION

It is important to keep in mind that a flood in a modern economy is expected to bring about a whole gamut of consequences. The costs of damage caused by extreme weather events (among which floods are a major category) have shown a rapid upward trend, both globally and in Europe. The scope and extremity of flood episodes point to the need to design and build a comprehensive system of flood protection measures in potential flood areas [Dráb, Říha 2001], [Drbal 2008], [Meyer, Messner 2005], [Říha et al. 2005], [Satrapa et al. 2011], [Vrijling et al. 1998], [Zeleňáková et al 2012], [Zeleňáková, Gaňová 2014]. The primary aim of flood risk management is the proposal of flood protection measures. The main objectives of management as well as the entire management cycle are regulated by Directive of the European Parliament and of the Council 2007/60/EC on the assessment and management of flood risks. The aim of the directive is to mitigate the adverse consequences for human health, the environment, cultural heritage and economic activity associated with floods. The objective of the paper is to develop and apply methodology for environmental risk assessment of flash floods in

Medzev, Bodva River catchment, eastern Slovakia and to select effective flood protection measures according to the objectives of flood risk management.

2. MATERIAL AND METHODS

2.1 Study area

The town of Medzev (Fig. 1) is found in the Košice District and its surrounding in the Košice Region. The River Bodva flows through the town with a left-side inflow from the Štóska, Porča, Piverský and Zlatná streams and a right-side inflow from the Grunt and Šugovský streams. The Bodva and the Zlatná and Piverský streams are assigned among the significant watercourses in water-management and at the same time are on the list among the managed watercourses [ENVIO 2013].

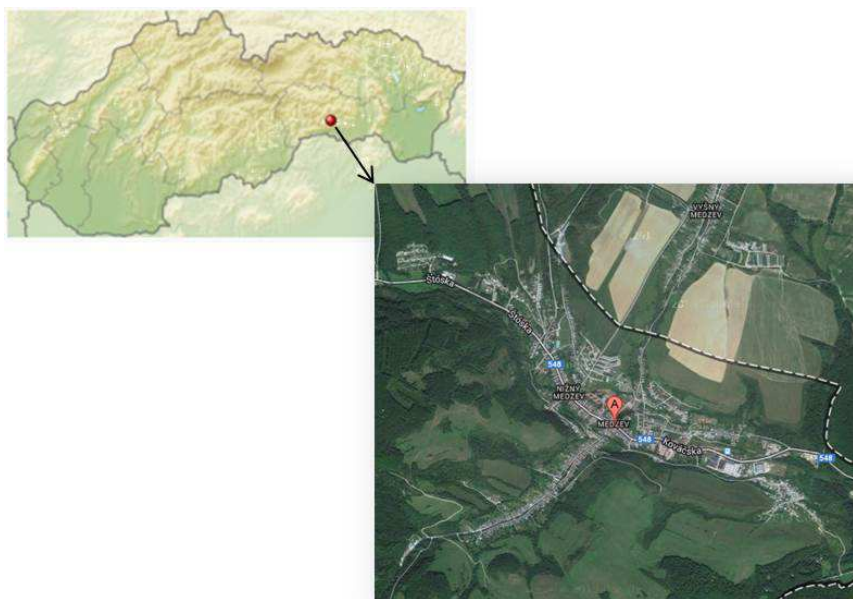


Fig. 1 Location of Medzev within Slovakia

Since Medzev is on the basis of preliminary assessment of flood risk ranked among areas with an existing flood risk, it is necessary to give priority to resolution of this area. In this area it is necessary to construct flood-protection measures which will be effective not only in terms of protection but also from economic, social and environmental points of view.

2.2 Damage to the environment

The concept of damage to the environment is understood to be “environmental damage”, which in connection with floods includes a wide scale of adverse impacts.

The principle philosophy of assessing damage to the environment comes from the fact that all three environmental elements evaluated (protected biotopes, water and soil) can be damaged by the impact of a whole range of floating hazardous substances from potential sources of contamination. Attention is therefore devoted to the quality of the water, exactly to the evaluation of sources of pollution situated in flooded area, which can cause the potential environmental damages in case of floods.

Damage to the environment or the consequence of floods on the environment is according to the point method classified into one of four categories – marginal, minor, intermediate and major (Tab. 1). The starting point for assigning a category of the consequence is categorization of potential sources of contamination influencing the quality of the water. At present no complete register of sources of contamination exists in the Slovak Republic; therefore, for the needs of this paper one of our own design was created. The individual sources of contamination are divided into two main categories: point and diffuse sources of contamination. Tab. 1 presents the divisions of the individual sources of contamination, their point classification and the weight indicating the importance of the component categories. When assigning points an inverse order is used; thus, the value 5 represents the greatest threat of contamination in the case of flooding. The individual weights of the component categories, which are standardized such that their sum is equal to one, are set in this same way. The individual points are set on the basis of a professional judgement.

The flooding of these objects can lead to leakage and the washing away of contaminating substances and thus to worsening the quality of surface and underground water and soils, which can lead to ecological catastrophes, such as damage to biotopes, the killing of fauna and flora as well as epidemics. Very serious damage of a long-term character is related to underground aquifers, which are used as sources of drinking water. The total consequence (Tab. 2) is calculated as the sum of the assigned points to the individual sources of contamination located in the flooded area for the given Q_N (probability of flood occurring) multiplied by the relevant weight, and this defines the negative impact on the environment [Gaňová 2014].

The Tab. 1 presents a description of the range of adverse consequences connected with environmental damage, together with the assigned point value level of the consequence. The total range is determined on the basis of all possible combination of the categories presented in Tab. 2. The number of combinations is 2159, which after arrangement are divided using the quartile method [Zeleňáková et al 2012] into the resultant four point ranges for each level of consequence.

Tab. 1 Category of consequences modified according to [Zvijáková 2013]

Level of consequence	Point range	Consequence	Description of consequence
1	0–6.85	<i>marginal</i>	Minimal or no environmental degradation.
2	6.86–12.25	<i>minor</i>	Disruption of biological communities which is reversible and limited in time and space.
3	12.26–17.65	<i>intermediate</i>	Disruption of biological communities which is extensive, but reversible or of limited severity.
4	17.66– 5.03	<i>major</i>	Extensive biological and physical disruption of entire ecosystems, which are not easily reversible.

The value of the consequence is considered as the determined threat of contamination of the environment during floods from all sources of contamination which enter into the calculation of environmental risk.

2.3 Measure of environmental risk caused by floods

The measure of environmental risk in consequence of floods is set on the basis of the calculated consequence on the environment for floods with different periods of recurrence, e.g. Q_5 , Q_{20} , Q_{50} and Q_{100} .

The numerical expression of the relationship for calculation of the average annual measure of environmental risk [-] for individual interval periods of recurrence is subsequently:

$$EnRp_i = \int_a^b D(Q)dP(Q) \approx \sum_{j=1}^n \left[\left(\frac{C_j + C_{j+1}}{2} \right) (P_{j+1} - P_j) \right] \quad (1)$$

where:

C_j sum of consequences set according to Tab. 2 [-]; the consequence is stated as “Point classification of threat” (column 4 in Tab. 2 based on authors` judge) x “Weight” (column 4 in Tab. 2) for different periods of recurrence, Q_5 , Q_{10} , Q_{50} , Q_{100} , and Q_{1000} .

P_j the probability of exceeding is given by relationship

$$P(Q) = 1 - N(Q) \quad (2)$$

and

$$N(Q) = 1 - e^{-\frac{1}{N}} \quad (3)$$

Q flow [$m^3/year$],

N, a, b values of the interval of the period of recurrence.

We select the individual component intervals of periods of recurrence (a , b) [Gaňová 2014], [Horský 2008]. The overall measure of environmental risk [-] is then given by the sum of the risks in individual component intervals $EnRp_i$, according to the determined consequence (3):

$$EnR = \sum EnRp_i \quad (4)$$

Thus determined measure of environmental risk caused by floods enables to assess the need for flood protection measures also with respect to damage to the environment and can be the starting point for assessing the effectiveness of measures for flood protection from this point of view [Dráb, Říha 2001].

2.4 Measure of acceptability of environmental risk

An expression of economic effectiveness with respect to damage to the environment is very complex. In this case we consider that the measure of environmental risk in consequence of floods is a dimensionless variable as it is a point range. Therefore, flood protection measures (FPM) effectiveness with respect to protection of the environment is determined as the measure of lowering environmental risk (MR) calculated in percentages according to formula (5):

$$MR = 100 - \frac{EnR(\text{postimplementationFPM})}{EnR(\text{preimplementationFPM})} \times 100 \quad (5)$$

where: EnR total measure of environmental risk [-].

The higher value of this parameter (a higher percentage) means higher FPM effectiveness with respect to protection of the environment.

3. RESULTS

In the flooded areas for the individual Q_N no sludge beds and waste dumps are found and likewise the sewage treatment plant lies outside the flood territory. A pumping station for fuel also lies outside of the flood territory. Therefore, a value of zero is assigned to this potential source of contamination (Tab. 2). An environmental burden assigned to category C (reclaimed/recultivated location) is located in the flood territories Q_{50} , Q_{100} and Q_{1000} . The individual Q_N is for this source in the component category C assigned a value of 0.36 (point value in Tab. 2). The Rosenberg industrial firm is also located in flood territories Q_{50} , Q_{100} and Q_{1000} . The enterprise is not in the meaning of Act no. 277/2005 Coll. assigned to any of the categories of A or B; therefore, in the scope of assessing the consequence it belongs to the component category “not assigned”. To the individual Q_N , specifically Q_{50} , Q_{100} and Q_{1000} , the value 1 is assigned to this line (not assigned) in Tab. 2. Given that Medzev has a sewerage system in place, it is assumed that the percentage of residents without sewerage is in a range from 0 to

40%; therefore, a value of 0.48 (Tab. 2) is assigned to each Q_N . The percentage share of flooded agricultural ground from the total flooded area does not exceed 40% with any overflow, and so the value of 0.36 (Tab. 2) is assigned for this source for each Q_N .

The total consequence is calculated as the sum of the points assigned to the individual source of contamination (column 4 in Tab. 2), located in the flooded area for the given Q_N (the probability of a flood occurring) multiplied by the relevant weight (column 5 in Tab. 2). A summary of the assigned points together with the calculated total value of the consequence (ΣC_i) is given in Tab. 2.

Tab. 2 Calculation of consequences of contamination on the environment

Labelling	Source of contamination	Component category of source of contamination	Point classification of threat	Weight	Q_5	Q_{10}	Q_{50}	Q_{100}	Q_{1000}
Point sources of contamination									
A1	Enterprises with hazardous substances present	Not assigned	5	0.2	0	0	1	1	1
		A		0.3	0	0	0	0	0
		B		0.5	0	0	0	0	0
A2	Sewage treatment plant	to 2000 EO	5	0.14	0	0	0	0	0
		2000 – 10 000 EO		0.21	0	0	0	0	0
		10 000 – 100 000 EO		0.29	0	0	0	0	0
		over 100 000 EO		0.38	0	0	0	0	0
A3	Pumping station	-	3	1	0	0	0	0	
Diffuse sources of contamination									
B1	Waste dumps	for inert waste	5	0.12	0	0	0	0	0
		for non-hazardous waste		0.29	0	0	0	0	0
		for hazardous waste		0.59	0	0	0	0	0

Labelling	Source of contamination	Component category of source of contamination	Point classification of threat	Weight	Q_5	Q_{10}	Q_{50}	Q_{100}	Q_{1000}
Diffuse sources of contamination									
B2	Sludge beds	-	3	1	0	0	0	0	0
B3	Population with no sewerage	0 – 40%	4	0.12	0.48	0.48	0.48	0.48	0.48
		40 – 60%		0.29	0	0	0	0	0
		60 – 100%		0.59	0	0	0	0	0
B4	Agriculture	0 – 40%	3	0.12	0.36	0.36	0.36	0.36	0.36
		40 – 60%		0.29	0	0	0	0	0
		60 – 100%		0,59	0	0	0	0	0
B5	Environmental burden	probable (A)	3	0.29	0	0	0	0	0
		confirmed (B)		0.59	0	0	0	0	0
		reclaimed/re-cultivated location (C)		0.12	0	0	0.36	0.36	0.36
Σ of consequences (C_j)					0.84	0.84	2.2	2.2	2.2

On the basis of Tab. 1 the calculated consequence for all Q_N is assigned to the category “*marginal consequence*” i.e., that the flooding of individual sources of contamination cause only minimal, respectively, no degradation to the environment.

Tab. 3 Resultant measure of lowering of environmental risk

Measure of protection of potential FPM	EnR (pre implementation FPM) (according to (1))	EnR (post implementation FPM) (according to (1); a is increasing)	Measure of lowering of environmental risk (MR) [%]
Q_5	0,317	0,228	28
Q_{10}	0,317	0,156	51
Q_{50}	0,317	0,041	87
Q_{100}	0,317	0,020	94
Q_{1000}	0,317	0	100

In Medzev the effectiveness of the FPM with respect to the protection of the environment is determined as the measure lowering the environmental risk (MR) calculated in percentages according to relationship (5). The resulting values are shown in the following Tab. 3.

From Tab. 3 it follows that construction of FPM, e.g., protection against floods of Q_{10} , the measure of environmental risk in consequence of flooding is reduced by up to 51%.

4. DISCUSSION AND CONCLUSIONS

The proposed methodological approach is applied in a modelled territory. Assessment of potential flood damage and subsequent determining of the measure of flood risk is carried out for the town of Medzev, which was in the scope of preliminary assessment of flood risk in Slovakia evaluated as an area with an existing potentially significant risk of flood. Given the preliminary results, we can state that in the studied location Medzev the building of FPM makes sense, mainly in relation to the protection of property and the environment. Because the actual proposed FPM, and thus their costs, are not known, it is not possible to assess this effectiveness. For determining effectiveness it is necessary to obtain documents on the proposed solutions of flood protection measures and subsequently assess the economic effectiveness of the individual assessed FPM variants. The obtained results can then be subsequently applied during the selection of the final FPM solution in the studied location mainly in decision-making process when the water managers will choose the degree of flood protection (eg. Q_{10} or Q_{100})

5. REFERENCES

- Act no. 277/2005 Coll amended Act no. 261/2002 Coll on prevention of significant industry accidents
- DRÁB, A., ŘÍHA, J. 2001. Application of risk analysis in flood protection measures assessment (in Czech). *Workshop: Extreme hydrological events in catchments*. Praha.
- DRBAL, K. et al. 2008. *Methodology for flood risk and damages determination in flooded area* (in Czech). Brno: T. G. Masaryk Water Research Institute, 72 p.
- ENVI, s.r.o. 2013. *Urban plan for Medzev* (in Slovak). [online]. Available at: <<http://medzev.sk/uzpmedzev-par.pdf>>.
- GAŇOVÁ, L. 2014. *Assessment and management of flood risks in selected river basins regarding the Directive 2007/60/EC* (in Slovak). Thesis. Kosice Technical University, 189 p.
- HORSKÝ, M. 2008. *Methods of potential flood damages assessment and its application in GIS* (in Czech). Thesis. Praha: CTU, 124 p.
- MEYER, V., MESSNER, F. 2005. *National Flood Damage Evaluation Methods, A Review of Applied Methods in England, the Netherland, the Czech Republic and Germany*. UFZ, Department of Economics.

- ŘÍHA, J. et al. 2005. *Risk analysis of flooded areas* (in Czech). Brno: CERM, 286 p.
- SATRAPA, L., FOŠUMPAUR, P., HORSKÝ, M., BROUČEK, M., NEŠVAROVÁ, P. 2011. Effectivity assessment of flood protection actions in strategic expert activity of program Flood prevention in Czech republic (in Czech). In: *River basin management and management of flood risks 2011*. Casta Papiernicka – Bratislava: Water Research Institute, 2011.
- Directive on the assessment and management of flood risks* (2007/60/EC). Official J, L288, pp. 27–34. Brussels: The European Parliament and the Council of the European Union, 2007.
- VRIJLING, J.K., VAN HENGEL, W, HOUBEN, R.J. 1998. Acceptable risk as a basis for design. *Reliability Engineering & System Safety*, 59(1), p. 141–150.
- ZELEŇÁKOVÁ, M., GAŇOVÁ, L., PURCZ, P. 2012. Flood risk assessment as part of flood defence. In. *SGEM 2012: 12th International Multidisciplinary Scientific GeoConference*, Albena, Bulgaria, STEF92 Technology Ltd., p. 679–686.
- ZELEŇÁKOVÁ, M., GAŇOVÁ, L. 2014. Flood risk assessment – approach for assessing environmental flood risk. In: *International Scientific Conference People, Buildings and Environment: 15.-17.10.2014*: Kroměříž, Brno: University of Technology, p. 568–576.
- ZVIJÁKOVÁ, L. 2013. *Environmental impact assessment of selected structures (flood protection measures) using risk analysis* (in Slovak). Thesis. Kosice Technical University, 213 p.

Acknowledgement

The contribution is written thanks to support of the project VEGA 1/0609/14.

Multicriteria analysis method for flood risk assessment

J. Kozubík, A. Dráb

(Institute of water structures, Faculty of civil engineering, University of Technology Brno, Žitkova 17, 602 00 Brno, Czech Republic, Kozubik.J@fce.vutbr.cz, Drab.A@fce.vutbr.cz)

Abstract

The flood risk multicriteria analysis is a topical issue which is engaged in the professional community in connection with the flood risk management process. According to the Directive 2007/60/EC of the European Parliament and Council (on the assessment and management of flood risks) and its transposition into Act no. 254/2001 Sb. (Water law) it is necessary to seek an appropriate flood protection measures (FPMs) to mitigate adverse effects of floods on human health, the environment, cultural heritage and economic activities.

For the complex assessment of FPMs variants, nature preservation, urban and architectural design, economic efficiency, heritage preservation and other factors are taken into account. Proposal of an appropriate FPMs necessarily involves the decision-making process which requires simultaneous consideration of all mentioned aspects. For this purpose multi-criteria analysis is suitable tool. This article presents one possible way to applicate multicriteria analysis methods to establish priorities for the progressive design and realization of FPMs.

Keywords

Břeclav, flood, multicriteria analysis, risk, PROMETHEE

1. INTRODUCTION

Directive 2007/60/EC defines the plans for flood risk management that aim to find appropriate measures to mitigate the adverse effects of floods on human health, the environment, cultural heritage and economic activity. Proposal of appropriate flood protection measures (FPMs) necessarily involves decision-making process requiring simultaneous consideration of all mentioned aspects. As a useful support tool for this purpose are the multi-criteria analysis methods as evidenced for example outputs of the project FLOODSITE [Meyer et al., 2007] or these articles [Meyer, Scheuer, Haase, 2009], [Gouldby, Samuels 2005], [Hutter, 2007], [Kienberger, Lang, Zeil, 2009], [Klijn, Samuels, Van Os 2008], [Kubal, Haase, Meyer, Scheuer 2009], [Brans, Mareschal 2005], [Samuels, Klijn, Dijkman 2006], [Schanze et al. 2008], [Brázdová, Říha 2014].

The following paper is a general description of the possible use of multi-criteria analysis in the process of flood risk management. The individual steps are described, analyzed and demonstrated in some practical examples. The article also includes brief description of methods of PROMETHEE II enabling multi-criteria flood risk analysis (MCA).

2. DEFINITION OF THE PROBLEM AND SOLVING METHOD

Decisions regarding proposed flood protection measures (FPMs) requires a comprehensive approach in the evaluation of a number of diverse criteria. At present, the greatest emphasis is on evaluating the economic effectiveness of FPMs and other aspects (eg. social, environmental, cultural) are considered only marginally. The aim of this chapter is to describe selected methods that allow multi-criteria analysis of the different forms of flood risk. MCA process can generally be divided into the following steps:

- problem definition and delimitation of solutions,
- determination and quantification of evaluation criteria,
- selection and application of methods of multi-criteria analysis,
- sensitivity analysis incl. assessment of uncertainties,
- evaluating the sequence of solutions and final recommendations.

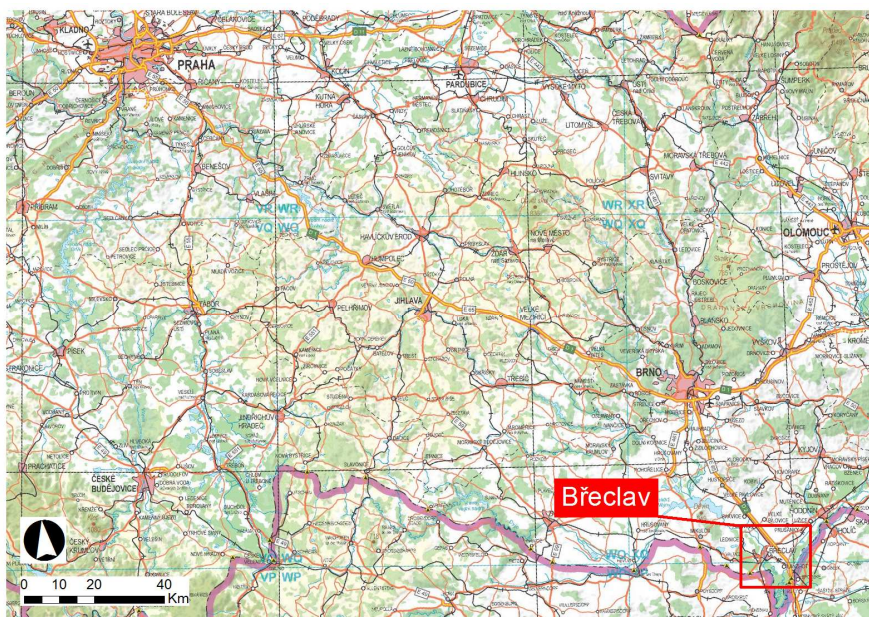


Fig. 1 Břeclav - area of interest in Czech Republic

At the beginning of the solution it is needed to clearly define the objectives, the assumptions for solutions and related requirements for necessary input data. Related to the flood risk management, in the following text we will focus on one of the possible case of using the MCA. It is prioritizing selected areas in the selected location for the design and subsequent implementation of the FPMs. The

aim of the multi-criteria analysis is to determine the sequence of the individual areas within the evaluated group (place) in terms of degree of flood risk.

To solve the problem, it is necessary to establish the appropriate criteria, which we understand as a benchmark for comparison or factor in assessing the options. Established assessment criteria should be made in relation to the method used MCA, since each method requires a specific range of input data and documents. General economic, social, cultural and environmental criteria need to be fleshed out in the relevant indicators, for example in the sense of [EC 2007].

The problem of multi-criteria decision-making is based on the assumption that there is a given set of possible options, the goal is to choose the option that fits the best into the given set of criteria. If a set of options given to the final roster is mentioned, then we talk about multi-criteria evaluation of alternatives. In the following we assume the decision-making under certainty - a condition where all the criteria values are realized with probability equal to 1. The multi-criteria evaluation of alternatives is a wide range of procedures, and the choice of appropriate methods based primarily on the level of knowledge about the preferences between criteria. To solve our problem we defined from the assumption that for the evaluation criteria measure of their importance in terms assigned of their weights is known.

There is a wide range of procedures for multicriterial evaluation and the choice of appropriate methods is based primarily on the level of knowledge about preferences among criteria [DRBAL 2011]:

- aspiration level - for those criteria the minimum (maximum) value must be known, which must variant for the maximization (minimization) reach the criterion to be acceptable (conjunctive method disjunctive method, PRIAM),
- ordinal information – a criteria for their arrangement of importance is known (lexicographical method, permutation method and ORESTE),
- cardinal information – a criteria for evaluating their importance assigned of their weights is known. There are three basic principles of working with the cardinal information:
 - principle of utility maximization (e.g. weighted sum method, AHP),
 - principle of minimum distance from the ideal options (eg. TOPSIS method),
 - principle of evaluating options based on preferential trade (eg. ELECTRE methods, PROMETHEE).

3. PRACTICAL APPLICATION OF METHODS OF MULTI-CRITERIA FLOOD RISK ANALYSIS IN BŘECLAV

3.1 Problem definition

For application of the method pilot site Břeclav watercourse Thaya (Fig. 1) was chosen. The aim of the multi-criteria analysis was to determine the sequence

of the functional areas taken from the urban planning documentation (UPD) in terms of degree of flood risk. The evaluation was based on quantified criteria listed in Tab. 1, which was calculated using equation (1). In addressing flood scenarios appropriate culmination flows Q_5 , Q_{20} , Q_{100} , Q_{500} have been considered. In order to ensure complete order subplots according to UPD were used for evaluation method of PROMETHEE II.

The results of multi-criteria evaluation method of PROMETHEE II are displayed in Fig. 3. Which are captured by the existing functional surfaces of UPD with different shades, depending on the value specified net flux ϕ . The value of ϕ determines the order of the respective functional areas, with the highest net flow ϕ correspond to areas with the highest levels of flood risk expressed according to Tab 1.

3.2 Evaluation criteria

All evaluation criteria are expressed as average annual flood risk, which is given by:

$$RI_i = \int_{p^1}^{p^2} D_i(p) dp \quad (1)$$

where p is the probability of achieving or exceeding the corresponding N -year peak discharge and $D_i(p)$ denotes the function of quantifying the potential flood damage, respectively the extent of affected structures. Method quantification function $D_i(p)$ varies depending on the evaluation criterion as shown in Tab 1.

Tab 1. Evaluation criteria within the meaning of [EC 2007]

i	Expressing risk RI_i	Unit	Expression matching function $D_i(p)$	Unit
1	The average annual loss per unit of the flooded area	RI_1 [CZK/m ² .year]	Property damage per unit area of the flooded area	[CZK/m ²]
2	Average annual number of population affected	RI_2 [people/year]	The number of affected population	[people]
3	The average annual number of affected cultural and historical monuments	RI_3 [objects/year]	Number of affected cultural and historical monuments	[objects]
4	The average annual number of interested potential pollution sources	RI_4 [sources/year]	The number of potential sources of accidental pollution of water in case of flooding during flood	[sources]

A more detailed description of the criteria is given in the following paragraphs.

3.2.1 Property damage

The principle of calculating property damage is based on the methodology of flood hazard maps and flood risk management [DRBAL 2009].

Potential direct material flood damages are determined by a procedure based on the application of curves damage (CD). Construction of the CD is based on a detailed analysis of flooding effects on individual categories of objects and component parts of their structures. Each CD is expressed in a certain range of values of potential damage. Upper and lower limit of damage is avoided due to the possibility of applying various failures of components of the structure of the resulting damage. Actual damage, expressing the costs of bringing the building to its original operating state moves within this interval.

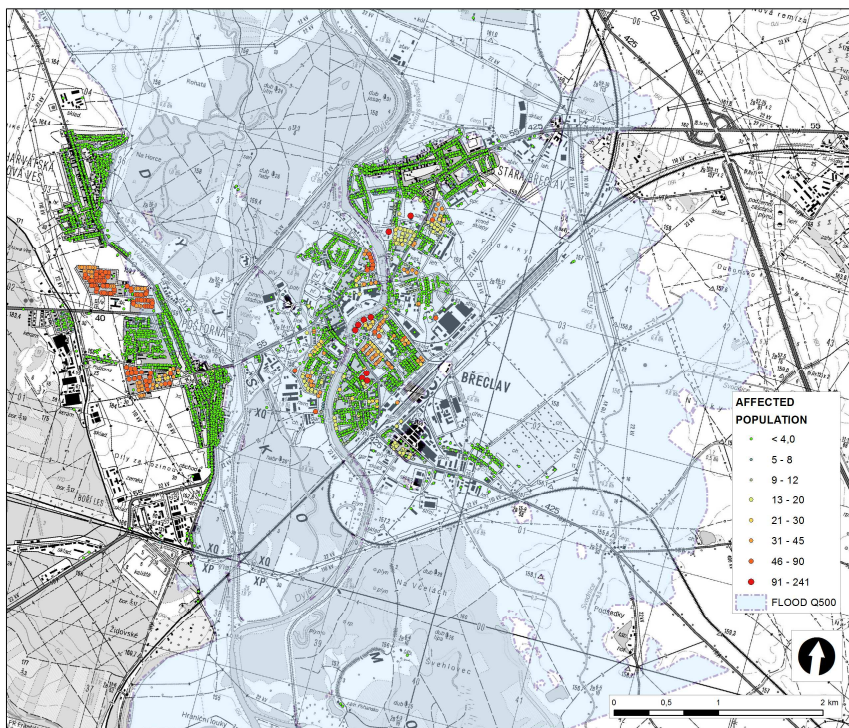


Fig. 2 Affected population

3.2.2 Affected population

The source for the number of people affected in the area of interest was the Register of Enumeration Districts and buildings administered by the Czech Statistical Office (CSO). Part of the register called “Buildings layer” with a house number [Štěpánková 2012], which contains a spatial localization of buildings with a house number in the form of definition point range, exists for the whole Czech

Republic and completeness is about 98.4% of the total registered number. This layer contains several dozens of attributes (for example the house number, street, cadastre, method of use and more). For the calculation of the persons that were affected the most important attribute was SUM_BYT (number of apartments in the building). Details about this layer are available on the CSÚ website [ČSÚ 2014].

But the number of apartments in the building is not sufficient because you need to have the right number of people (Fig. 2). For that you can take the advantage of the Geoportal CENIA [GEO 2014], a layer CENIA_OBYV_BYT (number of people per apartment), which contains cartogram showing the average number of residents per dwelling in the villages of the Czech Republic. For Breclav 2,477 (for example Prague 2,068 and 2,173 for Brno). Details about this layer are available on the website of the National Geoportal CENIA. We got total number of people at one address point by multiplying the number of dwellings in a given location and population per dwelling.

3.2.3 Cultural and historical monuments

Cultural monuments are among the sensitive objects, which in the framework of risk analysis requires special attention and define (classify) the risks arising from their exposure to the floods (eg. for the solved area Chateau Pohansko).

Part of the Heritage Fund of the Czech Republic, protected by law no. 20/1987 about state monument care, are registered in the Central list of cultural monuments of the Czech Republic (ÚSKP). The list includes:

- UNESCO,
- national cultural heritage (NKP),
- cultural monuments,
- listed territory,
- heritage protection zones.

3.2.4 Pollution sources

Pollution sources include industrial pollution and wastewater treatment plants.

Information about potential sources of industrial pollution were drawn from PRTR Environment (established under Law No. 76/2002) and Register of industrial pollution sources - part of the dangerous substance (RPZZ). RPZZ is focused on an inventory of waste and emissions of hazardous substances in the industrial sphere into the aquatic environment (surface water and sewer systems), and assessing compliance with the requirements of national laws and regulations, especially Government Decree no. 61/2003 as amended 23/2011.

The basic source of data on existing wastewater treatment plant (WWTP) - potential sources of municipal pollution - the database was created as a part of the project Identification of anthropogenic pressures on the status of water quality and aquatic ecosystems in the Morava and Thaya (VaV/SP/2e7/73/08). In this database there are recorded only sewage treatment plant for more than 2 000

population equivalent, which represents in the project area only 20 municipalities out of a total of 73.

Further localization WWTP was performed using the database ZABAGED and its attribute KC_TYPZASTAVBY (type of targeted buildings). Other information (eg. The type WWTP) are not recorded in the database.

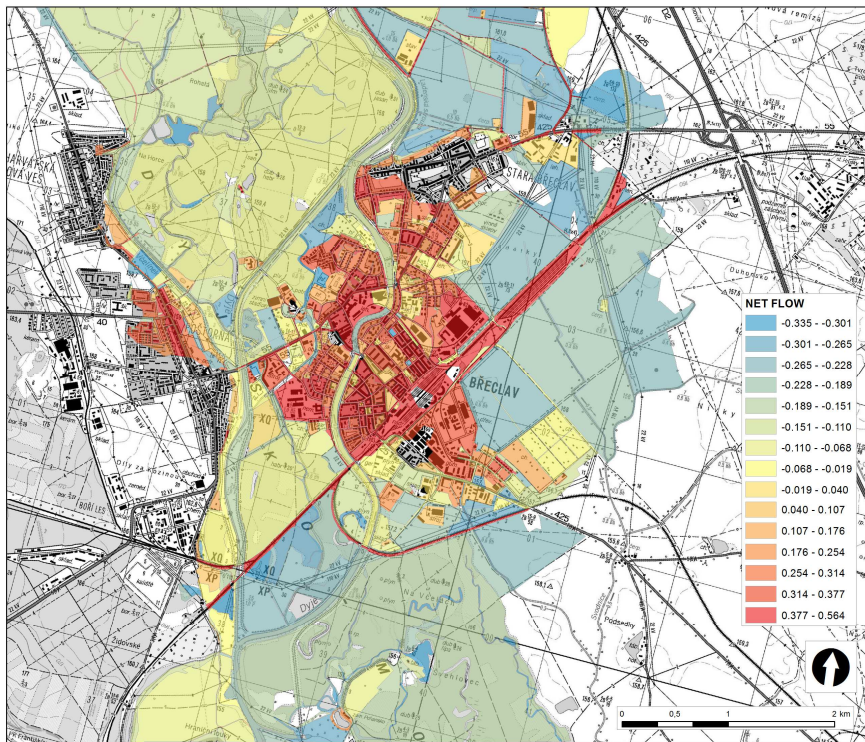


Fig. 3 Results of PROMETHEE II - net flow to areas of the UPD Břeclav

3.3 Selection and application of method

For evaluating the variant we used a method of PROMETHEE II, which is based on an approach based on the so-called preferential session. The aim of the evaluation was to determine the sequence of areas taken from the urban planning documentation in terms of the degree of flood risk. Outputs were published by GIS software and these layouts show areas with the highest net flow ϕ correspond to areas with the highest levels of flood risk.

4. CONCLUSION AND DISCUSSION

As a contribution there were presented sub-options of using the method of PROMETHEE II for multi-criteria analysis of flood risk. The procedures described above are particularly useful for assessing the current situation in the localities of interest when it is necessary to evaluate the most vulnerable areas in terms of flood risk, in order to set priorities for the subsequent implementation of flood control measures. The methods presented certain disadvantage, which is the fact that the so-called values of net flow resulting from the methods of PROMETHEE II are dimensionless and only serves as a benchmark for determining the order within the evaluated group of faces.

The net flow (Fig. 3) in any case do not represent an absolute measure of flood risk. The method is relatively easy to implement using GIS tools. Likewise, the evaluation results can be clearly presented in the form of maps, in which the order of assessed areas is expressed through the colour scale according to the value of the calculated net flow.

Another line of research in the field of application of methods of multi-criteria analysis of flood risk authors see especially in the more detailed elaboration of methods for expressing flood risk posed by the threat of people's cultural heritage, potential sources of water pollution and sensitive objects. A related issue qualified the weights of the individual evaluation criteria, which may significantly affect the results of the analyses.

5. REFERENCES

- BRANS, J.P., MARESCHAL, B. 2005. PROMETHEE methods. In: Figueira, J., Greco, S., and Ehrgott, M., (Eds.), *Multiple Criteria Decision Analysis: State of the Art Surveys*, Springer, New York, 2005, ISBN 0-387-23067 – X, pp. 163-195.
- BRÁZDOVÁ, M., ŘÍHA, J.: A simple model for the estimation of the number of fatalities due to floods in central Europe, *Nat. Hazards Earth Syst. Sci.*, 14, 1663-1676, doi:10.5194/nhess-14-1663-2014, 2014.
- ČSÚ 2014, Czech Stat. Office, http://www.czso.cz/csu/rso.nsf/i/budovy_s_cislem
- DRBAL, K., aj. *Metodika tvorby map povodňového nebezpečí a povodňových rizik*, VÚV T. G. M. Brno, 2009.
- DRBAL, K., aj. *Mapy rizik vyplývajících z povodňového nebezpečí v ČR*, VÚV T. G. M. Brno, 2011.
- ES 2007. Directive 2007/60/EC of the European Parliament and of the Council of 23 October 2007 on the assessment and management of flood risks, European Parliament, Council, 2007
- GEO 2014, Geoportál CENIA, <http://geoportál.gov.cz>
- GOULDBY, B., SAMUELS, P. 2005. *Language of Risk*. Report T32-04-01. FLOODsite Consortium.

- HUTTER, G. 2007. Strategic Planning for Long-Term Flood Risk Management. IPS - International Planning Studies. Vol. 12, No. 3, pp. 273-289.
- KIENBERGER, S., LANG, S., ZEIL, P. 2009. Spatial vulnerability units – expert-based spatial modelling of socio-economic vulnerability in the Salzach catchment, Austria, *Nat. Hazards Earth Syst. Sci.*, 9, pp. 767-778.
- KLIJN, F., SAMUELS, P., VAN OS, A. 2008. Towards Flood Risk Management in the EU: State of affairs with examples from various European countries. *International Journal of River Basin Management*, 6 (4). pp. 307-321.
- KUBAL, C., HAASE, D., MEYER, V., SCHEUER, S. 2009. Integrated urban flood risk assessment – adapting a multicriteria approach to a city, *Nat. Hazards Earth Syst. Sci.*, 9, 1881-1895.
- MEYER, V. et al. 2007. GIS-based Multicriteria Analysis as Decision Support in Flood Risk Management. Report T10-07-06. FLOODsite Consortium.
- MEYER, V., SCHEUER, S., HAASE, D. 2009. A multicriteria approach for flood risk mapping exemplified at the Mulde river, Germany. *Nat. Hazards* 48, 17–39, DOI: 10.1007/s11069-008-9244-4.
- SAMUELS, P., KLIJN, F., DIJKMAN, J. 2006. An analysis of the current practice of policies on river flood risk management in different countries. *Irrigation and Drainage*, 55, S141–S150.
- SCHANZE, J. et al. 2008. CRUE Research Report No. I-1: Systematisation, evaluation and context conditions of structural and non-structural measures for flood risk reduction. FLOOD-ERA Joint Report. ERA-NET CRUE.
- ŠTĚPÁNKOVÁ, P., aj. Potenciální povodňové škody a rizika v povodí Moravy a Dyje – projekt CEframe, VÚV T.G.M. Brno, 2012.
- 20/1987 Sb. o státní památkové péči
- 61/2003 Sb., o ukazatelích a hodnotách přípustného znečištění povrchových vod a odpadních vod, náležitostech povolení k vypouštění odpadních vod do vod povrchových a do kanalizací a o citlivých oblastech
- 76/2002 Sb. o integrované prevenci a o omezování znečištění, o integrovaném registru znečišťování a o změně některých zákonů (Integrated prevention law)
- 254/2001 Sb. o vodách a o změně některých zákonů (Water law)

Acknowledgment

This paper was made with the support of specific research project of Brno University of Technology no. FAST-J-15-2776 "Analysis of methods of multicriteria evaluation of flood risk".

Overview of water resource based human carrying capacity assessment models

M. Kuspilic, Z. Vukovic, I. Halkijevic

Water Research Department, Faculty of Civil Engineering, University of Zagreb, Andrije Kacica-Miosica 26, 10 000 Zagreb, Croatia, phone: +385 1 4639 610, fax: +385 1 4639 238, e-mail: mkuspilic@grad.hr, vukovic@grad.hr, halkijevic@grad.hr

Abstract

Human carrying capacity is defined as the maximum human population size which the environment can sustain indefinitely, given its resources. It is a threshold value which can be used as a measure of sustainability of a certain ecosystem. Water resources are a crucial element of any given ecosystem, as their availability precedes all other activities in the ecosystem. Unsustainable management of Earth's water resources has already caused environmental degradation and even destruction of certain local ecosystems. In order to prevent such events, it is necessary to define a boundary such as the water resource based human carrying capacity which will evaluate if the observed system has the ability to sustain human activities indefinitely. It is a difficult task, as it requires creation of a model which has to accurately evaluate the quantity, quality and availability of water resources, human water consumption and level of degradation of available resources caused by human activities. This paper contains an overview of most recent models created with the purpose of assessing the water resource based human carrying capacity.

Keywords

water resources, human carrying capacity, sustainability, carrying capacity assessment model

1. INTRODUCTION

Carrying capacity can be defined as a number of individuals of a given species that a given habitat can support without being permanently damaged. The concept is used to point out there is a limit to the growth of biological populations, and an analogy can be made for human societies – there is a maximum number of humans that can be supported indefinitely in a given environment. [Schroll et al., 2012]

If the human population exceeds the carrying capacity of its habitat, then either the resources required to meet the needs for human activities will be depleted, or the wastes produced will build to the point of poisoning the population, or both, and the population will crash. [Zhao et al., 2005]

Although exceedance of human carrying capacity will not result in extinction of the species, it may have drastic effects and alter our ecosystem in a way which will be able to sustain less human activities. [Motesharrei et al., 2014]

For this reason, human carrying capacity is an important tool for sustainability assessment of populated regions. Carrying capacity depends on the population size, availability of required resources, and the consumption rate of needed resources. Additionally, in order to accurately assess the carrying capacity of an observed system, all sustainability components; environmental, social and economic need to be taken into consideration.

Human carrying capacity is not a fixed value; technological advances and institutional measures which reduce the consumption rate of resources and assure the long term health of the ecosystem from which the resources are extracted will result in a higher human carrying capacity.

Scarcity of resources may be caused by natural processes or by human activities. Although we may not be able to affect natural processes, it is possible to regulate human activities which cause environmental degradation and pollution, effectively reducing the regional carrying capacity. In order to build evidence to support such actions, carrying capacity assessments can be very useful as they should provide a threshold value of sustainability.

2. WATER RESOURCE BASED CARRYING CAPACITY

Significant amount of human carrying capacity models have been introduced, from *World3* [Meadows, 1973] up to the latest, *Carrying capacity dashboard* [Lane et al.,2014] which only take into account land use as the crucial parameter for determination of maximum sustainable population. Although the models are very detailed and complex, availability of water resources is usually not covered, at least not directly.

In order to reduce the complexity of carrying capacity assessment and implement water availability as an important factor, water resources carrying capacity (WRCC) is introduced. WRCC represents the human population which the environment can sustain indefinitely, given its available water resources. In general, WRCC assessment regards water resources as the key element of sustainability, as insufficient water resources will hold back all other human activities. Since one of the essential resources for almost all of human activities is water, its availability usually precedes all other activities.

Liebig's law of the minimum states that growth is controlled not by the total amount of resources available, but by the scarcest resource (limiting factor). In the following figure (Fig.1), a graphical representation of this concept is given, where the capacity of the barrel is limited by its shortest section.

Liebling's law can be implemented in WRCC assessment methods, where water resources can be considered as the limiting factor of growth. This assumption may not be true for some regions, as food, clean air or raw materials may be the limiting factor of growth in those cases. However, for all regions water availability is an important measure of sustainability. Even if water resources are not the limiting factor they usually represent an integral part of sustainability assessment.

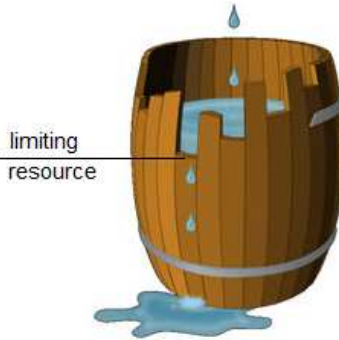


Fig. 1 Graphical interpretation of Liebling's law of minimum

2.1 Water resources carrying capacity definition issues

Unfortunately, WRCC still has no clear definition, and some authors have a different view of the concept. Two predominant definitions have been used in order to define this concept. WRCC is expressed as one of the two following values:

- (1) Maximum infinitely sustainable population size of a region given its available water resources
- (2) Largest infinitely sustainable development scale of a region given its available water resources

First definition is the one which relates to the original (ecological) concept of carrying capacity, a value which is ultimately expressed in measurement units such as person, resident etc.

Second definition is more closely linked to the economic aspect of sustainability and is most often expressed in measurement units of currency, as a maximum revenue which can be generated by given water resources if they are sustainably managed. [Liu et al., 2013, Song et al., 2011]

3. MOST RECENT WATER RESOURCES CARRYING CAPACITY MODELS

Most research regarding WRCC assessment has been done in China, as its large population and high economic growth put a lot of strain on the environment. Increased demand for water caused by population and industry as well as increased pollution of available water resources threatens the sustainability of many regions, especially arid ones. [Cheng et al., 2010, Min et al., 2011]

Multiple assessment attempts have been examined, and three have been selected as they are representative of most recent trends in regional WRCC assessment.

These assessment methods have been analyzed in order to evaluate the validity of achieved results.

- (1) *Li* proposes a simple equation as a method of determining the maximum sustainable population. Its simplicity makes it a good macroscopic indicator of regional sustainability, although it may not be applicable to large heterogeneous areas. [Li, 2012]
- (2) *Dang et al.* proposed a more complex model, where two values of carrying capacity were calculated. One was designed to assess the carrying capacity of analyzed region by examining available water resources and their consumption, while the other took into consideration the effect of water consumption rate and pollution on environmental sustainability. Out of these two, the lower value was selected as the computed WRCC. [Dang et al., 2014]
- (3) *Dou et al.* proposed the most comprehensive method of assessing the WRCC based on large scale system theory and optimization method. Unlike the previous two, this method defines the carrying capacity as the maximum socioeconomic scale, and its results are expressed as an index defined as the ratio of the current GDP (Gross domestic product) and the highest sustainable GDP. [Dou et al., 2015]

All of the models attempted to calculate WRCC according to its own definition of the concept for a period in the future, some have even analyzed the predicted WRCC trends. Methods used for prediction of population or industry growth were not analyzed in this paper, only the methods of assessing the WRCC, whether it applied to current or a future predicted period.

3.1 Available water resources assessment

Crucial component of WRCC assessment is an accurate estimation of volume of available regional water resources. According to the scope of the task, its temporal and spatial distribution may be important for the analysis as well. Data regarding water resources needs to be gathered from credible sources or by reliable measurements in order to accurately determine the amount of available water generated from precipitation, groundwater as well as surface water which inflows into the analyzed area.

All assessment models analyzed in this paper collected the data from adequately reliable resources, such as deliverables given by ministries, national statistical institutions and scientific institutions.

Three different approaches have been observed in the assessment of available volume of water resources:

1. Mean annual value of available surface water and groundwater was used in the calculation, neglecting its temporal and spatial variation

2. Mean annual value of available surface water and groundwater was computed, as well as total volume of available water available in drier periods, with the probability of occurrence of 5 [%] and 25 [%], in order to assess the WRCC. Spatial variation in occurrence of water resources has been taken into account by dividing the analyzed area into smaller regions.
3. Dynamic temporal and spatial variation of availability of water resources has been taken into account, in order to determine the worst case scenario regarding the availability of water resources

Spatial availability of water resources has been considered by Dang et al. and Dou et al. assessment methods, while Li did not factor this into their model.

Temporal availability of water resources has been properly considered by Dou et al., while other models only took into account mean yearly values of available volume of water (Li) or other statistical values (Dang et al.).

Pollution of water resources is considered as a factor which reduces the amount of available water by Dang et al. and Dou et al., while Li fails to take this effect into consideration.

Selected methods were analyzed according to three factors: their ability to accurately assess available water resources, water consumption and restraints which need to be imposed in order to achieve sustainability.

3.2 Assessment of water consumption caused by human activities

Much like available water resources assessment, amount of water consumed by human activities is a crucial part of the assessment models, and all observed models have gathered data from credible sources.

Water consumption was analyzed by all authors by different categories: industrial, agricultural and municipal (domestic).

Municipal (domestic) water consumption was calculated by all methods with the use of the water consumption quota (expressed in [unit of volume/person*day]) which was multiplied with the number of inhabitants of the analyzed regions. Distinctions have been made between the consumption quota of the rural and urban population. Duo et al. and Dang et al. took into consideration the differences in population density of the regions, while this was not the case with the method proposed by Li.

Parameter called industrial output per unit of water [unit of water / unit of currency] was used in the estimation of amount of water consumed by industry and agricultural activities in the method proposed by Li. Although introduction of this value significantly simplifies the WRCC estimation process, as the amount of water used by industry and agriculture can be estimated by multiplying the introduced parameter with the income (gross product) generated by these sectors, there is a strong possibility this will lead to unreliable results.

Duo et al. and Dang et al. gathered the statistical information on water consumption of industry and agriculture from credible institutions and calculated

the total amount of water consumed by these sectors, which should result in very accurate results.

Temporal variation in the water consumption was not considered by any of the models, while spatial variation was considered in more complex models (Duo et al., Dang et al.).

3.3 Assurance of social, economic and environmental sustainability

Sustainability can be achieved only if its three key aspects are fulfilled: economic, social and environmental sustainability. Chosen methods have been studied for their ability to determine if water resources are used in a way to help fulfill these three sustainability traits. Sustainability elements were considered by all authors by imposing restraints.

3.3.1 Environmental sustainability

Li defined the amount of required “ecological water”, a minimal amount of water needed for supporting the ecological cycle.

Dang et al. also determined the amount of water needed for the indefinite existence of the ecological system. Additionally, pollution of water resources was also taken into account in the assessment of sustainability as well as spatial distribution of these factors. Amount of wastewater generated by human activities, its COD levels and the self- purification capacity of the river have been used in order to determine the impact of anthropogenic pollution. An indicator of ecological sustainability was calculated based on these values.

Duo et al. obtained the value of ecological water demand from the statistical data of water conservancy departments and implemented it into its dynamic model. Pollution of available water resources was quantified by its permanaganate index (CODMn), a value which determines the level of organic pollution. In order to assess if sufficient protection of the ecosystem is achieved, maximum value of CODMn concentration has been defined as a threshold value.

3.3.2 Economic sustainability

No indexes of economic stability or sustainability were calculated by any of the analyzed methods. Industrial and agricultural water demand was calculated and implemented in all the models, but an assumption has been made that by all authors that this consumption rate is caused by a sustainable economic system, which may not be true.

3.3.3 Social Sustainability

Although it is difficult to find a link between aspects of social sustainability such as social equality, justice etc. and water resources, management of water resources does have an impact on the quality of life, which is an integral part of social sustainability.

Social sustainability was not considered or evaluated by Li or Dang et al. Dou et al., however, did implement two socioeconomic restraints, a minimal value of

GDP per capita and a minimal amount of grain produced per capita. These minimal living standards were used to assess if adequate quality of living is achieved by current water resources management.

4. CONCLUSIONS

Water based resources carrying capacity (WRCC) is a new, still not sufficiently defined concept. Although, according to the biological and ecological definition of carrying capacity, it should be defined as a maximum infinitely sustainable population size of a region given its available water resources, consensus had not been reached on its definition. Many authors still regard it as a maximum sustainable economic scale (GDP) achieved by sustainable water resources management. Regardless of this fact, all methods recognize the concept as a threshold value of sustainability which can be achieved by management of water resources.

Proposed methods of WRCC assessment range from simple ones to complex systems which give a more comprehensive view of water resources management. Simple methods can be used as macroscopic indexes, as a very crude assessment of sustainability of water resources management, but should not be used for large regions with significant differences in spatial water availability and consumption. More complex models provide a better overview of regional WRCC in these cases, although they require more time and resources for their completion.

Majority of the proposed models have a very comprehensive analysis of available regional water resources and the water consumption patterns of all sectors (industry, agriculture and domestic use).

Additionally, authors of most models also recognize the importance of a healthy ecosystem as a basis for sustainability. Different methods have been used in order to assess if the ecosystem's water resources are able to sufficiently replenish under different anthropogenic stresses, such as water abstraction and pollution.

Threshold values of environmental sustainability have been clearly defined by most authors, but economic and social aspects of sustainability have not been considered, or only marginally by available models.

Allocation of water resources towards a sustainable economic system was not considered by any of the methods, and assurances if water resources are being managed in a way to achieve an acceptable level of quality of life was considered by only one model. Most improvements need to be made in assessing the threshold values of these two components of sustainability, social and economic.

Water resources carrying capacity assessment importance is reflected in its ability to define the maximum level of human activities the ecosystem can sustain indefinitely, while achieving a predetermined quality of live, especially in regions where water availability is a limiting factor of growth. It can be used as a valuable tool in sustainable water management practices, and available methods, although

incomplete to a certain degree, can give a valuable insight into achieved level of regional sustainability.

5. REFERENCES

- CHENG, L., 2010. System dynamics model of Suzhou water resources carrying capacity and its application. *Water Science and Engineering*, 144-155 p.
- DANG, L., XU Y., WANG Z., 2014. The Population Carrying Capacity of Water Resources in Yulin City. *Asian Agricultural Research*, 85-91 p.
- DOU, M., MA J., LI G., ZUO Q., 2015. Measurement and assessment of water resources carrying capacity in Henan province, China. *Water Science and Engineering*, 1-12 p.
- LANE, M., DAWES, L., GRACE, P., 2014. The essential parameters of a resource-based carrying capacity assessment model: An Australian case study. *Ecological Modelling*, 220-231 p.
- LI, M., 2012., The Calculation and Analysis of Water Resource Carrying Capacity in Chongqing, China, *International Journal of Remote Sensing Applications*, 20-23 p.
- LIU, H., HAN H., ZHAO S., 2013. Analysis and Assessment of the Regional Water Resources Carrying Capacity Model. *International Journal of Advancements in Computing Technology*, 764–770 p.
- MEADOWS, L., 1973. Dynamics of Growth in a Finite World: A technical report on the global simulation model World 3, Thayer School of Engineering, Dartmouth College
- MIN D., ZHENGE X., LIMIN P., YUNHAI Z., XIUFENG X., 2011. Comprehensive Evaluation of Water Resources Carrying Capacity of Jining City. *Energy Procedia*, 1654 -1659 p.
- MOTESHARREI S., RIVAS J., KALNAY E., 2014. Human and nature dynamics (HANDY): Modeling inequality and use of resources in the collapse or sustainability of societies. *Ecological Economics*, 90-102 p.
- SCHROLL, H., ANDERSEN, J., KJAERGAARD, B., 2012. Carrying capacity: An Approach to Local Spatial Planning in Indonesia. *The Journal of Transdisciplinary Environmental Studies* vol. 11, no.1, 27-39 p.
- SONG, X., KONG F., ZHAN C., 2011. Assessment of Water Resources Carrying Capacity in Tianjin City of China. *Water Resources Management*, 857-873 p.
- ZHAO, S., LI, Z., LI, W., 2005. A modified method of ecological footprint calculation and its application. *Ecological Modelling* 185, 65-75 p.

Considering Uncertainties in Design of Stormwater Infiltration Facility

D. Duchan, J. Říha

Brno University of Technology, Faculty of Civil Engineering, Institute of Water Structures,
Veveří 95, 602 00 Brno, E-mail: duchan.d@fce.vutbr.cz, riha.j@fce.vutbr.cz

Abstract

For a hydraulic design of a facility for rainwater infiltration, i.e. a design of the volume of the infiltration facility, the so-called coefficient of infiltration is introduced, determined by an infiltration test. The use of the coefficient of infiltration brings a number of uncertainties into the solution, arising particularly from different conditions in carrying out the infiltration test and in operating a real infiltration facility. This paper presents an analysis of factors that influence the process of infiltration and relating uncertainties that influence the determination of the storage volume of the infiltration facility. The effect of the individual factors on the design of the infiltration facility was analysed using numerical simulations by the software HYDRUS-2D. The uncertainties are expressed using partial reliability coefficients.

Keywords: *stormwater management - infiltration facility - coefficient of infiltration –limit states*

1. INTRODUCTION

The rainwater management in an urbanised territory is traditionally carried out using a system of urban drainage. This method leads to overdimensioning and temporary overloading of sewers. An alternative approach to the integrated control of rainwater prefers the accumulation and infiltration of rainwater at the place of its formation [Griseček et al. 1996], [Watkins 1997]. At the present time, this approach is applied using directives and regulations. In the Czech Republic (CR), the requirements for rainwater infiltration are enshrined in the building law [Act No. 183/2006 Coll.] and in the water law [Act No. 254/2001 Coll.]. In the last decades, guidelines and standards have been developed abroad for the design of infiltration facilities [ATV-DVWK 2007], [Bloomberg, Strickland 2012], [DWA 2005] and [SMGM 2014]. In the Czech Republic, these are the Czech technical standards CSN 75 9010 and TNV 75 9011.

The standard CSN 75 9010 describes geological and hydrogeological surveys, the result of which is the determination of the coefficient of infiltration. The standard also gives a procedure for designing the volume of infiltration facilities.

The issue of infiltration and flow of water in the unsaturated zone was elaborated in a number of studies which were a basis for compiling relevant

software products. The problems of water flow in the saturated and unsaturated zones and their modelling were elaborated for example in the studies [Bear, Verrujit 1992], [Lu, Likos 2004], [Šimůnek et. al 2006] and [Šejna, Šimůnek 2007]. For the use of numerical models it is necessary to obtain the required geological and hydrogeological information about the structure of the groundwater (GW) body, the properties of porous materials in the zone of infiltration, their deposition and the regime of GW at the site. In case of a design for smaller or less important facilities, the extent of the geological survey is usually limited; the use of GW flow models is practically excluded for the reason of a lack of financial resources.

The design for the volume of infiltrated water and an infiltration facility is carried out using variables characterizing the infiltration capacity of soil - the coefficient of infiltration [CSN 75 9010], hydraulic conductivity [DWA 2005] or infiltration rate [Bloomberg, Strickland 2012]. The parameters of infiltration are generally determined on the basis of the results of infiltration tests. It is also considered that such determined parameters sufficiently represent the conditions at a site, i.e. the permeability of a GW body, the homogeneity and anisotropy of materials, the moisture content of soil, the state of GW table and the depth to the impermeable basement.

Practical experience shows that the determined value of the coefficient of infiltration does not reflect the real state and relating uncertainties and may lead to the underestimation of the volume of the designed infiltration facility, particularly during a long-lasting operation of the facility. The recommended coefficient of safety $f \geq 2$ is not specified in detail.

The following text analyses the factors influencing the reliability of design for the storage volume of an infiltration facility. The effect of the individual factors was quantified by extensive numerical calculations made by the software product HYDRUS-2D [Šejna, Šimůnek 2007], as well as by a professional estimate. The uncertainties of the individual parameters entering into the calculation are expressed using partial coefficients of reliability.

2. THE VOLUME OF THE INFILTRATION FACILITY

2.1 Discussion about the procedure according to CSN 75 9010

The storage volume of an infiltration facility V_{VZ} is determined as:

$$V_{VZ} \geq \max_{t_c=0, t_{c,max}} (V_S - V_{VSAK}), \quad (1)$$

where V_S is the volume of precipitation per the time t_c , V_{VSAK} is the infiltrated volume per the time t_c and t_{max} is the maximum duration time of substitute rain (e.g. 72 hours according to CSN 75 9010).

$$V_{VZ} \geq \max_{t_c=0, t_{c,max}} \left[\frac{h_d}{1000} \cdot (A_{red} + A_{VZ}) - \frac{1}{f} \cdot k_v \cdot A_{VSAK} \cdot t_c \cdot 60 \right] \quad (2)$$

where V_{VZ} is the storage volume of the infiltration facility (m^3), h_d is the total design precipitation (mm) with the duration t_c (min) and the periodicity, A_{red} is the plan view of the drained area (m^2), A_{VZ} is the area of the infiltration facility (m^2), A_{VSAK} is the infiltration area (m^2), f is the coefficient of safety $f \geq 2$ [CSN 75 9010].

In the relation (2), all variables are subject to uncertainties, however the coefficient of safety is related only to the infiltrated volume. Practical experience suggests that most designers determine the coefficient $f = 2$, namely for economical reasons. The size of the coefficient requires a more detailed discussion; it is determined on the basis of an infiltration test and is defined as follows:

$$k_v = \frac{Q_{ZK}}{A_{ZK}} \quad , \quad (3)$$

where Q_{ZK} is the volume of infiltrated water during the trial infiltration test or the inflow of water into an trial object and A_{ZK} is the infiltration area in a test object, specified in the standard. For the design of an infiltration facility, the flow rate Q_{VSAK} of infiltrated water is determined according to CSN 75 9010 from the relation:

$$Q_{VSAK} = \frac{1}{f} \cdot k_v \cdot A_{VSAK} \quad . \quad (4)$$

The coefficient of infiltration k_v is determined by an infiltration test with a recommended duration of 24 hours. Other requirements for infiltration tests are specified in [CSN 75 9010]. Practical experience shows that the test duration of 24 hours is seldom achieved; the common duration of infiltration tests is 6 to 8 hours.

The amount of infiltrated water Q_{ZK} changes during the infiltration test and, at the same time, the area A_{ZK} can also change. The coefficient of infiltration is thus a time-dependent variable during the infiltration test:

$$k_v(t) = \frac{Q_{ZK}(t)}{A_{ZK}(t)} \quad . \quad (5)$$

Nevertheless CSN 75 9010 does not state how to evaluate the coefficient of infiltration in such a case. One of the possibilities is to derive the total infiltrated volume of water by a numerical integration of the time dependent inflow of water into an trial object during the test. Because both the coefficient of infiltration and the infiltration area change with time, Q_{ZK} is also a function of time. Using the basic relationships of GW hydraulics [Bear, Verrujit 1992], the infiltrated flow rate can be expressed by means of the equation [Lu, Likos 2004]:

$$Q_{VSAK}(t) = \int_{A_{ZK}(t)} \mathbf{q}(x, y, z, t) \cdot dA, \quad (6)$$

where \mathbf{q} is the vector of the specific flow rate that is defined for the saturated and unsaturated zones as:

$$\mathbf{q} = \mathbf{K}(\theta) \cdot \text{grad } h(\theta), \quad (7)$$

where \mathbf{K} is the tensor of the saturated/unsaturated hydraulic conductivity, h is the piezometric head and θ is the moisture content of soil. By substituting the equations (6) and (7) in the relation (4), it yields:

$$k_v = \frac{1}{A_{ZK}} \int_{A_{ZK}} \mathbf{K}(\theta) \cdot \text{grad } h(\theta) \cdot dA. \quad (8)$$

All the variables in the equation (8) are time t and the position (x, y, z) dependent. The hydraulic gradient depends on the shape and properties of the infiltration area, i.e. it depends on the shape of the infiltration facility, on the geological composition of the strata, on the boundary and initial conditions, i.e. on the water level in the infiltration facility, the level of the impermeable base, the GW level and the initial moisture content of soil. $\mathbf{K}(\theta)$ and $\text{grad } h(\theta)$ can be determined, for example, using numerical modelling of flow in the unsaturated zone [Lu, Likos 2004], [Šimůnek et. al 2006] and [Šejna, Šimůnek 2007].

Another option that shifts the design of the volume of the infiltration facility to the safe side is to derive the coefficient of infiltration from the value achieved at the end of the infiltration test. Fig. 1 shows that the $k_v(t)$ decreases with time and is dependent on the test duration.

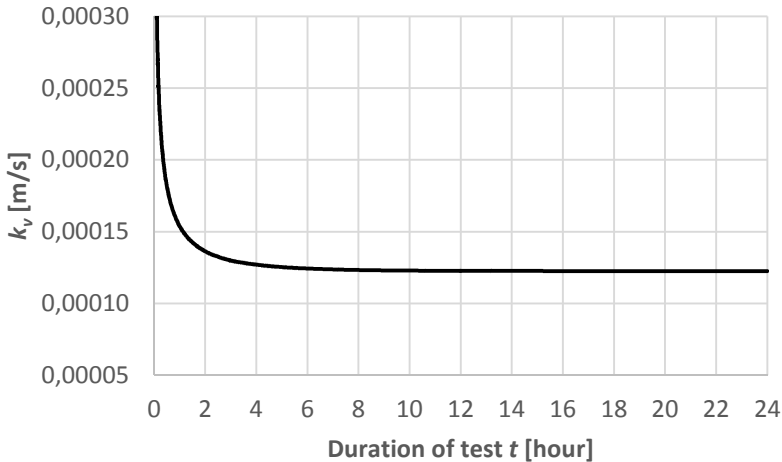


Fig. 1 Example of the time pattern of the coefficient of infiltration

2.2 Design of volumes of the infiltration facility with incorporation of uncertainties

The performance of a geological survey and field tests is usually not extensive, mainly in case of smaller installations in which the budget is limited. In practice, numerical models are used for designing infiltration facilities less often than simplified procedures applying the coefficient of infiltration k_v . The coefficient is determined using an infiltration test that usually reflects only instantaneous local

conditions. When using the coefficient of infiltration, it is considered that it expresses characteristics such as hydraulic conductivity, inhomogeneity and anisotropy of the GW body. An important factor in determining the coefficient of infiltration is the duration of an infiltration test. The coefficient of infiltration according to CSN 75 9010 should be evaluated at the end of the test after 24 hours; in practice, however, the length of the test is usually shorter. Due to this fact, the over-evaluated coefficient of infiltration is usually obtained.

Uncertainties are brought into the solution by the changing initial moisture content of soil, the position of the GW level and the position of the impermeable basement as well. Another factor influencing the course of infiltration is the size of the infiltration facility, its spatial arrangement and type (an infiltration furrow, an infiltration well, perforated piping). These factors are usually different for the designed infiltration facility and for the test at which the coefficient of infiltration was determined. The text below quantifies the uncertainties in the determination of the coefficient of infiltration. The objective was to express these mutually independent uncertainties. The individual uncertainties were expressed using partial coefficients of reliability for 3 typical soils – sand, loamy sand and sandy loam.

When undertaking a practical design the standard CSN EN 1990 recommends that the storage volume of the infiltration facility be determined using the condition of the limit state. This can be expressed in a more general form as follows:

$$\gamma_{VZ} \cdot V_{VZ} > \gamma_n \cdot \max_{t_c=0, t_{c,max}} (\gamma_S \cdot V_S - \gamma_{VSAK} \cdot V_{VSAK}) \quad (9)$$

where V_{VZ} is the storage volume of the infiltration facility, V_{VSAK} is the volume of infiltrated water and V_S is the volume of precipitation water. In the condition, in a broader concept, the left side represents the “resistance” of the object and the right side “loading”. The maximum of the term in parentheses on the right side of the relation (9) is determined with a whole range of the duration times t_c of the design rain. The following partial coefficients are introduced into the condition (9):

- γ_{VZ} for geometric uncertainties of the volume of the flood-control storage,
- γ_n of the significance of the facility,
- γ_S expresses the reliability of the volume of precipitation water,
- γ_{VSAK} expressing uncertainty in the volume of infiltrated water.

3. DETERMINATION OF RELIABILITY COEFFICIENTS

3.1 Storage volume of the infiltration facility

During the construction and operation of an infiltration facility the storage volume may decrease. The reasons can be an inaccurate calculation, e.g. in infiltration contour furrows or ponds, imperfect construction, silting.

Larger deviations in the storage volume due to an inaccurate calculation practically do not appear in technical elements such as rectangular reservoirs, wells or boreholes. A certain error may occur in topographically more complicated areas such as infiltration belts, contour furrows or reservoirs. In case of subsurface facilities it is necessary to subtract the volume of fillings such as plastic elements or a coarse-grained soil fill. The design volume can also be decreased by imperfect construction, by using another filling material, etc. A significant reduction of the volume can result from silting. It is necessary to assess the amount of arriving sediment load, the efficiency of a cleaning device in front of the facility, and the possibility of the periodical removal of deposit from the device.

The design and choice of the size of the coefficient $\gamma_{VZ} \leq 1$ (the reliability guarantee of the design volume) should take account of the method of construction and the possibility of technological deficiencies such as bulging of formwork, partial filling of flood-control storage by the material of the slopes, etc. In well-designed and periodically maintained objects that were constructed with high quality, the coefficient $\gamma_{VZ} = 0.95$ can be considered; the safe value is $\gamma_{VZ} = 0.90$.

3.2 Expression of the significance of the facility

It is useful to place the infiltration facility into three classes by its size, social and economic significance. The significance of the object is expressed using the coefficient of significance γ_n ; its value is determined on the basis of the analysis of social and economic significance of the object, by the degree of a threat to the territory and by the amount of damage incurred in case of overloading the facility. The values of the coefficient of significance can also be derived on the basis of probability analysis by evaluating the losses arising from a collapse of the function of the object. A certain guide can be the values of the coefficient given in Tab. 1.

Tab. 1 Classes of significance of objects

Class of significance	Description of significance of facility	γ_n
I	Facilities with great economic and social significance; if overloaded or put out of operation, considerable damage will occur	1.05
II	Objects with medium economic and/or social significance	1.02
III	Objects a failure of which results only in negligible damage	1.00

3.3 The volume of storm water

The volume of storm water is identified according to [Bareš et al. 2013] or [TNV 75 9011] using procedures of the hydrology of sewage systems. The corresponding uncertainties are connected with determining the drained area and its reduction and determining the runoff coefficients which significantly depend on the history of precipitation and the saturation of the surface by water at the beginning of the design episode. Certain inaccuracy is connected with provided design precipitation totals or rainfall intensities with given duration.

The coefficient γ_s , expressing the reliability of the volume of rainfall water, can differ according to the ruggedness of the drained area and on its permeability. A certain role is played by the reliability of provided data on precipitation totals. For practical designs the coefficient should be chosen $\gamma_s = 1.20$ for smaller areas with precipitation-gauge stations, $\gamma_s = 1.40$ for larger more rugged areas.

3.4 The volume of infiltrated water

The coefficient $\gamma_{VSAK} \leq 1$ expressing uncertainty in the volume of infiltrated water is formal in the condition (9); in practice it is necessary to express uncertainties for individual factors corresponding to the instantaneous conditions in the GW body. The following conditions are discussed:

- the duration time of the infiltration test γ_t ,
- the position of the impermeable basement and the GW table γ_h ,
- the instantaneous degree of saturation of soil γ_{sn} ,
- the size and shape of the infiltration facility γ_z ,
- the ageing of the facility (choking, degradation) γ_c ,
- the characteristics of the GW body (anisotropy, inhomogeneity) γ_a .

The coefficient γ_{VSAK} is then expressed using partial coefficients of reliability:

$$\gamma_{VSAK} = \gamma_t \cdot \gamma_h \cdot \gamma_a \cdot \gamma_{sn} \cdot \gamma_z \cdot \gamma_c \quad (10)$$

They can be determined using statistical evaluation of a sufficient number of field measurements, methods of analogy and numerical modelling or expert estimates.

In this study, the partial coefficients in the relation (10) were determined by numerical simulations in the software HYDRUS-2D [Šimůnek et. al 2006], [Šejna, Šimůnek 2007], which enables the solution of the flow in the saturated and unsaturated zones, assuming a two-dimensional approximation of flow. The formulation and a detailed description of the solution are beyond the scope of this text, therefore the readers are referred to the literature sources given above.

Numerical simulations were made for 3 typical materials with properties according to Tab. 2 for the infiltration facility according to CSN 75 9010, Ann. G.

Tab. 2. Properties of materials

Soil	θ_s	θ_r	α [1/m]	n	k_s [m/s]
Sand	0.430	0.045	14.5	2.68	$8.25 \cdot 10^{-5}$
Loamy sand	0.410	0.057	12.4	2.28	$4.05 \cdot 10^{-5}$
Sandy loam	0.410	0.065	7.5	1.89	$1.23 \cdot 10^{-5}$

In Tab. 2, θ_s means the moisture content of saturated soil, θ_r is the residual moisture content, α is the reciprocal of the input value of air, n is the shape coefficient of the water retention curve [Van Genuchten 1980], and k_s is the saturated hydraulic conductivity. The following paragraphs describe the derivation

of the partial reliability coefficients in (10) with the fulfilment of independence of the conditions in their determination.

3.5 The duration time of the infiltration test

The recommended length of the infiltration test according to CSN 75 9010 is 24 hours. Numerical tests show that after this period the evaluated coefficient of infiltration does not change anymore (Fig. 1). For this reason the 24-hour length of duration of the infiltration test is considered to be referential. The coefficient γ expressing the effect of the length of duration of the test is defined as follows:

$$\gamma_t(t) = \frac{k_v(t)}{k_{v24}}; \quad t < 24 \text{ hours} \quad (11)$$

where $\gamma(t)$ is the partial coefficient of reliability relative to the length of duration of the infiltration test, k_{v24} is the coefficient of infiltration determined after 24 hours of the test and $k_v(t)$ is the coefficient of infiltration determined at the time t . The coefficient $\gamma(t)$ was determined under the conditions of infinite depth to the impermeable basement without the effect of the GW table. The relationship $\gamma(t)$ according to (11) for typical soils is depicted in Fig. 2. The graph shows that for less permeable materials the coefficient of infiltration obtained from a shorter infiltration test should be reduced; e.g. for sandy materials it is sufficient that the test duration is about 8 hours when infiltration becomes steady.

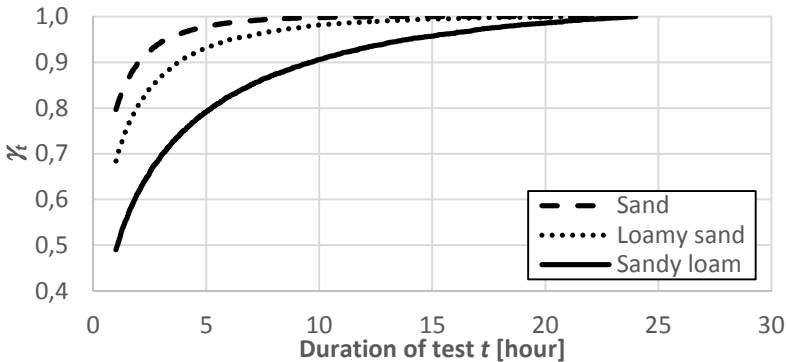


Fig. 2 Relationship $\gamma(t)$ for typical materials

3.6 Effect of impermeable basement and groundwater table depth

Different depths of the GW table and of the impermeable base beneath the infiltration facility influence the volume of infiltrated water and the coefficient of infiltration. For different combinations of depth to the impermeable basement and depth to the GW table, the coefficient γ_{h_i} was determined from the relation:

$$\gamma_{h_i} = \frac{k_{v24_h}(h_{GW}, h_{IS})}{k_{v24}} \quad (12)$$

where $k_{v24,h}(h_{GW},h_{IS})$ is the coefficient of infiltration after 24 hours for the corresponding depth h_{GW} to the GW table and the depth h_{IS} to the impermeable basement beneath the infiltration facility. k_{v24} is the coefficient of infiltration after 24 hours influenced neither by the position of the GW table nor by the level of the impermeable basement. The relationships of the coefficient of the partial reliability $\gamma_{h,i}$ for sand according to the equation (12) are depicted in Figs. 3.

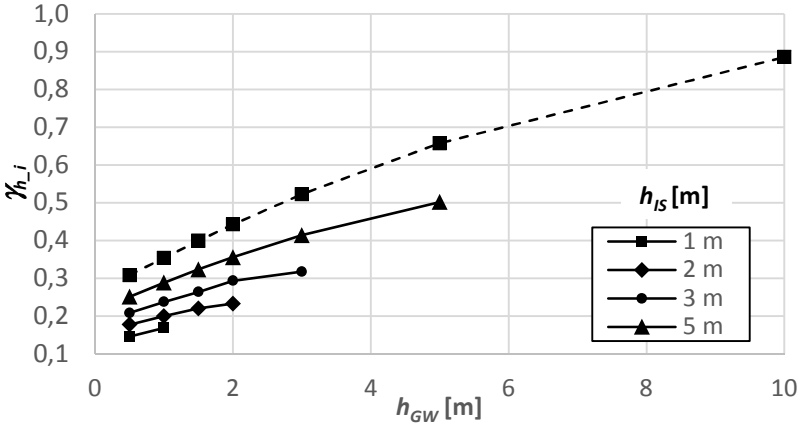


Fig. 3 Relationship $\gamma_{h,i}$, example for sand

For determining the coefficient γ_h it is necessary to determine the coefficient $\gamma_{h,i}$ for the conditions of the infiltration test ($\gamma_{h,ZK}$) and the conditions of the infiltration facility ($\gamma_{h,VSAK}$). The resulting coefficient γ_h is calculated from the relation:

$$\gamma_h = \frac{\gamma_{h,VSAK}}{\gamma_{h,ZK}} \quad (13)$$

3.7 The effect of the degree of saturation (moisture content) of soil

The instantaneous initial degree of saturation of soil plays a certain role in carrying out an infiltration test and also in the infiltration of rainwater in the already-constructed infiltration facility. Uncertainty in the initial degree of soil saturation is reflected by the coefficient of reliability γ_{sn} expressed for typical soils for the infiltration test duration of 24 hours. It is expressed by the following ratio:

$$\gamma_{sn} = \frac{k_{v24}(S_w)}{k_{v24}(S_{WR})} \quad (14)$$

where $k_{v24}(S_w)$ is the coefficient of infiltration for the given initial degree of saturation S_w , $k_{v24}(S_{WR}) = k_{v24}$ is the coefficient of infiltration for the material with the initial degree of saturation S_{WR} corresponding to the residual moisture content θ_R . The relationship between the coefficient γ_{sn} for typical materials and the degree of saturation is shown in Fig. 4.

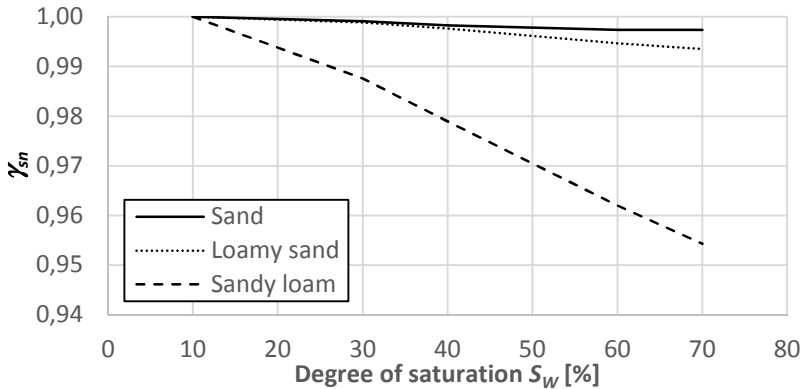


Fig. 4 Relationship γ_{sn} for typical materials

3.8 The effect of the shape and size of the infiltration facility

The infiltration test should be carried out according to [CSN 75 9010] on an trial pit or borehole specified in Annex G of the standard. Deviations in the shape and dimensions of the designed infiltration facility and equipment in the infiltration test can cause a difference in the velocity and volume of infiltrated water. With the aim to quantify the effects above, a number of scenarios of configuration with different geometric parameters of the infiltration facility were numerically calculated. The evaluation of the calculations indicated differences in the determined coefficient of infiltration in a range of 3 to 4%. The partial coefficient of reliability relating to different geometric dimensions of trial and designed infiltration objects, therefore, can be considered with the value $\gamma_c = 0.95$.

3.9 The effect of ageing of the facility

The ageing of the infiltration facility is governed by clogging of surrounding soil. Its course was studied e.g. by Kovács [1981]. His measurements show that clogging takes place especially in the layer about 0.50 m thick beneath the surface of infiltration; permeability decreases with time towards the surface of the infiltration facility, in which hydraulic conductivity can drop by up to several orders of magnitude after about 7 days. The coefficient γ_c should be chosen with regard to the efficiency of water pre-treatment in front of the entrance to the infiltration facility and/or to the possibilities of its regeneration. It is recommended that γ_c be chosen at least at 0.8; in case of impossible regeneration and unreliable pre-treatment, even at $\gamma_c = 0.1$.

3.10 The effect of anisotropy and inhomogeneity

When conducting the infiltration test, it is assumed that the determined coefficient of infiltration already implies the effect of anisotropy of the permeable filtration environment. In the event that inhomogeneity could be expected in the form of alternation of more permeable layers with less permeable ones beneath the

infiltration facility, a relationship was derived between the coefficient γ_a and the ratio of the hydraulic conductivity of the less permeable layer located 0.5, 1, 2 and 3 m beneath the level of infiltration (beneath the bottom of the infiltration facility) to the material in which the infiltration was conducted (Fig. 5). In case of a difference in the hydraulic conductivity of approximately horizontal layers (larger than five-fold), it is necessary to consider the layers as relatively impermeable and to use the procedure applying the relations (12) and (13).

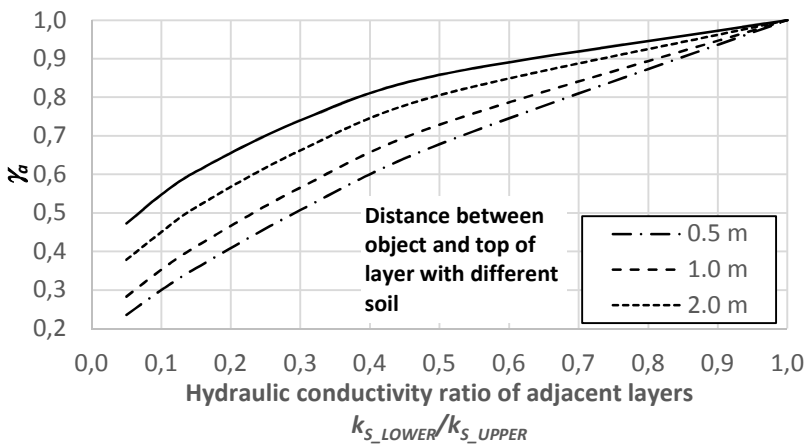


Fig. 5 Relationship γ_a for conditions of hydraulic conductivities of underlying layers, example for sand

4. COMPARISON OF TWO DESIGN APPROACHES

For demonstrating the above-given approaches - according to CSN 75 9010 and using the method of limit states, an example of the calculation of the storage volume of an infiltration facility is presented. The input parameters are based on the example D3 in the CSN 75 9010. A drained area is located on the Brno territory, the reduced orthographic projection $A_{red} = 560 \text{ m}^2$. The coefficient of infiltration is $k_v = 1 \cdot 10^{-6} \text{ m/s}$, concerning sandy loam. The coefficient of safety of infiltration is considered as $f = 2$ and the rainfall periodicity $p = 0.2 \text{ year}^{-1}$. In case of the procedure according to limit states, different conditions were chosen in conducting an infiltration test and in the operation of the infiltration facility:

In the infiltration test, the depth $h_{GW} = 4.0 \text{ m}$ of GW table beneath the bottom of a trial pit, the depth $h_{IS} = 5.0 \text{ m}$ of the impermeable basement beneath the pit bottom, the infiltration test lasted $t = 8 \text{ hrs}$. The initial degree of saturation is $S_w = 0.3$, which approximately corresponds to the moisture content 0.123.

In the infiltration facility, the GW table is considered to be $h_{GW} = 1.5 \text{ m}$ beneath the bottom of the facility, the position of the impermeable basement $h_{IS} = 3.0 \text{ m}$ beneath the facility. The initial soil saturation can reach up to $S_w = 0.7$. At a depth of 2.0 m beneath the bottom of the facility, a layer was encountered

with half the hydraulic conductivity than when drilling the trial pit. For the given conditions, the following values of the partial coefficients were determined using the above-depicted graphs supplemented with expert estimates:

- for geometric uncertainties in the flood-control storage $\gamma_{VZ} = 0.95$,
- for the significance of the facility $\gamma_n = 1.02$,
- for the reliability of the volume of precipitation water $\gamma_S = 1.20$,
- for the duration time of the infiltration test $\gamma_t = 0.88$,
- for the position of the impermeable base and GW table $\gamma_h = 0.57$,
- for the instantaneous degree of saturation of soil $\gamma_{sn} = 0.95$,
- for the size and shape of the infiltration facility $\gamma_z = 0.95$,
- for the ageing of the facility (choking, degradation) $\gamma_c = 0.80$,
- for the characteristics of the GW body $\gamma_a = 0.80$.

The calculation of the storage volume V_{VZ} of the facility was determined for design precipitation totals with the duration from 5 minutes to 72 hours according to the eq. 2 in CSN 75 9010 and according to the condition (9) incorporating partial uncertainties. The relationship expressing the required storage volume as a function of the rainfall duration is shown in Fig. 6. The maximum volume of the facility according to CSN 75 9010 is 19.9 m^3 and using the procedure proposed is 29.9 m^3 . It is obvious that the storage volume of the infiltration facility determined according to CSN comes out under-dimensioned by roughly 10 m^3 .

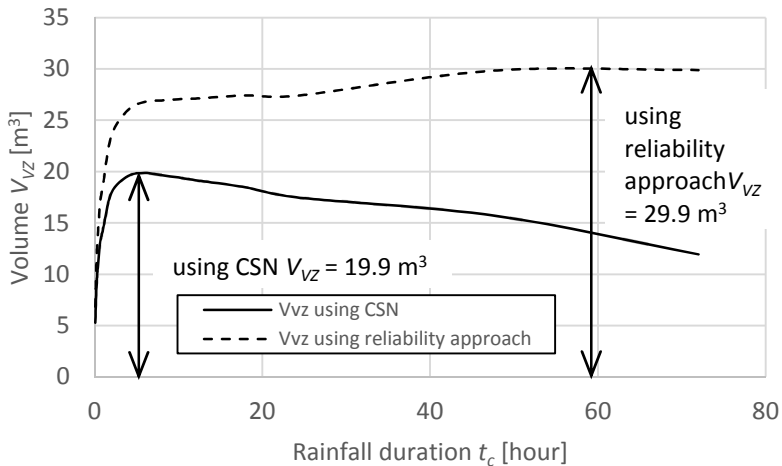


Fig. 6 Comparison of two design approaches

5. DISCUSSION AND CONCLUSIONS

A procedure is recommended in CSN 75 9010 for determining the storage volume of an infiltration facility, in which the coefficient of infiltration k_v is introduced. According to the standard it “characterises the infiltration capability of

the soil in a studied site". In practical calculations CSN 75 9010 recommends to reduce determined coefficient of infiltration by the coefficient of safety $f \geq 2$. The analysis carried out in more detail shows that numerous input variables are involved in the design, loaded by uncertainties arising from not meeting design parameters of the infiltration facility, from the reliability of hydrological data and particularly from the limited extent and reliability of the survey.

This paper defines the individual variables involved in the calculation, and analyses the factors that influence the design of the storage volume of the infiltration facility. The effect of each factor was quantified using extensive numerical calculations made by the software product HYDRUS-2D, [Šimůnek et. al 2006], [Šejna, Šimůnek 2007]. Uncertainties in the determination of the storage volume are expressed by partial reliability coefficients quantified for three typical soils.

The proposed procedure taking account of uncertainties in each parameter is demonstrated on an example of comparison. The results of the calculation show that the procedure according to [CSN 75 9010] can ultimately lead to the significant under-dimensioning of the storage area, particularly by over-evaluating the infiltration capability of the infiltration facility.

6. REFERENCES

- Act No. 183/2006 Coll. on Land-Use Planning and the Building Code as amended.
Act No. 254/2001 Coll. Water Act and certain acts as amended.
ATV-DVWK. 2007. Handlungsempfehlungen zum Umgang mit Regenwasser, GfA. ATV Merkblatt M153. 36 p.
BAREŠ, V., KABELKOVÁ, I., STRÁNSKÝ, D. 2013. TNV 75 9011 Precipitation water management, Part 3: Dimensioning of Objects and Facilities. Water management, 11/2013, p. 383 - 386.
BEAR, J., VERUJIT, A. 1992. Modeling Groundwater Flow and Pollution. D. Reidel Publishing. Comp. Dordrecht, Holland. 414 p.
BLOOMBERG, M. R., STRICKLAND, C. H. Guidelines for the Design and Construction of Stormwater Management Systems, NY City Department of Environmental Protection and Department of Buildings. 137 p.
ČSN EN 1990 (73 0002) Eurocode: Principles for Structural Design.
ČSN 75 9010. 2012. Stormwater soakaways.
DWA 2005. Planung, Bau, und Betrieb von Anlagen und Versickerung von Niederschlagswasser. Arbeitsblatt DWA-A 138. Deutsche Vereinigung für Wasserwirtschaft, Abwasser und Abfall e. V. 61 p.
GRISHEK, T. et al., 1996. Urban groundwater in Dresden. Hydrogeology J., Vol. 4, No.1, p. 8-63.
KOVÁCS, G. 1981. Seepage hydraulics, Akadémiai Kiadó, Budapest, 730 p
LU, N., LIKOS, W. J. 2004. Unsaturated Soil Mechanics, John Wiley & Sons, New Jersey, 556 p.

- SMGM. 2014. Stormwater Management Guidance Manual Version 2.1. Planning & Research. Philadelphia Water Department. 378 p.
- ŠIMŮNEK J., VAN GENUCHTEN, M. TH., ŠEJNA, M. 2006. The HYDRUS Software Package for Simulating the Two- and Three-Dimensional Movement of Water, Heat, and Multiple Solutes in Variably-Saturated Media, Praha, 241 p.
- ŠEJNA, M., ŠIMŮNEK, J. 2007. HYDRUS (2D/3D): Graphical User Interface for the HYDRUS Software Package Simulating Two- and Three-Dimensional Movement of Water, Heat, and Multiple Solutes in Variably-Saturated Media, published online at www.pc-progress.cz.
- TNV 75 9011. 2013. Sustainable stormwater management.
- VAN GENUCHTEN, M. TH. 1980. A Closed-form Equation for Predicting the Hydraulic Conductivity of Unsaturated Soils. *Soil Sci. Soc. Am. J.*, Vol. 44, 1980, p. 892 - 898.
- WATKINS, D. C. 1997. International practice for the disposal of urban runoff using infiltration drainage system. In: *Groundwater in The Urban Environment*, Vol. 1, Proceedings of the XXVII Congress held in Nottingham. Rotterdam, A. A. Balkena, p. 205-210.

Acknowledgement

This study has been prepared as a part of the project TACR No. TA02020386 *The Use of the Methods of Infiltration and Their Evaluation in Conjunction with the Comparison of Results with Laboratory Tests on Different Types of Soil and a Model for a Design of Infiltration Reservoir* and of the Task LO1408 AdMaS UP *Advanced Construction Materials, Structures and Technologies*.

Hydraulic assessment of flood protection measures in Small Carpathians

A. Janík, A. Šoltész

Department of Hydraulic Engineering, Faculty of Civil Engineering, Slovak University of Technology
in Bratislava, Radlinského 11, 810 05 Bratislava, Slovak Republic, phone: +421 2 59 274 571, fax:
+421 2 59274 565, e-mail: adam.janik15@gmail.com, andrej.soltesz@stuba.sk

Abstract

This article is dealing with mathematical modelling of flood wave passing in the Píla town. To ensure the flood protection detention reservoirs have been designed. The proposal is based on reconstruction of the flood wave on Gidra stream in June 2011. The model of water courses has been created according to geodetic and hydrological data in HEC – RAS 4.1.0 simulation package. The capacity flow in the Gidra stream river bed was evaluated. The designed detention reservoirs were checked by design flood wave and their effect from flood protection point of view has been evaluated. Their potential volume was also computed and compared to each other.

Keywords

flood, mathematical modelling, flood protection measures, design flood wave, detention reservoir

1. INTRODUCTION

Flash floods also called storm or sudden floods are a specific type of rain floods which typical sign is an intensive increase of water level in the river in a short time period (usually couple of hours). Mostly there are floods on small streams in upper parts of river basins and their starters are extreme storm rainfalls. Rainfall intensity and duration limits are not possible to determine exactly because they are dependent on many factors such as type and shape of landscape, soil water saturation and nonetheless they depend on anthropogenic activity (inadequate operation in the landscape).

Due to the extremely short time of flood beginning, it is very difficult to alarm inhabitants and for carrying out operative flood protection measures like mobile flood-protection barriers, is too late. That is the reason why it is necessary to prepare against such floods appropriate flood-protection measures which do not need any operation and work automatically.

2. MATERIAL AND METHODS

People start noticing the seriousness of flood protection usually when the flood appears. No exception is the town Píla which was affected by destructive flood in

year 2011. After this flood many buildings, roads and pavements had to be repaired but the flood protection was still non-existent.

Through the town flows stream called *Gidra* which is a right-sided inflow of *Dolný Dudváh*. Its length is 38,5 km and wells in Small Carpathians in height above sea level of 470 metres. *Gidra*’s most significant inflow above town *Píla* is right-sided *Kamenný* stream. Before *Gidra* enters residential area of the *Píla* town and close past the inflow with *Kamenný* stream a stream-gauging station is situated.



Fig. 2 River basin of *Gidra* above the *Píla* village

On 7.6.2011 storm areas were formed above Slovakia and the most intensive storm activity was in the afternoon in region of Small Carpathians (on its south-east side hills that are part of *Trnava* and *Pezinok* district). 51-100 mm rain falls in this area and in the most exposed places the amount exceeded to 100mm. The dangerous phenomenon was not the rainfall itself, but the long duration of very intensive rain.

As a result of this rainfall were catastrophic floods which affected many river basins in mentioned region. The most critical situation was on streams *Gidra*, *Parná* and *Vištucký* stream where water levels rose up to much higher limit than the level equivalent to third stage of flow activity in less than 2 hours. First peak occurred on 7.6. at 17:00 in *Píla* on stream *Gidra* where water level culminated on 226cm. Immediately after reaching culmination the water level started to decline

rapidly. Water level of Gidra has achieved quite fast the level adequate to first stage of flow activity but the next wave of rain caused repeated increase of water level. This was the reason of second flood wave but of a smaller range. After second culmination the water level on stream Gidra started to decrease until it dropped under the value of first stage of flow activity in afternoon hours.

Later was the culmination flow determined as a value of $Q_{culm} = 44,5 \text{ m}^3 \cdot \text{s}^{-1}$ and according to designed values of N-yearly flows it represented significance of more than 1000-year flow.

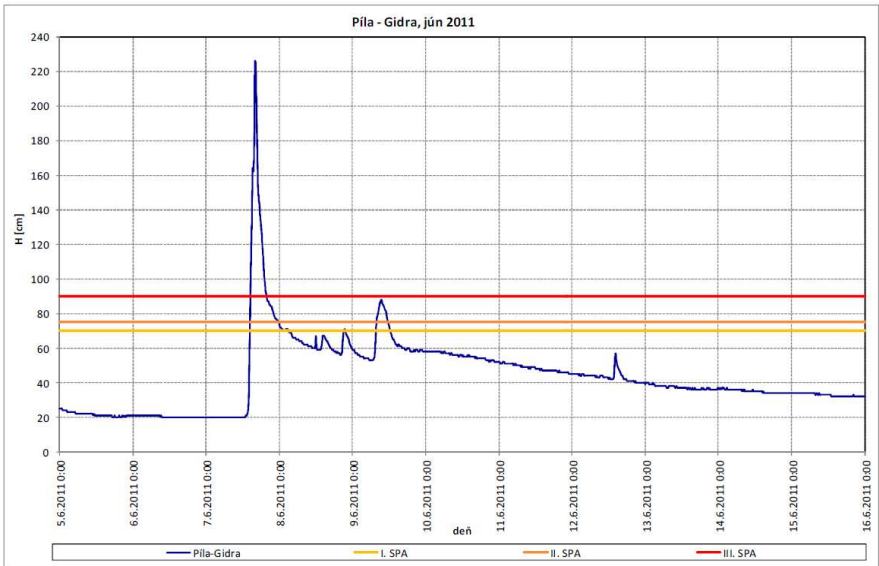


Fig. 2 Flood wave development on Gidra stream in June 2011

Two types of geodetic data were available: survey of Gidra stream bed in Píla town and two valleys of Gidra and Kamenný stream surveyed by 3D scanning.

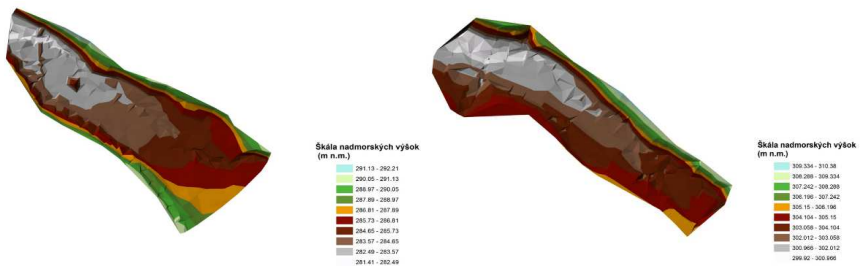


Fig. 3 Illustration of the 3D scans in basins of Gidra and Kamenný stream

Geodetic survey in Píla represented 72 profiles including seven bridges. The geometry of the model survey was completed by parameters of a possible third detention reservoir, which could be situated approximately 1000 m upstream on Gidra above scanned valley. All necessary data were gathered by classical survey of cross sections in landscape. Accordingly 5,1 km long model of Gidra stream with 2,1 km long inflow of Kamenný stream was created.

Roughness of river basin was defined in model by Manning coefficient. Values from previous thesis that concerned reconstruction of flood on Gidra stream in June 2011 and its impact on levels of the ground water have been used. Specifically the number $n=0,05$ for channel and for inundation number $n=0,5$ was used. It is necessary to mention that these values are not realistic and do not correspondent with current condition of the stream. They consider circumstances such as presence of big rocks in channel during flood or circumfluence of obstacles (stems or buildings in closeness to flow) by arisen water level.

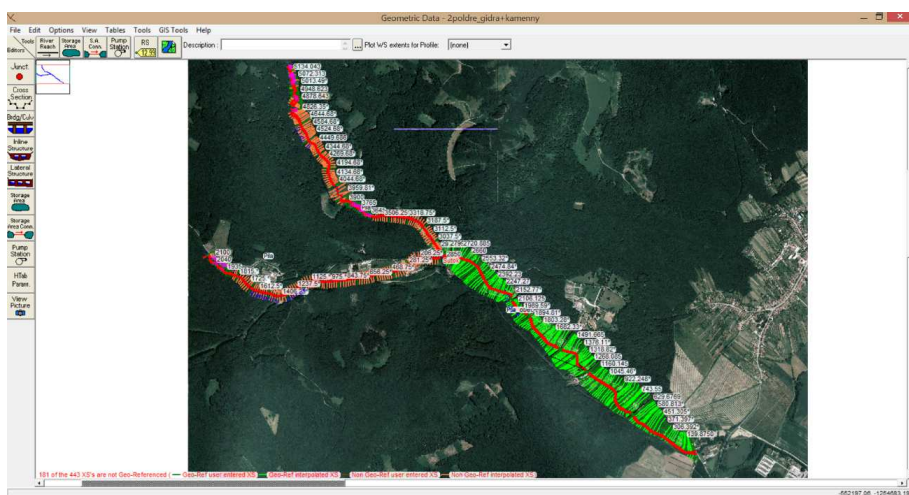


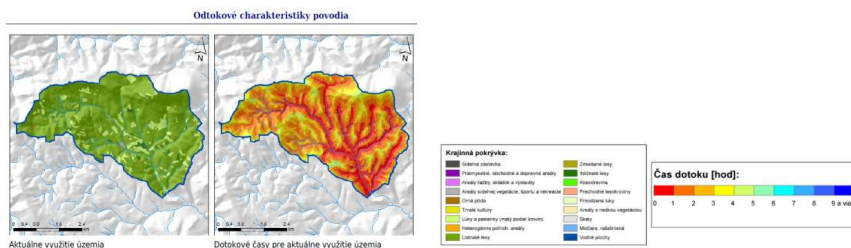
Fig. 4 Geometry of the Gidra and Kamenný stream in HEC-RAS programme

One of possible hydrologic basis of my thesis was a recording of position of water level during the flood on Gidra in June 2011. We decided not to use it for following reasons:

- Flood on Gidra in June 2011 was presumably affected by breaking of blocked fence which caused flood wave, which would not shape in same situation without the obstacle. These fences were conducted crosswise various streams and caused a barrier in flow during flood.
- These records of flood wave were under junction of Gidra and Kamenný stream and it would be problematic to divide this flood wave into two

separate streams so that the progress of water level past junction corresponded the recording.

Designed flood waves were created based on modelling of summer flood waves in basins without observations as a hydrologic basis. Mentioned flood waves are caused casual rainfall with set probability of repeating (100 years rainfall) and meridian flow caused by the rainfall having the same probability of repeating. For the two identified profiles on Gidra and Kamenny stream were created sub-basins by GIS based programme where the slope and vegetation cover were analysed. Runoff was then analysed by adding rainfall to the programme. As a result, designed flood waves with exact volume for specific profiles were created, in form of record of flow in time (Fig.5).



Čas koncentrácie [hod]	4
Návrhová intenzita zrážky I_n [mm.h ⁻¹]	13.5
Koeficient odtoku [-]	0.46
Návrhový prietok Q_n [m ³ .s ⁻¹]	13.74
Rozdiel prietokov	0
Objem návrhovej vlny [m ³]	399773.5938

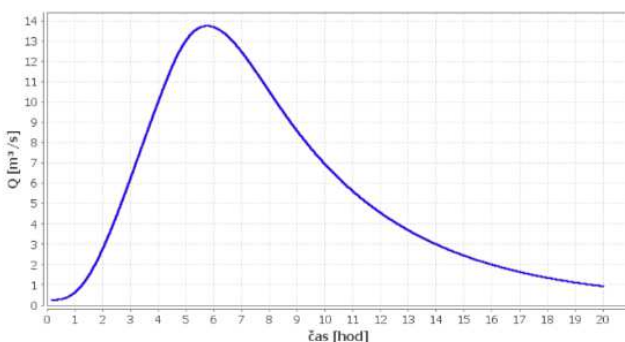


Fig. 5 Design flood wave for the profile of detention reservoir on Gidra stream

In the vicinity of Píla town flow into Gidra and Kamenný stream various smaller tributary streams which discharge is normally almost trivial (usually few

litres per second). Even though during flash floods can small stream become influential inflow and that is the reason for involving it into the hydraulic model.



Fig. 6 Map of streams and their inflows and proposed detention reservoirs over the Píla town

The limited profile in view of capacity of the channel was one of the seven bridge profiles in town. It turned out that the most critical section of stream is footbridge in rkm 32,006 which profile was almost completely clogged with water by flow of $15,3 \text{ m}^3 \cdot \text{s}^{-1}$. Bridge in rkm 31,127 was also critical and by mentioned flow had under bridge deck only 25 cm spare space before clogging.

As a basis to boundary conditions for unsteady flow above mentioned flood waves have been used. Upper boundary conditions were formed as a recording of flow in time and we used downstream boundary condition on Gidra from steady flow which is the normal depth assigned as a longitudinal slope. After successful simulation of flood we obtained data which could be used as a comparison for effect achieved on modelled detention reservoirs. We adjusted the model so that the flood waves on Gidra and Kamenný stream met on their junction at the same time, what indicates the worst possible case of flood on these two streams. The flood wave on stream Kamenný stream arrived to junction at 6:15 and flood wave on Gidra arrived at 6:00. By synergy of those waves arose in stationing 2799 m (the gauging station profile) wave with culmination flow $25,59 \text{ m}^3 \cdot \text{s}^{-1}$ at 6:15.

After calculating the simulation of flood without proposed measures we proceeded to design of detention reservoirs. We did not try to propose detention reservoirs to ensure complete flood protection of village. Instead of that, not too high reservoirs have been proposed in given locations.

I did not propose safety spillways for detention reservoirs. Because of that, dam crest of detention reservoir in my case means crest of emergency spillway. In

reality it would mean that detention reservoirs would be taller by emergency elevation of dam crest above maximum water level in detention reservoir.

Proposed detention reservoirs:

- detention reservoir on the Kamenný stream (stationing 1840 m, rkm approx. 1,84):
 - dam crest altitude – 307,8 m a. s. l.
 - dam height – 7,8 m
 - diameter of the outlet structure – 1,1 m
 - length of the dam in crest – approx. 80 m



Fig. 7 Location of the proposed detention reservoir on the Kamenný stream

- Lower detention reservoir on Gidra (stationing 3625 m, rkm approx. 34,126):
 - dam crest altitude – 289 m a. s. l.
 - dam height – 6,8 m
 - diameter of the outlet structure – 0,95 m
 - length of the dam in crest – approx. 65 m



Fig. 8 Location of the designed lower detention reservoir on the Gidra stream

- Upper detention reservoir on Gidra (stationing 4740 m, rkm approx. 35,241):
 - dam crest altitude – 307 m a. s. l.
 - dam height – 8 m
 - diameter of the outlet structure – 1 m
 - length of the dam in crest – approx. 140 m



Fig.9 Location of the designed upper detention reservoir on the Gidra stream

These proposals are result of many attempts and errors (trial – error method), because during the flood waves passing the detention reservoir it was figured out that they will be overspilled. So the dam crest altitudes have been gradually increased using geodetic surveying data as well as increasing the diameter of outlet structures.

The result of the hydraulic modelling of detention reservoirs above the village Pila is the flattening of the flood waves. The comparison of results of a zero variant and the proposed variant with several detention reservoirs have been performed. The comparison has been done in specific profiles below detention reservoirs.

Upper detention reservoir on the Gidra stream reduced the original meridian flow in the comparative profile right below the designed detention reservoir from value $11,83 \text{ m}^3 \cdot \text{s}^{-1}$ to $5,66 \text{ m}^3 \cdot \text{s}^{-1}$. It also caused the delay of meridian flow by 3,75 h. The maximum water level in the detention reservoir was 306,75 m above sea level, what is 25 cm below the dam crest of the detention reservoir.

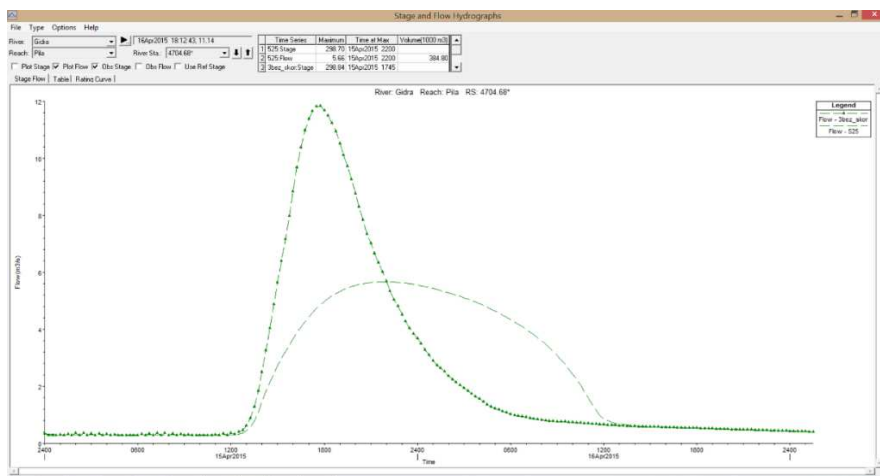


Fig. 10 Flattening of the flood wave on the Gidra stream below the designed detention reservoir

Behind the lower detention reservoir on Gidra was original meridian flow in comparative profile below the designed detention reservoir reduced from original value of $13,7 \text{ m}^3 \cdot \text{s}^{-1}$ to $4,76 \text{ m}^3 \cdot \text{s}^{-1}$. Delay of this meridian flow represented 10,5 h. The maximum water level in the detention reservoir was 288,94 m above sea level, what is 6 cm below the dam crest of the detention reservoir.

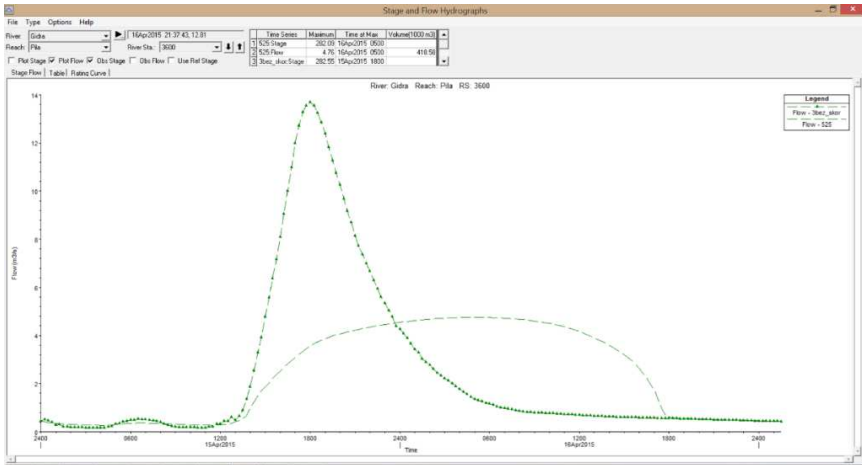


Fig. 11 Flattening of the flood wave on the Gidra stream below the designed detention reservoir

The designed detention reservoir on the Kamenný stream reduced the meridian flow in stationing 1815 m from original value $9,96 \text{ m}^3 \cdot \text{s}^{-1}$ to $6,78 \text{ m}^3 \cdot \text{s}^{-1}$ and caused its delay by 2,75 h. The maximum water level in the detention reservoir was 307,53 m above sea level and was 27 cm below the dam crest of the detention reservoir.

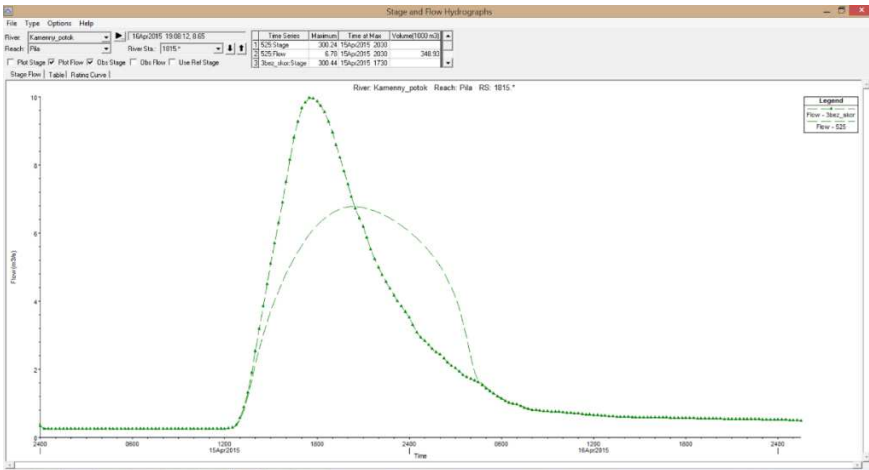


Fig. 12 Flattening of the flood wave on the Kamenny stream below the designed detention reservoir

By synergy of the detention reservoirs in the area below the junction of Gidra and Kamenný stream in stationing 2799 m, the meridian flow has been reduced from original $25,59 \text{ m}^3 \cdot \text{s}^{-1}$ to value $12,10 \text{ m}^3 \cdot \text{s}^{-1}$ and has been delayed by 1,25 hour.

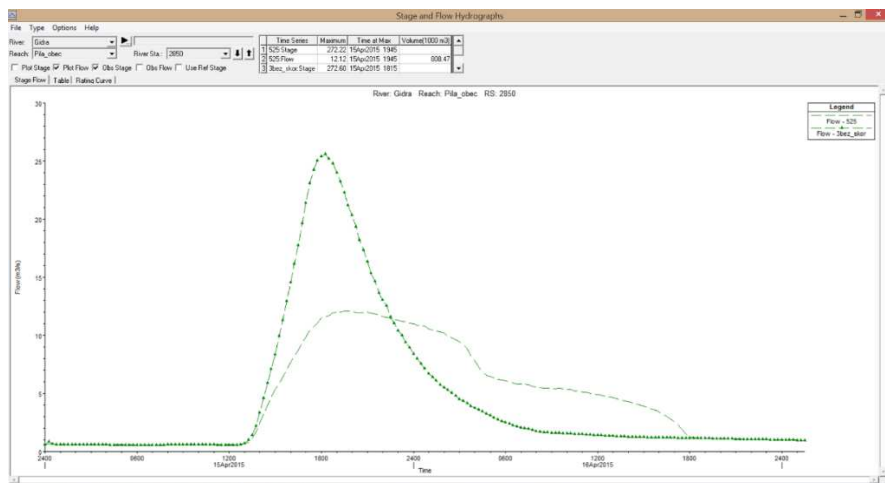


Fig. 13 Flattening of the flood wave below the junction of Kamenný stream and Gidra – in the profile of the SHMI gauging station

By this proposal a massive flattening of the flood wave has been achieved and meridian flow has been reduced by 52%. Proposal has accomplished a great improvement of the flood situation in the village Píla. In case of realising proposed flood protection measures the village would be safe from flooding. Specifically, the maximum flow through the village during a 100 years flood would be only $12 \cdot 10 \text{ m}^3 \cdot \text{s}^{-1}$.

3. CONCLUSION

By processing of the geodetic and hydrological data a creation of a mathematical model of Gidra stream river basin in the village and area nearly above the village was performed. The critical capacity flow of the Gidra stream was determined in a footbridge profile to be the value of $15.3 \text{ m}^3 \cdot \text{s}^{-1}$.

Flood protection measures using detention reservoirs have been proposed in the area above the village Píla with specific parameters. Afterwards these reservoirs have been involved in hydraulic model to test the efficiency of such measures during flood period given by design flood wave with likelihood of recurrence once per 100 years. After modelling and evaluation of results a veracious base for future flood protection realisation of the village Píla will be available.

4. REFERENCES

- BLAŠKOVIČOVÁ, Ľ. et al: Flash floods in Slovakia, flash flood on Gidra and Parná in June 2011. *Proceedings from conference: Risk and river basin management* [online] VÚVH 2012. Available on the internet: http://www.vuvh.sk/download/ManazmentPovodi_rizik/zbornikPrispevkov/Konferencia/Prispevky/SekciaC/Blaskovicova_Poorova_a%20kol.pdf
- PINDJAKOVÁ, T. : Reconstruction of flash flood on Gidra in Píla, June 2011 (article concept)
- PINDJAKOVÁ, T., KELČÍK, S., ŠOLTÉSZ, A. 2015. Simulation of flood progress on the Gidra river. *Pollack Periodica (in print)*.
- SHMÚ 2011. Flash flood on Small Carpathians streams in June 2011. Scientific article. Available on the internet: http://www.shmu.sk/File/HIPS/Prival_povoden_na_tokoch_Malych_Karpa_t_v_6_2011opr.PDF
- ŠOLTÉSZ .A.: Small Carpathian flood protection. Presentation. 2014. mapy.atlas.sk [online, available 29.4.2015] available on the internet: <http://mapy.atlas.sk/mapa/pila>
- Town Píla web page. Philippus [online, available 15.3.2015] available on the internet: <http://www.obecpila.sk>

Acknowledgement

This contribution was supported by the VEGA Grant agency under contract VEGA 1/10011/12.

Effect of soil erosion on filters behavior in hydraulic structures

S. Azirou², A. Benamar¹, A. Tahakourt²

¹ LOMC UMR 6294 CNRS- Havre university (France) Waves and Complex Media Laboratory (LOMC), UMR 6294 CNRS, Havre university, France.

² Construction Engineering and Architecture Laboratory (LGCA), Faculty of Technology, University of Bejaia, 06000 Bejaia, Algeria.

Abstract:

Cohesive soils with a large amount of fine particles are usually found in embankment dams. In order to prevent erosion of base soil and simultaneously to allow seepage, filters are designed and managed downstream of these structures. The filters grading is mainly designed using filter criteria [Sherard, Dunnigan 1985], which are based on relationships between the particle size (d_{85}) and the opening size of the filter (D_{15}). This paper reports experimental results obtained on the soil-filter system behaviour subjected to different hydraulic and geometrical conditions. The particles' transport and filtration of two clay soils through a granular filter are investigated. The importance of the effect of successive filtration on the porosity reduction under a constant load is evaluated. A comparison of the porosity and permeability reduction revealed extend of fine particles detachment and deposition during erosion process. Moreover, important results are developed for predicting a capacity of fine particles retention in filter's pores.

Keywords: erosion, flow, soil, filter, fine particles, porosity.

1. INTRODUCTION:

The construction of hydraulic structures (dams, levees) often involves the design of granular or geotextile filters devoted to protect the base soil (the core) against erosion due to seepage. As water flows through soil, fine particles of the core can be washed out under hydraulic loading, leading to internal erosion and likely, the failure of the structure. So, a correctly designed filter must retain loose soil particles and thus prevent piping, while it will be able to allow seepage water to flow and avoid the development of high internal pore pressures [Benamar, 2013, Kenney, Lau, 1985]. The detachment of fine particles and their subsequent transport throughout the porous network of the filter requires that the pore space is sufficient. This space is conditioned by the granular distribution, which in turn depends on the size of the grains, their form and their contact conditions. The main filter design criteria are empirical relationships based essentially on the representative size d_{85} (sieve size for which 15% of the weighed filter material is finer) of the soil to protect and the opening of filter pore D_{15} (sieve size for which 15% of the weighed filter material is finer). A series of laboratory observations on

sets of base soil-filter combination has usually led the researchers to recommend empirical relationships. Terzaghi [1922] was the first to give empirical criteria describing the importance of the grain size in the design of granular filters. This criterion was improved by other authors like Vaughan and Soars [1982], Sherard and Dunnigan [1989], Kenney and Lau [1985] and recently Lee et al. [2002]. In order to design a filter it is recommended to consider the most critical situation, the presence of a concentrated flow through the fine soil (dam core). In this case the particles are eroded when the hydraulic load exceeds the critical value of shear stress of the internal surface cracks. The filter behavior depends on the geometric requirements (grain size and pore distribution, fine particles size and concentration), water (velocity or gradient) and physicochemical processes. This process of filtration is affected by the deposition of particles on the upper surface of the filter or their capture in the porous medium. According to previous studies [Lee et al., 2002, 2005, Benamar, 2013, Lee et al. 2002], higher concentration of particles in the flowing suspension involves important deposition rate. Large concentration of particles causes increased capture rate and so rapid clogging. In this paper we have investigated various parameters affecting filtration behavior including: permeability, porosity and size of eroded particles, and their influence on the filter efficiency was evaluated.

2. MATERIAL AND METHODS:

2.1 Experimental set up and test procedure

The test performed in this study is based on procedures described by Sherard and Dunnigan [1985] devoted to simulate the filtration in cohesive soils with the presence of a crack. A similar apparatus is designed and presented in Fig 1. The so-called NEF test (no Erosion Filter) uses a permeameter (cell made of Plexiglas) which is 100 mm of diameter (25 mm soil thickness for fine soils, 100 mm thickness for coarse soils). In the apparatus a sample of fine soil (representing the core) is compacted above a layer of the granular filter previously selected. A hole (1 cm of diameter) is formed in the base soil which will induce a concentrated flow through the soil towards the filtering layer. The filter has a thickness which is ranging between 13 and 18 cm. The test involves injecting water (with controlled pressure) to the sample inlet to investigate erosion of base soil through the filter. The downward flow into the sample was applied with a maximum pressure of 140 kPa (1.4 bars). The pressure was increased by steps of 0.25 bars (25 kPa). The cell is equipped with a pressure gauge and the outlet is directed to a turbidity meter and a flowmeter.

After the filter was packed into the cell, the fine soil is compacted above the filter and then a hole is formed in its center. A flow at a very low pressure is applied through the soil-filter system and once saturation is reached, the water pressure is increased gradually. The water pressure was increased for each test from 25 kPa to 140 kPa. The eroded particles passing through the filter are detected by a turbidity meter placed downstream of the cell. A particle

concentration is derived using a previous correlation between fines concentration and turbidity (NTU). A flow meter is placed at the outlet of the column allows the record flow values continuously. The performance of the soil-filter combination is observed during a processing time of 5 to 10 minutes. The filter is considered effective if there is no particle transported by the flow through the filter after this period.

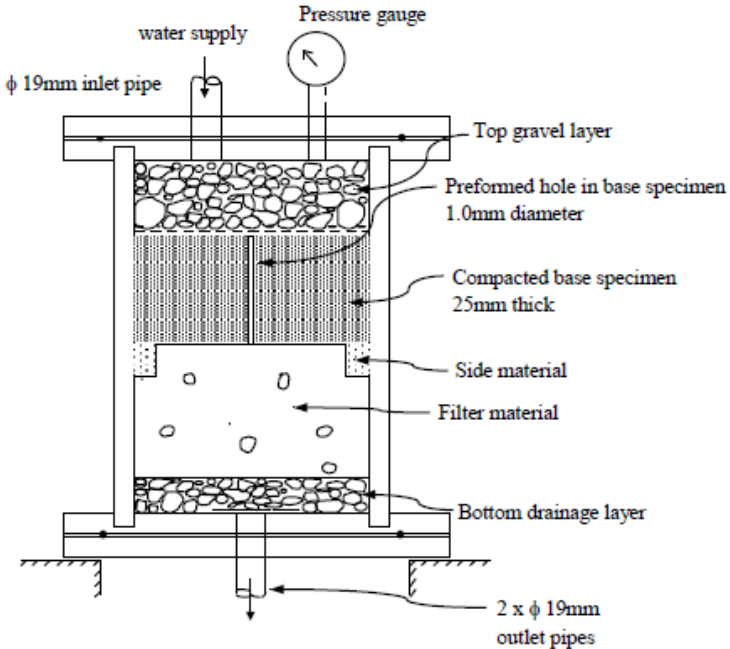


Fig. 1 General view of experimental apparatus [Sherard, Dunnigan, 1985]

2.2 Materials

The parametric study involves samples made of silt for the soil core and sand for the filter. The particle size distributions of the two materials are shown in Fig. 2. Two core soils were selected for erosion: silt 1 with a maximum particle size of $120\mu\text{m}$ and silt 2 (quite finer) whose maximal size is close to $106\mu\text{m}$. The two silts involve the same size d_{85} ($45.5\mu\text{m}$), which leads to the same ratio (D_{15} / d_{85}) of 11. For lower size than d_{50} , silt 2 contains more fines than silt 1.

The intrinsic characteristics of the two tested silts are listed in (Table 1). For mechanical properties, the plasticity index shows a difference between the two materials: Silt 1 is plastic ($I_p = 20$), while Silt 2 is slightly plastic ($I_p = 12$). From Fig. 2, the particle size distribution shows that Silt 2 contains less fines and is coarser than Silt 1.

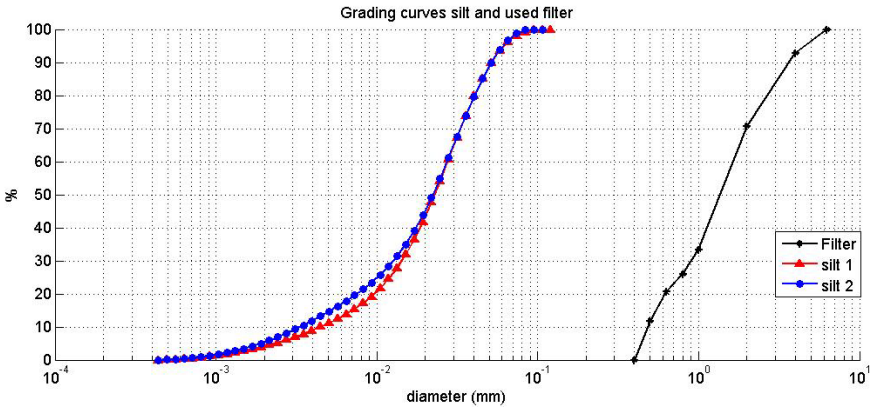


Fig. 2 Grain size distributions of used materials

The choice of filters for fine soils prone to suffusion or internal erosion is essentially based on the granulometric properties of materials. In our case the filter design was done in a way to meet the criteria proposed by the various authors (Tab. 2), [Locke 2001]. Terzaghi [1922] has been the first to propose a criterion to design the filter, followed by other approaches. The analysis of these different criteria reveals that that suggested by Sherard and Dunnigan [1985] is the most conservative criterion (Tab. 2). The filter used in the present study is efficient if fines grading involve a d_{85} size larger than $62 \mu\text{m}$. The diameter d_{85} ($45.5 \mu\text{m}$) of the two silts chosen was strictly smaller than the requested dimension given in Tab. 2 (right column), showing that filtration may not be efficient.

Tab. 1 Intrinsic characteristics of fine materials.

	plasticity			size (μm)				Grain	Retrait	Zêta
	W_L (%)	W_p (%)	I_p (%) (%)	D_{max}	D_{60}	D_{10}	<2 μm	γ_s (kN/m^3)	W_{sl} (%)	(mV)
Silt 1	37	17	20 (plastic)	120	30	4	6%	27.4	15	23.5
Silt 2	33	21	12 (Slightly Plastic)	106	28	3	5%	27.0	/	22.5

Tab. 2 Granulometric criteria applied to the designed filter

Author	Filter Criteria	Filter parameters	Fines size (μm)
Terzaghi [1922]	$(D_{15F}/d_{85B}) \leq 4$	$0.25D_{15F}$	140
Karpoff [1955] adopted by USBR	$5 < (D_{50F}/d_{50B}) \leq 10$ (sable fin)	Max= $0.2D_{50F}$ Min= $0.1 D_{50F}$	300 150
USACE [1971]	$(D_{15F}/d_{85B}) \leq 5$	$0.20D_{15F}$	112
Kenney and Lau [1985]	$(D_{15F}/d_{85B}) \leq 5$	$0.20D_{15F}$	112
		$0.25D_{5F}$	110
Sherard and Dunnigan [1985]	$(D_{15F}/d_{85B}) \leq 9$	$0.11D_{15F}$	62
Honjo and Veneziano [1989]	$(D_{15F}/d_{85B}) \leq 5.5$	$0.18D_{15F}$	101

3. RESULTS AND DISCUSSION

The filtration mechanism occurring in granular porous media is very complex, involving many processes and depending on several factors. One of them is the influence of silt type in filter efficiency. This parameter has enabled us to evaluate different parameters including: permeability, porosity and size of eroded particles.

3.1 Evaluation of the permeability change

After saturation of the filter in the cell, the measurement of the initial permeability is performed by a flow meter placed at the outlet of the column. This device enables us to save flow values throughout the test. The hydraulic conductivity is determined using Darcy's law presented in Eq. (1).

$$Q = -k \frac{A \Delta h}{L} \quad (1)$$

$$\Delta h = Z + \frac{\Delta P}{\rho g^2}$$

- $Z=0$ (reference level),
- Q = volume of flow,
- ρ = fluid density,
- k = permeability of the medium,
- A = apparent area of the material,
- ΔP = pressure difference.

To compare very easily the different parameters with several loads, curves of results are presented in dimensionless form (k / k_0). Figure 3 shows the evolution of the permeability of the filter according to the type of silt and the pressure applied to the inlet cell. Comparing two silts indicates that for a plastic soil (silt 1) erodibility is less than that of a slightly plastic soil (silt 2) which clogs the pores and leads to a drastic reduction of permeability. The permeability reduction (40%)

observed in the filter when used with silt 2 at a water pressure of 25 kPa is almost the same as that measured at 50 kPa when the filtration is processed for silt 1.

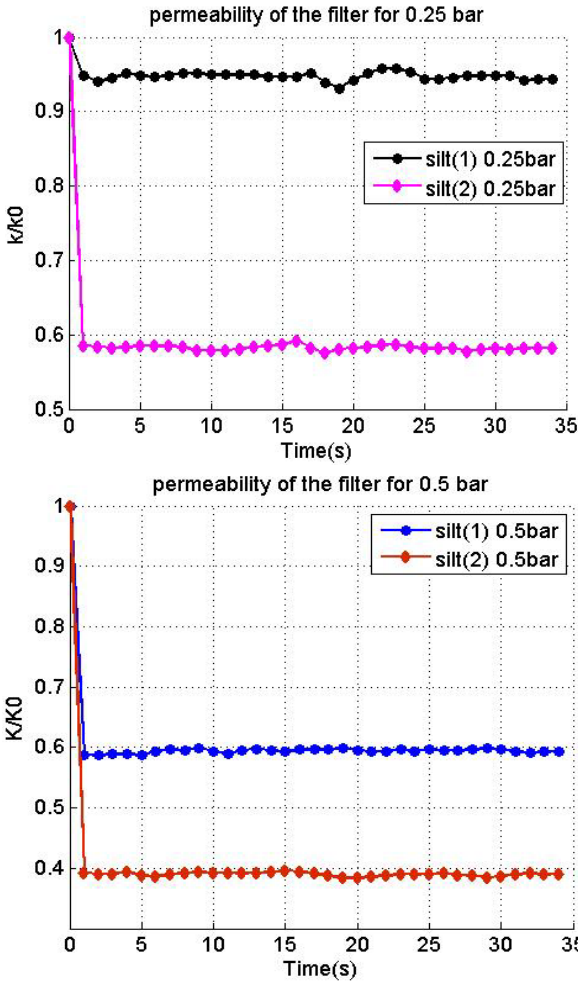


Fig. 3 Evolution of permeability ratio in the filter for two silts

The hydraulic load impacts heavily on the internal stability of fine soils. Figure 3 show that under a water pressure of 50 kPa permeability varies significantly compared to the permeability reduction obtained with previous pressure of 25 kPa. The reduction reaches 40% with silt 1 and then becomes 60% with silt 2 under a water pressure of 50 kPa. Such results suggest that silt 2 is more filtered than silt 1 under similar hydraulic conditions. The erodibility of silt 1 can be assumed to be

lower, inducing less particles flowing through the filter. The effect of water pressure on permeability reduction is due to previous deposition of particles within the filter and which not detached by the occurring higher pressure. This latter leads also to more particles removed from the core hole owing to increased shear stress on the hole surface. The curves from Fig. 3 illustrate that once permeability falls down in the beginning of filtration; its value remains constant, leading to a steady-state flow through the filter. So, no clogging risk occurs.

3.2 Porosity in the filter

Porosity is one of the most important parameters of concern in filtration process which includes the transport and deposition of particles in a porous medium. So, it is therefore important to investigate its evolution. Based on the experimental evaluation of the permeability of the filter for different silts tested, we were able to approximate the porosity n reduction according to the Eq. (2) of Kozeny, Carman, in [Nguyen, 2011]:

$$k = k_0 \frac{n^3 (1 - n_0)^2}{n_0^3 (1 - n)^2} \quad (2)$$

- k_0 = the initial permeability of the filter;
- k = the measured permeability;
- n_0 = the initial porosity;
- n = porosity corresponding to the permeability k ;

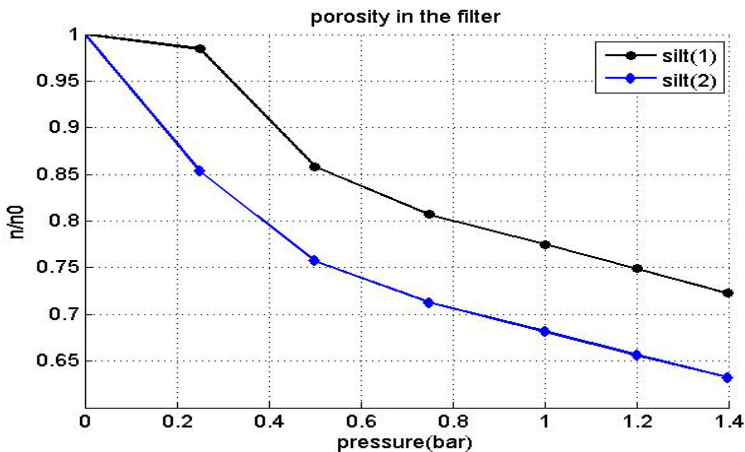


Fig. 4 Variation of the porosity in the filter under different loads.

The evolution of porosity was computed for different pressure ranges from 25 kPa to 140 kPa. Fig. 4 shows that the porosity decreases considerably when using

silt 2 than silt 1. These results can be related to clogging process in many pores by the flowing suspension containing a large amount of silt 2 particles, which reduces the hydraulic conductivity. If comparing the two silts, we conclude that during the first pressure steps the filter porosity in the presence of silt 2 is affected by a reduction ten times greater than that calculated with silt 1.

The erosion tests of the two kinds of silt show that the porosity decreases during loading (Fig. 4) and the effect of applied pressure decreases slightly when its amplitude increases. The porosity decrease in the filter is attributed to clogging process which occurs when detached particles are trapped within the filter.

3.3 Assessment of filter criteria

During the filtration tests we have separately collected samples of eroded particles through the filter for various water pressures for subsequent particle size analysis. The results can bring some knowledge about the maximal particle size which can flow through the filter without trapping.

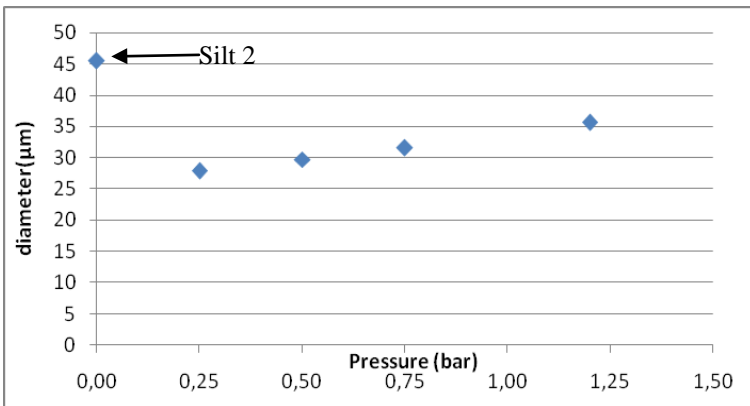


Fig. 5 d_{85} particle size of eroded fines versus applied pressure (silt 2)

In order to understand the filtration mechanism the distribution of sizes d_{85} for eroded (and not filtered) particles were plotted with respect to the grading curve of silt (Fig. 5). The results indicate that the fine fraction of silt particles are infiltrated since the size of particles collected ($<35 \mu\text{m}$) is widely smaller than that of silt ($45 \mu\text{m}$). According to initial size distribution of the two silts, this result suggests that only 40% of the eroded particles are filtered. The increase of the applied pressure generates increased size of eroded particles owing to higher shear stress applied on the internal surface of the hole. The d_{85} size (ranging between $28 \mu\text{m}$ and $38 \mu\text{m}$) of the infiltrated portion of fine particles (Fig. 5) is widely less than the filter opening ($550 \mu\text{m}$). These results confirm the criteria based on the filter size D_{15} but it remains that particles whose size is greater than d_{85} core soil (Fig. 6) requires larger opening filter.

Plotting the size distribution of recovered particles at the outlet of the filter column under different pressures (Fig. 6), it is shown that the detachment phenomenon of the fine particles in the base soil has the same shape with different rates, and d_{90} size is the same in the different cases of water pressure. Moreover, the lower portion becomes larger when increasing the hydraulic load, which generates strong extraction forces and even leads the particles previously retained. The recovered samples are finer than the initial particle size distribution in (silt 2). The effect of applied pressure is evident on the size distribution of recovered particles, since increasing pressure leads to recover larger sizes of particles. The analysis of the size distribution of retained particles within the filter at the end of the test shows that large size particles (coarse fraction) are retained by the filter. The grain size distribution of the filter material advocates the blocking of large silt particles in the voids formed by the grains.

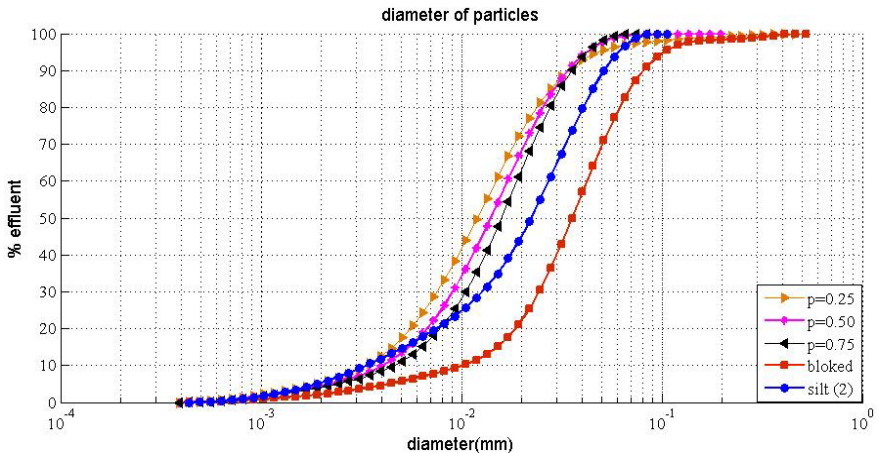


Fig. 6 Particle size distribution of the recovered samples (silt 2)

4. CONCLUSION

Two materials representing the base soil have been selected and tested with the aim of filtration mechanism investigation. The soil-filter system was subjected to increasing water pressure, geometric and hydraulic parameters were measured during and after filtration. The results of this experimental study lead to following main results:

Although the ratio (D_{15} / D_{85}) provided by the two silts is similar the filtration mechanism generates different results with the two samples.

Comparison of filter design criteria reveals that the relation proposed by Sherard and Dunnigan [1985] is the most conservative.

The plasticity of base soil influences greatly the filtration since slightly plastic soils (silt 2) are more erodible than plastic soils.

The hydraulic conductivity in the filter is of a great concern and leads to understand the filtration process but it remains a global parameter and knowing its spatial evolution along the filter becomes a necessity.

The permeability fall involves systematically a reduction in filter porosity.

The comparison of existing criteria in relation with d_{85} size of the recovered particles indicates that the large particles were filtered while the fines were infiltrated. Even if tested materials do not meet checked criteria, the filtration operates.

5. REFERENCES

- BENAMAR, A. 2013. Clogging Issues Associated With Managed Aquifer Recharge Methods: Soil Clogging Phenomena In Vertical Flow. IAH Commission On Managing Aquifer Recharge. Australia. 77 p.
- HONJO, Y., VENEZIANO, D. 1989. Improved filter criterion for cohesionless soils." J. Geotech. Engrg., 115(1), pp. 75–94.
- KARPOFF, K. P. 1955. The Use of Laboratory Tests to Develop Design Criteria for Protective Filters. American Society for Testing Materials, Vol. 55, pp. 1183-1198.
- KENNEY. T.C., LAU. D. 1985. Internal Stability Of Granular Filters. Can. Geotech. J., Vol. 22.
- LEE I. M., PARK Y. J., REDDI L. A. 2002. Particule Transport Characteristics and Filtration of Granitic Residual Soils from the Korean Peninsula. Can. Geotech. J. 39: 472-482 p.
- LOCKE. M. R. 2001. Analytical and Laboratory Modelling of Granular Filters for Embankment Dams. Doctor of Philosophy Thesis. University of Wollongong. Faculty of Engineering.
- NGUYEN. Q. T. 2011. Analyse Expérimentale Et Numérique De La Compaction Des Renforts Fibreux. Application Pour La Perméabilité. Thèse de Doctorat. INSA de Lyon. France.
- SHERARD. J. L., DUNNIGAN L. P. 1985. Filters and Leakage Control in Embankments Dams. American Society of Civil Engineers.
- TERZAGHI, K. 1922. Piping in Dams and Its Prevention Die Wasserkraft, Vol. 17, No. 24, pp. 445-449.
- USACE 1971. Dewatering and Groundwater Control for Deep Excavations. Technical Memorandum No. 5-818-5 (April), Office of Chief of Engineers, US Army, Washington D.C.
- VAUGHAN, P. R., SOARES, H. F. 1982. Design of filters for clay cores of dams. ASCE Journal of Geotechnical Engineering Division, January, Vol. 108 (GT1) pp. 17-31.

Investigations and Analysis of Levee Failures during recent Floods in Saxony and Saxony-Anhalt (Germany)

T. Heyer & J. Stamm

(Institute of Hydraulic Engineering and Technical Hydromechanics, TU Dresden – 01062 Dresden, Germany, torsten.heyer@tu-dresden.de)

Abstract

In recent years the German federal states of Saxony and Saxony-Anhalt were hit by several extreme floods (2002, 2006, 2010, 2013) leading to enormous damages in the range of billions of Euros. While the flood 2002 generated highest ever observed water levels mainly in Saxony, the flood 2013 generated maximum values at many gauges in Saxony-Anhalt. As a consequence many of the technical flood protection facilities were damaged and about 150 levee failures occurred during these floods. Against this background most of the levee failures were investigated by our institute and all available data was administered in a “levee failure database”. Besides the possibility of conducting a general descriptive analysis regarding the failures, this database also enables us to estimate the local failure probability of levees in future floods by using the method of logistic regression (“levee failure logit model”). Within this article, some results of the failure analysis of levees in Saxony and Saxony-Anhalt are presented. and the application of the levee failure logit model is demonstrated.

Keywords

Levee failure, Logistic regression, Reliability, Risk management, River floods

1. INTRODUCTION

In May 2013, exceptional precipitation caused extreme floods in the German federal States of Bavaria, Thuringia, Saxony and Saxony-Anhalt. At several river gauges of the Elbe catchment water levels were highest since records began or reached maximum alarm levels (Fig. 1). In consequence, flood protection structures were damaged resulting in heavy losses in economic terms and even human lives.

With regard to levee failures, about 40 cases were reported on the territory of Saxony and 12 cases in Saxony-Anhalt. Two of these, the levee failures at Breitenhagen (Saale River) and at Fischbeck (Elbe River) led to tremendous damages in the hinterland and thousands of people had to leave their homes (Fig. 2).

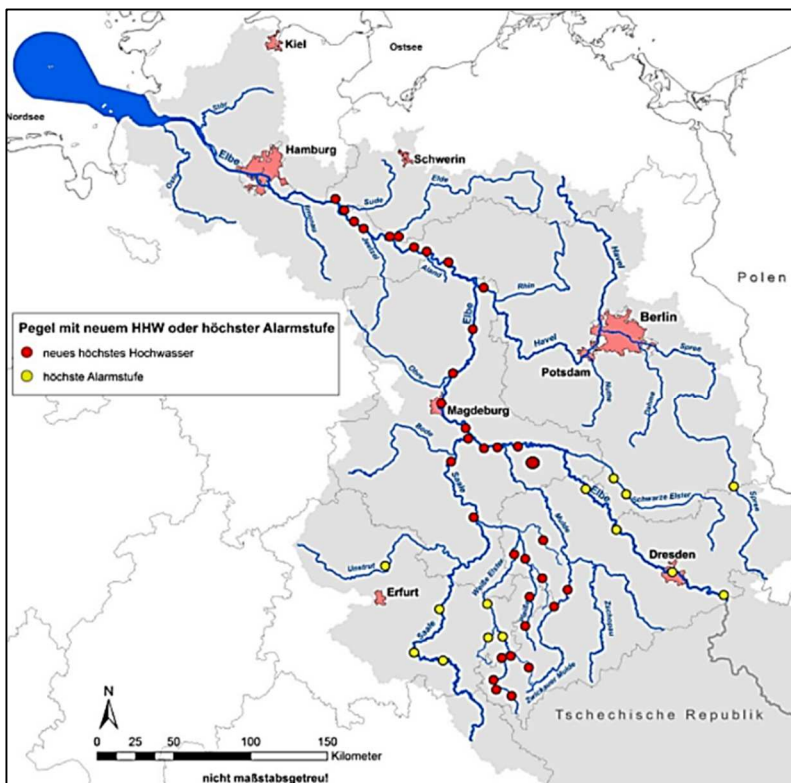


Fig. 1 River gauges in northeast Germany that reached highest, ever observed water levels (red) or maximum alarm levels (yellow) during the flood 2013 (source: FGG 2013)



Fig. 2 Levee breaches at Breitenhagen (Saale River) and Fischbeck (Elbe River)

Similar to a project that was conducted after the Elbe flood in 2002 (HORLACHER, HEYER & BIELAGK, 2005), in which a levee failure database was set up, our institute was asked to analyse all levee failures of the flood 2013 in northeast Germany, starting with the cases in Saxony-Anhalt.

Initially all relevant data and information had to be investigated, inspected and added to the levee failure database. Considering the parameters that could trigger or influence a levee failure, a large number of attributes are defined within each levee failure record, such as geographic location, cubature, degree of damage, inner structure, subsoil structure, vegetation, infestation by burrowing animals, breach geometry, to name but a few.

Based on this data the specific aims of the project were

- to characterise the conditions at the failed levee sections,
- to estimate the cause(s) of the initial failure,
- to test the so-called Levee Failure-Logit-Modell (LFLM) proposed by HEYER, HORLACHER & STAMM (2009) regarding its ability to predict levee failures

2. SIMPLE ANALYSIS

As the data availability for one of the twelve failures was poor, only eleven cases could be analysed in more detail. Some results of a simple analysis of the failures are presented in the following.

All failures occurred at rather old, homogeneous levees. In this regard, this type of levee should be rather referred to as “quasi-homogeneous” as many of them have been raised successively using the material available at this time. As a consequence, many of the existing, quasi-homogeneous levees (“old levees”) do not meet current safety standards. This holds particularly true for old levees protecting areas with low damage potential, where levee maintenance is usually reduced to an absolute minimum for financial reasons (Fig. 3).



Fig. 3 Typical breach appearance (left) at quasi-homogeneous levees (“old” levees) with distinctive stratification of the levee body (right)

From overlaying the assumed (in rare cases even exactly known) times of failure with the stage hydrographs of adjacent gauges it could be seen that all levees failed approximately during the passage of the corresponding flood peaks (Fig. 4). In reverse, all levees fulfilled their purpose until the exceedance of design load conditions. However, in some cases this was only be achieved by operational levee defence actions.

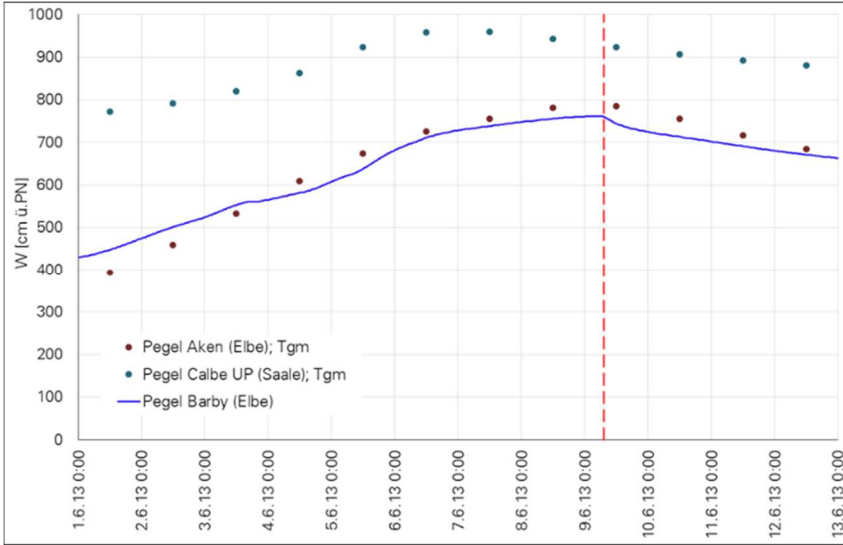


Fig. 4 Stage hydrographs of gauges adjacent to the levee failure at Breitenhagen (Saale River) and time of failure (red dashed line)

Referring to the degree of levee damage, in seven cases significant scours occurred with depths up to 3 m whereas in four cases only the levee body was eroded. In conclusion, in these four cases a subsoil participation could be excluded as trigger for the initial failure. On the contrary, the existence of scours does not imply that failure occurred due to initial subsoil processes, as scouring can also be the result of the flow process through the breach.

The widths (on crest level) of the investigated breaches varied from 10-140 m, showing a modal value in the class 10-20 m. This confirmed the result of the breach width evaluation presented in HORLACHER, HEYER & BIELAGK (2005) with the highest frequency of breach widths in the same class.

Although an analysis regarding the main failure modes and its triggers is always an estimate that, in the best case, is based on direct observations or measurements, we started an attempt in this project as well and came to the following conclusions:

- 1x Settlement on soft soil foundation,
- 3x Overtopping (erosion of inner slope)

- 1x Stability failure of inner slope
- 3x Piping in subsoil
- 2x Inner erosion in levee body
- 1x Hydraulic heave

3. LOGISTIC REGRESSION

Having established a comprehensive database about failed and non-failed levee sections as one of the results of the investigations after the flood 2002, the method of logistic regression offers best opportunities to use this valuable information from past experience for predictions of a levee's behaviour in future flood events.

Logistic regression is a statistical modelling approach used in multivariate data analysis. Although it has been widely used in other sciences, it is less common in civil engineering (Tab. 1).

Tab 1. Sample applications of logistic regression

Field	Variables, X	Response, Y
Medicine	age, smoker (y/n), blood pressure, ...	coronary heart disease (diseased/not diseased)
Sociology	age, social background, gender, ...	drug addiction (addicted/not addicted)
Transportation	age, season, distance, ...	means of transport (car/bike/public transport/...)

The application of logistic regression is preferable, whenever dependencies between several factors and observed events are undoubted, but the processes leading to the observation are uncertain. Regression models generally aim for the prediction of the outcome of a dependent variable (response variable), Y, given a set of influencing factors, X_i (Equation 1). Although not compulsory, logistic regression is often used, when the response variable has binary realisations (dichotomous variable), e.g. "failure" or "non-failure".

$$X_1, X_2, \dots, X_k \Rightarrow Y_{(0:1)} \quad (1)$$

A specific characteristic of logistic regression models is the ability to combine variables of different scale levels. Metric-scaled (cardinal) parameters are commonly used in engineering. Non-metric (categorical) parameters can be subdivided in nominal and ordinal variables (Tab. 2).

Tab 2. Scale levels

Scale	Properties	Example
<i>non-metric scales (categorical)</i>		
nominal	qualitative classification without ranking	gender (female/male)
ordinal	qualitative classification with ranking	quality (good/satisfactory/poor)
<i>metric scales (cardinal)</i>		
interval	with regular numeric distances; without fixed origin	temperature (celsius-scale)
ratio	with regular numeric distances; with fixed origin	kinematic parameters (velocity, weight, ...)

Whenever regression parameters are linked linearly, we refer to generalised linear regression models. The link between the combined regression parameters and the response variable is defined by a link function. In the case of logistic regression, the logistic function is used (Eq. 2).

$$P(z) = \frac{1}{1 + e^{-z}} \tag{2}$$

The logistic function given in Equation (2) belongs to the group of sigmoid functions. Since the functional values can be interpreted as probabilities in the range of $0 < P(z) < 1$ its usage is popular in probability theory. Therefore neither certain, $P(z) = 1$, nor impossible, $P(z) = 0$, events will be predicted.

Using this approach a logistic regression model computes the occurrence probability of an event, depending on the value of the parameter z , which is often called "logit". The logit z is an index that combines all regression parameters X_i by means of a linear sum. The logit of the n -th data sample with i influencing factors is calculated by using Eq. 3.

$$z_n = \beta_0 + \sum_{i=1}^k (\beta_i \cdot x_{ni}) \tag{3}$$

where

- z_n Logit for the n -th observation
- β_0 Constant
- β_i Regression coefficient of parameter X_i
- x_{ni} Value of parameter X_i in the n -th observation

While the values of the matrix X are the results of a levee (or levee breach) survey, the values of β will be determined within the model calibration. It is obvious that the applicability of a logistic regression model for a particular problem depends

strongly on the data availability and the selection of the characteristic regression parameters.

4. LEVEE FAILURE LOGIT MODEL

Based on the collected data of failed and non-failed levee sections, a so-called Levee Failure Logit Model (LFLM) was proposed by HEYER, HORLACHER & STAMM (2009) and developed further (HEYER, 2011) in order to predict the failure probability of individual levee sections in future floods depending on loads and local properties. As the data sample completely derives from surveys at old levees in Saxony and Saxony-Anhalt, the applicability of this model is limited to levees with similar characteristics. As this holds true for the levees that failed during the flood 2013 in Saxony-Anhalt, the goal was to test the LFLM for these locations by conducting an “ex-ante” (pre-flood) and an “ex-post” (post-flood) analysis (Tab. 3).

Tab 3. Applied levee failure logit models (status and purpose)

ID	Model status	Purpose
I	LFLM 2012	Computation of failure probabilities for extended data sample with original model (ex-ante-analysis)
II	LFLM 2014	Computation of failure probabilities for extended data sample with recalibrated model (ex-post-analysis)

In the original LFLM (HEYER, 2011), 24 parameters (11 metric, 7 nominal, 6 ordinal) were used for the failure probability predictions. Since not all of the information was available for the failed levee sections during the flood 2013, only 16 parameters could be included in the computations. The parameters used and the corresponding regression coefficients are summarised in Tab. 4.

Tab 4. Regression parameters and corresponding coefficients

i	Regression parameters X	Regression coefficient β	
		LFLM 2012	LFLM 2014
	Constant (β_0)	-10.636	-6.193
1	inner levee height	0.613	0.808
2	outer levee height	-1.704	-1.545
3	inclination of inner slope	0.443	0.387
4	inclination of outer slope	-0.079	-0.357
5	crest width	-0.167	-0.049
6	base width	-0.040	0.160
7	cross section area of levee body	0.162	0.069
8	discharge ratio ($Q_{\text{flood}}/Q_{\text{bankful}}$)	3.455	1.158

i	Regression parameters X	Regression coefficient β	
		LFLM 2012	LFLM 2014
9	width of foreland	-0.002	0.000
10	bridge connection	-8.079	-8.017
11	levee crossing	0.767	0.701
12	neighbouring water body	0.075	0.816
13	transverse structure	2.921	2.540
14	oxbow crossing	2.335	1.547
15	tree growth on/near levee	2.652	2.291
16	alluvial clay (thickness < 1 m)	1.990	1.724

It can be seen from Tab. 4 that the values of the regression coefficients change depending on the parameter values in the data sample, but also depending on the specified set of included parameters. By combining the regression parameters with the specific values of each record in the data sample according to Eq. 2 and 3, failure probabilities are computed in the range $0 < P_f < 1$. Using the definition that levee failure is predicted if $P_f > 0.5$ (otherwise “non-failure”) the results of the LFLM’s predictions can be summarised in contingency tables (Tab. 5 and 6).

Tab 5. Contingency table of model predictions vs. observations, LFLM 2012

		observation		total	
		failure	non-failure		
		yo=1	yo=0		
prediction	failure	yp=1	16	5	21
	non-failure	yp=0	29	608	637
total			45	613	658

Tab 6. Contingency table of model predictions vs. observations, LFLM 2014

		observation		total	
		failure	non-failure		
		yo=1	yo=0		
prediction	failure	yp=1	20	7	27
	non-failure	yp=0	25	606	631
total			45	613	658

It shows that with LFLM 2012 for 16 cases of the 45 observed failures (35.5 %) the prediction is correct and in total $16 + 608 = 624$ cases match the observed response of the levees, which leads to a hit ratio of 94.8 % (Tab. 5). After

recalibration (LFLM 2014) the hit ratio increased to 95.1 % and 20 of the observed failures were predicted correctly (Tab. 6).

Focussing on the predictions for nine of the twelve levee failures during the flood 2013 (three cases could not be included due to insufficient data), it can be seen from Tab. 7 that the original model (I, LFLM 2012) did not predict failure at these locations. However, the recalibrated model (II, LFLM 2014), which now contains the additional information of these locations, predicted failure in five of the nine cases. This demonstrates the possibility of updating the LFLM successively, being another advantage of this model type.

Tab 7. Computed failure probabilities at breached levees in flood 2013

No.	1	2	3	4	5	6	7	8	9
Name	SDL1	WB1	SLK1	ABI1	ABI2	BLK1	EE1	WB3	WB4
I	0.045	0.001	0.189	0.009	0.014	0.007	0.285	0.001	0.090
II	0.814	0.190	0.975	0.129	0.588	0.152	0.804	0.080	0.739

5. SUMMARY AND CONCLUSIONS

Motivated by the large number of levee failures that occurred during the recent extreme floods (2002, 2013) in northeast Germany, a levee failure database was established, initially for the purpose of simple descriptive statistical analysis only. Since extensive levee failure data is administered in this data base, the idea was to use this information further, in order to assess the reliability of levees in future flood events. For this purpose, the statistical method of logistic regression was used and the levee failure logit model (LFLM) proposed by HEYER (2011) was presented. The application of the LFLM was demonstrated using the example of the levee failures during the 2013 flood in Saxony-Anhalt. While the LFLM was not able to predict failures in the pre-flood 2013 state (LFLM 2012), predictions improved after recalibration (post-flood 2013) of the model. It proved that the LFLM provides a good opportunity to incorporate past event observations for levee failure predictions in future flood events. Perspectively, a constant updating of records regarding failed and non-failed levee sections is desirable in order to increase predictive capability and the confidence in the results of such models.

6. REFERENCES

FGG, 2013. Darstellung des Hochwassers 2013 im Einzugsgebiet der Flussgebietsgemeinschaft (FGG) Elbe.

HORLACHER H.-B., HEYER T. & BIELAGK U. 2005: Analyse der Deichbrüche an Elbe und Mulde während des Hochwassers 2002 im Bereich Sachsen, Tech. Report 2005/09, Institut für Wasserbau und Technische Hydromechanik, Technische Universität Dresden

HEYER, T., 2011: Zuverlässigkeitsbewertung von Flussdeichen nach dem Verfahren der logistischen Regression. Dissertation. In: *Wasserbauliche Mitteilungen, Heft 46*. Dresden (Germany)

HEYER, T.; HORLACHER, H.-B. & STAMM, J. 2009: Reliability analysis of river embankments using logistic regression In: *Proceedings „Long Term Behaviour of Dams“*. Graz (Austria)

Methodology for determination of rock mass characteristics for hydrotechnical tunnels

Z. Zafirovski, I. Peshevski, M. Jovanovski

(University Ss. Cyril and Methodius, Faculty of Civil Engineering Skopje, Partizanski Odredi 24, Skopje, Republic of Macedonia, e-mail: zafirovski@gf.ukim.edu.mk, pesevski@gf.ukim.edu.mk, jovanovski@gf.ukim.edu.mk)

Abstract

The analysis of stress-strain conditions is based on a large number of influential parameters of a rock mass that are very difficult to determine.

This paper includes analysis of a large amount of data derived from static and dynamic methods for ground investigation, drill holes and on site measurements. The methods used for investigation are particularly important since we tried to exceed the deterministic approach to analysis, because it does not always allow reliable information for adequate determination of input parameters; thus, the paper advocates the probabilistic approach to analysis.

The subject and methodology used in the paper are also mainly related to practical aspects, because final conclusions of investigations are obtained from analysis of a large amount of field and laboratory data, with experiences gained during the design process of hydrotechnical tunnels.

Keywords

rock mass, ground investigation, probabilistic approach, practical aspects, hydrotechnical tunnels.

1. INTRODUCTION

Geotechnical investigations present a very important part in the design of hydrotechnical tunnels. They are being performed from preliminary design phase, trough basic design and even in the phase of finalized constructions (Barton n., Lien , Lunde 1974). Some of the most important tests performed for rock mass characterisation include in situ tests as permeability (packer tests) and seismic wave velocity, laboratory tests as compressive strength, shear strength along joints, tensile strength, point load testing etc. (Hoek, E., Brown E.T. 1997). Since rock mass in most cases is anisotropic and discontinuous, it is usually very hard to adopt representative values for all geotechnical parameters and perform precise categorisation (Marinos, P; Hoek, E. & Marinos, V. 2006). Therefore we present statistical approach for adaptation of reliable parameters (Hoek, E. 2000). All results are from investigations performed for hydrotechnical tunnels in R.Macedonia in recent times.

2. RESULTS OF THE ANALYSIS

Results are statistically analyzed using computer program Statistica. For each analysis appropriate histogram is prepared, from where classes of parameter values can be deduced and their distribution. For example, presented are statistical analyses from compressive strength, point load index for rock masses from dam Sveta Petka, for phases before and during construction.

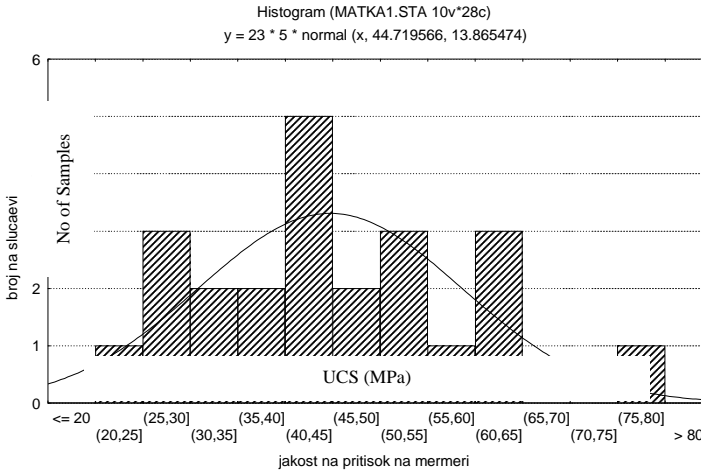


Fig. 1 Histogram of compressive strength values, results from investigation phase (Jovanovski et al. 2010)

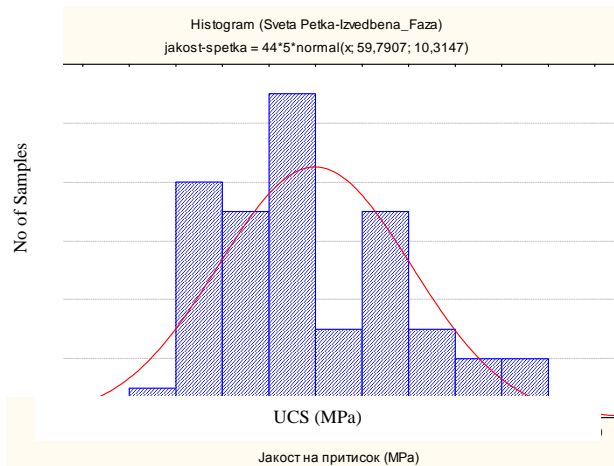


Fig. 2 Histogram of compressive strength values, results from construction phase (Jovanovski et al. 2010)

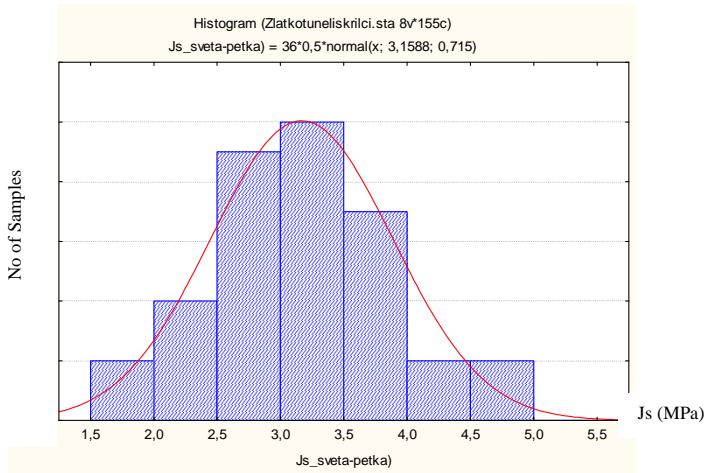


Fig. 3 Histogram of point load index values, results from investigation phase (Jovanovski et al. 2010)

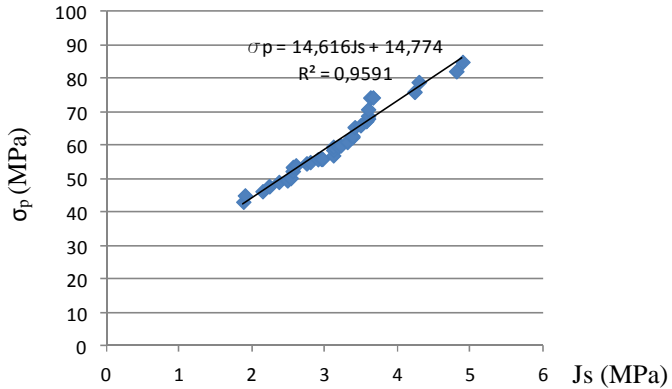


Fig. 4 Correlation between point load index and compressive strength, results from construction phase (Jovanovski et al. 2010)

Following figures show statistical analysis of results related to degree of fracturing and rock quality designation (RQD parameter).

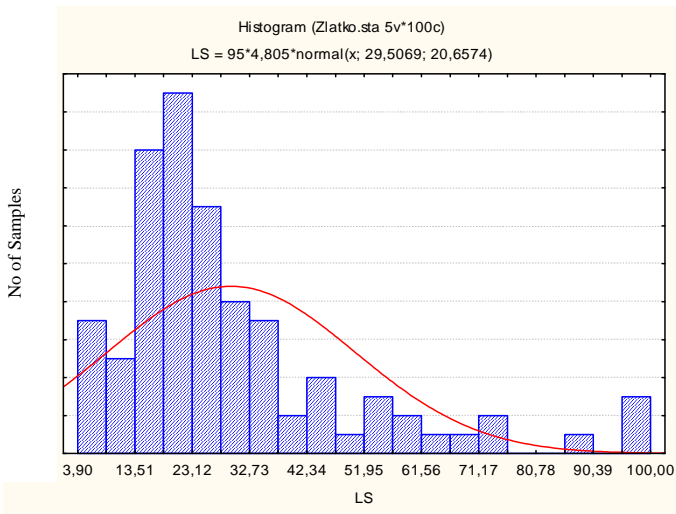


Fig. 5 Histogram of distribution of fracture density from drill hole data for dam Sveta Petka (Zafirovski et al. 2014)

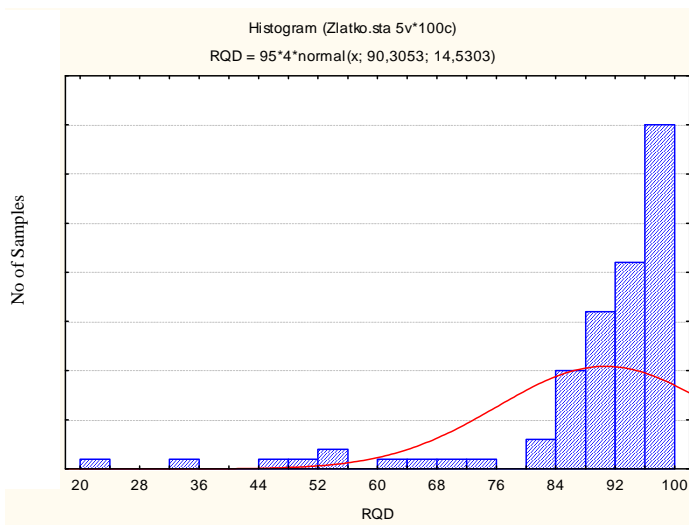
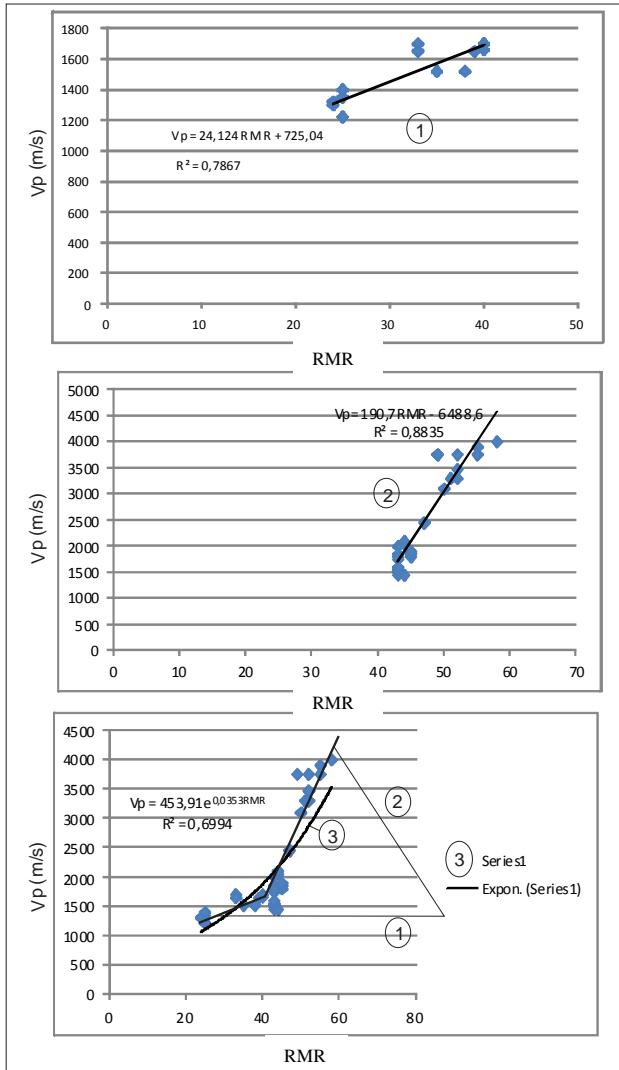


Fig. 6 Histogram of distribution of RQD parameter from drill hole data for dam Sveta Petka (Zafirovski et al. 2014)

From these histograms we can make better adaptation of most frequent values of parameters and interval of variation. Then decision can be made with which parameters we enter into the advanced designing which relies on these data.

It is obvious that the assessment of the class of rock mass for areas where we do not offer direct observations, it is necessary to establish a correlation relationship between the values obtained for the quality of the rock mass (eg RMR), with speeds of longitudinal elastic waves V_p (m/s). Some examples are shown on these pictures.



**Fig. 7 Correlation between RMR and speed of elastic waves $V_p \rightarrow$
 $RMR=f(V_p)$ (Zafirovski et al. 2014)**

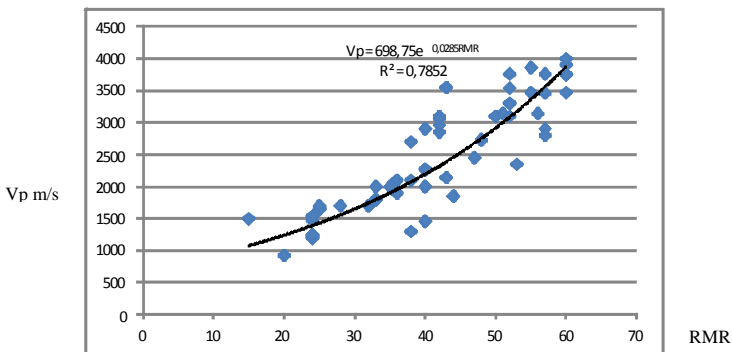
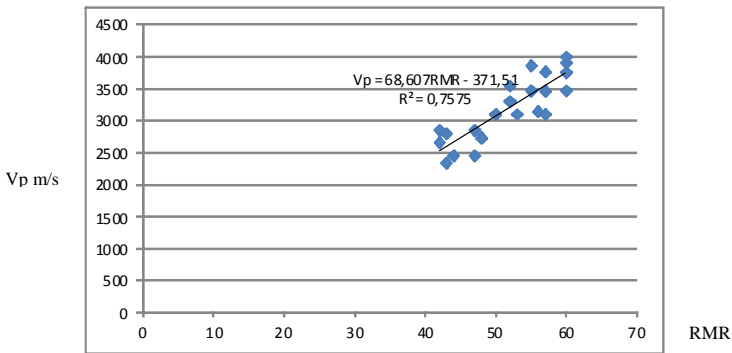
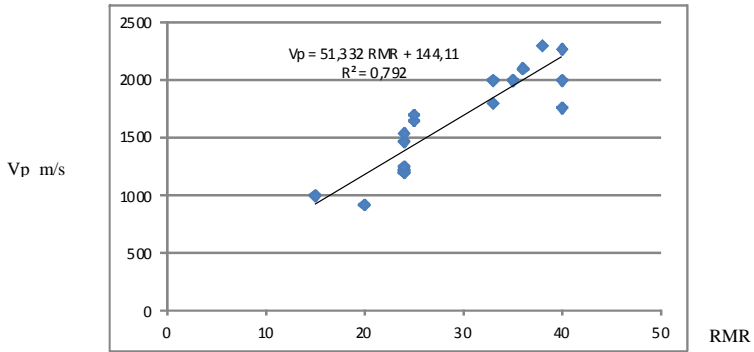


Fig. 8 Indirect correlation between the speed of elastic waves and modulus of deformation estimated by quality rocks $D \rightarrow D=f(V_p)$ (Zafirovski et al. 2014)

When there are direct measurements, they should also be used in appropriate analyzes, shown in figure 9.

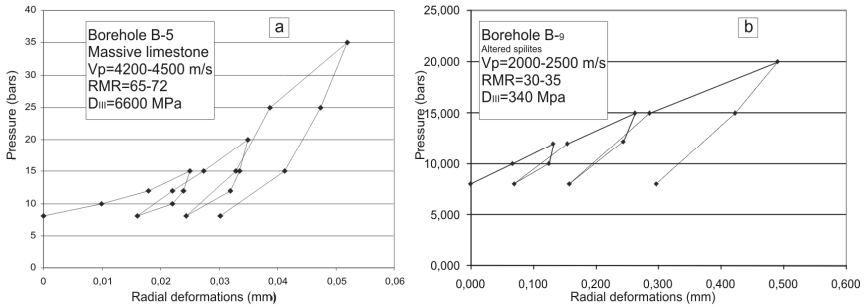


Fig. 9 Typical diagram of dilatometric tests (Zafirovski et al. 2012)

3. CONCLUSION

Statistical analysis of geotechnical data and correlations between analysed parameters are very important steps in any tunnel engineering project. Results from preliminary investigations can be considered as starting point, but their number should be increased in more advanced stages of design, and even checked in the phase of construction. With such approach we can calibrate correlations between geotechnical parameters and improve design.

The presented empirical–static–dynamic method for data extrapolation can be very useful tool in preparation of geotechnical models for further analyses in tunneling. Because of its verification, the suggested methodology must be critically re-examined meanwhile in terms of possibilities to apply it on other locations and other facilities in different geological media.

However, it will open doors and possibilities for further researches, considering that it is practically impossible to exhaust this scientific theme with only one paper. Analytical models for prognosis of possible intervals of deformation modulus D are useful as input data in numerical analysis for relatively shallow tunnels.

Also, the process of modelling must be harmonized with research and design phases. It is common to use simpler approaches in initial phases, which meet current quality and quantity of available data. Results of such kind of initial models for complex facilities can indicate the need for new data and they enable re-interpretation of existing data, what, in the other hand, influences the improvement of models or leads to new ideas for new model types.

Based on the aforementioned, we can conclude that there are many unlimited possibilities for further researches in this area. The purpose is to improve and confirm the methodologies suggested in this article, yet not only when it comes to tunnelling but also for other types of structures.

4. REFERENCES

- AFTES. 1993. Description of Rock Masses useful for examining the stability, Tunnels et ouvrages souterrains.
- BARTON, N., LIEN, R., LUNDE, J. 1974. Engineering classification of Rock masses for design in Tunnel support , Rock Mechanics Vol.6, No 4.
- HOEK, E., (2000): Rock engineering, Course notes by Evert Hoek. <http://www.rocksciennce.com>.
- HOEK, E., BROWN, E.T. 1997. Practical estimates of rock mass strenght. Intl. J. Rock Mech □ Mining Sci. □ Geomechanics Abstracts. 34(8), pp 1165-1186.
- HUDSON, J. A. 1993. Rock Properties, Testing methods and site Characterisation, Comprehensive rock Engineering.
- JOVANOVSKI, M., KRVAVAC-SPAGO, A., PESHEVSKI, I. 2010. Range of Engineering-geological properties for some carbonate rock complexes from Balkan Peninsula, Geologica Macedonica, Vol.24, No.1, pp.23-30, ISSN 0352-1206.
- MARINOS, P; HOEK, E., MARINOS, V. 2006. Variability of the engineering properties of rock masses quantified by the geological strength index. the case of ophiolites with special emphasis on tunnelling. Bull Eng Geol Environ (2006) 65, pp 129-142.
- VISSER, P. J. 1995. Application of Sediment Transport Formulae to Sand-dike Breach Erosion. Communication on Hydraulic and Geotechnical Engineering. Report No. 94-7, FCE, Delft University of Technology, 78 p.
- ZAFIROVSKI, Z., PEŠEVSKI, I., PAPIĆ, J. 2012. Methodology for extrapolation of rock mass deformability parameters in tunneling, FACTA UNIVERSITATIS - Scientific Journal Series Architecture and Civil Engineering, ISSN 0354 – 4605, Vol.10, No 3.
- ZAFIROVSKI, Z. 2014. Probabilistic approach for defining rock mass properties in stress – strain analysis in tunneling, DOCTORAL DISSERTATION.

Effect of designed material pits on filtration stability of the subsoil of polder Borša

D. Grambličková¹, E. Bednárová¹, M. Minárik¹, E. Kolesárová²
M. Bakeš³

¹ Department of Geotechnics, Faculty of Civil Engineering, Slovak University of Technology, Radlinského 11, 810 05 Bratislava, Slovakia, e-mail: danka.gramblickova@stuba.sk.

² Slovak Water Management Enterprise, branch office Trebišov, M. R. Štefánika 484/25, 0750 34 Trebišov, Slovakia, e-mail: Eva.Kolesarova@svp.sk.

³ Vodohospodarska vystavba s.p., Nobelova 7, 831 02 Bratislava, Slovakia, e-mail: martin.bakes@vzb.sk

Abstract

Polder Borša is situated in the East Slovakia Lowland, in the district Trebišov, near village Borša at confluence of Borša creek with river Bodrog. In recent years the polder has become a capacitive insufficient. Negative events were recorded during flood discharges on the circumferential dykes of polder, on the dykes of Borša brook as well as on the appurtenant structures. Therefore it was proposed reconstruction of the polder Borša including its circumferential dike.

The goal of this article is to assess the effect of the material pits excavation in the space of the existing polder on the changes in the filtration flow in the adjacent area during extreme hydrodynamic loading. The solution was carried out by finite element method.

Keywords

Reconstruction, Material pits, Stability, Dikes, Extreme hydrodynamic loading, Subsoil, Filtration velocity, Uplift, Finite Element Method

1. INTRODUCTION

Floods threaten humans for centuries. Their devastating effects are especially at risk of losses on human life. But they also sign under many situations threatening the quality of life and the environment. One way to accumulate flood discharges is the construction of polders [Rabatin, 2006]. For this purpose has been built in the past polder Borša. Polder Borša is situated in the East Slovakia Lowland, in the district Trebišov.

Due to changing hydrological conditions in recent years the polder has become a capacitive insufficient. Negative events (uneven settlement, overtopping of the dyke, seepages, failure of the spillway, breaching of the Borša brook dyke etc.) were recorded during flood discharges on the circumferential dykes of polder, on the dykes of Borša brook as well as on the appurtenant structures. Therefore was in 2007 proposed reconstruction of the polder Borša including reconstruction of its

circumferential dyke (Fig. 1). To the proposed reconstruction was in the space of the existing polder identified material pit for excavating materials. Material pit location is apparent from the scheme in Fig. 1. The goal of this article is to present lessons learned from the risk assessment of threats to the safety of the polder dikes and adjacent area due to mining of soils from the proposed material pits. The solution was carried out by finite element method [Thomas, Yuan, 1966] using programme Seftrans [Seftrans, 1996]. A detailed analysis is given in [Bednarova, Gramblickova 2007].

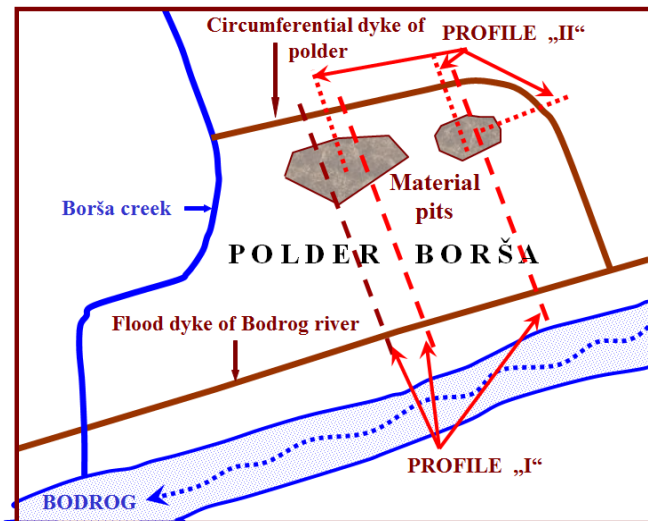


Fig. 1 Layout of the site

2. DYKES OF POLDER, ASSUMPTION OF CALCULATION

On Fig. 2 is presented cross section of the polder together with arrangement of objects. Circumferential dyke of polder is 578 m long; its 3 m wide crest reach elevation 100 m above sea level, inclination of slopes is 1:2. Distance of material pit from the right flood dyke of river Bodrog is 160 m, from circumferential dyke of polder 25 m and from left dyke of Borša creek about 65 m. Expected depth of material pit is 1.8 m (96 m above sea level), with a slope inclination of 1:2.

The surface layers of studied area (subsoil of Bodrog dyke, circumferential dyke of polder, and bottom of polder) are generally composed of silts and clays with class MS, CL, CS [Spisak, Varga, 2006]. Their thickness is variable and filtration coefficient around $5 \cdot 10^{-8} \text{ m.s}^{-1}$. Below them are situated loamy sand (SM), sometimes passing into fine-grained sands (SF) with filtration coefficient in the borders of $1.6 \cdot 10^{-5} \text{ m.s}^{-1}$ to $5 \cdot 10^{-6} \text{ m.s}^{-1}$. Analyses of available grain curves demonstrate their susceptibility to suffosion. The water table is in direct hydraulic

connection with the water level in the river Bodrog. According to the results of hydrogeological investigation in the studied area steady groundwater level is in a depth of about 2 m below the surface, on average about 96 m a. s. l. Considered backwater is 4 m above the average water level with duration of flood 40 days.

As a result of excavation of the soil from the bottom of the dry polder to the level of about 96 m a. s. l. existing seepage conditions of environment will change.

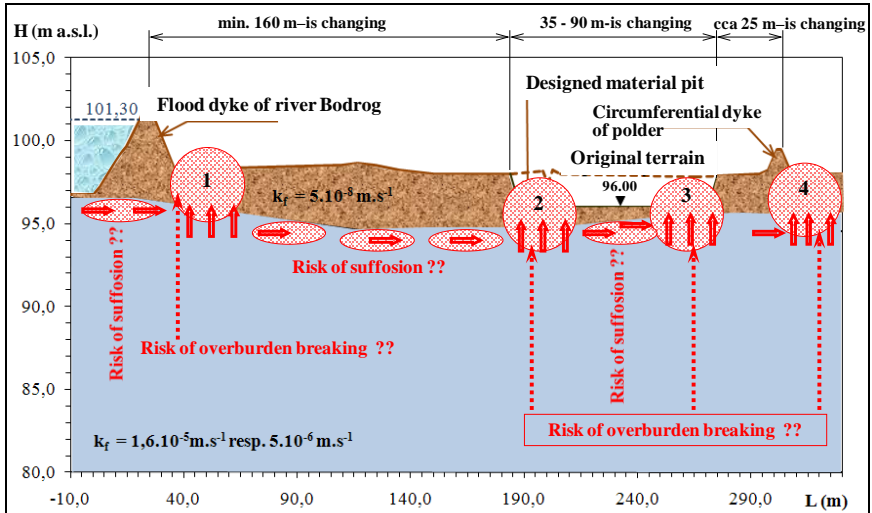


Fig. 2 Characteristic cross section, assumptions of calculation and risk factors

Impervious overburden layers with a relatively low coefficient of filtration (about 10^{-8} m.s^{-1}) will be at the material pit to a depth of about 1.8 meters excavated; thereby seepage paths in the subsoil of polder will locally shorten. Thus, to assess the safety of a flood protection dyke and the adjacent territory was necessary to verify the impact of designed material pits on filtration stability for two load cases:

- Under extreme flood conditions in the Bodrog River during floods (towards the dry polder) analyse seepage conditions of the right flood protection dyke and its subsoil. Stability of the dry reservoir bottom with the inlet of seepage water to the material pits was also observed. The solution was made in profiles "I" marked in Fig. 1 with dashed line.
- Under extreme hydrodynamic load (full reservoir of polder) analyse seepage conditions in circumferential dyke of polder, its subsoil and material pits. The solution was made in profiles "II" marked in Fig. 1 with dotted line.

3. ANALYSIS OF RESULTS

Geological composition of subsoil (contact of nearly impermeable overburden layer with the semi-permeable layer) indicates following potential risk factors (Fig.2):

- Risk of breaking of the overburden caused by uplift. The matter touched on both extreme hydrodynamic loading of the bottom of polder with flood discharges in Bodrog (sections "I") as well as loading of overburden layers near circumferential dykes of polder during its filling from the Borša Brook (sections "II"). On Fig. 2 are illustrated the most exposed areas of uplift for the first load state with numbers 1, 2, 3, for the second load cases it is a location labelled by 4.
- Risk of suffosion (Fig. 2) given the confirmed presence of sandy soils in the subsoil susceptible to suffosion. Analysis of the intensity of filtration flow was focussed to areas of Bodrog dyke subsoil, bottom of material pits (profiles "I") and subsoil of circumferential dyke of polder - towards the background - where as a result of excavation of soil in the immediate vicinity of the dyke implies the existence of shortened seepage path.

Uplifts were observed with regard to the height of backwater and duration of flood discharges. In this context, the dominant period is termination of the flood discharges. Filtration velocities are due to the maximum intensity of the hydrodynamic loading especially crucial in the early stages of flood discharges, therefore the analysis of their development was focused on this period.

3.1 Load state - extreme flood discharges in Bodrog riverbed profile „I“

Considered engineering-geological and morphological conditions of the adjacent area are shown on Fig. 2. Crest of the Bodrog flood protection dyke is at elevation of 101.80 m a. s. l., predicted flood level in Bodrog is at 101.30 meters a. s. l. Its height above the surrounding terrain is about 3.3 m; inclination of upstream and downstream slope of the dyke is 1:2. The bottom of the material pit is at an elevation of about 96 m a. s. l. Development of underground and seepage water flow was analysed assuming the coefficient of permeability of aquifers in the border $k_f = 1.6 \cdot 10^{-5} \text{ m.s}^{-1}$ to $5 \cdot 10^{-6} \text{ m.s}^{-1}$. Fig. 3 shows the time development (10 days, 40 days) of uplifts acting on overburden which permeability coefficient is $k_f = 1.6 \cdot 10^{-5} \text{ m.s}^{-1}$, what is the most unfavourable situation. Results of the development of the uplift pressure line as compared to the critical pressure horizon (red dashed line) indicate that even under these conditions does not originate conditions threatening the stability of the overburden against its breaking. This risk does not arise near downstream slope of the right-hand dyke of Bodrog (in Fig. area marked as "1"), as well as in the region of material pits (in Fig. area marked as "2" and "3"), where the original thickness of the overburden due to excavation of soils to a depth of about 1.8 m significantly decrease.

Development of seepage water levels indicate that during extreme discharges in Bodrog can be after the tenth day expected a slight increase of the water level above the bottom of the material pit. This was confirmed by providing filtration coefficient of sandy soils $k_f = 5 \cdot 10^{-6} \text{ m.s}^{-1}$.

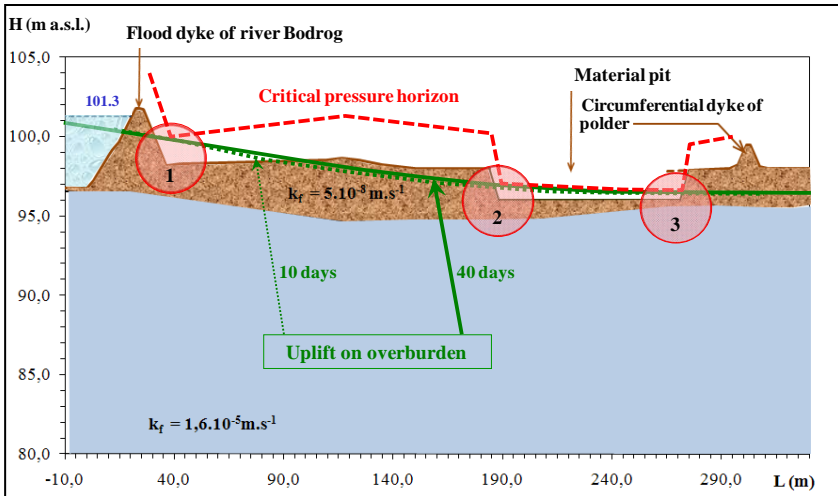


Fig. 3 Loading of overburden with uplift (profile „I“, $k_f = 1.6 \cdot 10^{-5} \text{ m.s}^{-1}$)

Analysis of filtration flow at the initial stage of extreme hydrodynamic loading of soils was focused on risky sub-regions - under a flood protective dyke of Bodrog and in the vicinity of material pits. Numerical results indicate that in assumed geological composition of the subsoil with the coefficient of sandy soil $k_f = 1.6 \cdot 10^{-5} \text{ m.s}^{-1}$ in the subsoil of a flood protection dyke of Bodrog occurred mainly gradients less than 0.2, which are less than the specified critical value $i_{crit} = 0.4$. Short-term local risk has been registered under the upstream toe of the dyke. The reason for this local phenomenon is not the existence of material pits, but the geological, hydrological and morphological conditions in the study area. In the area of material pits were not confirmed presumptions of origin of internal suffosion. Calculated hydraulic gradients here reached values less than 0.008.

3.2 Load state – full reservoir of polder - profile „II“

In the profile "II" are analysed parameters of filtration flow in the subsoil of polder and its circumferential dykes provided the full reservoir, with water at an elevation of about 99.60 meters a. s. l. As a result of the excavation of soil from the polder area to a depth of about 1.8 below the current ground level, i.e. to about 96 m a. s. l., seepage conditions will change. Shortening of seepage paths from the polder into adjacent surrounding areas includes consideration of the risk of breaking the overburden near downstream toe of the circumferential polder dykes (area "4" in Fig. 2) and risk assessment of internal suffosion.

It should be mentioned that the results of engineering - geological survey in this area confirmed the local presence of impervious overburden of lesser thickness. This weakness has a negative impact on the filtration mode in the subsoil. Moreover, during the excavation of soil for reconstruction of the polder, breaking of impermeable overburden layer in area of the bottom of material pits can be real. For the reasons outlined, we give this issue more attention in such negative, but realistic assumptions.

Fig. 4 shows the time development of uplifts acting on overburden, if there is a presence of sandy soils in the subsoil with filtration coefficient $k_f = 1.6 \cdot 10^{-5} \text{ m.s}^{-1}$, assuming the water level in polder at an elevation of 99.60 m a. s. l. When considering the composition of the subsoil and the position of the proposed material pits, the risk of exceeding the critical pressure horizon during 40 - day flood is on the limit of acceptability. In case of subsoil without material pits calculated pressure horizon is well below the critical values. The increase of uplifts in the subsoil to the acceptance limit is therefore evident influence of the material pits construction.

Similar results were also achieved from monitoring of the groundwater and seepage water levels. By excavation of material pits arise conditions for its partial wetting if the duration of flood discharges is 40 days.

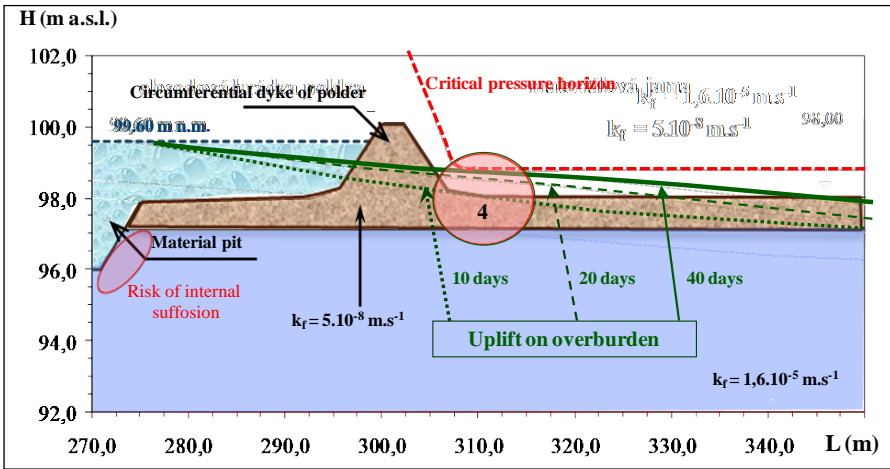


Fig. 4 Loading of overburden with uplift (profile „II“, $k_f = 1.6 \cdot 10^{-5} \text{ m.s}^{-1}$)

In the inlet parts of designed material pits were also confirmed locations with possible risk of internal suffusion. Hydraulic gradient here exceeds permissible value for about 2 days.

Calculated hydraulic gradients did not exceed critical values in the subsoil of circumferential dyke of polder and in the region of downstream toe of dyke.

4. RECONSTRUCTION OF THE POLDER BORŠA

Reconstruction of the polder Borša was implemented in the years 2008 - 2011. It was concentrated on increasing the stability of circumferential dyke of polder, where were during flood recorded seepages, outflows, breaching of dyke and flooding of surrounding agricultural land (grassland, arable land). The material for the reconstruction of dyke was excavated from the proposed material pits in the interior space polder. Fig. 5a illustrate material pit with partly excavated material. Water in material pit does not leak from the subsoil; it is the rest after flood on river Bodrog. Fig. 5b provides an overview of filled polder and Borša stream in 2010. Pumping of water from the Borša creek to Bodrog was part of the preparation for treatment work in 2010.



a) excavation of material from pit

b) filled polder and stream in 2010

Fig. 5 Reconstruction of the circumferential dyke, Photo: Tibor Karnay, 2010

Fig. 5b provides an overview of filled polder and Borša stream in 2010. Pumping of water from the Borša creek to Bodrog was part of the preparation for treatment work in 2010.

The original intention of the reconstruction was also an increase in volume of polder Borša by increasing the circumferential dyke. Due to the unsettled ownership relations to the adjacent properties it was not possible to implement this intention. Therefore, it was found a technical solution - construction of spillway on dike of the polder at km 0.210 to 0.510 with the length of 300 m, near the terrain depression. It is used to relieve the polder when is filled. The protection of the overflow area, chute and a part of the upstream side of the dam is strengthened with geosynthetic MacMat RA, which is covered with soil to a thickness of 100 mm and grassed.

Part of the investment project was also the reconstruction of riverbed of Borša creek. Its capacity was insufficient. Under excessive hydraulic loading here were also recorded seepages, outflows with symptom of suffusion, indicating risk of failure in stability of the riverbed. In km 0.0051 - 0.355 of the Borša creek on the left bank of the dyke was constructed crest spillway (Fig. 6). It serves to fill the

polder during the closure of the sluice at the confluence of the Borša creek and Bodrog.

In the flood conditions, when the sluice is closed and polder Borša is filled, water is pumped from Borša creek to Bodrog. This minimizes the risk of flooding of surrounding land through the spillway.



Fig. 6 Adjustment of the left-hand bank of the Borša creek dyke and the spillway, Photo: Tibor Karnay, 2011

5. CONCLUSIONS

Flood protection and safety of dikes is nowadays actual issue. Reliable function of flood protection measures may have a positive impact on mitigating the effects of floods. Indispensable part of ensuring reliable operation of technical measures (flood protection dikes, dikes of polders, dams etc.) is their continual monitoring. In case of presence of risk factors it is necessary to apply methods for verifying their safety and subsequent treatment.

In this paper is presented the application of finite element method in the safety assessment of the dikes of polder Borša, where due to the observation of multiple risk factors during floods was necessary its reconstruction.

6. REFERENCES

- BEDNAROVA, E., GRAMBLICKOVA, D. 2007. Effect of Material Pits on Filtration Stability of Polder Borša, SvF STU, Bratislava, 2007, 48p.
- RABATIN, T. 2006. BORŠA – reconstruction of polder. Project for construction permit. HYDROPROJSTAV, s.r.o., Košice, 2006
- SEFTRANS. 1996. A Simple and Efficient Two – Dimensional Groundwater Flow and Transport Model. Oxford, Durham, Prague, Dublin, 1996
- SPIŠAK, Z., VARGA, M. 2006. Borša – reconstruction of polder, Engineering-geological investigation. MONTANA, Košice, 2006
- THOMAS, S. D., YUAN, F. 1966. Groundwater and the Environment. Groundwater Modelling Case Studies. University of Durham, 1996

Acknowledgement:

This paper was supported by grant project VEGA No. 1/0318/13

Changes in groundwater level regime along channel due to surface water level fluctuations

P. Dušek

(Institute of Hydrology SAS – Račianska 75, 831 02, Bratislava, dusek@uh.savba.sk)

Abstract

Surface water fluctuations in streams can significantly affect the groundwater level regime in the surrounding aquifer. This effect is especially prominent in lowland areas without significant heterogeneity in the geological profile. The area of interest is located in the Rye Island, where a channel network was built to manage drainage and irrigation in the area, due to its very low slope. The regional geology consists mainly of gravel and sandy gravel fluvial sediments with high thickness, ranging from 350 to 400 meters. The selected channel Gabčíkovo – Topoľníky is one of the three main and most influential channels that affect the groundwater regime. The study was done using 1D and 2D surface water modelling with output data used in calibrated 3D numerical solution for simulating the groundwater regime. Several scenarios were assumed, including drought (zero or near-zero water level), high surface water level, and homogenous and heterogeneous geology.

Keywords

groundwater, stream, aquifer, interactions, models, simulation

1. INTRODUCTION

Žitný ostrov is an important agricultural site and is also an important source of drinking water. At the same time, thanks to the flat nature of the territory and the presence of a channel network is an ideal location for exploring the interaction of surface water and groundwater. The aim of this work is to assess the impact of fluctuations in the level surface flow of the irrigation and drainage channel Gabčíkovo – Topoľníky on the flow regime and groundwater levels in the surrounding aquifer using numerical simulations.

2. MATERIALS AND METHODS

2.1 Geography of Žitný ostrov

Rye Island is located in the south-western part of Slovakia, on the border with Hungary. Its boundaries are formed to the south by the Danube, to the north by Little Danube and the short section of the east it is bordered by the river Váh. The territory belongs geographically to the Danube basin. The island has an elliptical shape, its length is 84 km, the width is in the range of 15-30 km and total area of 1885 km² [Pásztorová et. al. 2013]. The island is the largest river island in Europe. The territory of the island is flat in nature. The slope of the territory is only 0.25

‰ [Velísková, Dulovičová 2008], with terrain height tend to fall in a south-easterly direction. The highest point of Rye Island is located near Šamorín (134 m a.s.l.) and the lowest is lying near Komárno (105 m a.s.l.).

2.2 Definition of the area of interest

The channel network of Žitný ostrov (Fig. 1) consists of seven main partially connected channels – Gabčíkovo – Topoľníky channel, Chotárny channel, Čalovo – Holiare – Kosihy channel, Aszód – Čergov channel, Čergov – Komárno channel, Dudváh channel and Komárňanský channel [Dulovičová et. al. 2013]. The total area of the irrigation and drainage channel network is 1469 km². The total length of the channel network is 1000 km. The density is approximately 1km of channels for 1.25 km². The most important and the most influential channels are Komárňanský, Chotárny and Gabčíkovo – Topoľníky channel.

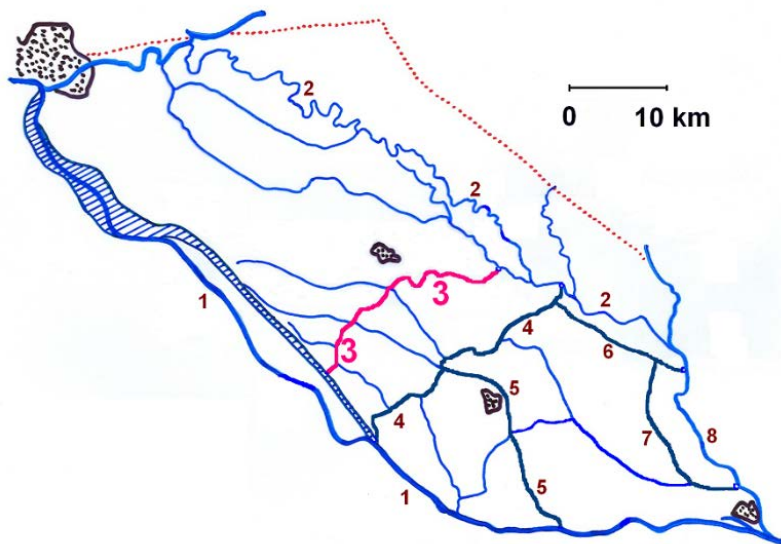


Fig. 1 Scheme of the channel network of Žitný ostrov (1–Danube; 2–Little Danube; 3–Gabčíkovo–Topoľníky channel; 4–Chotárny channel; 5–Čalovo–Holiare–Kosihy channel; 6–Aszód–Čergov channel; 7–Čergov–Komárno channel; 8–Dudváh channel; 9–Komárňanský channel) [Velísková, Dulovičová 2008]

Channel Gabčíkovo - Topoľníky is located in the central part of the Žitný ostrov (Fig. 2). It is donated with water seepage from the left-hand derivation channel of waterworks Gabčíkovo between the villages of Baka and Gabčíkovo. Diversion structure in the channel Gabčíkovo - Topoľníky is located in the left-hand bank of the derivation channel. Water is used in small hydropower plant

Small Gabčíkovo - S VII. Channel flows into Klátovský arm of Little Danube between the villages Topoľníky and Trhová Hradská. Its length is 28.7 km. On the channel there are two hydrometric stations, Gabčíkovo at river kilometre 25.7 with 10.7 km² catchment area and station Topoľníky at the 0.30 river kilometre with catchment area of 349.27 km², both within the competence of the Slovak Hydrometeorological Institute (SHMI). Directly in the area of interest there are 7 observation probes of SHMI for quantitative monitoring of groundwater from whom data were used to calibrate the model.

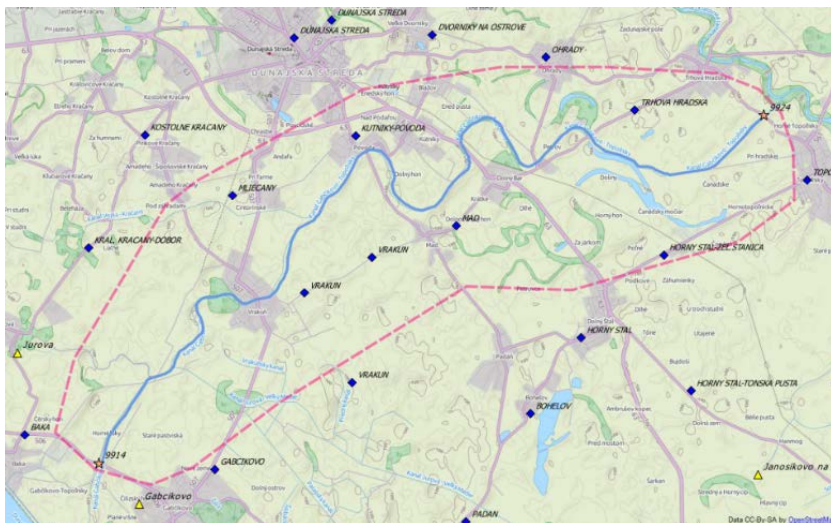


Fig. 2 The area of interest

Topography of the model area is of lowland nature, elevation ranges between 111.5 to 115.5 m a.s.l. The terrain lowers in northeast direction from river Danube to the Little Danube. At the same time the terrain lowers from northwest to southeast, parallel to the river Danube. The length of the model area is 18.16 km and the width is 6.07 km. The longitudinal slope is 0.2 ‰ and the lateral slope is 0.4 ‰ (Fig. 3).

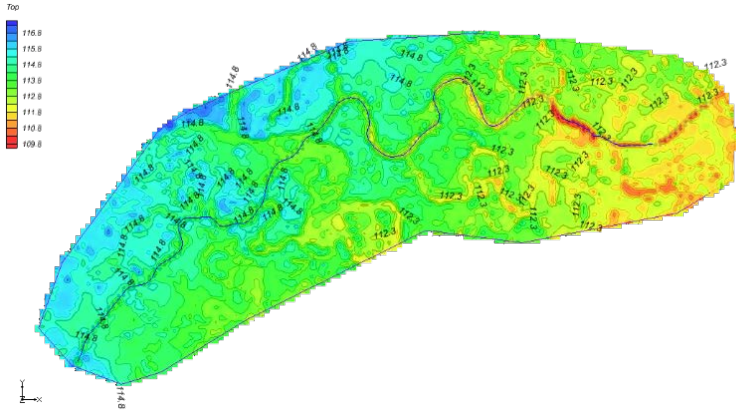


Fig. 3 Terrain topography of the model area

The area of interest can be from geological point of view classified as a part of Holocene alluvium of the Great Žitný ostrov. The geological structure is characterized mostly by quaternary fluvial sediments with thickness ranging from 200 to 500 meters [Káčer, et al. 2005] (Fig. 4). The groundwater level regime is influenced by the surface water levels in the channels and by the river Danube. Žitný ostrov is, due to the prominent occurrence of gravel in the geological profile, a significant collector of high quality groundwater, which is used as a drinking water. The saturated hydraulic conductivity in the area ranges from 7.10^{-4} do $8.10^{-5} \text{ m.s}^{-1}$ (Fig. 5).

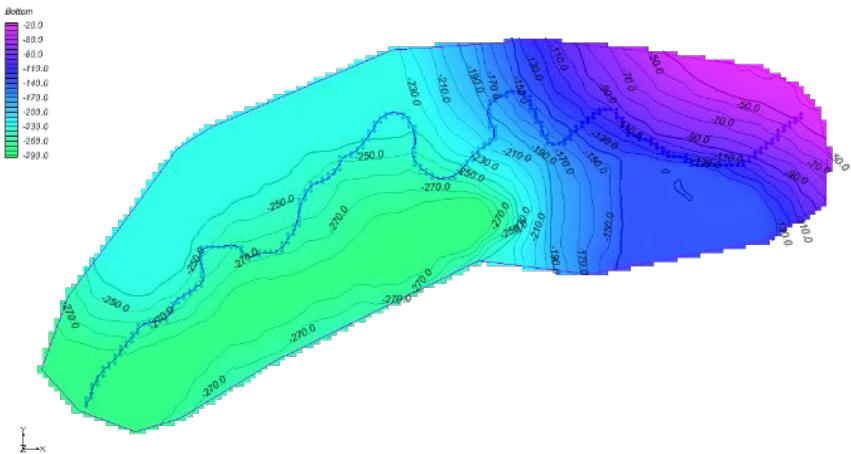


Fig. 4 The thickness of quaternary sediments in the model area

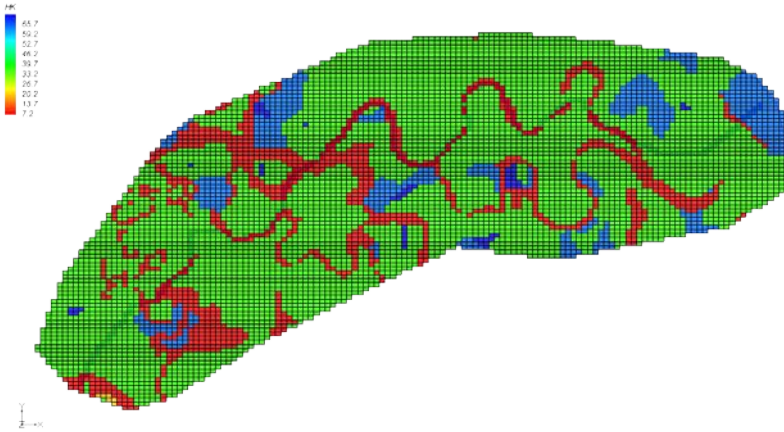


Fig. 5 Horizontal saturated hydraulic conductivity ($\text{m}\cdot\text{d}^{-1}$)

From the climatic point of view the area of interest belongs to the climatic zone A1 (according to the classification of M. Konček), which is characterized as warm, dry, with mild winters and longer sunshine [Faško, Štastný 2002]. The territory belongs to the warmest areas in Slovakia and is classified as an area of lowland climate. The average January temperatures are in the range of -4 to -1 °C, the average July temperatures are between 19.5 to 20.5 °C [Malík et al. 2011]. In the immediate surroundings of the channel Gabčíkovo - Topoľníky are two rain gauge stations, station 17600 - Gabčíkovo at an altitude of 113 m above sea level and station 17560 - Jurová at an altitude of 116 m above sea level. In 2013, the annual rainfall in the station Gabčíkovo was 640.8 mm and 670.2 mm in the Jurová station (Fig. 6).

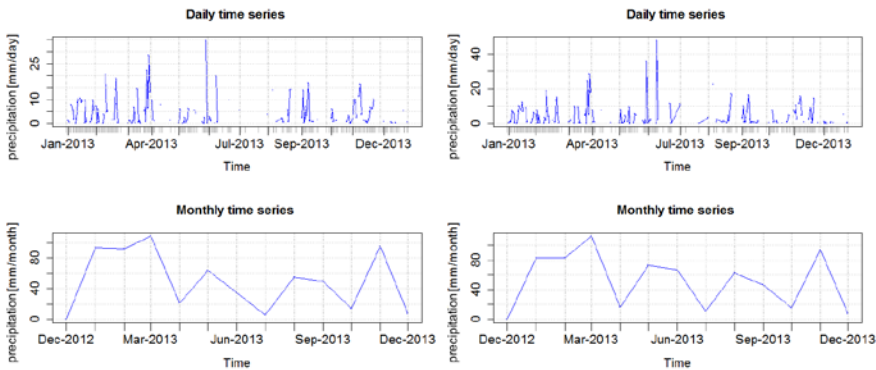


Fig. 6 Daily and monthly time series of precipitation in year 2013 for stations 17600 and 17560 [SHMI 2014]

2.3 Simulation of surface water flow

Simulation of surface water flow in the channel Gabčíkovo - Topoľníky was carried out according to known levels of the surface water at monitoring stations, and the topography of the channel cross-section profiles by the model GSSHA [Downer, Ogden 2006] GSSHA (Gridded Surface Subsurface Hydrologic Analysis) is a two-dimensional model using discretization of catchment area of interest by quadrangular elements. Part of the model is a one dimensional model of the surface water flow. The basic simulation outputs include depth level, velocity of the flow and the flow rate (discharge) at specified points. The output of the numerical model was used as an input parameter for subsequent numerical simulation of groundwater flow.

2.4 Simulation of groundwater flow for different surface water level scenarios

The flow of surface water and groundwater was simulated for three water levels in the channel during 2013, reflecting the maximum and minimum flow rates in a given year. On 1st May 2013 the flow in station 9914 Gabčíkovo was $1.37 \text{ m}^3 \cdot \text{s}^{-1}$ with the water at elevation 113 m a.s.l. and in station 9924 Topoľníky the flow was $1.92 \text{ m}^3 \cdot \text{s}^{-1}$ with water level at elevation of 109.59 meters a.s.l. On 12th of June 2013 the flow in station 9914 Gabčíkovo was $2.7 \text{ m}^3 \cdot \text{s}^{-1}$ with water level at elevation of 113.75 meters a.s.l. and in station 9924 Topoľníky the flow rate was $3.86 \text{ m}^3 \cdot \text{s}^{-1}$ with the water elevation at 111.17 m a.s.l. On 23th October 2013 the flow at station 9914 Gabčíkovo was $1.08 \text{ m}^3 \cdot \text{s}^{-1}$ with an elevation of 112.81 meters a.s.l. and in the station 9924 Topoľníky $0.73 \text{ m}^3 \cdot \text{s}^{-1}$ with an elevation of 109.39 m a.s.l. The simulation was created in a software package Aquaveo GMS 9.1 [Aquaveo 2013], which serves as a graphical frontend for several numerical models of groundwater flow, from which we used package MODFLOW - 2000 [Harbaugh et al. 2000]. It is a three dimensional model of groundwater flow. Groundwater levels in the day were defined by interpolation as the initial level of the model (starting heads), which also serves as a boundary condition as a specified constant level (specified head - CHD) [Aquaveo 2013], because the area has no natural filtration boundary. Channel Gabčíkovo - Topoľníky is specified as river body (river - RIV) [Aquaveo 2013]. River formations are represented by three figures - level, the height of the river bed and the parameter specified as conductance [Aquaveo 2013], which specifies the seepage of the bed sediments. The value of this parameter depends on the saturated hydraulic conductivity of bottom sediments (k), thickness (t) and the width of the bottom of the channel (w) (1).

$$Carc = \frac{k_t w}{L} = \frac{k}{t} w \quad (1)$$

Conductance parameter values were calculated from values of saturated hydraulic conductivity of bottom sediments in the channel Gabčíkovo - Topoľníky obtained by size distribution analysis of samples of bottom sediments. After

defining all the required parameters (boundary conditions for the field of filtration, topography, depth of the bottom of the aquifer, saturated hydraulic conductivity of the geology in aquifer, initial groundwater level, water level of surface flow, conductance of the river bed sediments, the inflow from rainfall) we approached the calibration of the model manually by editing the selected parameters, to achieve the best fit with the position of water level in observation wells in that day.

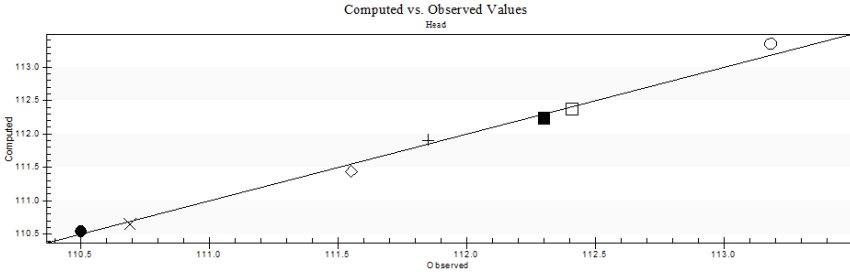


Fig. 7 The observed vs. computed head values – 1st scenario

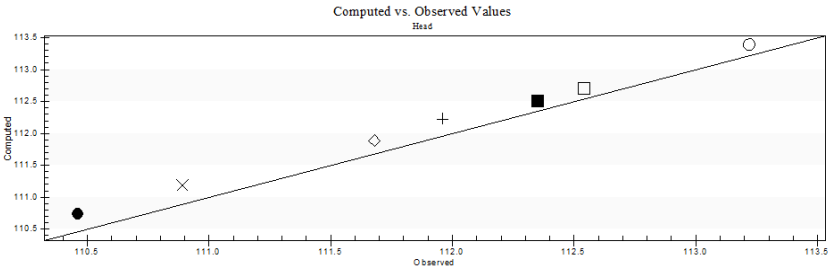


Fig. 8 The observed vs. computed head values – 2nd scenario

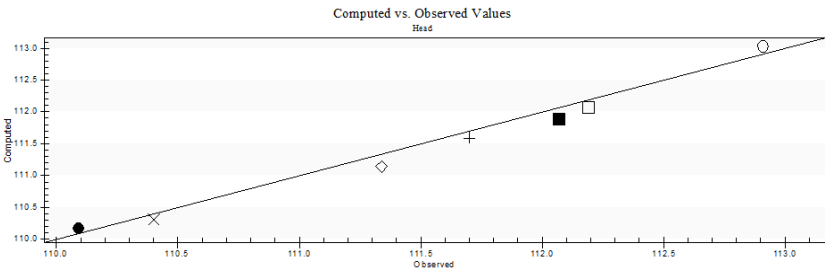


Fig. 9 The observed vs. computed head values – 3rd scenario

Deviation of the calculated values of groundwater level from the measured values determined the accuracy of the model. In the first scenario the deviations (errors) were calculated as values in the range of -0.17 to +0.11 m (Fig. 7). In the

second scenario, the dispersion of errors was in the range of -0.29 to -0.16 m m (Fig. 8). In the third scenario there was a variance of deviations between -0.11 m to 0,19 m (Fig. 9). Deviations from the observation values determined the accuracy of the calibrated model.

3. RESULTS

1st model scenario is characterized by the surface water level in the range from 113 m a.s.l. on the west end of the model to 109.59 m a.s.l. on the east end. The starting heads of the simulation range from 114.3 m a.s.l. on the west to 109.8 m a.s.l. to east. The computed groundwater heads range from 114 m a.s.l. to 109.5 m a.s.l., and there is a visible connection of the aquifer to the stream (Fig. 10).

2nd model scenario is characterized by the surface water level in the range from 113.75 m a.s.l. on the west end of the model to 111.17 m a.s.l. on the east end. The starting heads of the simulation range from 115 m a.s.l. on the west to 110 m a.s.l. to east. The computed groundwater heads range from 114.6 m a.s.l. to 110.3 m a.s.l.

The damming of the channel due to the higher surface water level on the east side of the model caused a significant change of the groundwater level regime (Fig. 11).

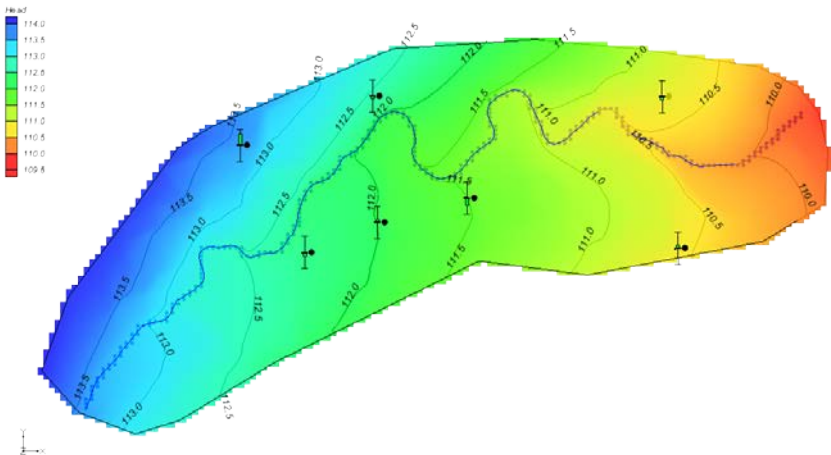


Fig. 10 The groundwater level regime – 1st scenario

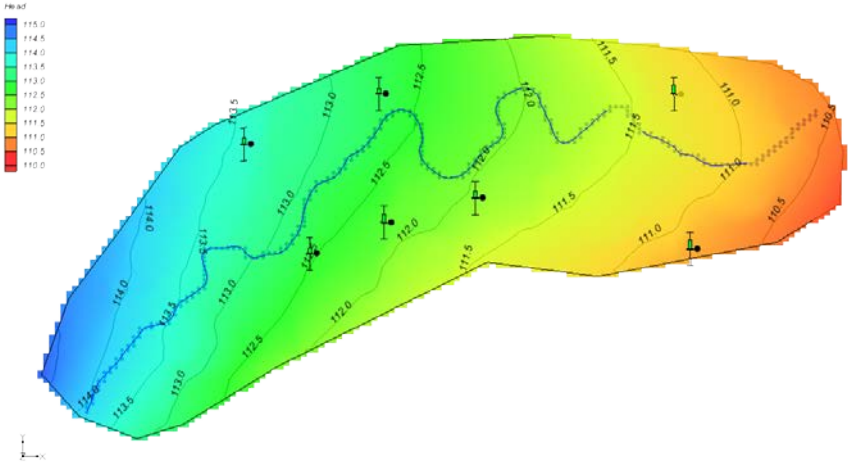


Fig. 11 The groundwater level regime – 2nd scenario

3rd model scenario is characterized by the surface water level in the range from 112.81 m a.s.l. on the west end of the model to 109.39 m a.s.l. on the east end. The starting heads of the simulation range from 114 m a.s.l. on the west to 109.3 m a.s.l. to east. The computed groundwater heads range from 113.8 m a.s.l. to 109.3 m a.s.l. The groundwater level regime is similar to the first scenario with the groundwater level change of 0.2 to 0.3 meters corresponds to the change in surface water level (Fig. 12).

The total water balance simulation models reflects the inflow and outflow of groundwater model. The inflow may consists of precipitation (Recharge), of inflow from constant level of head (boundary condition) on the boundary of the model (Constant Head), resp. if the channel is gaining or losing water from/to the aquifer (River leakage) (Tab. 1). For the first and the third scenario, the impact of depression of the surface water level (water level in the channel is lower than the level of the surrounding ground water) results in a gaining stream, so the aquifer is donating water to the channel. In the model MODFLOW the volume of flow from the aquifer to the stream (aquifer losing water volume) is expressed in negative values. In the 2nd scenario the channel partially infiltrates water into the aquifer, thus the inflow is expressed as a positive value.

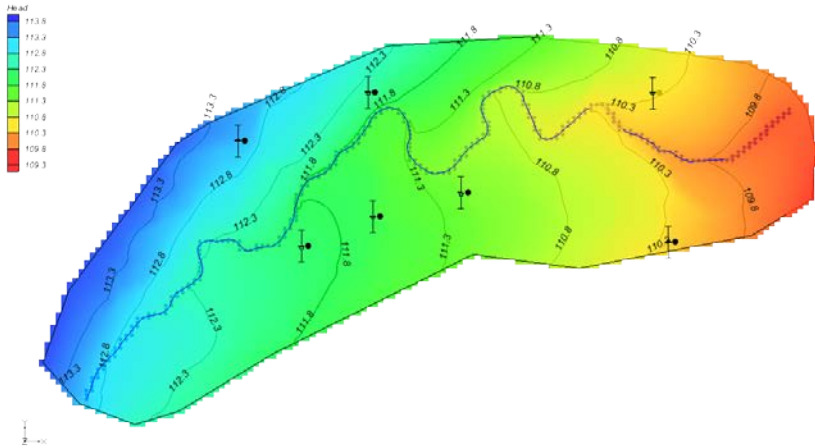


Fig. 12 The groundwater level regime – 3rd scenario

Tab 1. The total water balance of the numerical simulation (Flow Budget)

FLOW BUDGET	01/05/2013		12/06/2013		23/10/2013	
	FLOW IN	FLOW OUT	FLOW IN	FLOW OUT	FLOW IN	FLOW OUT
CONSTANT HEAD	92793	-33060	16419	-140610	69872	-45510
RIVER LEAKAGE	0	-1939412	3607	-13616	0	-158561
RECHARGE	134200	0	134201	0	134200	0
Total Source/Sink	226994	-227002	154227	-154227	204073	-204071

4. DISCUSSION AND CONCLUSIONS

The simulation results showed the impact of water level in the channel on the groundwater flow regime in the area, mostly in the riparian zone, where in the case of lower surface water level the channel creates a depression curve of the groundwater table and the channel is gaining water from the aquifer. In the case of higher surface water level in the channel (e.g. in the case of artificial damming of the flow due to irrigation, flood control or because of regulation of the flow in surrounding channels and rivers, etc.) there is a partial occurrence of the opposite effect, i.e. the stream is losing water to the aquifer. The channel, mostly in riparian zone, has a significant impact on the regime of the groundwater level.

5. REFERENCES

- AQUAVEO 2013. GMS User Manual (v9.1) – The Groundwater Modelling System, Aquaveo.
- DOWNER, C.W., Ogden, F.L. 2006. Gridded Surface Subsurface Hydrologic Analysis (GSSHA) User's Manual, Version 1.43 for Watershed Modeling System 6.1, System Wide Water Resources Program, Coastal and Hydraulics Laboratory, U.S. Army Corps of Engineers, Engineer Research and Development Center, ERDC/CHL SR-06-1, 207 pp.
- DULOVIČOVÁ, R., VELÍSKOVÁ, Y., BARA, M., SCHÜGERL, R. 2013. Assessment of the impact of riverbed sediment layer thickness along Chotárny channel on the interaction of surface water and groundwater, Acta Hydrologica Slovaca, Year 14, Volume 1, 2013, p. 126 – 134.
- FAŠKO, P., ŠTASTNÝ, P. 2002. Landscape atlas of Slovak republic, State Geological Institute of Dionýz Štúr, Bratislava.
- HARBAUGH, Arlen W., BANTA, Edward B., HILL, Mary C., MCDONALD, Michael G. 2000. MODFLOW-2000, The U.S. Geological Survey modular ground-water model – User guide to modularization concepts and the ground-water flow process, USGS.
- KÁČER, Š., ANTALÍK, M., LEXA, J., ZVARA, I., FRITZMAN, R., VLACHOVIČ, J., BYSTRICKÁ, G., BRODIANSKA, M., POTFAJ, M., MADARÁS, J., NAGY, A., MAGLAY, J., IVANIČKA, J., GROSS, P., RAKÚS, M., VOZÁROVÁ, A., BUČEK, S., BOOROVÁ, D., ŠIMON, L., MELLO, J., POLÁK, M., BEZÁK, V., HÓK, J., TEŤÁK, F., KONEČNÝ, V., KUČERA, M., ŽEC, B., ELEČKO, M., HRAŠKO, L., KOVÁČIK, M., PRISTAŠ, J. 2005. Digital geological map of Slovak republic at scale 1: 50 000 and 1:500 000, State Geological Institute of Dionýz Štúr, Bratislava.
- MALÍK, P., BAHNOVÁ, N., IVANIČ, B., KOČICKÝ, D., MARETTA, M., ŠPILAROVÁ, I., ŠVASTA, J., ZVARA, I. 2011. Complex geological information base for the needs of nature conservation and landscape management (GIB – GES), State Geological Institute of Dionýz Štúr, Bratislava.
- PÁSZTOROVÁ, M., VITKOVÁ, J., JARABICOVÁ, M., NAGY, V. 2013. Impact of Gabčíkovo Waterworks on the water regime of soils, Acta Hydrologica Slovaca, Year 14, Volume 2, 2013, p. 429 – 436.
- VELÍSKOVÁ, Y., DULOVIČOVÁ, R. 2008. Variability of bed sediments in channel network of Rye Island, IOP Conference Series: Earth and Environmental Science.

Acknowledgement

The research for this study was supported by the project VEGA č. 2/0058/15.

Experiences on the use of polymer coated steel net for the protection of dykes against the intrusion of beavers

P. Di Pietro¹, J.Adamec²

¹Maccaferri Deutschland GmbH – Kurfurstendamm, 226, 10719 Berlin, Germany
paolo.dipietro@maccaferri.de

²Maccaferri Central Europe s.ro. - Stvernik, 662 90613 Brezova pod Radlom Slovak Republic
jaroslav.adamec@maccaferri.sk

Abstract

Recent studies show an increase in the population of beavers, nutria and other rodents in vast regions of central Europe over the last 15 years. Unfortunately this caused in many instances considerable damages on large rivers along dykes and earthworks in the floodplain areas, leading to an increased risk of bank failures. However, most of these mammals belong to protected species. This work is aimed at showing positive experiences in cooperation with universities, research institutes and environmental agencies regarding measures to permanently safeguard the banks using composite erosion control systems with polymer coated steel wire net (as flexible reinforcement component) and a geosynthetic mat (to promote vegetation growth). The steel mesh component works as effective long term barrier against the intrusion of mammals, discouraging them from digging inside the core of the dyke. An analysis of the sensitive areas to be protected led also to define the characteristics of these interventions (length, shape, escape ways, population areas, etc). In summary, the study will also present several additional benefits when using polymer steel nets along dykes, such as:

- *high and durable erosion protection in overflow areas,*
- *promote fast and effective vegetation growth (increasing stability),*
- *surface protection against ice impacts (in northern regions).*
- *ease of installation, maintenance,*
- *ability to conform to irregular shapes of the slope.*

This work will also present the positive outcome of research studies along the dykes in Germany, Austria and in Italy.

Keywords

beavers, nutria, polymer coated steel net, geosynthetic mat, erosion control, dykes, flood protection, ice impact

1. INTRODUCTION

Beavers, Nutria and other rodents cause sometime fairly large damage on bank slopes, along dykes or in earthfilled embankments. In isolated cases such damages caused by these mammals could lead to an increased risk of global slope failures

with serious consequences of overflowing for the communities living in the area. However, one shall keep in mind that these species of rodents belong to protected species. Cavities created by beavers can be of high risk for the stability of the dyke. The highest risk is beavers digging through the impermeable layers. This leads to increased flow through the dyke, leading to erosion and water seeping through reaching the dry side.

According to a study published in 2011 [Kumutat 2011], [Schwab 2011] by the Bavarian State Office in charge of environmental protection, the beaver population across Germany was estimated in around 25,000 units, with increasing trend. An estimate across Europe in the same year was of approx 800.000 beavers. (Figs. 1 and 2).

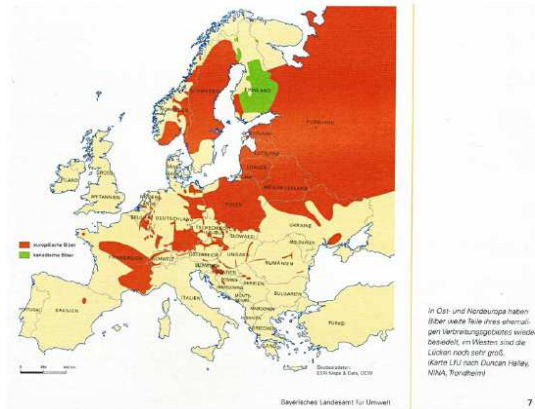


Fig. 1 Beaver population in Europe



Fig. 2 The Netherlands' beaver population is expected to grow from 700 to 7,000 by 2032

Measures to be undertaken to permanently prevent such effects depend on the sensitiveness of local authorities for potential hazards caused to people and to

infrastructures, as well as on costs required for the interventions and on the sensitiveness for the endangered species.

The correct approach consists in identifying critical areas of the dyke (Fig.3).



Fig. 3 Effects of beavers in floodway encroachment zones

The prevention against the intrusion of beavers, nutria, rodents and other protected species on dykes has been for over 15 years discussed and documented in studies carried out by academic Institutes and in works developed by the work of technical expert groups.

2. CONCEPT AND SUMMARY OF RESEARCH

Safe and durable protection against intrusion in dykes consists in identifying a suitable environmentally friendly barrier system. Steel meshes have been used to this purpose for decades. In recent times steel meshes combine the strength of the steel with the ability to promote vegetation provided by a three-dimensional geomat extruded during manufacture. The wire used for the steel mesh is protected a Zinc-Aluminum alloy and additionally by a polymer coating. The strength of the steel mesh will act as the impenetrable barrier for the rodents who will not be able to dig a hole through the steel net. The geomat will combine the antierosion function during flooding events, and by holding moisture will promote vegetation during the low flow season. These erosion mats may be delivered in rolled form and require very simple installation steps (Fig. 4).

In order to gain confidence about the effectiveness of steel meshes as beaver protection, several experiences were made in channels and dykes, some of which under the monitoring of technical Universities. To date there is wide experience that steel mesh systems perform satisfactorily to this purpose.



Fig. 4 Installation of beaver netting

2.1 Italy: guidelines from Ministry of Environment and long term studies after 10 years of observation

Italy had over the last decades a flourishing industry of fur. In the 1920's the population of beavers and nutria actually grew, to feed this sector of the industry. As modes changed in the 70's, and awareness for protecting endangered species grew, factories shut down and the animals released. This caused an increase of this population, which consequently led to more damages to embankments. Observations on slopes previously protected by stone-filled mattresses, showed no damages due to rodents, as opposed to other sections nearby where damages were visible. This was deemed as a proof that mammals were actually living in the area, but they could not damage slope sections protected with an armoured lining.

Based on these observations, the Ministry of the Environment, in coordination with the "National Institute for the Wild Fauna" and the "Institute for the Protection and Environmental Research (ISPRA)" [Cocchi, Riga 2005] promoted a long term study aimed at monitoring remediation measures against the intrusion of rodents into the canal banks. A testing canal (Zabarelle) in the Rovigo Province was chosen as representative of the large damages across the floodplain of the river Po (Fig. 5).

Steel meshes, with and without an extruded geomat, were installed in test sections in 2003. The initial survey allowed to capture and mark a number of nutria, and to apply a GPS-sender, in order to trace their paths. Results soon indicated that marked animals had moved to other sections.

In 2013 a second survey was arranged by ISPRA, to inspect these sections.

Observations showed that, where steel meshes with the extruded geomat had been applied, neither loss of fine materials in the water change zones nor damages to the steel net due to grass cutting were detected.

Where steel nets had been applied without the extruded geomat, losses of fine materials were noted. This was presumably due to the lack of the geomat at some locations where the eroded soil bank lost contact with the steel net, resulting in some damage during the grass cutting. The erosion function was not sufficiently provided by the open structure of the steel mesh alone. However, no intrusion of mammals was detected.



Fig. 5 Installation of beaver netting along Canale Zabarelle

2.2 Austria: Tests on effectiveness and implementation of 300,000 sqm of protection

For decades Austria experienced damages in waterways due to the intrusion of beavers. In 2008 the design of the protection measures along the river March (tributary of the Danube) took into consideration for the first time the effect of the beaver population with special reference to prevent potential damages. The analysis considered the variability of the species and types of mammals and rodents (quite large), hence the required strength characteristics of the protection netting, to resist to the bite and discourage even the strongest species from attempting to penetrate the protection.

Following these early studies, a first trial project was build using double twisted steel netting (300.000 m²) in a river bank application. The scientific study was part of a Diploma Thesis done for the Institute for Applied Geotechnics at the Technical University in Vienna under the guidance and coordination of the Prof. Dipl.-Ing. Dr. H. Brandl [Brandl, Szabo 2012]. Along with the observations and the experiences of the previous cases, the study encompassed an actual test done at the Research Center for Ethology at the Institute Konrad-Lorenz in Vienna.

The measures adopted were divided in two sections, where different protection systems (with and without steel nets) were used. The non metallic systems showed that after a short time a fairly large area of damages due to the bite of the rodents. Based on these findings, the technical university in Vienna concluded that the steel net types with the extruded geomat are the most recommended types of protection measures against beaver intrusion. The execution of the works was made in the years 2008-2013. They confirmed the expectations of a permanent protection against beavers.

In the recent years the beaver population further increased in Austria, extending in Upper Austria (Linz region).

Over the last years in the southern region as well (Carinthia) the beaver population has more than doubled.

2.3 Germany: protective measures against beavers along the Odra Dyke, District Sophienthal, Brandenburg 2013

Between October and December 2013, in cooperation with the State Agency for Environment, Health and Consumer Protection Frankfurt/Oder and the Water and Dike Association Oderbruch, Seelow beaver protection nettings were installed in a trial section approximately 175 m long, near the community Sophienthal (Fig.6).

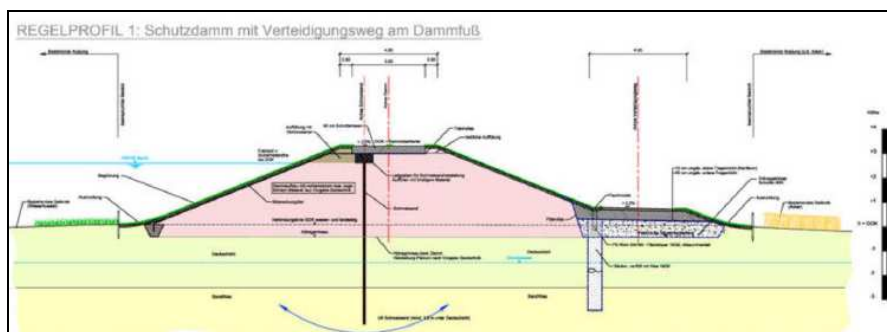


Fig. 6 Odra Dyke, Sophienthal – Cross section

Three different protection systems were installed:

- 1) Hexagonal steel wire mesh with integrated three-dimensional polymer matrix (MacMat R), covered by 5 cm top soil layer (Fig. 6, left bank).
- 2)

Hexagonal steel wire mesh, covered by 20 cm top soil layer. 3) Hexagonal steel wire mesh, covered by 20 cm top soil layer, connected to a stone mattress layer below in the water section.

The erosion net starts from the top of the dyke and ends on the water side, in the last case connected to the stone mattress below. Since further tunnels dug by beavers were detected in other sections nearby, the interventions were extended to these sections as well.

The execution of the works was under the supervision of the Institute of Hydraulic Engineering and Applied Hydromechanics (IWD) of the TU Dresden. IWD has been working for years on the task and supervised a Master Study on this topic in 2013.

3. NORMATIVE REQUIREMENTS FOR LONG LIFE

The use of steel nets in geotechnical and hydraulic applications pose questions of performance to corrosion. Galvanization (using Zinc-Aluminum alloys) provide an extended life, as the protection acts as retardant to corrosion by sacrificial nature. Additional polymer coatings applied on the galvanized wire provide a further extended protection. A newer generation of polyamide (PA6) in recent times introduced a further step in the life expectancy, allowing tests in severe saline conditions (ISO 9277) to exceed 6000 hrs of exposure without traces of red rust on the steel core inside.

An important reference in Europe is the EN 10223-3 [EN 10223-3] for double twisted steel wire meshes in civil engineering applications. The norm provides guidance concerning the life expectancy for steel mesh, defining for polymer coated steel wire mesh a minimum life of 120 years. In addition, guidelines in Germany [DVWK Merkblatt 247/1997] and Austria since 10 year already provide guidance concerning the use of steel nets as protection systems against beavers in dams and dykes.

However, DVWK 247/1997 has limited requirements for beaver nets with regard to corrosion protection and to their use (vertical barriers) making the systems effective only for limited time. Experience shows that in numerous sections of the dykes where vertical galvanized steel nets were used, the following effects were observed:

- Tunnels still present between the embankment and the vertical barrier, with evidence of flooding and partial collapse. Progressive erosion into the bank required vertical barriers to work as supporting elements. This caused deformation in the nets, and accelerated corrosion with loss of functionality.
- Tunnels ended at the vertical barrier. However this did not prevent beavers from digging new tunnels beyond the barrier into the berm, reaching in some instances even the toe of the main dyke.
- At high water flows, beavers could not reach the previously excavated tunnels, and made new ones directly into the body of the main dyke making their

stability critical as the upper portion has a smaller thickness. This triggered in some cases initial failures.

4. OTHER FEATURES OF BEAVER NETTINGS

4.1 Increased water conveyance

In accordance with the State Authority for Waterways (BAW) in Germany erosion protection systems consist mainly of a layer of loose stones laid on a sand mat (a thin layer of sand between two layers of geotextiles) acting as intermediate filter to prevent under piping through the voids of the larger rocks. Specifications for the stone size and for the layer thickness (0.50-1.0m) are of course determined by BAW according to their design recommendations [BAW]. As alternative to loose stones, steel meshes with the integrated geomat could in many cases be a sound alternative. Tests performed on these reinforced erosion blankets have shown the ability to resist to even high flows for a given period of time [Di Pietro, Urroz 1999], [Nemeth, Zanzinger 2009-2011]. The advantage of using a thin layer is also in the increased water conveyance, allowing a larger discharge in the river section.

4.2 Ease of maintenance

In case of accidental damage to the beaver erosion protection blanket, repair works would simply consist in the replacement of the damaged parts by attaching a panel of steel mesh on the surface. Connections are done with conventional steel rings, used for connecting rolls alongside.

4.3 Vegetation enhancement

In hydraulic works and the ability to develop a self-sustained vegetative layer with a solid rooting system to blend with the surrounding ecosystem has a special importance. Particularly susceptible to erosion are newly built sections when vegetation has not developed to a sustainable degree yet. The use of beaver protection with the integrated geomat allow a rapid establishment of vegetation [Di Pietro, Scotto, Guastini 2002], [Di Pietro, 2000].



Fig. 7 Growth of vegetation in beaver nettings

4.4 Protection against ice impacts

Embankment dykes in northern regions may often experience floods during the cold season, and be frequently exposed to the effect of ice blocks floating with the stream and impact against the banks (Fig.8). This results in damages to the bank slope and sometimes to partial failures. Steel nets with the geomat as beaver protection allow an armouring effect on the surface, further strengthened by the vegetative layer, which will grow through the mesh openings (Fig.7). This armouring effect will be particularly effective against the impact of ice blocks.



Fig. 8 Ice impacts along dykes

5. DISCUSSION AND CONCLUSIONS

Beaver protection nettings find in Germany an increasing interest in current dyke restoration projects. Projects in Brandenburg, Sachsen and Bavarian regions have been implemented successfully.

Extensive observations in areas protected by beaver nettings show that they protect against the several other types of animals, like rabbits, and wild pigs, who are frequently endangering the stability of the embankment as well. Beavers are discouraged from digging into the embankment and migrate to other areas.

However, these results raise questions concerning how beavers can populate in floodway areas without compromising structures designed to protect human lives.

The answer could be to build “ad-hoc” supporting structures in safe floodway encroachment zones where beavers could dig their tunnels without altering the embankment’s stability.

Trial projects have already started, and some authorities and research institutes have positively responded to this initiative. This is just a first step towards the development of a correct and more balanced approach to preserve our natural ecosystems to develop in harmony with the human needs.

6. REFERENCES

- BAW, Code of Practice .- Principles for the Design of bank and Bottom Protection for Inland Waterways (GBB), 2010, Bundesanstalt für Wasserbau
- BRANDL, H., SZABO, M. 2012. Vortragsfolien zum Themenbereich Hochwasser-schutzdaemme, Sicherung von Daemmen, Deichen und Stauanlagen, Vol. IV, Siegen
- COCCHI, R., RIGA F. 2005. Linee Guida per il controllo della Nutria (Myocastor Coypus), Quaderni per la conservazione della Natura: Min. Ambiente
- DI PIETRO, P. 2000. Soil bioengineering and ecological systems: how to handle erosion problems in natural and altered habitats, Geotechnical Fabric Report, September 2000, USA
- DI PIETRO, P., SCOTTO, M., GUASTINI, U. 2002. Stabilizing and waterproofing a levee in Italy, Geotechnical Fabric Report, August 2002, USA
- DI PIETRO, P., URROZ, 1999, Performance testing on a three-dimensional composite high strength soil erosion mat, Utah Water Research Laboratory, Proceedings from IECA Conference 1999 Nashville, TN, USA
- DVWK Merkblatt 247/1997, Bisam, Biber, Nutria: Erkennungsmerkmale und Lebensweisen – Gestaltung und Sicherung gefährdeter Ufer, Deiche, und Dämme, 1997
- EN 10223-3: 2013, Hexagonal Steel Mesh Products for Civil Engineering Purposes.
- KUMUTAT, C. 2011. Biber in Bayern – Biologie und Management, 2 Auflage 2011, Praesident des Bayerischen Landesamtes fuer Umwelt, Augsburg
- NEMETH, E., ZANZINGER, H. 2009-2011. Erarbeitung und Verifizierung von Auswahlkriterien fuer geosynthetische Erosionsschutzsysteme, AiF Research Project, SKZ/LWG 2009-2011
- SCHWAB, G. 2011. BN-Bibermanager Suedbayern, Auszug Vortragsfolien, Kuenzell 09-2011

Modelling of the impact on groundwater regime due to construction of the proposed hydraulic structure on the Danube River

M. Nahálkova, D. Baroková, A. Šoltész

Department of Hydraulic Engineering, Faculty of Civil Engineering, Slovak University of Technology in Bratislava, Radlinského 11, 810 05 Bratislava, Slovak Republic, phone: +421 2 59 274 571, fax: +421 2 59274 565, e-mail: mnahalkova@gmail.com, dana.barokova@stuba.sk, andrej.soltesz@stuba.sk

Abstract

The source of water for Bratislava urban area, satisfactory in terms of quality and quantity, is mainly groundwater from aquifer of Danube River sediments. They are water sources built on the left bank Danube islands Sihot' and Sedláčkov ostrov as well as water source on the right bank of the Danube River in Pečniansky les. The goal of the paper is a quantitative analysis of the groundwater regime in the mentioned areas, assessment of potential threats to water resources due to construction of the proposed hydraulic structure on the Danube River in the area of Bratislava ("Hydraulic structure Bratislava – Pečniansky les") and at last but not least design of the measures to reduce the negative impact caused by the construction of the hydraulic structure. The location of the mentioned hydraulic structure is in Bratislava between the highway bridge Lafranconi and the border to Austria at rkm 1872.21.

Keywords

groundwater flow, impact of the hydraulic structure, groundwater modelling, TRIWACO, water sources in Bratislava

1. INTRODUCTION

Water sources built on the Danube islands (Sihot' and Sedláčkov ostrov) and water sources, located on the right bank of the Danube in Pečniansky les have in terms of supplying the population in Bratislava with drinking water irreplaceable function. In order to keep the actual functions of water resources it is therefore necessary to assess the impact of the proposed construction of the multi-purposed structure "Hydraulic structure Bratislava – Pečniansky les" (HS) to these water sources. The issue of the impact of the construction on groundwater level regime is dealt with numerical model of groundwater flow TRIWACO – Flairs (Royal Haskoning, 2004), based on the finite element method.

2. MATERIAL AND METHODS

Source materials:

- morphological parameters;
- geological parameters – top and base of the aquifer;
- hydrogeological parameters – hydraulic conductivity;
- hydrological parameters – level regime of the Danube and Morava, daily rainfall and effective rainfall [Švasta, Malík 2006], measurement of groundwater levels, water abstraction from water resources.

2.1 Defining the model boundary

As a background for the model boundary the map of groundwater bodies in quaternary sediments [Kullman et al. 2003], the tourist map of the Small Carpathians and Bratislava and the map of the river network in Slovakia were used.

The model boundary is formed in the north of the River Morava and interfaces of the layers of groundwater bodies in quaternary sediments, in the east or River Danube and measuring objects of groundwater level in Petržalka, in the south (in Austria) passes in quaternary alluvial deposits of the Danube and in the north-west is formed by the Danube to the confluence with Morava.

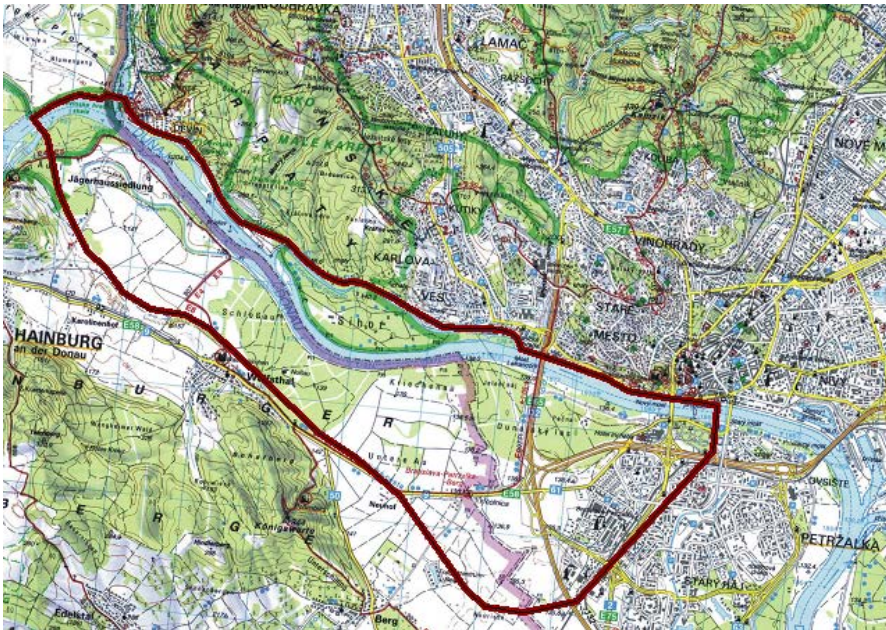


Fig. 1 Model boundary

2.2 Parametrization of the area

For parameterization of input values, such as terrain, base and top of the aquifer and hydraulic conductivity the triangular interpolation method (TinInt) was used.

2.3 Calibration of the groundwater flow model

Calibration of the model consisted in setting the hydraulic parameters of the river bed. Those parameters are the values of the hydraulic conductivity [Rosas et al. 2014] and drainage and infiltration resistance of rivers [Zaadnoordijk 2009], (Šlezinger, 2007). The result of calibration of steady-state flow was groundwater level regime (resp. piezometric head) in the area of interest corresponding to medium hydrological values. The simulation results – contour map of groundwater levels – are drawn in Fig. 2.

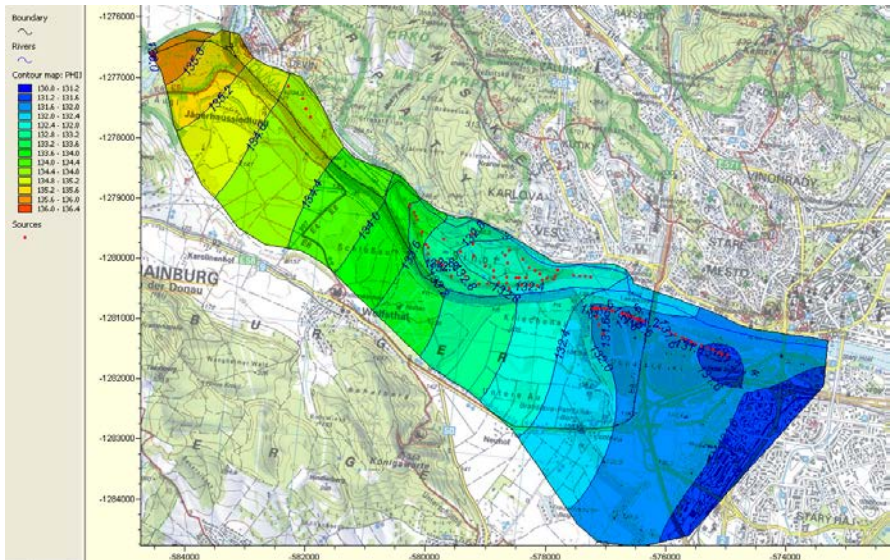


Fig. 2 Groundwater level contour map (m a. s. l.) – present time

From the groundwater level contour map is clear that the groundwater level and the direction of groundwater flow are directly dependent on water levels in the Danube River. In the vicinity of wells, however, the level and direction of groundwater flow is more influenced by pumping of water, especially on Sihot' and Pečniansky les where pumping is substantially greater than on Sedláčkov ostrov.

2.4 Simulation of groundwater level after the construction of the proposed HS

The simulation result, assuming steady-state flow after construction of the planned HS [Slovák 2010, Čomaj 2012] is the groundwater level (or piezometric water level) after the construction. Isolines of groundwater level are drawn in Fig. 3. The result of the simulation is also the determination of the depth of groundwater below the surface shown in Fig. 4.

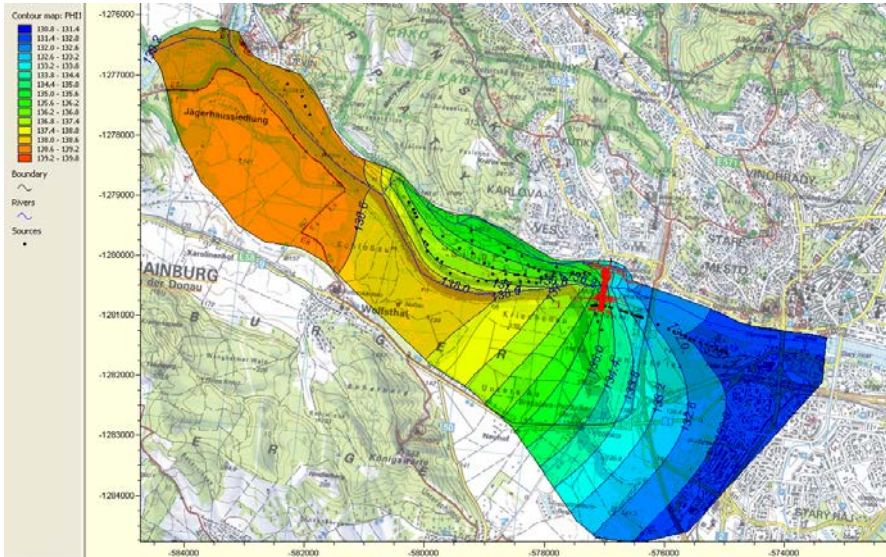


Fig. 3 Groundwater level contour map (m a. s. l.) prognosis after construction of the HS

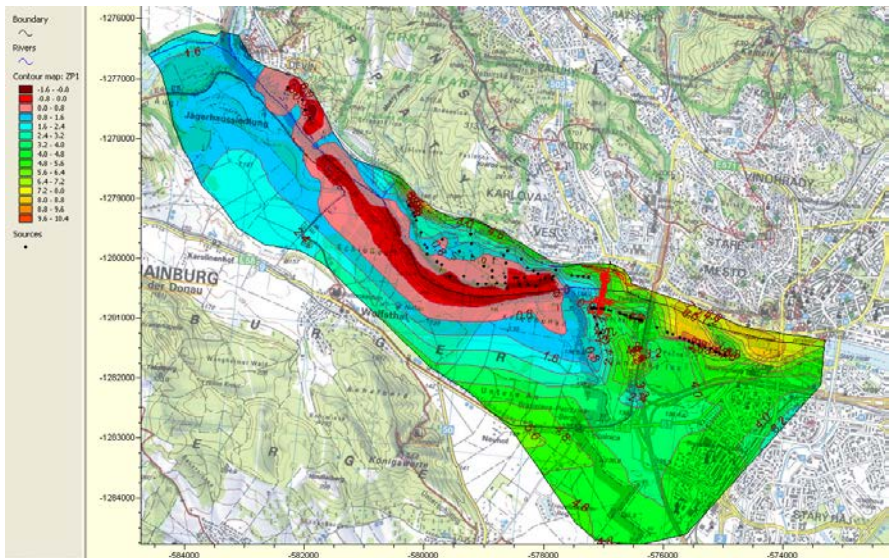


Fig. 4 Depth of groundwater below the surface after construction of the HS (red: flooded areas, pink: waterlogged area)

3. RESULTS OF THE SIMULATION

From the simulation it is clear that in terms of maintaining the functions of water resources the construction of the HS signify compromised functionality of some wells. Due to the construction of HS itself some wells in Pečniansky les would be destroyed. The simulation also shows that a part of the Sihot' could be flooded, and another part could be waterlogged. Due to the fact, that some parts could be flooded [Dráb, Říha 2010], significant portion of the wells on Sihot' (mostly wells near the Danube) would not be able to be used. On Sedláčkov ostrov all wells could be flooded.

For that reason, it is necessary to propose appropriate measures to mitigate or eliminate the negative consequences of construction of the HS, such as proposals for underground sealing wall.

Underground sealing wall has been positioned along the whole length of the Sihot' Island (from beginning of Karloveské rameno to its inflow into the Danube), further above the HD towards Petržalka and in Austria, in which took place along the Danube (Fig. 5). Its end would be around in rkm 1877.



Fig. 5 Situation of the location of the HS and underground sealing wall

The simulation result is the groundwater level (or piezometric water level) after construction of the HS and after realization of the underground sealing wall. Isolines of groundwater level are drawn in Fig. 6. The result of the simulation is also the determination of the depth of groundwater below the surface shown in Fig. 7.

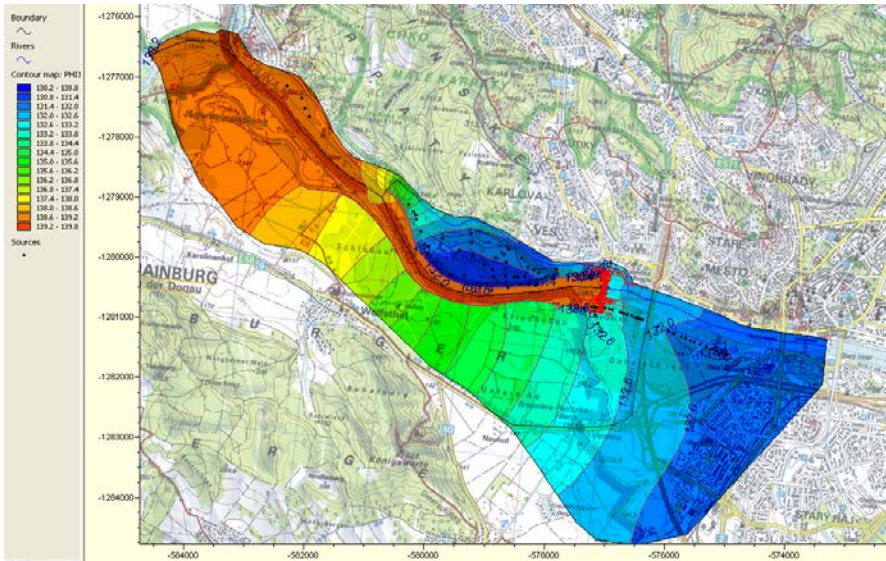


Fig. 6 Groundwater level contour map (m a. s. l.) after construction of the HS and realization of the underground sealing wall

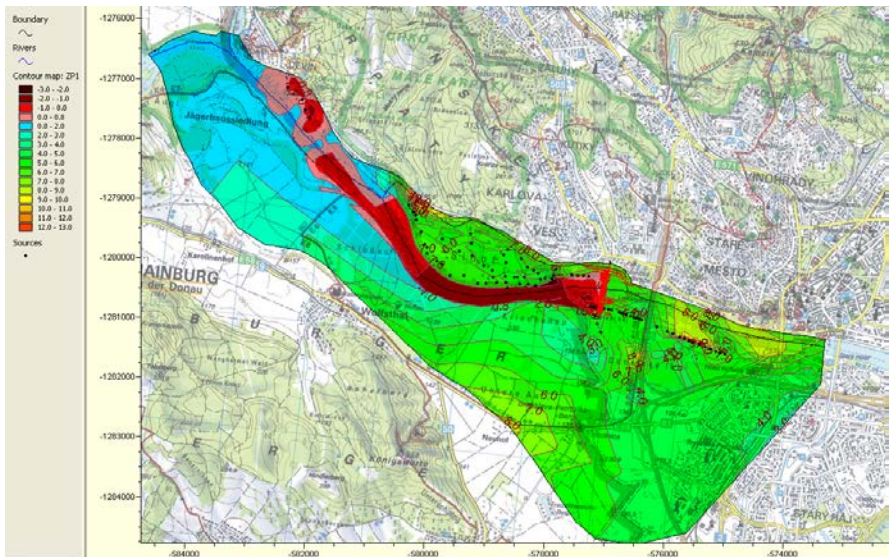


Fig. 7 Depth of groundwater below the surface after construction of the HS and realization of the underground sealing wall (red: flooded areas, pink: waterlogged area)

4. DISCUSSION AND CONCLUSIONS

The aim of the paper was the simulation of the groundwater flow before and after the construction of the proposed “Hydraulic structure Bratislava - Pečniansky les” followed by determining the effect of the HS on the groundwater level regime. Since it was found that the water sources on Sihot’ and Sedláčkov ostrov [Michalko et al. 2011] are in the state of compromised functionality, the next step was the proposal of the underground sealing wall to protect the areas from the negative effects of the proposed HS and the subsequent verification of the effects of this measure.

Due to construction of the underground sealing wall, five wells on Sihot’ would be destroyed (three of them are already not used). With such solutions there is some reduction in groundwater level (compared to zero variant) on Sihot’ and even a slight increase of the groundwater level in Pečniansky les.

5. REFERENCES

ČOMAJ, M. 2012. Locality of Danube drop structure near Bratislava: Wolfsthal or “Bratislava - Pečenský les”? [in Slovak: Lokalita dunajského stupňa u Bratislavy: Wolfsthal alebo “Bratislava - Pečenský les”?] Available from: <<http://www.projekt-baum.eu/vodne-dielo/ds-1014/p1=1126>>.

- DRÁB, A., ŘÍHA, J. 2010. An approach to the implementation of european directive 2007/60/EC on flood risk management in the czech republic. *Natural Hazards and Earth System Science*, Vol. 10, no. 9, p. 1977-1987.
- KULLMAN, E., MALÍK, P., PATŠCHOVÁ, A., BODIŠ 2005. Delinaeation of groundwater bodies on Slovak territory according to EU water framework directive 2000/60/EC [in Slovak: Vymedzenie útvarov podzemných vôd na Slovensku v zmysle rámcovej smernice o vodách 2000/60/ES.] *Podzemná voda*. Vol. XI, no. 5, s. 5–18.
- MICHALKO, J., BODIŠ, D., MALÍK, P., KORDÍK, J., FAJČÍKOVÁ, K., GROLMUSOVÁ, Z., VEIS, P. 2011. Potenciálne zdroje strategických množstiev podzemnej vody v Bratislavskom samosprávnom kraji. *Mineralia Slovaca*. Vol. 43, p. 449–462.
- ROSAS, J., LOPEZ, O., MISSIMER, T.M., COULIBALY, K.M., DEHWAH, A.H., SESLER, K., LUJAN, L.R., MANTILLA, D. 2014. Determination of hydraulic conductivity from grain-size distribution for different depositional environments. *Groundwater*. Vol. 52, no. 3, p. 399–413.
- ROYAL HASKONING. 2004. Triwaco User's Manual. Triwaco 3.x. Netherlands
- SLOVÁK, T. 2010. Shipping objects of Hadraulic structure Prčniansky les. [In Slovak: Plavebné objekty VD Pečenský les]. Diploma theses. STU iv Bratislava, FCE
- ŠLEZINGR, M. 2007. Stabilisation of reservoir bank an „armoured earth structure“, *Journal of hydrology and hydromechanics*, Vol. 55, no. 1, p. 64-69
- ŠVASTA, J., MALÍK, P. 2006. Spatial distribution of mean effective precipitation over Slovakia (In Slovak: Priestorové rozloženie priemerných efektívnych zrážok na území Slovenska). *Podzemná voda*. Vol. XII, no. 1, s. 65–77.
- ZAADNOORDIJK, W.J. 2009. Simulating Piecewise-Linear Surface Water and Ground Water Interactions with MODFLOW. *Ground Water*. Vol. 47, no. 5, p. 723–726.

Acknowledgement

This contribution was supported by the VEGA Grant agency under contract VEGA 1/10011/12.

Arch dam behaviour evaluation by comparison of numerical model and monitoring data

S. Mitovski, L. Petkovski, G. Kokalanov

Civil Engineering Faculty, Ss Cyril and Methodius University, blvd. Partizanski odredi no. 24, Skopje,
Republic of Macedonia,
e-mail: smitovski@gf.ukim.edu.mk, petkovski@gf.ukim.edu.mk, kokalanov@gf.ukim.edu.mk

Abstract

The assessment of dam's safety is complex task that has to be considered from numerous aspects by including of various factors. The following safety requirements are to be fulfilled in order to ensure the dam stability: (i) functional (considering the degree of satisfaction of the users' objectives), (ii) economic (considering the relation between costs and gains), (iii) hydrological (considering the acceptable risks for evacuation of the flood waters), (iv) hydraulic (considering the capacity of the conduits), (v) seepage (considering the intensity of the hydrodynamic parameters) and (vi) structural (considering the effects of static and dynamic loads). The application of the finite element method has lead to significant changes in the treatment of the arch dam stability, enabling non-linear spatial analysis, analysis of the arch dam for different loading states (gravity and water load, temperature effect), including the dam foundation within the analysis. Also, application of contact elements for simulation of the behaviour on the interface concrete-rock in the dam abutments and foundation as well as the behaviour on the interface concrete-grouting material in the joints in the dam body is enabled. The process of calibration of the results obtained by numerical analysis and monitoring data is continuous in the same time improving the numerical model and monitoring instrumentation. In this paper a comparison of part of the output results from the numerical model with monitoring data is illustrated on the case of St. Petka dam, a 64 m high arch dam on River Treska in Macedonia, commissioned in 2012.

Keywords:

arch dam, numerical model, monitoring data.

1. INTRODUCTION

The dams, having in consideration their importance, dimensions, complexity of the problems that should be solved during the process of designing and construction along with the environmental impact are lined up in the most complex engineering structures [Novak et al., 2007; Tančev, 2013]. The number of constructed large dams in the world in specific periods is presented in Fig. 1. The ICOLD Register of dams lists around 45,000 dams higher than 15 m. According to the rapid population increase, foreseen to reach 10 billion inhabitants

by the end of the century, more dams will have to be built in order various water demands to be satisfied.

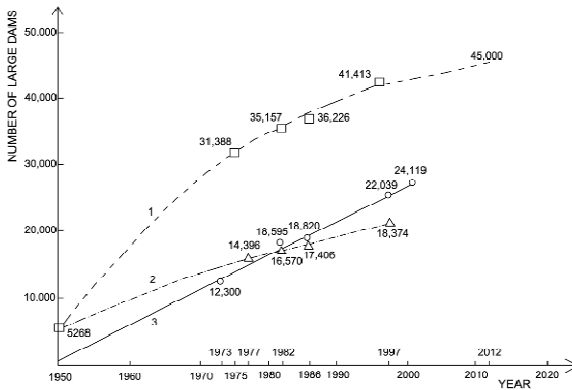


Fig. 1. Total number of constructed dam in the world [Jiazheng & Jing, 2000]. (1) Total number of dams in the world; (2) Number of large dams in the world except China; (3) Number of large dams in China.

Republic of Macedonia is located in the central part of the Balkan Peninsula, covering area of 25,713 km² with a population of about 2 million inhabitants. Its mountain relief, vast valleys and numerous long and narrow ravines distinguish the topography of the Republic of Macedonia. The rivers in Republic of Macedonia belong to three main river basins: (a) The Aegean basin, in which they flow out through the rivers Vardar and Strumica; (b) The Adriatic basin, to which they are taken away through the river Crn Drim (Black Drim); and, (c) The Black Sea basin, through the river Binachka Morava, which extends over a quite insignificant part. The biggest is the catchments basin of the River Vardar, which extends to some 20,525 km² or 80% of the territory of the Republic of Macedonia. Total available surface water resources in the Republic of Macedonia are assessed as about 3,300 m³ per capita annually.

The dam construction in Macedonia dates from 1938 when the Matka arch dam was constructed, located on the River Treska, in the vicinity of Skopje, still in service, since 2008 with double capacity, after the construction of a new power plant. To present are constructed 27 large dams [Tančev et al., 2013]. Different types of dams are represented, having in consideration the various geological, topographical and hydrological conditions, among which 18 are embankment dams, 8 concrete arch dams and 1 concrete multiple arch dam. The stored water is used for meeting the demands for water supply of population and industry, irrigation, production of electricity, flood and erosion control, provision of minimum accepted flows, recreation and tourism. The total stored water volume is about 2.4×10⁹ m³. The potential of the rivers in Republic of Macedonia is utilized to hardly 30%, and yet there is a permanent shortage of water for various

purposes. Due to this fact, as well as due to strongly expressed uneven distribution of water, it is indispensably necessary to construct new dams with reservoirs.

The assessment of the stability and the behaviour of dams during construction at full reservoir and during service period is of vital meaning. In August 2012 was commissioned Saint Petka arch dam, in nearby the city of Skopje, as final part of the cascade system on river Treska, along with dams St. Andrea and Kozyak (Fig. 2). The paper deals with static analysis of St. Petka dam, performed with application of the program package SOFiSTiK.

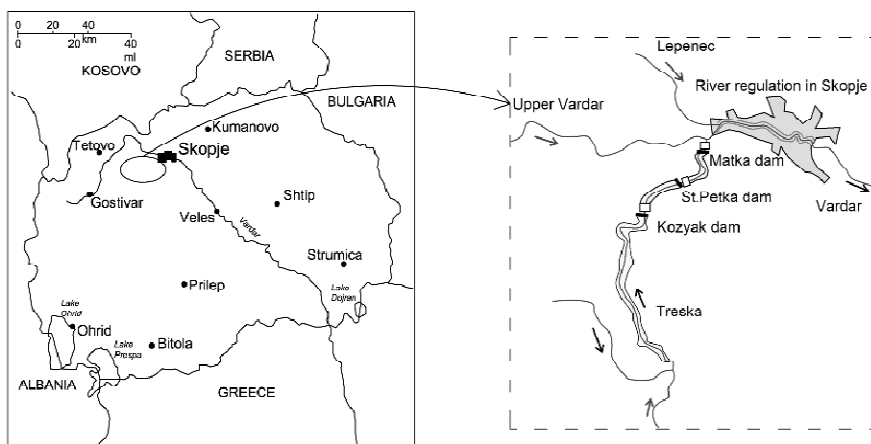


Fig. 2. Map of Republic of Macedonia and display of water resources system on Treska River, with 3 dams and HPP: Kozyak - St.Petka – Matka.

2. ST. PETKA DAM

St. Petka dam is double curved thin arch dam, with height of 64.0 m (Fig. 3). The crest elevation is at 364.0 masl, with crest thickness of 2 m and length of 115 m, while the lowest elevation is at 300.0 masl, thickness of 10.0 m. On the right bank the low quality zone of the rock foundation is replaced by concrete block, thus avoiding the weak foundation zones. The dam site is characterized by symmetric shape with steep slopes, apropos the left abutment is with inclination of 60°, while the right abutment has an inclination of 50°. The normal water level is at 357.30 masl, while the reservoir volume is $12.4 \times 10^6 \text{ m}^3$. The main purpose of the dam is electric power production.

3. DAM MODELLING

The static analysis of St. Petka dam is conveyed with application of the program package SOFiSTiK, based on the finite element method. The program offers possibilities for complex presentation of the structures and simulation of their behaviour as well and including in the analysis of certain specific phenomena

(automatic mesh generation based on given geometry, application of various constitutional laws, simulation of dam construction and reservoir filling in increments, simulation of contact behaviour, etc.).

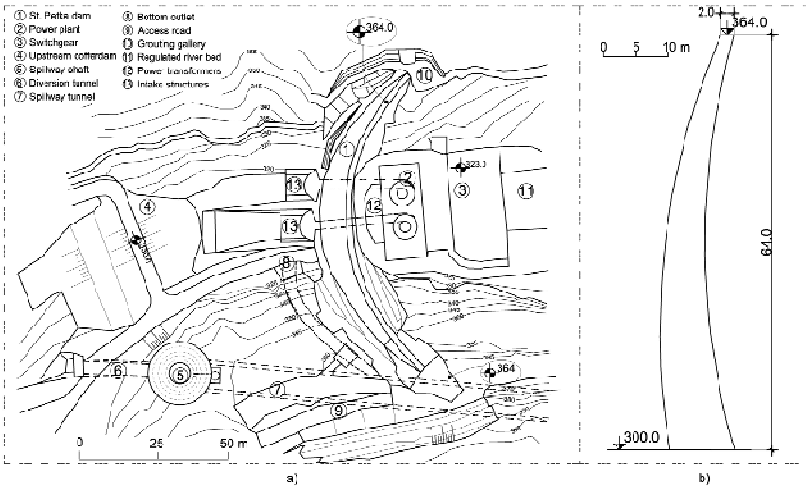


Fig. 3. St. Petka dam. a) Dam layout, b) Central cross-section.

In order to perform the numerical analysis following steps must be undertaken, conventional for this type of analysis: (1) choice of material parameters – constitutional laws (one of the most complex tasks during the analysis), (2) adoption of dam geometry and (3) simulation of the dam construction and reservoir filling.

3.1 Input parameters

The program SOFiSTiK offers rich library of constitutional models for the materials, such as standard (concrete, steel, timber, soil and rock), but also and non-standard with option of self input of specific parameters.

The terrain is composed of mainly of marble. The carbon schist appears as plates with mica sub-layers between them. At the upper zones of the dam site are detected diluvia and alluvial sediments, later excavated during the construction stage.

The geotechnical input data for the modelled three different zones of the rock foundation (Tab. 1) are adopted on base on overall data from the geotechnical investigations and control testing before and during construction process [Synthesis Elaborate, 2004]. An engineering-geological model of the terrain per parameter of deformability and shear strength is used, prepared on basis of the models per parameter of elastic waves velocity, obtained by geophysical methods before construction stage, as well and the model and section per parameter of weathering. Linear constitutional law is applied for the materials in dam foundation. The three main fault zones are also included in the rock foundation model.

Table 1. Zoning per parameter of velocity of elastic waves of the massive deformability.

Zone	v_p [m/s]	Deformation modulus at pressure D [MPa]	Poisson's coefficient μ
Fault zones	2500 – 3000	2500	0.30
Left bank	4000 - 4500	7000-8000	0.24
Right bank	3800 – 4000	5000-6000	0.26

The constitutional law for the concrete is adopted according to EC 2, CG 30 [ICOLD, 2009; Eurocode 2, 1992], based on performed probe and control testing of the concrete before and during construction stage.

The interface elements (springs) are applied in order to enable differential displacements in the dam joints and at the contact dam-foundation. The behaviour of the spring elements is described by two stiffness parameters: axial constant C_p and lateral constant C_l . The values for the lateral constant was adopted on base of laboratory and „in situ“ testing on the shear strength parameters by Hoek apparatus at the contact concrete-rock foundation and concrete-grout mixture in the dam joints (Fig. 4), as well on performed “in situ” testing of the rock mass deformability by applied vertical load. The adopted values are: $C_l=1 \times 10^6$ KN/m³ for contact dam-foundation and $C_l=5 \times 10^6$ KN/m³ for contact concrete-grout mixture, while same value is adopted for the axial constant $C_p=16 \times 10^6$ KN/m³.

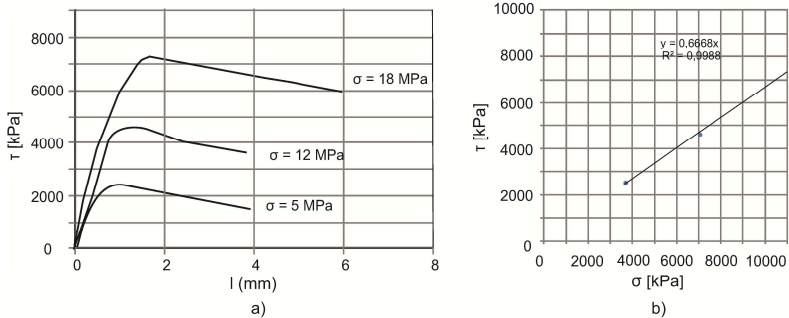


Fig. 4. Output results for testing sample 378 I/A, contact concrete-grout mixture at constant normal load of 6, 12 and 18 MPa. a) Dependence shear load-displacement $l=f(\tau)$, b) Dependence shear/normal load $\tau=f(\sigma)$.

3.2 Model geometry

The spatial analysis of St. Petka dam is performed in stages. The numerical model is composed of the dam body and the rock foundation. The rock foundation boundaries (in the same time boundary conditions for the model) are adopted according to literature [ICOLD, 1987]. More precisely, the numerical model is composed of dam body, limited by the dam site shape, and rock foundation, with

length upstream and downstream of the dam central cantilever in interval $(1 \div 2) H$, where H denotes dam height apropos a length of 100 m is adopted, while the rock foundation under the dam is adopted at depth of 65.0 m (Fig. 5a). By such parameters is defined the non-deformable boundary condition (displacements in X , Y and Z direction are fixed at the lowest section). The discretization is conducted by capturing of zones with different materials – concrete and rock foundation. Per crest length the dam is divided in vertical segments with length of 6-12 m. The segments are divided horizontally in 16 groups. The height of one segment is 4 m. By activation of different horizontal group it is possible to simulate the construction phases of the dam. The dam's thickness is divided in 6 layers (groups). In this way, the different distribution of the temperature along the thickness, measured from installed thermometers, are taken in the analyses adequately. The layers are created by specified number of volume bodies, constructed of one type of material. The concrete block, constructed to replace some weak rock zones in the right abutment of the dam site, is also included in the model (Fig. 5b). At the contact of the dam and the foundation as well and at the contact between two vertical blocks – in the dam joints are applied interface elements (Fig. 5c) in order to simulate the interaction at contact of materials with different deformable parameters.

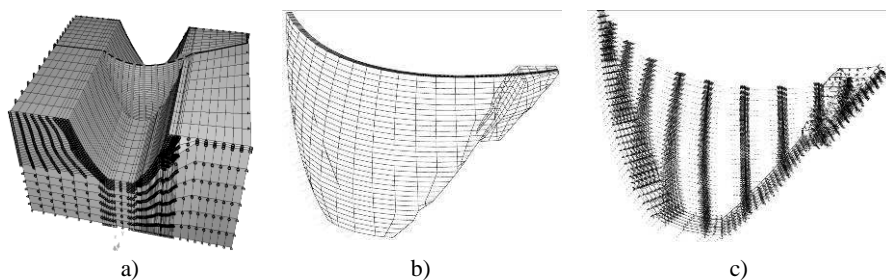


Fig. 5. St. Petka dam model. a) Spatial view from upstream side, b) Discretization of the dam body and the concrete block, c) Interface elements at contact dam-foundation and at contact concrete-grout mix in dam joints.

3.3 Dam loading

The analyzed loading states of the dam include state after dam construction and at first reservoir filling. The state after dam construction considers dead weight, temperature and grouting load, while the state at first reservoir filling considers dead weight, temperature, grouting load and hydrostatic pressure (applied on the upstream face of the dam and on the reservoir area). The dam joint grouting was performed in period March-April, 2012. The dam filling commenced in June 2012 and reached normal water elevation of 357.30 masl at end of July 2012. The temperature load is adopted in accordance with the monitoring data of the temperature in the dam body for the specified loading states apropos

previously specified time periods (Fig. 6). The grouting load, applied on the joint surfaces between two concrete blocks, was included in the analysis. The grouting was done in five stages in height of 12 m per stage, with grouting pressure of 7 bar at bottom and 5 bar at top of one grouting section of 12 m.

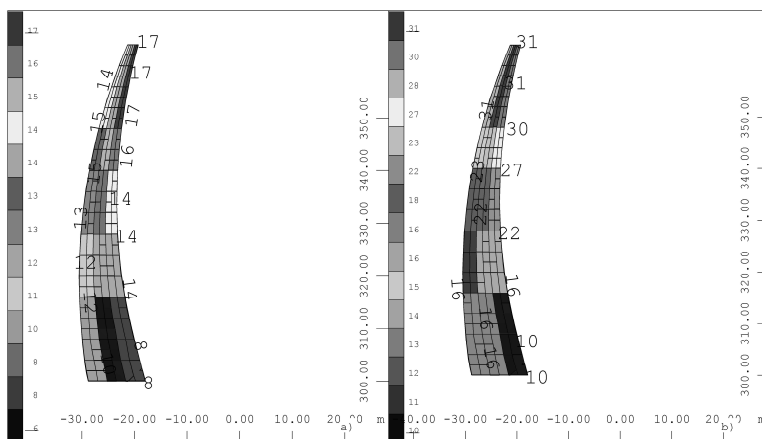


Fig. 6. Temperature load applied for various loading states.

4. OUTPUT RESULTS

The dam stability is assessed by analysis of the values and distribution of the principal stresses and displacements in the dam body. In Fig. 7a are displayed principal stress after dam joints grouting, while in Fig. 7b principal stresses at full reservoir. The stresses after dam grouting are mainly compressive, in the region of expected values and distribution, with maximal value of 8.5 MPa, located in the upstream contact of the dam and the foundation, typical for this type of dam and loading state. The stresses at full reservoir are also mainly compressive, with maximal value of 7.3 MPa, located also at the upstream toe of the dam.

The contour lines of the horizontal displacements (Y direction, „-“denotes displacement in upstream direction) after dam grouting are displayed in Fig. 8a, while in case of full reservoir in Fig. 8b. The dam in both cases deforms in upstream direction. For the case after dam grouting, the maximal displacement occurs at the upstream face of the dam, approximately at 60% of the dam height, value around 9 mm. At full reservoir the maximal displacement occurs at dam crest, value of 12 mm.

In Fig. 9a and 9b are displayed partial vertical displacements (temperature and water load effect) after dam grouting and at full reservoir („-“denotes settlement). The displacements due to the dominant temperature effect mainly are characterized with rising, with maximal values of order 11 and 15 mm appropriately. In the lower dam zone, approximately at 30% of the dam height occurs settlements, values of order 2 mm.

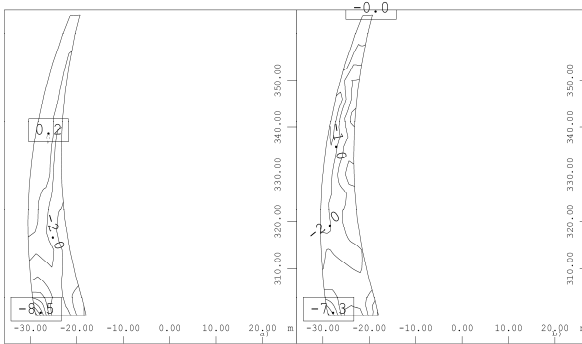


Fig. 7. a) Contour lines of principal stress σ_3 after dam grouting; b) Contour lines of principal stress σ_3 at full reservoir.

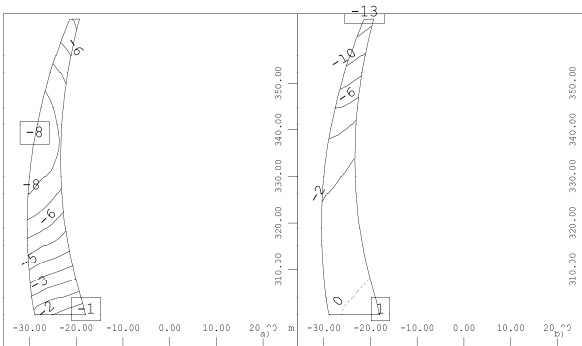


Fig. 8. a) Contour lines of summary horizontal displacements in Y – direction after dam grouting; b) Contour lines of summary horizontal displacements in Y – direction at full reservoir.

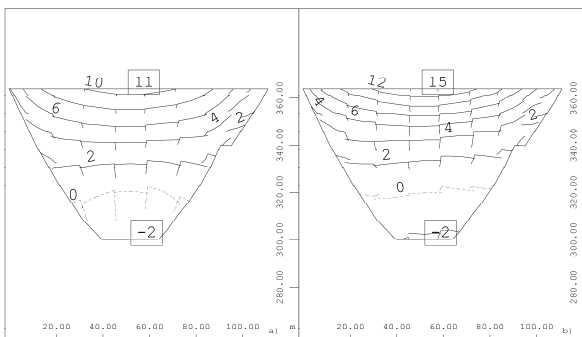


Fig. 9. a) Contour lines of partial vertical displacements in longitudinal section of the dam after grouting, b) Contour lines of partial vertical displacements in longitudinal section of the dam at full reservoir.

5. MONITORING DATA COMPARISON

The technical monitoring of the dams should fulfil two objectives: (1) to verify the conducted numerical analyses of the dam and to follow the dam behaviour in the service period, in order to detect eventual non-regular occurrences in the dam and the foundation, that could endanger the dam safety and (2) taking of timely and appropriate restoration measures. The concept of the technical monitoring system regarding the number of instruments, location, reading frequency etc. is primarily determined in dependence of the dam type and importance. St. Petka dam is equipped with monitoring equipment that enables measurement of data significant for dam behaviour interpretation and safety. In this case are analyzed measured data from the geodetic survey benchmarks, compared with calculated values in case of horizontal and vertical displacements. In Fig. 10 are presented curves of partial calculated and measured horizontal displacements for the period after dam grouting - reservoir filling. The measured values are from survey benchmarks placed on the downstream face of the central cantilever. The obtained displacements curves show good matching regarding the direction of dam deformation, as well and for the location of the occurred maximal displacements.

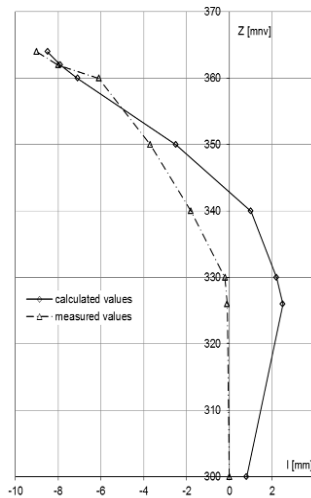


Fig. 10. Partial calculated and measured values in Y – direction at full reservoir for central cantilever section.

Fig. 11 presents the comparison curves for the partial calculated and measured vertical displacements of the dam crest for the specified period. The survey benchmarks are located along the dam crest. From the chart it can be concluded that calculated and measured values have similar pattern apropos the maximal displacement occurs in the middle part of the dam crest, while in direction of both banks the displacements values are decreasing.

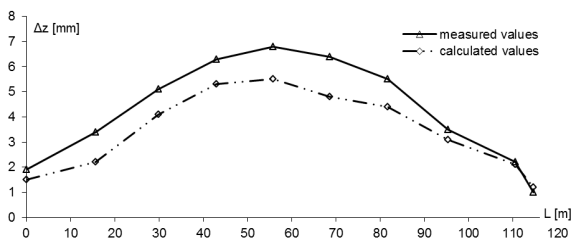


Fig. 11. Partial calculated and measured displacements along dam crest at full reservoir (“+” denotes rising).

6. CONCLUSIONS

The prediction of the behaviour of the concrete arch dams during construction and at full reservoir is essential for ensuring and providing interval data for the dam engineers – designers of these structures. The dam stability is assessed in case of principal stresses. Maximum allowable stresses for usual loading state of the dam (self weight, temperature and hydrostatic pressure) should be less than 1/3 of specified compression strength and according to the maximal calculated value of the principal stresses of 8.2 MPa, such criteria is met.

The comparison of the increment of the calculated and measured horizontal and vertical displacements was undertaken. Namely, the deformation pattern and displacements values for both calculated and measured values shows good matching, analyzed for the period after dam grouting till reservoir filling. The comparison analysis gives valuable findings for the dam behaviour, and it serves as base for calibration process of the numerical model and installed monitoring instruments.

7. REFERENCES

- EUROCODE 2, 1992. Design of concrete structures, European Committee for Standardization
- ICOLD Bulletin 145, 2009. The physical properties of hardened conventional concrete in dams.
- ICOLD Bulletin 30a, 1987. Finite element methods in design and analysis of dams
- NOVAK P., MOFFAT A. I. B., NALLURI C., NARAYANAN R. 2007. “Hydraulic structures”, Taylor & Francis Group, London
- SYNTHESIS ELABORATE on performed investigation and testing for concrete arch dam at dam site “St. Petka” on river Treska, 2004. Civil Engineering Institute “Macedonia”
- TANČEV L. 2005. “Dams and appurtenant hydraulic structures”, A.A. Balkema Publ., Taylor & Francis Group plc, pp. 195-196, London, UK
- TANČEV L. PETKOVSKI L. & MITOVSKI S. 2013. “Dam engineering in Republic of Macedonia: Recent practice and plans” International Symposium Dam engineering in Southeast and Middle Europe, Recent experience and future outlooks, Ljubljana, Slovenia

Flood zone modelling and flood losses estimation using GIS and numerical hydrodynamic models

N. V. Badenko¹, T. S. Ivanov¹, S. P. Kotlyar¹,

K. A. Osmolovsky¹, M. V. Petrosenko², V. A. Prokofyev¹

¹JSC VNIIG, Address: Gjatskaya str., 21, Saint-Petersburg, 195220, Russia

²EC Kronschtadt, Address: Kronschtadt, Posadskaya str.41, A, 197760, Russia

E-mail: maxpetrosenko@gmail.com

Abstract

Current paper represents process of methodology and software development for flood zone modeling and simplified damage evaluations in case of passing rare occurrence flood or hydraulic structure failure.

A software product called Hancock was developed for purposes of flood modeling. Approach allowing usage of this software together with geographic information systems is described in the paper.

Damage evaluation is carrying out based on simplified methodology, which doesn't include on-site researches and mostly relies on digital maps data and statistical data. GIS-based application was created for representing calculation results, visualizing and analyzing of flood zone and object identification on the map. Displaying damage caused by flooding depends on chosen flood scenario.

Future improvements of methodology described in the paper are associated with flood risk estimations and flood risk mapping.

Keywords

Flood losses, Flood modeling, Geographic information systems.

1. INTRODUCTION

Authors studied ways of using hydraulic modelling toolsets Hancock2D, Hancock25 (nonprofit hydraulic toolset, certified in Russia, developed at JSC VNIIG) and also widely used MIKE by DHI together with geographical information systems (GIS) ESRI ArcGIS for forecasting flood zones during flood passing and for estimation of flood losses. Having in mind flooding of European territories that happen so often, recent floods in Australia and Asia caused by heavy rains, and the Amur Region floodings in Russia in 2013, one may say that the study is fulfilled at the right time. The need of the study in Russia is also triggered by the requirements of the Ministry of the Russian Federation for Civil Defence, Emergencies and Elimination of Consequences of Natural Disasters [Recommendation 2010]. In [Recommendation 2010] it is claimed that for all HPPs there should be designed 3D models of the HPP, surrounding territory including all the forecasted flood zones for the most probable disaster scenarios, having all the objects affected by the

possible flooding indicated in the 3D model. The study of combining a certified hydraulic toolset with GIS software is the key to these tasks.

During flood passing some settlements located downstream of a set of HPPs in Russia were flooded by the discharges rarely used by HPP operators. Such territories should have been unsettled, but were settled in fact due to the approval from the administration, which was mistakenly given because the territories were not flooded for 20-30 years. So a need of a system that would allow an HPP operator, administration, emergency services to have the information about the objects that would be flooded in case of passing a 10 year, 50 year, 100 year flood in the upstream and downstream areas of HPP was considered by JSC VNIIG. The idea of creating a system that would allow a user to estimate the risk of flooding an object was also envisioned.

The approach presented in the paper is based on a one layer and a multi-layer model of hydrodynamics (layers quantity is set by researchers and is limited by the computer performance only) adapted to flow spreading along dry riverbed.

For input of topographic information and further visualization of results the model has been combined with the geographic information system ArcGIS 10.1 that minimizes manual input of the initial data and increases abruptly their accuracy, allowing to use a great number of sources for elevation data (SRTM data, raster and digital maps and etc.) The article also deals with development of sophisticated GIS based software for flood zone analysis, flood losses estimation, reports generation.

2. MATERIAL AND METHODS

2.1 Hancock2D, Hancock25D Tools For Flood Modelling

There is a number of different approaches to solve the task of flood modelling with the majority of which are based on one-dimensional or plane (2D) setting.

2D and 3D algorithms used in this work are made up on the method of the finite volume that allows to create numerical diagrams conservative by mass and pulse.

2.2 Plane (2D) Model of Hydro-Dynamics and Heat Transmission (Hancock2D Toolset)

The divergent form of the 2-D system of the shallow water equations for viscous liquid and for heat transmission in Cartesian coordinate system (x,y) is the following [Ivanov et.al. 2012], [Fracarollo et.al. 1996], [Nujic' 1995]:

$$\frac{\partial \mathbf{Q}}{\partial t} + \frac{\partial \mathbf{E}}{\partial x} + \frac{\partial \mathbf{G}}{\partial y} = \mathbf{S} \quad (1)$$

Where the vector of variables, fluxes and sources is written as:

$$\mathbf{Q} = \begin{bmatrix} h \\ hu \\ hv \\ hT \end{bmatrix}; \quad \mathbf{E} = \begin{bmatrix} hu \\ hu^2 + gh^2/2 \\ huv \\ huT + h\gamma_T \partial T/\partial x \end{bmatrix}; \quad \mathbf{G} = \begin{bmatrix} hv \\ huv \\ hv^2 + gh^2/2 \\ hvT + h\gamma_T \partial T/\partial y \end{bmatrix}; \quad (2)$$

$$\mathbf{S} = \begin{bmatrix} \Phi \\ ghS_{0x} - S_{fx} + hfv + \tau_x/\rho + h\gamma\nabla^2 u \\ ghS_{0y} - S_{fy} - hfu + \tau_y/\rho + h\gamma\nabla^2 v \\ \rho c (\Theta_\Phi + \Theta_{bot} + \Theta_S) \end{bmatrix} \quad (3)$$

In equation (2) and (3) is g free fall acceleration, h is water depth, u and v are components of the vector \mathbf{U} averaged by the velocity depth in Cartesian coordinate system; S_{0x}, S_{0y} are components of the bottom slope, $f = 1,458 \times 10^{-4} \sin(\varphi)$ is Coriolis parameter, φ is geographical latitude, τ_x, τ_y are components of the wind tangential stress on the free surface, ρ is water density, c is specific heat, ∇^2 is Laplace operator, Φ is mass source, T - water temperature average by depth, γ_T is coefficient of temperature conductivity in the horizontal direction including turbulent and disperse components. The components of the friction force vector on the bottom can be determined by Manning formula:

$$S_{fx} = C_f(h)hu|\mathbf{U}|; \quad S_{fy} = C_f(h)hv|\mathbf{U}|; \quad (4)$$

$$|\mathbf{U}| = \sqrt{u^2 + v^2}; \quad C_f(h) = \frac{gn^2}{h^{4/3}}$$

The numerical algorithm implemented in the Hancock2D toolset is described in [Prokofiev 2002] and is based on solving the equations system (1). The algorithm is implemented for the regular curvilinear quadrangular grid of finite volumes.

Multilayer analogue of the shallow water equations is described in [Prokofiev 2012]. Multi-layered system of shallow water equations takes into account the exchange of mass and impulse between the layers, the proportion of levels of the layers remains the same (see Figure 1).

2.3 Advantages Of Multilayer Hydrodynamic Modelling (Hancock25D toolset)

The Hancock25D toolset algorithm is described in [Prokofiev 2012]. In this article we only describe advantages of the new toolset:

1. Elapsed time of calculation for a multilayer model approximately equals the elapsed time of calculation for a one layer model multiplied by the number of rows.

2. Hancock25D uses multithreading and the algorithm design is optimized for running the program with more than one processor, allowing to achieve an up to 95% load for each processor.
3. The algorithm is conservative by mass and pulse which is important for heat transfer modeling and for wave tasks, specifically for modelling of breach waves.
4. The option of nonrectangular grids is available together with the “cut” technology that allows to avoid grid effects for the edges (grid roughness effects).
5. Algorithm uses RAM effectively, allowing to run the toolset on a computer with 4 GB RAM for the grids having for example dimensions of 5000×2000 elements in plane and having up to 5 layers (50 million of nodes).
6. The “vertical” grid is adaptive for the bottom and for the free surface. Even a 2-3 layer model allows to get useful results and one layer model automatically switches to a classical shallow water model.

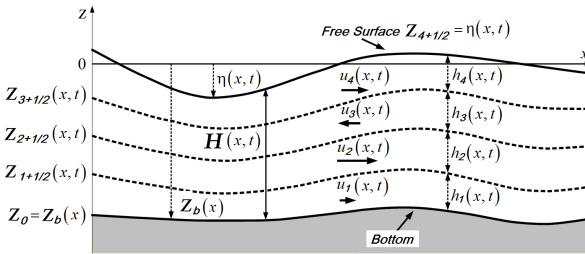


Fig. 1 Schematization of the flow to split vertically into 4 layers [Badenko 2000].

2.4 Method of integrating Hancock2D, Hancock25D Tools with GIS (ArcGIS 10.1)

In the given study the algorithm and methods of integration of hydraulic models in GIS were developed, allowing a researcher to get advantages at all stages of a study.

Usage of GIS allows to involve a wide range of sources at a stage of processing the terrain data [Badenko 2000]:

- Traditional topographic maps;
- data received by remote sensing;
- data received by results of aerial photography;
- Terrain laser scanning data;
- Pilot charts;
- Other data.

In the given section the integration of hydrological and hydraulic models into GIS is described. Hancock2D, and Hancock25D toolsets were used for the task. The

algorithm for using MIKE, HEC-RAS or analogical to Hancock2D tool River would be almost identical [Dráb et.al. 2010], [FEMA 2012]. MIKE tools (MIKE 11, MIKE 21, MIKE FLOOD) were also tested by the authors. Calculation in Hancock was carried out on the basis of the multilayer model (3-5 layers) and on a classical shallow water model.

The proposed methodology of fulfilling flood zone modelling and flood losses estimation includes of the following steps for each study area:

1. Creation of digital elevation models (DEM) using a set of initial data.
2. Import of DEM to numerical hydraulic modelling software, creation of numerical hydraulic model (Hancock/MIKE).
3. Fulfilling of modelling (Hancock/ MIKE).
4. Model verification.
5. Export of results from Hancock/MIKE to ArcGIS and creation of flood zone layers.
6. Flood losses estimation (scripts for ArcGIS).
7. Flood zone modelling results interpretation.

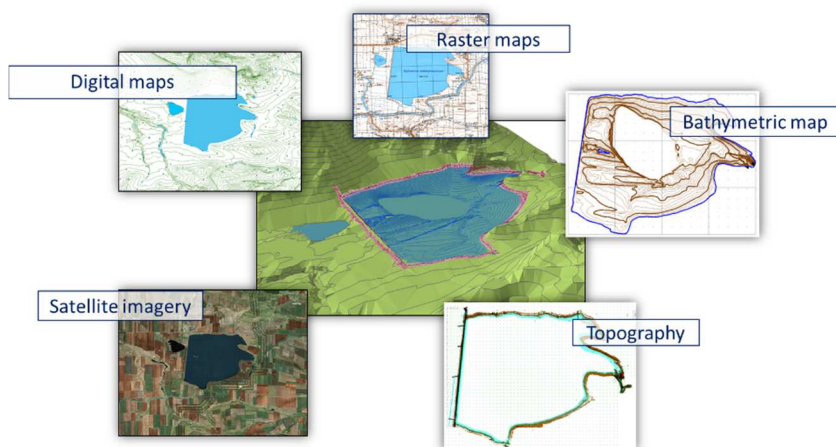


Fig. 2 Initial data for DEM creation

2.5 Creation of digital elevation models (DEM) using a set of initial data

For creation of digital elevation model and visualization of the results of modelling the authors are using ArcGIS 10.1. This allows to minimize manual input (digitization) of the terrain data and increase accuracy, allowing to use a great number of sources for terrain data (Raster and digital maps, remote sensing data, bathymetry, additional technical drawings of embankment dams and etc.) (Figure 2).

2.6 Import of DEM, numeric hydraulic modelling, export of results

The integration algorithm uses special procedures for the import/export of data. The algorithm is presented on Figure 3.

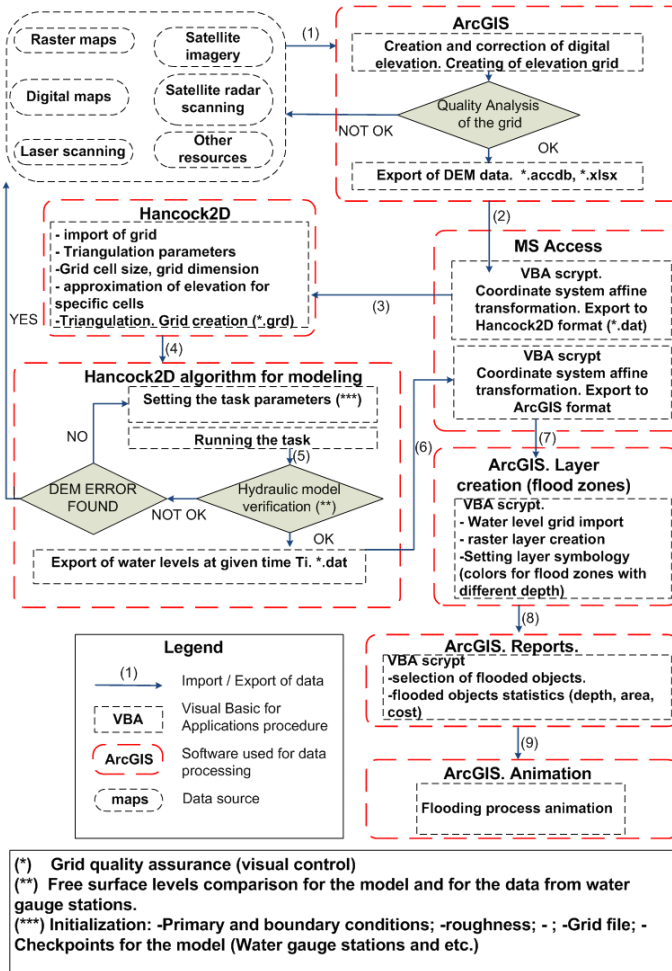


Fig. 3 Algorithm of integrating Hancock2D, Hancock25D tools with GIS systems (ESRI ArcGIS 9.3.1.)

After performing of calculations on numerical hydraulic and hydrological models, the data may be imported in GIS. This allows to make a flood zone layer in GIS and manage a spatial analysis of it with the usage of electronic maps, satellite imagery and etc.

This GIS based approach, allows fulfilling of modelling not in the schematic areas constructed on the map basis, but on the maps basis itself. This approach leads to accuracy of model and an exact coordinate binding of sources, to hydraulic engineering constructions and the objects in the flooded zone.

2.7 Numerical hydraulic modelling (Hancock2D, MIKE)

Hancock2D/MIKE21 allow a researcher to simulate flows in case of flooding and predict water level and velocity at each point of the study area. Both toolset provide a wide range of options for setting the scenarios of modelling.

The numerical algorithm implemented in the Hancock2D can be used not only for the regular curvilinear quadrangular grid of finite volumes, but also for irregular, triangular, flexible grids. MIKE 21 FLOW MODEL HD FM module also allows a user to fulfil a study with a flexible mesh.

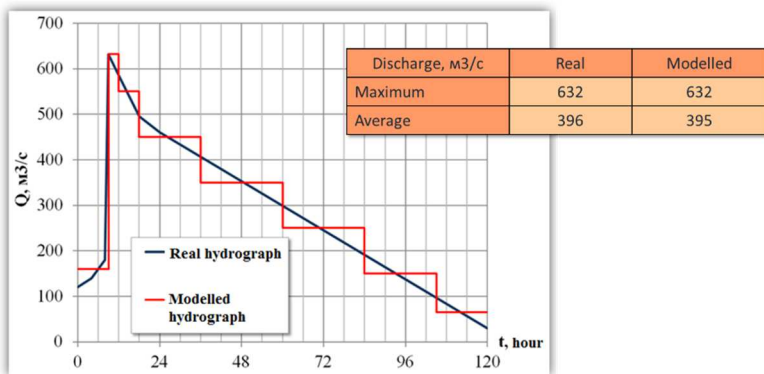


Fig. 4 Modelled hydrograph and a real hydrograph

According to authors experience, when a study area is relatively small (less than 10 million nodes of the grid), the river is not mountainous, and the shores are not steep, the regular mesh is the easiest for modelling and yet is effective. Using the flexible mesh takes more time for each study and should be used mostly for mountainous regions with meandering rivers.

Both Hancock2D and MIKE toolsets allow setting regions of the study area where the computation is not needed to save computation time and make computation faster. The simulation allows to predict flows and levels of water for every node of grid, the morphometry of river bed and viscosity are taken into account.

Time step is also set in Hancock2D/MIKE. The researcher has to specify the period for saving the result of modelling into a file.

The hydrograph for setting the discharge both for Hancock2D and MIKE is set via the time series and discharge rate for each interval as specified bellow (Figure 4).

2.8 Model verification

The verification of a model is usually done by comparing the modelled levels with the observed ones for a set of discharges. This is possible only for the points of the model and for the respective places on the river where the gauge stations are situated (Table 1).

Tab 1. Comparison of observed levels and the modelled levels for a gauge station on Zeya river.

Discharge, Q m ³ /s	Water level, Zeya river, m	Gauge station, Zeyskaya sloboda at Zeya river, m
3500	227.7	228.0
5500	229.6	229.1
6500	230.5	229.7
9500	231.6	231.0
11500	232.5	231.8

Analysis of table 1 shows that the model was well calibrated. For higher accuracy of the results there is a need of more accurate DEM and other initial data.

The following figure (Fig. 5) illustrates possibilities of comparing results of modelling with the satellite imagery captured at the time of flood passing. This procedure allows to verify the results and to find zones in the model where the DEM, discharges of the tributary rivers or some other initial data is not set correctly.

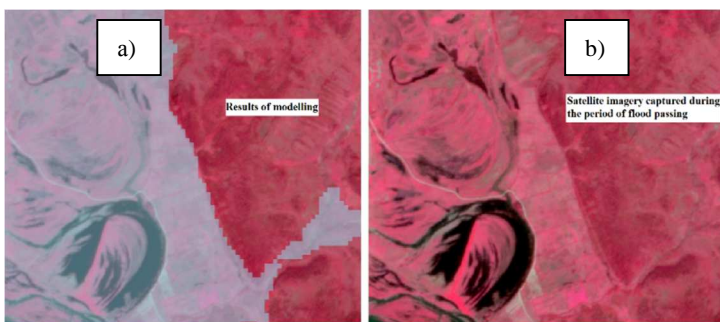


Fig. 5 Comparing the results. a) – Results of flood modelling, b) – Satellite imagery captured during the period of flood passing (Amur river).

2.9 Creation of flood zone layers and the aggregation layer

After the computation is finished the results from Hancock2D/MIKE can be exported to GIS. The authors have developed Python scripts for fulfilling this operation. The procedure is a simple export of X, Y coordinates and additional parameters such as water level, velocity and etc. For some study areas affine transformation are needed to avoid accuracy problems with the floating point

calculation and/or problems with coordinates that exceed the boundary of long integer data type.

The flood zones are created for a set of time intervals that were specified in the beginning of simulation. The water level and velocity vary for cells of the grid from one time stamp to another, but the most interesting for the researcher is the maximum speed and the maximum height of the flow during the full period of time. So authors have built a special aggregated layer where maximum level and velocity is stored for each cell (see figure 6). This allows to build a layer of flood zones by type of damage, as the damage for the buildings, roads, and other objects depending on the combination of level and velocity.

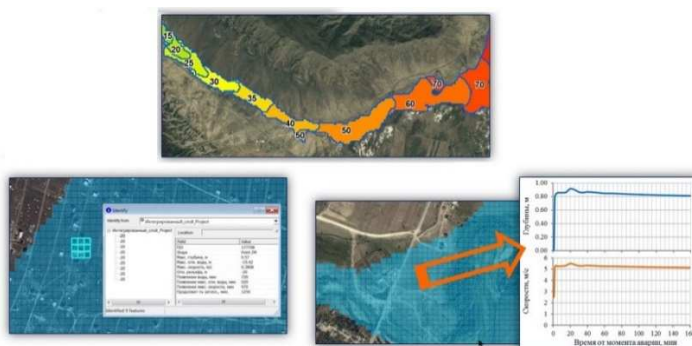


Fig. 6 Aggregated layer and charts of the velocity and depth changes during the simulated period.

3. RESULTS

3.1 Estimation of flood losses

Material [Recommendations 2007] was used for estimation of losses.

The authors approach is based on the automated identification of objects that would be flooded according to the results of modelling. As soon as the objects are identified the recommendations [Recommendations 2007] are used to estimate the total losses caused by the floodings. Figure 7 shows the principle of identification of objects of different types, the procedure is automated using GIS.

The flood zones are classified by zones of catastrophic, high, medium and low impact according to the water levels and velocity.

Usage of modelled flood zones together with the digital map's layers allows to build the flood zone maps, and to estimate flood losses for each scenario of a disaster as well.

Depending on quality of initial data associated with the study area and the size of grid cells the researcher can either make a more or less detailed estimation of flood losses.

The scripts developed for ArcGIS allow to specify the layers that would be used for estimation of flood zones. The technology can be used with recommendations other than Russian recommendations.

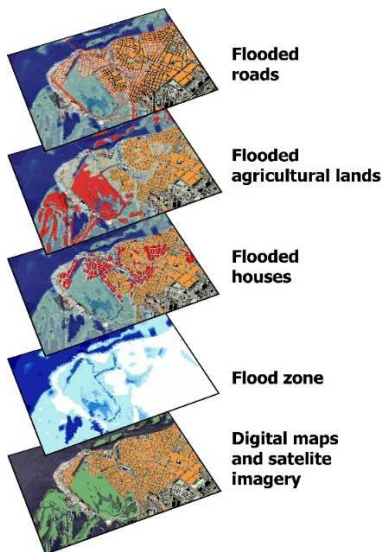


Fig. 7 Identification of objects that would be flooded according to the results of simulation.

3.2 Flood zone analysis in a sophisticated GIS based application

To make the analysis of flood zones easier for specialists, who are new to GIS, the authors have developed WEB-based application and also a Desktop application that works with the flood zone modelling results and provide basic features for navigation, identification, search and report generation for specialists in hydropower safety, administration, and other parties.

The above mentioned application FloodArea is module based. Architecture of this application FloodArea is presented on figure 8.

Except for the basic features the application includes the following instruments:

1. Selection of the study area and of scenario of modelling, creation of thematic maps for analysis of water levels, velocities or impact value;
2. obtaining characteristics of flooding at any point of study area;
3. object's measurement (length, area);
4. creation of lists of flooded objects grouped by type;
5. creation of screen shots with additional legends, notes and etc.;
6. creation of reports presenting information about the flooding;

The GIS developed by the authors may become a platform for storing the modelling data for MIKE, Hancock, storing and presenting the results of modelling, for creating the reports.

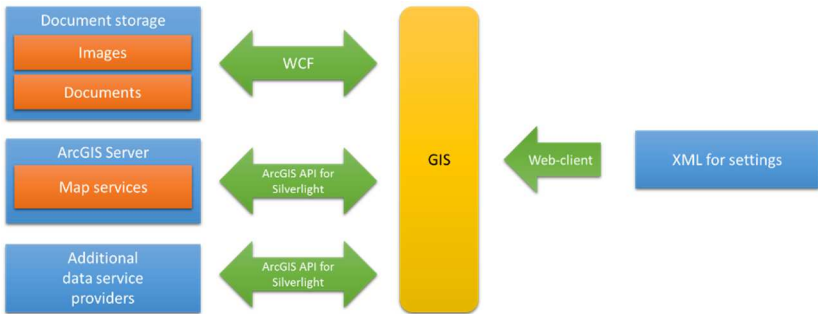


Fig. 8 Architecture of the GIS application

The interface of the application is presented on figure 9.

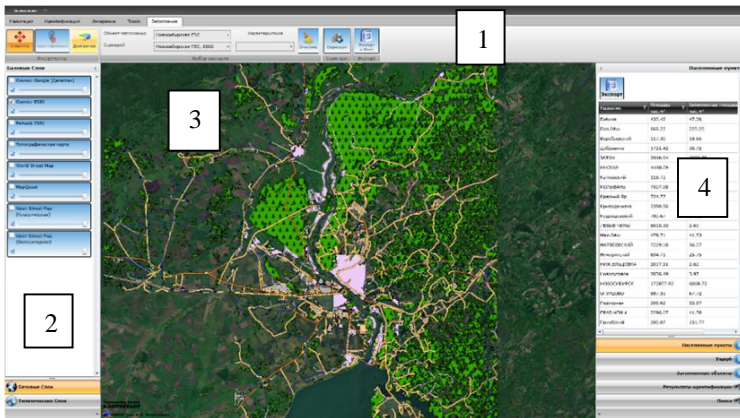


Fig. 9 1) Ribbon interface of the application with the basic panels, 2) contents of the map, 3) interactive map, 4) flooded objects list.

4. DISCUSSION AND CONCLUSIONS

1. Methodology for multiuser system for modelling of flood zones and flood losses estimation is presented.
2. This advanced system allowed to fulfill a study for a big set of objects with a concurrent model creation and computing (over 37 HPP with a set scenarios for each HPP).
3. A sophisticated GIS based tool for interactive analysis of flood zone modelling results was created. Software is using Microsoft Silverlight, WCF and ArcGIS API for Silverlight.

4. The GIS based tool developed by the authors can be used by specialist in hydraulic constructions, who are new to GIS.
5. Module based software is multilingual and can be used for other projects close to the study field.
6. GIS based application “FloodArea” was certified in Russia.

5. REFERENCES

- BADENKO, V.L. Scientific bases and methods of geographical information system implementation for environmental protection in the environmental management. Doctor of Science thesis, L.: 2000, -34 p.
- DRÁB, A., ŘÍHA, J., 2010. An approach to the implementation of European Directive 2007/60/EC on flood risk management in the Czech Republic, *Nat. Hazards Earth Syst. Sci.*, 10, 1977-1987, doi:10.5194/nhess-10-1977-2010.
- FEMA Flood risk report (for the Big Wood Watershed), 2012. URL: <http://www.bhs.idaho.gov/Pages/Plans/RiskMAP/Risk%20MAP%20Projects/Big%20Wood%20Watershed/BigWoodFloodReport.pdf>
- FRACAROLLO, L., TORO, E.F. Experimental and numerical assessment of the shallow water model for two-dimensional dam-break type problems.// *Journal of Hydraulic research*, 1995, vol. 33, №6.
- IVANOV, T.S., PROKOFYEV, V.A. 2012. Forecast of Flooded Zones During Flood Passing Based On Multi-Layer Hydrodynamic Model And GIS Technologies.// *International symposium on Dams for a changing world. ICOLD. Kyoto, 2012. Abstracts*
- NUJIC, M. Efficient implementation of non-oscillatory schemes for the computation of free- surface flows.// *Journal of Hydraulic research*, 1995, vol. 33, №1.
- PROKOFIEV, V.A. Application of Unified 3D Hydro-Thermal Model of a Reservoir for Estimation of HPP Construction Influence on Environment. //Proceedings of the international symposium on dams for a changing world – 80th annual meeting and 24th congress of ICOLD, KYOTO, Japan. 2012, section 5. pp. 69-75.
- PROKOFIEV, V.A. Modern numerical schemes based on control volume for the simulation of turbulent flows and dam breake modelling.// *Hydraulic Engineering*, 2002, №7.
- Recommendations #528/143 as of Oct,2 2007 by Ministry of the Russian Federation for Civil Defense, Emergencies and Elimination of Consequences of Natural Disasters
- Recommendations of the Ministry of Russian Federation for Civil Defense, Emergencies and Elimination of Consequences of Natural Disasters №2-4-60-6-14 as of June, 30th, 2010 «Methodical recommendations about issuing the statement of organization maintaining hydraulic engineering constructions»

Analysis of SHPP Brodraci influence on production of HPP Ozalj

E. Ocvirk, G. Gilja, J. Berbić

Water research dept., Faculty of civil engineering, University of Zagreb,
Andrije Kačića Miošića 26, 10000 Zagreb,
E-mail: ocvirk@grad.hr, ggilja@grad.hr, jberbic@grad.hr

Abstract

Hydro junction Brodraci on the river Kupa is part of flood protection system Srednje Posavlje focusing to protect the city of Karlovac. Final design of flood protection system includes utilisation of hydropower in form of small hydropower plant Brodraci (SHPP Brodraci). In this paper an analysis of the impact of the SHPP Brodraci backwater on the production of existing hydropower plant Ozalj (HPP Ozalj) is given. Within the analysed river reach is located confluence of tributary river Dobra. HPP Lešće operation on river Dobra affects the regime of the river Kupa between the SHPP Brodraci and HPP Ozalj. Available hydrologic data includes information from gauging stations on river Kupa upstream and downstream of analysed river reach and on river Dobra downstream of HPP Lešće. Assessment of HPP Ozalj's tailwater in the design state is based on the results of a detailed hydraulic flow model setup on hourly data and operating conditions on both HPP. Also are available hourly data for the year 2012 on production, the tailwater and the headwater at HPP Ozalj. For better description of the real conditions of production and thus a more accurate assessment of the impact efficiency curve for HPP Ozalj is analysed in detail. The main idea was to determine efficiency coefficient depending on available flow and head. Conducted analyses resulted in comparison of HPP Ozalj's production in the current and design state based on the defined hydrological regime and efficiency curve. Results show that the raising tailwater during low flow has no negative effect on the production of HPP Ozalj due to improved working conditions and increased efficiency coefficient.

Keywords

small hydropower plant, efficiency curve, backwater impact

1. INTRODUCTION

The subject of this paper is to determine the impact of future small hydropower plant (SHPP) Brodraci on Kupa, near the entrance to 21,9 km long flood relief channel Kupa-Kupa, on production of hydropower plant (HPP) Ozalj placed upstream. Primary design of SHPP Brodraci defines it as a run of the river HPP with installed discharge of 120 m³/s and generating capacity 2.8 MW at gross head of 4m (headwater at level +112,00 m asl (above sea level)). This location in flood

protection system of city of Karlovac is named hydro junction Brodarci and it redirects high waters of River Kupa to channel Kupa – Kupa. Around 700 m upstream from the channel Kupa – Kupa, river mouth of r. Dobra can be found. HPP Lešće on r. Dobra is also included in the analysis. It is placed 30 km upstream of SHPP Brodarci with installed discharge of 120 m³/s).

2. INPUT DATA ANALYSIS

The most interesting part of the analysis is defying the efficiency coefficient depending on head and discharge based on inputs. The SHPP Brodarci impacts the tailwater of HPP Ozalj. As shown in Table 1 there is only data on efficiency coefficient for one turbine depending on discharge. Efficiency coefficient, used in analysis, is defined based on data on heads, production of turbines and hourly discharges.

Tab 1. Review of database used in the analysis

Survey	Hydrologic data	Data from HPP Ozalj
Croatian Base Map 1:5000	HPP Ozalj: water levels (headwater, tailwater – hourly data)	Data on production of HPP Ozalj for 2012 in form of daily reports with hourly data
Topographic map of Croatia 1:25000	Gauging station Kamanje: water levels (daily data); discharge-water level curve	efficiency coefficient of turbine depending on discharge for 1 turbine
Channel bathymetry data	Gauging station Brodarci (r. Kupa): hourly data discharges and water levels	
	Gauging station Stative donje (r. Dobra): hourly data discharges and water levels	

Figure 2 shows „input data“ used in the analysis based on data from turbine producer (marked with green) and efficiency coefficient according to calculations made based on data from HPP Ozalj (marked with blue). The Figure 2 also shows a clear need for detailed analysis, which would estimate the effect of head decrease on production at small discharge. The problem that appears when analysing efficiency coefficient is that a wide range of efficiency coefficient appears in similar conditions.

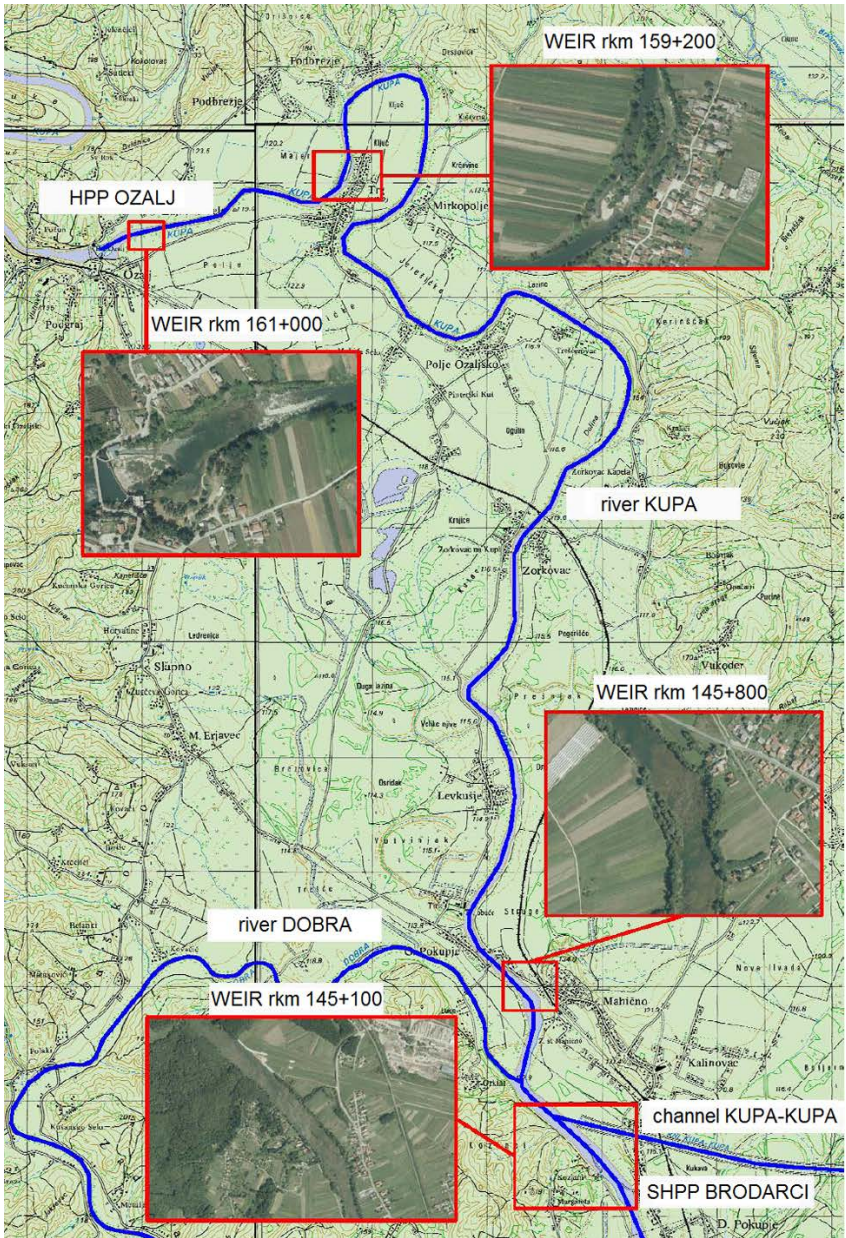


Fig. 1 General layout of analysed river section

The mathematical method of approximation and averaging oscillations is used to create efficiency coefficient used in further analysis (figure 3). The data was fitted using polynomial regression, resulting in 3d curve which fits the efficiency coefficient in the dependency of two input variables – discharge and gross head. In the manner of showing clear representation, the efficiency coefficient curve is represented using equipotential lines, in figure 3. It should be noted that further in paper term efficiency coefficient involves efficiency values of the power plant including the loss of the water turbine, generator and transformers of all turbines in operation at any discharge.

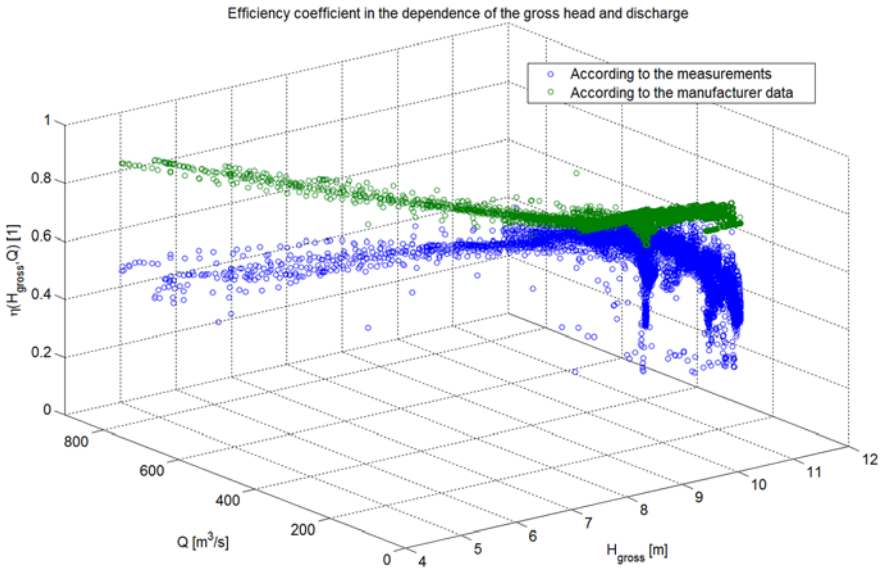


Fig. 2 Efficiency coefficient HPP Ozalj depending on head and discharge

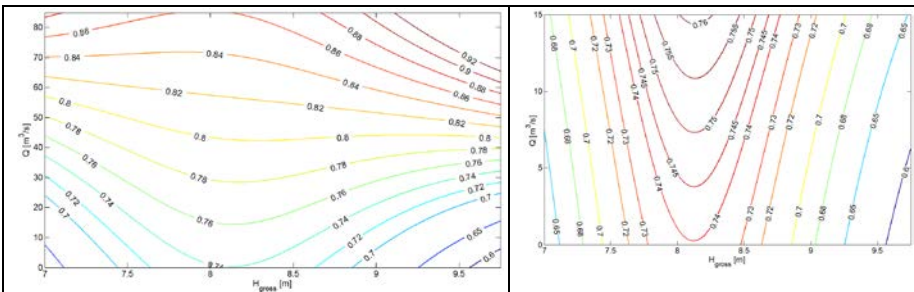


Fig. 3 Efficiency coefficient HPP Ozalj depending on head and discharge used in this paper

Hydraulic flow model is made as the basis for determine impacts of SHPP Brodarci on hydraulic regime of River Kupa in order to estimate the impacts of SHPP Brodarci on production of HPP Ozalj more precisely. Hydraulic flow model for current and future state was made with HEC-RAS. The model included r. Kupa from river station 144+900 (SHPP Brodarci) to river station 161+772 (HPP Ozalj tailwater) and r. Dobra from river mouth into Kupa (river station 145+700 Kupa) to river station 11+210 (gauging station Stative donje). The accuracy of calculations made by numerical model depends on the accuracy of used river geometry and hydrological boundary conditions. Calibration of the numerical model is reduced to the determination of the roughness coefficient and weir overtopping coefficients which affect the hydrological regime of the river Kupa and Dobra. Calibration is carried out on the basis of available data of the hydrological boundary conditions on the boundaries of the model - the water level and flow at Brodarci, Ozalj and Stative donje.

Based on the calibrated model, the calculation of the flow of the rivers Kupa and Dobra was made for current state with discharges from yr. 2012. Discharge range for r. Kupa was from 5 m³/s to 834 m³/s according HPP Ozalj input data, and from 9,5 m³/s to 1006 m³/s at gauging station Brodarci. Discharge range for r. Dobra at gauging station Stative donje was from 3,1 m³/s to 240 m³/s.

The input data analysis are divided into two input data subsets according to the dependence on the work of HPP Lešće: the data with the impact of the HPP Lešće and the data when HPP Lešće was not in operation.

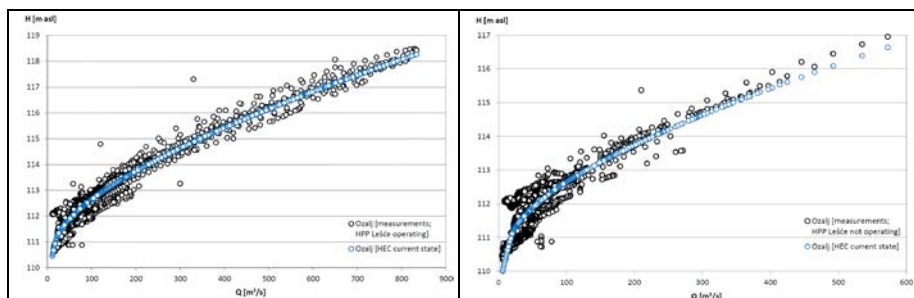


Fig. 4 Hourly flow and water levels from the input data (black) and the results of the numerical model (blue) at HPP Ozalj tailwater: HPP Lešće in operation (left) - HPP Lešće not in operation (right).

It is evident that the results of numerical models at location of the HPP Ozalj tailwater correspond well with the measurements. As shown in figure 4, the results of the model are in the middle of a cloud of oscillating water levels from measurement.

Results of numerical model for future state with headwater on SHPP Brodarci on level +112,00 m asl are shown in figure 5. These results are used to analyze changes in the hydrological regime of the river Kupa and Dobra in the case of

construction of SHPP Brodarci. The results are presented for the current and future state for two cases – HPP Lešće in operation and HPP Lešće not in operation. Figure 5 shows discharges in the zone of interest for the production of HPP Ozalj. The impact of the HPP Lešće is clearly visible with increase of the water level up to 30 cm.

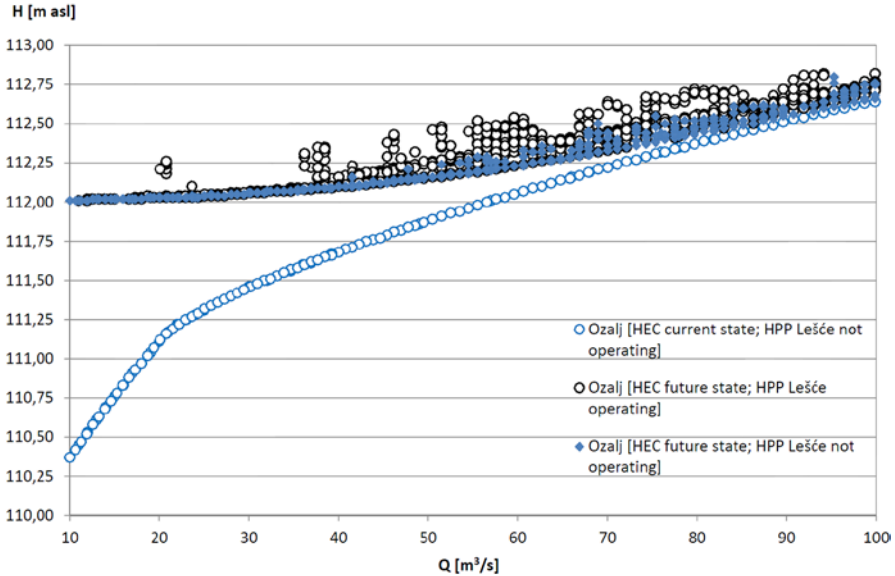


Fig. 5 HPP Ozalj tailwater in current and future state at lower discharges (below installed discharge)

Finally, Figure 6 shows the impact of the SHPP Brodarci backwater on HPP Ozalj depending on the discharge rate which is in the range of 2 m at an extremely small discharge ($5 \text{ m}^3/\text{s}$), approximately 1.5 m at a discharge of $10 \text{ m}^3/\text{s}$, 1.0 m at a discharge of $20 \text{ m}^3/\text{s}$, 60 cm at $30 \text{ m}^3/\text{s}$, 40 cm at $40 \text{ m}^3/\text{s}$, 10 cm at the discharge of $70 \text{ m}^3/\text{s}$. At a discharge of around $150 \text{ m}^3/\text{s}$ impact is completely lost in case when HPP Lešće is not in operation. But in the case when HPP Lešće is operating impact still exists, but due to the short duration through the year, doesn't have significant impact on production.

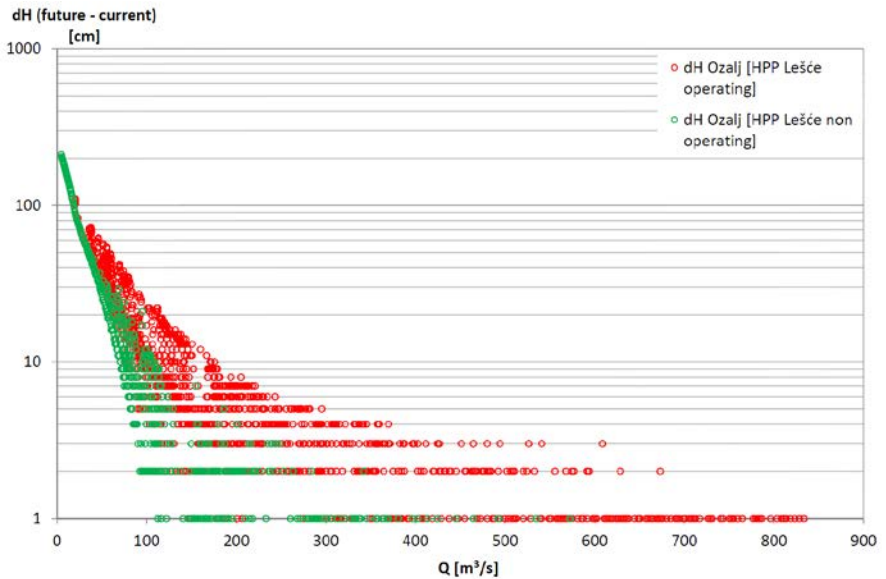


Fig. 6 SHPP Brodarci backwater impact on HPP Ozalj

3. IMPACT ON HPP OZALJ ENERGY PRODUCTION

Based on the results of the numerical model for the current state, an analysis of future production by the same criteria was made. Namely, before the use of numerical model results for the future state it is necessary to prove its applicability to the current state. For this reason the results of the numerical model for the current state were verified by comparing the actual production from 2012 and production on the base of numerical model water levels and efficiency coefficient shown in figure 3.

Calculation of production was carried out for two cases. As the first, to check the results of hydraulic models and in the paper defined efficiency coefficient, production in the current state was calculated. After that, production in the future state on the basis of numerical model was calculated. Calculation of energy production was carried according to the equation:

$$W = 9,81 \cdot Q_r \cdot H_b \cdot t_r \cdot \eta, \quad (1)$$

where: W (kWh) is energy production, Q_r (m^3/s) is discharge, H_b (m) is gross head, t_r (h) is discharge and associated gross head duration, η (1) is efficiency coefficient (turbine, generator, transformer, hydraulic loss in penstock).

The maximum used discharge is $85 \text{ m}^3/\text{s}$, although according to the data from HPP Ozalj can be concluded that HPP Ozalj occasionally worked with a larger discharge.

The results obtained by the procedure described above are shown in Table 2.

Tab 2. HPP Ozalj production

	2012. yr Input data from HPP Ozalj	2012. yr numerical model for current state	2012. yr numerical model for future state
Production [GWh]	22,356	22,309	22,248

According to the presented results it can be seen that the deviation in the HPP Ozalj production in the current state (from numerical model) compared to measured data is less than 1 %. That shows that numerical model and efficiency coefficient were determined correctly. Furthermore, production in future state doesn't change much because, as expected, increasing HPP Ozalj tailwater also increases the efficiency coefficient. In that case with smaller gross head at small discharges production stays almost the same.

4. CONCLUSION

In this paper, an analysis of the impact of future small hydropower plant Brodarci on the production of HPP Ozalj was made. For a better description of the real conditions of production and thus a more accurate assessment of the impact, hourly data obtained from HPP Ozalj on production, headwater and tailwater and average daily discharges were used.

SHPP Brodarci, designed as run of the river SHPP with headwater at +112 m asl, obviously has impact on upstream located HPP Ozalj tailwater. Based on the collected data the HPP Ozalj efficiency coefficient depending on discharge and gross head is determined.

Finally, a comparative calculation of production in the current and future state (according to numerical flow model) were obtained. Analysis shown in the paper confirmed that the development of hydro junction Brodarci with SHPP Brodarci will not have a significant negative impact on the production of HPP Ozalj.

5. REFERENCES

AKI 2014. *Preliminary design of SHPP Brodarci*, AKI, Zagreb
 CHOW, V. T. 1986. *Open-Channel Hydraulics*. McGraw-Hill, New York
 LAÍN, S., GARCÍA, M., QUINTERO, B., AND ORREGO, S. 2010. CFD Numerical Simulations of Francis Turbines. *Revista Facultad De Ingeniería Universidad De Antioquia*, 51, 24–33
 EGRE, D., AND MILEWSKI, J. C. 2002. *The diversity of hydropower projects*. *Energy Policy*, 30, 1225-1230

Temperature measurement methods on the water structures

O. Černý¹, J. Hodák²

¹VODNÍ DÍLA-TBD a.s., CREA Hydro&Energy, cluster of companies, research institutions and universities, Traubova 6, 602 00 Brno, Czech Republic, phone: +420 680 437 053, e-mail: cerno@vdtbd.cz

²CREA Hydro&Energy, cluster of companies, research institutions and universities, Traubova 6, 602 00 Brno, Czech Republic, phone: +420 777 769 360, e-mail: hodak@creacz.com

Abstract

Seepage regime measurement is one of the fundamental instruments for water structures safety surveillance and supervision. Modern temperature measurement methods were carried out on various water structures. Fibre optic temperature sensing was performed on the Moravská Třebová dam, ground temperature sensing by means of the hollow tubing and temperature sensor was done on the Spytihněv weir and thermo camera recording was tested on different types of water structure. Modern temperature sensing methods can be used as an important supplement instrument for water structures safety surveillance and supervision. A methodology for different methods is main output of this CREA Hydro&Energy IIa research project undertaken thanks to PROGRAM SPOLUPRÁCE-Klastry.

Keywords:

water structures safety, seepage, temperature measurement

1. INTRODUCTION

Seepage regime is one of the basic indicators monitored for assessing the safety and technical reliability of water structures. In the Czech Republic seepages are systematically monitored within the water structures safety surveillance and supervision from the 70's of the 20th century.

Seeping water has a significant effect on the static and seepage stability of the water retaining structures, on its deformation as well as deformation of the subsoil. Changes in seepage regime caused by internal erosion in most cases occur after a longer period of time, often with no visible expression on the surface of the dam. The internal erosion of the embankment dam is one of the frequent causes that can lead to the destruction of the dam. Identification of the potential problem zones at an early stage of the seepage development may help to implement appropriate measures in time.

Seepages of the dams and their subsoil are monitored mainly by measuring their quantity or temperature, a turbidity and material outlet is observed and when necessary a chemical analysis is performed. The measurement of the amount of

seeping water is carried out at the outlet of the drainage system or in the drainage manholes. Other devices for monitoring of the water head and seepage regime are observation boreholes located within the dam or underneath.

On the dams following methods based on temperature measurements are used:

- temperature monitoring of the water outlet from the drainage systems,
- temperature measurement of the water (or material of the dam) in observation wells,
- the use of fiber optic cables in monitoring of the seepage regime,
- ground temperature measurement by means of hammered probes.

This article discusses the use of fiber optic cables, ground temperature measurement and also possible use of the infrared thermography (IRT) in dams monitoring.

1.1 Ground water temperature in soil and embankments

Surface water temperatures and ground temperatures show seasonal variation caused by the climate. The maximum and the minimum of the temperature at the ground and surface water are occurring approximately at the same time. Due to the low thermal conductivity of the soil a phase shift between the fluid temperature and the temperature of the ground material develop with increasing depth. Also the amplitude of the seasonal temperature decreases with the depth. Therefore, ground temperatures show different seasonal variations than surface water temperatures (Fig. 1). If surface water is seeping through the ground, ground temperatures are changing due to the heat transport and thus ground temperatures assimilate to the temperature of the seepage water.

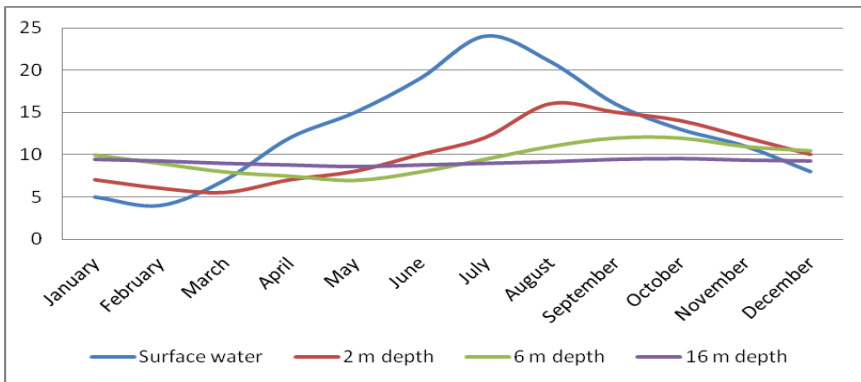


Fig 1: Example of the phase shift a amplitude decrease of the surface water a and undisturbed ground temperatures at 2 m, 6 m and 16 m depth

2. FIBRE OPTICAL SEEPAGE DETECTION SYSTEM

Optical fibre is a transmission medium composed of glass (quartz) or a plastic fibre (POF), which transmits signals via the light in the direction of its

longitudinal axis. There are many fibre optic sensors. One is a DTS (distributed temperature sensing). The optical fibre is in this case a temperature sensor which allows by a single measurement to obtain several thousand temperature values.

DTS method offers the possibility to measure the ambient temperature along fibre optical cables of a few kilometre length continuously with high accuracy. Compared to the conventional measuring method DTS gives a much higher information density and improves the evaluation of the temperature distribution in big constructions.

2.1 Seepage detection with the use of DTS

DTS can be used for the detection of the inner erosion paths as well as for the determination of the temperature distribution in concrete structures. For the deployment in water retaining structures and concrete temperature monitoring cables of usually 10 mm diameter are used. These cables possess a great mechanical strength and are fit for construction site conditions. For the implementation of the temperature measurements the fibres in the cable are connected to the laser. The measurements can be performed quasi continuously as well as in optional time intervals.

There are two measurement methods, namely:

Temperature gradient method

Absolute temperature distribution is determined along an optical fibre. This method can be used where is a temperature difference between the reservoir water and the dam material. To guarantee this a sufficient distance between the fibre optic cable and the reservoir water must be kept to ensure a corresponding temperature difference over an extended amount of time. The leakage is detected by a significant drop of the temperature gradient between the water and the ground temperature. The ideal position of such a measuring system is naturally on the downstream side of the sealing system, since normally anomalies are there well developed.

Heat-pulse method

In this method a hybrid cable is used which enables the heating by sending an electric current. The temperature increase is directly dependent on the heat capacity and conductivity around the cable. Flowing water, which has a higher thermal conductivity than the soil prevents higher temperature increase around the cable compared to locations without increased seepage. Therefore, clearly visible temperature anomalies arise in these areas during the process of heating.

This method leads to a considerable extension of DTS applications for seepage localisation. Through the described procedure nearly any sealing system can be verified regardless of seasonal temperature variations. The requirement of a spatial – respectively a heat transport delaying – distance between the fibre optical cable and the water body is no longer necessary.

2.2 Seepage detection with DTS on Moravská Třebová dam

On Moravská Třebová dam was during its reconstruction installed surveillance DTS system using hybrid fiber optic cable to carry out a test measurement of heat pulse method. Fiber optic cable was laid along the newly constructed toe drain (Fig. 2) and new construction of the spillway. It was important to coordinate the fiber optic cable installation with the progress of reconstruction works.



Fig. 2 – Fibre optic cable installation along a new toe drain

Measurement

Initial measurement took place on 25th of November 2014. During the measurement reservoir was empty which is appropriate for the reference measurement. The main task of measurement, in addition to testing the system itself, was to perform a reference measurement for "dry" unaffected conditions against which subsequent measurements can be compared to for the most accurate data interpretation and determination of the seepage zones.

During the measurements absolute temperature, temperature differences before and after the cable heating and the effective thermal conductivity were monitored. Different temperature along the cable in its individual parts was detected. The reason was different thickness and composition of the backfill material and different water saturation along the cable.

Large temperature dispersion reflects unaffected dry conditions along the toe drain and saturated environment with different material and thus thermally more conductive environment along the spillway.

No significant anomalies were observed during the reference measurement.

2.3 DTS usability in the Czech Republic

Consideration using both methods of seepage regime monitoring at water retaining structures by optical cables is necessary already in the phase of the

project preparation of structure construction or reconstruction or its repair. It is not a method for investigation, but the placement of fibre optic cable is possible at the new construction or during interventions in the structure of existing dams. In some cases, e.g. cable installation along the toe drain, it is possible to install cable without major interventions into the construction of dam. For the deployment in water retaining structures and concrete temperature monitoring cables of usually 10 mm diameter are used. These cables possess a great mechanical strength and are fit for construction site conditions.

Installation of fibre optic cable is not too complicated. The most important is the choice of the location of the cable itself, which must be based on general knowledge of the water behaviour in geotechnical and building structures and their cooperation (e.g. the potential flow paths on the contact of different structures and soils, etc.).

Generally, the heat pulse method has a significantly higher spectrum of usage compared to the temperature gradient method.

Temperature gradient method

This method is applicable where there are different temperatures of seeping water and the environment in which an optical cable is installed. Optical cable must be installed in sufficient distance from the water reservoir, river, etc., to ensure adequate temperature reduction of the material (e.g. soil) compared to the retaining water for a longer period. Locations with an increased seepage will show a temperature anomaly compared to areas with steady flow seepage regime.

This method is applicable for long-term seepage monitoring. For a trustworthy evaluation a regular measurements would be essential. From their comparison a possible changes in seepage regime can be assessed. The advantage is that standard optical cables can be used and measurement only requires a standard electric current 230V.

Heat pulse method

It is not possible to list complete possible situations where cable optic monitoring, especially the heat pulse method, can be applied. It is always necessary to take into account the specific conditions of individual water structures. Examples of possible uses of installation optic cable are following:

- behind the sealing components;
- along the toe drains of earthfill dam;
- at the contact of the construction facility and earthfill materials of the dam body.

For the fundamental design apart from the cable placement it is necessary to take into account:

- overall required length of cable plus reserve 10 to 20% of the cable for connection to the splice boxes (at the ends of the cable or for cable connection) in which are located all the electrical and optical interfaces

required for laser temperature measurement and heat pulse method application - heating cable;

- choice of the measuring point which would be easily accessible and considering the need of sufficient power supply;
- cable installation with respect to the progress of construction works;
- cable must be protected from damage by machinery; backfill with permeable material rather than using a plastic sleeve is suitable;
- security measuring point against its damage;
- if possible reference measurement after cable installation is appropriate with undisturbed conditions prior to reservoir filling. The following measurements are compared to the reference one for most accurate data interpretation and determination of the seepage regime or anomalies.

However, the disadvantage remains the high cost of measurement. Currently it could be recommended for reconstruction of waterworks. If already implemented interventions into the construction of water structures, fibre optic cables installing does not represent extra high investment. Optical cables can then be used for regular monitoring or to have it ready for use in the future. In situations where there will be observed phenomena indicating seepage regime change it would be possible to measure the optical cables. This may provide useful information for a correct assessment of the situation and help choose most effective measure.

3. GROUND TEMPERATURE MEASUREMENT BY MEANS OF HAMMERED PROBES

It is a method which in our country, according to the known documents, has not yet been tested. The first test application took place in the framework of our temperature research project on Spytihnev weir.

This method is applicable only to the earth-fill dams, dikes, etc. In a series of hammered probes (low profile boreholes) temperature profile is measured by means of temperature sensors. Fig. 3 schematically shows an example of the dam with the placement of temperature probes.

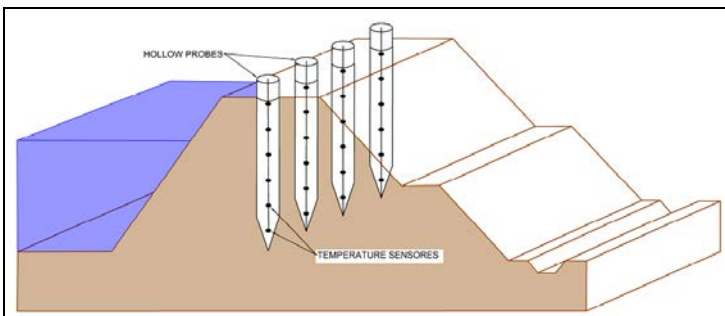


Fig. 3 – Schematic principle of the grand temperature measurement

The output is then temperature recordings, graphical progressions along the depth of boreholes and temperature map of the study area, which can identify areas with temperature anomalies representing increased seepage.

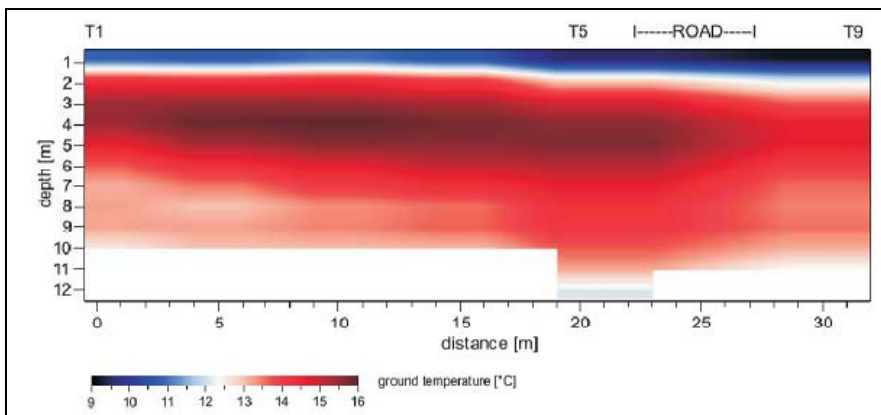


Fig. 4 – Temperature profile – example of the output from temperature probes measurement

3.1 Spytihněv weir right abutment investigation

Pilot measurements in the Czech Republic on the Spytihněv weir was performed in cooperation with GTC Kappelmeyer research organization which is involved in research and development of measurement techniques which allows temperature measurement in fine-grained soils and embankments up to a depth of 30 m.

Installation of the temperature measuring probes in the right abutment of the Spytihněv weir on the Morava River took place on 26th of November 2014. It included 10 temperature probes to a depth of between 10 m to 13 m. The aim of the survey was to clarify the origin of seeping water which is observed in the right abutment concrete pillar. It was expected that seeping water could come from the river or canal lock located along the weir.

Temperature measurement in probes was done with a cable with sensors in 1 m distance. No significant temperature anomalies in the embankment showing possible seepage from the canal lock or river was identified.

However, ground temperatures were particularly disturbed between 8 and 10 m below ground level. The measurement used indicated that this anomaly is likely to be caused by a possible flow of slightly thermal groundwater. This assumption is supported by the fact that the temperature of seeping water from concrete pillar at the time of measurement was 13,1 °C with a slight sulphur odour. For more accurate results to already obtained information it was advised to make a chemical analysis of surface water in the river and seepage water.

3.2 Probes investigation usability in the Czech Republic

Usage is limited to earthfill dams with fine-grained materials. It is an investigation method that can be used for localization of the dam body with increased seepage in cases where traditional measurements and observations show a change in seepage regime or long-term unsatisfactory seepage regime is monitored.

Despite to the fact that it is an “invasive” method with mechanical impact to the dam body, since a very small diameter probes are used it doesn't have a negative impact.

4. WATER STRUCTURES THERMOGRAPHY MONITORING

Thermography, measurement of surfaces temperatures using thermo cameras, is not yet used in water structures monitoring. This method was first tested in this research project focused on different methods of temperature measurements on water structures. Its use was verified on various types of dams.

Water structures especially those retaining water have compared with the structures of housing specific function, technical design, used materials atc. Contrary to the heated buildings water structures usually don't separate spaces with different temperature, respectively their function is not heat insulating. Thermal characteristics of waterworks structures should be stable during long-term monitoring with natural changes caused by different climatic conditions, particularly changes of seasons.

For heated buildings the best time for thermographic measurement is winter with biggest difference between the temperature inside and outside the building. Due to thermal stratification of water in reservoirs in winter seepage on downstream face is reflected as temperature increase compared to undisturbed surrounding frozen surface and contrary seeping water is cooling the surface in the summer. On the water structures were specifics of thermography tested under different climatic and operating conditions in different season but also on the different types of dam structures.

Most detailed survey was carried out on the Upper reservoir of Dlouhé Stráně Power Station where it was possible to perform measurements in different operating conditions as well as with fully empty reservoir. It is a reservoir with an asphalt upstream surface sealing. Thermography survey was also conducted on concrete gravity Mohelno dam and reservoirs which belong under Povodí Moravy, s.p. management, concrete dam Vranov, stone masonry dam Jevišovice, earthfill dam Karolinka and others. At Fig. 5. an example of thermography snapshot of Dlouhé Stráně upper reservoir is shown.

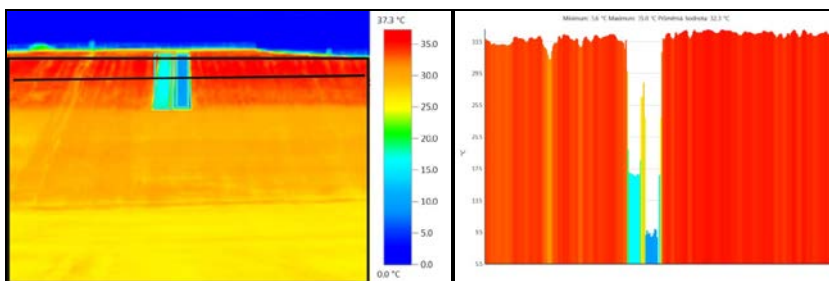


Fig. 5 – Dlouhé Stráně water structure - test surface painting on the western reservoir slope

4.1 Thermography usability in the Czech Republic

Thermography is in terms of technical demands and usability a simple method that can be in the geographic and climatic conditions of the Czech Republic used for dams monitoring. It may be recommended for measurement within the technical and safety surveillance and supervision because it can bring additional information to the overall knowledge of water works objects and construction behaviour. It can also be applied under suitable conditions as the first step in seepage detection as it is a very simple inexpensive method without mechanical intervention in the construction.

For the most accurate evaluation of thermal imaging it is necessary in addition to thermo recording itself also record data which can output or more precisely its diagnostic influence. In particular, the following information are important:

- air temperature at the time of thermo scanning and even before if the structure surface could had been influenced by the temperature development;
- cloudiness during thermo scanning and before it if the structure surface could had been affected by previous sun exposure;
- wind force near the structures during thermo scanning;
- water level in the reservoir during the thermo scanning or its movement before prior to it;
- water temperature development in the reservoir and outlet form drainage system for several days or weeks prior to thermo scanning;
- humidity (too high humidity condensed into mist or fog significantly affect the measurement);
- when scanning the upstream face of the dam it is important to know the evolution of the water level in the reservoir for several hours prior to scanning.

Earthfill dams

Thermal scanning should be performed in the summer and winter months when there is highest difference between the temperature of the water in the reservoir and the temperature earthfill dam material.

Dams and dikes overgrown with trees, bushes, self-seeding trees or in built-up area can't be thermo scanned properly. The surface of the dam itself is not possible to capture by scanning.

Also in cases where the grass surface of the dam is too high uncut or with grown weed thermo scanning shows temperatures of the grass cover rather than the surface of the dam. It is ideal if the dam surface has grass cover high 5 to 10 cm.

Earthfill dams with upstream asphaltic concrete sealing

At these water structures thermo scanning can focus on upstream slope/face of retaining structure for leaks detection. Furthermore, it is suitable for temperature measurement of surfaces (asphaltic concrete) of both downstream and upstream. Temperature regime has a significant influence on the deformational behavior of the structure therefore it is suitable for long-term monitoring at different operating and climatic conditions.

Deformation of the top layer of asphaltic concrete shell (cracks, blisters), which can retain water shows relatively large temperature differences compared to the surrounding dry by sun heated undistorted surface. There are also significant temperature differences of asphaltic concrete shell surface on more and less sunlit sides of the reservoir.

Significant changes in surface temperatures can appear during a single day. The highest temperatures are always under a clear sky and sunlight perpendicular to the surface. The influence of sunlight is essential. With the cloudy or semi cloudy sky when sunshine quickly changes with overcast skies and in combination with cold wind flow quick and relatively significant surface temperature fluctuations are observed.

Thermography is sufficiently accurate method for water structures surfaces absolute temperatures monitoring. This was proved by comparing the results from thermo scanning to results obtained with surface contact thermometer. However it is always necessary to comply with principles of thermography and observed outer conditions which can influence obtained data interpretation.

Temperature measurement accuracy of "detailed" thermo scanning on short distances can be considered proved. While scanning of the larger areas from distance can be slightly affected by external influences such as particularly the warm ray light of the sun and/or the cold ray light of the sky and their reflection from water surface. Nevertheless affect on the results is in units of degrees. Other factors affecting results accuracy can be the state of the surface such as grain structure, purity, vegetation mosses, plants etc.

For most accurate data interpretation and to avoid unsubstantiated conclusions in some cases it is appropriate to perform repeated scanning and scanning under

different angles. Also a regular scanning of some structures could contribute to better knowledge of their behavior and influences that affect the behavior of these structures.

Concrete and masonry dam

For thermal scanning of concrete and masonry dams similarly applies principles and possibilities of use as for dams with asphaltic concrete shell sealing mentioned above. It is a similar building materials in terms of properties such as emissivity and the ability to reflect and absorb heat.

It is always necessary to take into account the specifics of the individual water structure in terms of both their construction and technical design and specific operating and environmental conditions.

5. REFERENCES

- DUSEK, M., MAZANEC, M., 2012. Physical principles of optic and optic-fibre sensor, *Centrum pro rozvoj výzkumu pokročilých řídicích a senzorických technologií, Ústav automatizace a měřicí techniky, VUT v Brně.*
- KAPPELMEYER GTC, 2003. Sensitive inspection and monitoring of embankment dams, GTC Kappelmeyer GmbH.
- LATAL, J., KOUDELKA, P., HANACEK, F., SISKA, P., 2010. Introduction into the Raman effect based Distributed Fiber Optic Systems for Temperature Measurement, VŠB-TU Ostrava, FEI.
- REASERCH REPORT, 2015. Temperature measurement methods on the water structures, research report, CREA Hydro & Energy, April 2015.

Using high-precision total station operating in ATR mode and robust adjustment of geodetic networks for safety supervision over waterworks¹⁾)

T. Macháček¹, V. Krnáč²

¹VODNÍ DÍLA-TBD a.s., CREA Hydro&Energy, cluster of companies, research institutions and universities, Traubova 6, 602 00 Brno, Czech Republic, phone: +420 777 769 325, e-mail: machacekt@vdtbd.cz

²CREA Hydro&Energy, cluster of companies, research institutions and universities, Traubova 6, 602 00 Brno, Czech Republic, phone: +420 773 785 997, e-mail: krnac@vdtbd

Abstract

High precision terrestrial geodetic measurement is one of fundamental instruments for water structures safety surveillance and supervision. This work is devoted to research the usability of high precision Leica TM30 total station, operating in ATR (automatic target recognition) mode for determining the displacements and deformations of waterworks. Data sets of geodetic measurements on dams Josefův Důl, Řimov, Nechanice and Vrchlice was survey for observed points and reference net points on each of waterwork in one or more stages. Measured data was offset as a spatial or planar geodetic network using computer program EasyNet. This program has a sophisticated analysis of measurement data and for least squares adjustment of geodetic networks use robust methods of analysis for the exclusion of outliers and gross errors of measurement. The result is a new methodology for measuring especially horizontal displacements, which uses a new measurement technologies and computational processing. This process is more efficient and achieves more accurate and stable results than conservative displacement measurement methods, for example, the line of sight or forward intersection. A methodology for correct measurements was developed. This work is the output of CREA Hydro&Energy IIa research project undertaken thanks to PROGRAM SPOLUPRÁCE-Klastry.

Keywords

ATR, dam monitoring, Leica TM30, robust analysis, spatial network adjustment, stage displacements, waterwork

1. INTRODUCTION

This paper deals with deformation measurements exact total station using the technology ATR (automatic target recognition) for the purposes of monitoring dams. Water works are regularly geodetic measurements in the performance of technical and safety supervision. We have tried to develop a new method for determining the horizontal (or spatial) deformations that would be automated as much as possible, correspond to the current state of modern measuring and

computing and in practice replacing previously used methods of conservative geodetic deformation measurements.

2. METHODS OF MEASUREMENT DISPLACEMENTS WITH TOTAL STATION

Deformation measurements are historically divided for terms of the methods and instruments for determining the separate horizontal and vertical displacements. In practice, for measuring vertical displacements due to the high achievable accuracy uses a high-precision levelling.

Measurement of horizontal displacements on the waterworks is currently carried out with precise theodolites and total stations. Measured are slope distances, zenith angles and horizontal angular directions. Based on the configuration of waterwork are chosen adequate methods for measuring the observed points of the waterwork and its components and checking the stability of the reference points. These measurements have a stage character and between stages differences measured values are calculated corresponding displacements.

2.1 Network reference points

The reference network consists of stabilized points outside the zone anticipated deformations which serves as an opinion to the measurement object being tracked. These points are usually with heavy stabilization (reinforced concrete pillar, casing pipe), the station head with mounted equipment for forced centring.

In networks of small-scale is stability checked by measuring the opinions of orientation and locking points, larger networks are the opinions of measurement points observed supplemented by other reference points that serve to improve the shape of the network in terms of increased accuracy and stability calculation. These networks are measured length and directions in suitable combinations of visible and measured data are aligned by least squares method (LSM) in the form of free or fixed geodetic network.

Monitor the stability of the reference points of the network is needed to evaluate their own shifts observed points and the evaluation of the deformations of individual parts of the waterworks.

The basic methods for measurement of reference networks are as follows:

- Planar geodetic network (2D).
- Spatial geodetic network (3D).

2.2 Observed points

Observed points are fitted in the monitored area and represent the measured object. Stage measurements can be determined with displacements of individual points and follow up the deformation of the object being tracked.

In practice, most of the deformation measurements carried out by conservative methods, which correspond to the level of measurement and computer equipment during the construction of various water works (Wild T3, Kern Mekometer):

- Line of Sight.
- Direct distance measurements.
- Intersection of angles.

The result of these measurements is one dimensional shifts determined in a direction perpendicular to the direction (line of sight), or oriented in the direction (measured length). They are only a part of true displacement vector and limits further interpretation of this data.

2.3 The proposed upgrade of the existing methods for measuring displacement

Our proposed and tested method replaces the existing procedures deformation measurements on waterworks polar geodetic network focused by precise total station with ATR. Replaces measurement methods (mostly horizontal displacements) have carried theodolites and total stations. For this technology, it is necessary to change the instrumentation measurement points so that they can be fitted in the measurement of reflective prisms. For observation points are measured horizontal directions, zenith angles and slope distances and allow the calculation of 2D vector in the horizontal plane or spatial 3D vector displacement, also including point height. The achieved accuracy is higher than in the previous methods, excess quantities are used for alignment. This measurement method is commonly used for measuring the reference networks as part of our research has been newly established to measure their own displacements and deformations of monitored objects.

From the principle of measuring ATR is also possible to determine the vertical component of the displacement (simultaneous determination of position and height of the displacement vector components from homogeneous data), in some cases can replace measurements of vertical displacements by accurate levelling. The limiting factor for the accuracy and reliability of the results is the effect of vertical refraction.

Assuming the observed polar focus points can be converted to a conservative method of alignment using ATR data in the form of a plane or space geodetic network. It seems most appropriate method of robust alignment when the calculation can search for and eliminated remote measurements with robust analyses. For own calculations was chosen by EasyNet, which compared with conventional programs for adjustment of geodetic networks has the support measurements in rows and groups, analysing measured data and the possibility of a robust compensation.

3. TOTAL STATION WITH ATR TECHNOLOGY

For the measurement, it is necessary to have a motorized total station with ATR system. Available precision total stations have very similar characteristics of precision measuring horizontal directions, zenith angles and lengths. Machines for the highest standard of accuracy angular accuracy of 0.15 [mgon] and length accuracy better than $1 + 1$ ppm [mm]. Larger differences are in the performances of ATR (range of lengths measurable plan, support polar measurement data in rows and groups).

For testing the proposed methodology was used machine Leica TM30, which has a usable range of ATR 2-3000 m. A sufficient capacity to discern a disturbing reflection from the other prisms to target (minimum lateral distance of prisms is 0.3 m for 200 m, the ability to narrow the field of ATR view for 0,52 gon with TargetView to increase the detection rate of correct prism without risk of interference reflections from surrounding prisms).



Fig. 1 Leica TM30, Stanovice dam

3.1 ATR Technology principle

ATR system allows automatic focus centered prism. Rough searches prism describes the optical axis of the telescope spiral and ATR system emits a laser beam until the optical sensor (CCD or CMOS) receives a sufficiently strong reflected signal. After analysing the reflected laser beam is calculated intensity and spot size of light emitted relative to the centre of the sensor is determined deviations offset targets in vertical and horizontal direction by means of actuators,

the device is rotated in the right direction. To optimize measuring time machine shooting at a target with a certain tolerance, and the remaining difference is corrected numerically.

To use the function of ATR is necessary that the prism found in the visual field of the telescope. If the view of the telescope contents more prisms, there is a problem for older devices with detection targets.

3.2 Reflecting prisms

For measurement with ATR, it is necessary to fit the measured points with reflective prisms. Points of reference networks are mounted tribrachs (adapted to the system used forced centring) with a pin and a reflecting prism. It is necessary to ensure the quality and accuracy of the equipment used (hysteresis of tribrachs, prism parameters). Observed points are signalled by miniprisms adapted for temporary or permanent signalling points. ATR targeting accuracy depends on other parameters (constants of prisms, anti-glare coating, rotating beams at the target, etc.). For the measurement of deformations is not suitable to use a 360° prisms and reflecting labels targeting accuracy and reliability is insufficient.

4. PROCESSING OF POLAR GEODETIC NETWORKS

A large amount of measured data requires appropriate tools for their analysis and computational processing and automated as much as possible the process of elaboration of the measurement to final interpretation of computed displacements.

The processing results of measurement of stage shifts are observed points that represent the behaviour and eventual deformation of monitored objects. If the variables in the network greater than the necessary number, may be used in the alignment network of redundant measurement used to control and achieve a higher precision of search displacements. For your own calculation is used geodetic network least squares method (LSM), resulting in a balanced values of the measured data and the resulting coordinates. The net is placed in the output coordinate system by using the conditions as fixed or free network.

4.1 Robust adjustment of geodetic networks LSM

When testing the proposed method was alignment measured data in various programs for computer data processing as the most proven application EasyNet (version 3.2.1.).

It is an application that is used for the processing and evaluation of high-precision measurement engineering geodesy, the classic terrestrial surveying values (oblique lengths of horizontal directions and zenith angles), arranged in rows and groups and subsequent evaluation in the form of spatial geodetic network. A significant advantage of the application is to implement methods for automatic detection and exclusion of remote measurement, which is based on a robust analysis of geodetic measurements and statistical testing of residues.

Robust analysis is used for further calculation work (Helmert transformation) and allows direct and exact search demonstrable shifts e.g. when testing the stability of the reference points of the network.

Another unique tool is a sophisticated apriori analysis of measured quantities, which allows a detailed analysis of the input data before the actual alignment. To facilitate the work program supports the work with the projects outputs in the form of reports, graphical output, extensive options of calculation and export parameters.

By default, the program serves to compensate for spatial geodetic networks. In some cases, the height is not needed and exact measurement of the 3D network is uneconomical for logistical reasons. Measured data can be converted into the calculation plane, a disadvantage of this process is higher laboriousness data preparation and absence of analysis of measured zenith angles.

4.2 Stage processing - statistical evaluation of displacements

The outputs of the alignment of each stage are always the coordinates of points and covariance matrix describing the standard deviation of individual coordinates and their interdependencies (weights matrix and apriori or aposteriori unit standard deviation).

Standard deviation of displacements is determined by applying the law hoarding standard deviations, determined shift should always be assessed in terms of statistical detection threshold. Compared with a marginal shift for the chosen significance level used probability distribution is dependent on the choice of the unit when calculating the standard deviation covariance matrix (Normal or Student's distribution). More complex statistical evaluation in 2D and 3D is complicated (Helmert curve and surface), simplified solutions using confidence ellipses and ellipsoids is only an approximation, which is valid only under certain conditions. Development of statistical evaluation will be the subject of further work in this area. Now it is tested by Easynet Analyser, which is used for practical and user-friendly evaluation of stage displacements. When measuring and evaluating changes in points (deformation) is required to work with the covariance matrix characterizing completely precision of coordinates. Without this information cannot be properly assessed verifiability shift.

5. RESULTS

The method deformation measurements waterworks with ATR total station and the subsequent alignment of robust data in the form of a planar or spatial geodetic network was verified by testing as a suitable alternative to the existing methods. For each application, it is necessary to create a specific project of measurement that takes into account the configuration of measurement points, a range of location and used instruments.

We have tried to develop a comprehensive practical measurement procedure, which is to a large automatic, as well as computer processing in EasyNet. The

calculation is itself in danger of the incorrect choice of parameters that can devalue the quality of measurement. The combination of high levels of reliability, robust analysis and too height accuracy of measured quantities can cause the exclusion of a large number of measurements, which will be identified as outliers. Then for alignment can be exploited only a fraction of the measured data and accuracy after alignment may not correspond to the actual state of the network and the accuracy achieved will greatly overstated. The program addresses the robust alignment based on user-specified parameters and therefore it is necessary to take all steps to control the calculation and use of the available analysis and control mechanisms. Due to the complexity of an objective evaluation of geodetic measurements, it is necessary to draw attention to the need to evaluate the resultant displacements experienced expert in the field of alignment of geodetic networks, whose knowledge will assess everything in a broader context and determine the relevance of the outcome in relation to specific cases of geodetic measurements.

5.1 Measuring with ATR total station

For testing was used Leica TM30. ATR achieved accuracy is comparable with manually targeted, except for the very close targets, which can be manually focus more accurately (in relation to other residual measurement errors can be neglected, this fact). Speed measurements given used ATR and motorization with piezo servos, is very fast and reliable targeting under standard conditions perfect.

ATR targeting may complicate obstacles intentions, mostly vegetation. It is necessary intentions cleaned before measuring and inspected for sharpening the entire length of intentions. If this preparation ignored, may result from reduced angular accuracy, which is evident when comparing the selection of standard deviations and apriori accuracy of the machine.

Other options to reduce ATR accuracy is measured reflecting prisms pollution problems may be even drops of water or snow. In practice, this factor was apparent during measurements underground 100% humidity and a large temperature gradient when there is condensation on the face of prisms.

The last factor is the improper placement of reflective prisms. If there are multiple prisms close together, ATR cannot filter out interfering signals from surrounding prisms and targeting does not. This can be avoided by selecting the appropriate configuration points. By using the existing instrumentation, this situation occurs occasionally. A possible solution is to split the file into more contentious warps of directions so as to increase the required transverse distance between the prisms.

5.2 Alignment of geodetic network

Calculations were performed in Easynet 3.2.1 and 3.3.3. Much effort was spent selecting parameters for robust alignment. Calculations were performed for most locations in multiple variants in order to find the best solution in terms of accuracy

reached, use of the measured data and achieve fair precision aligned coordinates, which would correspond to the configuration of the network and equipment used.

Robust levelling regularly provide overvalued precision aligned coordinates, which is due to robust job analysis (excluding remote measurements with increasing precision alignment) and a large number of redundant measurement (due to processing individual values of all measured groups). If the main source of error in measuring the random deviations (normal distribution), the method of calculation in order. According to our experience, but measurements in multiple groups does not affect the systematic component of actual errors and therefore it is necessary in the qualitative evaluation of caution. In an effort to obtain relevant accuracy we are adjusted to compensate for the input data by averaging the measured groups or intentionally offended a priori accuracy of measured quantities. This adjusted compensation had already made adequate precision, the drawback is laborious data preparation, and their complications affecting the function of a robust analysis in case of intentionally degraded accuracy.

Tab 1. Results of alignment EasyNet – Kamenička dam

1. stage 2014, Leica TM30									
Point	X [m]	Y [m]	Z [m]	σ_x	σ_y	σ_z	σ_x	σ_y	σ_z
				apriori [mm]			aposteriori [mm]		
L	183,1253	0,0000	102,6349	0,18	0,11	0,09	0,15	0,09	0,07
P	0,0008	0,0000	99,9996	0,14	0,16	0,06	0,11	0,13	0,05
O1	11,8572	15,2909	96,8084	0,28	0,29	0,10	0,22	0,24	0,08
O2	8,0292	19,2350	100,5063	0,20	0,33	0,07	0,16	0,27	0,06
1	138,6683	4,9465	93,5753	0,44	0,08	0,14	0,35	0,07	0,11
2	112,1465	1,1136	93,5893	0,30	0,11	0,11	0,24	0,09	0,09
3	92,1274	-0,0351	93,5911	0,30	0,13	0,11	0,24	0,10	0,09
4	72,3605	1,4683	93,6033	0,30	0,13	0,10	0,24	0,11	0,08
5	55,2671	3,8398	93,5776	0,43	0,13	0,12	0,34	0,11	0,09
sample standard deviation			$\sigma_{x,y,z}$	0,30	0,18	0,10	0,24	0,15	0,08

The final option is robust alignment with all data, real apriori estimation accuracy (based on the accuracy of the machine, measurement the extent of the locality and the analysis of measured variables) and subsequent treatment of aposteriori accuracy of alignment correction coefficient which corresponds to our hypothesis about the actual accumulation of errors during polar measurements in rows and groups. Like a numerically correct version is the use of more stringent levels of significance in statistical evaluation of stage between displacements.

The advantage of a robust alignment will take effect if a file is infected coarse measurement data or systematic errors. In practice, it is often the influence of refraction, which is otherwise hardly recognizable. If sufficient homogeneity and accuracy of measured values is influence of robust analysis in alignment for the resulting coordinates and their accuracy small.

Tab 2. Parameters alignment EasyNet – Kamenička dam

option robust analysis:	Huber 1%	accuracy		used	internal	external
remote measurements	5/108	σ_j	[mgon]	0,20	0,16	-
horizontal angle	0/36	σ_z	[mgon]	0,20	0,17	0,74
zenith angle	5/36	σ_{s^*}	[mm]	0,80	0,07	0,06
slope distance	0/36	coordinate accuracy after network alignment:				
unit aposteriori error	0,805	σ_{xy}	[mm]	0,25	apriori	
redundant measurement:	78	σ_{xy}	[mm]	0,20	aposteriori	
empirical unit error	0,503	σ_{xy}	[mm]	0,35	final accuracy	
used unit error	0,577	σ_z	[mm]	0,14		

5.3 Calculation and statistical evaluation displacements, interpretation of results

For the monitoring displacements and deformations are the most important carrier of information being sought between the vectors of stage displacements ie. the change of position (in the plane or space) between the assessed stage and the previous or basic stage, which represents the initial state of the observed object.

The proposed method of calculation, it is assumed for each shift of weighted calculation of standard deviation shift and evaluate its detection threshold using tolerances. The procedure uses a balanced and coordinate appropriate covariance sub-matrix of individual points and can be applied in the plane and space. The statistical evaluation is possible to add a graphical representation of the network, including summaries of measurement error or confidence ellipses for documenting the accuracy of individual network points and balanced depiction of displacement vectors. Any verifiability of individual displacement vectors can be expressed eg. different color. This procedure is the subject of further work, practical applications being developed will allow extension application EasyNet (EasyNet Analyser), which in addition to the above-described steps in the processing of stage measurements will allow further statistical testing of balanced outcomes (eg. the stage length changes in the spatial geodetic network).

LEGEND:

Scale confidence ellipses: 1:5000
Scale vectors: 1:5000
Significance level of ellipses: 1%

— alignment EasyNet, stage 2013
— alignment EasyNet, stage 2014
— displacement vectors, EasyNet

Scale of confidence ellipses and vectors



0 2 4 6 8 10 mm

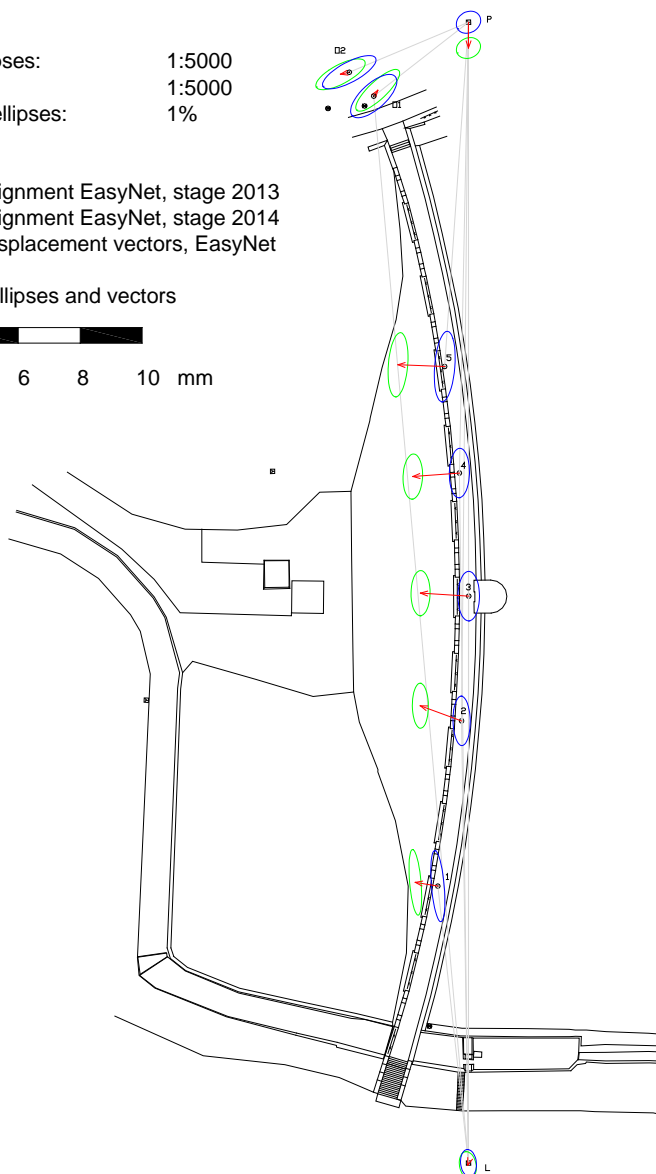


Fig. 2 Displacements with confidence ellipses, Kamenička dam

6. CONCLUSION

Scope of this paper does not permit a comprehensive evaluation of the solved problems. This is stated in a research report of the project CREA Hydro & Energy, and created a methodology for application of a test method in practice, mentioning concrete solutions to specific problems. The proposed method has proven itself and the process used i.e. The machine Leica TM30 for data acquisition using the ATR and the settlement program Easynet can be recommended.

Potential for further development is mainly achieved evaluation accuracy of points and "mezietapová" balanced analysis of the achieved displacements and their detection threshold. The proposed methodology can be modified for other jobs engineering geodesy, which foresee the precise measurement of total station with ATR-targeted (deformation measurements of buildings, crane rails, etc.).

7. REFERENCES

- HAMPACHER M., ŠTRONER M., 2011, Processing and analysis of measurements in civil engineering, Prague, Czech Technical University in Prague
- KRNÁČ V., MACHÁČEK T., 2015, Research methods for geodetic measurements, Brno, CREA Hydro&Energy, o.s.
- TŘASÁK P., 2013, Simulation, modeling and statistical processing of geodetic measurements, dissertation, Prague, Czech Technical University in Prague

Acknowledgement

Acknowledgement to doc. Ing. Martin Štroner Ph.D. and Ing. Pavel Třasák Ph.D. from the Department of Special Geodesy FSv CVUT in Prague with valuable consulting and software provide EasyNet to test the proposed method and to Ing. Pavel Dobrovolný and Bc. Jana B. Hejduková for cooperation in the development of methods and participation in experimental measurements.

The effect of flow regime on navigation near the Water Structure

A. Palkovičová

(Department of Hydraulic Engineering, Faculty of Civil Engineering, University of Technology in Bratislava, Radlinského 11, 810 05 Bratislava, Slovak Republic , e-mail: andrea.palkovicova@stuba.sk.)

Abstract

The article deals with analysis of the impact in operation mode of some water structures on the navigation. At the multipurpose water structures, some dynamic functions of a hydroelectric powerplant can endanger the safety of navigation. Therefore, it is important to know how to qualify and quantify the individual effects of the operation mode in the other functions of the water structure and then optimize the operation mode. A suitable tool for research and verification of the nautical conditions is particularly a simulation of a mathematical model or a physical model of an appropriate scale in the laboratory.

Keywords

Mathematical modelling the flow parameters, waterways, vector field of flow mode, movement of vessels, Hydraulic Structure Gabčíkovo.

1. INTRODUCTION

Water structures on navigable waterways improve the parameters of fairway at a higher level than the intervention to river by adjusting the regulatory type. By heaving a water level, it can increase the navigation depths, which are the key parameters of the fairway and in most cases even the width of the fairway and the radius of curvature. The result of better parameters of the fairway represents the transport capacity increase of the waterways. At the multipurpose water structures involving more objects than just a lock, hydroelectric power plant or weir, there appears the flow influence caused by the operation of these objects and the influence of routing of vessels by the forces of the flowing water. Optimal a safety movement of the vessels on the flowing water, as well as the navigation and controllability relates with the size of flow amount change at the operations of weir or hydroelectric power plant, the time course of this operation mode, slope level of water surface and direction of a moving vessel in the channel. The result of the adverse impact of the flow mode on vessels can be the collision with another vessel, the impact on the functional object of the water structure or the impact on the banks of waterway.

Currently, the research and verification of nautical conditions on navigable watercourse uses mainly mathematical modelling. For financial and time demands

of the laboratory hydraulic model research there are often chosen the methods of mathematical modelling. Mathematical model represents the idealization of actual physical system in a form of mathematical expressions which is mostly expressed in a form of partial differential equations in the engineering practice. By using the simulations, we can examine the response of the mathematical model to changes in input data and correct the operating parameters of the real water structures.

2. COMPLEXITY OF MOVEMENT OF VESSELS IN THE AFFECTED SECTION

Mainly at the derivation channels it is running short of a significant influencing of the navigation operation by the energy operation. The regulatory hydroelectric power plants which are being used to cover the electric system load influence at the most of the navigation. In these cases, it is needed by a research to determine the limit of the possible manipulation operation of hydroelectric power plant or propose some measures to allow align the interests of navigation operation and energy operation.

In terms of potential threats of safety navigation and transport capacity restrictions, the most critical area of is the stretch of transition from free tracks into the lock. The navigation width in this section is significantly limited. At the short section of the fairway, there narrows from the navigation width of open track to width of the lock. The vessel has to reduce its speed, which is the speed of floating vessel on the vacant track so that it would be able to slow down its movement to arrive into the lock or possibly would stop moving safety and completely at the area of lock cut when it is not possible to enter into the lock. At the same time the vessel cannot move with smaller speed than the value of minimum manoeuvring speed of this area. When a vessel reduces its speed and becomes less controllable, the force effect of water flow velocity field is most apparent on the vessel. Decisive is the influence of a mainly flow transverse components that act transversely to the direction of the vessel movement. The water flow pushes vessel away from the ideal route, giving rise the danger of already mentioned collisions (Fig.1).

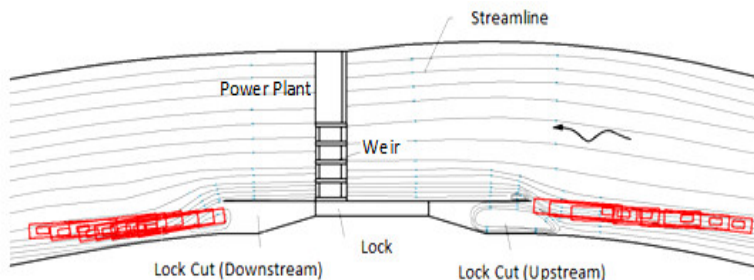


Fig. 1 The scheme of navigation level with the possible vessel path

A lock cuts have minimize the described complications of the vessels movement between the open track and the lock and negative impacts on the safety of navigation. Their primary function is to create conditions for a smooth and safe passage of vessels from open track water way to a confined space of the lock and in the opposite direction. Another important task of lock cut is to create a protected area for waiting vessels when the lock is occupied or the lock cut serves as protective or emergency dock.

3. MODELLING THE FLOW PARAMETERS AT THE HPPG

For the current situation at the international Danube waterway, it is important that the short stretch of a river passing throughout Slovakia ensures a sufficient maritime safety and transport capacity. The field of Hydroelectric Power plant Gabčíkovo (HPPG) operation impact on the navigation safety at the relevant section of River of Danube should be examined (Fig.2). The operation of the HPPG (without existing lower degree Nagymaros) works in continuous operation with level regulation. Continuous operation of the HPPG represents a uniform processing flow, which determines Hydroenergetic Dispatch Trenčín during 24 hours according to flow forecasts. Regulate operation is carried out under the "Conditions of the Regulatory Operation" and represents the using of Hrušov reservoir storage and upstream of derivation channel during the changes in the flow mode of the Danube. Mathematical modelling provides a useful tool to simulate the current operating conditions the HPPG.



Fig. 2 Hydraulic Structure Gabčíkovo

As a mathematical model, I chose freeware software 2D River which was developed at the University of Alberta. It is two-dimensional, depth averaged

hydrodynamic and fish habitat model developed specifically for use in natural streams and rivers. It is a Finite Element model, based on a conservative Petrov-Galerkin up-winding formulation. It features subcritical-supercritical and wet-dry area solution capabilities. Ice covers with variable thickness and discontinuous ice covers can be modelled. It has been verified through a number of comparisons with theoretical, experimental and field results (Ghanem et al, 1995a; Waddle et al, 1996, Christison et al). River 2D is a modelling system for modelling the water flow mode with free surface and allows to solute exactly the steady and unsteady two-dimensional turbulent flow of water in areas with a complex geometry. The theoretical basis provide three equations based on physical laws - the law of conservation of mass and momentum conservation law and the equations are expressed in the form of partial differential equations:

Conservation of mass:

$$\frac{\partial H}{\partial t} + \frac{\partial q_x}{\partial x} + \frac{\partial q_y}{\partial y} = 0 \quad (1)$$

Conservation of x-direction momentum:

$$\frac{\partial q_x}{\partial t} + \frac{\partial}{\partial x}(Uq_x) + \frac{\partial}{\partial y}(Vq_x) + \frac{g}{2} \frac{\partial}{\partial x} H^2 = gH(S_{0_x} - S_{f_x}) + \frac{1}{\rho} \left(\frac{\partial}{\partial x} (H\tau_{xx}) \right) + \frac{1}{\rho} \left(\frac{\partial}{\partial y} (H\tau_{xy}) \right) \quad (2)$$

Conservation of y-direction momentum:

$$\frac{\partial q_y}{\partial t} + \frac{\partial}{\partial x}(Uq_y) + \frac{\partial}{\partial y}(Vq_y) + \frac{g}{2} \frac{\partial}{\partial y} H^2 = gH(S_{0_y} - S_{f_y}) + \frac{1}{\rho} \left(\frac{\partial}{\partial x} (H\tau_{xy}) \right) + \frac{1}{\rho} \left(\frac{\partial}{\partial y} (H\tau_{yy}) \right) \quad (3)$$

where H is the depth of flow, U and V are the depth averaged velocities in the x a y coordinate direction respectively, q_x and q_y are the respective discharge intensities, g is the acceleration due to gravity, ρ is the density of water, S_{0x} and S_{0y} are the bed slopes in the x and y directions, S_{fx} and S_{fy} are the corresponding friction slopes and τ_{xx} , τ_{xy} , τ_{yx} and τ_{yy} are the components of the horizontal turbulent stress tensor.

3.1 Method of mathematical modelling

The River 2D software consists of four modules: R2D_Bed - initial topography, R2D_Mesh - generate computing grid, R2D_Ice - ice cover model and River2D - simulation according to specified boundary and initial conditions. The areas examined by this software represent approximately three kilometres section of the upstream channel just above the VEG and approx. two km stretch of downstream channel just below VEG. The basis for the formation of the mathematical model was the geometry of the channel (Fig.3) in the transverse and longitudinal directions and measurement of flow and level for the flow, which formed the model boundary conditions.

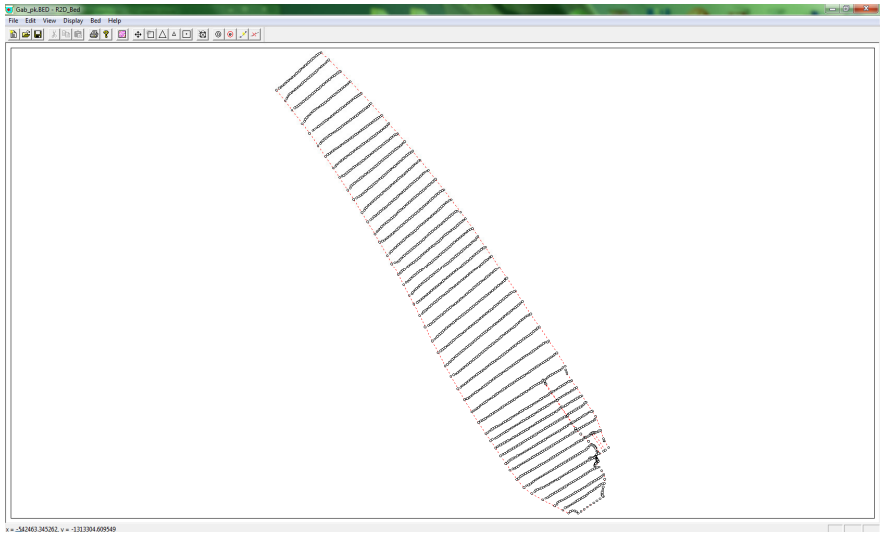


Fig. 3 The geometry of the channel above HPPG with the external border of the solving area

The most important output of the mathematical model simulating of spatial flow close the water structures with navigation mode is the flow velocity field. When water is flowing in the study area the complex current circumstances appears, that are being measured with a lot of difficulties on the physical moths - the direction of the velocity vector can be only estimated. The results of simulations of a mathematical model can be viewed by contours, colour range, or as vectors. More accurate results can be achieved by thickening the local grid, but this significantly extends the computation time (Fig.4).

Figure 5 shows the flow rate of the model area above the HPPG at a flow rate $3400 \text{ m}^3 \cdot \text{s}^{-1}$ with detail the inlet to the upper lock cut. Figure 6 shows the direction of the vectors which twister directly to separating wall. Downstream movement of vessels while the velocity is reducing could be influenced towards the separating wall. The flow simulation is carried out under the conditions of non-perforated separating wall at the upstream lock cut. Figure 7 shows the final vector field of flow mode at the area below the HPPG for a discharge $3400 \text{ m}^3 \cdot \text{s}^{-1}$. It is visible that there is a twisting stream of flow before the entrance to the lower lock cut and thus vessels would be affected by a force action of this stream of flowing water.

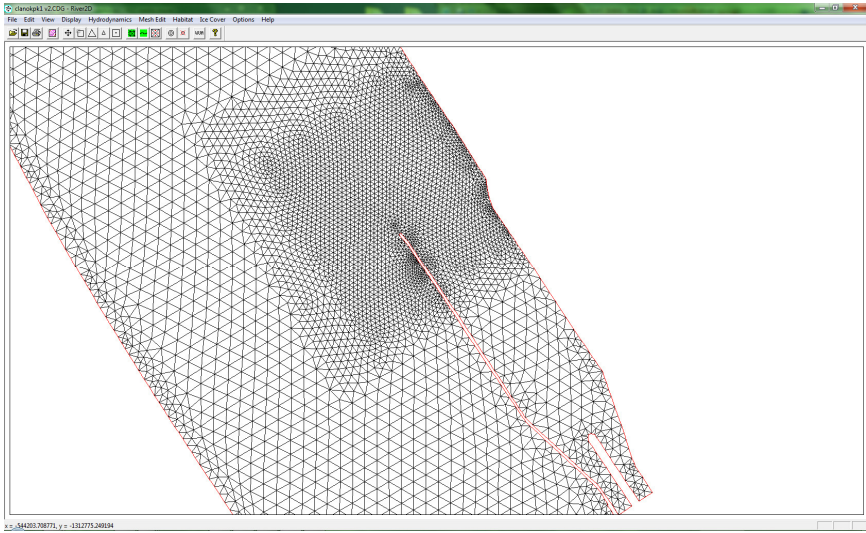


Fig. 4 Grid in the channel above the HPPG with local thickening of grid

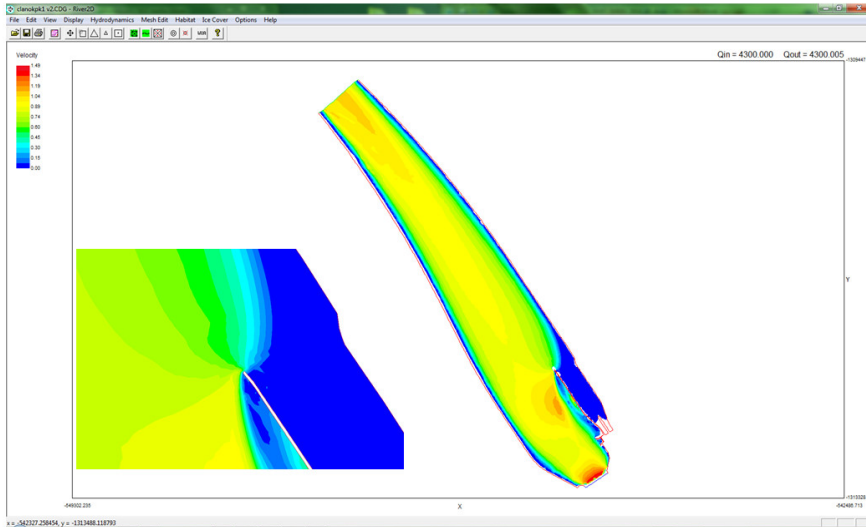


Fig. 5 Flow velocities visualised by colour scale

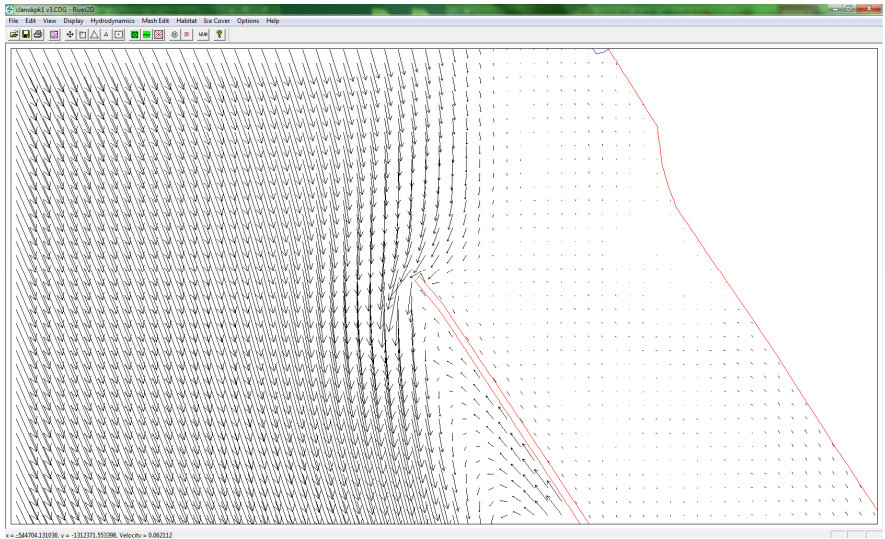


Fig. 6 Vector field of the flow, inflow to the upper lock cut

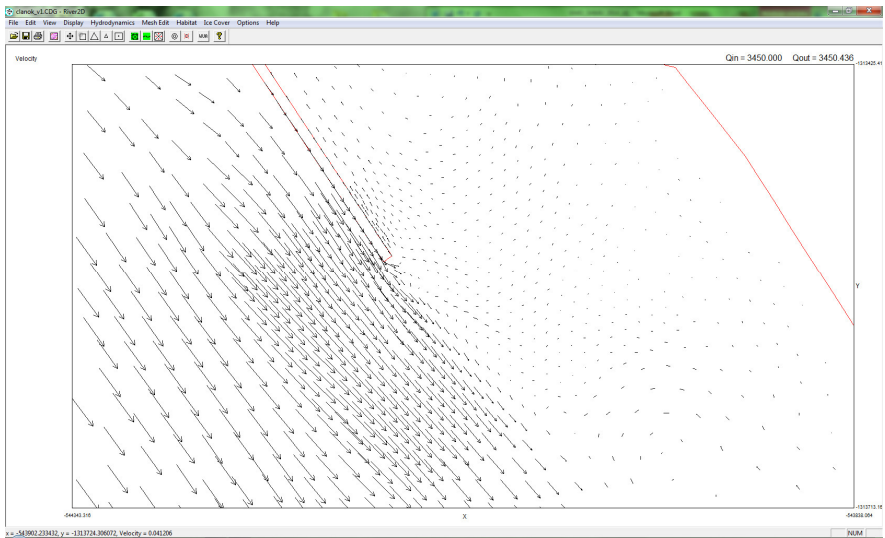


Fig. 7 Vector field of the flow, inflow to the down lock out

4. CONCLUSION

The operation of hydraulic objects of the water structures leads to affecting the navigation conditions. Safe movement of vessels on the waterway - their ability to manoeuvre is related to the direction, orientation and size of the velocity vector flow, water level slope and the time course of these parameters. The experiences of navigation point to the fact that the influence of flow mode to the trajectory of vessel movement is expressed in the immediate vicinity of the lock and lock cuts. Especially downstream vessels are at greater risk of the loss of manoeuvre ability when they are slowing down their speed and the threat of risk collision is there. By constructing the mathematical model and simulations themselves at different flow regimes hydroelectric power plants the parameters of flow velocity field near the lock cuts are identified. On the basis of assessing the operation of hydraulic structures for navigation safety, it is possible to form the measures to minimize negative impacts or even eliminate them. And thus find the optimal parameters of operation of hydroelectric power plant so dynamic functions of this power plant in the energy system would not be disrupted while the safety of the navigability is not limited by the regulatory of the power plant operation.

5. REFERENCES

- BLACKBURN, J., STEFFLER, P. 2007. *River2D, Two-Dimensional Depth Averaged Model of River Hydrodynamics and Fish Habitat, River2D Tutorial – The Basics*, Alberta: University of Alberta.
- KUTIŠ, V. 2006. *Basic of Modelling and Simulations*. Bratislava: Institute of Computer Science and Mathematics, Faculty of Electrical Engineering and Information Technology STU in Bratislava.
- MOŽIEŠIK, E., ČEPCOVÁ, Z. 2009. *Conflict Situations in Operation Mode of Waterworks*. Bratislava: The ESF Project of Hydroinformatics in Bratislava.
- MOŽIEŠIK, E. 2010. *Flow Limits of Changes Through the Degree Gabčíkovo Regarding to Sefeness of Navigation on the Danube*. Bratislava: International Scientific Conference on Safety of Hydraulic Structures.
- MOŽIEŠIK, E. 2012. *Lock Cuts on Navigable Waterways*. Monograph. Bratislava: Faculty of Civil Engineering STU in Bratislava.
- MOŽIEŠIK, E., VALENTA, P., ŠULEK, P., SLABÁ, V. 2002. *Modelling of Flow Mode and Vessels Movement in Areas of Waterworks*. Piešťany: Conference of Navigation Days.
- MOŽIEŠIK, E. 2003. *The Interaction of the Operation of the Waterworks and Navigation*. Edition of the Scientific Works, Book num.14. Bratislava: Faculty of Civil Engineering STU in Bratislava.
- MOŽIEŠIK, E. 2008. *Water Management Model of Hydraulic Structure Gabčíkovo Operation Mode*. Final Report. Bratislava: Faculty of Civil Engineering STU in Bratislava.

- PALKOVIČOVÁ, A., KVĚTON, R., MOŽIEŠIK, Ľ. 2013. *Mathematical Modelling of Extreme Changes in Flow Mode to the Waterwork Gabčíkovo*. Bratislava: 13th International Symposium on Water Management and Hydraulic Engineering.
- PALKOVIČOVÁ, A. 2012. *The Effect of Shoutdown of the Hydroelectric Powerplant Gabčíkovo on the Water Level and Flow Mode of the Danube with Respect to Navigation*. Bratislava: Diploma thesis. Faculty of Civil Engineering STU in Bratislava.
- PALKOVIČOVÁ, A. 2012. *The Research in the Development Program of the Waterways in Slovakia*. Bratislava: 12th Conference of Young Water managers. SHMU in Bratislava.
2010. *The Temporary Manipulation Order for Hydroenergy Project G-N in the Slovak Republic, updating VIII*. Retrieved form http://www.gabcikovo.gov.sk/SVD_G-N.h.

Acknowledgement

This article was created with the support of the Grant Agency VEGA, number 1/0660/12.

Kolárovo Water Structure - selected results of the hydraulic research

Možiešik, L., Orfánus, M., Rumann, J., Šulek, P., Dušička, P.

(Department of Hydraulic Engineering, Faculty of Civil Engineering, University of Technology in Bratislava, Radlinského 11, 810 05 Bratislava, Slovak Republic , e-mail: ludovit.moziestik@stuba.sk, martin.orfanus@stuba.sk, jan.rumann@stuba.sk, peter.sulek@stuba.sk, peter.dusicka@stuba.sk)

Abstract

Department of Hydraulic Engineering, Faculty of the Slovak Technical University in Bratislava held since 2013 an extensive model research, which was part of the preparation of the implementation of Water Structure Kolárovo (WSKo) on the River Váh. The article presents selected results of research on the optimization of the WSKo design with regard to navigation safety and transport capacity of WSKo objects. The article is based on the issues and content of an article [Možiešik, Šulek, Orfánus, 2012].

Keywords

Navigation, hydraulic research, mathematical modelling, physical modelling.

1. INTRODUCTION

River Váh is the largest national Slovak river (the whole river is located at the territory of the SR), which has at the network of waterways of European importance label E81. WSKo is a precondition of navigability of the lower section of Vah in Komárno (junction with the Danube River) - Sereď (rkm about 80). The situation with the development of water projects is in Fig. 1- red marked, which are in the stage of preparation for construction, and black marked as existing water structures in full operation. Information about the wider context concerning the navigability of the lower Váh are given in [Možiešik, Šulek, Orfánus, 2012], in the following text will be information on the research.

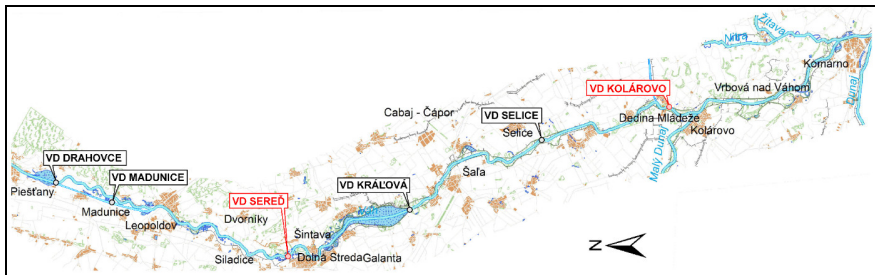


Fig. 1 Situation of the lower Váh River, section Piešťany – Komárno

2. AIM AND CONTENT OF THE RESEARCH

Research must propose the water structure project, which

1. Ensure adequate parameters of the navigation corridor between water structure Selice (VSSe) and WSKo in accordance with the relevant international regulations for class VIa waterways.
2. Till realization of the lower degree of the Gabčíkovo - Nagymaros Water Structure (SVD GN) will support the assurance the Danube navigable depth at the min. 2,8 meters with a minimum navigable discharge, after the realization of the lower degree of of the Gabčíkovo - Nagymaros Water Structure of the depth min. 3,8 m.
3. WSKo will satisfy the requirements for safe and sufficient capacity for the navigation operations for all large vessels up to a size of convoy type consisting of two vessels type DE IIa and tug. VSKO will ensure safe crossings of the small vessels, self-propelled boats.
4. VSKO will be designed so as to fulfill the engineering, environmental and energy requirements.
5. Weir will be designed to be able to regulate the level and discharge in the range of navigation limits. At discharges higher than max. navigable the waterway will be disrupted and the weir will adjust its operation of water flow needs. With a view to minimizing the costs of constructing the WSKo will be at flood flows overflowed without decreasing the capacity of the profile.

On the basis of these objectives has been identified methodology of research - a means to achieve the objectives were simulations of water flow on physical model and mathematical models of flow.

The research consisted mainly of the following components:

1. Proposal of WSKo location.
2. Measurement and surveying for calibration purposes in situ.
3. Construction of digital terrain models of Váh river bed in the current and planned state, modeling of water flow in the segment of Váh at section VDSe - Komarno on 1D mathematical model of flow (HEC-RAS) to identify the level regime.
4. Construction of the physical model of the input proposal in hydraulic laboratory and creating a mathematical model geometry of the input proposal for two-dimensional and three-dimensional modeling.
5. Measurement and evaluation of flow parameters (velocity and direction) in area of the WSKo in the range of navigation discharges and water levels in conditions of proposed design at the physical model.
6. Calibration of 2D and 3D mathematical models of water flow based on the measurements provided at the physical model according the 3.

7. Measurement and evaluation of flow parameters (velocity and direction) in area of the WSKo in the range of navigation discharges and water levels in conditions of proposed design at the mathematical model.
8. Evaluation of the impact of flow on nautical conditions and the navigation security of the proposed design of the WSKo at the physical model.
9. Evaluation of the impact of flow on nautical conditions and the navigation security of the proposed design of the WSKo at the mathematical model.
10. Correction of the proposed design geometry parameters and layout of the structure and its objects based on the results of the evaluation according to points 8 and 9.
11. Cyclic repetition of "mathematical simulation and evaluation of flow parameters - assess the impact on the flow of nautical terms - correction of prior design parameters and layout of the structure" to identify the optimal solution.

Verify the final design completed under the point 11 on the physical model.

VSKO will forms the objects for water management, navigation and power operation - the weir, shiplocks, hydroelectric power, fish passage and the object for small and sport boats.

3. PHYSICAL AND MATHEMATICAL MODELS

Physical model parameters were adjusted to the size of objects (eg. A ship lock has interior dimensions 120x24 m), discharge range of navigation (10 – 460 m³/s) and the parameters of the waterway (corridor width of min. 80 m). Given the nature of research and the proposal itself of WSKo is the physical model designed within the Froude criterion of model similarity, the model is built in geometry scale 1:50. The project is in Fig. 2 and the construction of the model is shown in Fig. 3. Ground plan dimensions of the model are 45x15 meters.

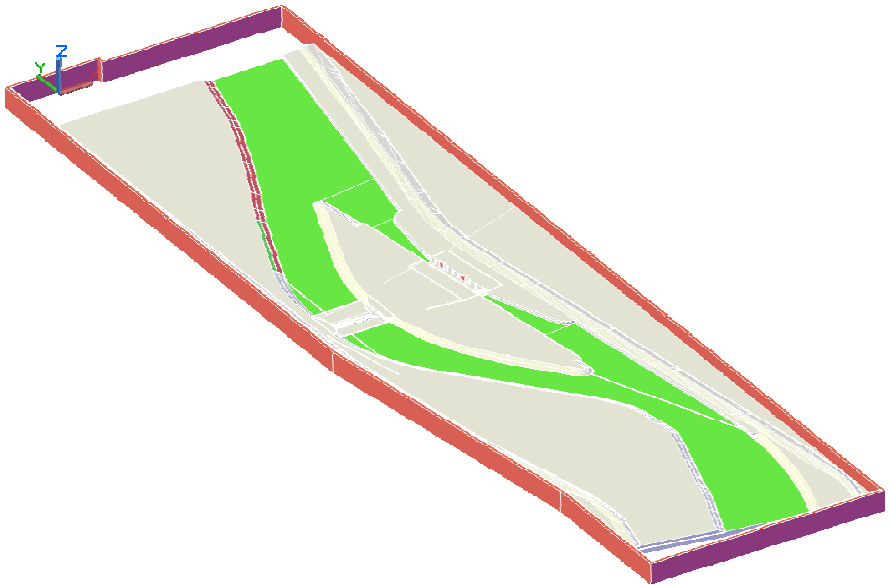


Fig. 2 3D visualisation of the physical model geometry



Fig. 3 Physical model construction

In mathematical modeling were applied software packages such as HEC-RAS (1D), River2D, mike21 (2D) and FLOW3D (3D). During calibration, the model followed by the first 1D has been calibrated on the present state of the field-work. Thus established roughness parameters were used for 1D model of the planned state trough following modifications of the river bed. 1D simulation and

measurement of the input physical model were then used to define the boundary and initial conditions for 2D and 3D simulations.

4. MEASUREMENTS AND SIMULATIONS

The criterion for assessing the safety of the vessels, the parameters of flow velocity field in the entrance area to the ship lock approach of the ship lock (the PLK). Especially important are the parameters of velocity vectors at the entrance to the upper approach - there is the influence of transverse components of velocity as the most dangerous for floating vessels, it can cause deflection of the vessel from the safe corridor followed by collision. Therefore, the optimization goal was the minimization of the components of velocity vectors, especially cross.

Measurements and simulations were carried out especially for the most unfavorable conditions for navigation vessels - at max. navigable discharge velocity measuring device was used by an American company FlowTracker® SONTEK / YSI, Inc. After measuring the velocity field of the flow parameters and their evaluation for physical models the corrections of layout design were carried out. The impact of these corrections was examined by simulations on 2D and 3D models of flow and subsequently verified by physical model. On mathematical models were tested dozens of variants and recommended modifications were verified on a physical model.

5. CORRECTIONS AND MODIFICATION OF THE INPUT PROPOSAL OF WSKO

After measuring of the input proposal of WSKo, it was stated that the lower approach is for shipping safe enough even at max. navigable discharge as transverse components of the flow are less than 0,3 m/s (spot max. 0,21 m/s), longitudinally max. 2,2 m/s. Therefore, in the lower approach no other modifications were needed.

At the upstream side of WSKo were modifications necessary because the flow parameters exceeding recommended limits.

During the optimization process of the WSKo proposed layout were step by step modified following features:

1. modification of left river bank of the Váh River in upper approach (2 modifications),
2. shape of the dividing island between the weir and ship lock,
3. shape of the island at the tributary of the shifting of the Nitra River.

Modifications and corrections are shown on Fig. 4.

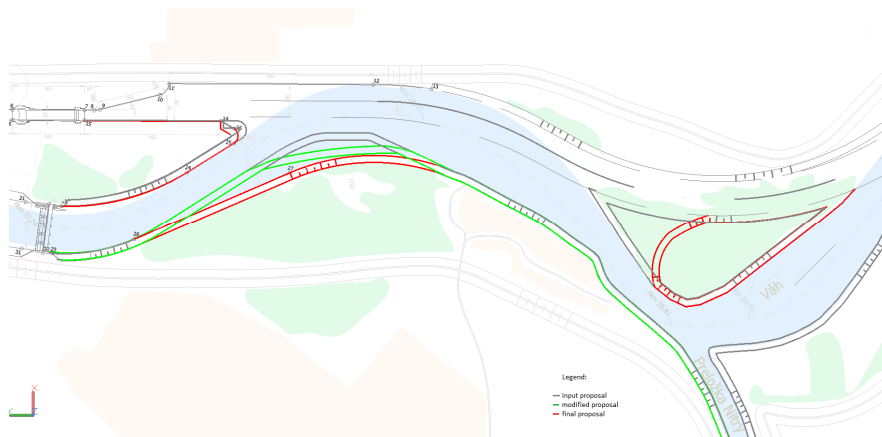


Fig. 4 Modifications and corrections of the input proposal of the WSKo

On physical model the parameters were measured for the input design, for design modification to the first line of the left bank of the Váh River and definitive adaptation of the model through the further correction line of the left bank, modified gridiron shape of the dividing island between the weir and ship lock and shape of the island at the tributary of the shifting of the Nitra River.

On mathematical models were seeking optimal line of the left bank, the shape of the dividing island between the weir and ship lock (tens of shape) and the shape of the island at the tributary of the shifting of the Nitra River (about 10 shapes).

Optimization criterion was minimization of the operating parameters of the flow vectors. The following figures documented results of measurements and simulations.

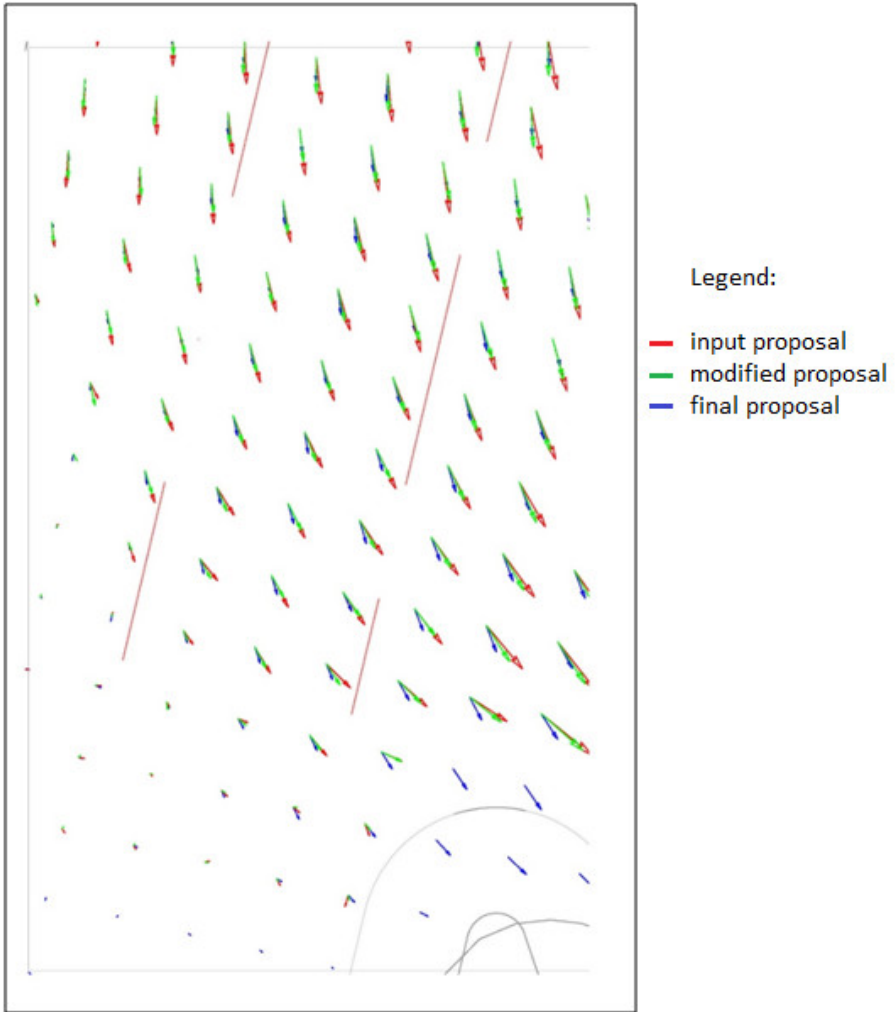


Fig. 5 The results of measurements on the physical model input, modified and final proposals layout

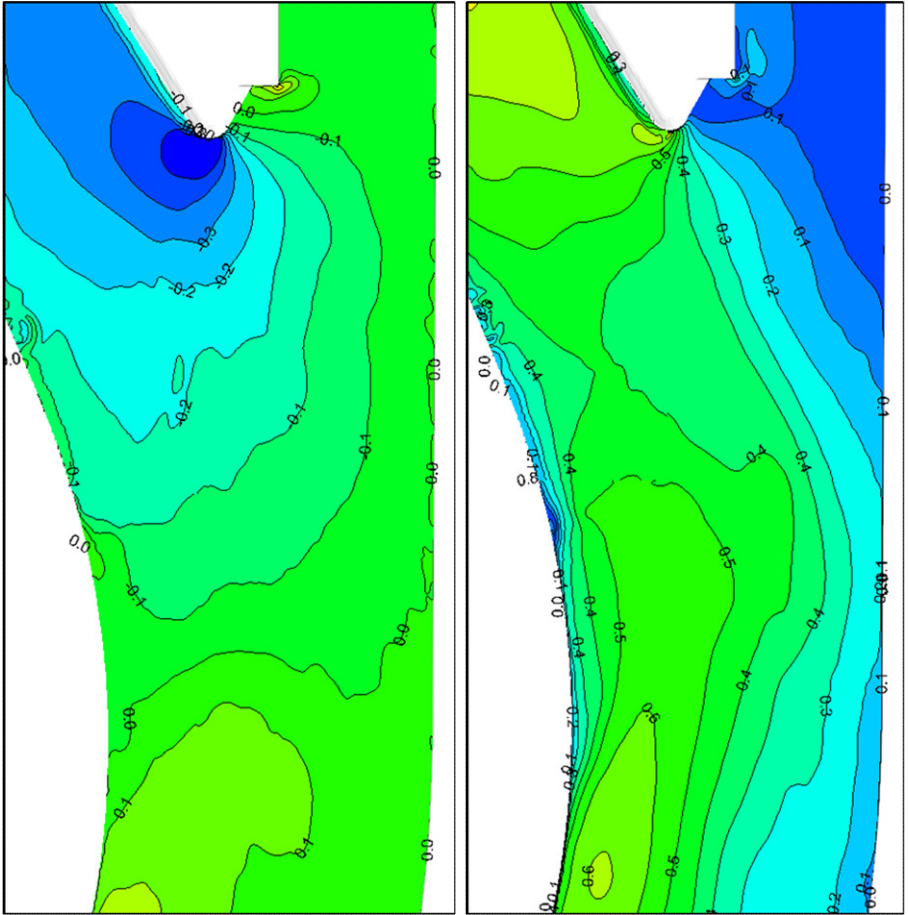


Fig. 6 The transverse component of the velocity and overall velocity model visualization of the shorter shape of the dividing island between the weir and ship lock at a depth of half of the maximum draft (3D model) - an example of simulation in finding optima

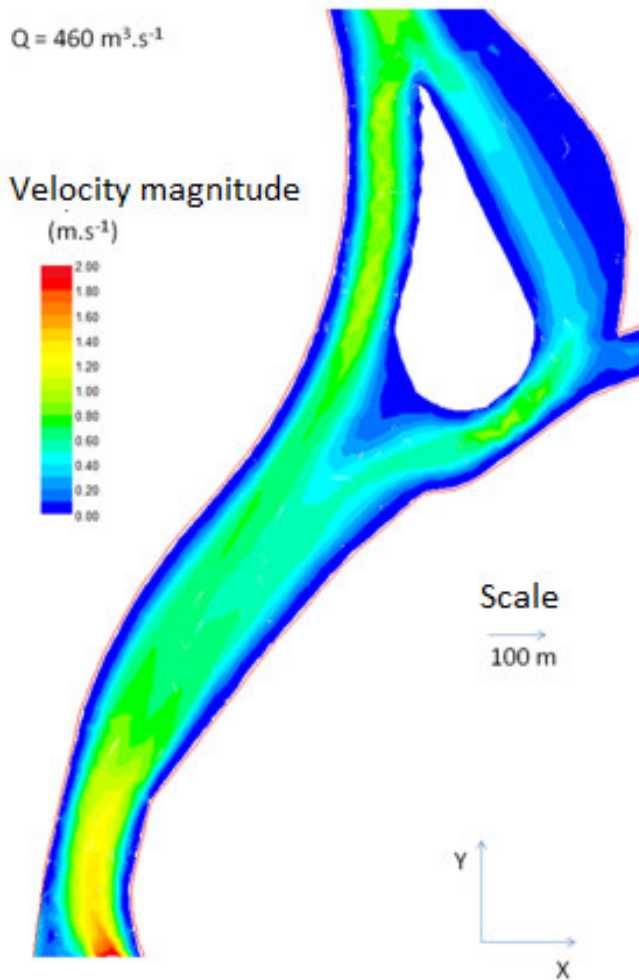


Fig. 7 Simulation to find the shape of the island at the tributary of the shifting of the Nitra River

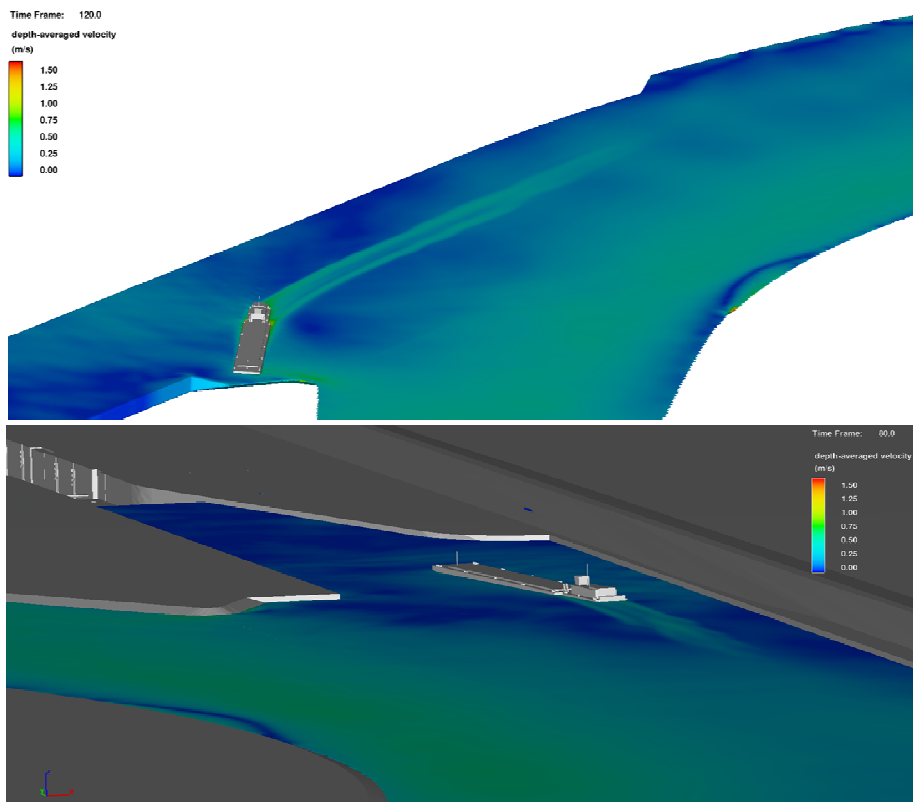


Fig. 8 Examples of simulations of the vessel trajectory (Flow 3D)

6. CONCLUSION

This article describes the implementation of hydraulic modeling research performance and some results of the research concerning in particular the navigation aspects of the Water Structure Kolárovo operation.

Research has optimized layout of WSKo particularly with regard to navigation safety and transport capacity. Gradually it managed to eliminate the effect of channel parameters of the waterway and its other components, so that flowing water with its parameters are safe and the navigation is not compromised in its entirety navigational flow limits.

The resulting design of WSKo is shown in Fig. 9.

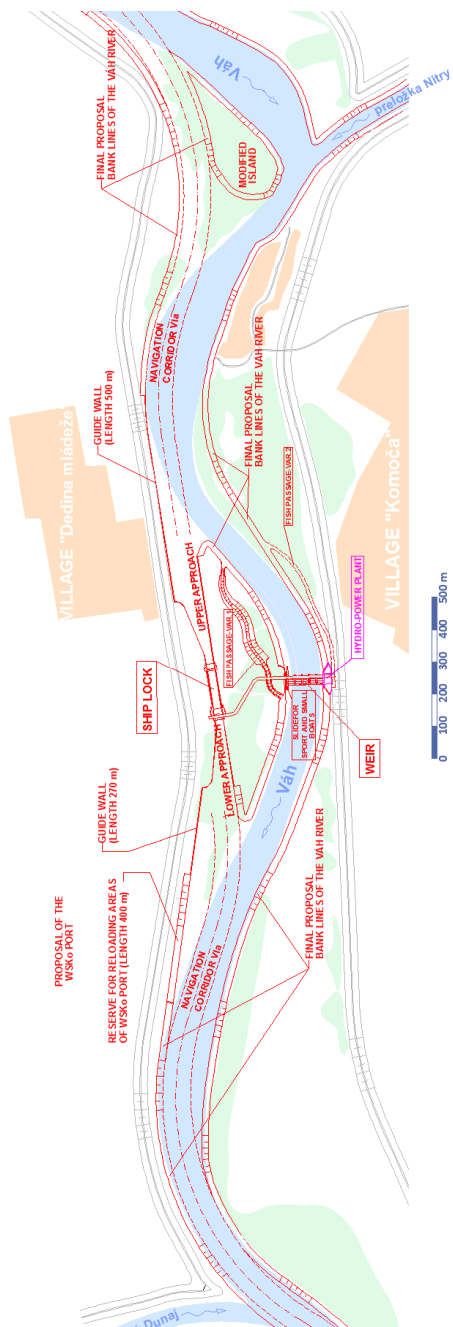


Fig. 9 The situation of resulting design of WSKo

7. REFERENCES

- FLOWSCIENCE, INC. 2011. Flow 3D v10 Users manual. Santa Fe : Flow Science Inc, 2011.
- GABRIEL, P., LIBÝ, J., FOŠUMPAUR, P., 2008. Hydraulický výzkum vodního díla Děčín. Praha. ISBN 978-80-85900-85-9.
- MOŽIEŠIK, L., DUŠIČKA, P., ŠULEK, P., ORFÁNUS, M., RUMANN, J., 2013. Modelový výskum dispozičného riešenia vodného diela Kolárovo na Váhu s ohľadom na nautické podmienky a podmienky plavebnej bezpečnosti. Správa z výskumu. Bratislava.
- MOŽIEŠIK, L., ŠULEK, P., ORFÁNUS, M., 2013. Kolárovo water structure – preparation of the research and design proposals. Water management and hydraulic engineering - thirteen international symposium, Book abstracts. Bratislava.
- MOŽIEŠIK, L., ŠULEK, P., ORFÁNUS, M., 2012. Výskum prípravy, projektu a realizácie plavebného stupňa vodného diela Kolárovo na Váhu: Záverečná práca.
- MOŽIEŠIK, L., 2012. Rejdy plavebných komôr na splavných vodných tokoch. STU Bratislava. ISBN 978-80-227-3847-7.

Acknowledgement

This article was created with the support of the Grant Agency VEGA, number 1/0660/12.

Monitoring of the embankment dam and effectiveness of remedial measures by EIS method

J. Parilkova, I. Pavlik, M. Novak, J. Vesely

(Brno University of Technology, Faculty of Civil Engineering, Veveri 331/95, 602 00 Brno, Czech Republic, parilkova.j@fce.vutbr.cz,

GEOtest, Inc., Šmahova 1244/112, 627 00 Brno, Czech Republic, ivo.pavlik@geotest.cz,

ENVICONS, s.r.o., Hradecká 569, 533 52 Pardubice – Polabiny, Czech Republic,
michael.novak@envicons.cz,

Brno University of Technology, Faculty of Civil Engineering, Veveri 331/95, 602 00 Brno, Czech Republic, vesely.j@fce.vutbr.cz.)

Abstract

This paper summarizes the monitoring of embankment dam near the village Jevíčko, which was built as a new structure. At the time of construction, there were problems with locally increased soil moisture and a different level of compaction. Based on the tests and inspections, it was decided to continuously monitor the embankment dam. On the dam, which is shaped like the letter "L", were designed four monitoring profiles. To monitor the changes occurring in the soil as a result of water loading of dam indirect method of measuring electrical impedance spectrometry was chosen. Measurements were performed using special measuring apparatus developed and implemented in the Laboratory of Water Management Research Department of Water Structures FCE, BUT as result of solution applied research projects of the international program EUREKA. After remediation of detected trouble sites was determined her efficiency.

Keywords

embankment dam, fault, monitoring, electrical impedance spectrometry

1. INTRODUCTION

For the needs of the Czech Anglers' Union seated in the municipality of Jevíčko, (the owner of the structure), a pond has been constructed at a selected site near the above-mentioned municipality (Fig. 1). The fishpond is located at the exit towards the municipality of Krenov. The site is part of the hydrogeological zone "Boskovice Furrow", which is a narrow, asymmetrical, tectonically predisposed depression between the Bohemian-Moravian Highland and the Brno Massif. It is filled by Permo-Carboniferous sediments of large thickness, which are locally covered by sediments of Cretaceous, Neogene and Quaternary age [Slavik, 2005]. Soils of the Quaternary cover are represented predominantly by clayey loams of deluviofluvial origin. Not far from the newly constructed fishpond, there is the spring area "Pod Zadnim Arnostovem", which is used for supplying drinking water to the town of Jevicko. According to the opinion of the hydrogeologist

RNDr. Josef Slavik, dated 14 March 2005, the operation of the structure, i.e. fish farming, with all accompanying processes (fishpond fertilisation, fish feeding) will have no adverse, qualitative or quantitative effect on the given water resource.

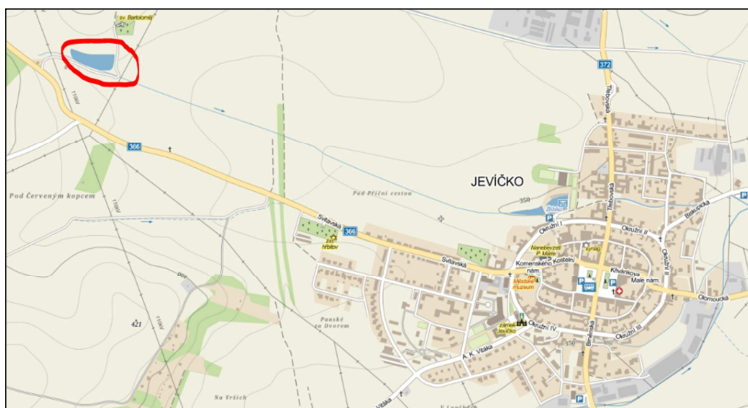


Fig. 1 Layout of the municipality of Jevíčko and marking the fishpond (public base maps)

1.1 Description of the embankment dam

The embankment dam of the fishpond is constructed homogeneous earthfill of the shape of the letter “L” with upstream slope being 1:3 and downstream slope being 1:2. The planned width of the dam crest was 2,5 m, but due to the modifications made it differs locally. The length of the dam crest is 150 m. The elevation of the dam crest is 380,50 m a. s. l. (above sea level) and the maximum height of the dam above the valley bottom is 2 m. The upstream slope is lined with 2,5 m coarse riprap where the water surslope touches the slope along the length of the slope. After lining, the downstream slope of the dam, the crest and the upstream slope are spread with topsoil and planted with grass. Topsoil and subsoil 30 cm thick were removed from the area of the basement of the earth-fill dam [Project documentation, 2005].

The water area of the fishpond is 0,56 ha and the volume of water is 7,800 m³, the bottom lies chiefly at the level of the original terrain. The water level determined by the upper edge of the plank wall in the gullet (monk) is determined at an elevation of 380,00 m a. s. l. [Project documentation, 2005]. The fishpond has other usual facilities such as emergency spillway etc.

The dam was built of soil excavated from the bottom of the constructed fishpond. During the construction of the earth-fill dam, which took place at two stages, there were problems with compaction and moisture of the soil. Check tests of the compaction of the dam body were carried out at the end of each stage. The results were given in [Pařilková and Pavlík, 2010]. Because of the concerns about the impact of technological indiscipline (primarily the dam reach between profiles

2 and 3), it was decided to start monitoring of the dam body in four profiles (Fig. 2). Using electrical impedance spectrometry (EIS) was measured electrical impedance, especially electrical conductance which corresponds with water content in the soil and from geotechnical parameters it was especially granulometry, plasticity and compaction of the soil.

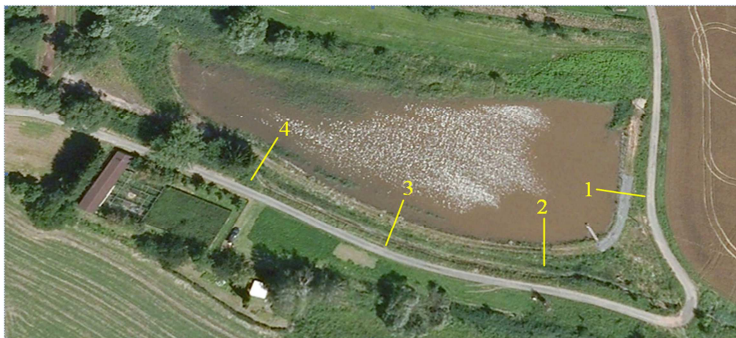


Fig. 2 Location of the monitoring profiles (public base maps)

The first profile lies in the centre of the front part of the dam. Here, the dam is formed by sandy loam of Class F4 CS. This soil is very suitable for homogeneous dams by ČSN 75 2410 – “Small Water Reservoirs”. With regard to the satisfactory results of tests of compaction of the dam body, we did not expect dam leaks here, which should also be proved by measurement on probes in this area.

The second profile has been determined in the place where the dam is formed from sandy loam of Class F3 MS – F4 CS. This soil is also very suitable for homogeneous dams. However, here, check tests have identified insufficient compaction of the dam body. Because of that the monitoring system EIS was installed here.

The third profile is located to the middle of longer line "L" letter. Here, the surface layer of the dam is formed by clayey loam with high plasticity of Class F7 MH, which is little suitable for a homogeneous dam. Here, the check tests of compaction were satisfactory. The measurement of moisture verified what effect the little suitable clayey loam has on the dam permeability.

The last, **fourth profile** is located at the end part of the dam. Here, in its upper part the dam is formed by very suitable sandy loam of Class F4 CS. In the first stage of the dam construction, insufficient compaction of the dam body was detected here. The monitoring of this profile verified whether the remedial measures (re-compaction of the soil, change of the dam body height) were properly made and if there are leaks of water in the lower levels of the dam.

2. MONITORING METHODS AND PROBES

When studying soil-fluid systems, electrical impedance spectrometry (EIS) can give accurate, error-free kinetic and mechanistic information using a variety of techniques and output formats. For this reason, EIS is becoming a powerful tool in the study of soil environment with different degree of water saturation. In principle electrical impedance is measured which is the basic property characterizing electrical alternating-current circuits. Electrical impedance is always higher than or equal to the real electrical resistance R in the circuit. Apparent resistances, i.e. inductance – the reactance X_L of an inductor and capacitance – the reactance X_C of a capacitor, form the variable and thus frequency-dependent part of electrical impedance. Electrical impedance, therefore, is composed of the real and imaginary parts. The real part is formed by the resistance R , which is frequency-independent. The imaginary part is formed by the reactance X , which is frequency-dependent. Electrical impedance \mathbf{Z} can be expressed using the Ohm relation for alternating-current circuits, i.e. the relation between the phasor of electrical voltage \mathbf{U} and the phasor of electrical current \mathbf{I}

$$\mathbf{Z} = \frac{\mathbf{U}}{\mathbf{I}}. \quad (1)$$

The frequency characteristic of electrical impedance \mathbf{Z} can be expressed as a function of a complex variable in the algebraic (component) form

$$\mathbf{Z} = R + jX. \quad (2)$$

Other electrical parameters, which can be calculated from both measured parts, is possible to find in [Callegaro, 2012, Kanoun, 2011]. In this paper some results through electrical conductivity G (the inverse parameter to the resistance R) are shown, this parameter corresponds with water content of the soil, and through susceptance B , which can characterize consolidation of the soil, granulometry and other [Novák, 2012, Gardavská, 2014]. Both parameters are included in electrical admittance (inverse parameter to electrical impedance)

$$\mathbf{Y} = G + jB. \quad (3)$$

Because EIS is indirect monitoring method, always must be done calibration of the electrical parameter to the parameter which describes studied environment or process. This way is sometimes very long and data interpretation can do only people with qualification. Therefore is possible also other view – in context of the problems to see the relative changes of measured parameters.

EIS techniques developed through the project within the EUREKA program is very modular [Radkovský, 2014, Pařílková and Radkovský, 2011, Pařílková and Stoklásek, 2008]. It is possible to change monitoring frequency (detection of environment characteristics), excitation amplitude of the signal (sensitivity, reduction errors caused by the measurement technique), but also number of sensors (geometry of monitoring).

2.1 Probes

From the physical point of view, the probes of the EIS method can be characterised as passive sensors that change their characteristic property under the action of the measured variable. Change in the property is thus a degree of the value of the measured non-electrical variable. In terms of connection, a two-terminal connection was used in measurement, while adhering to the principle of the close contact of the probe sensor with the surrounding medium. Two-terminal connection does not eliminate the effect of voltage loss on the resistance of the supply cables and on the contact resistance between the sensors and the measured medium. It is, however, sufficiently sensitive and accurate for changes in observed electrical impedance.

The probes are mounted on the upstream and downstream slopes of the embankment dam of the fishpond, currently about 0,5 m below the edge of its crest. The measuring probe is formed by two tubes fitted with 7 passive sensors. Conductive material (a measuring electrode) alternates with non-conductive material (an insulant) in lengths $d = 0,15$ m regularly. The measuring electrodes are made of stainless tubes with walls 0,002 m thick and with an outer diameter of 0,025 m; a polyamide tube of the same parameters was used as an insulant. The total length of the probes is $h = 2,0$ m. The spacing between the electrode tubes is $L = 2,0$ m.

Conductors ensuring the transmission of the exciting signal (electric current) and the measuring signal (electric voltage) are conveyed through the centre of the tubes to the individual measuring electrodes. To avoid the penetration of moisture to the area of conductors (parasitic electrical resistance), the individual parts of the probe are connected with a silicone non-conductive sealing material which also seals the probes in their surface layer. The conductors are fitted with labels and terminated with a connector.

2.2 Evaluation of measurement

At each monitoring profile on the dam of the fishpond at Jevicko, two probes are always installed (Fig. 3). One probe, with rods labelled 1 and 2, is on the downstream slope of the dam, and the other probe, with rods labelled 3 and 4, is located at the opposite level on the downstream slope of the dam.

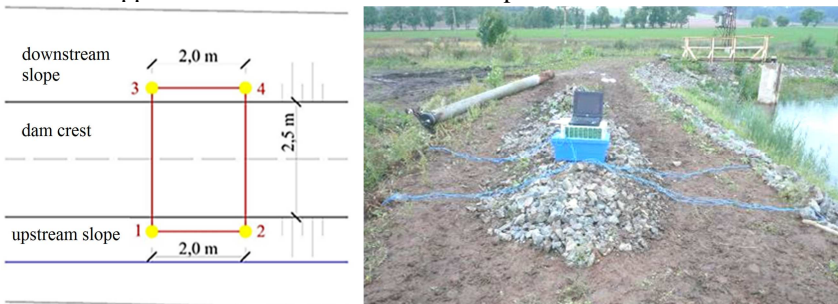


Fig. 3 Position of the probes in profile, monitoring scheme and situation

3. RESULTS

The installation of probes and, at the same time, the first measurement took place on 25 September 2008; the last one was done in December 2012. Monitoring was performed with frequency once per month. Already in the first measurement, changes caused by different soil composition and compaction were shown at the individual profiles (Fig. 4). Because the dam was constructed before the EIS apparatus installation, the monitoring started without the possibility of device calibration to the moisture. Therefore, the results are shown as conductance maps which correlate with soil moisture changes.

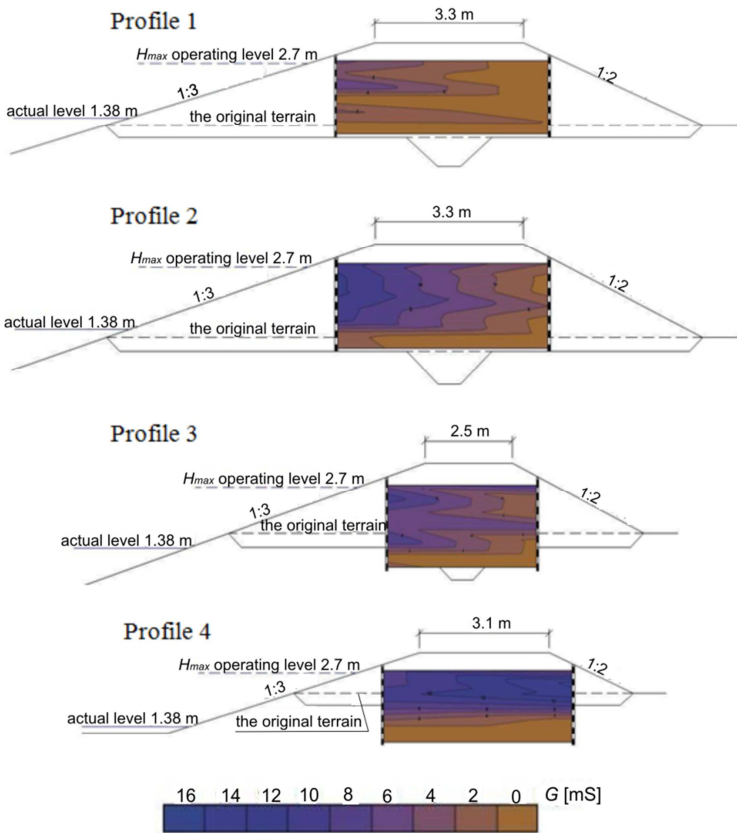


Fig. 4 Electrical conductance G (blue colour means higher water content of the soil, brown colour means lower water content) at cross-section profiles measured after probes' installation (the numbering of the profiles from 1 to 4 is the same in the figure 4, 5, 6 and 7)

The depth of water in the fishpond ranged approximately at a level of 2 m. The fishpond was not fully filled until June 2009. The possible problems with seepage in profiles 2 and 3 were observed from the beginning of the measurement. In July 2010, prolonged rainfall totals have caused increase of water level in the pond and subsequent flooding of probes installed on the upstream side of the embankment dam. It was a short-term event, therefore, in assessing the electrical conductance there were not significant changes, but the problem in profile 2 and 3 was obvious (Fig. 5). Based on the results of monitoring, the dam was raised in a section between profiles 1, 2 and 3 in October 2010 and compacted by travel, thus interrupting the process of suffosion. The disturbed place, however, was not sufficiently remediated because imperfect compaction was revealed by a small inrush of water on the downstream slope of the dam in April 2011. After further dam remediation between profiles 2 and 3 already seepages did not appear [Novák, 2012; Gardavská, 2014].

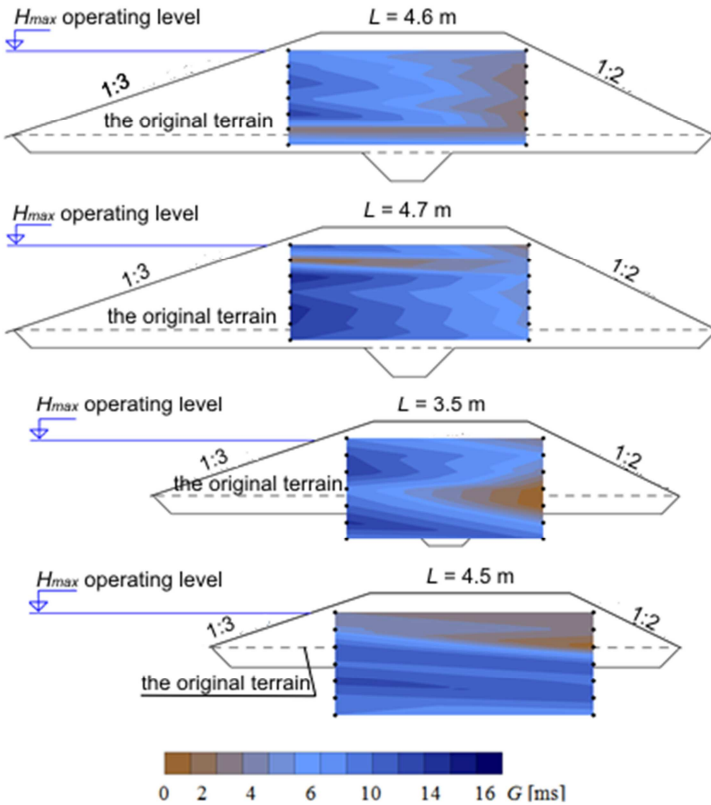


Fig. 5 Electrical conductance at cross profiles 1 to 4 after short-term flood

In October 2011, the fishpond began to be emptied for fish harvesting. The electrical conductance after emptying is depicted in Fig. 6. Again, the highest content of water is evident in the soil close to the upstream slope at profile 2. At cross profiles and on the downstream slope of the dam, the value of electrical conductance stabilised probably to that corresponding to the naturally moist soil. At profile 1, which is exposed to the prevailing winds, a trend of drying of the upstream slope of the dam can be observed.

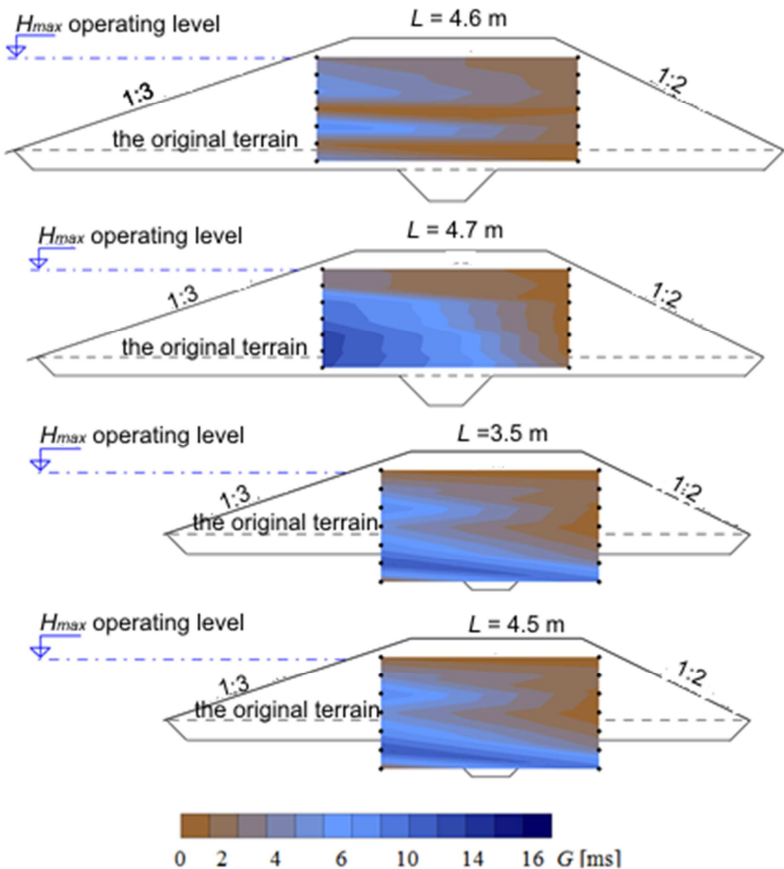


Fig. 6 Electrical conductance at cross-section profiles 1 to 4 of the fishpond after emptying

Together with electrical conductance susceptibility of the soil was measured. This parameter describes soil inhomogeneities and signals a problem in profile 2 (Fig. 7).

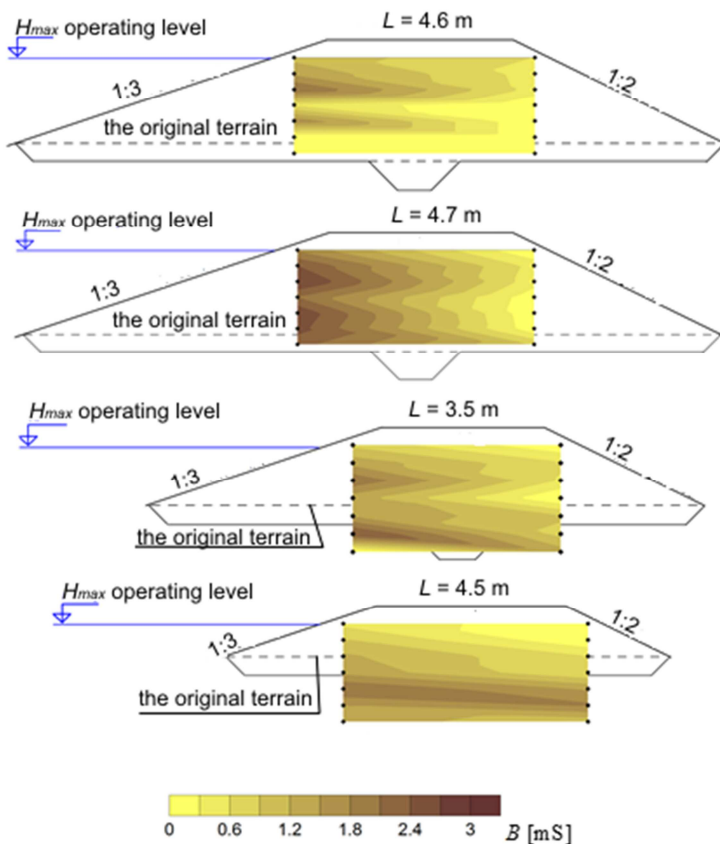


Fig. 7 Susceptance of the soil in cross-section profiles 1 to 4

4. CONCLUSIONS

Monitoring of the earthen dam of the fishpond near the municipality of Jevicko has shown the suitability of the EIS method and the constructed measuring apparatus for monitoring the water content in the body of embankment dam and hence its stability and the safety of its operation. In the given case, insufficient soil compaction was detected in some parts of the dam, remedial measures were implemented and their efficiency was also reflected in the results of monitoring. The operation of the fishpond has shown that compaction was sufficient only in the upper parts of the dam; at greater depths, higher values of electrical conductance can be observed, i.e. a higher water content in soil. Because the soil was analysed at the individual profiles, it is possible to compare well the values of electrical conductance. For example, at the first profiles, sandy clay of Class F4

CS was used; it was compacted well since the first stage of construction. This has led to the assumption that no privileged pathways should be formed in the given part of the dam. Monitoring has confirmed this assumption, although an increased activity of aquatic animals, probably water voles, was visually observed on the upstream slope of the dam. The monitoring apparatus and the detected results have helped to identify local anomalies in the body of the dam and thus timely to draw attention to the necessity of their remediation, which has been accepted by the owners of the fishpond and accomplished.

5. REFERENCES

- CALLEGARO, L. 2012. *Electrical Impedance: Principles, Measurement, and Applications*. CRC Press, ISBN 9781439849101, 308 p.
- GARDAVSKÁ, Z. 2014. Monitoring of filtration processes in earth dams. *Doctoral thesis*. BUT FCE. 141 p.
- KANOUN, O. 2011. *Lecture Notes on Impedance Spectroscopy: Measurement, Modeling and Applications*, Volume 1. CRC Press, ISBN 9780415684057, 110 p.
- NOVÁK, M. 2012. Evaluation of changes in pond dam monitored by EIS method. *Bachelor's thesis*. BUT FCE, 63 p.
- PAŘÍLKOVÁ, J., PAVLÍK, J. 2010. Construction – research, development and production of an automated system of monitoring of changes in soil moisture content using the EIS method. *Externally examined reports of the project OE240 for the year 2009*. Brno.
- PAŘÍLKOVÁ, J., RADKOVSKÝ, K. 2011. Z-meter III – User's Manual. Print Copy General, Ltd., 32 p.
- PAŘÍLKOVÁ, J., STOKLÁSEK, R. 2008. Manual – ZScan 2A. Print Česká reprografická, Ltd., 26 p.
- RADKOVSKÝ, K. 2014. Description of the new Z-meter IV. *EUREKA 2014*. ISBN 978-80-214-4883-4, 27-31 p.
- SLAVIK, J. 2005. Jevicko – Czech Anglers Union, fishpond – opinion of a hydrologist.
- PROJECT DOCUMENTATION, 2005. Regulations of operation and handling for the water reservoir of the Local Organisation Jevicko of the Czech Anglers Union.

Acknowledgement

This paper has been created with the financial support of the MŠMT (Ministry of Education, Youth and Sports) of the Czech Republic in the solution of the international projects E!7614 and E!4981 in the programme EUREKA.

CLASSIFICATION OF DAM FAILURES FOR ADOPTING LIMIT STATES

K. Adam , J. Vrabel

Brno University of Technology, Faculty of Civil Engineering, Institute of Water Structures, Veveří 95,
602 00 Brno, Czech Republic

Abstract

The formalized method for the safety analysis of dams following the particular limit states is not described in any available literature yet. Adopting uniform method involves classification of possible failures of dams. This article describes the approach for classification of possible failures of hydraulic structures, namely dams. First the databases of both theoretically possible and real cases of failures was created for both gravity and embankment dams. Then the formalized list of failures was assembled based on potential failures with focus on case studies. This list of failures will assist for the further safety analysis of hydraulic structures using the limit states method.

Keywords

Limit states, dam failure, hydraulic structures.

1. INTRODUCTION

The formalized method of the safety analysis for complex assessment of hydraulic structure using the limit states hasn't been published in any available references yet. To create such a method it's necessary to identify possible failures and divide them according to the failure mechanism. This article reports the process of listing of all possible failures based on both case studies and theoretically possible failures for selected types of hydraulic structure.

The aim of this article is to unify case studies and theoretically possible failures to complete formalized list which will be significant for safety assessment of hydraulic structures namely dams.

The process contains these parts: first the types of dams which are suitable to deal with according to region (middle Europe) were selected. Second the articles, lectures and other references about failures of dams were studied (Chap. 2). That conclude to a list of failures (Chap. 3) based on own database of failures with respect of 3 groups of different importance (global, local and serviceability failures). A list of failure divided by selected types of dam shows that some failures are repeating (same principal) for different type of structures, this concludes to sorting by types of failure giving us the final list of formalized failures (Chap. 4).

The detailed analysis was performed for structures as follows, concrete dams, masonry dams, embankment dams with body sealing, homogeneous dams and embankment dams with slope sealing. In this article the analyses of both concrete and embankment dams with central sealing are presented. The formalized list of failures can also be used for other hydraulic structures such as polders, weirs, flood protection structures, tailing dams, hydro tunnels, lock chambers and structures for energy and sailing purposes.

2. PRESENT STATE REVIEW

In the 1947 the International Commission on Large Dams published the first list (database) of the dam failures, which has contained about 202 cases [Fry, Vogel, Royet, Courivaud 2012], [Foster, Fell, Spannagle 2000]. The database was focused on dams with the body height above 15 m, or the body height of 10 to 15 m under the condition of the dam crest length greater than 500 m or the dam reservoir volume above 10^6 m³ or the outlet discharge greater than 2000 m³/s or dams of unconventional design [Foster, Fell, Spannagle 2000]. In the 1995 the ICOLD has published the Bulletin 99, which presents the statistic of failure according to the type of dam. ICOLD currently offers the largest database of dam failures [Fry, Vogel, Blais, Courivaud 2004]. This database has some disadvantages for our purpose, because it doesn't content failures of smaller dams. ICOLD databases often serves as a base for another authors for an example [Zhang, Xu, Jia 2007] and [Jandora, Riha 2008]. Very precise study of the both concrete and masonry dam failures presents [Douglas, Spannagle, Fell 1998], the study also refers the statistical assessment of failures according to various factors. Similar study but focused on embankment dams presents [Foster, Fell, Spannagle 1998]. Both overview and analysis of the world's major failures of dams shows [Saxena, Sharma 2005], [Bosela 2013]. Different approach of failures assessment according to failure risk and failure starter shows [Almog, Kelham, King 2011]. The most significant failures of dams are described in [Broža, Kratochvíl, Peter, Votruba 1987], [Říha 2004] and [Říha, Švancara 2006].

The assessment against the structural failure is described in the Eurocodes noted as 2 and 7. In the Czech Republic the same standards are noted as [ČSN EN 1992] and [ČSN EN 1997-1]. The Eurocode defines the limit states, which are states when the structure has no longer the required parameters. These states can be marked as failures. According to the Eurocodes there are 2 types of limit states, the ultimate limit state (ULS) and the serviceability limit state (SLS).

3. TYPES OF DAM FAILURES

Failure of the installation is defined as the termination of its ability to perform required functions. For our purpose the failures were classified as follows:

- group G – global failures leading to complete dam collapse,
- group L – local failures leading to local defects,
- group P – failures leading to loss of serviceability.

Global failures represents the worst case scenario. Both local failures and loss of serviceability mainly involves operational restrictions. Failure from both groups L and P may lead to global failure if they are not dealt with.

3.1 Concrete dam failures

The list of failures of concrete dams were assembled including the historical documented cases. Basic types of failure corresponds with both ultimate limit states and serviceability limit states according to [ČSN EN 1992]. The assessment of the dam body against the uplift can be handled by [ČSN EN 1997] (UPL ULS). General assessment of concrete hydraulic structures is described in [ČSN 73 1208].

The failures for concrete dams are as follows.

3.1.1 Collapse of dam blocks

Collapse of dam blocks belongs into group of global failures and is caused by block sliding, block uplifting or block overturning. These failures can be described as sudden and entire failure of structure. They have usually fatal consequences and they are often signalized by local failure. Examples of these failures are shown in Fig. 1 and Fig. 2.



Fig. 1 Bayless Dam (Austin dam) (1911), block sliding [Vogel, 2014]



Fig. 2 Gleno dam(1923), collapse of dam block [Herzog, 1999]

3.1.2 Foundation failure

The foundation failure belongs into group of global failure. The progress of foundation failure depends on both strength and resistance of foundation material and also on hydraulic gradient. Piping occurrence is necessarily precedent by local exceeding of bearing capacity of foundation.

The progress of the piping is indicated by both pressure and seepage regime changes.



Fig. 3 Malpasset Dam(1959), foundation failure [Duffaut, 2013]



Fig. 4 Ashley Brook Dam (1909), foundation failure [Vogel, 2013]

3.1.3 Exceeding of concrete strength

Exceeding of concrete strength (tensile, pressure, shear) is local failure and it usually don't lead straight to global failure, it leads to redistribution of forces in material and to local failures, i.e. cracks. Although local failure can lead to global failure without the proper failure treatment.

Concentrated local leakage can occur along the working joints, when the concrete is processed and placed poorly. This type of failure mainly occurs on the roller compacted concrete dams see Fig. 5.



Fig. 5 Rialb Dam (2006), leakage through the crack [photo: Řiha]



Fig. 6 Folsom dam (1995), gate failure [Vogel, 2014]

3.1.4 Exceeding of foundation strength capacity

Exceeding of strength (compressive, tensile and shear) of foundation material is local failure and depends on type of material of foundation. The principle of failure for solid mass rocks is analogous with failure of concrete material. Both stress and strain in foundation are directly connected to stress and strain in dam body (foundation must be considered like part of dam construction).

Failure by local internal erosion in foundation is caused by washing out of small particles of foundation material or grout curtain. This could lead to degradation of the foundation material and also cause a good condition for seepage pass occurrence.

3.1.5 Loss of serviceability

Examples of loss of serviceability are as follows. **Mutual displacement of dam blocks** are caused by variable static loads of dam blocks and also by variable properties of foundation material. Mutual displacement can cause the loss of serviceability of various parts of dam structure such as facing of dam crest, devices that comes through more then one dam block, sealing of the expansion joints, etc.

Mutual displacement of dam body and foundation are between the dam body and relatively fixed foundation. These displacement can be indicated by occur of slip surface.

Deformation, damage or loss of operability of the appurtenant works can cause uncontrolled discharge through the work or else loss of capacity of reservoir, see Fig. 6.

Degradation of the grout curtain can decrease the safety of dam. The purpose of grout curtain is to elongate filtration path and lower both hydraulic gradient and pressure in the foundation. Due to degradation of the grout curtain, hydraulic conductivity of it is increasing and causes increase of pressure in foundation on downstream face.

Drainage system reduces the water pressure in the sub-base. Its damaging or degradation can cause an increase of water pressure in the sub-base and lower the safety of the dam.

3.2 Embankment dams with central core sealing

Second example of a list of failures was concluded for embankment dams with central core and it content example of case studies of failure. Some failures form list could be compared with ultimate limit state (ULS) or serviceability limit state (SLS) in Eurocode 7 [ČSN EN 1997-1].

Global failures (G) of embankment dams with central core contain: failures of stability and accidental cracks; failure caused by accidental seepage; failure due to hydraulics extremes; and failures caused by accidental seepage. Failures belong to group of local failures (L) contain local hydraulic failures and local structural failures: local exceeding of concrete and soil stress; local failure due to accidental seepage; and local failure caused by external factor. Serviceability failures (P) of embankment dams with central core are divided to failures of measurement equipment and appurtenant works; failure of sealing and settlement.

3.2.1 Failure of stability

A failure of stability means slopes stability of embankment dams or create slip surface which indicate global instability of dam and sub-base. Shape of slip surface is a general and takes position through dam body, sub-base or both of

them. A position slip surface could be affected by the interface of two materials (e. g. if they have different parameters). Accidental cracks belong to global failure of stability. Appearing of cracks relates to settlement, displacement or slides and could be on dam core, body or sub-base.

3.2.2 Failure caused by accidental seepage

Global failure caused by accidental seepage (e. g. erosion, suffosion) is often caused by more than one aspect: critical hydraulic load (critical hydraulic gradient, critical pore pressure forces), soil resistant parameters and stresses. Example of failures is suffosion on the interface of fine grade core and dam body or on interface of cohesive and noncohesive (soil) structures, e. g. seepage along bottom outlet. This failure is mentioned in Eurocode 7 [ČSN EN 1997-1].

This type of failure isn't unpredictable often, but the process of developing cloud be very rapid (Teton 1976). In case of long term the development of failure cloud progress a years (Mostišťe, Fig, 9). Obvious local deformation due to accidental seepage has been appeared before global failure.

3.2.3 Failure due to extreme hydraulics events

Hydraulic failure (mostly overtopping) could cause global instability of dam body or some local failure. Global failure due to overtopping has been described as a state when surface erosion starts and the breach reach the upstream edge of dam crest and decrease level of a crest in whole cross section.

For example periodical wind waves, exceeding of spillway capacity or improper emergency operation during hydraulics extremes could cause failure due to overtopping.



Fig. 7 Metelský rybník (2002), failure by overtopping [photo: Říha]



Fig. 8 Pocheň (1997), overtopping and surface erosion [photo: Žatecký 1997]

3.2.4 Failures due to pore pressure forces

This type of failure could be caused by two driving forces, uplift forces on low permeable layer and volume forces by leakage through permeable volume of soil. The examples of failures by uplift forces are uplifting impermeable soil layers or

construction made of cohesive material (varved clay, dam galleries, conduits, lock chambers, slab of stilling basin, etc.). Effect of volume forces is heave, for example heave of embankment toe or heave of unsealed excavation bottom. Difference between failures by these driving forces is in permeability, heave occurs in noncohesive and more permeable soil.

3.2.5 Local structural failures

First part of local failures (L) is structural. Like other local failures structural failures don't evoke immediate risk but could lead to global failures of dam. This failure contains local failure of appurtenant works (made from concrete), and local stability failure of slope embankment or sub-base (e.g. local slips, cracks or local deformation due to seepage).

Important part of local failure is deformation of embankment dam by vegetation, animals and caused by human. This situation often helps to global failures based on accidental seepage.



Fig. 9 Mostišť (2004), piping through dam core [photo VD - TBD a.s.]

3.2.6 Local hydraulic failure

Local hydraulic failures relate to short term hydraulic extreme like wind waves on reservoir water surface, flooded downstream slope or toe and obviously heavy precipitation. Local failure due to periodical overtopping also belongs to this type of failure.

3.2.7 Serviceability failures

Failures of serviceability contain three main parts: failure of measurement equipment and appurtenant works, failures of sealing and settlement. For example inclination of water supply tower affects the operation of valve or gate. Also gated emergency spillways could be affected by serviceability failure. Second type of serviceability failure is degradation of sealing system of a dam or sub-base, e. g. grouting curtain or dam core. And settlement during and after construction or significant displacement also belongs to serviceability failures. For example the vertical displacement could cause local lowering of dam crest, or the horizontal structures which are passing through the dam body (bottom outlet, grouting gallery) could be affected by significant displacement.

4. SUMMARY OF FORMALIZED FAILURES OF DAMS

Tab. 1: Formalized list of failures

Failure/group *)		Detail of the failure	Consequence
Sliding	G	Slip surface through - dam body - along foundation joint - sub-base	Occur of slip surface, breaching, loss of overall stability
		- slopes of reservoir.	Landslide.
Overturning	G	Overturning of dam body or its major part.	Loss of stability.
Uplift	G L	Uplifting of the structure or impermeable soil layer.	Uplift or overturning of a part of structure.
Heave	L	Breaching of permeable soil layer due to pore water pressure.	Internal erosion (boiling), sliding of structure.
Internal erosion	G	Piping.	Deformations, structural collapse.
	L	Suffosion/fluidization, erosion	Local instability of particles.
Surface erosion (overtopping, precipitation, scouring)	G	Long term overtopping, exceeds of scouring strength.	Breaching, scouring of slope, crest or foundation.
	L	Short term overtopping.	Local scouring of slope, crest or foundation.
Exceeding of material strength	L	Exceeding of strength of sub-base/structure material.	Cracks.
Deformation of structure	P	Mutual displacement of parts of structure, structure and sub-base or significant displacement (soil).	Failure of sealing of joint, higher leakage.
Leakage/seepage	P	Higher leakage through the dam body, around the structure of appurtenant works.	Water losses and filling difficulties.
Failure of appurtenant works	P	Blockage or malfunction of bottom outlet, emergency spillway (ice, sediments).	Breach, spate, manipulation restrictions.
Degradation of material of structure	P	Degradation of concrete, masonry, rockfill, leakage into dam body.	Degradation of reinforcement, changes of material properties.
Degradation of sub-base material	P	Clogging, degradation of grout curtain.	Increasing of pressure in foundation, internal erosion.
Degradation of instrumentation	P	Ageing of boreholes/instrumentation, siltation of pipes, malfunction of devices.	Measured values out of prognosis.

*) G – global failure, L – local failure, P – loss of serviceability

The list of formalized failures of dams mentioned in chapter 3 is shown in Tab. 1. Every group of failures is possible to specify according to the type of dam, but the principal of failure is similar.

5. DISCUSSION AND CONCLUSIONS

The list of possible failures is not uniform in any available literature. Several authors describe the possible failures but some failures are not properly discussed. In this article the process of formulation of uniform list of possible failures for selected types of dam is presented. The list includes both the historical failures, and potentially possible failures. The formalized list is a synthesis of failures defined separately for every selected type of dam. The synthesis were performed because of the repeating of failures of same principle for different types of dam. For example the failure by sliding is the same for concrete and masonry dams or weirs. The structure of the formalized list also respects the division of limit states types according to the Eurocode, thus the list is prepared for further application of assessment of the dam safety using the limit states.

6. REFERENCES

- ALMOG, E., KELHAM, P., KING, R., 2011. Modes of dam failure and monitoring and measuring techniques. *Environment Agency, Horison House*, Deanery Road Bristol, BS1 5AH, ISBN: 978-1-84911-230-7. 2011.
- BOSELA P. A., BRADY P. A., DELATTE, J. N., PARFITT, M. K., 2013. Failure Case Studies in Civil Engineering. Published by the American Society of Civil Engineers.
- BROŽA, V., KRATOCHVÍL, J., PETER, P., VOTRUBA, L., 1987. Přehrady. SNTL, Praha, 1987.
- ČSN 73 1208 Betonové konstrukce vodohospodářských objektů.
- ČSN EN 1992-1-1 (73 1201) Eurokód 2: Navrhování betonových konstrukcí.
- ČSN EN 1997-1 (731000) Eurokód 7: Navrhování geotechnických konstrukcí.
- DOUGLES, K., J., SPANNAGLE, M., FELL, R., 1998. Analysis of Concrete and Mansonry Dam Incidents. The University of New South Wales, Australia.
- DUFFAUT, P., 2013. The traps behind the failure of Malpasset arch dam, France in 1959. *J. of Rock Mech. and Geotech. Engineering*, 5(5), pp. 335–341.
- FOSTER, M., FELL, R., SPANNAGLE, M., 1998. Analysis of Embankment Dams Incidents. The University of New South Wales, Australia, 1998.
- FOSTER, M., FELL, R., SPANNAGLE, M., 2000. The statistics of embankment dam failures and accidents. *Canadian Geotechnical Journal*, 37(5), p.1000–1024.
- FRY, J-J. VOGEL, A., ROYET, P., COURIVAUD, J-R., 2012. Dam failure by erosion, *In: lessons from ERINOH data bases*. 2012, ICSE6 Paris, p. 273-280.

- FRY, J-J. VOGEL, A., BLAIS, J-P., COURIVAUD, J-R., 2004. Dam Accident Data Base DADB - The Web Based Data Collection of ICOLD. London.
- HERZOG, M. A. M., 1999. Practical Dam Analysis. Thomas Telford, 250 p.
- ICOLD Bulletin 99, 1995. Dam failure statistical analysis.
- JANDORA, J., ŘÍHA, J., 2008. The Failure of Embankment Dams due to Overtopping. Brno University of Technology. ISBN 978-80-214-3527-8.
- ŘÍHA, J., ŠVANCARA, J., 2006. The failure of the Mostiště embankment dam. *Proc. of the 14th Conference of the British Dam Society: Improvements in Reservoir Construction, Operation and Maintenance*, pp. 391-403.
- ŘÍHA, J. 2004. Comments on failures of small dams in the Czech Republic during historical flood events. *In: Long-term Benefits and Performance of Dams - Proceedings of the 13th Conference of the British Dam Society and the ICOLD European Club Meeting*, pp. 597-608.
- SAXENA, K. R., SHARMA, V. M., 2005. Dams Incidents and Accidents. A.A. Balkema Publishers, ISBN 90 5809 701 3.
- VOGEL, A., - LAUGIER, F., - BOURDAROT, E., 2014. Failures of masonry or concrete dams by overtopping. *Proc. of The 1st International Seminar on Dam Protection against Overtopping and Accidental Leakage, Madrid*.
- VOGEL, A., 2013. Internal erosion dam failure cases. *Proceeding European Working Group on Internal Erosion 21st Annual Meeting, Vienna*.
- ZHANG, L. M., XU, Y., JIA, J. S., 2007. Analysis of earth dam failures – A database approach, *ISGSR2007 First International Symposium on Geotechnical Safety & Risk, 2007 Shanghai China*, p. 293-302.

Acknowledgement

This study is part of projects FAST-J-15-2838 project of specific research “A Comparison of Safety of Concrete Dams for Individual Scenarios of Failure according to the Safety Levels and Limit States” and FAST-J-15-2756 project “Evaluation of the Stability of Slopes of Dams of Small Water Reservoirs in Relation to the Requirements of CSN 75 2410”.

Restoration of the stilling basin of the Drtjščica dam

N. Humar¹, A. Kryžanowski²

¹Hidrotehnik d.d., Ljubljana, Slovenia, Humar.nina@gmail.com

²Faculty of civil engineering, Ljubljana, Slovenia, Andrej.kryzanowski@fgg.uni-lj.si

Abstract

The Drtjščica dam and the reservoir represent the most important part of the flood protection system in the motorway section to the northeast of the city of Ljubljana. The reservoir is designed as a relief system for retention of peak discharges of flood waves, enabling higher flood safety for the entire area along the motorway. The dam is an earth dam with a central clay core, having a height of 18 m and a crest length of 256 m. The evacuation of water through the dam cross-section is through a shaft overspill and the bottom outlet into the channel of the Drtjščica stream. In September, 2010 a flood event occurred, when the high waters were in the range of the designed maximum flow. During the evacuation of flood water extensive erosion-induced damage to the stilling basin of the bottom outlet and the right part of the toe of the dam occurred. After the conditions steadied, the damaged structures were rehabilitated in the matter of priorities, together with the proposal of minor improvements of the original design, where this proved justified. After the event, an analysis of the conditions during the flood event was performed, where it was found that the damages were the result of several factors: firstly, there were exceptional operational conditions that exceeded the normal operational conditions, secondly, the end-part of the bottom outlet was inadequately designed, and, thirdly, the hydraulic conditions downstream of the dam were inadequate. For determination of the final solution a comprehensive redesign of the evacuation structures on the dam will be needed, taking into account the conclusions of the analysis of the 2010 event.

Keywords

Bottom outlet, damage, earth fill dam, erosion, flood, scour protection, stilling basin

1. INTRODUCTION

The Drtjščica system was built in 2002 in order to ensure flood safety in the area of the new motorway section. The building of the motorway caused a considerable loss of floodplains in Radomlja valley area, and as a result the flood threat to urban areas and road connections in the impact area increased. During the design stage of the protection measures the construction of the dam with a reservoir and diversion through the relief tunnel seemed to be the most appropriate and effective. Due to the lack of space and relatively dense settlement, the building of a reservoir in the Radomlja valley was not an option; therefore both

the dam and the reservoir were built on the Drtijiščica River, the left tributary of the Radomlja River.

The reservoir with a total capacity of 6,7 hm³, the dam, the intake sill with gates on the Radomlja River and the water tunnel are connected into a system, which during high flows of the Radomlja River partly diverts water through the diversion tunnel to the Drtijiščica valley, while after the Radomlja River levels are lowered it controls the discharge into the Drtijiščica River and onwards into the Radomlja River (Fig.1).

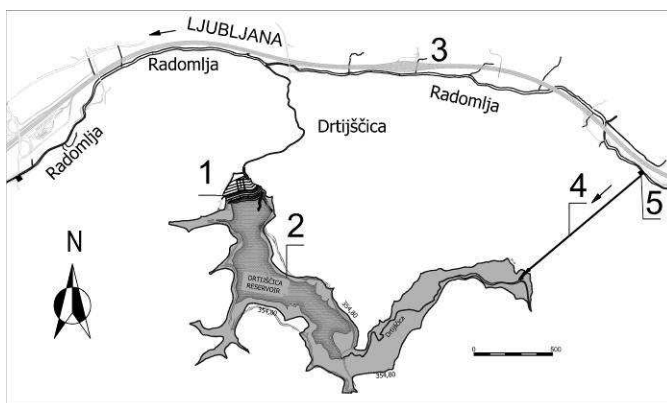


Fig. 1 Drtijiščica system for improvement of flood situation and protection (1- dam, 2- reservoir, 3- motorway, 4- diversion tunnel, 5- intake works)

2. DESCRIPTION OF THE DRTIJIŠČICA DAM

The main structures in the system are the dam of Drtijiščica and the Gradišče reservoir. The dam is situated approx. 2.3km upstream the Drtijiščica and Radomlja Rivers confluence. The dam is a zoned earth dam consisting of a central impervious core of greasy grey clay, reaching to the semi-pervious alluvial layers and shale bedrock. The maximum height of the dam is 18,2 m. The air side of the dam is in a slope of 1:4, lined with four berms of a width of 2,5 m and covered with turf. The slope of the upstream side of the dam is 1:3, lined with three berms. The length of the crest along the dam axis is 256 m. In the bottom, the width of the dam is 150 m. The dam is founded in the less pervious alluvium (at the right abutment), which on the left side of the right abutment passes into shale bedrock. The sealing of the dam cross-section in the more pervious alluvial subsoil is performed with a two-line grout curtain, in a length of 66 m and a depth of 20 m (Fig. 2).

The role of the semi-dry reservoir is multifunctional. The primary function of the reservoir is the flattening of the flood wave, while the permanent accumulation should also provide a site for fishing and other water and water-side activities. The level of permanent accumulation is at 344,80 m a. s. l., its capacity is 0,9 hm³ and

it offers fishing and other aquatic and water-side opportunities. Maximum water level is at 354,80m a. s. l. At this elevation the reservoir flood control capacity is 5,6 hm³ which should be enough to ensure flood safety of the motorway section and improve the flood safety of the settlements downstream of the dam which were, prior to the building of the reservoir, flooded during heavy rains. The reservoir capacity, whose water intake should at this elevation fit the 10 000-year flood, was based on the 100-year return period of the Drtijiščica River flow, estimated at 43 m³/s and 45 per cent of the Radomlja River flow with a 100-year return period, being 30 m³/s, which is diverted through a tunnel into the Drtijiščica River and further into reservoir.

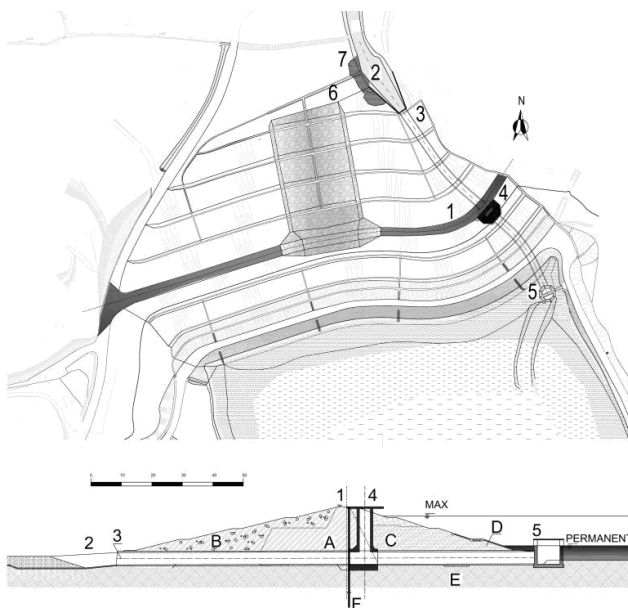


Fig. 2 The Drtijiščica dam ground plan and characteristic cross-section (1-crest of dam, 2- stilling basin, 3- bottom outlet, 4- gate chamber, 5- shaft spillway, 6- spillway chute, 7- scour hole, A- core, B- clayey gravels, C- soil, D- riprap, E- foundation of dam, F- grout curtain)

During normal operation conditions the control of the water level in the reservoir and the outflow through the bottom outlet further into the Drtijiščica River is performed via a drawoff tower with a shaft spillway. At the right abutment of the dam cross-section axis there is a shaft with a sluice gate, which helps to adjust the flow downstream of the dam, when in the control cross-section on the Radomlja River the elevation exceeds 325,8m a. s. l. (and the need for storage emerges) and until the total of the Drtijiščica River flow and the flow of the Radomlja River into reservoir does not exceed 73 m³/s.

Below the dam the bottom outlet of a rectangular cross-section of dimensions 4x3,5 m ends in a flared outflow of a length of 14 m, which is lined with reinforced concrete floor and side wing walls. In the final part of this section the stilling basin changes from the rectangular into trapezoidal cross-section, which has a bottom width of 10 m, a height of 2,46 m, with the banks lined with dry-laid masonry in a slope of 1:1. The total length of the stilling basin and the transition into the lower river bed ending with the rock/concrete 0,8 m long sill is 28,31 m. Further on, the river bed cross-section is of a simple trapezoidal shape with a cross-section width of 6 m and a height of 1,46 m.

In exceptional cases, when the natural inflow into the reservoir exceeds the capacity of the bottom outlet to such an extent that the possibility of overflow becomes real, as an extreme measure the activation of an emergency spillway in a width of 40 m is planned, located in the central part of the dam, whose spillway elevation is at 352,45 m a. s. l [Humar and Kryżanowski, 2012]

3. DESCRIPTION OF THE 2010 EVENT

The Drtijščica system is designed in a way that, despite the considerable torrential character of the Drtijščica and Radomlja Rivers, a safe operation and sufficient storage is ensured for retention of flood surcharge. During the time of its operation, from the construction to the onset of the extreme event in September 2010, the reservoir performed its function without any particularities. The largest fluctuations in the reservoir did not exceed 1,5 m, despite the increased water levels of the Drtijščica and Radomlja Rivers. The September 2010 event, however, was characterized by previous heavy and prolonged rain in the wider catchment area of the Radomlja River, when the peak flood flows of the Drtijščica and Radomlja Rivers coincided, and the flows came very close to the estimated values of 100-year return period flows. The level in the reservoir, filled between 17 and 19 September, reached the planned maximum level on 19 September.

According to the weather forecasts, the conditions in the following days were not about to improve, and the fear of dam overtopping existed. Because of the bad forecast and consistent with the contingency protocol for extreme operational conditions, a decision was made to activate the bottom outlet and start the precautionary drawdown of the reservoir. The overtopping over the emergency spillway, as an extreme protection measure, was out of the question, so the first priority was to ensure the safety of the dam.

Since the inflow into the reservoir did not cease, the bottom outlet was opened, and on 19 September it started to work with full capacity. With the full capacity of the bottom outlet, the water level in the stilling basin increased, it started to flood the banks, and an indentation appeared at the toe of the dam. In a mere six hours a large scour hole emerged, spreading approximately to a third of the toe of the dam (Fig. 3). When the flows decreased, the conditions started to settle down, and the outflow from the bottom outlet could once again be controlled; after the outlet was reduced, and the retention water level was restored, the size of the scour hole did

not change significantly. An inspection of the dam, bottom outlet and the stilling basin lead to the following conclusions:

- The most critical part of the stilling basin is the left bank on the stretch between the concrete outlet and the transition into the lower river bed. In this stretch, a complete failure of the protection of the left bank in dry laid riprap and its consolidation with wooden piles occurred, including the retrograde scour hole, which extended over approximately 1/3 of the dam (on the dry side).
- On the right bank of the same stretch of the stilling basin there were no significant damages reported.
- To see if there were any structural displacements when the storage reservoir was full, extensive surveying was performed after the conditions went back to normal. On the dam itself no deviations compared to previous observations were found, and it was established that during the extreme event the dam stability was at no point under threat.



Fig. 3 The scour hole on the left side of the stilling basin prior to refurbishment works



Fig. 4 Outflow from the bottom outlet during the floods in September 2010

Based on the surveying of the scour hole and the study of archive materials, however, a hydraulic jump was established, which was contrary to expectations. There was a sudden shift of the outflowing water level in the stilling basin upwards towards the left bank, while along the right bank depression with return flow occurred (Fig. 4). At the time of the event the phenomenon was explained as a result of the impoundment caused by tailwater, since it was evident that the Drtiščica natural river bed, which narrows down considerably downstream of the dam, was not able to convey such high flows. Only later it was found that the phenomenon was the result of several factors that could not be influenced at the onset of the event [Humar and Kryžanowski, 2012].

4. IDENTIFYING THE CAUSE OF DAMAGE

Until the September 2010 event, the operation of the bottom outlet and the stilling basin was within expectations. Because of the reservoir capacity, the flows and the outflow via the bottom outlet could be adjusted within the planned values. The progression of the September 2010 events and the damage done to the stilling basin gave us an insight into the dynamics of the processes that occur during large outflows from the bottom outlet. When analyzing the phenomena on the outflow, the poorly chosen combination of design plan and the choice of the bottom outlet and the plunge pool material became evident, while at the same time it was confirmed that the erosion processes are encouraged by the design itself. The analysis of the September 2010 events also included the inspection of project documentation, and a re-evaluation of the assumptions underlying the hydraulic calculations of the evacuation structures. We identified the following inconsistencies in preparation of project designs, which contributed, among other things, to the damage on the dam:

- The hydraulic calculations of the bottom outlet consider only free-surface flow. This applies to operating conditions where the reservoir water level is within the retention water level range, while the intake shaft is not submerged and acts as an overfall spillway. In this case, the bottom outlet's maximum discharge capacity is $52 \text{ m}^3/\text{s}$. By raising the reservoir water level and, as a result, activating the volume intended for flattening the flood wave, the intake shaft is submerged and the bottom outlet discharge is fully pressurized. In line with the design specifications, the maximum permitted flow rate is $73 \text{ m}^3/\text{s}$. Outlet discharge is regulated by a gate installed in the vertical shaft, approximately in the central part of the bottom outlet. The gate operates automatically, depending on the water downstream the dam (the gauging site is approx. 2 km downstream the dam profile) and the reservoir water level. There are no gate operating rules, and also no discharge-head curve is available for the individual gate operating maneuvers. Gate operation is based on the known inflow from the Radomlja River and the monitoring of reservoir water level dynamics, while the operator has no data on the Drtijiščica inflow.
- In order to ensure a better foundation of the bottom outlet construction, the path of the bottom outlet under the dam was designed in a fine "S" curve, while the outflow was directed towards the left bank. The design characteristics of the bottom outlet accelerate the swirl of the current field entering the bottom outlet through the shaft overspill. Furthermore, the orientation of the outflow, lying on the crown of the bend, additionally potentiates the direction of the current field towards the left bank of the stilling basin, bordering the toe of the dam, which could conditionally explain the larger damage of the left bank of the stilling basin and the river bed downstream of the dam.

- The outflow from the bottom outlet is designed as a concrete channel that symmetrically expands into the fortified stilling basin. The concrete wing walls form an angle of 15° with the bottom outlet axis. The stilling basin bottom is deepened by 1 m. The pool is trapezoidal and lined with quarry stone, as requested by nature conservation services during the environmental permit application process. The circumferential channel walls at the transition are 3,05 m high, which coincides with the height of the bottom outlet, and then they wedge out to the level of the plunge pool at 2,5 m. In view of functionality, the stilling basin design is hydraulically extremely unfavorable. The angle of the channel flaring exceeds the recommended angle of 7° [Agroskin et al, 1973], failing to result in the formation of a steady hydraulic jump across the channel cross-section; instead, a sinuous water current is generated, which is directed into the walls of the channel. The situation at Drtiščica continues to deteriorate also due to the installation of the evacuation structures, since the course of the bottom outlet is in a slight arch, directed towards the left side of the channel. Due to the special natural conservation requirements, the plunge pool, too, has a trapezoidal design, and due to design requirements, the concrete channel passing into the stilling basin is also trapezoidal. Because of the changing concrete channel cross-section at the bottom, the functionality of the stilling basin designed in this way is questionable.
- With the exception of the direct outlet works, the rest of the plunge pool and the outgoing channel are shaped as a reinforced trapezoidal channel. At the outflow from the plunge pool, the channel cross-section gradually changes from the rectangular to trapezoidal shape of the natural channel. No major regulatory actions on the downstream channel were taken, even though the nominal flows during flood water evacuation significantly exceed the flow characteristics of the Drtiščica extreme flows, as estimated in the project documentation. When analyzing the in-bank capacity below the dam we found that the channel could only convey flows up to $8 \text{ m}^3/\text{s}$. Overtopping occurs during higher flows, and extensive floodplains are formed below the dam. The overtopping also decreases the water level at the sill at the outflow from the stilling basin, which affects the functionality of the stilling basin.
- Approximately 120 m below the dam the river bed enters a narrow canyon cross section, which additionally hinders the stream conveyance and directly influences the conditions in the stilling basin, because upon the entry into the canyon, an impoundment is formed, spreading up to the stilling basin. In this way the water that should flow down the river bed becomes a constriction to the incoming water rushing down from the bottom outlet with great force and velocity. Asymmetric flow emerges, which is on the left side oriented in flow direction, while along the right bank upstream flow and swirling against the main flow of the outflowing water occur.

The asymmetric hydraulic jump and the sinuous current in stilling basins were discussed by [Bribiesca and Sánchez, 1999]. In the case of the sinuous current in the stilling basin, the current field rotates into one or another direction, and along one of the banks return flow occurs. With the return flow along one of the banks a return mechanism is set off (circling of water in horizontal direction), when the flow along one of the banks moves against the stream, while along the other bank it flows downstream. A new stable situation is established, where the water level in the stilling basin up to the contact between the return and normal flows is higher at the bank where there is no return flow. In the case of asymmetric flow the deviation in the y-direction does not exceed 20 per cent of the total depth of water in the pool, which is why an approx. 20 per cent heightening should suffice on the side with the level increase. The analysis revealed that because the submergence was too low, an asymmetric repelled hydraulic jump was generated, which was, due to the course of the bottom outlet, directed at the left bank. By taking into account the discharge and hydraulic characteristics of the stilling basin during the event, the hydraulic jump height was estimated at 5 m; under given conditions, by considering the asymmetry of the hydraulic jump, this meant an overtopping of the channel wall by about 2 m. The estimated overtopping coincided with the overtopping during the event, and the size of the later damage at the toe of the dam (Fig. 5). The recommendations on the needed heightening were taken into account when designing the measures for restoration of the scour hole and evaluation of the needed heightening of the left side of the plunge pool.

5. REHABILITATION MEASURES

The rehabilitation measures were divided into two stages: In the first stage, during 2010–2011 the emergency rehabilitation measures were performed, in order to restore the normal operation of evacuation structures, and simultaneously the restoration of all erosion-induced damages on the dam. During the rehabilitation, field observations and literature recommendations were taken into account. In the second stage a model will have to be made, based on the data obtained by additional observations of the phenomena in the stilling basin and the measurements done in the river bed downstream of the dam.

In the first stage, the heightening of the bank and the toe of the dam bordering the bank was performed. The slope protection was heightened on the left side of the stilling basin. Next to the heightened slope protection, where the recommendations from the literature were considered, the rock riprap was laid in concrete. Considering the progression of processes in the stilling basin, an additional reinforcement of the right bank was not necessary. Since in the literature more or less isolated cases are discussed, in the case of Drtijiščica dam a hydraulic (physical) model should be made, which would address the direction of the outflow and the shape of the river bed downstream of the dam, as well as the shape of the bottom outlet, the flaring on the outflow from the outlet and, last but not least, the phenomenon of asymmetric flow.

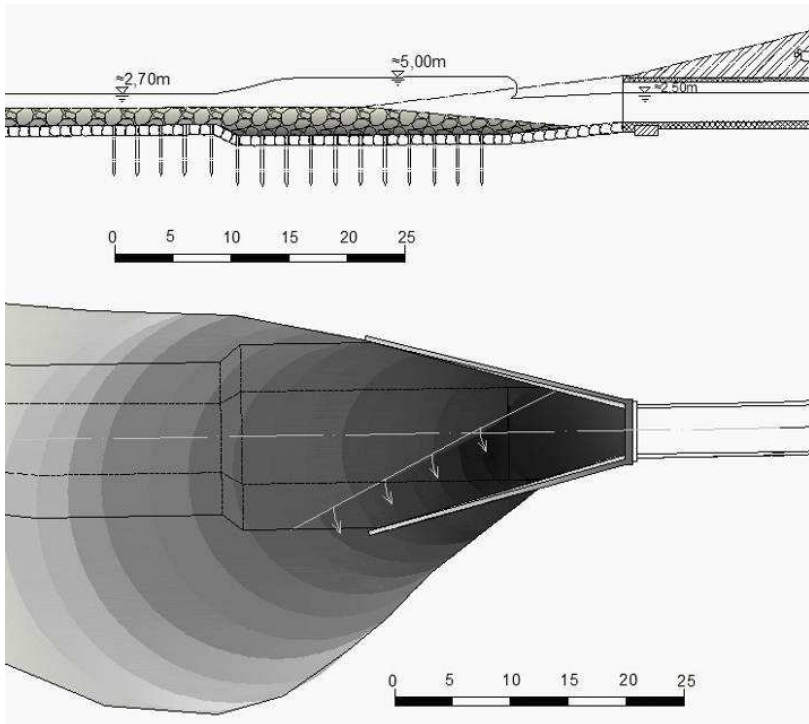


Fig. 5 The estimated overtopping (above) basin caused by the asymmetric hydraulic jump (below) in the stilling basin

It should be emphasized that the solution put in place at the stage of rehabilitation of the scour hole was a temporary one, while for a final solution the phenomenon will have to be analyzed with a physical model, which is planned for the second stage of the rehabilitation measures. In the latter stage the stilling basin works will have to be optimized, as well as the stretch of the river bed downstream, considering the obvious fact that under extreme circumstances the existing river bed fails to ensure sufficient conductivity. Only a detailed analysis will help to confirm the calculations and suitability of the solution decided upon, and contribute to the final solution of the design problem and improvement of the dam itself.

6. CONCLUSIONS

In relation to the evacuation structures on the Drtjščica dam, at the planning stage the functionality of the technical design was subordinate to the requirements of the environmentalists for sustainable planning, which is a frequent occurrence in the design of water works in Slovenia. When planning the evacuation structures, some design elements were adopted that are typically used in planning

of small or medium regulation structures, which have turned out to be completely inappropriate in the case of large dams. Here, one should further identify those design elements of the Drtjžšćica dam that should be exposed as a case of engineering practice to be avoided in the future:

- The design of the stilling basin in the trapezoidal cross-section represents in the sense of sustainable planning an added value to the space, while in the hydrotechnical sense it represents a weak point and a latent danger in ensuring the stability and safe operation of the stilling basin and the resulting safety of the entire construction.
- The design of the path of evacuation objects on the Drtjžšćica dam was subordinate to finding a soft transition between the bottom outlet and the river bed downstream, which is why the outflow part of the outlet and the stilling basin are location-wise in a most unfavorable part of the curve, which additionally contributes to the increase of intensity of erosive action in the stilling basin with additionally induced effects in the river bed downstream. When designing the path of the evacuation structures in the hydraulic calculations one should optimize the entire section, including the river bed downstream the outlet, since only in this way could one properly design the structures and security and take into account the natural characteristics of the river bed and the flow downstream of the dam.
- In cases similar to the one discussed in this paper, where the shape of the river bed downstream of the dam cannot be changed significantly, and the impact of the narrowing cannot be reduced completely, the impact of the characteristics of the water regime downstream of the dam must be considered in the model and later in the design of additional measures for the optimization of dam operation in the case of large events, thereby ensuring a higher safety of this and similar structures.

7. REFERENCES

- AGROSKIN, I., I., DIMITRIJEV, G., T., PIKALOV, F., I., 1973. *Hydraulics*, Tehnička knjiga, Zagreb.
- BRIBIESCA, J., L., S., SANCHEZ J.G. 1999. Asymmetric flows in stilling basins with trapezoidal cross-sections, *Dam Engineering*, Vol. 9, No 4.
- HUMAR N., KRYŽANOWSKI A. 2012. The Drtjžšćica case study - restoration of the stilling basin for improvement of hydraulic conditions. 24th *International Congress on Large Dams*, Kioto, pp. 404-418.

Use of gabion structures as flood mitigation in hydraulic works

J. Adamec, L. Lichý

(MACCAFERRI CENTRAL EUROPE s.r.o., Štverník 662, 906 13 Brezová pod Bradlom, Slovakia,
e-mail: jaroslav.adamec@maccaferri.sk, lubos.lichy@maccaferri.sk)

Abstract

In the light of ongoing climate changes and the related increased incidence of floods of different nature confirms the need to invest in flood prevention systems and the need for the application of new, flexible technical resources available within the safety works during the floods. One of the structures, materials and technologies which in the long term prove its suitability for the whole spectrum of possible measures of flood protection are gabion structures.

Keywords

floods, double twisted wire mesh, durability, gabion, mattresses,

1. INTRODUCTION

On the topic of floods are applicable generally known experiences and predictions expressed in the sentence: "Floods have been, they are and will be." Adverse effects of climate change only confirm these truths. (Fig.1)

In the Slovak Republic for the years 1996 - 2005 appeared floods which killed more than 50 people and damages caused by the floods reached the property of citizens, municipalities and state the amount of more than 560 mil. €.

In the year 2010, which can be characterized as a year of extraordinary occurrence of flood damages reached to municipal property about 160 mil. €. 150 mil. € was damage to agricultural and forestry assets, 50 mil. € to property of citizens. The estimated damage could be round up to 500 mil. €.

Endangering the lives and health of the population followed by potentially huge material damages caused by flooding have led the Ministry of Environment to the preparation of strategic documents for planning of the use of EU funds for the programming period 2014 - 2020, major part of this funds will be used also for flood protection. The Operational Program Environmental quality is set as a Priority 2 - Adaptation to the adverse effects of climate change with a focus on flood protection and within investment priority 1 "Promoting investment in climate change adaptation, including the ecosystem approach."

Construction technologies will need to focus on high quality level, in the wider sense of the term, which means ensuring their smooth and reliable operation, high resistance to extreme loads and high requirements to integrate structures into the natural environment, speed of construction and a reasonable prices.



Fig. 1 Floods in Banská Bystrica (SK), 1974 [photo: registry of Central Slovakia Museum Banska Bystrica]

2. FLOOD MITIGATION

Preventing the negative impact of floods or mitigate them is the most significant possible measure for flood protection. These are measures of a technical and biotechnical character that slow river basin runoff into watercourses, increase retention capacity of river basins, create artificial retention areas - thus flatten the course of the flood wave, increase the flow capacity of the river beds of watercourses. The preventive measures include the engineering, planning and administrative provisions relating to flood services, which are not subject of this article.

Concreteness of the technical and biotechnical methods, structures, construction elements, building materials used in emergency and preventive flood protection measures are the result of long-term development and to professional public are generally known. Many of flood mitigation works consist of modification of water flows, streams, technical and biotechnical measures in river basins aimed to increase water retention capabilities and prevent erosion phenomena in the basin and in watercourses, construction of polders, dikes.

All the above measures for flood protection implemented preventive, emergency or are made from different types of structures, materials and different technologies, on which are placed certain specific conditions resulting from the location of installation in watercourses, including environmental requirements.

One of the materials and technologies, which in the long term prove their feasibility for the whole spectrum of possible measures for flood protection are gabion structures.

3. GABION STRUCTURES IN RIVER SECTOR

140 years of experience the Officine Maccaferri company, linked to the scientific research of use of gabion structures on hydraulic works has reached a state that these structures are often used, demonstrating their reliability, stability, durability and ability to fit in the natural environment (Fig. 2).

Gabion is a wire-stone element in the shape of a cube or cuboid, made of hexagonal double twisted wire mesh, filled with natural or quarry stone or suitable recycle. Gabion is formed by bottom and side elements, lid and diaphragms premanufactured in one element. According to the dimensions they can be divided into gabion baskets, mattresses and sack gabions.

Gravity gabion structures are built in a simple modular way, filled directly on the site with suitable aggregates is a way to ensure minimal porosity. Each of the elements must be self-supporting and dimensioned to be stable block.

Objects generally act like gravity structures. Due to this fact one of the main requirements is to reach average density of the finished structure. From gabion baskets it is possible to create almost any shape structure. If keeping in accordance with the design principles it is very durable system, where one of the best features is the ability to blend in with the surrounding natural environment.



Fig. 2 Historical longitudinal gabion wall at river, year 1906 [photo Maccaferri Central Europe]

Major advantage of these structures compared to conventional concrete or reinforced concrete structures is its drainage function, which significantly reduces the water pressures on the structure. Another advantage is that the gabion wall is

able to absorb large deformations without breaking. If deformations are few centimeters, but even tens, the structure still retains its functionality compared to concrete structures, which would no longer withstand the deformation. The use of gabion structures of hexagonal double twisted wire mesh had been from the beginning always historically connected with the function of gravity retaining wall with an emphasis on flexibility and its ability to withstand major deformation thanks to double twisted joints. It is this ability of gabion structures made from double twisted mesh, which has incomparable advantage compared to structures made from welded steel panels, which are vulnerable exactly in the weld points, where mechanical fault appears and is afterwards spreading to the rest of the structure.

3.1 Classic Gabion

It is used to build retaining walls, vertical structures, dams on rivers (Fig. 3, 4). Classic gabion is made of double twisted steel wire mesh with standard wire diameters 2.7 and 3.0 mm with a mesh type 8x10. Originally it was protected only with a simple coating of zinc deposition, today it is considered as the simplest treatment, as minimal standard nowadays is Galmac coating (Zn + 5% Al), which has roughly double durability. A suitable coating for hydraulic application is Galmac + organic PVC coating. The top level is a PA6 coating. An important reference is the [EN 10223-3; 2013] for double twisted steel wire meshes used in civil engineering applications. The norm provides guidance concerning the life expectancy for steel mesh, defining for polymer coated steel wire mesh a minimum assumed life of 120 years.

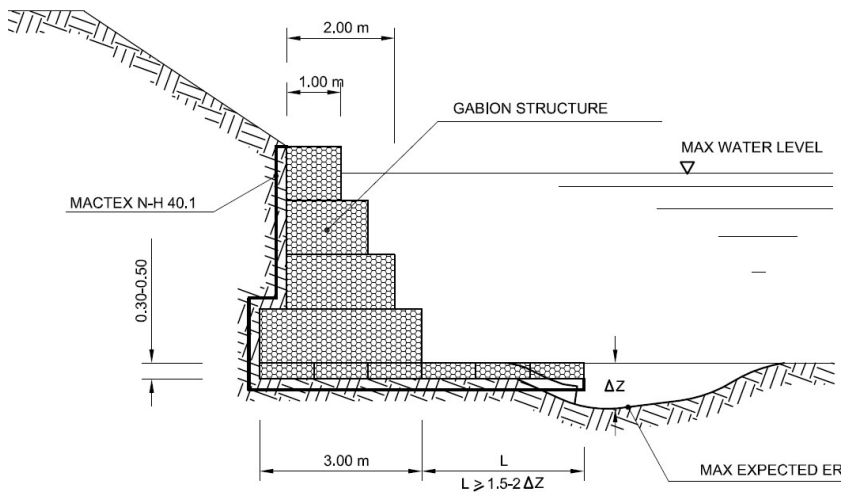


Fig. 3 Example of gabion river wall [photo Maccaferri Central Europe]



Fig. 4 Gabion river wall at Oravský Podzámok, Slovakia

3.2 Sack Gabion

Sack gabions are cylindrical baskets made of hexagonal double twisted wire mesh with a mesh type 8x10, wire diameter 3,0 mm. They are filled of stones directly on the site. They form flexible and permeable structures used for hydraulic applications like protection of toe of the river embankment, groins (Fig. 5) and various emergency works. Sack gabions are supplied with reinforcing steel wires embedded during the manufacturing process to enable ease of its closure during installation.

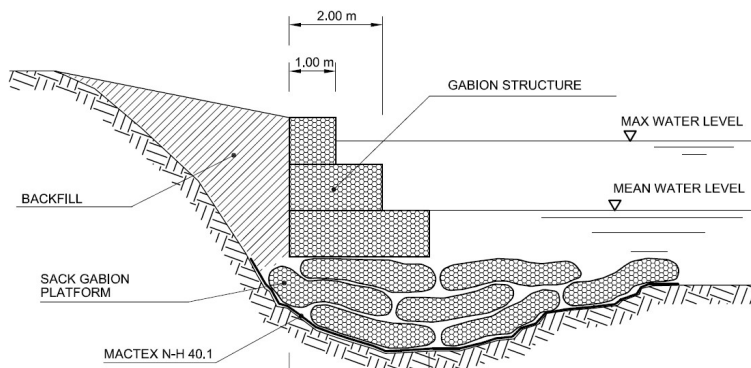


Fig. 5 Example of use of sack gabions with gabion wall [photo Maccaferri Central Europe]

3.3 Gabion SF (Strong Face)

Baskets made of hexagonal double twisted wire mesh, the gabion is divided into cells by diaphragms which are inserted approximately every 1 m. Due to the need for increased abrasion resistance and ensuring higher rigidity of the front face of gabion, the front face is supplied from a mesh type 8x10, wire diameter of 3,9 mm. The coating is Galmac. Gabion SF (strong face) is a patented product of MACCAFERRI, finds its application as retaining walls, in high velocity rivers, dams and other structures in hydraulic sector.

3.4 Gabion mattresses

Baskets whose height is significantly lower than their width and length are called mattress. Their width is typically 2.0 m, length of 3.0 to 6.0 meters, height of the baskets is 17, 23 and 30 cm. RENO mattresses are made from wire diameter of 2.2 mm and a mesh type 6x8. Depending on the required service life and the environment in which they are located, appropriate surface finish has to be selected. Heavy zinc coating, Galmac, Galmac + PVC or the best performance Galmac + PA6. RENO mattresses are manufactured with integrated double diaphragms in order reach better handling, speed of installation and stiffness of mattress. RENO mattresses are used primarily for reinforcing slopes and protecting against erosion (Fig.6). They are suitable and economical substitute for stone rip-rap (Fig.7). Mattresses are filled with stones directly on the site, where they form flexible and permeable structures.

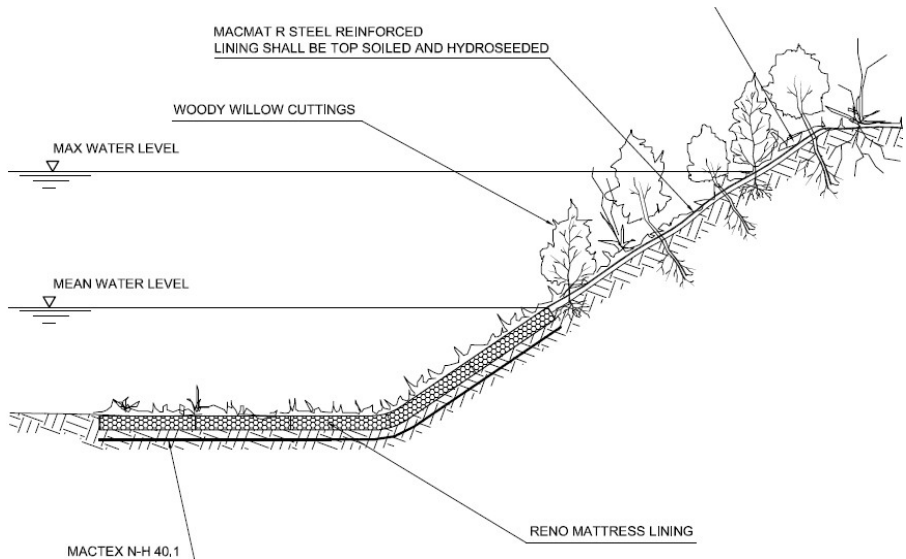


Fig. 6 Example of use of RENO mattresses [photo Maccaferri Central Europe]

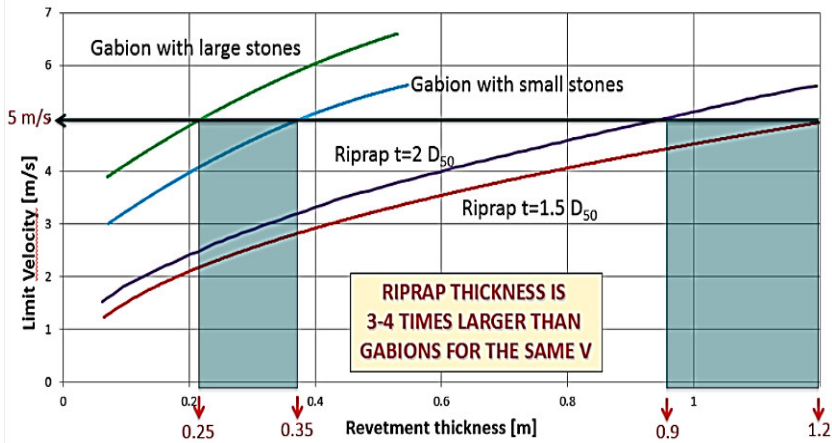


Fig. 7 Gabion lining vs Rip-Rap lining for $v = 5$ m/s flow

3.5 Gabion structures in emergency works

The wire-stone gabion structures in emergency works in time of danger during floods have been used only partially. This is mainly due to the lack of information among the professionals in hydraulic sector in Slovakia, whereas abroad are those structures in such situations commonly used.

Both already described gabions and mattresses are used, but above all newly developed precast and prefilled wire gabions CUBIROCK and high speed assembly multicellular unit FLEXMAC are more often used.

3.5.1 CUBIROCK - prefilled gabion

By modification of the classical gabion for special constructions like emergency works during floods and for situation where quick installation is required, gabion CUBIROCK was created. This gabion is supplied to the affected area already filled with stone, what gives a huge time advantage during emergency works. It is manufactured from robust wire 3,9 mm, which ensures a very good stability and rigidity of unit.

CUBIROCK can be filled in a quarry, or even directly at the installation location on a special vibrating table. In the unit there are mounted certified synthetic lifting straps which make the unit easy to manipulate. Installation of prepared units is very fast, with one group of only three people, one crane and relevant transport capacity (Fig. 8).

The advantage is the high stability of these elements in extreme situations with significantly lower amount of required material and therefore also the cost. For eight hours, it is possible to build more than 200 m³ wall. Further possible

applications of prefabricated gabion is also building provisional bridges, walls or smaller bridge abutments.



Fig. 8 Installation of CUBIROCK gabion [photo Maccaferri Central Europe]

3.5.2 FLEXMAC

FLEXMAC® DT multicellular structure suitable for rapid building of anti-flood barriers and serves as ideal replacement for bagging (Fig. 9, 10). The units are made of double twisted hexagonal mesh type 8x10. The mesh is reinforced by vertical steel rods, lined from inside face with non-woven geotextile with a minimum weight of 250 g/m². The geotextile lining enables FlexMac to be filled with locally available materials such as sand, general fill or other materials. These can be easily placed within the structure using mechanical means or by workers. Units are supplied in bundles and wrapped in plastic for protection during freight and storage.

After temporary use, FlexMac can be folded up and efficiently stored for another emergency. It can be a temporary or permanent solution. When used as a permanent solution after the emergency has passed, it would be covered and re-vegetated in harmony with the environment. The versatility, simplicity and rapid deployment make it ideal for emergency situation.

The great advantage of FlexMac™ DT is clear when compared with traditional sand bags. In 3 hours, 30 people can construct a 10 m embankment using sand bags, compared with 5 people constructing a 60 m embankment using FlexMac units. To deploy and assemble a single unit requires only 2-3 people and 20-30 seconds.



Fig. 9 Filling of FLEXMAC unit [photo Maccaferri Central Europe]



Fig. 10 Application of FLEXMAC system [photo Maccaferri Central Europe]

4. RESUME

Aim of this article was to describe solutions made of hexagonal double twist steel wire mesh and their use in hydraulic sector. Considering the fact that majority of these solution have been on the market for over 100 years, with thousands reference structures, enormous research and development, Maccaferri decided in order to collect all old and new information to create a new book called “Use of gabion in hydraulic sector”.

Manual is aimed to describe basic applications of different solution, determine material characteristics, new forms of coatings and also main design principles.

The manual is a unique tool for designers, clients and all professionals in this sector.

5. REFERENCES

- BS EN 10223-3, 2013. Steel wire and wire products for fencing and netting. Hexagonal steel wire mesh products for civil engineering purposes
- LUKÁČ M., BEDNÁROVÁ, E., 2006. Navrhovanie a prevádzka vodných stavieb, Sypané priehrady a hrádze. JAGA GROUP, s.r.o. Bratislava.
- MACURA, V., HALAJ, P., 2013. Úpravy a revitalizácia vodných tokov, STU Bratislava.
- MINISTERSTVO ŽIVOTNÉHO PROSTREDIA SR, 2014. 3. návrh Operačného programu Kvalita životného prostredia na obdobie 2014-2020. *Available at: <http://www.minzp.sk/služby/moznosti-financovania-projektov/p0-2014-2020/operacny-program-kvalita-zivotneho-prostredia.html>* [6/2015].
- SŇAHNIČAN, J., PODKONICKÝ, L., 2014. Drôtokamenné konštrukcie v systéme ochrany pred povodňami. *In: Inžinierske stavby 2*, 2014, pp 16-19.
- TELIŠČÁKOVÁ, D., 2014. Štyridsať rokov po povodni je Bystrica stále v ohrození. *Pravda.sk. Available at: <http://spravy.pravda.sk/domace/clanok/333672-styridsat-rokov-povodni-je-bystrica-stale-v-ohrozeni/>* [6/2015].

Influence of Genetic Algorithms Parameters on the Optimization of Hydrothermal Coordination Problem

P. Šulek, T. Kinczer, P. Dušička

Department of Hydraulic Engineering, Faculty of Civil Engineering, Slovak University of Technology in Bratislava, Radlinského 11, 810 05 Bratislava, Slovak republic, phone: +421 2 59 274 571, fax: +421 2 59274 565, e-mail: peter.sulek@stuba.sk, tomas.kinczer@stuba.sk , peter.dusicka@stuba.sk

Abstract

At present, Genetic algorithms (GAs) belong to one of the most popular heuristic optimization methods. GAs are used for the solution of many optimization problems in fields of economy and chemistry, as well as many other fields, e.g. energetics, especially when dealing with complex problems of hydrothermal coordination of thermal and hydro plants. Despite the fact that GAs are suitable for the solution of complex large scale optimization problems, the quality of achieved results depends on the so-called GA parameters. The paper describes the influence of GA parameters on the results of the optimization of hydrothermal coordination problem in hydrothermal system consisting of one thermal and one hydro plant.

Keywords

sensitivity analysis, genetic algorithms, hydrothermal coordination, optimization, hydro plant

1. INTRODUCTION

A hydro plant (above 10 MW of installed power) hardly ever operates for individual consumer. It submits the produced energy to single energetic system. In such a system in most cases, hydro plants (HP) function together with thermal plants (TP), the so-called hydro-thermal system. Thus, the operation planning of individual elements of hydro-thermal system must respect the common target defined by the common whole system optimization criterion, the so-called hydrothermal coordination (HTC). HTC is a complex optimization problem, to the solution of which methods of optimal control of systems are used. Except the numerical optimization methods (e.g. linear, or more precisely, nonlinear programming) modern heuristic optimization methods (e.g. genetic algorithms, simulated annealing) are also used. The application of both approaches is often connected with difficulties resulting from the fact that the function expressing HTC problem is characterized by complicated course of surface and several local extremes. In case of large-scale problems, numerical optimizing methods can demonstrate many difficulties (e.g. the so-called „curse of dimensionality“), even though they show high efficiency with less complex problems. Therefore, to solve

the large-scale problems, heuristic methods are more appropriate. *Genetic algorithms* (GAs) are significant representatives of these methods. GAs are algorithmic models inspired by principles of natural selection which can be observed in the nature. Organisms have mechanisms influencing their ability to survive and reproduce, with the result of more perfect organisms. By similar mechanisms, GA searches for the best solution of a problem, i.e. by means of *selection*, *crossover* and *mutation* operators it searches for the most perfect individual, or more precisely, a chromosome (optimal solution) from a population. The evaluation consists of the definition of the so-called *fitness* of given chromosome, which means the value of objective function defining its quality in relation to the optimal solution. GA allows the population created on the basis of aforesaid operators to develop during many generations, gradually excluding individuals with low fitness from the evolution. Combining individuals with higher fitness, chromosome with the highest fitness is obtained. Genes of this final solution represent the searched elements of the vector of the solution, or more precisely, the elements of the matrix of the optimization problem solution. A more detailed description of the method can be found e.g. in [Goldberg 1989]. The possibilities of GA application and solution of HTC problem were published in [Gil et al. 2003], [Šulek and Cipovová 2010], [Troncoso et al. 2008], [Zoumas et al. 2004].

Despite many advantages (the possibility of complexity of the target function form, bigger number of searched variables), GAs also have several disadvantages. The disadvantage of its application is relatively high risk of getting trapped in local extremes and rather complicated definition of penalty functions. Unlike some representatives of common optimizing methods (e.g. simplex method, characterized by certain linearity of solution), results of solutions done by GA often depend on the setting of many parameters. Among some of the basic GA parameters, the following ones can be included:

- N_P – *population size*, i.e. number of individuals (chromosomes) in a generation, given that the first generation of population is generated randomly and represents the initial state of the solution,
- N_G – *maximum number of generations*, i.e. number of generations in which the population evolves, given that the number of individuals in each generation is the same,
- P_{cross} – *crossover probability* of individuals defines the probability of genetic information interchange between two selected individuals (parents) from the population. The result of the crossover of two parents are two offspring. In accessible literature the value of crossover probability $P_{cross} = 0.75$ is recommended.
- P_{mut} – *mutation probability* of an individual defines the probability of mutation of a small part of genotype of a new offspring). The recommended value of the parameter is set in the range 0.05~0.1.

In the next section, the influence of GA parameters setting on achieved results of HTC problem by means of GA in the hydrothermal system comprising of 1 hydro and 1 thermal plant, more precisely from HP Žilina and TP Nováky, is calculated.

2. MATERIAL AND METHODS

2.1 Formulation of HTC problem

The simplest and most general criterion for optimal operation of hydrothermal system (i.e. HTC problem) is to optimize the system payoff (e.g., the total operational cost) while subjected to constraints accompanying this criterion in given time period. It is the so-called *economic dispatch* (ED), where optimal division of load in the system on individual plants is ensured. HTC problem in hydrothermal system composed of 1 VE and 1 TE can be, for 24 hour time period (within so-called *peak shaving method* (PS method)), described with linear objective function

$$F = \sum_{i=1}^{24} Dem_i Q_{HP,i} \rightarrow \max \quad (1)$$

where i is time interval (hour) index, Dem_i the total load demand of hydrothermal system in i -th hour [MW], $Q_{HP,i}$ the discharge through VE Žilina in i -th hour [m³/s] (variables). Values Dem_i can be interpreted also as price evaluation (so-called pricing) of produced electric power.

Note: Linear form of the function describing HTC problem is chosen due to the possibility to compare the results of the solution using GA with the results of solutions obtained by the application of simplex method (SM) which, when given the input parameters, always finds the global extreme of the optimization function.

PS method [Wu et al. 1989], [Wu et al. 1991], [Simopoulos et al. 2007] is based on the condition that the production of electric energy by VE should be allocated in peak parts of system's load curve. The solution of HTC problem using PS method gives satisfactory results particularly with the condition that during the whole planning time period, the same configurations of thermal units with stable convex cost characteristics are available.

2.2 Model of hydrothermal system HP Žilina – TP Nováky

The task of the model (optimization model) was to define economic dispatch for TP Nováky and HP Žilina. Input parameters of the model of hydrothermal system are taken from handling and operating rules of HP and TP and from the real operation of HP Žilina.

Tab 1. Hourly Load Demand Dem_i [MW]

Hour	Load	Hour	Load	Hour	Load	Hour	Load
1	114	7	113	13	136	19	138
2	114	8	119	14	134	20	133
3	114	9	125	15	131	21	130
4	113	10	130	16	132	22	124
5	114	11	136	17	138	23	120
6	113	12	138	18	140	24	114

Parameters of thermo system (TP Nováky - ENO B):

- Maximum power output : 440 MW.
- Minimum power output : 50 MW.

Parameters of hydro system (HP Žilina):

- Number of units : 2 type Kaplan (symmetrical installation).
- Maximum power output : 72 MW.
- Minimum power output : 12 MW.
- Maximum water discharge : 300 m³/s.
- Maximum reservoir storage volume : 3.918 mil.m³.
- Reservoir's initial storage volume: $V_{in}=2.766$ mil.m³.
- Reservoir's final (target) storage volume: $V_{fin}=2.766$ mil.m³.

Tab 2. Inflow to the reservoir forecast [m³/s]

Hour	Inflow	Hour	Inflow	Hour	Inflow	Hour	Inflow
1	65	7	70	13	70	19	80
2	65	8	70	14	70	20	70
3	65	9	70	15	65	21	65
4	70	10	70	16	75	22	65
5	75	11	70	17	90	23	60
6	75	12	70	18	90	24	60

Flow to the biocorridor counts with the value 2.5 m³/s.

The solution of HTC problem (1) is represented by the vector $s=(Q_{HP,1}...Q_{HP,24})$. Values of the elements of the vector s (i.e. operation plan of VE Žilina in one hour range) are the result of the function maximization (1) which must be modified by constraining conditions (2)~(4) based on constraints defined in handling regulation of HP Žilina.

$$0 \leq Q_{HP,i} \leq 300 \quad (2)$$

$$0 \leq V_i \leq 3,918 \quad (3)$$

$$V_0 = V_{in} = 2.766, V_{24} = V_{fin} = 2.766 \quad (4)$$

The water balance for reservoir during hour i is given by:

$$V_i = V_{i-1} - 3600Q_{HP,i} + I_i \quad (5)$$

where V_i is reservoir storage volume at the end of an hour i [m^3], I_i is inflow rate including the evaporation losses, leakage and other non-energy withdrawals [m^3].

GA application

In general, GAs solve non-constrained optimizing problems. In case of their application for HTC problem solution, the target function (1), the so-called fitness function must be adjusted to constrained form. One of the most common ways of its transformation is the penalty function when fitness function and its limits are transformed into the pseudo fitness function. When solving the maximization of the function (1), the pseudo fitness function can be written as follows

$$\varphi = \underbrace{\sum_{i=1}^{24} Dem_i Q_{HP,i}}_{Fitness} - W_{pen} \underbrace{\left(s_1 \frac{pen_1(\cdot)}{\max(pen_1(\cdot))} + s_2 \frac{pen_2(\cdot)}{\max(pen_2(\cdot))} \right)}_{Penalization} \rightarrow \max \quad (6)$$

$$pen_1(V_i, 0) = \begin{cases} \sum_{i=1}^{N_1} (0 - V_i)^2 & | V_i < 0 \\ 0 & | V_i \geq 0 \end{cases} \quad (7)$$

$$pen_2(V_{24}, 2.766) = \begin{cases} \sum_{i=1}^{N_2} (V_{24} - 2.766)^2 & | V_i < 2.766 \\ 0 & | V_i \geq 2.766 \end{cases} \quad (8)$$

where $pen_{1,2}$ are penalty functions expressing limits (3) and (4), W_{pen} is penalty weighting factor and $s_{1,2}$ are stringency factor for the violation of the constraints. By means of mutual proportion of individual factors, it is possible to “tighten” or “loosen” individual limits of the task. Constraint (2), i.e. limits of variable $Q_{HP,i}$ are defined as lower and upper boundary of the interval from which GA can select individual genes (elements of the vector of the solution \mathbf{s}).

If the strictness of observing the boundaries in the equation (6) is the same for all constraints (e.g. $s_1=s_2=1$), the value of penalty weighting factor W_{pen} significantly influences the process of selection of the most fit individual (optimal solution). It is a complex problem to set the value W_{pen} and sometimes multicriteria approach is used. The value W_{pen} should be set in such way that the

pseudo fitness function φ never reaches the value greater than the global maximum F_{max} . That means that each solution which does not observe the constraints shall be penalized in such way that it should be worse than the solution which observes the constraints. This can be ensured by sufficiently high value of W_{pen} . However, penalty which is too high can cause early convergence of the solution. In Fig. 3, typical course of pseudo fitness function (6) by means of GA for three values $W_{pen}=10^9$, 10^{10} and 10^{11} is calculated. Individual (optimal solution) was let to develop in a population of 5000 individuals in 1000 generations. Values $P_{cross}=0,75$ and $P_{mut}=0,02$ are values recommended in the literature. From the results of the simulation it is evident that with the lowest value of W_{pen} , the solution converges to the “false” optimum. The achieved value F_{max} is higher than the value of real global maximum, i.e. $F_{max}=233\ 052$ (value solved by simplex method), what is caused by not observing the condition $V_{Z24} \geq 2.766$. With the highest value W_{pen} all constraints are observed. However, the solution too early converges to the value lower than the real maximum. The best result for the given set of inputs is achieved for $W_{pen}=10^{10}$, by which all constraints are observed and at the same time, the value of the solution is the closest to the real maximum. For this reason, in next calculations, the value of penalty weight is $W_{pen}=10^{10}$.

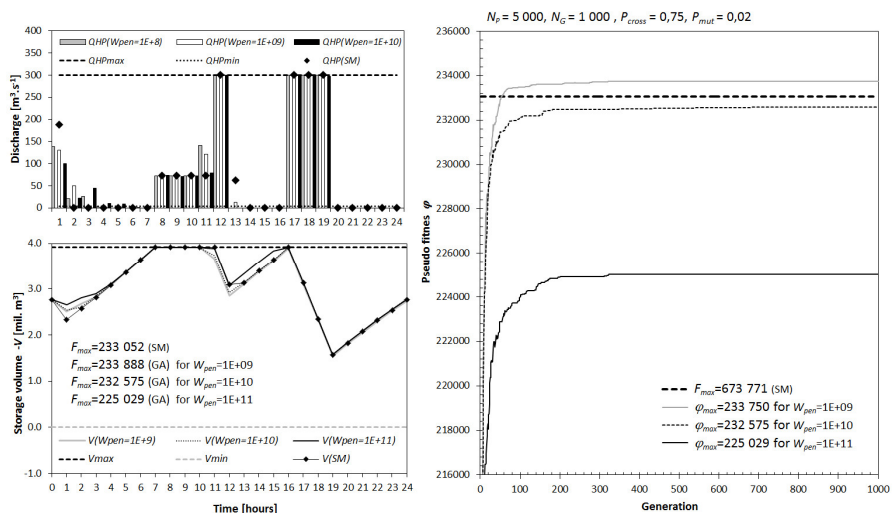


Fig. 3 Influence of penalty weighting factor W_{pen} on the results of pseudo function maximization

Based on the aforesaid relations according to the flow chart in Fig. 4, optimizing model of hydrothermal system HP Žilina – TP Nováky integrating *dll* file with GA, which forms part of the product Genetic Server by NeuroDimension Systems, Inc., was formed, using the programming language Visual Basic. The

result of the solution of HTC problem (1) is then represented by the vector $^{FIN}s=(Q_{HPi})_{24}$, i.e. the best individual from the final population.

By means of the optimization model, sensitivity analysis of the influence of population size N_p , crossover probability P_{cross} and mutation probability P_{mut} on the results of HTC problem solution in hydrothermal system HP Žilina – TP Nováky was performed.

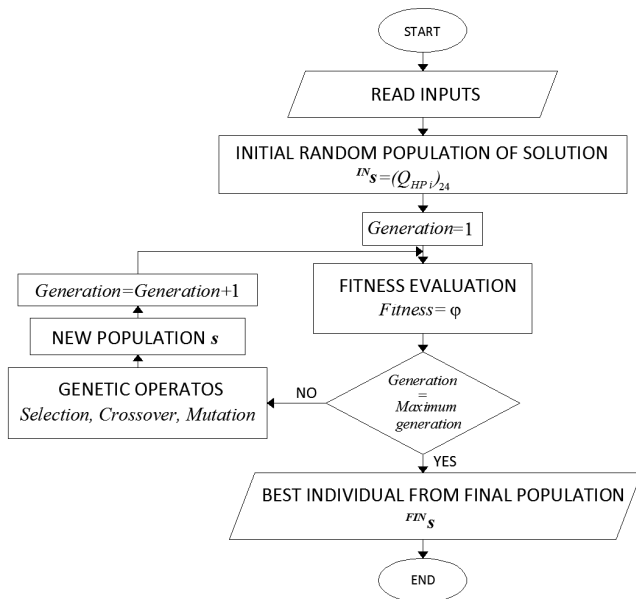


Fig. 4 Flow chart of the GA simulation

3. RESULTS OF SENSITIVITY ANALYSIS

3.1 Population size

The results of sensitivity analysis of the influence of GA population size N_p on the results of pseudo fitness function maximization (6) are displayed in Fig. 5. Achieved values of maxima of pseudo fitness functions represent the average of 50 GA simulations for each value N_p . Simulations in which not all requested constraints were observed were excluded from the evaluation. From the evaluation it is evident that satisfactory results can be achieved by values $N_p=2000$ and higher approximately in 1000th generation. In the following generations, no significant improvement of solution arises; only the simulation time is longer.

3.2 Crossover and mutation probability

In Fig. 6, the influence of crossover probability P_{cross} and mutation probability P_{mut} on achieved values of maxims of pseudo fitness function φ calculated by the average of 50 GA simulations for all combinations P_{cross} and P_{mut} is calculated. Simulations in which not all requested constraints were observed were excluded from the evaluation. The results clearly demonstrate that the value P_{mut} has more significant influence on the final solution than the value P_{cross} . Optimal results are reached approximately with the value $P_{mut}=0,05$. The influence of the value of crossover probability on the results was not proven. According to many authors, the crossover operator is often subject of opposing opinions, as well as the subject of the question if it should be used at all, since for some members of Academia it bears a certain undertone of sex. The opponents of crossover consider it as the “breaker” of promising individuals and use the crossover operator in the same way as mutation with very little probability.

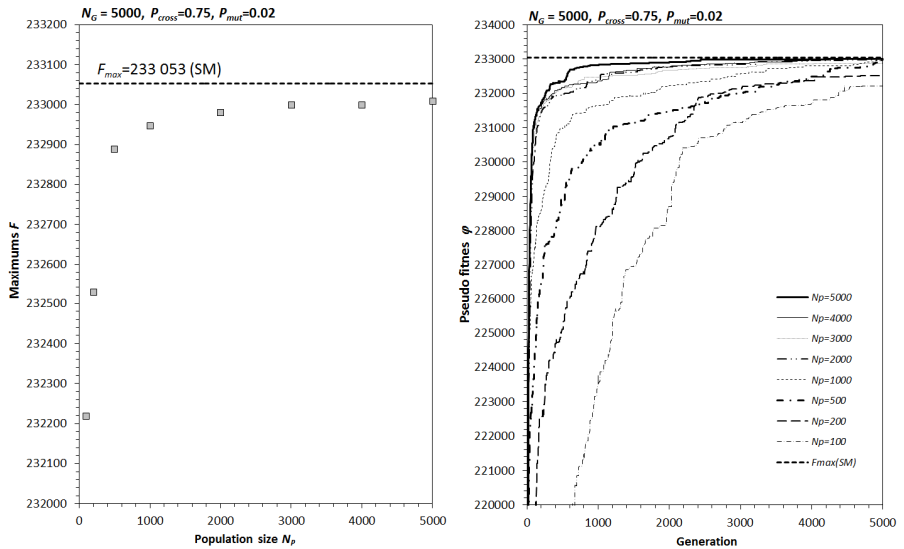


Fig. 5 Influence of population size on results of pseudo fitness function maximization

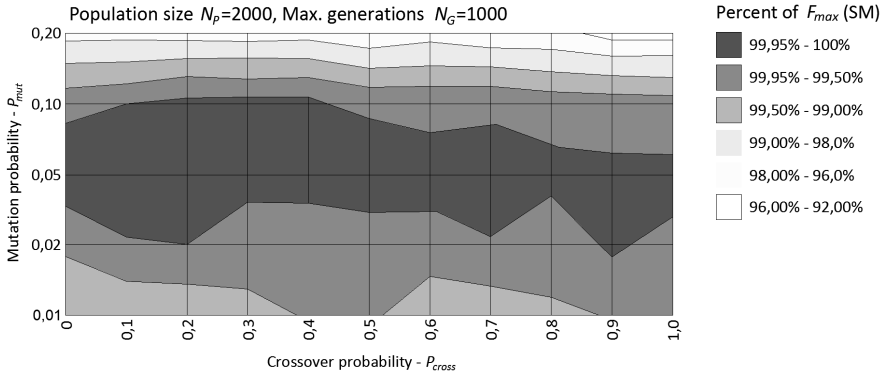


Fig. 6 Influence of P_{cross} and P_{mut} on results of pseudo fitness function maximization

4. DISCUSSION AND CONCLUSIONS

The paper contains results of the research of the influence of GA parameters on the optimization of HTC problem in hydrothermal system with on hydro plant and one thermal plant. The target function describing HTC problem was adjusted and solved in linear form (1) in order to compare the results of the solution using GA with the results of solutions obtained by the application of simplex method which, when given input parameters, always finds global extreme of the optimization function. For the given set of inputs, the influence of individual GA parameters on 50 simulations was evaluated as follows:

- with the parameter **population size** N_P , satisfactory results were achieved with the values $N_P=2000$ and higher approximately in 1000th generation, while in the following generations no significant improvement of solution arises; only the simulation time is longer,
- with the parameter **crossover probability** P_{cross} and **mutation probability** P_{mut} from the results of sensitivity analysis clearly demonstrate that the value P_{mut} has significantly greater impact on the resulting solution as the value P_{cross} , while the results approaching the global maximum of the solution the most were reached approximately with the value $P_{mut}=0.05$. The influence of values of crossover probability was practically not demonstrated. Results attained by sensitivity analysis proved that for given set of inputs, GA demonstrates the highest efficiency with the parameters close to parameters recommended in literature (i.e. $P_{cross}=0.75$ and $P_{mut}=0.05\sim 0.1$).

5. REFERENCES

- GIL, E., BUSTOS, J., RUDNICK, H., 2003. Short-term hydrothermal generation scheduling model using a genetic algorithm. *IEEE Trans Power Syst.* 18(4), pp. 1256–64.
- GOLDBERG, D., E., 1989. Genetic Algorithms in Search. *Optimization and Machine Learning*, New York, Addison-Wesley.
- SANTOS, J., M., 2008. Evolutionary techniques applied to the optimal short-term scheduling of the electric power production. *European Journal of Operational Research* 185, pp.1114–1127.
- SIMOPOULOS, D., N., KAVATZA, S., D., VOURNAS, C., D., 2007. An enhanced peak shaving method for short term hydrothermal scheduling. *Energy Conversion and Management* 48, pp. 3018–3024.
- ŠULEK, P., CIPOVOVÁ, K., 2011. Heuristic optimization methods for hydro plants generation scheduling. *In: Current events in hydraulic engineering. - Gdańsk: Wydawnictwo Politechniki Gdańskiej*, ISBN 978-83-7348-375-0. pp. 266-276.
- TRONCOSO, A., MARTINEZ-ALVAREZ, F., RIQUELME, J., C., AGUILAR-RUIZ, J., S., 2008. LBF: A Labeled-Based Forecasting Algorithm and Its Application to Electricity Price Time Series. *In: Eighth IEEE International Conference on Data Mining, 2008*, pp. 453 – 461.
- WU, R., N., LEE, T., H., HILL, E., F., 1989. An investigation of the accuracy and the characteristics of the peak-shaving method applied to production cost calculations. *IEEE Trans Power Syst.* 4(3), pp. 1043c9.
- WU, R., N. - LEE, T., H. - HILL, E., F., 1991. Effect of interchange on short-term hydrothermal scheduling. *IEEE Trans Power Syst.* 6(3), pp. 1217–23.
- ZOUMAS, C., E., BAKIRTZIS, A., G., THEOCHARIS, J., B., PETRIDIS, V., 2004. A genetic algorithm solution approach to the hydrothermal coordination problem. *IEEE Trans Power Syst.* 19(2), pp. 1356 – 1364.

Application of artificial intelligence methods in solving problems of hydrotechnics.

S. Kelčík, R. Květon

(Radlinského 11, 810 05 Bratislava 1, radomil.kveton@stuba.sk, stanislav.kelcik@stuba.sk)

Abstract

Aim of the article was to create essential elements of an expert system (ES) that provides effective support for a dispatching control of Water work Gabčíkovo – Nagymaros (SVD-GN). Solution of this problem was focused on reaching maximal operation safety of SVD-GN during flood discharges. The thesis resulted in parts of an expert system that consists of an inference engine, database and knowledge base during flood discharges for supporting the dispatching control of the Water work Gabčíkovo – Nagymaros (SVD-GN). The operation parameters of SVD-GN are a part of the external database including structure operation and prepared manipulation of discharge through SVD-GN. From steering matrix which was generated before, it is possible to provide the dispatcher with aggregate information from database and knowledge base. Dispatcher is also provided with information about expected impact of intended manipulation on operation parameters of SVD-GN along with information about possibilities and its real feasibility on structures of SVD-GN.

Keywords

Expert system, Water work Gabčíkovo – Nagymaros, dispatching control support

1. INTRODUCTION

With the increasing complexity of water structures (WS) and with the growing volume of input data there is increasing demand on the management of these water structures. Therefore, the question is, whether some of the dispatching decisions could be move to the automated management systems or provide increased support of the dispatching decisions.

The use of tools and procedures of the **Artificial intelligence** (AI) is nowadays increasingly applied while addressing not only theoretical, but mainly practical technical problems. Typical areas in hydrotechnics are the tasks associated with the optimization of the operation of WS in normal operation and with the increase of the operational safety of WS in special cases. Considerable attention is therefore address to the problems of acquisition, representation and to the use of special, expert knowledge. Based on this, **expert systems (ES)**, whose strength lies precisely in the quality and scope of knowledge were created.

Expert systems consist of (Fig. 1):

- Knowledge Base – contains the knowledge and experience of experts, contained for example in an operational regulation in water works.
- Data Base – all data to the given case, not only historical but also hypothetical, which are obtained for example by means of modelling research or mathematical modelling (MM).
- Inference Engine – its role is to effectively manage a process of information usage and data databases in order to resolve particular task in optimal and especially safe way.

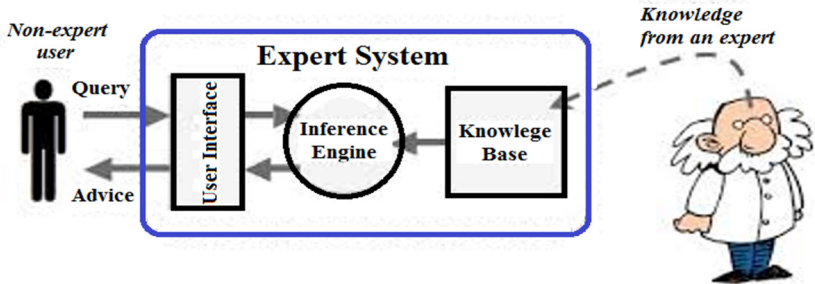


Fig. 1 Diagram of a standard expert system (<http://www.igcseict.info>)

The module, which links variable external interfaces, is missing in the system defined like this. The Diagram of the extended expert system with the integrated contact with the external interfaces is shown on the figure below (Fig. 2).

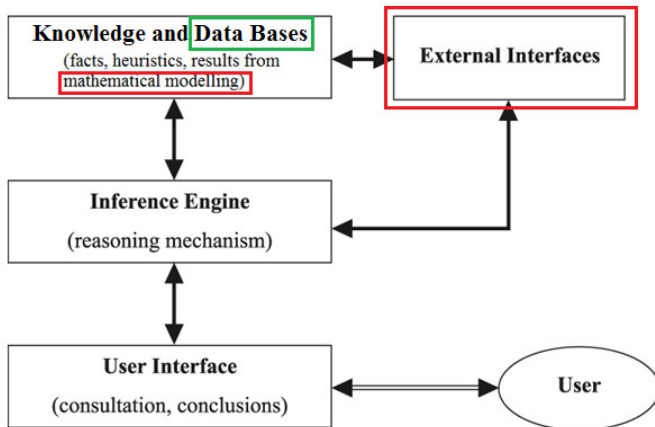


Fig. 2 Diagram of an extended expert system (expertsystem101.weebly.com)

External interfaces may provide:

- Results of external measurements from water works.

- Derived data, such as water flow or slope of water.
- Information on an operating status of WS on the water works.
- The prognosis of the development of the major hydraulic characteristics of the water flow, such as potential increase in flood flows (forecasting service of the Slovak Hydrometeorological Institute).

Expert system can provide through the external interfaces information for the autonomous control systems installed on the water facilities, information on implemented and upcoming changes in the water flow below WS for the central management authorities established by the state – Flood Commissions.

2. THE AIM OF THE PAPER AND ADDRESSED TASKS

The aim of the article is to establish essential elements of an expert system ensuring the efficient support of the dispatching management of the water work Gabčíkovo – Nagymaros (SVD-GN) reaching the maximum operation safety during flood flows. To achieve this goal a set of tasks was addressed and solved:

- The hydraulic analysis of the flood wave in 2013 (2002).
- Modeled section of the Danube, Devín – Medved'ov was divided into two separate modeled areas – area above the WS and WS itself.
- Creation of the models, their calibration and application on selected areas. Analysis of the WS of SVD-GN operated during the flood flows, digitalization of the operational parameters from operation manual and creation of the tools for providing of the operational data derived from the WS.
- Generation of the various operational scenarios to the knowledge base for the flood flows from $Q = 6\ 100$ to $11\ 100$ (more than Q_{100}) $\text{m}^3 \cdot \text{s}^{-1}$.
- Development of tools for a multivariate search and interpolation in various scenarios.

3. THE AREA OF INTEREST

The area of interest in the application of AI methods for the needs of navigation of the flood flows through the SVD-GN can generally be divided into 2 parts (Fig. 3):

- Area A – above the SVD-GN, from the profile where the measurements of the water level takes place to the profile above the SVD-GN. In this section the transformation of the flood wave is assumed. It also serves as an entry flow to the B area.
- Area B – the SVD-GN itself, which consists of the WS and their interconnection, which define their interaction.

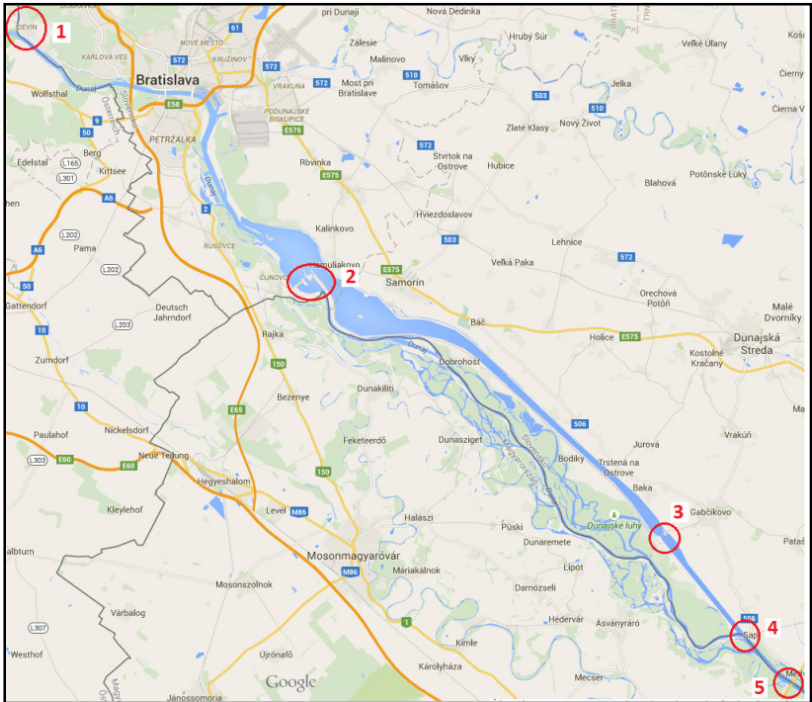


Fig. 3 The area of interest for the application of AI methods (source www.google.sk/maps/)

For the calculation purposes the area was divided into two models (Fig. 4):

- Model of the area A, implemented in HEC-RAS environment.
- Model of the area B, HDM 2012, model developed to address the hydraulic tasks of the operation of channel hydroelectric power stations. Version 2002 of the model was successfully implemented to address the challenges of the channel hydroelectric power stations on the river Váh as well as in the addressing the subtasks for the SVD-GN. The great advantage of the HDM compared to the modelling environment of HEC-RAS is that it has directly integrated WS (such as hydropower plant), which are not available in HEC-RAS.

The dominant facility is the Gabčíkovo hydroelectric power plant (VEG). During the standard water flows, its main task is to effectively use the flow in the Danube to generate electricity and to ensure the navigation on the Danube through two navigation chambers. During the flood situations its task is to navigate the water flows through the eight turbines in power mode until the head on VEG is at least 13m. Then the turbines are shut down and decrease of the flow is replaced with the flow through the navigation chambers.

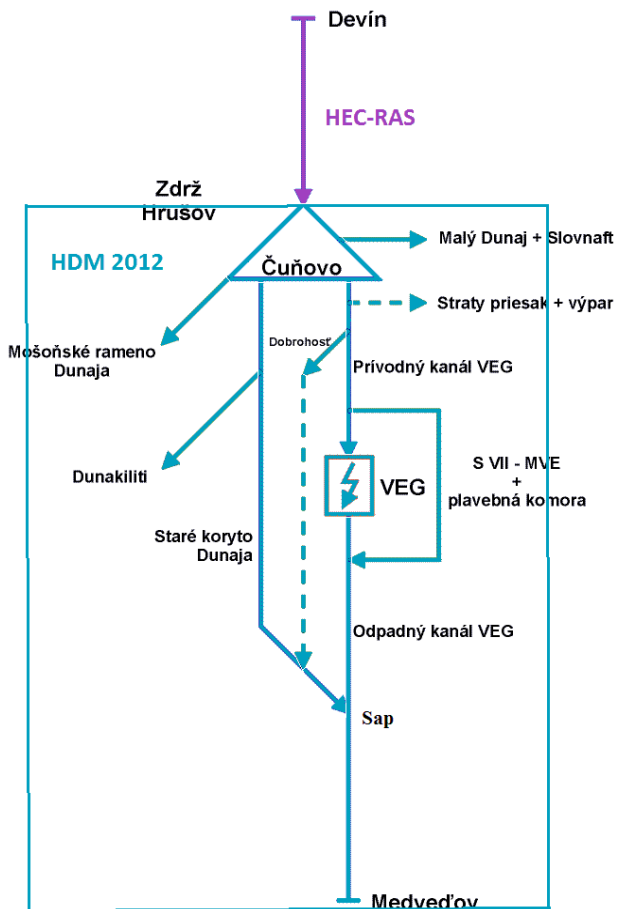


Fig. 4 Hydraulic diagram of the area of interest A and application of mathematical models

4. ANALYSIS OF THE WATER STRUCTURES

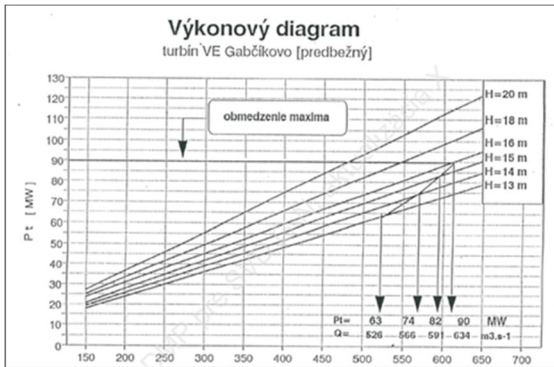
For the purpose of an obtaining the relevant data to the database and knowledge base of ES, the analysis of the WS of SVD-GN was conducted in order to digitize operating parameters of the objects involved in the navigation of the water flows through the SVD-GN and to create tools for the inference engine of ES.

The main operating parameters of VEG are shown in the table (Tab. 1Tab.). Figure 5 shows data digitization process and the setting of a specific possible minimum and maximum flow through the VEG allowing the insertion of these data into the database of ES and for inference engine of ES to gain the flow capacity for a particular head at VEG. The inference engine of ES had an access to the data of

the minimum and maximum flow through a single turbine, as well as the maximum and minimum available flow through all turbines for particular head.

Tab. 1 VEG main operating parameters

VEG	IX. DMP	X. DMP	units
number of TG	8		[pcs]
Type	kaplan 4-K-15G		
Installed capacity	90 x 8 = 720	90 x 8 = 720	[MW]
Absorption capacity	413 to 636	413 to 636	[m ³ .s ⁻¹]
max. upper water stage	131.1	131.1	[m a.s.]
min. upper water stage	128.5	128.5	[m a.s.]
min. upper water stage during state of emergency	128.2	128.2	[m a.s.]
min. usable head	13	13	[m]
min. possible head (in case of emergency)	12.5	12.88 (12,70)	[m]



H [m]	Q _{min} [m ³ .s ⁻¹]	P _{min} [MW]	Q _{max} [m ³ .s ⁻¹]	P _{max} [MW]
20		78	480	90
18	413	68	545	90
16	413	62	634	90
15	413	57	591	82
14	413	54	566	74
13	413	51	526	63

VEG	number of TG		H	1 turbine		Q _{VEG}	
	Inst.	operating	head	min Q _{tur}	max Q _{tur}	min Q _{VEG}	max Q _{VEG}
units	[pc]	[pc]	[m]	[m ³ .s ⁻¹]	[m ³ .s ⁻¹]	[m ³ .s ⁻¹]	[m ³ .s ⁻¹]
	8	4	13.25	413	536	1652	2144

Fig. 5 The digitization of the data from the VEG turbines power diagram and the determining of the specific flow

5. GENERATION OF THE STEERING MATRIX

Filling out the ES databases with the steering matrix data ensures efficient support for dispatching control of the SVD-GN. Data for the various scenarios were based on the operation manual and supported with the practical experience from the flood in the year 2013. The result is steering matrix with 11 x 5 vectors of hydraulic parameters in the decisive sections of the SVD-GN. The demonstration of the

steering matrix for the flows $Q_C = 6100 \text{ m}^3 \cdot \text{s}^{-1}$ and $Q_C = 11100 \text{ m}^3 \cdot \text{s}^{-1}$ are shown in tables Tab. 2 and Tab. 3

Tab. 2 Cross section of the steering matrix for $Q_C = 6100 \text{ m}^3 \cdot \text{s}^{-1}$

Q_C [$\text{m}^3 \cdot \text{s}^{-1}$]		Stupeň Čunovo			Stupeň Gabčíkovo			Sap	Medved'ov	
Staré koryto [$\text{m}^3 \cdot \text{s}^{-1}$]	VEG [$\text{m}^3 \cdot \text{s}^{-1}$]	Hl. horná [m n.m.]	Hl. dolná [m n.m.]	Spád [m]	Hl. Horná [m n.m.]	Hl. dolná [m n.m.]	Spád [m]	Hladina [m n.m.]	Hladina [m n.m.]	Q [$\text{m}^3 \cdot \text{s}^{-1}$]
2100.00	4000.00	131.10	125.62	5.48	130.62	115.63	14.99	115.43	114.69	6100.00
2600.00	3500.00	131.10	126.10	5.00	130.74	115.63	15.11	115.44	114.69	6100.00
3100.00	3000.00	131.10	126.56	4.54	130.83	115.63	15.20	115.45	114.69	6100.00
3600.00	2500.00	131.10	127.00	4.10	130.89	115.63	15.26	115.46	114.69	6100.00
4100.00	2000.00	131.10	127.42	3.68	130.95	115.63	15.32	115.47	114.69	6100.00

Tab. 3 Cross section of the steering matrix for $Q_C = 11100 \text{ m}^3 \cdot \text{s}^{-1}$

Q_C [$\text{m}^3 \cdot \text{s}^{-1}$]		Stupeň Čunovo			Stupeň Gabčíkovo			Sap	Medved'ov	
Staré koryto [$\text{m}^3 \cdot \text{s}^{-1}$]	VEG [$\text{m}^3 \cdot \text{s}^{-1}$]	Hl. horná [m n.m.]	Hl. dolná [m n.m.]	Spád [m]	Hl. horná [m n.m.]	Hl. dolná [m n.m.]	Spád [m]	Hladina [m n.m.]	Hladina [m n.m.]	Q [$\text{m}^3 \cdot \text{s}^{-1}$]
7100.00	4000.00	131.10	129.56	1.54	130.62	119.01	11.61	118.75	117.69	11100.00
7600.00	3500.00	131.10	129.86	1.24	130.74	119.01	11.73	118.76	117.69	11100.00
8100.00	3000.00	131.10	130.15	0.95	130.84	119.01	11.83	118.77	117.69	11100.00
8600.00	2500.00	131.10	130.42	0.68	130.93	119.01	11.92	118.78	117.69	11100.00
9100.00	2000.00	131.10	130.69	0.41	130.99	119.01	11.98	118.79	117.69	11100.00

Tab. 4 Interpolation of the steering matrix for particular rate $Q_C = 9250 \text{ m}^3 \cdot \text{s}^{-1}$

Q_C [$\text{m}^3 \cdot \text{s}^{-1}$]		Stupeň Čunovo			Stupeň Gabčíkovo			SAP	Medved'ov	
Staré koryto [$\text{m}^3 \cdot \text{s}^{-1}$]	VEG [$\text{m}^3 \cdot \text{s}^{-1}$]	Hl. Horná [m n.m.]	Hl. dolná [m n.m.]	Spád [m]	Hl. horná [m n.m.]	Hl. dolná [m n.m.]	Spád [m]	Hladina [m n.m.]	Hladina [m n.m.]	Q [$\text{m}^3 \cdot \text{s}^{-1}$]
5250.00	4000.00	131.10	128.30	2.80	130.62	117.87	12.75	117.66	116.69	9250.00
5750.00	3500.00	131.10	128.66	2.44	130.74	117.87	12.87	117.66	116.69	9250.00
6250.00	3000.00	131.10	129.02	2.08	130.84	117.87	12.97	117.66	116.69	9250.00
6750.00	2500.00	131.10	129.34	1.76	130.93	117.87	13.05	117.66	116.69	9250.00
7250.00	2000.00	131.10	129.65	1.45	130.99	117.87	13.12	117.66	116.69	9250.00

Exceed of the critical rates of the operational parameters in individual scenarios is color-coded. For example in table 4, the decrease of the head on the VEG below the 12,88 m (the defined level for the short-term decrease of the minimal rate of the head) is marked with the color red. With the orange the decrease of head on the interval of 12.88-13 m is marked.

5.1 Multivariate data interpolation in a steering matrix

ES inference engine allows us in the first interpolation to generate the section of steering matrix for the particular inflow $Q_C = 9250 \text{ m}^3 \cdot \text{s}^{-1}$ (Tab. 4). In the second step the calculation for the particular basic parameters $Q_C = 9250 \text{ m}^3 \cdot \text{s}^{-1}$ and $Q_{VEG} = 2800 \text{ m}^3 \cdot \text{s}^{-1}$ (Tab 5) was made.

Tab. 5 Interpolation of the steering matrix for particular flow $Q_{VEG} = 2\ 800\ m^3.s^{-1}$

Q_C [$m^3.s^{-1}$]	9250	Stupeň Čunovo			Stupeň Gabčíkovo			SAP	Medveďov	
Staré koryto [$m^3.s^{-1}$]	VEG [$m^3.s^{-1}$]	Hl. Horná [m n.m.]	Hl. dolná [m n.m.]	Spád [m]	Hl. horná [m n.m.]	Hl. dolná [m n.m.]	Spád [m]	Hladina [m n.m.]	Hladina [m n.m.]	Q [$m^3.s^{-1}$]
6450	2800	131.10	129.15	1.95	130.88	117.87	13.01	117.66	116.69	9250

5.2 Interconnection between the data from the steering matrix with the ES databases

Cross connection of the results from steering matrix with the knowledge base gives an user the data on the main operating parameters on the WS SVD-GN. It also provides the data on the possibility of implementation of the required flow on the individual facilities SVD-GN.

In the Tab. 6, the data from the steering matrix $Q_C = 9\ 400\ m^3.s^{-1}$ and $Q_{VEG} = 2\ 100\ m^3.s^{-1}$ are shown. These data are further used for the dispatching decisions.

Tab. 6 Data obtained from the steering matrix for $Q_C = 9\ 400\ m^3.s^{-1}$ and $Q_{VEG} = 2\ 100\ m^3.s^{-1}$

$Q_{Devin} - Q_{Str}$ [m ³ /s]	9400	Stupeň Čunovo			Stupeň Gabčíkovo			SAP	Medveďov	
Staré koryto [$m^3.s^{-1}$]	Q_{VEG} [$m^3.s^{-1}$]	Hl. Horná [m n.m.]	Hl. Dolná [m n.m.]	spád [m]	Hl. Horná [m n.m.]	Hl. Dolná [m n.m.]	spád [m]	Hladina [m n.m.]	Hladina [m n.m.]	Q [m ³ .s ⁻¹]
5400,00	4000,00	131,10	128,41	2,69	130,62	117,97	12,65	117,75	116,77	9400,00
5900,00	3500,00	131,10	128,77	2,33	130,74	117,97	12,78	117,75	116,77	9400,00
6400,00	3000,00	131,10	129,12	1,98	130,84	117,97	12,88	117,75	116,77	9400,00
6900,00	2500,00	131,10	129,44	1,66	130,93	117,97	12,96	117,75	116,77	9400,00
7400,00	2000,00	131,10	129,74	1,36	130,99	117,97	13,02	117,75	116,77	9400,00
7300	2100	131,10	129,68	1,42	130,98	117,97	13,01	117,75	116,77	9400

The submatrix in table 6 gives us the instructions, on which interval of the flow through VEG should we look for the solution of the problem for the redistribution of the flow through the SVD-GN (between 2000 and 2500 $m^3.s^{-1}$) with the preferred energy use using existing hydro potential on VEG.

Required flow $Q_{VEG} = 2\ 100\ m^3.s^{-1}$ may only be transferred through the turbine flow with 4 or 5 TG (Table 7 marked with green).

Tab. 7 The feasibility of the flow through the facilities of the VEG

Number of Turbines	H	Q _{min}	Q _{max}	Q	implementability
[pc]	[m]	[m ³ .s ⁻¹]			
1	13,01	413	526,40	2100	0
2	13,01	826	1052,80	2100	0
3	13,01	1239	1579,20	2100	0
4	13,01	VEG	2105,60	2100	1
5	13,01	2065	2632,00	2100	1
6	13,01	2478	3158,40	2100	0
7	13,01	2891	3684,80	2100	0
8	13,01	3304	4211,20	2100	0

Chambers					
installed	operating	Upper stage	Q _{I,PLK}	ΣQ	implementability
[pcs]		[m a.s.]	[m ³ .s ⁻¹]		
2	1	130,98	1288,9	1288,9	1

Bypasses of the chambers					
installed	operating	H	Q _{I,obt}	ΣQ	implementability
[pcs]		[m]	[m ³ .s ⁻¹]		
2	1	13,01	612,1	612,1	1

Tab. 8 The feasibility of the flow through the facilities on the Čunovo level

Central weir				
Weir sections	operating	Upper stage	ΣQ	implementability
[pcs]		[m a.s.]	[m ³ .s ⁻¹]	
3	3	131,10	3960	1

Weir in by-pass				
Weir sections	operating	Upper stage	ΣQ	implementability
[pcs]		[m a.s.]	[m ³ .s ⁻¹]	
4	4	131,10	1418,2	1

Weir in inundation					
Weir	operating	Upper stage	Q _{1pole}	ΣQ	implementability
[pcs]		[m a.s.]	[m ³ .s ⁻¹]		
20	20	131,10	244,2	4883,7	1

Water power station Čunovo					
turbines	operating	H	Q _{1tur}	ΣQ	implementability
[pcs]		[m]	[m ³ .s ⁻¹]		
4	4	1,42	100	400	0

ΣQ _c	10261,9	[m ³ .s ⁻¹]
-----------------	---------	------------------------------------

Alternative solution is to navigate the flow through the navigation chambers and bypasses of the navigation chambers, however they only have maximum capacity of $1\,901\text{ m}^3\cdot\text{s}^{-1}$ (one navigation chamber is out of service). For this reason, it is not possible to completely replace the outage of the turbine flow with the flow through the navigation chambers and bypasses of the navigation chambers while the decrease of the head on VEG is below the 13 m. The desired flow $Q_{SK} = 7\,300\text{ m}^3\cdot\text{s}^{-1}$ may be transferred through Central weir and Weir in inundation (Table 8). Weir in by-pass does not need to be open yet. On the Čunovo hydropower plant minimum head of 3,5m was not reached and for this reason it was not possible to implement the turbine flow through the hydroelectric power plant. Mentioned solution of making decision based on the steering matrix and the knowledge base together with the data from ES was developed and tested in Microsoft Excel spreadsheet.

6. CONCLUSIONS

This work outlines the proposal and the creation of the essential elements of the expert system to support the dispatching management of the SVD-GN during flood flows through the water structures with the concrete application on the SVD-GN. Implemented procedures can be applied on any other water structures. However when applying procedures mentioned above on another water structures, the complex questions addressed in this paper also need to be answered. The steering matrix system is completely universal and does not depend on any mathematical model of the water structures.

7. REFERENCES

- DUŠIČKA, P., KVĚTON, R.: Hydrodynamický model VE Gabčíkovo. In 10 rokov prevádzky VE Gabčíkovo : Gabčíkovo, 2002, s. 285--291.
- KAMENSKÝ, J., KVĚTON, R.: Hydrologické a hydraulické aspekty protipovodňovej ochrany : časť 1 - Povrchové vody v tokoch/Hydroinformatika, 2007.
- KVĚTON, R.: Matematické modelovanie prúdenia vody v otvorených korytách. Bratislava: Nakladateľstvo STU, 2012. ISBN 978-80-227-3810-1.
- KVĚTON, R., ORFÁNUS, M.: Hydroinformatika. Skriptá. Slovenská technická univerzita v Bratislave. Pripravené na publikovanie 2015
- PALKOVIČOVÁ, A., KVĚTON, R., MOŽIEŠIK, L.: Mathematical modelling of extreme changes in flow mode to the water work Gabčíkovo. In WMHE, Proceedings of the 13th Intern. Symposium. Bratislava, 2013 s. 197-210.
- VV, š.p.: Dočasný manipulačný poriadok pre sústavu vodných diel Gabčíkovo-Nagymaros na území Slovenskej republiky Aktualizácia X. 2015
- VV, š.p.: Dočasný manipulačný poriadok pre sústavu vodných diel Gabčíkovo-Nagymaros na území Slovenskej republiky Aktualizácia IX. 2012

Acknowledgement

This contribution was supported by the VEGA Grant agency under contract VEGA 1/10011/12.

Modeling of long-term sedimentation in the Osijek port basin

G. Gilja, N. Kuspilić

(Faculty of civil engineering, University of Zagreb, Kačićeva 26, 10000 Zagreb, Republic of Croatia, ggilja@grad.hr)

Abstract

On Drava River's rkm 14+110 closure dam was constructed across the upstream end of the old bendway that is being preserved for Osijek port basin. During high water conditions when water level rises part of flow is diverted from main channel over closure dam. Overtopping of dam consequently disrupts water and sediment regime in port Osijek basin. Aim of this paper is to determine long-term sediment yield that enters the port carried by the flow over dam and conditions under which it deposits, changing port's morphology during the process. This process is analyzed thought 8-year period, from 2005 until 2013. Paper presents modelling method for calculation of layer thickness for suspended sediment deposited in port basin. Bed forming sediment is extracted from total sediment inflow in port basin using Reynolds number as common parameter in sediment rating curves for port basin and gauging profile. For each sediment fraction conditions of its deposition are determined based on particle fall velocity, transport velocity and water column depth. Hydraulic flow conditions are calculated from measured hydrograph using 1D computations. Since sediment rating curve doesn't depict reliable relationship corresponding to flow sediment regime is analyzed for three characteristic scenarios (mean, minimum and maximum) according to data. Results are given as longitudinal profile of volume for deposited suspended sediment and compared to measured change in bathymetry for set time period.

Keywords

Closure dam, bedload sediment, sediment transport, settling velocity

1. INTRODUCTION

On Drava River's rkm 14+110 closure dam "G" was constructed across the upstream end of the old bendway, spanning the full width of watercourse. Role of closure dam is to deflect Drava River's flow towards meander cut-off, thereby increasing efficiency of its evolution process. Closure dam is constructed as rockfill dam with crest elevation set on 82 m a. s. l., and it shields old bendway from flow for discharges under 650 m³/s.

Diversion of primary flow through constructed cut-off enabled use of old bendway as basin of port Osijek. New port Osijek is situated on right hand riverbank, from Drava River station 12+600 to 14+450, and has entrance on

downstream end of towhead. Length of port basin from entrance to closure dam is circa 1700 m, with average width of 160 m and area 20.4 ha.

Sediment is carried by flow into port basin when water elevation upstream is higher than dam crest and Drava Rive flow is divided: it partially flows through cut-off and partially inflows into port basin overtopping closure dam. Taking into account fact that crest of closure dam as constructed doesn't absolutely shield port Osijek from flow, water and sediment regime downstream of closure dam can be considered disturbed when referenced to natural conditions.

This paper presents results of flow and sediment regime analysis for port of Osijek. Analyses are based on long-term field survey data and data from adjacent gauging stations. Aim of this paper is to quantify changes in riverbed morphology induced by construction of closure dam and meander cut-off by analyzing conditions under which suspended sediment is deposited. Two approaches are used: (1) distribution of settling velocity over suspended sediment fractions and (2) application of 1-D numerical sediment transport model. Timespan used for this paper covers 8-year period, from construction of closure dam in October 2005 until June 2014.

2. METHODOLOGY

Entrainment and deposition of suspended sediment that causes morphological changes in port of Osijek is quantified using two aforementioned methods whose precision is evaluated by comparing results after 8-year period with in-situ measured bathymetry. Hydraulic geometry of Osijek port river reach is compared to natural conditions which are presumably in equilibrium at beginning and at the end of simulation. Trend of developing hydraulic geometry is used for prediction of further morphological changes in port basin.

2.1 Available data

Input for analysis is flow regime data, coupled with suspended sediment concentration and known bathymetry at the beginning and end of simulated time period. Available data consist of:

- river bathymetry of defined river reach – collected on the beginning and the end of simulated period;
- water elevation measurements on two gauging stations that are positioned on boundaries of numerical model;
- hydrological – hydraulic regime of defined river reach described through collected flow velocity profile on several occasions throughout simulated time period;
- suspended sediment concentration measurement;
- granulometric curves for both suspended and bedload sediment.

In order to describe hydrological regime of Drava River water elevation data from GS Belišće was converted in mean daily discharges using discharge curve.

GS Belišće is located on river station 53+800, and since there are no tributaries between there and defined reach, calculated discharges are suitable for flow description. Flow hydrograph data for modeled time period covered great span of discharges, from low to high flow, which almost covers full span of discharges collected from gauging station's start of operation. In following table summary of flow data for analyzed time period is given and compared to historic data (Tab. 1):

Tab 1. Summary of discharge data for GS Belišće

Characteristic discharge	Historic data from year 1962. Q [m ³ /s]	Modeled period from 2005. to 2014. Q [m ³ /s]
Q_{MIN}	160	224
Q_{AVG}	556	547
Q_{MAX}	2232	2017

Hydrological – hydraulic regime of defined river reach is described through collected flow velocity profiles on 13 occasions throughout simulated time period, from August 2009 until October 2014. Data collected during this period also included flow distribution between cut-off and port basin. Flow distribution curve for port basin flow is calculated as:

$$Q_{PORT} = -5.35 \cdot 10^{-4} \cdot Q^2 + 1.7188 \cdot Q - 870.88 \text{ [m}^3\text{/s]}, \quad (1)$$

where: Q_{PORT} is flow over closure dam [m³/s], Q is Drava River discharge [m³/s].

For description of sediment transport regime measured data on gauging station GS Donji Miholjac, located on river station 80+500, was used. On this gauging station suspended sediment data is periodically sampled several times per year, resulting with 80 measurements since year 2000. Suspended sediment data correlates well with discharge, so suspended sediment curve is developed from paired data in following form: P [kg/s] = $f(Q)$.

Correlation between discharge Q and suspended sediment yield P is not strong, therefore collected data have no distinctive trend and are characterized with large data scatter. Since data scatter is too large to be represented accurately with one curve, three characteristic scenarios for suspended sediment curve were developed: (1) minimum suspended sediment load $Q_{S(MIN)}$; (2) average suspended sediment load $Q_{S(AVG)}$ and (3) maximum suspended sediment load $Q_{S(MAX)}$. Equations defined for each of three scenarios are:

$$P = 9 \cdot 10^{-6} \cdot Q^{2.1851} \text{ [kg/s]} \text{ for } Q_{S(MIN)}, \quad (2)$$

$$P = 1.3 \cdot 10^{-4} \cdot Q^{1.8541} \text{ [kg/s]} \text{ for } Q_{S(AVG)}, \quad (3)$$

$$P = 5.18 \cdot 10^{-3} \cdot Q^{1.3757} \text{ [kg/s]} \text{ for } Q_{S(MAX)}, \quad (4)$$

where: P = suspended sediment load [kg/s], Q = Drava river discharge [m³/s].

Collected data and defined equations are given on the following figure (Fig. 1). Granulometric curve of suspended sediment reveals that it consists mainly of silt and sand, with mean particle diameter $d_{50} = 0.15$ mm.

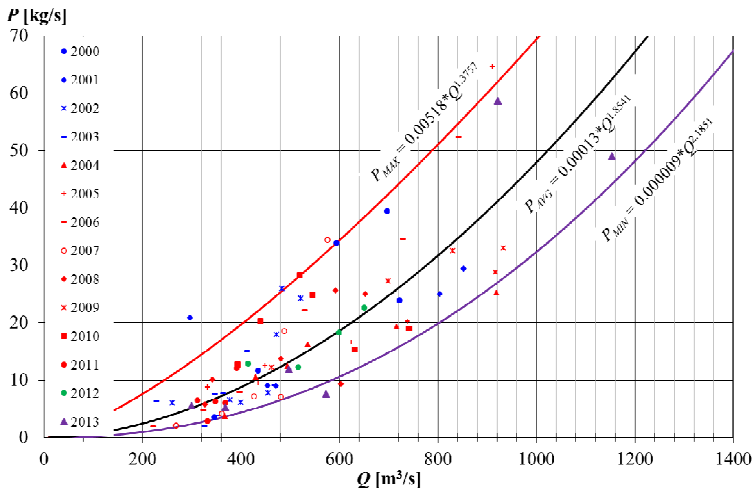


Fig. 1 Characteristic curves for scenarios of suspended sediment load

2.2 Sediment regime in port basin

Sediment yield that enters port basin carried by flow overtopping closure dam is calculated as fraction of total suspended sediment yield corresponding to ratio of overtopping flow to total flow. Suspended sediment consists of two components: bedforming, which is deposited in port basin and wash, which is transported downstream. In order to define amount of sediment deposited in port basin sediment outflow must be subtracted from sediment inflow.

Since flow conditions at gauging station Donji Miholjac and port basin differ significantly sediment entrained by flow cannot be calculated using suspended sediment curve defined at GS Donji Miholjac (Fig. 1). Therefore, suspended sediment load must be correlated with flow variables that are independent of river profile. Suspended sediment transport generally depends on the Reynolds number because pattern of flow around settling particles is controlled by the viscosity of the fluid and flow around them [Cheng 2004, Liu 2014]. Available data doesn't cover temperature of water, therefore Reynolds number is calculated without viscosity as it is presumed to be constant. Suspended sediment curves equations are as follows:

$$P = 9 \cdot 10^{-6} \cdot Q^{2.1851} \text{ [kg/s] for } Q_{S(MIN)}, \quad (5)$$

$$P = 1.3 \cdot 10^{-4} \cdot Q^{1.8541} \text{ [kg/s] for } Q_{S(AVG)}, \quad (6)$$

$$P = 5.18 \cdot 10^{-3} \cdot Q^{1.3757} \text{ [kg/s] for } Q_{S(MAX)}, \quad (7)$$

where: U is profile velocity [m/s], R is hydraulic radius [m].

These relationships are used for estimation of sediment transport capacity of port basin, *i.e.* suspended sediment outflow and subsequently amount of sediment deposited in port basin. Since suspended sediment inflow cannot be unanimously determined from available data, analyses of its deposition are conducted for three scenarios: minimum, average and maximum. Results from settling velocity method and numerical model will be compared to measured data in order to determine most appropriate method.

2.3 Settling velocity

Conditions under which suspended sediment is deposited is defined for each fraction separately, based on known settling velocity, horizontal speed of particle which is set equal to mean profile velocity and flow depth. Sediment particle settling velocity is one of the important parameters used in most sediment transport functions or formulas [Yang 2006]. In this paper van Rijn's equation was used. Van Rijn approximated the US Interagency Committee on Water Resources' curves for settling velocity using three equations, depending on particle size [van Rijn 1984]. Suspended sediment is divided into five fractions with regards to their different diameter which influences settling velocity. Fractions are divided in such a way that every fraction contains same amount of sediment, *i.e.* 20 %. For every fraction settling velocity is calculated using appropriate equation of mean particle diameter for that fraction, which is in turn used to describe settling of sediment in that fraction. Following table (Tab. 2) contains calculated settling velocities for each fraction.

Tab 2. Calculated settling velocities for each sediment fraction

sediment fraction	mean particle diameter d [mm]	settling velocity W [cm/s]
$d < 20 \%$	0.045	0.18
$20 \% < d < 40 \%$	0.09	0.74
$40 \% < d < 60 \%$	0.15	1.65
$60 \% < d < 80 \%$	0.17	2.03
$80 \% < d < 100 \%$	0.21	2.80

Time required for particle to vertically pass through water column is calculated by dividing flow depth with settling velocity for each hydrological event. Then this time is multiplied with flow velocity in order to calculate horizontal distance traveled by particle before depositing (settling length). For each fraction total sediment mass is calculated entering the port basin and then is calculated length it travels before depositing. This results in longitudinal profile of deposited sediment mass. Settling length curves depending on flow are given for each sediment fraction in following figure (Fig. 2):

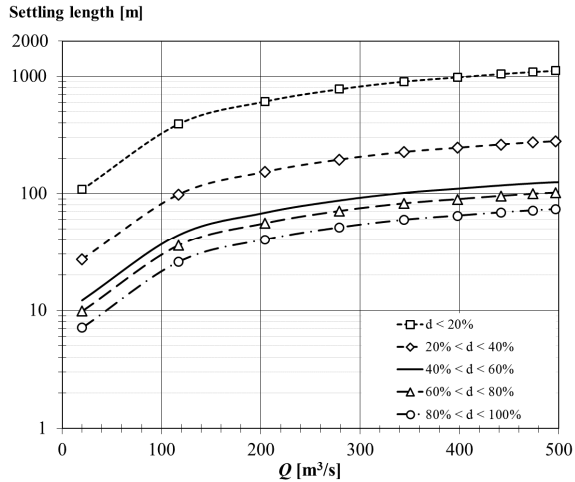


Fig. 2 Settling length for deposition of sediment fractions under variable flow conditions

2.4 Numerical model

In order to describe flow regime on defined river reach for defined time period 1-D numerical model was used. Model was set up using measured bathymetry data on river cross-sections, water levels on downstream model boundary and discharge on the upstream. Calibration of Manning's roughness coefficient was done for 13 aforementioned measurements of flow velocity profile during which water surface elevation was collected on each cross-section. Model was run for a range of discharges, resulting in longitudinal velocity and water depth profile used in sediment deposition calculations. Results of calibrated numerical model are used for description of flow regime in form of averaged variables on each cross-section: profile velocity U , hydraulic radius R , flow area A and mean depth h .

Global Drava River model is set-up from mouth of Drava River to gauging station GS Osijek, located on river station 20+000 km. For all hydrological events in modeled period, daily discretized, model is run in order to obtain longitudinal water surface profile.

Based on hydraulic regime calculated using hydrodynamic model, sediment transport can be calculated for defined river reach, as well as its influence on channel morphology through erosion and deposition processes. For this type of calculation model with smaller domain was set-up describing port basin. This model is set up on 18 cross-sections, spanning from closure dam to port entrance, with downstream boundary condition set on Drava River's natural profile, as shown on following figure (Fig. 3).

Downstream boundary condition for sediment transport model, water surface elevation, was extracted from results of global model. Sediment inflow was calculated through relation with Reynolds number as described in previous

chapters for flow situations that overflow the closure dam. For sediment transport calculation Toffaleti's formula for large sand-bed rivers was used [Toffaletti 1969]. Toffaleti's formula is based on the concepts of Einstein's total load function with several modifications, defined as total river sand discharge for range of bed size material from 0.062 to 16 mm. The function is not heavily dependent on shear velocity or bed shear. Instead, it was formulated from regressions on temperature and an empirical exponent that describes the relationship between sediment and hydraulic characteristics. A distinctive approach of the Toffaleti function is that it breaks the water column down into vertical zones and computes the concentration of each zone with a simple approximation of a Rouse concentration profile. Transport for each zone is computed separately. This approach is, obviously, most appropriate for transport with significant suspended load such that a vertical Rouse distribution includes significant concentrations in the water column. The function has been used successfully on large systems like the Mississippi, Arkansas, and the Atchafalaya Rivers [Brunner 2010].



Fig. 3 Port basin profiles used for analyses plotted on orthophoto image

2.5 Hydraulic geometry

The term “hydraulic geometry” connotes the relationships between the mean stream channel form and discharge both at-a-station and downstream along a stream network in a hydrologically homogeneous basin. Leopold and Maddock (1953) expressed the hydraulic geometry relationships for a channel in the form of power functions of discharge as:

$$B = a \cdot Q^b; h = c \cdot Q^f; U = k \cdot Q^m, \quad (8)$$

where: B is channel width [m]; a, b, c, f, k, m are parameters.

The at-a-site hydraulic geometry entails mean values over a certain period, such as a season, or a year. According to Langbein (1964), Langbein and Leopold (1964), and Yang, et al. (1981) among others, the mean values of the hydraulic

variables of equations (8) are known to follow necessary hydraulic laws and the principle of the minimum energy dissipation rate. As a consequence, these mean values are functionally related and correspond to the equilibrium state of the channel. This state is regarded as the one corresponding to the maximum sediment transporting capacity. The implication is that an alluvial channel adjusts its width, depth, slope, velocity, and friction to achieve a stable condition in which it is capable of transporting a certain amount of water and sediment. Marked changes in the channel form and associated hydraulic geometry can occur over a short period of time in the absence of exceptionally high flows and in a channel with high boundary resistance. This suggests that the approach to quasi-equilibrium or establishment of a new equilibrium position is relatively rapid.

In order to determine current state of riverbed and potential for future development hydraulic geometry of river profiles in equilibrium is calculated, as well as hydraulic geometry of port basin profiles for beginning and end of modeled period. Hydraulic geometry of Drava River was investigated over five year period, with calculation for each year and average discharge for that year. River cross-sections used for calculation were selected from reach upstream and downstream from defined reach, and in meander cut-off. These values are compared to results of hydraulic geometry of port basin profiles in order to evaluate future development of port basin.

3. RESULTS AND DISCUSSION

Results of conducted analyses were used to determine portion of suspended sediment load that is most likely to enter in port basin, to evaluate which method gives more accurate prediction of morphologic changes in port basin and to estimate trend of future morphological port basin development. Results of modeling show that two applied methods produce significantly different output.

Both methods estimate most intensive deposition in first 200 m downstream of closure dam, although settling method produces far greater values of deposited sediment. Measured bathymetry doesn't reflect this trend, as sediment mass is distributed more evenly over the length of port basin. Further downstream HEC method estimates continuous trend of reducing deposition with increasing distance. Settling method shows different trend: in first 200 m fractions $40\% < d < 100\%$ are deposited and later downstream rest of particles deposit, with increasing trend as more distance is needed for smaller fractions to settle. This trend is also visible from measured data. For both measured geometry and settling method deposition ends after 1000 m. One of the measured profiles shows significant erosion which could be result of possible sand dredging, but this anomaly is not explained. HEC model for minimum and average scenario in this area shows erosion as consequence of disbalance caused by previously deposited sediment and later deposition on port entrance. Maximum scenario model is oversaturated with sediment and it predicts deposition on full length of port basin. Following figure (Fig. 4) shows longitudinal profile of port basin for which

sediment mass balance was depicted as a change in flow area and hydraulic depth on each profile.

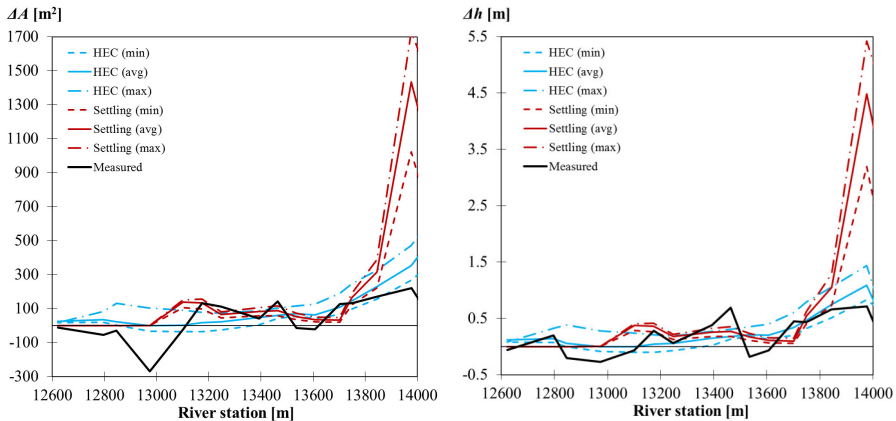


Fig. 4 Longitudinal profile of bed change representing sediment mass balance: profile area (left) and hydraulic depth (right)

Most applicable method for overall sediment mass balance is HCE method for minimum inflow scenario, which predicts 55 % greater deposition compared to measured data (49234 m³). If profiles with anomalies in measurement are disregarded this scenario shows even better results: it overestimates deposited sediment on first 1000 m by only 13 %. For this part of reach measured amount of deposited sediment is 74798 m³. Other two HEC models on this reach overestimate deposition by 65 % for average scenario and 142 % for maximum scenario. For all three scenarios used with settling methods overestimations of deposited sediment are greater, ranging from 147 % for minimum to 348 % for maximum scenario.

Both used methods do not represent turbulence, which is present in field conditions, and therefore influences sediment transport. Turbulence is most intense in area downstream of closure dam, and it prevents sediment deposition which both applied methods cannot take into account. Therefore in this area methods overestimate amount of deposited sediment, which is 53953 m³. Most applicable method for first 300 m is also HEC method for minimum inflow scenario, overestimating deposition for 28 %.

When difference between presumed scenarios separately for each method is analyzed, settling method is less sensitive to inflow mass of sediment, as it deposits total amount of sediment in basin. HEC method is more sensitive to inflow scenarios because it predicts extensive deposition in port basin entrance. Results of analyses are shown to be under expected confidence interval for sediment transport methods [van Rijn 1984], and correlate with previous analyses conducted on Drava River [Gilja *et al.* 2009]. Since for all parts of port basin best representation of sediment regime is minimum sediment inflow scenario, it is safe

to assume that sediment is not uniformly mixed throughout water profile and column. This must be taken into consideration when relationships for sediment inflow are calculated.

After it has been shown that sediment regime under varying flow regime can be reliably represented using 1-D models, temporal development of riverbed has been analyzed using principles of hydraulic geometry. Hydraulic geometry was determined for port basin profiles on the beginning of modeled period, in 2005, and at the end in 2014. Geometry of equilibrium profiles is collected in period from 2009 to 2014 for profiles located on natural reach of Drava River enclosing analyzed reach. For comparison of Drava River development cut-off profiles were used, collected in 2005 when cut-off was built and also in period from 2009 to 2014. Results for mean flow velocity and hydraulic depth are given in following figure (Fig. 5). On each figure expected relationship is plotted as dashed line through equilibrium profile points.

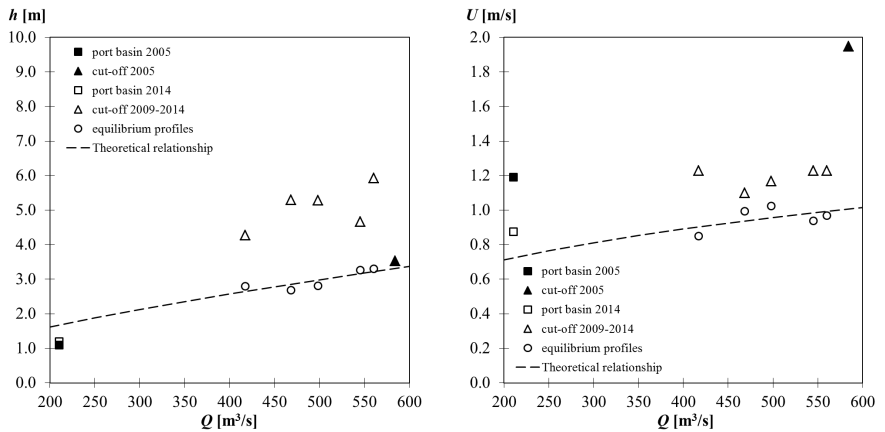


Fig. 5 Hydraulic geometry for hydraulic depth (left) and velocity (right)

When hydraulic geometry for hydraulic depth is compared to theoretical relationship it seems that cut-off profiles are distancing from equilibrium with passing time and that port basin profiles are streaming towards equilibrium but at slow pace. This trend is not consistent with hydraulic geometry for mean flow velocity, where both cut-off and port basin profiles in year 2014 are much closer to equilibrium line than in 2005.

This discrepancy in trend regarding reaching equilibrium is consequence of high boundary resistance, *i.e.* on river banks there exist trees whose roots stabilize banks and prevent erosion. Therefore, flow energy is dissipated mostly on riverbed, causing it to deepen faster than it can widen. Therefore, hydraulic geometry approach must be coupled for all three relationships (depth, width and velocity), rather than focusing on single one. This is especially important if available data covers period after high flows which rapidly modify riverbed morphology.

Based on defined hydraulic geometry we can assume that adaption of riverbed geometry to flow and sediment regime is still active process. Since flow is constrained in port area and limited as only part of flow passes through it, riverbank erosion cannot be expected, rather occurrence of bars along left bank which will impose on normal port operation.

4. CONCLUSION

Results of presented analyses show that two selected methods are applicable for calculating sediment mass balance in reaches with tranquil flow, such as ports. HEC method estimated amount of deposited sediment better than settling method, although only minimum sediment inflow scenario gave reliable results. On the other hand, settling method approximated spatial distribution of deposited sediment better. As expected, both methods underperformed in area where intense turbulence occurs and sediment deposition was overestimated by majority of methods.

Both methods are severely dependent of sediment load that enters the port, *i.e.* boundary condition. This is especially true for settling method because it deposits almost total amount of sediment that enters the model domain. In order to achieve reliable results of sediment distribution that inflows into the port would have to be verified with field data. Based on results, it can be concluded that both methods are moderately applicable for estimation of sediment regime in port basin. Results are well within confidence interval for sediment transport formulas, and total amount of deposited sediment from mass balance can be used in further analyses.

5. REFERENCES

- BRUNNER, G.W. 2010. HEC-RAS River Analysis System Hydraulic reference manual. USACE, Davis, CA, 411 p
- CHENG, N.S. 2004. Analysis of bedload transport in laminar flows. *Advances in Water Resources*, 27(9), pp 937-942.
- GILJA, G., BEKIĆ, D., OSKORUŠ, D. 2009. Processing of Suspended Sediment Concentration Measurements on Drava River. *Proceedings of the 11th WMHE Symposium (Popovska, C.)*, University Ss. Cyril and Methodius, Skopje, pp 181-192
- LIU, X. 2014. New Near-Wall Treatment for Suspended Sediment Transport Simulations with High Reynolds Number Turbulence Models. *Journal of Hydraulic Engineering*. 140(3), pp 333-339.
- TOFFALETI F.B. 1969. Definitive Computations of Sand Discharge in Rivers, *Journal of the Hydraulics Division, ASCE*, vol. 95, pp. 225-246
- VAN RIJN, L.C. 1984. Sediment Transport, Part I: Bed Load Transport. *Journal of Hydraulic Engineering*. 110/11, pp 1431-1456
- YANG, C.H. 2006. Erosion and Sedimentation Manual. U.S. Department of the Interior, Bureau of Reclamation, Sedimentation and River Hydraulics Group, Denver, Colorado, 618 p.